Bulky Ligand Systems Containing Pi-Acidic Aryl and Carboranyl Groups

Peace, Richard John

Bulky Ligand Systems Containing Pi-Acidic Aryl and Carboranyl Groups

by

Richard John Peace, B.Sc. (Dunelm)

Grey College, University of Durham

A thesis submitted in part fulfilment of the requirements for the degree of Doctor of Philosophy at the University of Durham

August 1996

STATEMENT OF COPYRIGHT

DECLARATION

The work described in this thesis was carried out in the Department of Chemistry at the University of Durham between September 1993 and August 1996. All the work is my own, unless stated to the contrary, and it has not been submitted previously for a degree at this or any other University.

FINANCIAL SUPPORT

The Engineering and Physical Sciences Research Council (EPSRC) are gratefully acknowledged for providing a grant for the work described herein.

ABSTRACT

Bulky Ligand Systems Containing Pi-Acidic Aryl and Carboranyl Groups

This thesis describes studies into the synthesis and coordination chemistry of ligands containing bulky π-acidic groups. Both π-acidic aryl and carboranyl groups have been investigated.

Chapter One highlights electronic and structural aspects of ligands investigated and computational techniques employed.

Chapter Two describes the synthesis of aromatic systems bearing nitrogen substituents and trifluoromethyl groups, with a view to their use in the synthesis of new ligands. The π-interaction between the nitrogen substituent and aromatic ring has been investigated and is found to vary considerably with the nature of the substituent and position of the CF_3 groups on the ring.

Chapter Three describes the synthesis of molybdenum compounds containing CF_3 substituted aryl-imido ligands. The presence of the π-acidic group is found to decrease π-bonding from the ligand to the metal which results in changes in the reactivity of such complexes.

Chapter Four describes the synthesis of nitrogen-substituted carboranes 1-NHX-2-R-1,2-$C_2B_{10}H_{10}$ (R = Me, Ph; X = 2-R-1,2-$C_2B_{10}H_{10}$, NHAr, OH, H) and 1-NX-2-R-$C_2B_{10}H_{10}$ (R = Me, Ph; X = O, NAr). The structures of many of these compounds are described and the π-interaction between the cage and substituent investigated. This π-interaction determines the orientation of the substituent relative to the cage and causes changes in the geometry of the cage. The ^{11}B NMR shift of the atom directly opposite the nitrogen substituent is found to give an accurate indication of the *exo* π-bond order. In light of these observations data from other systems have been re-examined.

Chapter Five describes the incorporation of carborane containing ligands into metal systems. The π-acidic carboranyl group reduces π-bonding from the ligand to the metal. The consequences of this on the structure and reactivity of these complexes are discussed.

Chapter Six gives experimental details for Chapters Two to Five.

Richard John Peace (August 1996)

ACKNOWLEDGEMENTS

Firstly I must thank Ken Wade for his advice and inspiration during my three years, and Vernon Gibson for his encouragement and for starting me out in the right direction. I must also thank Hugh MacBride for his help, suggestions and stories. Mark Fox, Wendy Gill and Andy Hughes are also thanked for many useful discussions, Brian Hall for all his help, and everyone else in lab 104/106 for humouring me and making the last three years so enjoyable.

Ray-the-glassblower and Gordon-the-glassblower have been wonderful, particularly for seeming delighted at the sight of yet more NMR tubes. Joe must not be forgotten for seeming happy to let things leave stores, nor Jimmy for making life interesting. The work of Alan Kenwright, Ian McKeag and Julia Say is gratefully acknowledged. The hard work of Andrei Batsanov, Judith Howard, Christian Lehmann and Jing Wen Yao at Durham and Bill Clegg and Mark Elsegood at Newcastle in solving the crystal structures in this thesis has been invaluable.

I must thank Stella for all her support, love and understanding and the numerous animals for the squeaks, hairs, bits of hay and bitten furniture. Finally I must thank my parents for their support, both moral and financial, throughout my six years at Durham.

ABBREVIATIONS

$\Sigma\angle X$	Sum of bond angles around atom X
18-C-6	18-crown-6, 1,4,7,10,13,16-hexaoxacyclooctadecane
Ar	Aryl
C_i, C_o, C_m, C_p	C atom at *ipso*, *ortho*, *meta* or *para* position in aromatic ring
COSY	Correlation spectroscopy
dme	1,2-dimethoxyethane
Fmes	Fluoromes group, 2,4,6-$(CF_3)_3C_6H_2$
Ftol	Fluorotol group, 2-$(CF_3)C_6H_4$
Fxyl	Fluoroxyl group, 3,5-$(CF_3)_2C_6H_3$
HETCOR	Heteronuclear correlation spectroscopy
^{i}Pr	Iso-propyl group, $CHMe_2$
IR	Infra Red
L	General two electron ligand
Me	Methyl
MO	Molecular orbital
NMR	Nuclear Magnetic Resonance
Ph	Phenyl
PS	Proton sponge, 1,8-N,N,N',N'-tetramethylnapthalenediamine - 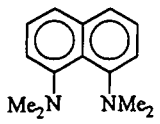
R	Any hydrocarbon group
RHF	Restricted Hartree Fock
TBDMS	Tertiarybutyldimethylsilyl group, Si^tBuMe_2
^{t}Bu	Tertiary butyl group, CMe_3
thf	Tetrahydrofuran
TMS	Trimethylsilyl
Tol	Tolyl, 4-Me-C_6H_4
VSEPR	Valence shell electron pair repulsion
X	General one electron ligand
XCbY or 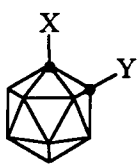	1-X-2-Y-1,2-$C_2B_{10}H_{10}$

KEY TO COMPOUND NUMBERING

1	$FmesN_2Ph$	**20**	PhCbNO
2	$FmesNH_2$	**21**	MeCbNO
3	FmesNHNHPh	**22**	$(PhCb)_2NH$
4	$FtolNH_2$	**23**	$(MeCb)_2NH$
5	$1\text{-}NH_2\text{-}3,5\text{-}(CF_3)_2C_6H_3$	**24**	$(PhCb)_2N^-$
6	$1\text{-}NH_2\text{-}2\text{-}(CF_3)C_6H_4$	**25**	$MeCbN_2Ph$
7	Aniline	**26**	$PhCbN_2Tol$
8	$Mo(NFmes)_2(OTMS)_2$	**27**	MeCbNHNHPh
9	$Mo(NFtol)_2Cl_2\cdot dme$	**28**	PhCbNHNHTol
10	$Mo(NFxyl)_2Cl_2\cdot dme$	**29**	MeCbNHOH
11	$Mo(NFmes)_2Cl_2$	**30**	PhCbNHOH
12	$Mo(NFmes)_2Cl_2\cdot 2py$	**31**	$MeCbNH_2$
13	$Mo(NFmes)_2Cl_2\cdot dme$	**32**	$PhCbNH_2$
14	$Mo(NFmes)_2Cl_2\cdot 2dme$	**33**	$[Mo(NCbMe)_2Cl_4][Et_3NH]_2$
15	$Mo(NFtol)_2(PMe_3)_3$	**34**	$Mo(NAr^i)_2(OCbPh)_2$
16	$Mo(NFmes)_2(PMe_3)_3$	**35**	$Mo(NAr^i)_2(OCbMe)_2$
17	$Mo(NFxyl)_2(PMe_3)_2$	**36**	$Mo(NtBu)_2(CbMe)_2$
18	$Mo(NFmes)_2(PMe_3)_2(C_2H_4)$	**37**	$Mo(NAr^i)_2(CbMe)_2$
19	$Mo(NFtol)_2(PMe_3)_2(C_2H_4)$	**38**	$Mo(NAr^i)_2(1,2\text{-}C_2B_{10}H_{10})$

All lines drawn on graphs in this thesis are intended merely to guide the eye. Error bars on distances determined by X-ray diffraction represent three times the e.s.d. unless stated otherwise.

Selected bond lengths and angles from crystal structures are given in the text. Full tables of bond lengths, bond angles and atomic coordinates are given in Appendix C.

TABLE OF CONTENTS

CHAPTER ONE

INTRODUCTION

CHAPTER TWO

π-ACIDIC AROMATIC SYSTEMS WITH NITROGEN SUBSTITUENTS

CHAPTER THREE

IMIDO LIGANDS CONTAINING π-ACIDIC AROMATIC GROUPS

CHAPTER FIVE

LIGAND SYSTEMS CONTAINING ICOSAHEDRAL CARBORANES

CHAPTER SIX

EXPERIMENTAL DETAILS

APPENDIX A

ADDITIONAL DATA FROM CHAPTER TWO

APPENDIX B

ADDITIONAL DATA FROM CHAPTER FOUR

APPENDIX C

CRYSTAL DATA

APPENDIX D

COURSES, LECTURES, COLLOQUIA AND CONFERENCES ATTENDED

Chapter One

Introduction

1.1 INTRODUCTION

The work described in this thesis is an investigation of novel ligands containing π-acidic groups i.e. groups which can accept electrons into a vacant π orbital. Both fluorinated aromatic and carboranyl systems have been investigated as π-acids.

If a substituent bearing a lone pair (e.g. NH_2, OH) is bonded to a π-acid the lone pair can form a dative π-bond to this group. This is evident in multiple bond character between the π-acid and substituent and in changes in the bonding within the π-acidic group itself. Factors which influence the extent of this π-interaction have been investigated.

Species of the form RNH_2 and ROH (R = aryl or carboranyl group) have been used to form metal complexes in which the π-acidic group is bound to a transition metal via an atom bearing a lone pair (i.e. MNR, MOR). This lone pair can be involved in π-bonding to either the metal or the π-acid - there will be competition for the lone pair. Hence the π-acidic group will reduce the availability of the lone pair for π-bonding to the metal and this is reflected in both the structure and reactivity of such complexes.

Much of the work in this thesis involves, or is directed towards, the synthesis of a number of common ligand types. Section 1.2 of this chapter gives a summary of these ligands and the effect that steric and electronic factors have on such complexes. This is not intended to be comprehensive, but to highlight areas of particular relevance. Section 1.3 describes orientational preferences in metal complexes containing π-donor ligands. Section 1.4 describes some of the computational techniques used to study these compounds.

1.2 LIGAND TYPES

1.2.1 ALKOXY AND ARYLOXY LIGANDS OR

Alkoxy and aryloxy ligands (OR) consist of an alkyl or aryl group bound to a metal via an oxygen atom. Such ligands can be terminal or bridging (Figure 1.1). The steric nature of R will dictate which mode is preferred, bulky substituents preventing the formation of an alkoxide bridge.[1] This is evident in the volatility of such compounds. $Zr(OCH_3)_4$ is involatile due to a high degree of polymerisation. With increasing bulk of the alkyl group the degree of polymerisation decreases, $Zr(OEt_2)_4$ subliming at 180°C, 10^{-4} Torr, $Zr(O^iPr)_4$ distilling at 160°C, 0.1 Torr and $Zr(O^tBu)_4$ distilling at 52°C, 0.1 Torr.

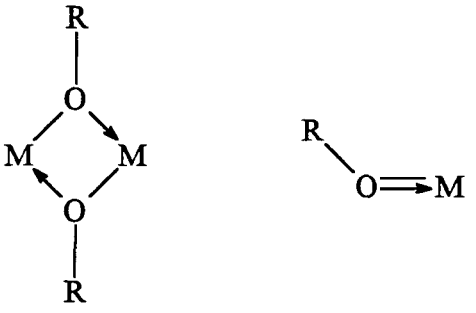

Figure 1.1 Bonding modes in alkoxides and aryloxides

The OR ligand can function as a one electron donor to a metal or, by using the lone pairs on oxygen, a three or five electron donor. For a terminal OR ligand the M-O bond will consist of a σ-bond and up to two π-bonds. The frontier orbitals on oxygen are shown in Figure 1.2.

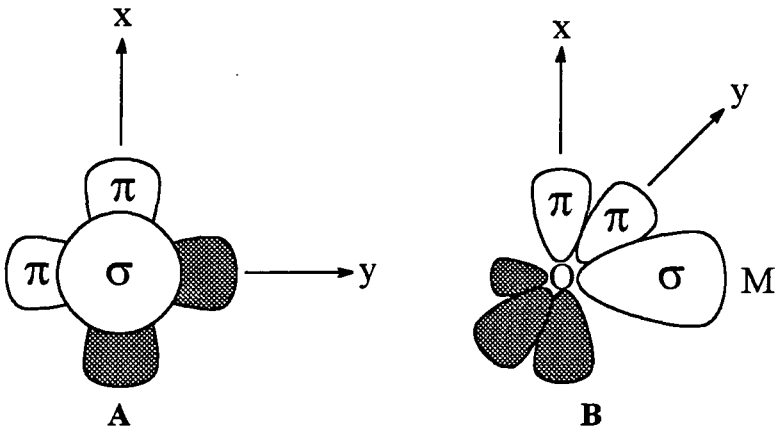

Figure 1.2 **π and σ-donor orbitals on oxygen viewed down M-O bond (A) and from side (B)**

Only rarely are both lone pairs used for π-bonding to the metal. In the compound $(^tBu_3CO)_2ZrMe_2$ both lone pairs are used resulting in a short Zr-O distance and large Zr-O-C angle, almost linear, with an sp hybridised O atom.[2] More commonly M-O-C angles are about 140° with less M-O π-bonding.[3] The extreme case is represented by $(dppe)_2Pt(OMe)Me$ in which there are no vacant π-orbitals on the metal resulting in a Pt-O-C bond angle of about 120°.[4]

The inclusion of bulky, electron withdrawing aryl groups in aryloxides has led to the isolation of a number of metal complexes containing low coordinate metal centres. These include $[Tl(OC_6H_2(CF_3)_3)]_2$ and $[In(OC_6H_2(CF_3)_3)]_2$ (Figure 1.3),[31,32] the first structurally characterised examples of two coordinate Tl(I) and In(I). The stability of these low coordinate complexes is attributed to a combination of the bulk and electron withdrawing nature of the $C_6H_2(CF_3)_3$ group.

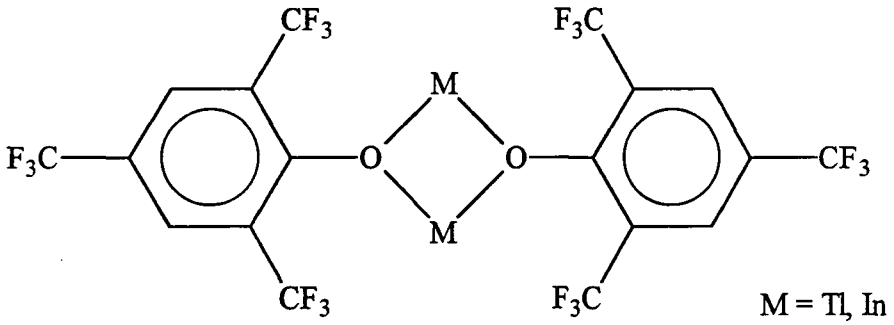

Figure 1.3

Alkoxides have found use in metal complexes with catalytic behaviour. One such group of complexes is the 'Schrock' type ROMP (Ring Opening Metathesis Polymerisation) initiators of the form $M(OR)_2(NR')(CHR'')$ (M = Mo, W). It has been found that the nature of the group R of the alkoxide ligand affects both the activity of the initiator and the stereochemistry of the resulting polymer.[5]

1.2.2 METAL AMIDE LIGANDS NR_2

Amide ligands can be either terminal or bridging and sources of either one or three electrons. The tendency to form bridged structures is less than for alkoxides due to the greater steric crowding at the nitrogen atom compared to that at the oxygen atom. $Zr(NMe_2)_4$, although largely monomeric in solution,[6] is found to be dimeric in the solid state (Figure 1.4).[7]

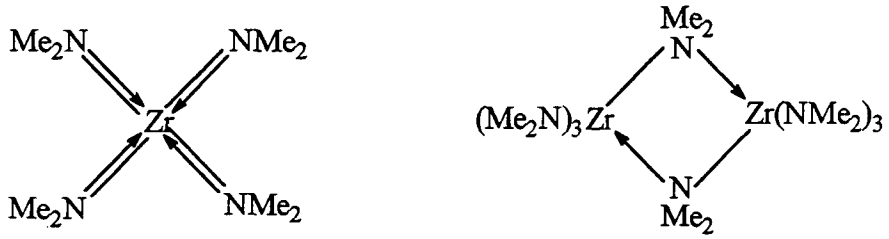

Solution
(Terminal Amides)

Solid State
(Terminal and Bridging Amides)

Figure 1.4 Solution and solid state structures of $Zr(NMe_2)_4$

Such compounds undergo aminolysis to form new metal amides releasing the corresponding amine (Equation 1.1).[4,6,8] The steric bulk of both R and R' will determine the extent to which substitution will take place. For example, treatment of $Zr(NMe_2)_4$ with $HNEt_2$ yields $Zr(NEt_2)_4$ whereas HN^iPr_2 yields $Zr(NMe_2)_2(N^iPr)_2$.[6]

$$M(NR_2)_n + xHNR'_2 \longrightarrow M(NR_2)_{(n-x)}(NR'_2)_x + xHNR_2$$

Equation 1.1

A bridging amide group functions as a one electron ligand to one metal using the lone pair in the formation of a bridging dative σ-bond to the other. In a terminal amide the lone pair will form a π-bond to the metal resulting in a planar nitrogen environment (Figure 1.5).

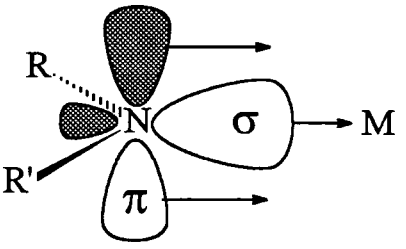

Figure 1.5 π and σ-donor orbitals in terminal amides

It has proved difficult to synthesise dialkylamides of the later transition metals. This is attributed to the bonding properties of the ligand which, being a strong π-donor ligand, will form strong bonds only to the early π-acceptor transition metals, but weaker bonds to the later π-donor metals. The use of silylamides $N(SiMe_3)_2$ has allowed the synthesis of such compounds for all first row transition metals[9,10,11,12] and several lanthanides.[13] Their stability is attributed to the bulk and π-acidity of the silyl group.

The steric bulk of certain dialkylamides and disilylamides has been used to allow the isolation of transition metal complexes with unusually low coordination numbers including $Cr(N^iPr_2)_3$,[14] $M(NSiMe_2)_3$ (M = Sc,[10] Ti,[11] V,[12]). Disilylamides have also proved to be bulky enough to allow the isolation of three coordinate lanthanide complexes $Ln(N(SiMe_3)_2)_3$.[13] Four coordinate actinide complexes including $U(NEt_2)_4$ and $ThCl(N(SiMe_3)_2)_3$ have also been synthesised.[15,16]

1.2.3 IMIDO LIGANDS NR

As with both alkoxides and amides, imido ligands can be both bridging and terminal (Figure 1.6). The imido ligand NR^{2-} is both isoelectronic and isolobal with the alkoxide ligand RO^- and can act as either a one, three or five electron donor (using a neutral electron counting formalism).

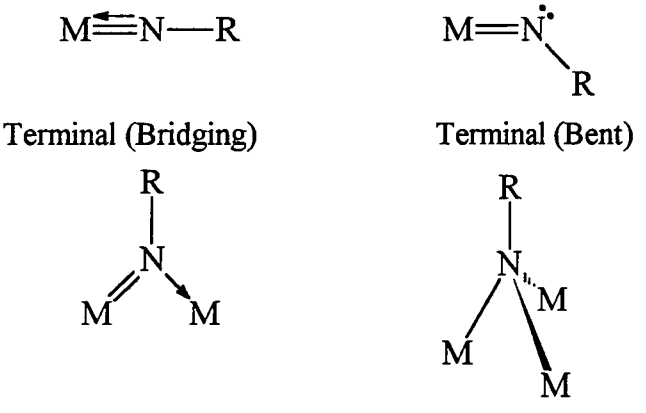

Figure 1.6 Imido bonding modes

A terminal imido ligand will form a σ-bond and up to two π-bonds to the metal. If two π-bonds are formed to the metal centre the imido group will be linear, a bent imido ligand implying that only a single π-bond to the metal is formed. Frequently the bonding is intermediate between these two cases with a M-N bond order of between 2 and 3.[17] Such bond angles are susceptible to steric effects and prove to be a poor indication of bonding, M-N-R bond angles between 150° and 180° can be considered to represent 'linear' imido groups.[18] $Mo(NPh)_2(S_2CNEt_2)_2$ represents the only example of a structurally characterised 'bent' imido group, having one linear (Mo-N-C 169.4(4)Å) and one bent (Mo-N-C 139.9(4)Å) imido ligand.[19] There are examples of imido ligands which, due to a lack of orbitals on the metal of suitable symmetry,[20] cannot form two π-bonds to the metal and possess a lone pair localised on nitrogen despite their linearity.[21]

As with alkoxides the steric and electronic nature of the substituents affects the structure and reactivity of such complexes. For example, the reduction of $Mo(NR)_2Cl_2$.dme in the presence of PMe_3 gives an imido bridged dimer $[Mo(N^tBu)(\mu\text{-}N^tBu)(PMe_3)]_2$ when R = ^{t}Bu (Figure 1.7A) but monomeric $Mo(NAr^i)_2(PMe_3)_2$ (Figure 1.7B) when R = Ar^i (2,6-^{i}Pr-C_6H_3).[22] This is thought to be due to the greater bulk of the Ar^i group. Similarly, treatment of $Mo(NR)_2Cl_2$·dme with EtMgBr in the presence of PMe_3 yields the mono-phosphine complex $Mo(N^tBu)_2(PMe_3)(C_2H_4)$ but bis-phosphine $Mo(NAr^i)_2(PMe_3)_2(C_2H_4)$.

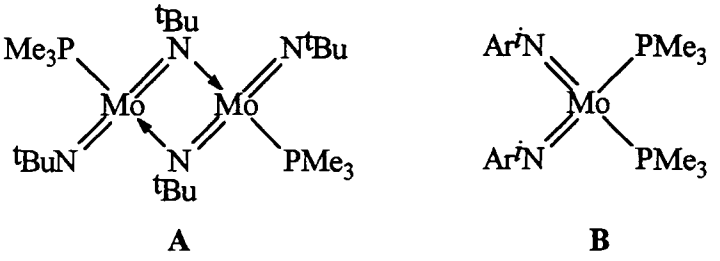

A **B**

Figure 1.7

1.3 ORIENTATIONAL PREFERENCES FOR π-DONOR LIGANDS

The formation of a π-bond between a ligand and metal centre requires vacant d-orbitals on the metal of the required symmetry of which there are a limited number. In compounds with more than one such ligand there will be competition for the available orbitals, the strongest π-donor determining the orientation of the others.[23] π-Donor ligands can be divided into three classes for such purposes. Π_1 ligands possess a single π-symmetry orbital e.g. alkenes, amides, carbenes. Π_2 ligands have two degenerate π-symmetry orbitals e.g. NR, OR, Cl, Cp. $\Pi_{2'}$ ligands have two π-symmetry orbitals which are non-degenerate e.g. alkynes.

Given these ligand classes the orientations in a pseudo tetrahedral complex can be predicted. Other geometries can be reduced to tetrahedral, e.g. by considering three ligands in an octahedral geometry to be a single composite ligand.

Figure 1.8 summarises orientation preferences in compounds containing π-donor ligands. For a compound containing a dominant Π_2 donor the π-symmetry orbital of a Π_1 ligand will point towards the Π_2 ligand. If there are two dominant Π_2 ligands this π-symmetry orbital of the Π_1 ligand will point between these two ligands.

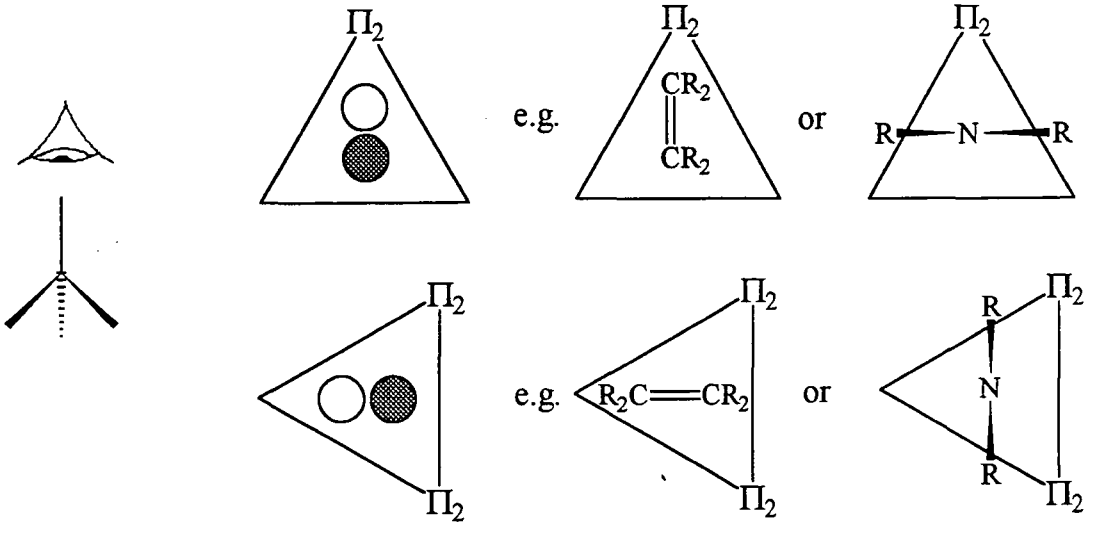

Figure 1.8 Orientations of π-donor ligands in tetrahedral complexes (viewed down Π_1 - metal axis)

1.4 Quantum Chemistry And Molecular Modelling

1.4.1 Introduction

The principles of quantum mechanics and their application in the determination of the electronic structure of molecules, and hence associated properties such as molecular geometries and energies, have been understood since the early decades of the century. Only within the last 30 years or so with the advent of computers have such calculations been possible without gross simplifications. As the power of computers continues to increase rapidly and the reducing cost of such machines increases their availability it becomes feasible to perform such calculations on increasingly more complex molecules and higher levels of theory. Such calculations have led to an increase in the understanding of chemical bonding and other properties.[24]

Simplifications and approximations are still required. There are many different levels of theory and the time required for calculations increases with the complexity of the theory, as does the associated cost. The level of theory used has to be matched to the size of molecule, the information required and the time and cost which can be justified. In general the simpler theories perform better in predicting trends than in calculating absolute quantities such as total energies. This section describes the different methods used in this thesis.

1.4.2 Ab Initio Methods

Ab initio calculations, meaning "from the beginning", are generally considered to be the most accurate of molecular orbital calculations and are certainly the most computationally expensive. There are several different levels, the simplest of which is Restricted Hartree Fock and is the most commonly used for large molecules. A number of assumptions are made. Amongst these is the Born-Oppenheimer approximation which separates the motions of electrons from that of nuclei and hence the electrons are treated as moving in a field created by nuclei in fixed positions. The molecular orbitals which are calculated are expressed in terms of basis functions which resemble atomic orbitals. This is often known as the LCAO-MO method (Linear Combination of Atomic Orbitals). There are a number of terms which describe the

motion of the electrons, the most difficult computationally is that describing the repulsion between two electrons. In the Hartree-Fock method this is overcome by treating each electron as moving in the average field of all other electrons (and the nuclei). Such a method requires a knowledge of the positions of all other electrons - these are not known initially and the problem is clearly insoluble mathematically. In practice the initial wavefunctions are guessed and modified by an iterative procedure until no further change occurs within set limits - the field is "self consistent" and such calculations are thus known as SCF (Self Consistent Field) calculations. Such a method neglects the correlation between the motion of electrons and more advanced methods have been developed to account for this but are computationally more complex and not feasible for large molecules.

The results obtained from such methods will obviously depend on the basis functions used to describe the AO's. This *basis set* must be flexible enough to accurately describe the orbitals, though the greater the number of functions the more expensive (though more accurate) the calculation. Such functions consist of combinations of gaussian functions. STO-3G is simplest of basis sets in common use and describes each AO in terms of three gaussian functions. Higher levels include contracted and diffuse functions to allow the functions to effectively change size e.g. 3-21G and 6-31G. Also included in some basis sets are functions of a higher quantum number which allow displacement of AO's from the nucleus. Such basis sets are denoted by a * e.g. 3-21G*. This is particularly important for elements such as sulphur and phosphorus which require d-orbitals to accurately describe certain compounds, such functions being absent in many basis sets.

1.4.3 Semiempirical Methods

These methods use empirical parameters in the calculation of wavefunctions and are hence much faster than *ab initio* methods.[25] These parameters are determined by a fitting procedure using a number of known compounds, the parameters being altered until a calculated value (frequently heat of formation) matches that determined experimentally. The results from such calculations can be as good as results from *ab initio* calculations. Results are usually best for molecules similar to those considered

for the initial parameterisation. MNDO[26], AM1[27] and PM3[28] are the most commonly used methods. These methods use the 'core approximation' which treats the valence electrons as moving in a field due to the nucleus and core electrons which are represented by a single function. AM1 is based on the MNDO method with a modified description of the core and leads to improvements in the calculation, particularly the treatment of hydrogen bonding. PM3 represents a different method of parameterisation for MNDO calculations, leading to an improvement on MNDO calculations. AM1 has been used in this thesis as it is more accurate than MNDO and is parameterised for boron[29] which PM3 is not. These methods rely on a SCF calculation.

Hückel theory is the most basic of calculational methods and treats only the π-system of molecules. Extended Hückel[30] includes also σ-bonding and although being relatively simple can produce useful results. It is parameterised for far more elements than AM1 and as it does not use an SCF procedure is far faster.

1.4.4 Mulliken Population Analysis

Mulliken population analysis is a method by which properties such as bond orders and atomic charges may be calculated, hence returning some familiar chemical concepts to such MO calculations. These must be treated with some care as the method for assigning an electron in an MO to a particular atom is arbitrary. They are particularly useful for describing *trends* in a series of similar compounds rather than producing absolute values.

1.4.5 Geometry Optimisation

Using MO calculations it is possible to calculate equilibrium geometries. Structural parameters are varied until a minimum in energy is achieved - a procedure known as geometry optimisation. Care must be exercised as the procedure will only find the nearest minimum and not necessarily the lowest minimum. If the lowest energy configuration is in doubt it is wise to perform a calculation at a lower level in a number of orientations to determine the approximate geometry before proceeding at a higher

level. Geometries calculated by this method correspond to an isolated gas phase molecule.

Such calculations can be very lengthy and often only part of a molecule is optimised, the rest being fixed to a geometry calculated from standard bond lengths and angles or determined by X-ray diffraction. Such approximations usually give good results particularly in establishing trends or approximate orientations.

1.5 REFERENCES

1 D.C. Bradley, *J. Organomet. Chem.*, **1982**, *239*, 17

2 H. Weingold, P.C. Wailes, A.P. Bell, *J. Organomet. Chem*, **1972**, *34*, 155

3 M.H. Chisholm, I.P. Rothwell, *"Comprehensive Coordination Chemistry"*, Volume II, pp 336-364, Pergamon Press, 1987

4 M.H. Chisholm, D.M. Hoffman, J.C. Huffman, *Inorg. Chem*, **1984**, *23*, 3683

5 W.J. Feast, V.C. Gibson and E.L. Marshall, *J. Chem. Soc., Chem. Commun.*, **1992**, *16*, 1157

6 D.C. Bradley and I.M. Thomas, *J. Chem. Soc.*, **1960**, 3857

7 M.H. Chisholm, C.E. Hammond, J.C. Huffman, *Polyhedron*, **1988**, 7, 2515

8 D.C. Bradley and I.M. Thomas, *Can. J. Chem*, **1962**, *40*, 449; D.C. Bradley and M.H. Chisholm, *Acc. Chem. Res*, **1976**, *9*, 273; M.F. Lappert and A.R. Sanger, *J. Chem. Soc. (A)*, **1971**, 874

9 H. Burger and U. Wannagat, *Monatsh. Chem.*, **1963**, *94*, 1007; H. Burger, C. Forker and J. Goubeau, *Monatsh. Chem.*, **1965**, *96*, 597.

10 D.C. Bradley and R.G. Copperthwaite, *Chem. Commun.*, **1971**, 765

11 E.C. Alyea, D.C. Bradley and R.G. Copperthwaite, *J. Chem,. Soc., Dalton Trans.*, **1972**, 1580

12 D.C. Bradley, R.G. Copperthwaite, S.A. Cotton, J. Gibson and K.D. Sales, *J. Chem. Soc., Dalton Trans.*, **1973**, 191

13 D.C. Bradley, J.S. Ghotra and F.A. Hart, *J. Chem. Soc., Chem. Commun.*, **1972**, 349; D.C. Bradley, J.S. Ghotra and F.A. Hart, *J. Chem. Soc., Chem. Commun.*, **1973**, 1021

14 E.C. Alyea, J.S. Basi, D.C. Bradley and M.H. Chisholm, *Chem. Commun.*, **1968**, 495

15 H. Gilman, R.G. Jones,.E. Bindschader, D. Blume, G. Karmas, G.A. Martin Jr., J.F. Nobis, J.R. Thirtle, H.L. Yale, F.A. Yoeman, *J. Am. Chem. Soc.*, **1956**, *78*, 2790

16 D.C. Bradley, J.S. Ghotra and F.A. Hart, *Inorg. Nucl. Chem. Letters*, **1974**, *10*, 209

17 T.R. Cundari, *J. Am. Chem. Soc.*, **1992**, *114*, 7879

18 A. Bell, W. Clegg, P.W. Dyer, M.R.J. Elsegood, V.C. Gibson and E.L. Marshall, *J. Chem. Soc., Chem. Commun.*, **1994**, 2247

19 E.A.Maata, R.A.D. Wentworth, B.L. Haymore, *J. Am. Chem. Soc.*, **1979**, *101*, 2063

20 R. Hoffmann, J.W. Lauher, *J. Am. Chem. Soc.*, **1976**, *98*, 1729

21 J.E. Bercaw, G. Parkin, A. Van Asselt, D.J. Leahy, L. Whinnery, N.G. Hua, R.W. Quay, L.M. Henling, W.P. Schaeffer, B.D. Santarsiero, *Inorg. Chem.* **1992**, *31*, 82; R.R. Schrock, J.T. Anhaus, T.P. Kee, M.H. Schofield, J. Am. Chem. Soc., 1990, 112, 1642; R.G. Bergman, F.J. Hollander, P.J. Walsh, J. Am. Chem. Soc., 1988, 110, 8729

22 P.W. Dyer, V.C.Gibson and W. Clegg, *J. Chem. Soc. Dalton Trans.*, **1995**, 3313

23 V.C. Gibson, *J. Chem. Soc. Dalton Trans.*, **1994**, 1608

24 W.J. Hehre, L. Radom, P.v.R. Schleyer, J.A. Pople, "Ab Initio Molecular Orbital Theory", John Wiley and Sons, **1986**; A. Hinchliffe, "Computational Quantum Chemistry", John Wiley and Sons, **1988**; S.R. La Paglia, "Introductory Quantum Chemistry", Harper and Row, **1971**

25 J.A. Pople, D.L. Beveridge, "Approximate Molecular Orbital Theory", McGraw-Hill, **1970**

26 M.J.S. Dewar, W. Thiel, *J. Am. Chem. Soc.*, **1977**, *99*, 4899,

27 M.J.S. Dewar, E.G. Zoebisch, E.F. Healy and J.J.P. Stewart. *J. Am. Chem. Soc.*, **107**, *3902*, 1985

28 J.J.P. Stewart, *J. Comp. Chem.*, **1989**, *10*, 209; *J. Comp. Chem.*, **1989**, *10*, 221

29 M.J.S. Dewar, C. Jie, E.G. Zoebisch, *Organometallics*, **1988**, *7*, 513

30 R. Hoffmann, *J. Chem. Phys.*, **1963**, *39*, 1397; R. Hoffmann, W.N. Lipscomb, *J. Chem. Phys.*, **1962**, *36*, 2179 and 3489; J.H. Ammeter, H.B. Burgi, J.C. Thibeault and R. Hoffmann, *J. Am. Chem. Soc.*, **1978**, *100*, 3686

31 M. Scholz, M. Noltemeyer, H.W. Roesky, *Angew. Chem., Int. Ed. Eng.*, **1989**, *28*, 1383

32 H.W. Roesky, M. Scholz, M. Noltemeyer, F.T. Edelmann, *Inorg. Chem.*, **1989**, *28*, 3829

Chapter Two

π-Acidic Aromatic Systems With Nitrogen Substituents

2.1 INTRODUCTION

1,3,5-tris(trifluoromethyl)benzene ('fluoromes', pronounced 'fluoromess' for fluoromesityl) has been the subject of much attention in recent years due to its ability to stabilise unusual coordination environments through the combination of both its steric bulk and electron withdrawing nature. A survey of the existing chemistry of this group (see Section 2.1.1) reveals its use as a ligand to both main group and transition metals, either directly by a M-C σ-bond or via a non-metal (e.g. O, S, P). There are, however, no reports of fluoromesityl compounds with nitrogen substituents despite the importance of aryl nitrogen compounds as ligand precursors.

Many common methods of placing a nitrogen substituent onto an aromatic ring are not feasible in this case due to the nature of the fluoromes group. For example, electrophilic nitration would be difficult due to the deactivating and *meta* directing nature of the CF_3 groups which will not facilitate nitration at a hindered *o*-position. This chapter describes the synthesis of 2,4,6-tris(trifluoromethyl)aniline **2** via the reduction of 2,4,6-tris(trifluoromethyl)azobenzene **1**. The synthesis of 2,4,6-tris(trifluoromethyl)hydrazobenzene **3**, also a reduction product of the azobenzene, is also described.

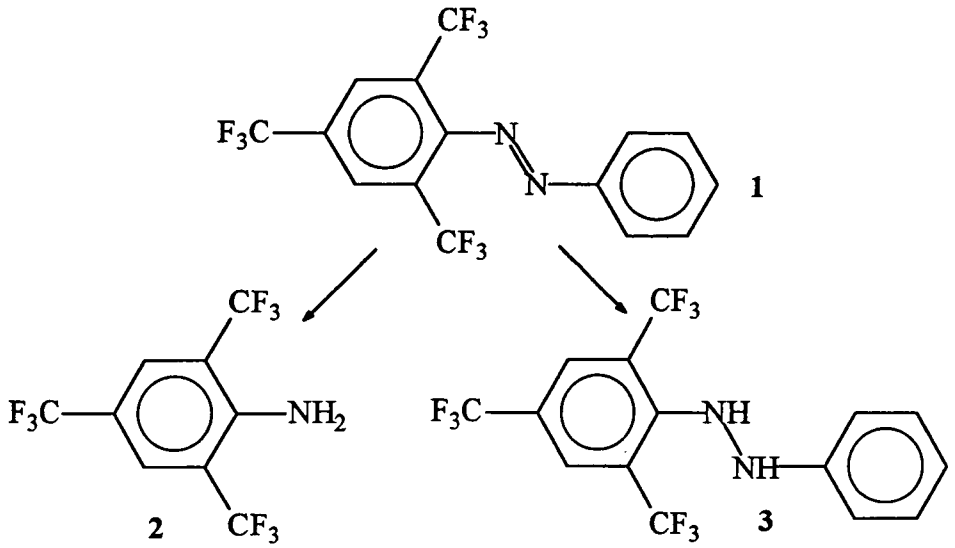

Scheme 2.1

The interaction between aromatic systems and such azo[1,2], hydrazo[3] and amino[4,5,6] functionalities has been of interest for many years. Other CF_3 substituted anilines such as 1-NH_2-2-CF_3-C_6H_4, 1-NH_2-4-CF_3-C_6H_4 and 1-NH_2-3,5-$(CF_3)_2$-C_6H_4 are readily

available commercially and although both less bulky and less strongly electron withdrawing still offer potential as interesting ligands and hence have also been considered here.

2.1.1 SUBSTITUTED 2,4,6-TRIS(TRIFLUOROMETHYL)PHENYL COMPOUNDS

2.1.1.1 DIRECT METAL-CARBON σ-BONDS

There are many compounds in which the fluoromes ring is directly bonded to a metal by a M-C σ-bond. The reaction of ^{n}BuLi with fluoromes generates 1-lithio-2,4,6-tris(trifluoromethyl)benzene[7] (Lifmes) which has proved to be an extremely versatile reagent. The reaction of Lifmes with metal halides has led to the synthesis of a wide range of compounds with a fluoromes group as a ligand. Recent examples of main group metals include Ga[8] , Sn[9], Pb[10] and Bi[11]. There are fewer transition metal complexes, these include M(Fmes)$_2$ (M=Zn[12], Hg[7], Cu[7], Ni[13], Co[13]), Cufmes, Cr(PMe$_3$)$_2$(Fmes)$_2$[14] and M(N^{t}Bu)$_2$(Fmes)$_2$ (M=Cr, Mo)[14]. Many of these compounds have unusually low coordination numbers which in some cases are stabilised by weak M···F interactions in addition to the steric bulk.

2.1.1.2 OXYGEN SUBSTITUENTS

The action of bis(trimethylsilyl)peroxide on Lifmes followed by subsequent treatment with HCl has been shown to generate 1-hydroxy-2,4,6-tris(trifluoromethyl)benzene[15] which has not been structurally characterised. The compound has proved useful in the synthesis of novel aryloxides stabilising unusual coordination environments in metals. These compounds include both main group (Na[16], K[16], Mg[17], Tl[15], In[18]) and transition metals (W[17], Mn[17]).

2.1.1.3 SULPHUR SUBSTITUENTS

1-Mercapto-2,4,6-tris(trifluoromethyl)benzene has been synthesised by the reaction of sulphur with Lifmes[7] followed by hydrolytic cleavage of the Li-S bond. The thiolate residue has been used as a ligand to many metals including both main group (Zn[19], Pb[19], In[20]) and transition metals (Mn[19]). Although the thiol itself has not been structurally characterised the structure of the disulphide (Fmes-S)$_2$[21] is known.

2.1.1.4 PHOSPHORUS SUBSTITUENTS

A phosphorus substituent may easily be introduced onto the fluoromes ring by the reaction of Lifmes with a phosphorus chloride, typically phosphorus trichloride. This has led to the synthesis of a range of phosphorus substituents on the fluoromes ring, many of which are surprisingly stable for P(III) compounds. Examples include Fmes-PCl_2,[22] Fmes-PH_2,[22] Fmes-P=P-Fmes[23] and Fmes-P=CCl_2[24]. Such compounds have been used as ligands in complexes such as $M(CO)_5(FmesP)_2$ (M = Mo, W)[22] and $PtCl_2(PEt_3)(FmesP{=}CCl_2)$[24] in which the ligand is bound to the metal via a phosphorus atom in an η^1 fashion.

2.2 2,4,6-TRIS(TRIFLUOROMETHYL)AZOBENZENE

2.2.1 SYNTHESIS OF 2,4,6-TRIS(TRIFLUOROMETHYL)AZOBENZENE

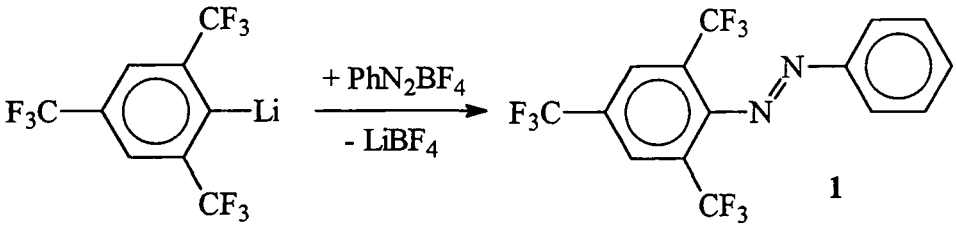

Equation 1

Many methods are known for the synthesis of azobenzenes. Many of these employ aromatic compounds with a nitrogen atom already on the ring, e.g. by the oxidation of anilines. Such methods are clearly not applicable in this case as the synthesis of the azobenzene is viewed primarily as a method of introducing a N substituent onto the ring. The reaction of the readily synthesised Lifmes with dry PhN_2BF_4 led to the isolation of red crystals of 2,4,6-tris(trifluoromethyl)azobenzene (**1**) in moderate yield (Equation 1).

The $^{13}C[^1H]$ NMR of the compound reveals an unusual feature which is also present in other fluoromes compounds described in this thesis. Both the carbon atoms of the CF_3 groups and the *ortho* and *para* carbon atoms of the ring are coupled to the fluorine atoms ($J \approx 270$ and 30 Hz respectively). However, only the CF_3 carbon atoms are coupled to the hydrogens on the ring ($J \approx 5$ Hz), despite the greater number of bonds between these and the CF_3 group (3 bonds) as opposed to the *ortho* and *para* carbon atoms (2 bonds).

2.2.2 THE MOLECULAR STRUCTURE OF 2,4,6-TRIS(TRIFLUOROMETHYL)AZOBENZENE

The evaporation of a hexane solution of **1** led to the formation of red monoclinic crystals which were found to be suitable for an X-ray structure determination. The structure was solved by Prof J.A.K. Howard and Dr A.S. Batsanov within this department. The molecular structure is shown in Figure 2.1 and selected bond lengths and angles in Table 2.1.

1 is found to adopt the trans configuration which is known to be the most stable in azobenzenes. The CF_3 substituent in the *p*-CF_3 shows a rotational disorder which is

frequently seen in CF_3 groups. Under 170 K, **1** undergoes a phase transition, probably linked to the ordering of that group.

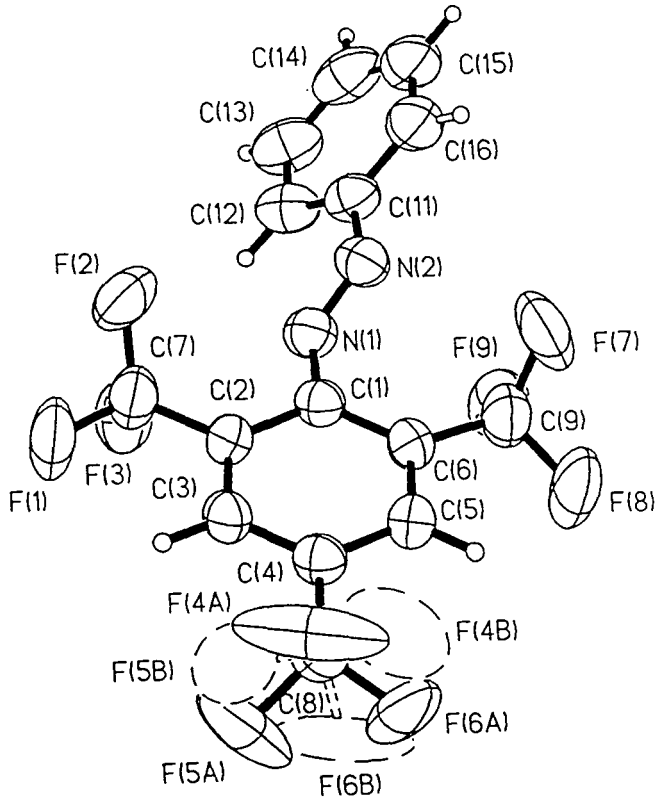

Figure 2.1 Molecular structure of 1

Atoms	Bond Length / Å	Atoms	Bond Angle / °
N1-N11	1.228(6)	C1-N1-N2	112.6(5)
N1-C1	1.443(7)	N1-C1-C2	115.9(5)
N2-C11	1.453(8)	N1-C1-C6	125.1(5)
C1-C2	1.401(7)	C11-N2-N1	112.7(5)
C6-C1	1.406(7)	N2-C11-C12	125.0(5)
C11-C12	1.388(9)	C16-C11-N2	113.9(6)
C16-C11	1.381(9)		

Table 2.1 Selected bond lengths and angles for 1

2.2.3 AM1 CALCULATIONS ON 2,4,6-TRIS(TRIFLUOROMETHYL)AZOBENZENE

AM1[25] molecular orbital calculations were performed using the MOPAC 6.0 package[26] and coordinates derived from the molecular structure. Two calculations were performed, one with no optimisation of atomic positions and the other with optimisation of all atoms. Selected data from these calculations are given in Table 2.2, further data are given in Appendix A.

Atoms	X-ray Structure	Calculated Geometry	Atoms	X-ray Structure	Calculated Geometry
N1-N2	1.228(6)	1.226	C1-N1-N2	112.6(5)	120.3
C1-N1	1.443(7)	1.434	C1-N2-N1	112.7(5)	120.5
C11-N2	1.453(8)	1.434			
			C6-C1-N1-N2	52.5	81.9
			C12-C11-N2-N1	6.5	4.4

Table 2.2 Selected data from AM1 calculations on 1

There are small differences between the bond lengths in the two structures, the greatest being 0.031Å. The single major difference is the twist angle between the plane of the azo group and that of the fluoromes ring which may be conveniently described in terms of the C_o-C_i-N1-N2 torsion angle θ (Figure 2.2). This is much greater in the calculated gas phase structure (81.9°) than that in the solid state structure (52.5°) (Figure 2.3), an observation which is consistent with previous results[27,28]. Azobenzene is almost planar in the solid[29] having a twist angle of between 7° and 18°. In the gas phase[30] the preferred angle is thought to be around 30°.

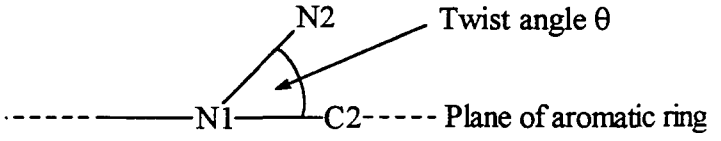

Figure 2.2 Twist Angle Between Azo Functionality and Aromatic Ring

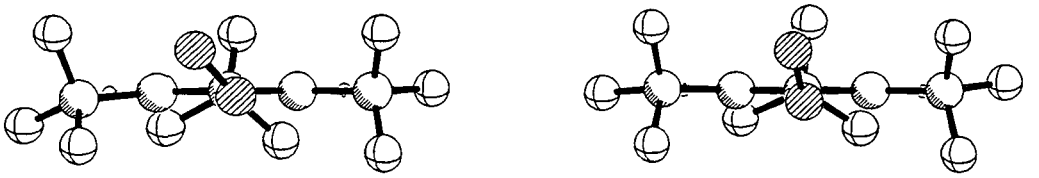

A **B**

Figure 2.3 X-ray (A) and calculated (B) structures of 1 (phenyl group removed for clarity)

The solid state structure reveals that both sides of the fluoromes ring are inequivalent as the second nitrogen of the azo functionality is closer to one side. The solution state ^{1}H and ^{13}C NMR spectra suggest no such distinction due to rotation about the C-N bond being rapid on an NMR time scale.

2.2.4 BONDING IN 2,4,6-TRIS(TRIFLUOROMETHYL)AZOBENZENE

The steric and electronic nature of the two aromatic groups differ considerably and the orientations of these groups with respect to the azo linkage reflect this. The major difference is in the C_o-C_i-N_A-N_B torsion angle (Figure 2.2), the twist for the fluoromes group (θ = 52.5°) being substantially greater than that for the phenyl group (θ = 6.5°). Similar observations have been made for other azobenzenes (Ar-N=N-Ar) with relatively planar conformations for sterically unhindered azobenzenes (e.g. Ar = Ph[29], θ = 12°; C_6F_5[31], θ = 4.2°; 2,4,6-$Me_3C_6H_2$[32], θ = 3.2°) and greater deviations from planarity where bulky *ortho* substituents are present (e.g. Ar = 2,4,6-$Bu^t_3C_6H_2$ [33], θ = 38°; 2,4,6-$(NO_2)_3C_6H_2$ [34], θ = 39°). There is little variation in the C-N and N-N bond lengths in azobenzenes, those in **1** being comparable to average values[35] of 1.255Å and 1.431Å for the N=N and C-N bonds respectively.

AM1 calculations reveal a small π-contribution to both C-N bonds with π-bond orders of 0.081 for the Fmes-N bond and 0.089 for the Ph-N bond. This is consistent with previous work indicating interactions between the π-system of the ring with both the π-system of the azo group and the N lone pair.[27] The relative contribution of each will depend on the orientation of the azo group. In a conformation with the azo linkage in the plane of the ring the interaction will involve the azo π-system. MO calculations have shown that in this conformation the azo group withdraws electrons from the ring.[36] The lone pair will contribute increasingly with increasing distortion from this

conformation which can be viewed as a donation of electrons to the ring. Figure 2.4 illustrates these interactions (no representation of the molecular orbitals which may be involved is intended).

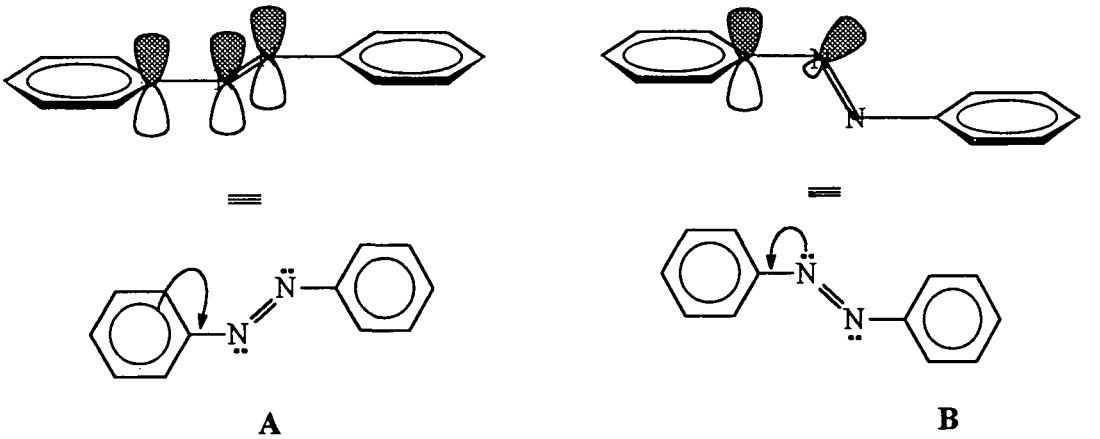

A **B**

Figure 2.4 Interaction of azo functionality with aromatic ring via interaction between aromatic π-system (A) in the planar conformation and nitrogen lone pair (B) in an orthogonal conformation

The presence of the CF_3 groups on the fluoromes group will favour an interaction with the lone pair, a donation of electrons from the azo linkage to the ring, over an interaction with the azo π-system which is associated with a withdrawal of electrons from the ring. This should favour a conformation with the azo linkage orthogonal to the plane of the ring over a planar conformation. There is no evidence, however, that the fluoromes group exhibits a greater distortion in the solid than other sterically hindered azobenzenes. Likewise decafluoroazobenzene[31] in the solid state shows no greater tendency towards orthogonality than azobenzene despite the electron withdrawing pentaflurophenyl groups. It appears that the distortions in azobenzenes are almost purely steric in nature. The C1-N1 and C11-N11 bond lengths and π-bond orders are almost identical despite the difference in conformations. This supports the previous conclusion that the efficiency of conjugation is affected little by the orientation.[28]

2.3 2,4,6-TRIS(TRIFLUOROMETHYL)ANILINE

2.3.1 SYNTHESIS OF 2,4,6-TRIS(TRIFLUOROMETHYL)ANILINE

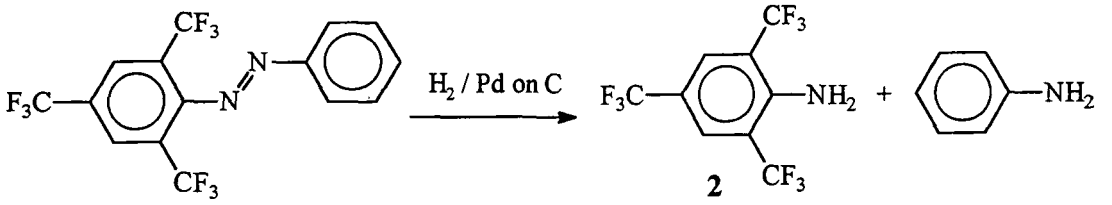

Equation 2

Reduction of **1** with H_2 at 1 atmosphere and 5% Pd/C catalyst in ethanol at 70°C led to the formation of **2** (Equation 2). The solvent could not be removed under reduced pressure or by distillation as the high volatility of **2** caused the product to remain in the solvent. The product was finally removed by precipitation from ethanol solution with water. Pure **2** was obtained after removal of the aniline by-product by either recrystallisation from pentane or sublimation (1 atm, 30°C).

2.3.2 MOLECULAR STRUCTURE OF 2,4,6-TRIS(TRIFLUOROMETHYL)ANILINE

A sample of **2** in a sealed vessel at room temperature and pressure formed crystals within 24 hours which proved suitable for an X-ray diffraction experiment. The structure was solved by Prof J.A.K. Howard and Dr C.W. Lehmann within this department. The molecular structure is shown in Figure 2.5 and selected bond lengths are given in Table 2.3 and angles in Table 2.4.

Bond	Bond Distance / Å	Bond	Bond Distance / Å
	Molecule A		*Molecule B*
N1-C6	1.358(6)	N11-C11	1.357(7)
C6-C1	1.417(7)	C11-C12	1.409(7)
C5-C6	1.415(7)	C16-C11	1.409(6)
C1-C2	1.381(7)	C12-C13	1.379(7)
C4-C5	1.368(7)	C15-C16	1.384(7)
C2-C3	1.394(7)	C13-C14	1.391(7)
C3-C4	1.386(7)	C14-C15	1.377(7)

Table 2.3 Selected bond lengths for 2

Bond	Bond Angle / °	Bond	Bond Angle / °
	Molecule A		*Molecule B*
H1A-N1-H1B	124(6)	H11A-N11-H11B	122(6)
H1A-N1-C6	113(4)	H11A-N11-C11	118(4)
H1B-N1-C6	124(4)	H11B-N11-C11	120(5)
$\Sigma\angle N^{\dagger}$	361(14)	$\Sigma\angle N$	360(15)
N1-C6-C5	122.2(5)	N1-C11-C12	121.2(4)
N1-C6-C1	121.7(4)	N1-C11-C16	121.4(4)

Table 2.4 Selected bond angles for 2

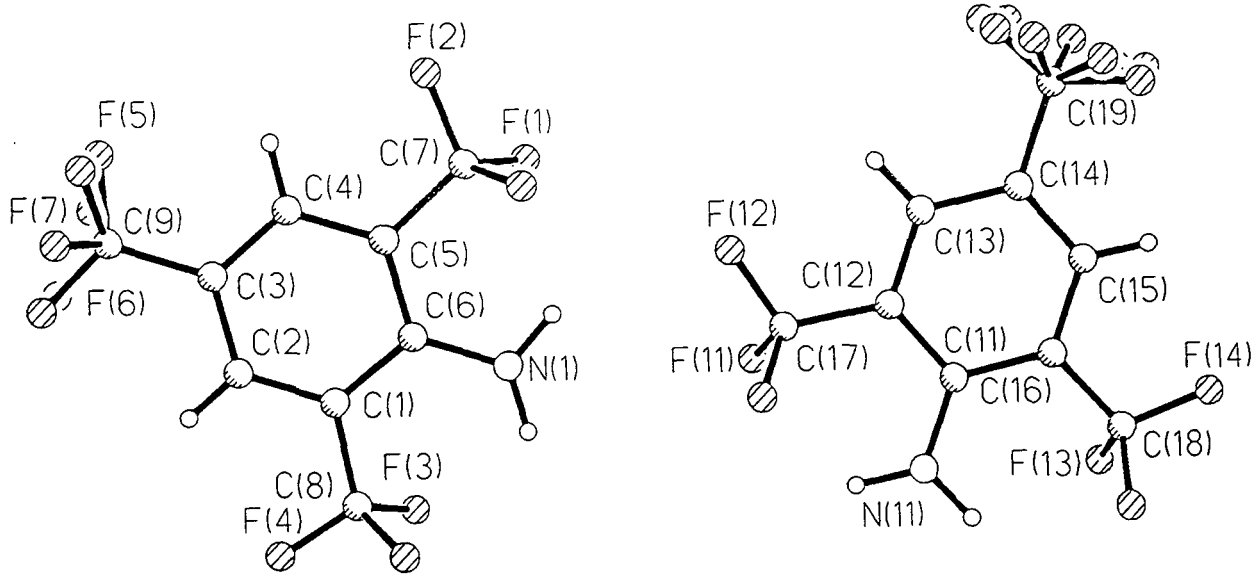

Figure 2.5 Molecular structure of 2

The assymetric unit of **2** comprises two molecules. In both the *p*-CF_3 groups show rotational disorder. Both molecules lie on a crystallographic mirror plane containing all atoms except two fluorine atoms from each CF_3 which are related to one another by the mirror plane. The hydrogen atoms of the amine group participate in weak intra

† Despite large e.s.d's on H positions the sum of these angles must be 360° as all atoms lie on the same crystallographic plane.

molecular contacts with the *o*-CF_3 groups (H···F 2.28-2.43 Å). There is also an intermolecular contact between H11B and F18 on the molecule related by a translation (½+x, ½-y ½-z). These interactions may help to stabilise the ordered positions of the *o*-CF_3 groups.

2.3.3 AM1 CALCULATIONS ON 2,4,6-TRIS(TRIFLUOROMETHYL)ANILINE

AM1[25] molecular orbital calculations were performed using coordinates derived from the molecular structure. As with **1** two calculations were performed, one with no optimisation of atomic positions and the other with optimisation of all atoms. Table 2.4 contains selected data from the AM1 calculations. Further data, including bond orders and atomic charges, are given in Appendix A. There are only small differences between the two either in bond lengths or orientation indicating that the configuration of **1** in the solid is not affected greatly by either crystal packing or intermolecular forces neither of which are present in the calculated gas phase structure.

Parameter	X-ray Structure	Calculated Structure	Parameter	X-ray Structure	Calculated Structure
N-C_i	1.358(7)	1.360	H-N-H	123(4)	118.7
C_i-C_o	1.413(7)	1.430	H-N-C_i	119(5)	120.6
C_o-C_m	1.378(7)	1.389	$\Sigma\angle$N	360.0	358.0
C_m-C_p	1.387(7)	1.396			

Table 2.5 Comparison of geometries for both X-ray and calculated structures of 2

2.3.4 BONDING IN 2,4,6-TRIS(TRIFLUOROMETHYL)ANILINE

Aniline **2** is similar to other anilines bearing strongly electron withdrawing groups[4,5] in that the bonds around the N atom are coplanar and in the plane of the ring. The C-N bond length (1.358) is comparable to the average[35] for planar anilines of 1.355Å. The AM1 calculation reveals a C-N π-bond order of 0.30. Planarity in such anilines is attributed to the stabilisation of lone pair delocalisation onto the ring by electron withdrawing substituents (e.g. nitro groups, see Figure 2.6). Clearly the CF_3 groups will have a similar effect (Figure 2.7) although this will arise from an *inductive* withdrawal of electrons rather than the *resonance* effect observed for nitro groups. In contrast to these planar anilines, parent aniline, with no electron withdrawing groups,

has a pyramidal nitrogen and longer C-N distance of 1.392(6) Å in the solid state[6]; theoretical calculations[4,37]and electron diffraction studies support this conformation for gas phase molecules. The average[35] C-N distance for anilines with a pyramidal amino group is 1.394Å whereas anilines with protonated nitrogen, in which there is no possibility for C-N π-bonding, have an average C-N distance of 1.465Å.

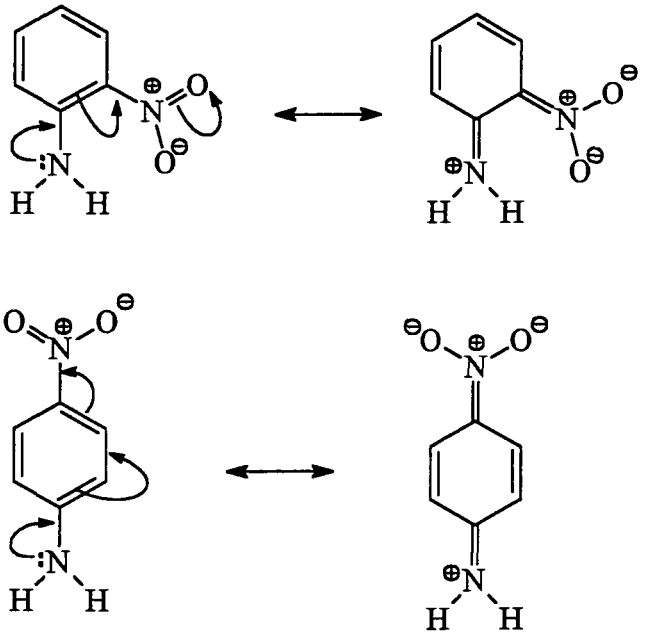

Figure 2.6 **Resonance description of the stabilisation by *o*- and *p*-nitro of delocalisation of amino lone-pair onto ring**

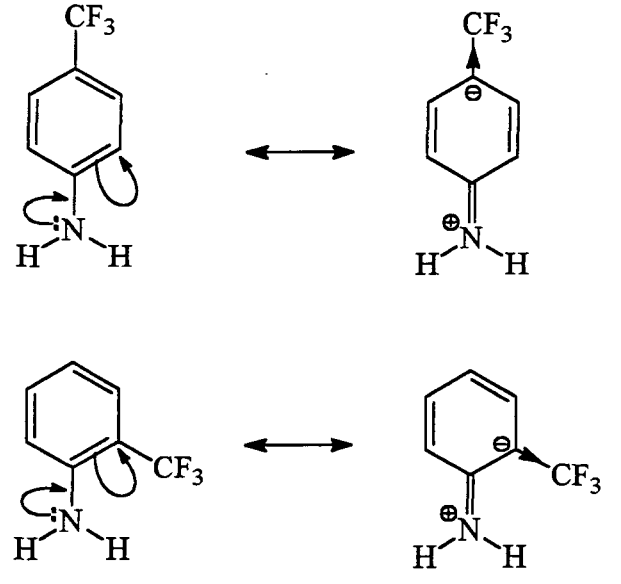

Figure 2.7 **Stabilisation of delocalisation of amino lone-pair onto ring by inductive effect of CF_3 groups**

Although the AM1 calculations reveal a negative charge on the nitrogen and not the positive charge which would be expected from a consideration of the resonance forms, this is due to an inductive effect arising from the higher electronegativity of nitrogen than carbon, a factor not reflected in the resonance forms which consider only the π-system.

Although the CF_3 groups will exert an electron withdrawing effect on the nitrogen atom via a σ-inductive effect it is clear from the results of the AM1 calculations and the rehybridisation of the N atom to sp^2 that the fluoromes ring is acting as a π-acid.

2.4 2,4,6-TRIS(TRIFLUOROMETHYL)HYDRAZOBENZENE

2.4.1 SYNTHESIS OF 2,4,6-TRIS(TRIFLUOROMETHYL)HYDRAZOBENZENE

Reduction of **1** in diethyl ether at room temperature with zinc and hydrochloric acid in a two phase system led to rapid decolourisation of the solution and the formation of 2,4,6-tris(trifluoromethyl)hydrazobenzene **3** (Equation 3).

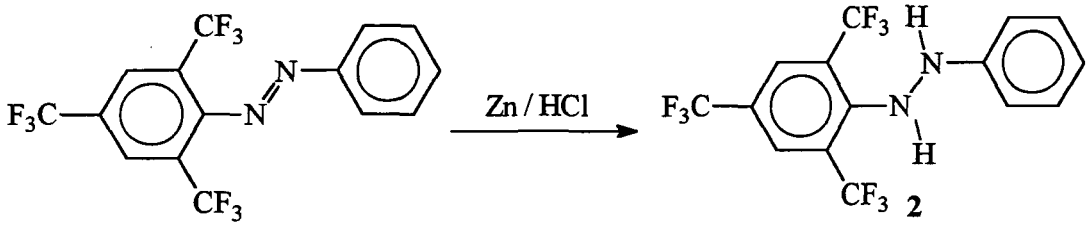

Equation 3

The compound was found to oxidise over a period of weeks in air with the red colour of the azo compound **1** becoming evident. Such oxidation is also observed in 1,2-diphenylhydrazine. No such conversion was observed in samples stored under nitrogen.

2.4.2 MOLECULAR STRUCTURE OF 2,4,6-TRIS(TRIFLUOROMETHYL)HYDRAZOBENZENE

Evaporation of a hexane solution of **3** yielded colourless monoclinic crystals that were found to be suitable for X-ray diffraction. The structure was solved by Prof. J.A.K. Howard and Dr A.S. Batsanov within this department. The molecular structure is shown in Figure 2.8 and selected bond lengths in Table 2.6 and angles in Table 2.7.

The asymmetric unit of **3** comprises two independent molecules, A and B, related via a pseudo-translation (0.5x, 0.1y, 0). In molecule A, the *p*-CF_3 group shows only minor disorder, fluorine positions F41, F51, F61 having occupancies of ca. 90% and F42, F52, F62 of 10%. On the other hand, in molecule B the same group is completely disordered. The electron density cross section map through the supposed positions of the fluorines (Figure 2.9) surprisingly reveals four peaks differing from each other by a 90° rotation, and from the benzene ring plane by a 45° rotation around the C4B-C8B bond. Attempts to rationalise this picture as an overlap of 2, 3 or 4 orientations of the CF_3 group with different occupancies were unsuccessful, none of them giving R(F) below 0.12 (cf. R=0.2, if these fluorines were completely neglected). Finally, this group had to be introduced into the refinement as a continuous distribution of electron density, albeit chemically meaningless, which brought R down to 0.061.

H1 participates in a bifurcated H-bond with F7 and F9 (H···F 2.34 - 2.38Å) and H2 in a similarly bifurcated contact with F3 of its own and translationally equivalent molecules (H···F 2.54 - 2.71Å), which may help to stabilise the ordered positions of these CF_3 groups.

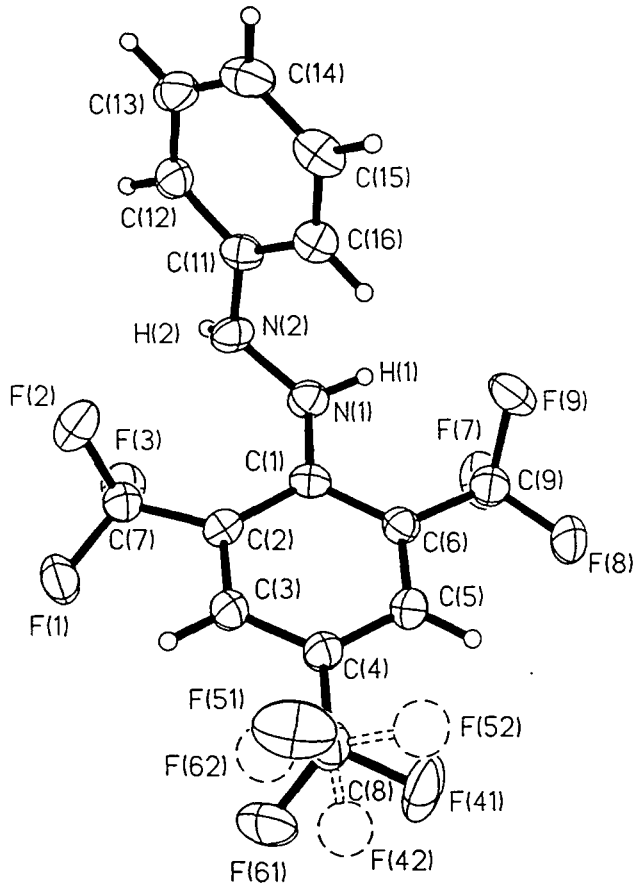

Figure 2.8 Molecular structure of 3 (molecule A)

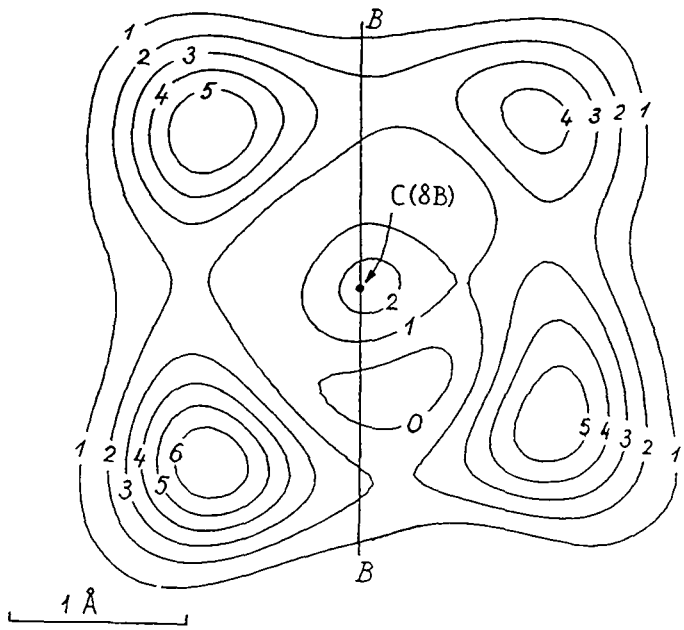

Figure 2.9 Electron density map of *p*-CF_3 of molecule B

Atoms	Molecule A	Molecule B	Average
N1-N2	1.395(4)	1.401(4)	1.398(4)
N1-H1	0.90(4)	0.92(4)	0.91(4)
N2-H2	0.86(4)	0.86(4)	0.86(4)
C1-N1	1.389(4)	1.386(4)	1.388(4)
N2-C11	1.411(4)	1.411(4)	1.411(4)

Table 2.6 Selected bond lengths for 3

Atoms	Molecule A	Molecule B	Average
C1-N1-N2	119.4(3)	118.6(3)	119.0(3)
C11-N2-N1	118.9(3)	119.3(3)	119.1(3)
C1-N1-H1	116(3)	118(2)	117(2)
C11-N2-H2	119(3)	112(3)	115.5(3)
N1-N2-H2	111(3)	120(3)	115.5(3)
N2-N1-H1	117(2)	115(2)	116(2)
N1-C1-C2	123.1(3)	123.3(3)	123.2(3)
N1-C1-C6	119.5(3)	119.4(3)	119.5(3)
N2-C11-C12	117.3(3)	117.9(3)	117.6(3)
N2-C11-C16	122.9(3)	122.5(3)	122.7(3)

Table 2.7 Selected bond angles for 3

2.4.3 AM1 Calculations on 2,4,6-tris(trifluoromethyl)hydrazobenzene

AM1[25] molecular orbital calculations were performed using coordinates derived from the molecular structure. As with **1** two calculations were performed, one with no optimisation of atomic positions and the other with optimisation of all atoms. Table 2.8 contains selected data from the AM1 calculations. Further data, including bond orders and atomic charges, are given in Appendix A. There are no major differences between either bond lengths or angles between the two structures indicating that the configuration of **3** in the solid is not greatly affected by either crystal packing or intermolecular interactions.

Bond Length / Å	X-ray Structure	Calculated Structure	Bond Angle / °	X-ray Structure	Calculated Structure
N1-N2	1.398(4)	1.379	C1-N1-N2	119.0(3)	118.2
C1-N1	1.388(4)	1.417	C11-N2-N1	119.1(3)	117.9
C11-N2	1.411(4)	1.436	C1-N1-H1	117(2)	111.6
C1-C2	1.425(4)	1.422	C11-N2-H2	115.5(3)	109.9
C6-C1	1.417(4)	1.427	N1-N2-H2	115.5(3)	106.7
C11-C12	1.398(4)	1.410	N2-N1-H1	116(2)	112.2
C16-C11	1.391(4)	1.409	$\Sigma\angle$N1	352(7)	342.0
			$\Sigma\angle$N2	350(9)	334.5

Table 2.8 Comparison between bond lengths and angles in the X-ray structure of 3 (average) and the calculated structure

2.4.4 BONDING IN 2,4,6-TRIS(TRIFLUOROMETHYL)HYDRAZOBENZENE

Compared to the wide range of substituted azobenzenes and anilines there is a distinct lack of structurally characterised hydrazobenzenes (1,2-diarylhydrazines). This may be due to their instability towards oxidation to the corresponding azobenzene which limits their potential uses.

There appears to be little difference in the orientation of the fluoromesityl and phenyl groups of **3** and the phenyl groups of hydrazobenzene[3] with respect to the N substituent. In all cases it is analogous to that in aniline with the lone pair aligned parallel to the aromatic π-system.

Although the N atoms are not planar they do show some degree of flattening, the sum of the angles around N of about 349-352° (cf. 352° in hydrazobenzene) lying nearer to that for planar sp^2 nitrogen (360°) than pyramidal sp^3 nitrogen (328.4°), and greater than that in aniline (342°).

H1 lies in the plane of the fluoromes ring whereas N2 lies out of the plane. This is not seen for the other end of the molecule where both H2 and N2 lie out the plane of the phenyl ring. This is almost certainly due to repulsion between N2 and the nearest CF_3 group which leads to these two groups bending away from each other as evidenced by the bond angles (Figure 2.10).

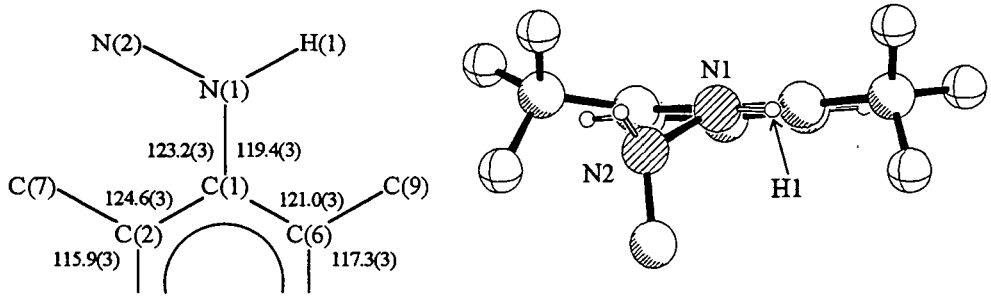

Figure 2.10 Selected angles for (2)

On the basis of the short C-N distance in hydrazobenzene (1.386(4)) it has previously been suggested that there is significant donation of the nitrogen lone pair into an antibonding orbital of the aromatic ring. The orientation of the substituents is analogous to that in anilines with the lone pair parallel to the p-orbitals of the aromatic π-system. Although there is only a small difference between the C-N distances in **3** (1.388(4)Å for the fluoromes group, 1.406(4)Å for the phenyl group) the AM1 calculations suggest a stronger π-bond between the fluoromes and the nitrogen (0.203) than between the phenyl and the nitrogen (0.108). Delocalisation of the lone pair onto the ring will be greater for the fluoromes group due to the same effect discussed for **2**.

2.5 AM1 Calculations on Other Anilines with Trifluoromethyl Substituents

A variety of anilines with CF_3 substituents on the ring are available commercially, although none have both *o*-positions substituted and hence do not offer the properties of fluoromes. These include 1-NH_2-2-CF_3-C_6H_4 (**4**), 1-NH_2-3,5-CF_3-C_6H_3 (**5**) and 1-NH_2-4-CF_3-C_6H_4 (**6**), the steric and electron withdrawing properties of which will depend on the number and position of the CF_3 groups.

2 is unusual amongst such anilines in that it is a solid at room temperature and although the structures of these other anilines would be of interest the time and effort required to obtain a solid state structure cannot be justified. The geometries calculated by MOPAC using AM1 parameters for **1**, **2** and **3** do not differ considerably from those found in the solid state, in fact some small differences would be expected as the geometries calculated relate to isolated molecules with no crystal packing forces. As it appears that this method has a high degree of accuracy for this type of compound it

seems likely that the structures of **4**, **5** and **6** calculated by this method would provide an accurate indication of the actual structures. The calculated structures for **4**, **5** and **6** are shown in Figure 2.11. Bond lengths and bond orders are given in Appendix A. A summary of selected bond lengths and angles is given in Table 2.9. The initial geometries for the calculations were derived from the X-ray structure of **2** with CF_3 groups either moved to appropriate positions or replaced with H atoms.

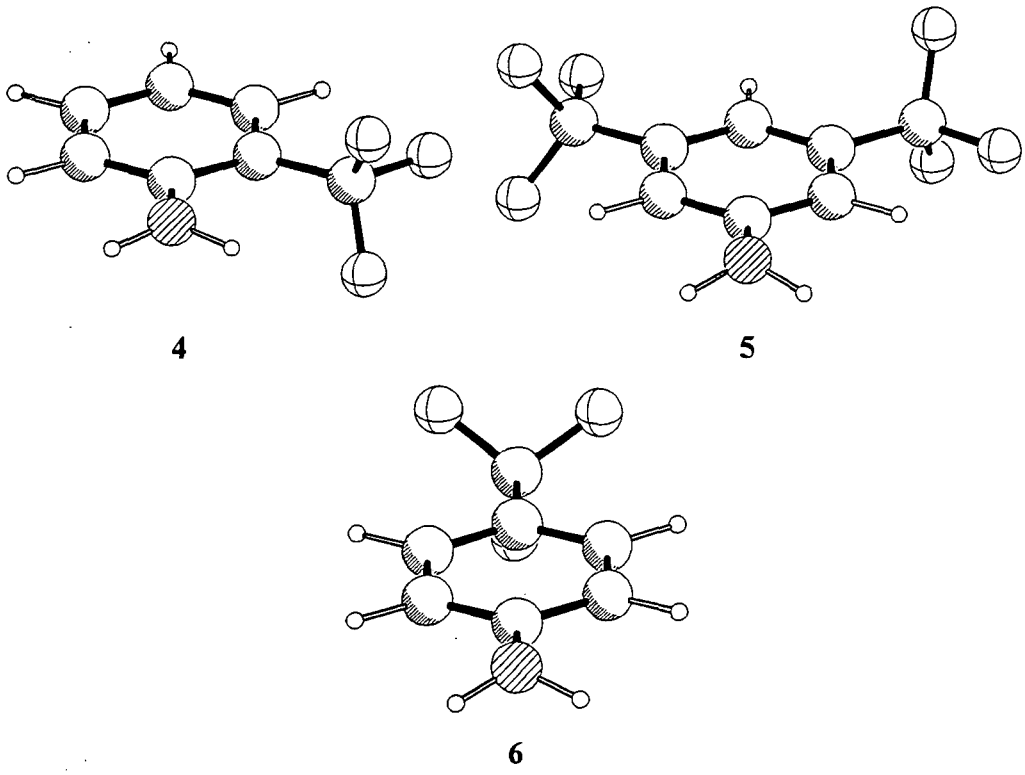

4 **5**

6

Figure 2.11 AM1 optimised geometries of 4, 5 and 6

	C-N Distance / Å	Σ∠N / °
4	1.377	354.5
5	1.393	345.2
6	1.387	347.7

Table 2.9 Selected data for structures of 4, 5 and 6

2.6 AM1 CALCULATIONS ON ANILINE

The structure of aniline **7** has been determined by X-ray and electron diffraction, and also several different calculational methods although not the AM1 method used here. Bond orders derived from these methods cannot, however, be compared directly to

those obtained by the AM1 method for compounds **1-6**. To provide such bond orders an AM1 calculation has been carried out using the coordinates obtained by the previous X-ray diffraction study, both with and without the optimisation of atomic coordinates. The calculated molecular structure is shown in Figure 2.12. Bond lengths and angles for both the X-ray and AM1 optimised structures, calculated bond orders and calculated atomic charges are given in Appendix A. Selected data are given in Table 2.10.

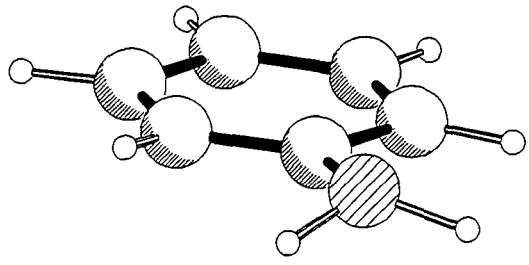

Figure 2.12 AM1 structure of aniline 7

	AM1 Structure	X-ray Structure
C-N distance / Å	1.392(6)	1.399
C_i-C_o distance / Å	1.396(6)	1.415
C_o-C_m distance / Å	1.379(7)	1.390
C_m-C_p distance / Å	1.381(7)	1.394
$\Sigma\angle$N / °	342(11)	341.8

Table 2.10 Selected data for aniline

2.7 AM1 CALCULATIONS ON OTHER FLUOROMES COMPOUNDS

It will be seen in Chapter 4 that the atoms bonded to a nitrogen substituent on a carborane cage (1-X-2-R-1,2-$C_2B_{10}H_{10}$, X = nitrogen substituent) has a profound effect on the π-bonding between the N and carborane. It would be expected that similar observations would be made in the fluoromes system. The geometries of FmesNHOH and FmesNO have been calculated using the AM1 method. Although the synthesis of these compounds should be possible sufficient time was not available.

The calculated structures for FmesNHOH and that for FmesNO are shown in Figure 2.13. Selected bond lengths and angles are given in Table 2.11, further data can be

found in Appendix A Initial geometries were taken to be those of **2** and **1** respectively with atoms replaced or removed as required.

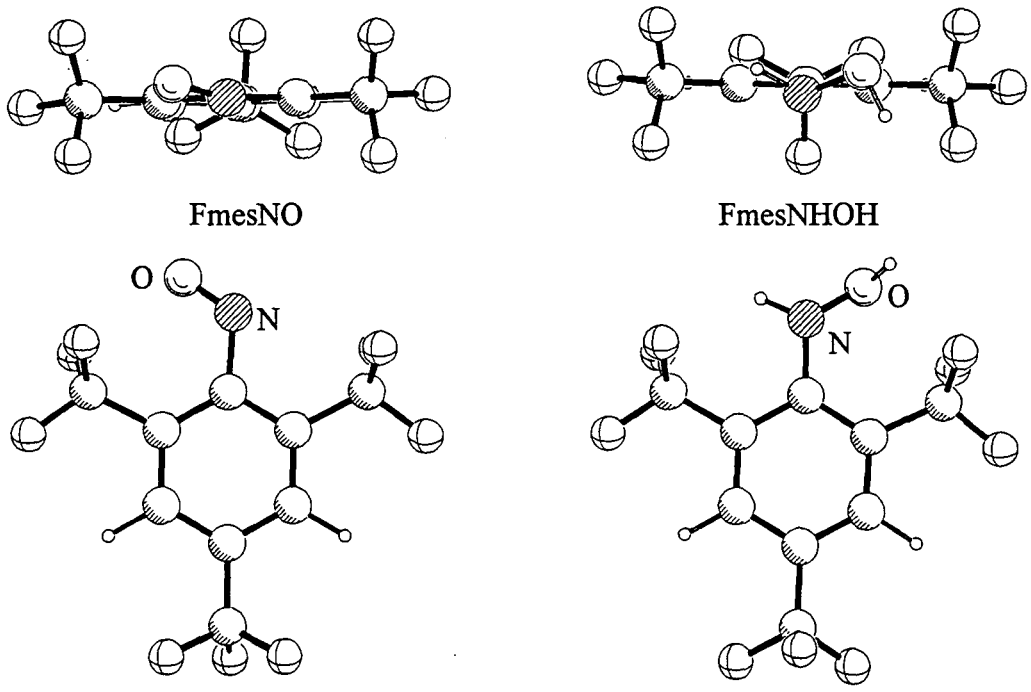

Figure 2.13 Calculated molecular structures for FmesNO and FmesNHOH

	FmesNO	FmesNHOH
N-C1 bond length / Å	1.477	1.421
N-O bond length / Å	1.150	1.332
$\Sigma\angle N$ / °	119.7	335.11
N-C1 π-bond order	0.068	0.151

Table 2.11 Selected Data for FmesNO and FmesNHOH

2.8 EXO-π-BONDING BETWEEN π-ACIDIC ARYL GROUPS AND NITROGEN SUBSTITUENTS

Compounds **1** - **7** constitute a series consisting of an aromatic ring bound to a nitrogen substituent in which there exists π-bonding between the ring and substituent, the extent of which depends on both the nature of the nitrogen substituent and the other groups attached to the ring.

Compounds $FmesN_2Ph$ **1**, $FmesNH_2$ **2**, FmesNHNHPh **3** and aniline **7** form two series in which the substituents on the ring are the same and the substituent varies. The π-bonding increases in the order:-

	1	<	**3**	<	**2 / 7**
Fluoromes Group	0.081	<	0.203	<	0.300
Phenyl group	0.089	<	0.108	<	0.138

Azobenzene **1** exhibits less C-N π-bonding between the azo linkage and the fluoromes or phenyl group than the other compounds although the difference between the π-bonding to the phenyl groups in **1** and **3** is small (and reversed if π-bond orders for the calculated geometries are used). The difference between the C-N π-bonding for the fluoromes groups of **1** and **3** is much larger. This reflects the fact that the π-bonding in **1** is affected little by the CF_3 groups whereas there is a much greater effect in **3**.

There is considerably more C-N π-bonding in the anilines (**2** and **7**) than in hydrazine **3**. This is due to the influence of the other atoms on the N. In **2** there are two H atoms on the N, whereas in **3** there is one N and one H, the N being of higher electronegativity than the H atoms. This will decrease the electron density on the donor N hence reducing the π-donor capacity. This is the same effect as is responsible for the lower bascicity of hydrazine (pK_a 7.95) compared to that of ammonia (pK_a 9.24), and the lower bascicity of hydroxylamine (pK_a 5.96) compared to both. Both hydrazine and hydroxylamine are often observed to be stronger nucleophiles than ammonia. This is sometimes attributed to repulsions between lone pairs on adjacent

atoms, however this does not explain the order of basicities and is now thought to be due to the combined effect of the lone pairs in stabilising the transition state. Clearly it is basic strength and not nucleophilic strength which can be related to the degree of π-bonding in the aromatic systems.

For the fluoromes group there is an additional effect. Repulsion between N2 and the *o*-CF_3 group in **3** will prevent the conformation for which π-bonding would be greatest with N1, N2 and H1 lying in the plane of the fluoromes ring. No such effect is present in **2** where N1, H1 and H2 all lie in the plane of the aryl ring.

This electronegativity effect can be observed in the calculated structures of the fluoromes compounds. Figure 2.14 shows the effect of the electronegativities of the atoms bonded to N on the C-N π-bond order. This is expressed as a sum of Pauling electronegativities of atoms bonded to N, counting doubly-bonded atoms twice. This is discussed further in Chapter 4. It can clearly be seen that the C-N π-bond order decreases as the electronegativity of atoms on nitrogen increases and is consistent with the bond lengths observed in the X-ray structures of **1**, **2** and **3**.

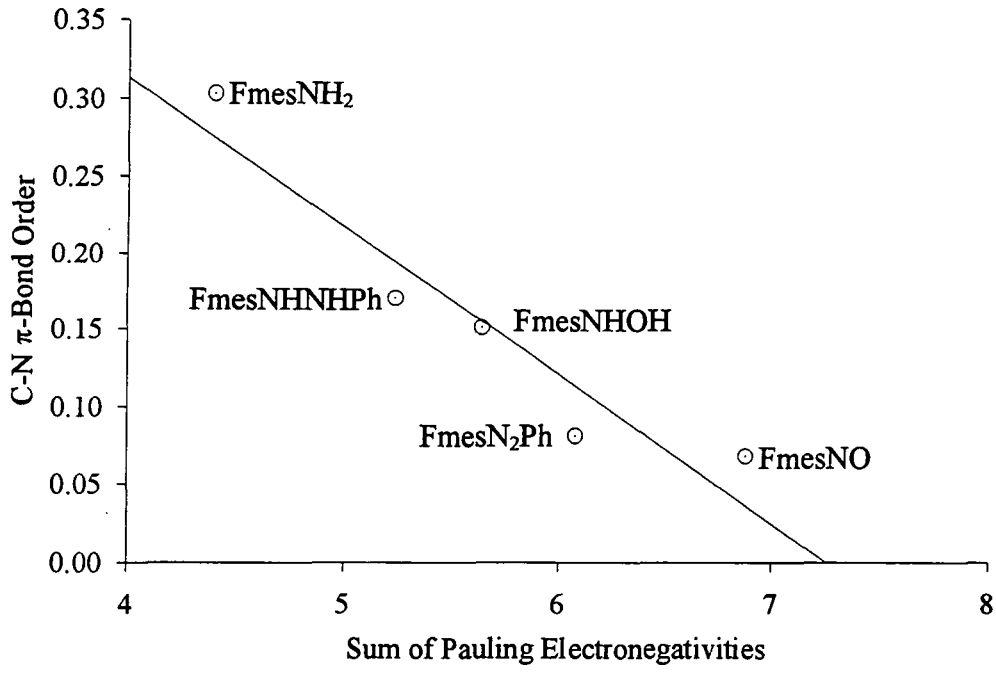

Figure 2.14

The anilines FmesNH$_2$ **2**, 1-NH$_2$-2-CF$_3$-C$_6$H$_4$ **4**, 1-NH$_2$-3,5-CF$_3$-C$_6$H$_3$ **5**, 1-NH$_2$-4-CF$_3$-C$_6$H$_4$ **6** and aniline **7** constitute another series in which the N-substituent remains the same and the substituents on the ring vary. This reveals the effect of the number and position of CF$_3$ groups on the π-acidity. This discussion will refer to the calculated gas phase structures for consistency, the arguments are not altered however if the X-ray structures are used where available. The order for π-bonding in these compounds is

	7	<	**5**	<	**6**	<	**4**	<	**2**
π-Bond Order	0.135		0.156		0.174		0.209		0.303
Charge on NH$_2$	+0.037		+0.061		+0.070		+0.078		+0.147

4 displays less π-bonding than **2**, clearly due to the reduced number of CF$_3$ groups reducing the π-acidity. Interestingly both **4** and **6** display more π-bonding than **5** despite the lesser number of CF$_3$ groups. This shows the greater effect of a CF$_3$ group at an *o*- or *p*-position compared to a *m*-position with a single CF$_3$ group at one of these positions having a greater effect than two *m*-CF$_3$ groups. This can be rationalised by a consideration of the resonance forms which suggest a localisation of negative charge at the *o*- and *p*-positions (Figure 2.15), charge is not localised at the *m*-positions and hence the lesser effect. Comparison of **5** and **7** clearly shows that the *m*-CF$_3$ groups do still have an effect. Hence the effect of *o*-CF$_3$ > *p*-CF$_3$ > *m*-CF$_3$ > H. This order is also reflected in the overall charge on the NH$_2$ group, the positive charge increasing as the delocalisation onto the ring increases.

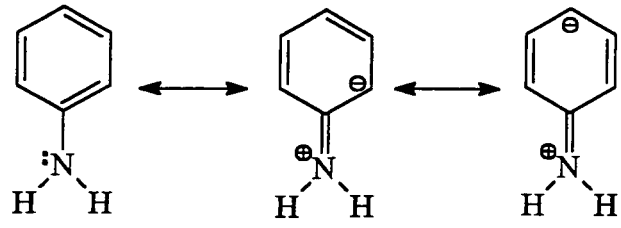

Figure 2.15 Resonance description of the delocalisation of the nitrogen lone pair of aniline onto the phenyl ring

This increase in π-bonding is also seen in the sum of the bond angles to the substituents on the N atom with an increasing tendency towards 360° with increasing π-bonding ranging from 341.8° in **7** to 360.0° in **2** (Figure 2.16). Values are for calculated structures due to the large errors on the positions of the hydrogen atoms in

the X-ray diffraction experiments. This is reflective of a change in hybridisation of the N lone pair from sp^3 to p which will allow greater π-bonding.

π-Acidity appears to be more significant than inductive effects in the withdrawal of electrons from the amino group. Hence a CF_3 group has a similar effect in an *o*- or *p*-position and a much reduced effect in a *m*-position.

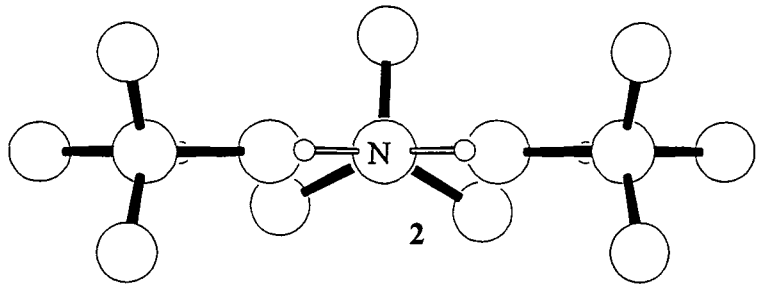

2 $\Sigma\angle N = 358.0°$

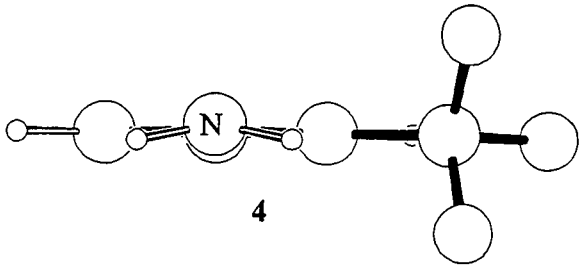

4 $\Sigma\angle N = 354.5°$

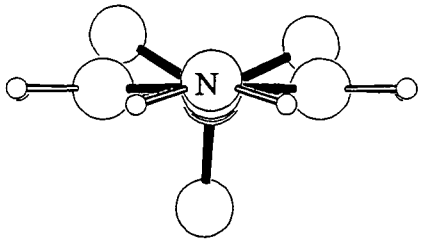

6 $\Sigma\angle N = 347.7$

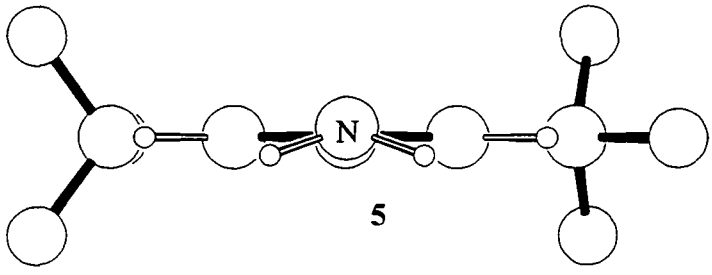

5 $\Sigma\angle N = 345.2°$

7 $\Sigma\angle N = 341.8°$

Figure 2.16 Calculated Structures of 2, 4, 5, 6 and 7 of aniline viewed down C-N bond. Arranged in order of C-N π-bonding (decreasing down the page)

2.9 EFFECTS OF EXO-π-BONDING ON THE AROMATIC RING

It has previously been noted in a series of anilines that as the C-N bond length decreases due to increased π-bonding the C_i-C_o bond lengthens. This has been attributed to a weakening of the C-C π-bonds as suggested by the resonance forms describing the delocalisation of the nitrogen lone pair onto the ring (Figure 2.15). There is no mention, however, of a similar lengthening of the C_m-C_p bond or a shortening of the C_o-C_m bond which the same argument would predict.

While there is no significant difference between the C-C bond lengths in the X-ray structures of **1**, **3** and **2**, the π-bond orders calculated from the X-ray structures do show significant changes in all the C-C bonds which are consistent with the above argument and are shown in Table 2.12. There is little change in the σ-bond order. It is significant that the greatest change is observed for the C_i-C_o, the bond in which changes in length have been noticed in the X-ray structures.

	C-N distance \ Å	C_i-C_o	C_o-C_m	C_m-C_p
1	1.443(7)	0.418	0.456	0.444
3	1.398(4)	0.354	0.468	0.430
2	1.357(7)	0.312	0.478	0.421

Table 2.12 π-Bond orders in fluoromes rings of 1, 2 and 3

The same trend is observed in the π-bond orders in the aromatic rings of the structures calcualated by the AM1 method in this chapter (Figure 2.17). There is a notable deviation in the data for **4** (marked on graph) from the trend of the other data. Whereas in all the other compounds both sides of the ring have the same substituents **4** has different substituents on each side of the ring. This leads to the predominance of one structure (Figure 2.18) in the resonance description of the delocalisation which results in weakening of both C_i-C_o bonds (hence this point falls on a line with the other points) but different effects on the other bonds which in the other compounds are equivalent.

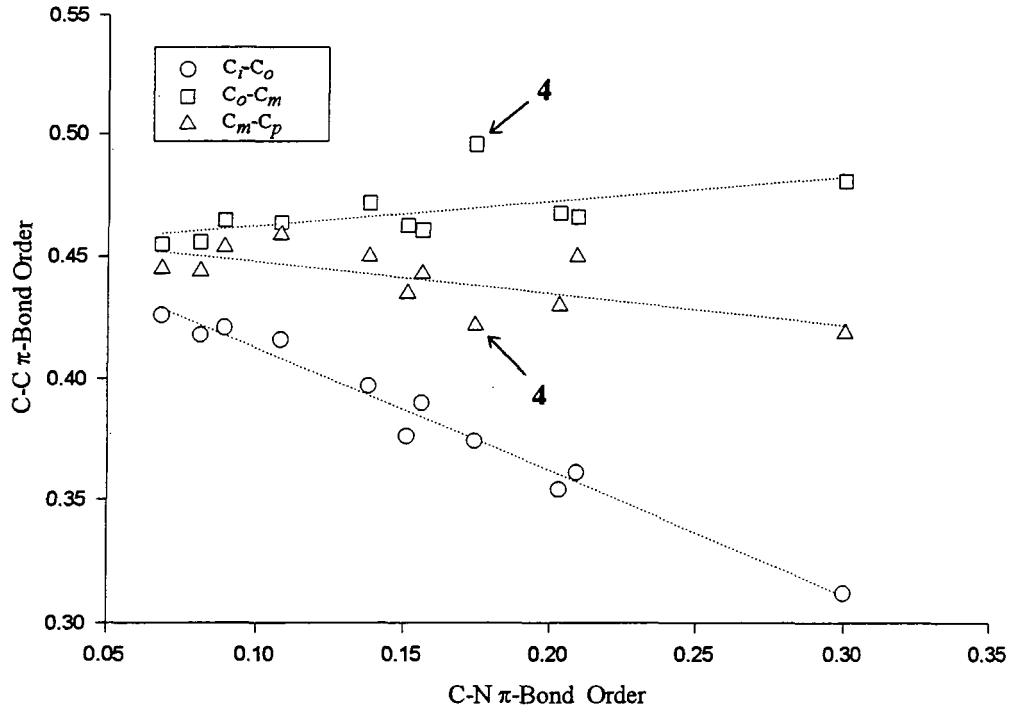

Figure 2.17 Variation in π-bond orders with C-N π-bond order

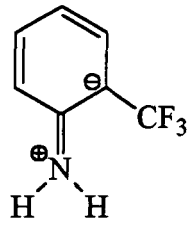

Figure 2.18 Predominant resonance form in 4

It appears that such π-bond order changes only have a small effect on the actual bond lengths. This may be due to constraints imposed by the cyclic system, changes in bond lengths will necessitate changes in the bond angles which will in turn strain the ring. It is not necessarily the case that the bond lengths do not change, merely that the X-ray diffraction technique is insufficiently accurate to detect the changes.

The calculated C-C bond lengths of compounds **1-7**, however, do reflect the changes in bond lengths expected (Figure 2.19). These changes are small and observable because of the higher precision (although not necessarily higher accuracy) of the

calculation compared to that of the X-ray experiment; the error on bond lengths in an X-ray structure would normally be too large for such differences to be observed.

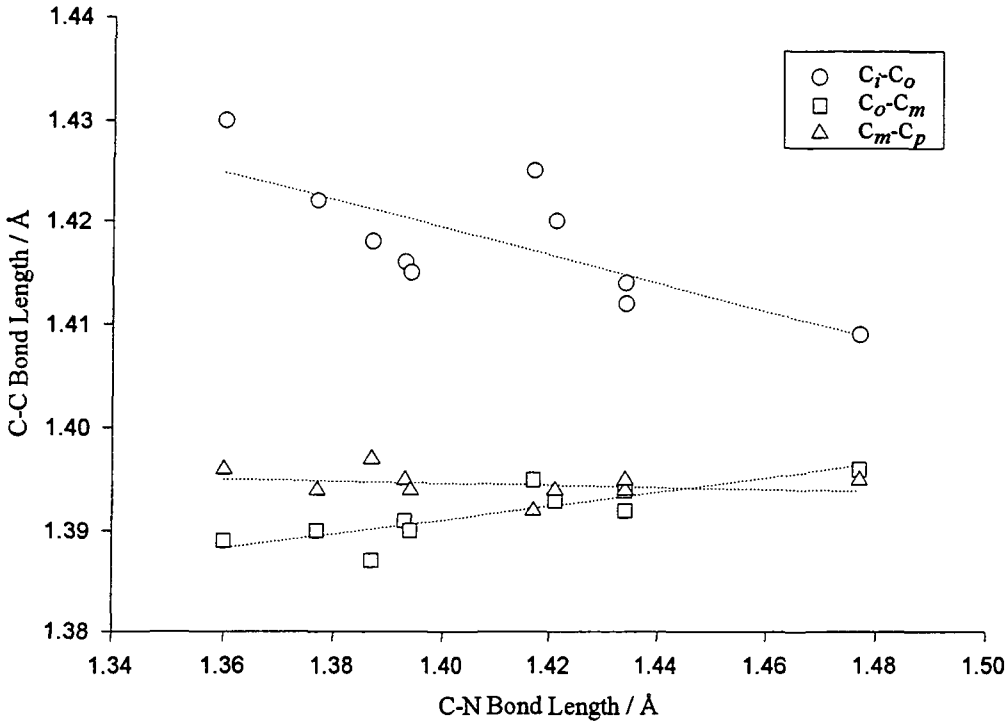

Figure 2.19 Variation in calculated C-C distances with C-N bond length

The greater effect observed in the bonds adjacent to the point of substitution can be explained in the following manner. The more the p-orbital perpendicular to the plane of the ring, i.e. that contributing to the aromatic π-system, becomes involved in π-bonding to the nitrogen atom, the less it can be involved in the π-bonding within the ring. Hence the π-bonds to this atom are weakened more than the C_m-C_p bond bonds within the ring.

2.10 ^{13}C NMR Shifts

The ^{13}C shifts of aromatic rings are well known to be sensitive to substituents. For example, the introduction of an electron donating susbstituent onto the ring will cause a shift to lower frequency in the *o*- and *p*-carbons. This is commonly known as the Mesomeric effect and is due to an increase in charge on these atoms (Figure 2.15) leading to an increased shielding. The shift is most clearly seen for the *p*-carbon as it is most remote from the position of substitution and hence is less susceptible to other effects of the substituent (e.g. inductive effects). Clearly the greater the delocalisation

of a lone pair onto the ring the greater this effect will be. This is reflected in the ^{13}C NMR shift for compounds **1**, **2** and **3** (Table 2.13). There is an increasing shift to lower frequencies with increasing π-bonding (as evidenced by decreasing C-N bond length and increasing C-N bond order).

Compound	C_o	C_m	C_p
	Fluoromes Group		
1	129.8	127.8	124.0
3	116.6	129.1	120.6
2	115.3	128.0	118.6
	Phenyl Group		
1	129.4	123.6	133.4
3	129.5	112.7	121.4

Table 2.13 ^{13}C NMR shifts (ppm) for *o*-, *m*- and *p*-carbon atoms for 1, 2 and 3

2.11 CONCLUSIONS

The degree of π-bonding between a N substituent and an aromatic ring through delocalisation of the lone pair onto the ring depends on the nature of the substituent. Such π-bonding is found to be greater for an amino group than a hydrazo group (NHNHR). π-Bonding between an azo linkage and an aromatic group is approximately the same as a hydrazo group where the aromatic ring is an unsubstituted phenyl ring, but less if the aromatic group is fluoromes. This reflects an involvement of the π-system of the azo linkage.

CF_3 groups on the ring will increase delocalisation of the lone pair onto the ring both through inductive effects and by increasing the π-acidity of the aromatic system. Of these the π-acidity appears to be most significant. The effect of *o*- and *p*-CF_3 groups is much greater than *m*-CF_3 groups.

These interactions will clearly affect the ligand properties of such compounds through a reduction of the availability of lone pair electrons for bonding to a metal centre. Consequences of this are investigated in Chapter 3.

2.12 REFERENCES

1 C.J. Byrne, D.A.R. Happer, M.P. Hartshorn and H.K.J. Powell, *J. Chem. Soc, Perkin Trans. 2*, **1987**, 1649; C.J. Byrne and D.A.R. Happer, *Aust. J. Chem*, **1993**, *46*, 887-894

2 C.L. Forber, E.C. Kelusky, N.J. Bunce, M.C. Zerner, *J. Am. Chem. Soc.*, **1985**, *107*, 5884

3 D.C. Pestana and P.P. Power, *Inorg. Chem.*, **1991**, *30*, 528

4 D.B. Adams, *J. Chem. Soc. Perkin Trans 2*, **1987**, 247; D.B. Adams, *J. Chem. Soc. Perkin Trans. 2*, **1993**, 567

5 J.R. Holden, C. Dickinson, C.M. Bock, *J. Phys. Chem*, **1972**, *76*, 3597 and references therein.

6 M. Fukuyo, K. Hirostu, T. Higuchi, *Acta Cryst* **B38**, 1982, 640-643

7 G. E. Carr, R. D. Chambers, T. F. Holmes and D. G. Parker, J. Organomet. Chem., **1987**, *325*, 13

8 R.D. Schulter, A.H. Atwood, R.A. Jones, M.R. Bond and C.J. Carrano, *J. Am. Chem. Soc.*, **1993**, *115*, 2070; R.D. Schulter, H.S. Isom, A.H. Cowley, D. A. Atwood, R.A. Jones, F. Olbrich, S. Corbelin and R.J. Lagow, *Organometallics*, **1994**, *13*, 4058

9 H. Grützmacher, H. Pritzkow and F.T. Edelmann, *Organometallics*, **1991**, *10*, 23

10 S. Brooker, J-K. Buijink and F.T. Edelmann, *Organometallics*, **1991**, *10*, 25

11 K.H. Whitmire, D. Labahn, H.W. Roesky, M. Noltemeyer and G.M. Sheldrick, *J. Organomet. Chem.*, **1991**, *402*, 55

12 S. Brooker, N. Bertel, D. Stalke, M. Noltemeyer, H.W. Roesky, G.M. Sheldrick, F.T. Edelmann, *Organometallics*, **1992**, *11*, 192

13 M. Belay and F.T. Edelmann, *J. Organomet. Chem*, **1994**, *479*, C21

14 V.C. Gibson and co-workers, unpublished work

15 H.W. Roesky, M. Scholz, M. Noltemeyer, F.T. Edelmann, *Inorg. Chem.*, **1989**, *28*, 3829

16 S. Brooker, F.T. Edelmann, T. Kottke, H.W. Roesky, G.M. Sheldrick, D. Stalke and K.H. Whitmire, *J. Chem. Soc., Chem. Commun.*, **1991**, 144

17 H.W. Roesky, M. Scholz, M. Noltemeyer, *Chem. Ber.*, **1990**, *123*, 2303

18 M. Scholz, M. Noltemeyer and H.W. Roesky, *Angew. Chem. Int. Ed. Engl*, **1989**, *28*, 1383

19 D. Labahn, S. Brooker, G. M. Sheldrick, H.W. Roesky, *Z. Anorg. Allg. Chem.*, **1992**, *610*, 163

20 N. Bertel, M. Noltemeyer and H.W. Roesky, *Z. Anorg. Allg. Chem.*, **1990**, *588*, 102

21 A. Edelmann, S. Brooker, N. Bertel, M. Noltemeyer, H.W. Roesky, G.M. Sheldrick and F.T. Edelmann, *Z. Naturforsch., Teil B*, **1992**, *47*, 305.

22 K.B. Dillon and H.P. Goodwin, *J. Organomet. Chem.*, **1992**, *429*, 169

23 D. Stalke, K. Keller, F.T. Edelmann, M. Scholz and H.W. Roesky, *J. Organomet. Chem*, **1989**, *366*, 73

24 K.B. Dillon and H.P. Goodwin, *J. Organomet. Chem.*, **1994**, *469*, 125

25 M.J.S. Dewar, E.G. Zoebisch, E.F. Healy and J.J.P. Stewart, *J. Am. Chem. Soc.* **1985**, *107* 3902; M.J.S. Dewar and E. G. Zoebisch, *Theochem.*, **1988**, *180*, 1

26 J.J.P. Stewart, MOPAC 6.0, Frank Seiler Research Lab., USAF Academy, Colorado, 1992.

27 C.J. Byrne, D.A.R. Happer, M.P. Hartshorn and H.K.J. Powell, *J. Chem. Soc, Perkin Trans. 2*, **1987**, 1649; C.J. Byrne and D.A.R. Happer, *Aust. J. Chem*, **1993**, *46*, 887.

28 C.L. Forber, E.C. Kelusky, N.J. Bunce, M.C. Zerner, *J. Am. Chem. Soc.*, **1985**, *107*, 5884

29 J. A. Bouwstra, A. Schouten, J. Kroon, *Acta Cryst.* **1983**, *C39*, 1121-1123

30 M. Traetteberg, I. Hilmo, K. Hagen, *J. Mol. Struct.*, **1977**, *39*, 231

31 K. Chinnakali, Hoong-Kun Fun, *Acta Cryst*, **1993**, *C49*, 615

32 E.J. Gabe, Yu Wang, L.R.C. Barclay, J.M. Dust, *Acta Cryst*, **1981**, *B37*, 978

33 Y. Le Page, E.J. Gabe, Yu Wang, L.R.C. Barclay, H.L. Holm, *Acta Cryst.*, **1980**, *B36*, 2846; L.R.C. Barclay, J.M. Dust, S. Brownstein, E.J. Gabe, *Org. Mag. Res.*, **1981**, *17*, 175

34 E.J. Graeber, B. Morosin, *Acta Cryst.*, **1974**, *B30*, 310

35 F.H. Allen, O. Kennard, D.G. Watson, L. Brammer, A.G. Orpen, R. Taylor, *J. Chem. Soc. Perkin Trans. II* **1987**, S1

36 W. J. Hehre, L, Radom and J. A. Pople, *J. Amer. Chem. Soc*, 1972, **94**, 1496

37 G. Schultz, G. Portalone, F. Ramondo, A. Domenicano, I. Hargitai, *Struct. Chem.*, **1996**, *7*, 59

Chapter Three

Imido Ligands Containing π-Acidic Aromatic Groups

3.1 INTRODUCTION

This chapter describes the synthesis of a range of bis(imido)molybdenum compounds where the imido group contains a phenyl ring bearing CF_3 substituents. As demonstrated in Chapter 2 the effect and position of these CF_3 groups will affect the π-acidity of the aromatic group which will in turn affect the availability of the lone pair on N for π-bonding to the metal. This is manifested in both the structure and reactivity of these complexes.

Much of the interest in bis(imido) complexes of Group 6 metals arises from their similarity, through isoelectronic and pseudoisolobal relationships,[1,2] to the widely used Group 4 metallocenes (see Section 3.2).

Many methods have been devised for the synthesis of transition metal imido complexes. Some of the more important methods are considered in Section 3.3.

3.2 THE PSEUDO-ISOLOBAL RELATIONSHIP

A simple MO treatment of the frontier orbitals of both the cyclopentadienyl ($C_5H_5^-$) and imido ligands (NR^{2-}) reveals a close resemblance, with both having one filled orbital available for σ bonding to the metal and two filled π-symmetry orbitals (Figure 3.1). In addition to these the cyclopentadienyl ligand has two unfilled orbitals of δ-symmetry available for metal-ligand back bonding, although for early transition metals with no filled δ-symmetry orbitals these are unlikely to be of significance.

While such a description of the imido ligand is good to a first approximation, the interaction of the lone pair on N and a substituent such as an aryl group will remove the degeneracy of the π-symmetry orbitals.

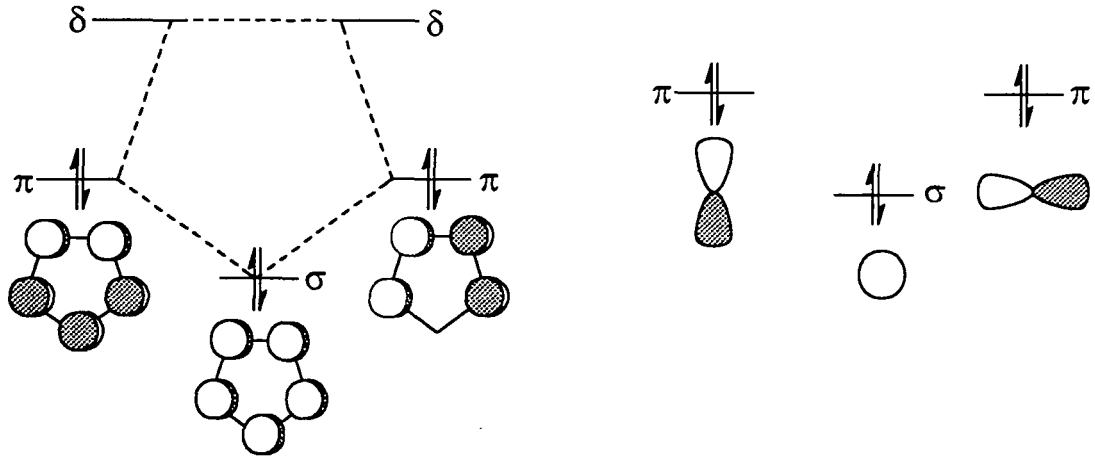

Figure 3.1 Representation of frontier orbitals for $[Cp]^-$ and $[NR]^{2-}$

Using a neutral formalism for electron counting the cyclopentadienyl ligand donates $5e^-$ to the metal whereas the imido ligand donates only $4e^-$. Hence a Group 4 metallocene fragment $[Cp_2M]$ will be both isoelectronic and pseodo-isolobal with a Group 5 half-sandwich compound [CpM(NR)], the additional electron on the Group 5 metal compensating for the fewer electrons supplied by the imido ligand, hence retaining the overall electron count. By a similar argument both these fragments are isoelectronic and pseudo-isolobal with a Group 6 bis(imido) fragment $[M(NR)_2]$ (Figure 3.2).

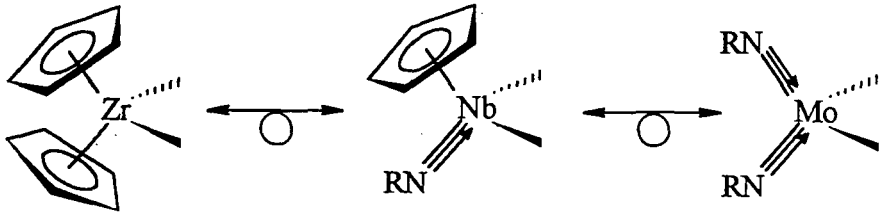

Figure 3.2 The Isolobal Relationship

In view of this relationship and the widespread use of Group 4 metallocenes both in organic synthesis and polymerisation reactions, the bent metallocenes of Group 5 and bis(imido) compounds of Group 6 have been the subject of much study in recent years. These studies have revealed that, while similarities do exist, considerable differences in reactivity are observed. The structures of such compounds, however, are closely

related[3]. The nature of the imido group, both sterically and electronically, is found to influence the reactivity of such compounds significantly.[4]

3.3 SYNTHESES OF IMIDO COMPLEXES

Imido compounds are frequently synthesised from primary amines or their derivatives. Such methods are convenient as a wide range of such compounds is available.

A simple one-pot reaction for the synthesis of bis(imido) molybdenum compounds was devised by Schrock and co-workers, utilising readily available primary amines or anilines. This provides an easy entry point into such chemistry, yielding compounds of the form $Mo(NR)_2Cl_2.dme$ which, through replacement of the chlorines, can be converted into a variety of other compounds including the family of 'Schrock' type initiators for Ring Opening Metathesis Polymerisation (ROMP) of the form $Mo(NR)(CHR)(OR)_2$.[5] The original synthesis[6] employs $[NH_4]_2Mo_2O_7$, subsequent modifications[7] have employed Na_2MoO_4 (Equation 3.1) which gives excellent yields of material with sufficient purity not to require subsequent purification. It has been shown that the use of a mixture of amines or anilines can lead to mixed bis(imido) complexes $Mo(NR)(NR')Cl_2.dme$.[8]

$$\begin{matrix} Na_2MoO_4 + 2RNH_2 \\ + 4Et_3N + 11TMSCl \end{matrix} \xrightarrow{70°C,\ 12\ hrs} \begin{matrix} 3TMSCl + 4HNEt_3Cl \\ + 4TMS_2O + 2NaCl \\ + Mo(NR)_2Cl_2.dme \end{matrix}$$

Equation 3.1

Another method of synthesising such compounds is via imido exchange[9,10] with an existing imido compound (e.g. Equation 3.2). Although useful, the efficiency of such reactions is dependent on the amine used. In many cases a mixture of products is formed which requires separation.

$$\underset{0\%}{Mo(N^tBu)_2(O^tBu)_2} \underset{^tBuNH_2}{\overset{Ar^iNH_2}{\rightleftharpoons}} \underset{65\%}{Mo(N^tBu)(NAr^i)(O^tBu)_2} \underset{^tBuNH_2}{\overset{Ar^iNH_2}{\rightleftharpoons}} \underset{35\%}{Mo(NAr^i)_2(O^tBu)_2}$$

Equation 3.2

Silylated amines ($RNHSiR'_3$) are frequently employed in such syntheses and their use has led to a variety of complexes including $Mo(NAr^i)_2Cl_2$·dme,[11] $Mo(N^tBu)_2(OTMS)_2$[12] and $Cr(N^tBu)_2(OTMS)_2$.[12,13] Again the nature of the product is dependent on both the metal and the amine.

Isocyanates are also used to generate imido complexes. For example, both $Mo(NAr^i)_2Cl_2.THF$[14] and the base free $Mo(N^tBu)_2Cl_2$[15] are generated by the reaction of the appropriate isocyanate with MoO_2Cl_2.

3.3.1 IMIDO EXCHANGE INVOLVING FmesNH₂

Previous work[9] has shown that imido exchange can only occur on heating $Mo(NR)_2Cl_2$·dme compounds with primary amines if the solvent used is dme. Equimolar amounts of $FmesNH_2$ and $Mo(N^tBu)_2Cl_2$.dme were dissolved in dme and sealed in an NMR tube. Even after prolonged heating at 70°C for several weeks the ^{19}F NMR spectrum of the solution revealed that no reaction involving $FmesNH_2$ had occurred. This complete lack of reactivity may be due to the reduced basicity of the $FmesNH_2$ due to the delocalisation of the lone pair.

A similar exchange reaction has been shown to occur with $Mo(N^tBu)_2(O^tBu)_2$ regardless of solvent.[10] Equimolar amounts of $FmesNH_2$ and $Mo(N^tBu)_2(O^tBu)_2$ were dissolved in C_6D_6 and sealed in an NMR tube. After 24hrs at room temperature peaks were seen in the ^1H NMR spectrum which suggested the possible formation of $^tBuNH_2$ and $Mo(N^tBu)(NFmes)(O^tBu)_2$ (Equation 3.3), the peak integrals suggested the ratio of $Mo(N^tBu)_2(O^tBu)_2$ to $Mo(N^tBu)(NFmes)(O^tBu)_2$ to be 2:1. Purification of this product did not prove possible. A similar reaction with two equivalents of $FmesNH_2$ showed no signs of the species $Mo(NFmes)_2(O^tBu)_2$, only the mono-substituted product being evident.

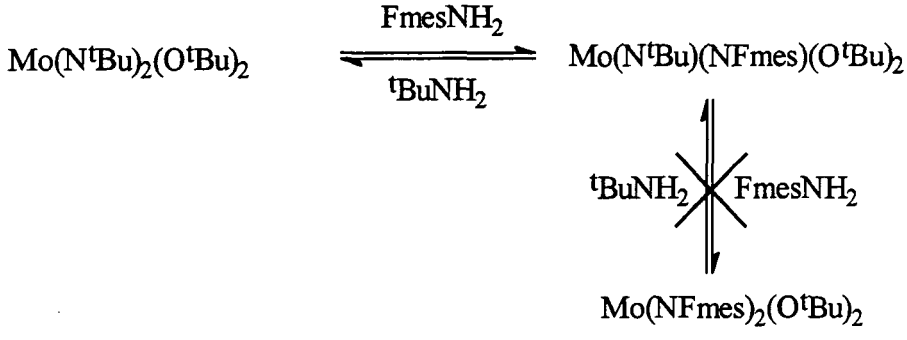

Equation 3.3

The reaction between $Mo(N^tBu)_2(O^tBu)_2$ and two equivalents of Ar^iNH_2 (Equation 3.2) yielded 35% $Mo(NAr^i)_2(O^tBu)_2$ and 65% $Mo(N^tBu)(NAr^i)(O^tBu)_2$ whereas the reaction with two equivalents of $C_6F_5NH_2$ yielded only 50% of $Mo(N^tBu)(NC_6F_5)(O^tBu)_2$ and no $Mo(NC_6F_5)_2(O^tBu)_2$.

Clearly such reactions with electron withdrawing anilines give poor yields of the corresponding imido species, probably due to a reduction in the stability of the system with increasing electron withdrawing strength of the aryl group which will decrease N-Mo π-bonding.

3.3.2 SYNTHESIS OF $Mo(NFmes)_2(OTMS)_2$

$$2FmesNH_2 + Na_2MoO_4 + 4Et_3N + 6TMSCl \longrightarrow 2TMS_2O + 4HEt_3NCl + 2NaCl +$$

2

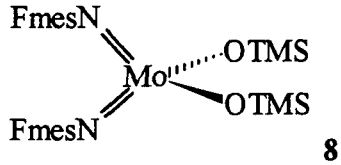

8

Equation 3.4

The reaction of $FmesNH_2$ with Na_2MoO_4, Et_3N and TMSCl in dme yielded a volatile viscous orange oil (Equation 3.4). This proved to be $Mo(NFmes)_2(OTMS)_2$ (**8**) as opposed to the product $Mo(NFmes)_2Cl_2$.dme which would normally be formed in such a reaction. Figure 3.3 shows the part of the mass spectrum obtained for **8** showing the parent ion and the calculated isotope pattern.

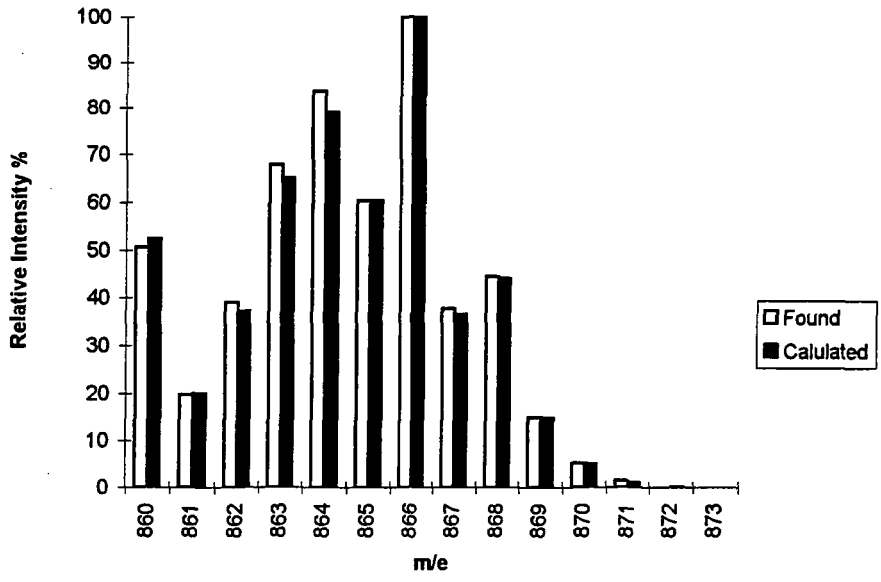

Figure 3.3 Mass spectrum and calculated isotope pattern for 8

The reason for this unusual reaction product is unclear. The effect cannot be purely steric arising from the *o*-CF_3 groups, as similarly bulky amines and anilines (e.g. Ar^iNH_2, ^{t}$BuNH_2$) do not show such reactivity. Likewise it is unlikely to be a purely electronic effect as $C_6F_5NH_2$ does not show this reactivity, again yielding the expected dichloride. It appears that the unusual reactivity of the $FmesNH_2$ arises from a combination of electronic and steric effects. Such factors are known to influence this reaction. The reaction of $[NH_4]_2[Mo_2O_7]$ with $Me(CF_3)_2CNH_2$ under similar conditions did not lead to an isolable product.

The formation of siloxides in reactions of this type is not unknown. The reaction of Ar^iNH_2 with the hydrated molybdate salt $Na_2MoO_4{\cdot}2H_2O$ led to the formation of what appeared to be Mo(NAr^i)$_2$Cl(OTMS).[16] A similar reaction employing Re_2O_7, ^{t}$BuNH_2$ and TMSCl yielded Re(N^{t}Bu)$_3$(OTMS), subsequent treatment with HCl generated Re(N^{t}Bu)$_2$Cl$_3$. It is likely that siloxides such as **8** are intermediates in the more typical reaction and which, for some reason, do not react further with the fluoromes groups present.

3.3.3 SYNTHESIS OF Mo(NFtol)$_2$Cl$_2$·dme

$$Na_2MoO_4 + 2FtolNH_2 + 4Et_3N + 8TMSCl \xrightarrow{70°C,\ 12\ hrs} 4HNEt_3Cl + 4TMS_2O + 2NaCl +$$

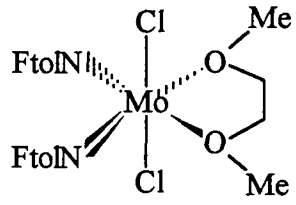

9

Equation 3.5

The reaction of FtolNH$_2$ with Na$_2$MoO$_4$, Et$_3$N and TMSCl in dme gave Mo(NFtol)$_2$Cl$_2$·dme (**9**) in high yield and purity (Equation 3.5). This compound has previously been synthesised via the analogous route employing [NH$_4$]$_2$[Mo$_2$O$_7$].[17] The combined steric and electronic effects of fluorotol are clearly insufficient to produce the unusual reactivity of the fluoromes group and hence the more usual product is formed in this reaction.

3.3.4 MOLECULAR STRUCTURE OF Mo(NFtol)$_2$Cl$_2$·dme

Orange needles of **9** suitable for X-ray diffraction were obtained by the cooling of a Et$_2$O solution. The structure was solved by Prof J.A.K. Howard and Jing Wen Yao within this department. The molecular structure is shown in Figure 3.4, selected bond lengths and angles are in Table 3.1. The complex adopts a highly distorted octahedral geometry typical of such compounds with *trans* Cl ligands and the imido groups mutually *cis*. The Cl1-Mo1-Cl2 shows a large deviation from linearity (160.11(4)°) caused by repulsion between the Cl ligands and the imido groups. Repulsion between the two multiply bonded imido ligands leads to an opening up of the N1-Mo-N2 bond angle to 102.7(1)°. The 'bite' angle of the dme ligand (69.75(9)°) is comparable to that in Mo(N^{t}Bu)(NAr^i)Cl$_2$·dme (69.29(9)°).[16] The Mo-Cl bond lengths (average 2.390(1)Å) are somewhat shorter than those in Mo(N^{t}Bu)(NAr^i)Cl$_2$·dme (average 2.4048(6)Å). This reflects the π-acidity of the fluorotol group reducing N-Mo π-bonding which is compensated for by a strengthening of the Mo-Cl bonds. Both of the C-N-Mo bond angles are within the accepted range for a 'linear' imido group.

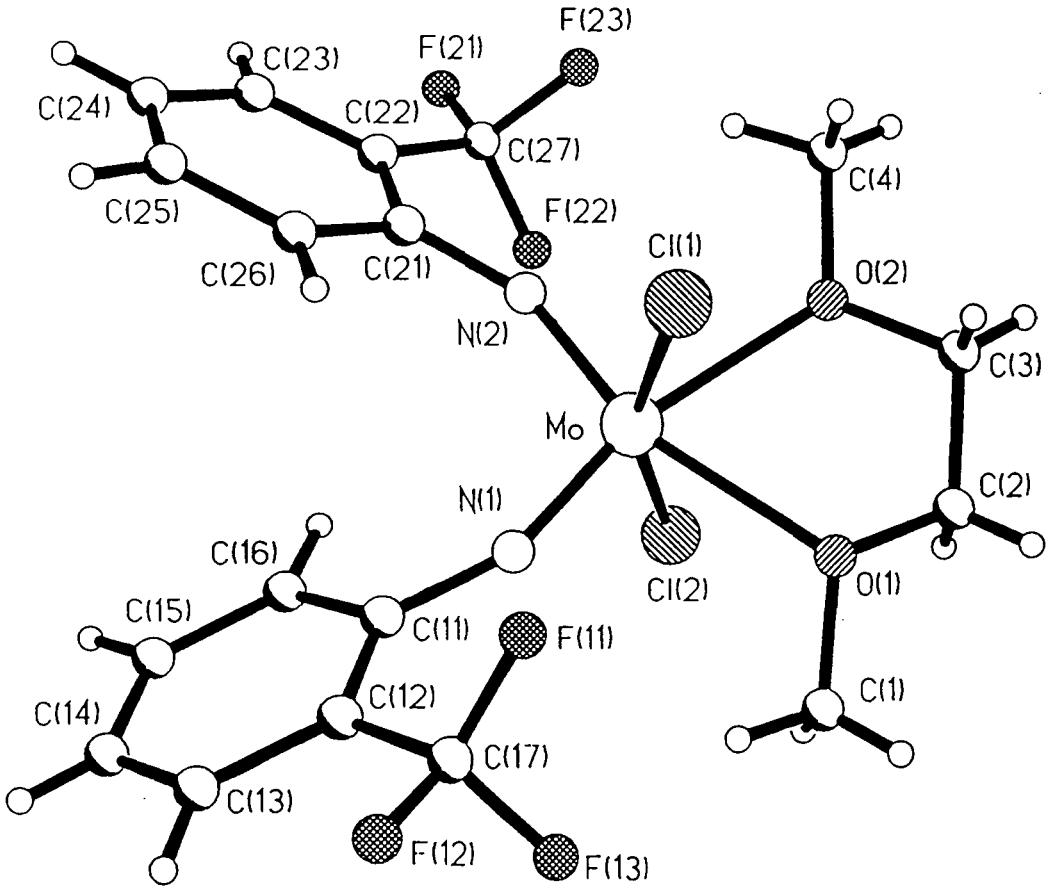

Figure 3.4 Molecular structure of 9

Bond	Bond Length / Å	Atoms	Bond Angle / °
Mo1-Cl1	2.393(1)	Cl1-Mo1-Cl2	160.11(4)
Mo1-Cl2	2.387(1)	N1-Mo1-N2	102.7(1)
Mo1-N1	1.747(3)	Cl1-Mo1-N1	96.35(9)
Mo1-N2	1.745(3)	Cl2-Mo1-N1	95.11(9)
N2-C21	1.393(4)	Cl1-Mo1-N2	94.82(9)
N1-C11	1.383(4)	Cl2-Mo1-N2	98.46(9)
Mo1-O1	2.353(2)	O1-Mo1-O2	69.75(9)
Mo1-O2	2.345(2)	O2-Mo1-N2	92.4(1)
		O1-Mo1-N1	95.2(1)
		C11-N1-Mo1	157.0(3)
		C21-N2-Mo1	153.6(2)

Table 3.1 Selected bond lengths and bond angles in 9

3.3.5 SYNTHESIS OF Mo(NFxyl)$_2$Cl$_2$·dme

$$Na_2MoO_4 + 2FxylNH_2 + 4Et_3N + 8TMSCl \xrightarrow{70°C,\ 12\ hrs} 4HNEt_3Cl + 4TMS_2O + 2NaCl +$$

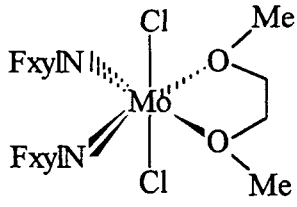

10

Equation 3.6

$FxylNH_2$ reacts with Na_2MoO_4 in the presence of TMSCl, Et_3N and dme to form Mo(NFxyl)$_2$Cl$_2$·dme **10** (Equation 3.6) although in poorer yield than often obtained in such reactions.

3.3.6 SYNTHESIS OF Mo(NFmes)$_2$Cl$_2$

$$Mo(NFmes)_2(OTMS)_2 \xrightarrow{2BCl_3} 2B(OTMS)Cl_2 +$$

8

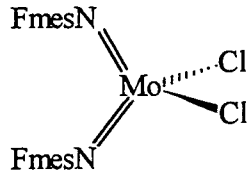

11

Equation 3.7

While **8** is an interesting compound it is not easy to handle and not as useful as a reagent as the Mo(NR)$_2$Cl$_2$·dme family of compounds. It has been shown[18] that Cr(N^{t}Bu)$_2$(OTMS)$_2$ can be converted to Cr(N^{t}Bu)$_2$Cl$_2$ by chlorination with BCl_3. Treatment of **8** with BCl_3 in CH_2Cl_2 immediately produced a red solution. Removal of the solvent and subsequent recrystallisation from heptane yielded Mo(NFmes)$_2$Cl$_2$ as a red crystalline solid in good yield (Equation 3.7).

3.3.7 MOLECULAR STRUCTURE OF Mo(NFmes)$_2$Cl$_2$

On cooling a saturated solution of **11** in pentane to -25°C red crystals formed which proved suitable for an X-ray structure determination. The structure was solved by Prof J.A.K. Howard and Jing Wen Yao of this department. The molecular structure is shown in Figure 3.5, selected bond lengths and angles are collected in Table 3.2. The complex is found to adopt a distorted tetrahedral geometry in the solid, the greatest deviation from an ideal tetrahedron being the Cl1-Mo-Cl2 bond angle (115.53(6)°).

The Mo-Cl bond lengths are shorter than those in **9**. This is indicative of the lower electron count on the metal centre (formally $16e^-$ in **11**, $20e^-$ in **9**). Again the C-N-Mo bond angles are within the accepted range for a 'linear' imido group, there is a distinct deviation from linearity. It is unlikely that this is due to a stereochemically significant lone pair on the nitrogen atom as this is not present in the free aniline. It would appear this deviation arises purely from steric and crystal packing effects, emphasising that such angles are a poor indication of the nature of bonding between the N and Mo.

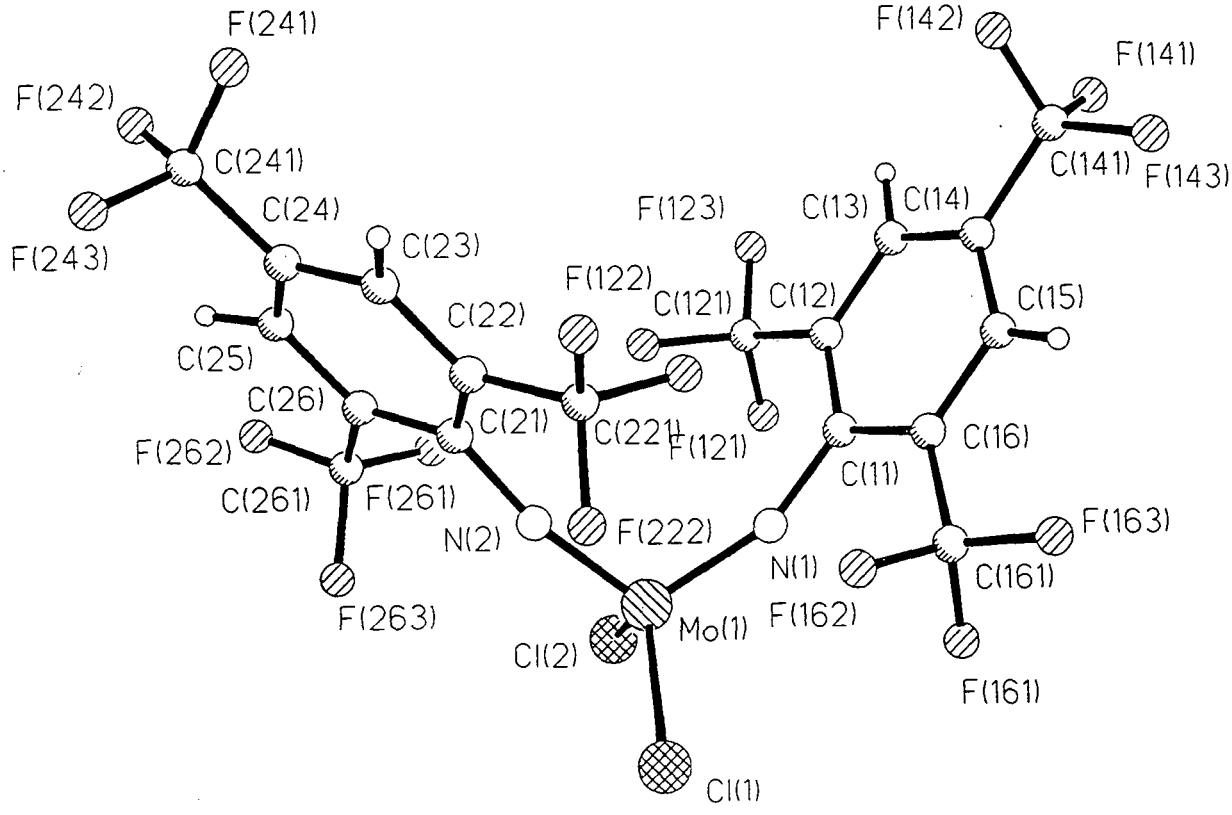

Figure 3.5 Molecular structure of 11

Atoms	Bond Length / Å	Atoms	Bond Angle / °
Mo1-Cl1	2.2524(12)	Cl1-Mo1-Cl2	115.53(6)
Mo1-Cl2	2.2588(13)	Cl1-Mo1-N1	107.62(12)
Mo1-N1	1.736(3)	Cl1-Mo1-N2	107.32(11)
Mo1-N2	1.745(3)	Cl2-Mo1-N1	108.94(11)
N1-C11	1.387(5)	Cl2-Mo1-N2	107.98(11)
N2-C21	1.396(5)	N1-Mo1-N2	109.3(2)
		Mo1-N2-C21	167.8(3)
		Mo1-N1-C11	156.9(3)

Table 3.2 Selected bond lengths and bond angles for 11

3.3.8 Synthesis of $Mo(NFmes)_2Cl_2 \cdot 2py$

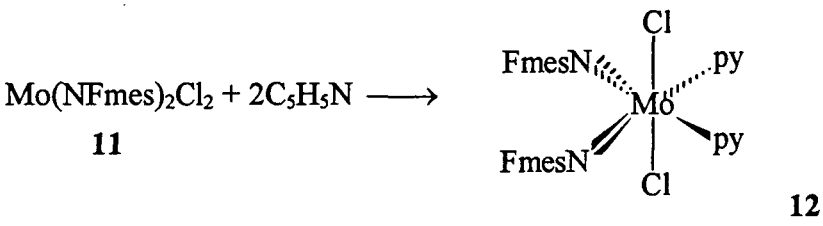

Equation 3.8

Treatment of **11** with pyridine in pentane led to the formation of a dark solid which proved to be the pyridine adduct $Mo(NFmes)_2Cl_2 \cdot 2py$ (**12**) (Equation 3.8). Such adducts are frequently formed with coordinatively unsaturated compounds and can be considered analogous to the $Mo(NR)_2Cl_2 \cdot dme$ compounds in that they can be considered as $Mo(NR)_2Cl_2.2L$ type complexes.

3.3.9 Molecular Structure of $Mo(NFmes)_2Cl_2 \cdot 2py$

On cooling a warm solution of **12** in pentane slowly to room temperature dark purple crystals formed which proved suitable for an X-ray diffraction experiment. The structure was solved by Prof J.A.K. Howard and Jing Wen Yao within the department. The molecular structure is shown in Figure 3.6 and selected bond lengths and bond angles in Table 3.3.

The complex adopts a highly distorted octahedral geometry analogous to that for the $Mo(NR)_2Cl_2 \cdot dme$ compounds with imido ligands mutually *cis*, Cl atoms mutually *trans* and the pyridine ligands occupying the coordination environment of the bidentate dme ligand. There is a large deviation in the Cl-Mo-Cl bond angle from linearity and also an opening up of the angle between the two imido-Mo bonds as in the structure of **9**.

The Mo-Cl bonds (average 2.3757(14)Å) are longer than those in **11**, reflective of the higher electron count of the metal (formally $20e^-$ as opposed to $16e^-$ in **11**).

Atoms	Bond Lengths / Å	Atoms	Bond Angles / °
Mo1-Cl1	2.3738(13)	Cl1-Mo1-Cl2	154.74(5)
Mo1-Cl2	2.3776(14)	N1-Mo1-N2	102.4(2)
Mo1-N4	2.385(4)	N2-Mo1-N4	88.6(2)
Mo1-N3	2.354(4)	N3-Mo1-N4	81.47(13)
Mo1-N2	1.774(4)	N1-Mo1-N3	87.6(2)
Mo1-N1	1.774(4)	Cl1-Mo1-N1	98.65(13)
N1-C11	1.372(6)	Cl1-Mo1-N2	98.03(12)
N2-C21	1.379(6)	Cl1-Mo1-N3	81.80(10)
		Cl1-Mo1-N4	78.54(10)

Table 3.3 Selected bond lengths and angles for 12

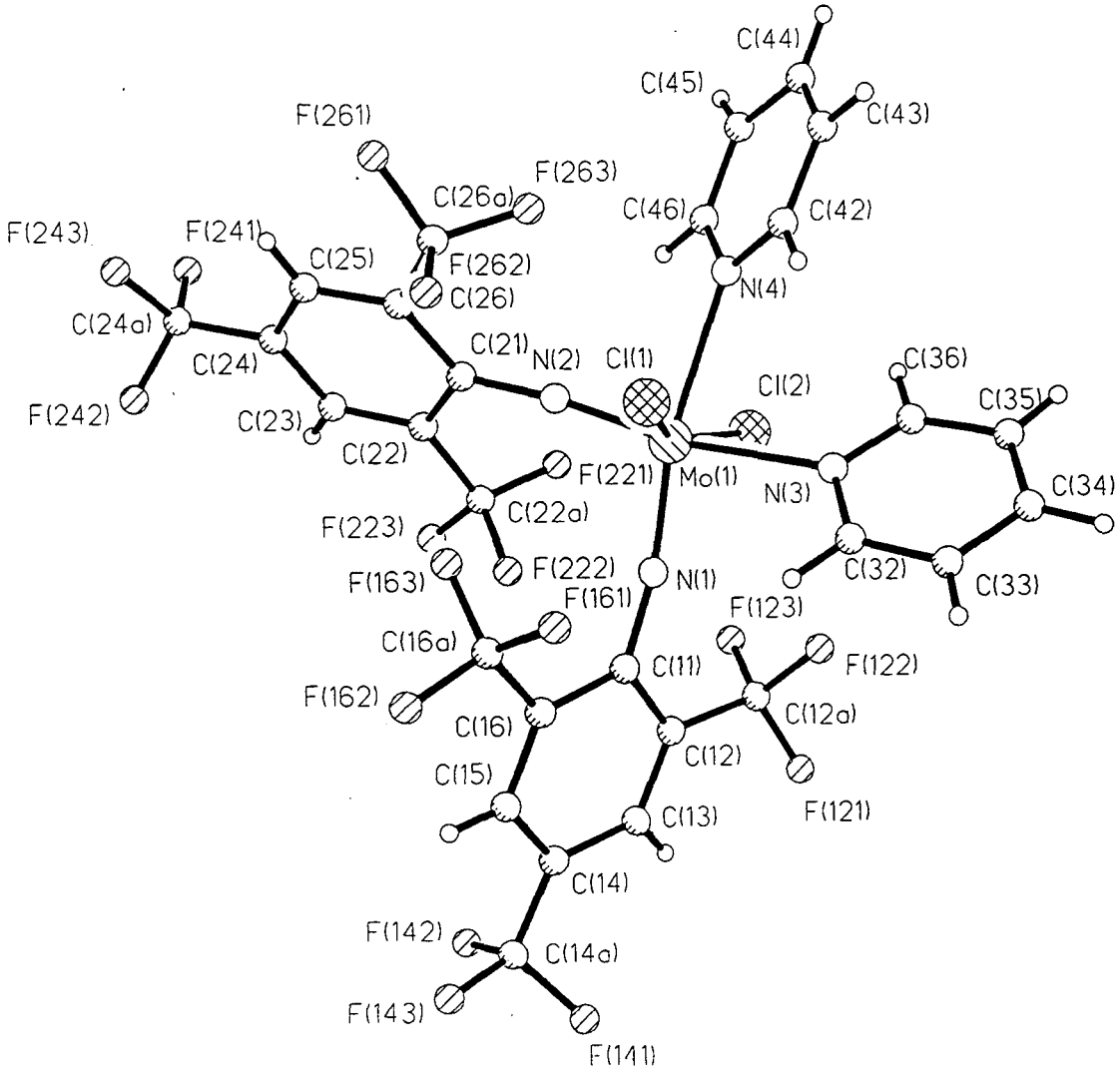

Figure 3.6 Molecular structure of 12

3.3.10 REACTION OF $Mo(NFmes)_2Cl_2$ WITH DME

$$Mo(NFmes)_2Cl_2 + dme \longrightarrow Mo(NFmes)_2Cl_2{\cdot}dme + Mo(NFmes)_2Cl_2{\cdot}2dme$$

11 **13** **14**

Equation 3.9

The addition of dme to a solution of **11** in pentane caused the simultaneous formation of an orange powder and a red crystalline solid. The ^1H NMR spectra indicated both to be **11** with coordinated dme, the red solid crystalline solid being $Mo(NFmes)_2Cl_2{\cdot}dme$ (**13**) and the orange powder having a ratio of dme:fmes of 1:1 suggesting $Mo(NFmes)_2Cl_2{\cdot}2dme$ (**14**) (Equation 3.9). The formation of **13** is unremarkable being analogous to **9**. The formation of **14** however is harder to rationalise as two bidentate dme ligands will clearly result in a highly crowded system. The formal electron count of **13** is $20e^-$, coordination of a further dme ligand will result in a $24e^-$ system and is clearly not required to satisfy the $18e^-$ rule. It is feasible that the dme ligands are monodentate and although this will clearly reduce the steric requirements of the two dme ligands there is no apparent advantage of this system over the single bidentate dme ligand in **13**.

3.4 PREPARATION OF Mo(IV) PHOSPHINE COMPLEXES

The reduction of Cp_2MCl_2 (M = Ti, Zr) with Mg in the presence of tertiary phosphine generates the reduced species $Cp_2M(PR_3)_2$.[19,20] The same method has been employed to generate the isoelectronic and pseudo-isolobal complexes $CpNb(NAr^i)(PMe_3)_2$,[21] $W(NAr^i)_2(PMe_2Ph)_2$[1] and $Mo(NAr^i)_2(PMe_3)_2$.[4] Reduction of $Mo(N^tBu)_2Cl_2{\cdot}dme$ under the same conditions leads to dimeric $[Mo(N^tBu)(\mu\text{-}N^tBu)(PMe_3)]_2$,[4] illustrating the effect of the imido substituents on reactivity.

Such compounds have proved to be useful as synthetic precursors and react with, amongst other things, unsaturated hydrocarbons generating complexes with η^2-bound ligands such as $Mo(NAr^i)_2(PMe_3)_2(C_2H_4)$,[4] $Mo(N^tBu)_2(PMe_3)(C_2H_4)$[7,22] and $W(NAr)_2(PMe_2Ph)(C_2H_4)$.[1] Again, the first two examples underline the difference in reactivity arising from the differing imido groups which is thought to be largely steric in origin.

3.4.1 SYNTHESIS OF Mo(NFtol)$_2$(PMe$_3$)$_3$

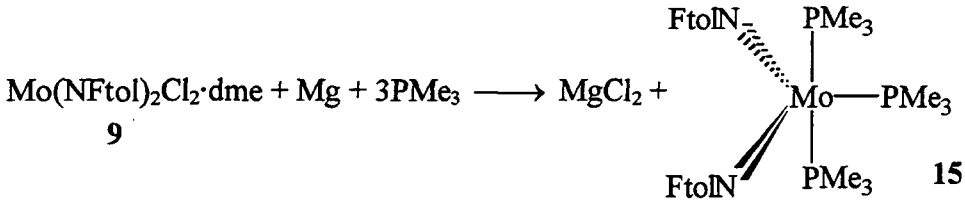

Equation 3.10

The reduction of **9** with magnesium in the presence of PMe_3 in THF led to formation of $Mo(NFtol)_2(PMe_3)_3$ (**15**) (Equation 3.10). Green crystals of **15** obtained from pentane solution rapidly formed an orange powder on drying under nitrogen. This orange powder redissolved to give a green solution which proved still to be **15**, hence this colour change appears to be a dichroic effect. This dichroic effect could also been seen in solutions of **15**, the green solution appearing orange around the fringes of the solution.

3.4.2 MOLECULAR STRUCTURE OF Mo(NFtol)$_2$(PMe$_3$)$_3$

Green crystals of **15** obtained by the cooling of a pentane solution proved to be suitable for an X-ray structure determination. The structure was solved Prof J.A.K. Howard and Dr A.S. Batsanov within the department. The molecular structure is shown in Figure 3.7 and selected bond lengths and angles are collected in Table 3.4.

The complex is found to adopt a highly distorted trigonal bi-pyramidal geometry in the crystal. The imido ligands occupy equatorial sites, the angles between the two N-Mo bonds being 146.5(2)° showing repulsion between the two multiply bonded ligands as in compounds **9**, **11** and **12**. The P1-Mo-P3 bond angle (166.70(4)°) shows that the axial phosphine ligands bend away from the CF_3 groups and equatorial phosphine ligand. The Mo-P bond lengths clearly show the inequivalence of the equatorial and axial phosphine ligands, the bond to the equatorial phosphine being 0.07Å shorter than the other two. These bonds are longer than those in the compound $Mo(NAr')_2(PMe_3)_2$ (Mo-P 2.401(5)Å) There are two signals in the ^{31}P solution NMR (ratio 2:1) indicating that this structure is retained in the solution without exchange of ligands between axial and equatorial positions at room temperature on the NMR time scale.

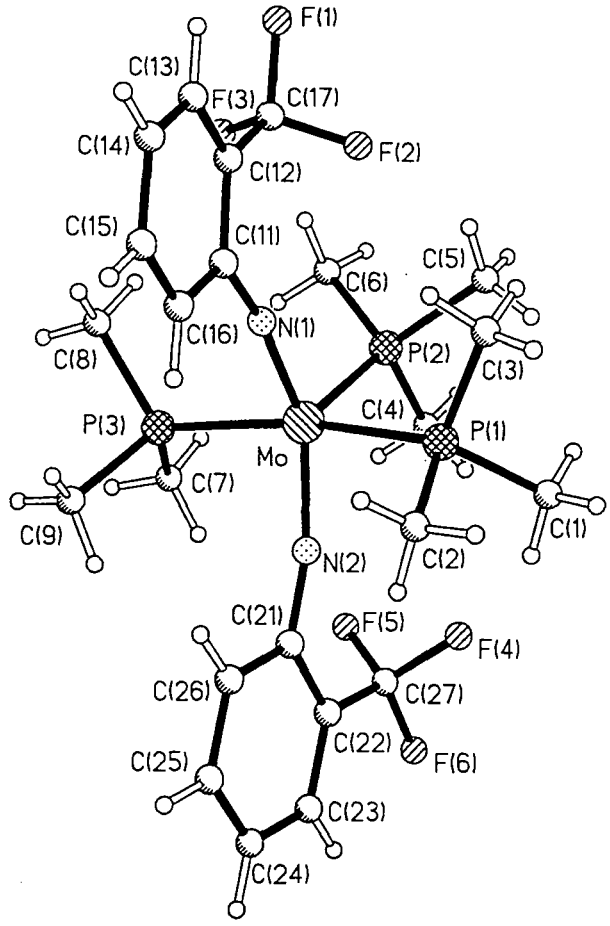

Figure 3.7 Molecular structure of 15

Atoms	Bond Lengths	Atoms	Bond Angles
Mo1-N1	1.826(3)	N1-Mo1-N2	146.5(2)
Mo1-N2	1.848(3)	N1-Mo1-P2	103.2(1)
Mo1-P1	2.495(1)	N2-Mo1-P2	110.4(1)
Mo1-P2	2.419(1)	P1-Mo1-N1	89.2(1)
Mo1-P3	2.481(1)	P1-Mo1-N2	87.1(1)
		P1-Mo1-P2	96.69(4)
N1-C11	1.376(5)	P3-Mo1-N1	90.3(1)
N2-C22	1.360(5)	P3-Mo1-N2	86.0(1)
		P3-Mo1-P2	96.38(4)
		P1-Mo1-P3	166.70(4)

Table 3.4 Selected bond lengths and angles for 15

3.4.3 SYNTHESIS OF Mo(NFmes)$_2$(PMe$_3$)$_3$

$$Mo(NFmes)_2Cl_2 + Zn + 3PMe_3 \longrightarrow ZnCl_2 +$$

11

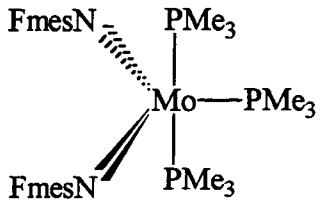

16

Equation 3.11

Treatment of **11** with Mg in the presence of PMe_3 in a reaction analogous to Equation 3.10 yielded a dark paramagnetic product. However, a similar reaction employing Zn as the reducing agent in place of Mg led to the isolation of a red/green dichroic crystalline solid which proved to be Mo(NFmes)$_2$(PMe$_3$)$_3$ **16**.

The ^{31}P solution NMR spectrum at room temperature indicates two phosphine environments (ratio 2:1) consistent with a structure equivalent to that of **15** in the solid. On warming these signals broaden until at 344K they disappear into the baseline due to exchange of ligands between inequivalent positions. The ^{1}H NMR spectrum at room temperature indicates that the *meta* protons on the fluoromes ring are equivalent, the ^{19}F NMR spectrum however indicates that the *o*-CF_3 groups are inequivalent at room temperature with two broadened resonances being seen. This again indicates a structure similar to that for **15** with the fluoromes groups lying in the equatorial plane, which results in two environments for the CF_3 groups (Figure 3.8) the rotation about C_i-Mo being slow on an NMR time scale. On cooling to 198K these peaks sharpen due to a reduced rate of rotation (Figure 3.9 **A**). On warming these peaks broaden (Figure 3.9 **B** and **C**) until at 313K they are very broad and are only just discernible as separate peaks (Figure 3.9 **D**). At 323K the peaks have coalesced to form a single broad peak (Figure 3.9 **E**). On further warming this single peak sharpens further as the rate of rotation increases (Figure 3.9 **F**). These data allow the calculation of the free energy of rotation of the fluoromes ring.[23] The rate constant of rotation, k, at the coalescence temperature (T_c) can be obtained using the equation $k=\pi(\Delta\nu)2^{-½}$ ($\Delta\nu$ = separation (in Hz) of the two peaks at the slow exchange limit). This case is complicated in that the chemical shifts of the *o*-CF_3 groups appear to be temperature dependent, the peak separation being 1.5 ppm at 193K and 2.0 ppm at 253K. This

yields values of k of 1254 s^{-1} and 1636 s^{-1} respectively. From these values it is possible to obtain the free energy of rotation of the aryl group using the equation:

$$\Delta G^{\ddagger} = -RT_c[\ln (k/T_c) + \ln (h/K)]$$

R = molar gas constant, 8.314 $Jmol^{-1}K^{-1}$

K = Boltzmann's constant, 1.381×10^{-23} JK^{-1}

h = Planck's constant, 6.626×10^{-34} Js^{-1}

T_c = Coalescence temperature, K

This yields a free energy of rotation of 60.2 $kJmol^{-1}$ using the value of $\Delta\nu$ at 193K and 59.5 $kJmol^{-1}$ using the value of $\Delta\nu$ at 253K. These values are similar to that determined for $Mo(NAr')_2(PMe_3)_2$ (55.0 $kJmol^{-1}$).

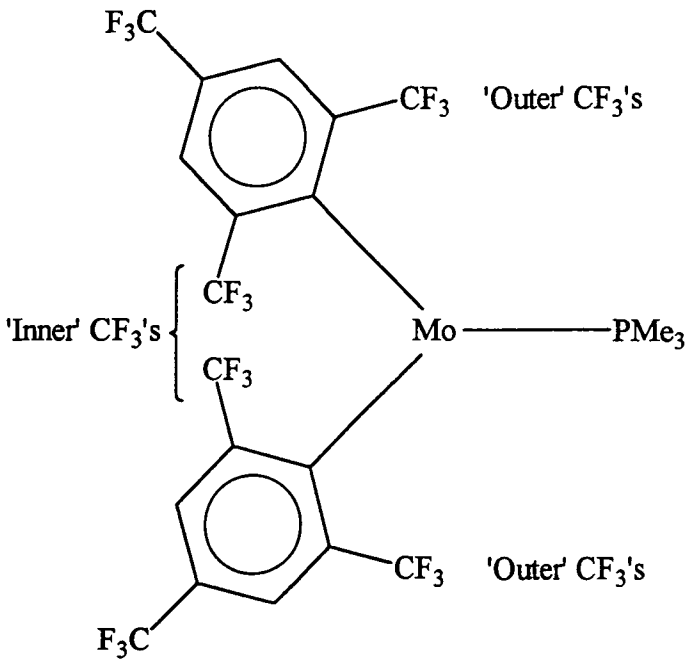

Figure 3.8 Compound 16 viewed down the time averaged P-Mo-P axis

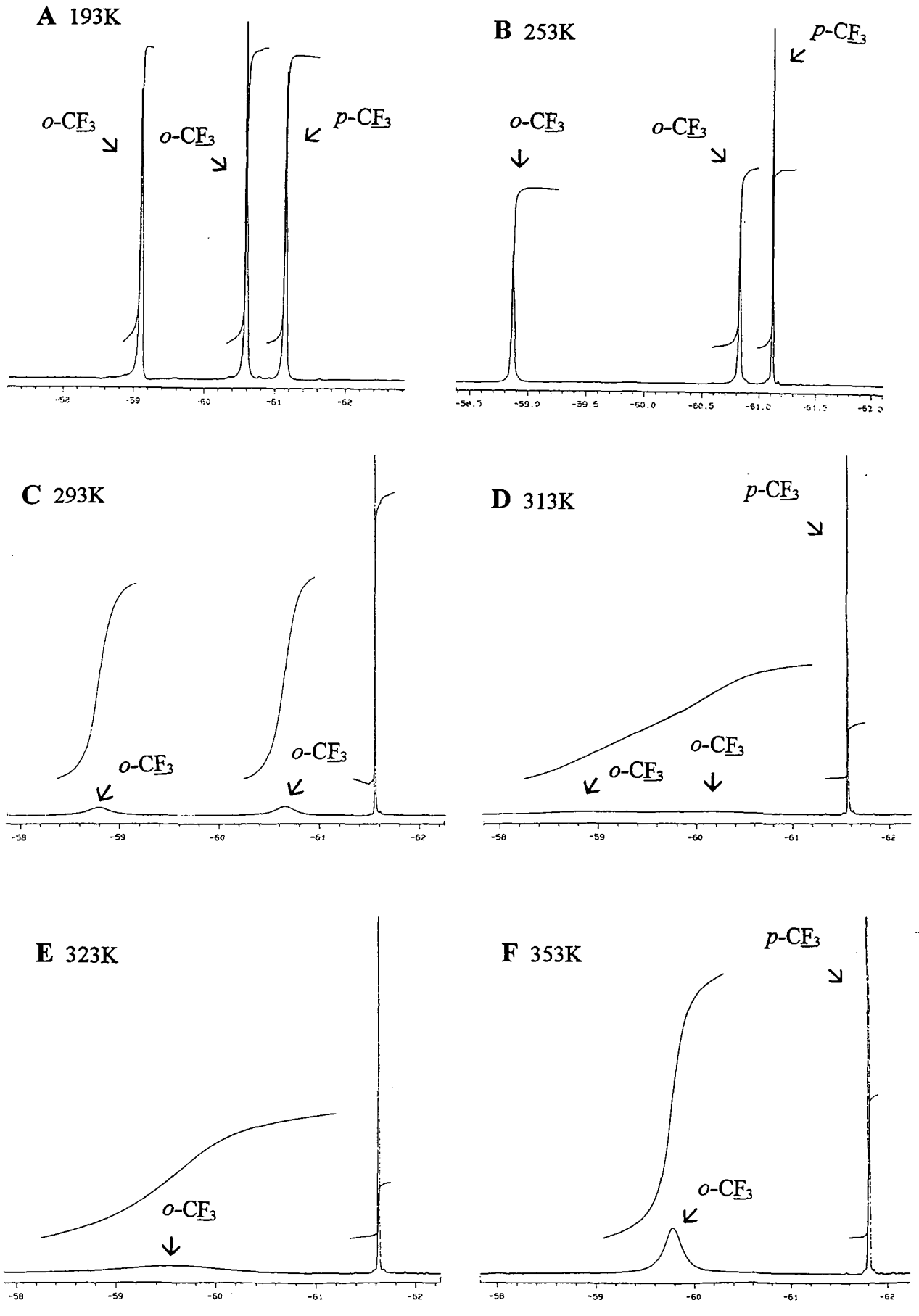

Figure 3.9 Variable temperature 376 MHz ^{19}F NMR spectra of 16

Both **15** and **16** represent the first examples of tris phosphine complexes $Mo(NR)_2(PR_3)_3$. Previous work has shown that the reduction of $Mo(NAr^i)_2Cl_2$·dme under similar conditions leads to the formation of the bis-phosphine complexes $Mo(NAr^i)_2(PMe_3)_2$. With $Mo(N^tBu)_2Cl_2$·dme the imido bridged dimer $[Mo(N^tBu)(\mu\text{-}N^tBu)(PMe_3)]_2$ is formed. The coordination of an additional phosphine ligand in **15** and **16** compared to $Mo(NAr^i)_2(PMe_3)_2$ is clearly not a steric effect as the Ar^i group is similar in steric bulk to Fmes and bulkier than Ftol. The π-acidic nature of both Fmes and Ftol will decrease the electron density on the Mo compared to the equivalent compound with Ar^i, due to reduced N-Mo π-bonding. The coordination of an additional phosphine ligand will compensate for this and occurs despite the additional steric crowding. Whilst sensitive to moist air, both **15** and **16** are far less sensitive than $Mo(NAr^i)_2(PMe_3)_2$, no doubt due to a combination of both steric protection and increase in the formal electron count reducing the electrophilic nature of the metal centre.

3.4.4 Synthesis of $Mo(NFxyl)_2(PMe_3)_2$

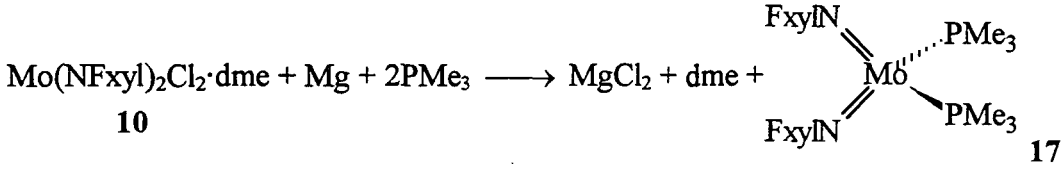

Equation 3.12

The reduction of **10** with Mg in the presence of PMe_3 led to the formation in poor yield of a solid which was shown by ^1H and ^{31}P NMR spectra to be $Mo(NFxyl)_2(PMe_3)_2$ although small peaks in both ^{19}F and ^{31}P NMR spectra indicated that the compound was not pure. The coordination of only two phosphines, as opposed to the three in the case of **15** and **16**, can be attributed to the weaker π-acidity of the Fxyl group compared to that of Fmes and Ftol (Section 2.8). The isolation of this bis-phosphine complex demonstrates that the existence of tris-phosphine complex **15** is not purely due to the reduced steric hindrance of the Ftol group compared to the Ar^i group which also forms the bis-phosphine complex. If reduced steric bulk alone was the factor responsible for the coordination of three phosphine ligands, then the reduction product of **10** would also be expected to have three phosphine ligands.

3.4.5 SYNTHESIS OF $Mo(NFmes)_2(PMe_3)_2(\eta^2\text{-}C_2H_4)$

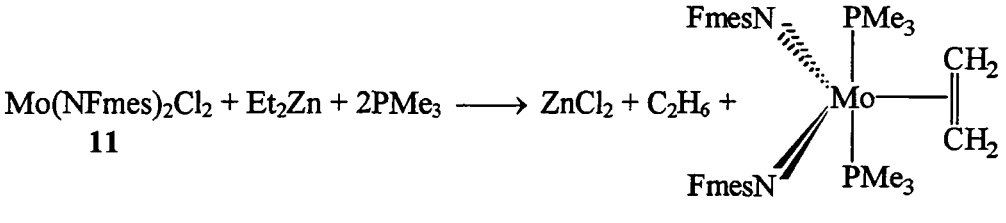

Equation 3.13

The reaction of $Mo(NR)_2Cl_2$·dme with EtMgBr in the presence of PMe_3 has been shown to generate Mo(IV) species with η^2 ethylene ligands.[4,7,22] When dichloride **11** was treated with EtMgBr in the presence of phosphine, no identifiable products were isolated. The reaction was repeated with Et_2Zn in place of the Grignard reagent (Equation 3.13). On work up a blue crystalline product was obtained which proved to be $Mo(NFmes)_2(PMe_3)_2(\eta^2\text{-}C_2H_4)$ (**18**). The compound was surprisingly stable for such an Mo(IV) species, decomposing in moist air only over a period of days.

Crystals of **18** were obtained and an X-ray structure determination carried out by Prof. J.A.K. Howard and Jing Wen Yao within this department. The data was of insufficient quality for meaningful bond lengths and angles to be calculated. The molecular geometry (Figure 3.10) is analogous to that for $Mo(NAr^i)_2(PMe_3)_2(\eta^2\text{-}C_2H_4)$, with both fluoromes groups lying in the equatorial plane, phosphine ligands in axial positions and the ethylene ligand in an equatorial site with the C-C bond perpendicular to the equatorial plane. This orientation can be rationalised in terms of competition for π-symmetry orbitals on the metal.[3]

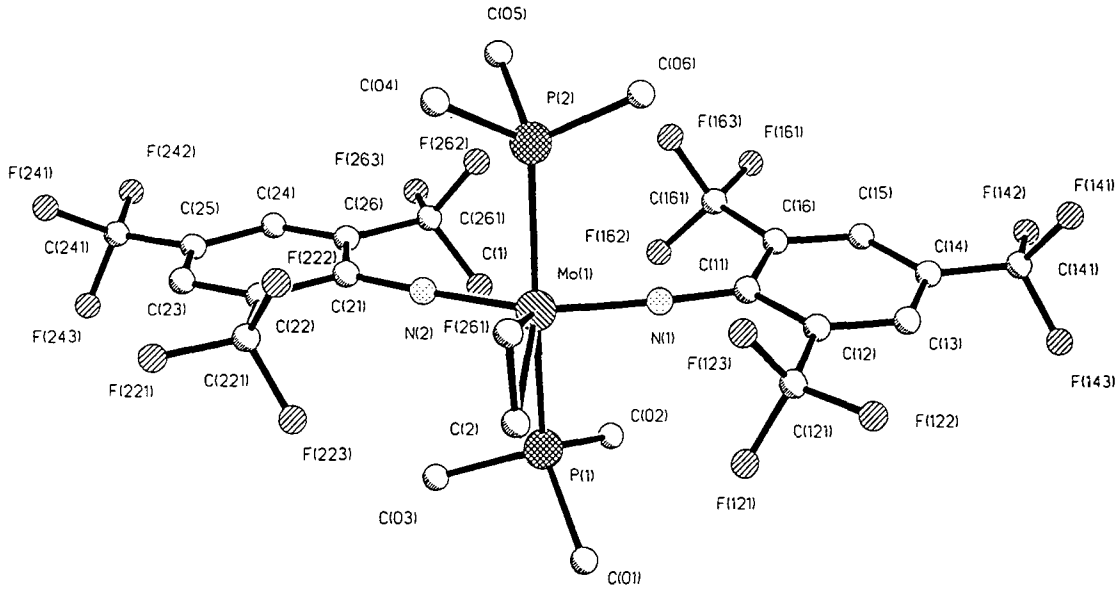

Figure 3.10 Molecular structure of 18

The ^{31}P NMR is consistent with this structure showing only one phosphorus environment in solution. The ^{13}C NMR of the Me groups on the phosphine appear as triplets due to coupling to ^{31}P (Figure 3.11). This is consistent with two *trans* phosphines and arises for a large coupling between the two phosphine ligands due to the trans orientation.

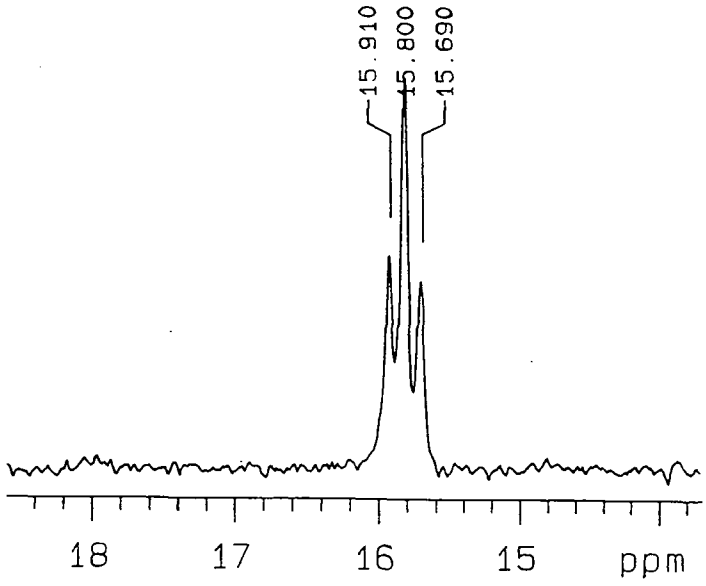

Figure 3.11 ^{13}C NMR of PMe_3 ligands

The ^{1}H solution NMR spectrum at room temperature shows the *m*-Hs on the aryl group to be inequivalent and the ^{19}F NMR spectrum also shows the *o*-CF_3 groups to be inequivalent due to restricted rotation of the fluoromes group as in *tris*-phosphine **16**. On warming to 363K the signals due to these CF_3 group broaden but do not coalesce (Equation 3.12) as the corresponding signals in **16** do. This is not seen as the greater separation of the peaks leads to a much higher value for k of 4637 s^{-1} i.e. the rate of rotation required for the peaks to coalesce is much higher than for **16**. Assuming a similar value for $\Delta G^{\ddagger}$ the temperature required for the coalescence of the peaks would be considerably higher than for **16**. The resonances due to the *o*-CF_3 groups are not seen in the ^{13}C NMR spectrum at room temperature, presumably due to broadening caused by the restricted rotation.

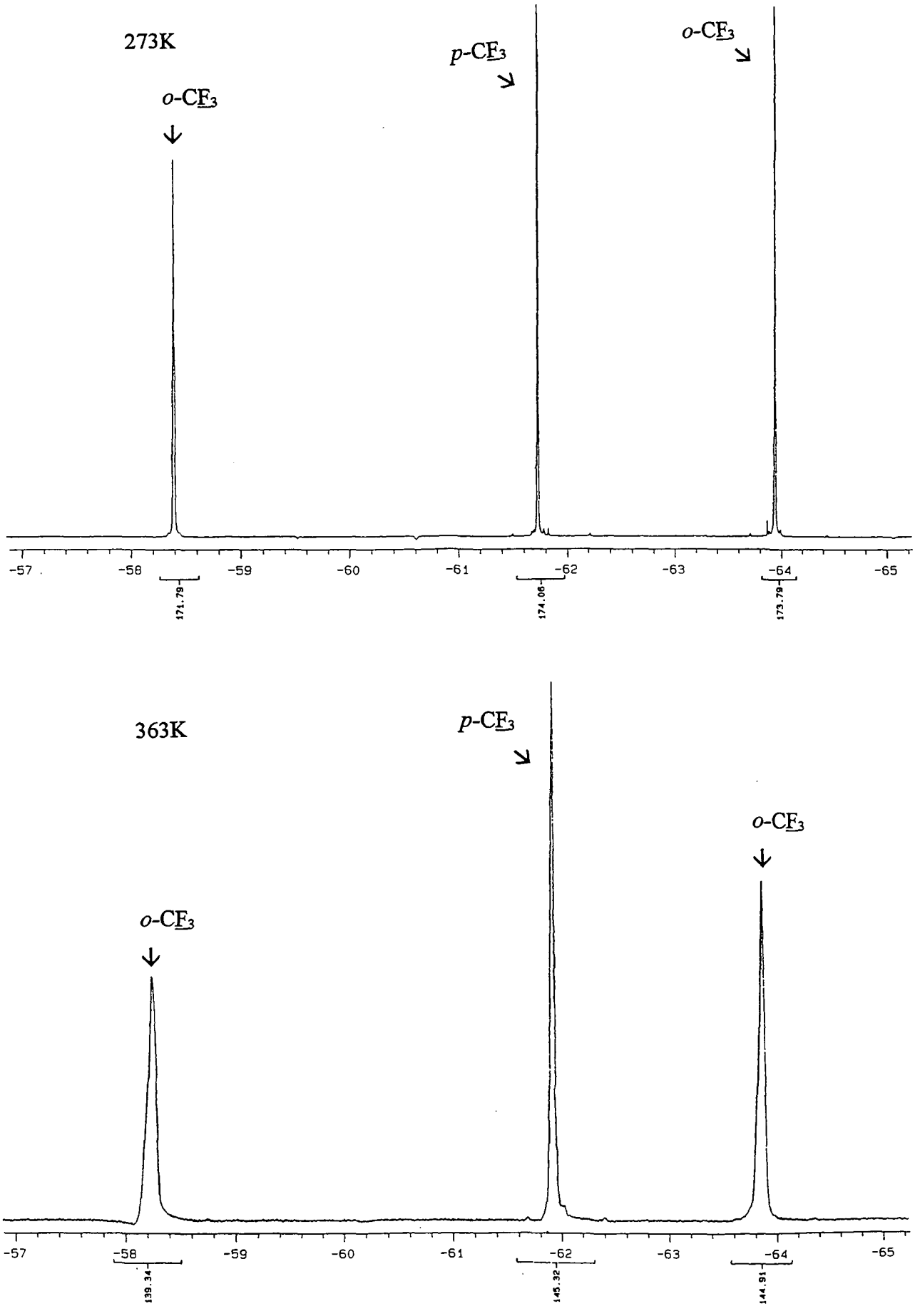

Figure 3.12 Variable temperature 376 MHz ^{19}F NMR spectra for 18

3.4.6 SYNTHESIS OF Mo(NFtol)$_2$(PMe$_3$)$_2$(η^2-C$_2$H$_4$)

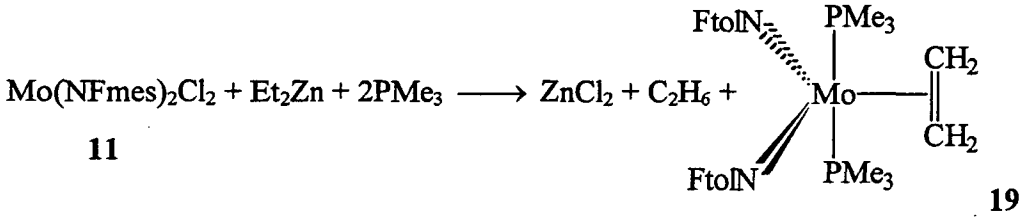

Equation 3.14

The reaction of Et_2Zn with $Mo(NFtol)_2Cl_2$·dme in the presence of excess phosphine resulted in the formation of $Mo(NFtol)_2(PMe_3)_2(\eta^2\text{-}C_2H_4)$ (**19**). It is expected that the conformation of this complex is as that in **18**. Both ^1H and ^{13}C and ^{19}F NMR spectra indicate that both imido groups are equivalent. The C atoms of the methyl groups of the phosphines appear as triplets in the ^{13}C NMR confirming that the phosphines are indeed mutually *trans*.

3.5 π-BONDING IN ARYL-IMIDO COMPLEXES

Formally 'linear' imido ligands display π-bonding between the N 'lone pair' and the metal atom. As the lone pair in compound **8** to **14** is also involved in π-bonding to the aryl ring there will be competition for the lone pair. Increasing N-Mo π-bonding should result in reduced N-C π-bonding and hence a shortened N-Mo bond should correspond to a lengthened C-N bond. This is seen in Figure 3.13 although the errors on the C-N distances are large in relation to the differences (error bars indicate the e.s.d). Also included are data for the pentafluoroimido ligand from the compounds $Mo(NAd)(NC_6F_5)Cl_2$·dme and $Mo(NAd)(NC_6F_5)(CHCMe_2Ph)_2$ (Ad=adamantyl) in which the C_6F_5 group is also a π-acid.

Similar trends have been noted for pentafluorophenoxy (C_6F_5O) ligands in which the electron withdrawing effect of the aromatic system reduces the availability of electrons for π-bonding to the metal. As with this system, competition for the lone pair is seen and shorter M-O distances correspond to lengthened C-O distances.[24]

Such trends are not seen in all aromatic systems. The NAr^i ligand, for example, shows no such trend, as although there will be some degree of interaction between the N lone pair and ring, this is insufficient to affect Mo-N distances to an extent great enough for

such trends to be seen. Mo-N bond lengths for this ligand do tend to be longer than those for N^{t}Bu ligands, and this has been attributed to reduced π-electron availability in the aromatic ligand due to lone pair delocalisation.[16]

This relationship allows the effect of the auxiliary ligands on the Mo atom to be assessed. $Mo(NFmes)_2Cl_2$ **11** displays significantly less C-N π-bonding than the parent $FmesNH_2$. Coordination of two pyridine ligands to **11** to form **12** will increase the electron density on the central Mo atom producing a formally "20e⁻" system. Less Mo-N π-bonding will be required to stabilise the system resulting in a longer N-Mo bond (1.774(4)Å in **11**, 1.837Å in **12**). This in turn will allow more C-N π bonding and the C-N distance shortens from 1.376(6)Å in **11** to 1.368(5)Å in **12**.

A similar effect is seen for the fluorotol group in $Mo(NFtol)_2Cl_2$·dme **9** and $Mo(NFtol)_2(PMe_3)_3$ **15**. The C-N distance in **9** (1.388(4)Å) is longer than that calculated by the AM1 method in Section 2.5 for the parent aniline $FtolNH_2$ (1.377Å) implying reduced C-N π-bonding. The C-N distance in **15** (Å) however is almost identical to that calculated for the free aniline. This shortening of the C-N bond on going from **9** to **15** is accompanied by a lengthening of the N-Mo bond from 1.746(3)Å to 1.837(3)Å. The similarity between the C-N bond lengths in $FtolNH_2$ and **15** does not imply that there is no N-Mo π-bonding, merely that it is of insufficient magnitude to affect the π-bonding to the ring.

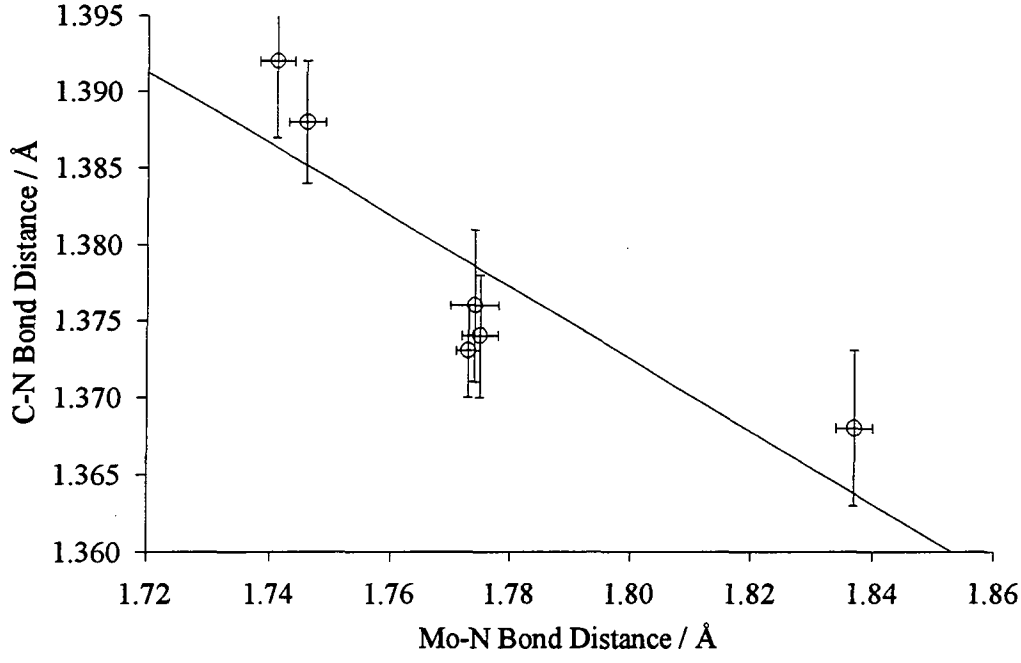

Figure 3.13 Relationship between C-N and N-Mo bond distances in Mo-NAr imido complexes

3.6 ^{13}C NMR OF ARYL-IMIDO COMPLEXES

It was noted in Section 2.10 that the ^{13}C NMR shifts of the *o*- and particularly *p*-carbon atoms of the fluoromes ring reflect the degree of multiple bonding between the ring and nitrogen substituent. As this is altered by coordination to a metal the ^{13}C NMR shifts of these compounds should alter accordingly. Figure 3.14 shows this trend for those compounds which have been structurally characterised with decreasing frequency of the ^{13}C NMR shift with decreasing C-N distance. Table 3.5 summarises these shifts for the N substituted fluoromes compounds. Two lines are perceptible, both apparently including the point for $FmesNH_2$ **2**. The ^{13}C shift of the *p*-C is clearly governed by other effects, in addition to the degree of C-N π-bonding and could be related to coordination to the metal. A lack of data prevents further conclusions relating to this effect to be drawn.

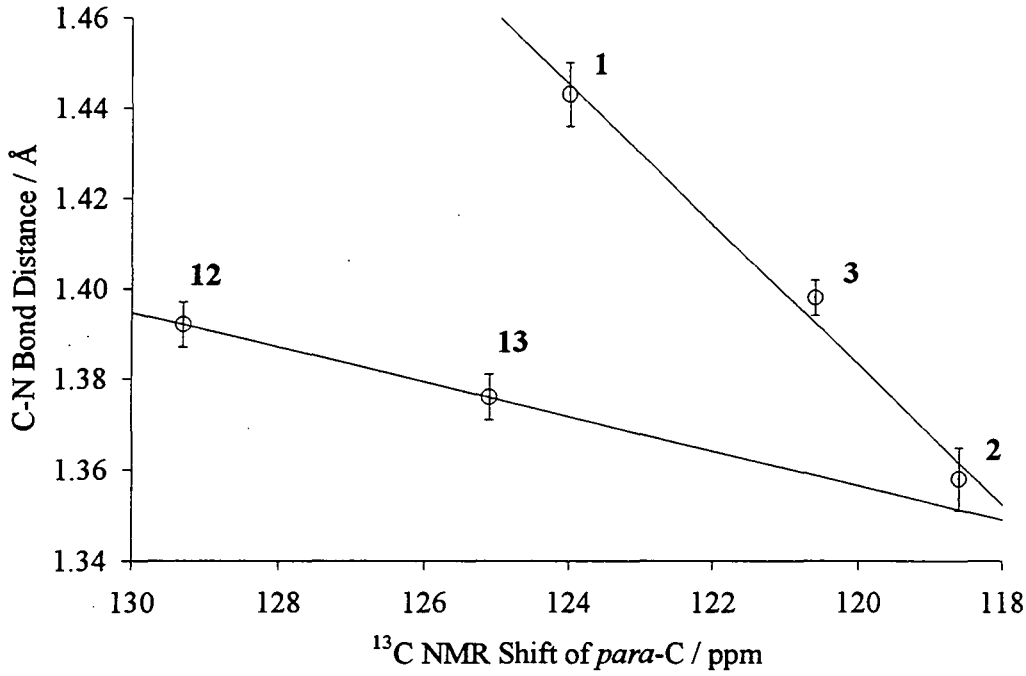

Figure 3.14 **Relationship between C-N bond distances and ^{13}C NMR shifts for N-substituted fluoromes compounds**

Compound	*o*-C	*p*-C	Solvent
Fmes-N=N-Ph	129.8	124.0	$CDCl_3$
Fmes-NHNH-Ph	116.6	120.6	$CDCl_3$
$FmesNH_2$	115.3	118.6	$CDCl_3$
8	125.6	125.5	$CDCl_3$
8	125.11	125.00	C_6D_6
11	126.6	129.3	$CDCl_3$
12	124.4	125.1	$CDCl_3$
13	125.5	126.7	$CDCl_3$
14	127.2	128.5	$CDCl_3$
16	†	116.9	C_6D_{12}
16	†	115.7	C_6D_6
18	118.9	121.4	C_6D_{12}
18	117.8	120.8	C_6D_6

Table 3.5 **^{13}C NMR shifts (ppm) for N substituted fluoromes compounds †This peak is not seen (see Section 3.4.5).**

This relationship between the ^{13}C NMR shift and C-N bond length can be used to assess the degree of both C-N and N-Mo π-bonding in compounds which have not been structurally characterised. For example the ^{13}C NMR shift of the *o*- and *p*-carbon atoms of dme adduct **13** are to slightly higher field than the pyridine adduct **12,** indicating slightly greater N-Mo π-bonding to compensate for the poorer oxygen donor ligand. The ^{13}C NMR shift of the tris phosphine complex **16** indicates a similar amount of N-C π-bonding as in the free aniline $FmesNH_2$, an observation consistent with the similar C-N bond lengths in $FtolNH_2$ and **15**.

This effect is similar to that previously noted for *tert*-butyl imido ligands where the difference in ^{13}C NMR shift for the α- and β-carbons gives an indication of the electron density on the imido nitrogen and hence the extent of N-Mo π-bonding.[25]

3.7 CONCLUSIONS

The π-acidity of CF_3 aryl groups established in Chapter Two is seen to influence the reactivity of systems containing such groups as imido ligands through a reduction of N-Mo π-bonding. This leads to a preference for higher coordination numbers to compensate for this, despite the resulting steric crowding.

Both the π-acidic aryl groups and metal centre compete for π-bonding from the nitrogen lone pair. This is reflected in the relationship between C_i-N and N-Mo bond distances which vary with the auxiliary ligands on the metal centre, and the consequent changes in electrophilicity, and hence demand from the metal for N-Mo π-bonding. Such changes are reflected in the ^{13}C NMR shift of the aryl rings which provide an indication of the extent of lone pair delocalisation onto the ring.

The ^{13}C NMR shifts of the aryl C atoms are seen to reflect the C-N distance as demonstrated in Section 3.6. Hence such ^{13}C NMR data give an indication of the degree of both C-N and N-Mo π-bonding.

3.8 REFERENCES

1 D.S. Williams, M.H. Schofield, J.T. Anhaus and R.R. Schrock, *J. Am. Chem. Soc.*, **1990**, *112*, 6728.

2 D.S. Williams, M.H. Schofield and R.R. Schrock, *Organometallics*, **1993**, *12*, 4560.

3 V.C. Gibson, *J. Chem. Soc. Dalton Trans.*, **1994**, 1607.

4 P.W. Dyer, V.C. Gibson, W. Clegg, *J. Chem. Soc., Dalton, Trans.*, **1995**, 3313.

5 R.R. Schrock, K.B. Yap, D.C. Yang, H. Sitzman, L.R. Sita and G.C. Bazan, *Macromolecules*, **1989**, *22*, 3191; R.R. Schrock, J.S. Murdzek, *Macromolecules*, **1987**, *20*, 2640; R.R. Schrock, W.J. Feast, V.C. Gibson, G. Bazan, E. Khosravi, *Polymer Commun*, **1989**, *30*, 258; R.R. Schrock, V.C. Gibson, G.C. Bazan, H.N. Cho, *Macromolecules*, **1991**, *24*, 4495.

6 H.H. Fox, K.B. Yap, J. Robbins, Shi'ang Cai, R.R. Schrock, *Inorg. Chem*, **1992**, *31*, 2287.

7 P.W. Dyer, V.C. Gibson, J.A.K. Howard, B. Whittle, C. Wilson, *J. Chem. Soc., Chem. Commun*, **1992**, 1666.

8 A. Bell, W. Clegg, P.W.Dyer, M.R.J. Elsegood, V.C. Gibson, E.L. Marshall, *J. Chem. Soc., Chem. Commun*, **1994**, 2247; V.C. Gibson, E.L. Marshall, *unpublished results*; P.W. Dyer, *PhD Thesis, Durham*, **1993.**

9 V.C. Gibson, E.L.Marshall, *unpublished work.*

10 M. Jolly, *PhD Thesis, Durham*, **1994.**

11 R.R. Schrock, J.S. Murdzek, G.C. Bazan, J. Robbins, M. DiMare and M. O'Regan, *J. Am. Chem. Soc.*, **1990**, *112*, 3875.

12 W.A. Nugent, *Inorg. Chem.*, **1983**, *22*, 965.

13 W.A. Nugent and R.L. Harlow, *Inorg. Chem.*, **1980**, *18*. 777.

14 N. Bryson, M.T. Youinou and J.A. Osborn, *Organometallics*, **1991**, *10*, 3389.

15 G. Schoettel, J. Kress and J.A. Osborn, *J. Chem. Soc., Chem. Commun.*, **1989**, 1062.

16 P.W. Dyer, V.C. Gibson and B. Whittle, Unpublished results.

17 J.H. Oskam, H.H. Fox, K.B. Yap, D.H. McConville, R O'Dell, B.J. Lichtenstein and R.R. Schrock, *J. Organomet. Chem*, **1993**, *459*, 185.

18 A.A. Danopoulus, Wa-Hung Leung, G. Wilkinson, B. Hussain-Bates and M.B. Hursthouse, *Polyhedron*, **1990**, *21*, 2625.

19 L.B. Kool, M.D. Rausch, H.G. Alt, M. Heberhold, U. Thewalt and B. Wolf, *Angew. Chem. Int. Ed. Engl.*, **1985**, *24*, 394.

20 L.B. Kool, M.D. Rausch, H.G. Alt, M. Heberhold, B. Honold and U. Thewalt, *J. Organomet. Chem.*, **1987**, *320*, 37; T. Takahashi, D.R. Swanson and E. Negishi, *Chem. Letters*, **1987**, 623.

21 V.C. Gibson and U. Siemeling, *J. Organomet. Chem.*, **1992**, *426*, C25.

22 P.W. Dyer, V.C. Gibson, J.A.K. Howard, B. Whittle, C. Wilson, *Polyhedron*, **1995**, *14*, 103.

23 J. Sandström, Dynamic NMR Spectroscopy, Academic Press, London, 1984

24 R.G. Abbot, F.A. Cotton, L.R. Falvello, *Inorg. Chem.*, **1990**, *29*, 514; C.J. Willis, *Coord. Chem. Rev.*, **1988**, *88*, 133.

25 W.A. Nugent, R.J. McKinney, R.V. Kasowski, F.A. Van Gartledge, *Inorg. Chim. Acta.*, **1982**, *L91*, 65.

Chapter Four

Icosahedral Carboranes as π-Acids

4.1 ELECTRON DEFICIENT CLUSTERS

The term "electron deficient" in this context is used to describe a situation in which there are too few electrons to allow the bonding to be described in terms of 2-centre 2-electron bonds (2c2e). The atoms in such compounds adopt a clustered structure to make the best use of the available electrons, with an electron pair being shared between more than two atoms, hence the term cluster.

The concept of a 3-centre 2-electron (3c2e) BHB bond was introduced by Longuet-Higgins[1] to rationalise the bridged structure of diborane. This concept was extended to 3c2e BBB bonds by Lipscomb[2] and used extensively to describe the bonding in a series of higher boranes in terms of 3c2e BHB and BBB and 2c2e BH and BB bonds.

The bonding in larger clusters such as $B_{12}H_{12}^{2-}$ can be described in terms of these localised bonds although there are often a large number of canonical forms.[3] The bonding is considered to be *delocalised* and is better described in term of molecular orbitals. Because each skeletal boron atom has attached to it one hydrogen atom, by an exo bond pointing radially outwards, the boron atoms are considered to be sp hybridised with one sp hybrid used for bonding *exo* to the cage, the remaining sp hybrid (radial to the cage, pointing inwards) and 2 p orbitals (tangential to the cage) being used for cluster bonding (Figure 4.1). In the case of boron one electron is used for *exo*-bonding and the remaining two for cluster bonding.

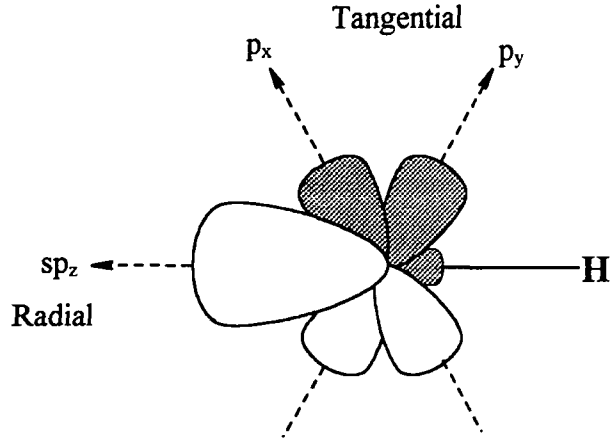

Figure 4.1 Tangential and radial orbitals of a BH cluster unit used for skeletal bonding

The structures of such compounds can be rationalised in terms of the number of electrons involved in skeletal bonding. The atoms of a cluster are considered to

occupy the vertices of a deltahedron (i.e. a polyhedron with triangular faces). The number of vertices of the deltahedron will be one less than the number of electron pairs contributing to cluster bonding[4]. This results in an electronic structure in which all the bonding levels are filled.

e.g. $B_{12}H_{12}^{2-}$

12 × BH units	= 12 × 2e⁻	= 24e⁻
Negative charge	= 2e⁻	= 2e⁻
Total skeletal electrons		= 26e⁻ ≡ 13 e⁻ pairs ⇒ 12 vertices

Hence $B_{12}H_{12}^{2-}$ has the structure of a 12 vertex deltahedron, an icosahedron, with all vertices being occupied. This argument was originally used the other way round to show that an icosahedral cluster would require 13 filled MO's.[5] A consequence of the dependence of structure on skeletal electron count is that if a vertex atom is removed, the structure will remain equivalent if *the electrons contributed by that vertex atom to cluster bonding remain associated with the cluster*. Hence $B_{11}H_{11}^{4-}$ and $B_{10}H_{10}^{6-}$, which can considered to be derived from $B_{12}H_{12}^{2-}$ by the removal of BH^{2+} units, both have 13 skeletal electron pairs and hence would have structures based on the icosahedron with one vertex and two vertices respectively (Figure 4.2). Clusters with all vertices occupied are termed *closo* (from the Greek meaning 'cage-like'), those with one vertex unoccupied *nido* ('net-like') and those with two unoccupied *arachno* ('web like').

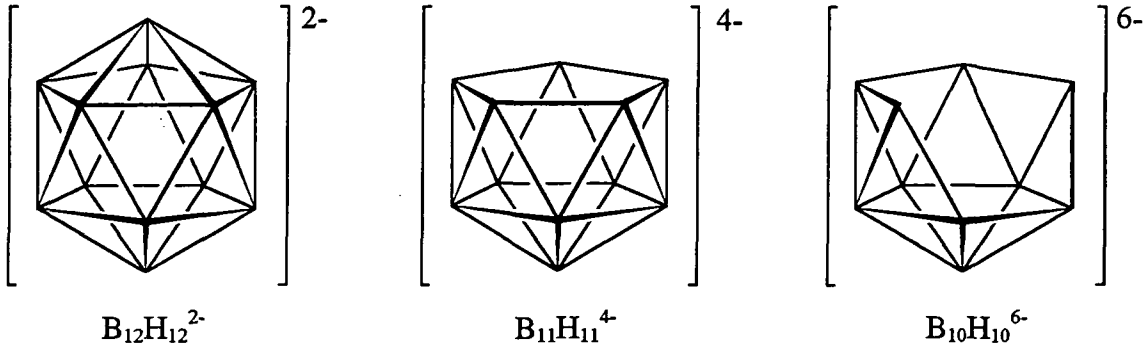

Figure 4.2 Structures of $B_{12}H_{12}^{2-}$, $B_{11}H_{11}^{4-}$, $B_{10}H_{10}^{6-}$

By a similar logic a vertex atom can be replaced by another atom providing that the number of atomic orbitals and skeletal electrons remains the same. A BH^- unit may be

replaced by an isolobal CH unit (or in general a CR unit) with retention of their icosahedral structure. Hence $C_2B_{10}H_{12}$ has a structure based on an icosahedron. Such clusters, known as carbaboranes or carboranes, are the subject of this chapter.

4.2 ICOSAHEDRAL CARBORANES

Carboranes were first reported in the 1950's during research into the potential of boranes as rocket fuels. Of these compounds one of the most extensively studied is the $C_2B_{10}H_{12}$ system (dicarbadodecaborane or "carborane").[6] This has three possible isomers, all of which have been prepared (Figure 4.3). These are known as the 1,2, 1,7 and 1,12 isomers referring to the position of the carbon atoms by the standard numbering scheme shown in Figure 4.4. These are commonly known as the *ortho*, *meta* and *para* isomers. A simplified representation used in this thesis is shown in Figure 4.5. In the remainder of this thesis the term carborane is used to refer to the *ortho* isomer and the abbreviation XCbY to refer to 1-X-2-Y-1,2-$C_2B_{10}H_{10}$. The solid lines shown in such diagrams are not intended to represent bonding in the cluster but merely indicate the overall shape and connectivities.

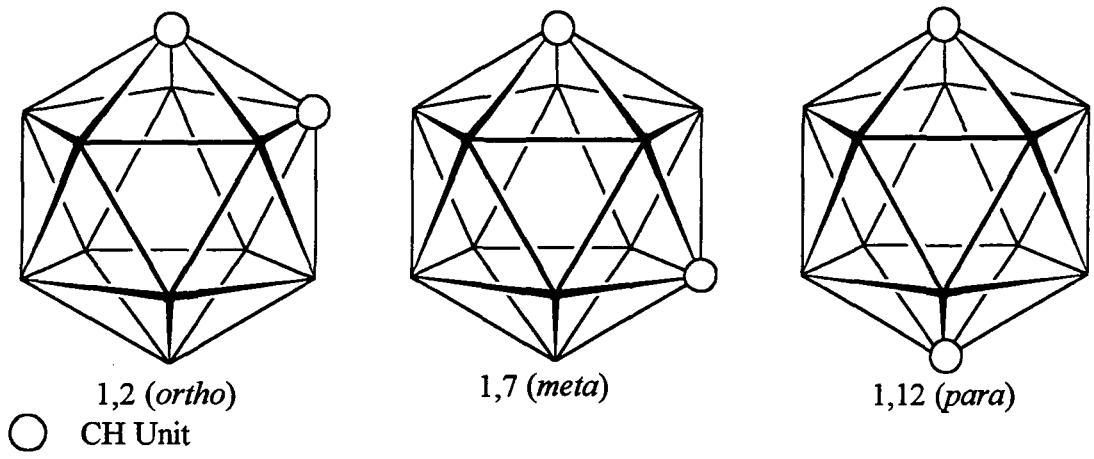

Figure 4.3 Isomers of $C_2B_{10}H_{12}$

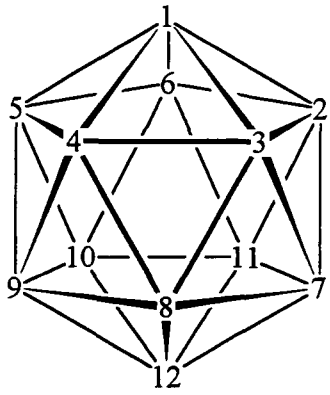

Figure 4.4 Standard Numbering Scheme

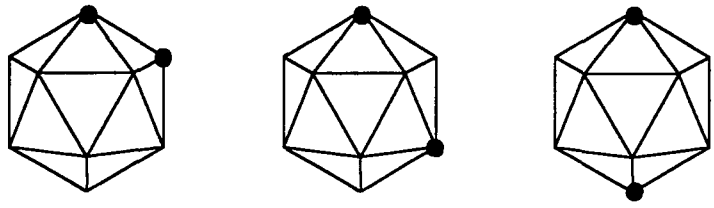

Figure 4.5 Simplified representations of *ortho* , *meta* and *para* isomers

The *ortho*-isomer is synthesised directly by the reaction of acetylene with Lewis base adducts of decaborane ($B_{10}H_{12}$·2L). The *meta*- and *para*-isomers are synthesised from the *ortho*-isomer by thermal isomerisation (460°C and 620°C) respectively.[7] The formation of the *para*-isomer is accompanied by a large degree of decomposition, resulting in the much higher cost of this isomer. This isomerisation occurs due to a tendency for similarly charged atoms to adopt positions with the greatest separation to minimise the overall dipole[8], the *para*-isomer being of lower energy than the *meta*-isomer, which in turn is lower in energy than the *ortho*-isomer

The chemistry of these compounds is similar in many respects to that of organic aromatic compounds and the term "pseudo-aromatic" is often applied to them. Unlike the smaller boranes these clusters are stable to both oxygen and moisture and extremely stable to heat which has led to their commercial use in high temperature polymers. The *ortho*-isomer has received the greatest attention and a large number of compounds substituted at both C and B atoms are known. Such substituents can interact with the cage in a manner similar to that observed in aromatic compounds (see examples in Chapter Two) with delocalisation of electrons from electron-rich

substituents onto the electron deficient cage. This chapter focuses on *ortho*-carboranes bearing π-donor substituents on a carbon atom and the formation of dative π-bonds between the cage and substituents.

4.3 Synthesis of Icosahedral Ortho-*Carboranes*

Ortho-carborane is formed by the reaction of acetylene with Lewis base adducts of decaborane, $B_{10}H_{10}L_2$. The use of substituted acetylenes RCCR' leads to the formation of substituted carboranes although the number of substituents which are possible is limited to those that will tolerate the conditions of the reaction (Equation 4.1).

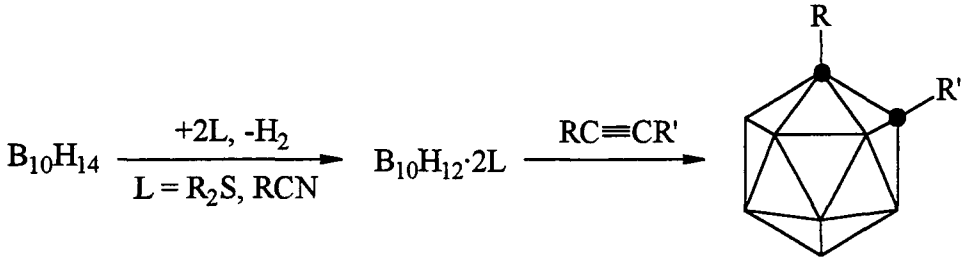

Equation 4.1

1-Phenyl-1,2-dicarbadodecaborane (phenyl-*ortho*-carborane or PhCbH) can be synthesised in this manner from phenylacetylene.[9] 1-Methyl-1,2-dicarbadodecaborane (methyl-*ortho*-carborane or MeCbH) is formed by a modified method which avoids the use of gaseous propyne. The reaction of propargylbromide (3-bromo-propyne) with $B_{10}H_{12}$·2L gives 1-CH_2Br-*ortho*-carborane which is treated with magnesium to produce 1-Br$MgCH_2$-*ortho*-carborane which isomerises to MeCbMgBr, hydrolysis of which gives the desired MeCbH.[10]

Substituents can be attached directly onto the preformed cage and such a strategy is necessary where the corresponding acetylene would either react with decaborane or result in poor yields. The lithio derivative of the cage is most commonly used in such substitutions although magnesium derivatives have been used and copper derivatives are required in some cases. Several examples of such reactions are shown in Scheme 4.1. Many other examples are evident throughout this chapter. Such strategies rely on the acidity of the hydrogen on the cage carbon atoms arising from the electron-

withdrawing effect of the cage. Treatment with n-butyl lithium removes this acidic proton to yield the lithio-carborane.[11]

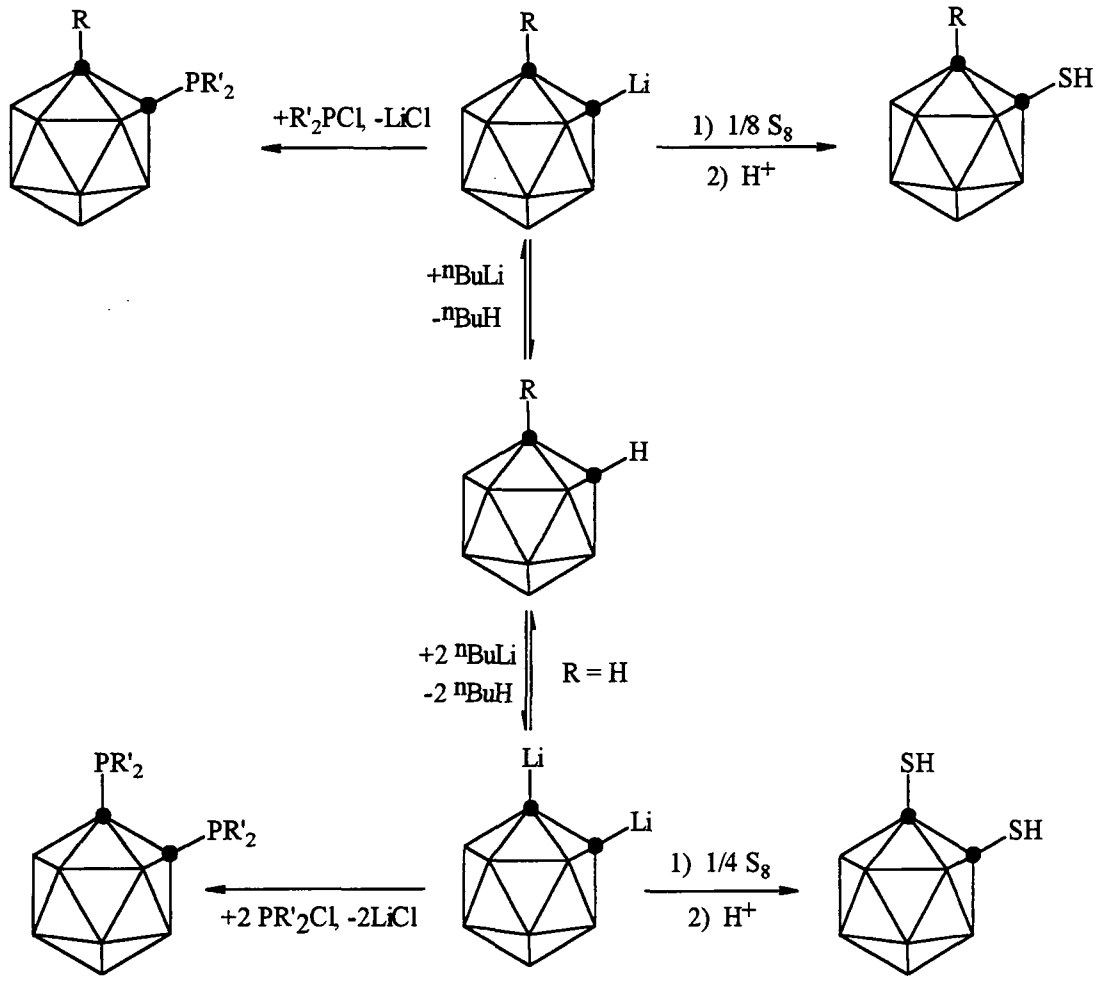

Scheme 4.1 Examples of substitution of carborane cages

Unless substitution at both carbon atoms is desired it is usual to employ a carborane with a substituent on the other carbon (e.g. phenyl or methyl) as this prevents unwanted disubstitution of the cage. TBDMS (^{t}BuMe$_2$Si) groups are sometimes used as a protecting group to prevent disubstitution.[12] They can then be removed easily to allow further substitution at the other carbon atom.

The presence of a substituent on both carbon atoms is also advantageous for the characterisation of such compounds by X-ray diffraction. Both boron and carbon have a similar number of electrons causing them to diffract X-rays in a similar manner and resulting in difficulty in distinguishing between BH and CH environments, although this is sometimes possible. The presence of a substituent on both carbon atoms avoids

such problems. Recent work has determined the structures of the parent unsubstituted *ortho-* *meta-* and *para*-carboranes by co-crystallisation with HMPA (hexamethylphosphoramide). This results in hydrogen bonding interactions between the O of HMPA and the cage CH thus preventing disorder and allowing the C atoms to be identified.[13]

4.4 Boron Nuclear Magnetic Resonance

Boron has two common isotopes, ^{11}B and ^{10}B. Both are suitable for NMR spectroscopy having nuclear spins of I = 3/2 and 3 respectively. ^{11}B is most commonly used as it has the higher natural abundance (79.7%), higher receptivity, narrower line widths and shorter relaxation times. A variety of NMR techniques are possible. $^{11}B\{^1H\}$ and $^{11}B[^1H]$ reveal the number of equivalent positions and the number of H atoms on the B. ^{11}B COSY experiments reveal which B atoms are magnetically coupled and hence which are directly bonded. For an *ortho*-carborane with different substituents on the two C atoms and only H's on B atoms 6 peaks should be seen, 2 of intensity equivalent to 1B (B9 and B12) and 4 equivalent to 2B (B4, 5; B3, 6; B8, 10; B7, 11), these pairs of atoms being related by symmetry. If both C atoms bear the same substituent the number of peaks is reduced to 4, 3 equivalent to 2B (3, 6; 8, 10; 9, 12) and 1 equivalent to 4B (4, 5, 7, 11).

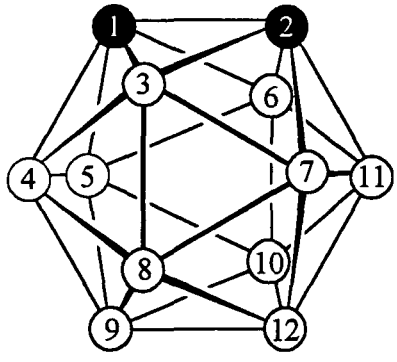

Figure 4.6 Numbering scheme for *ortho*-carborane, viewed to show equivalent boron sites. Carbon atoms shown in black

The ^1H NMR resonances of the BH protons are broadened due to coupling to the quadupolar B atoms and consequently are observed as a single extremely broad resonance amongst which individual peaks cannot be distinguished. A $^1H\{^{11}B\}$ experiment can be performed to remove this coupling to allow the observation of these

protons. A ^{1}H-^{11}B HETCOR experiment is also possible which reveals which H and B atoms are directly bonded.

Using these techniques it is possible to assign ^{11}B and ^{1}H resonances with a high degree of certainty. However, it is rarely possible to make a completely unambiguous assignment of the resonances. For example, it may be possible to assign a peak to one of the pairs of atoms adjacent to only one C atom, i.e. B4, 5 or B7, 11, but impossible to assign the peak to a particular pair. The same problem arises for B9 and B12. B8 and B10 can be distinguished without ambiguity as they are the only atoms bonded to all other types of B atom. Likewise B3 and B6 are the only atoms not bonded to either B9 or B12. Further complications arise if peaks overlap which is not uncommon.

^{11}B NMR shifts have proved notoriously difficult to predict and rationalise.[14] Despite this a number of trends have been identified. Of these the "Antipodal Effect" is of the greatest magnitude. This relates to the effect of a substituent atom or cluster atom on the NMR chemical shift of the atom *directly opposite*, the so called *antipodal* atom.

For a series of carboranes in which only the substituent varies it has been shown that it is the electron donor capacity of the substituent which determines the magnitude of the antipodal shift. This has been attributed to an increase in electron density at the antipodal position and the resultant increase in nuclear shielding. This is often compared to the "Mesomeric Effect" observed with aromatic compounds.[15]

This increase in electron density suggested by the ^{11}B NMR is not reflected in chemical reactivity. This has been rationalised by considering the tangential and radial p-orbitals separately. An increase in electron density in the tangential orbitals leads to increased nuclear shielding and a shift to lower frequency. These tangential orbitals are thus known as "NMR active" and do not appear to determine the chemical reactivity which depends on the electron density in the radial orbitals ("chemically active").[16]

4.5 EXO-π-BONDING IN ICOSAHEDRAL CARBORANES

Previous work has shown that multiple bonds can form between the carborane cage and substituents. This leads to dramatic changes in cluster bonding. Deprotonation of PhCbOH with "proton sponge" (PS, 1,8-N,N,N',N'-tetramethylnapthalenediamine) leads to the formation of the anion $PhCbO^-$ (Figure 4.7).[17]

The crystal structure of this anion reveals a short C-O distance, which at 1.25Å corresponds to a partial C-O double bond (~1.20Å). Consistent with this is the C-O stretching frequency in the IR spectrum which at 1460 cm^{-1} is intermediate between that for a single C-O bond (~1200 cm-1) and a double C=O bond (~1700 cm^{-1}). This can be rationalised in terms of delocalisation of the negative charge, formally on the oxygen atom, onto the electron deficient cage to form a dative π-bond. The actual structure is closer to structure B shown in Figure 4.7 than structure A.

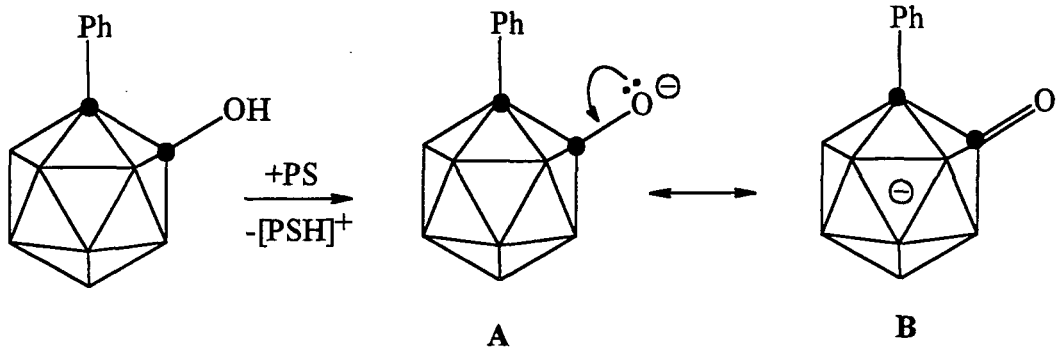

Figure 4.7 Deprotonation of PhCbOH

Also observed is a lengthening of the C-C cluster bond from 1.64Å in PhCbH to 2.00Å. This can be explained by a consideration of the number of skeletal electrons. Delocalisation of the lone pair increases this skeletal electron count from 13 pairs in the parent compound to formally 14 pairs. This will cause the cluster to tend towards a *nido* residue of a docasahedrom (13 vertex cluster). As more electronegative atoms tend to be situated at positions of lower connectivities (i.e. electron rich environments) the two C cluster atoms will be situated at the edge of this newly forming open face. As previously mentioned the lowest energy state will occur when the C atoms are separated as much as possible and so these atoms will move apart as the new face forms (Figure 4.8). This has been reproduced experimentally[18] by reduction of *ortho-*

carborane with sodium napthalide to give $Na_2C_2B_{10}H_{12}$. Although the structure of this is not known, several examples of such 13 vertex clusters are known with a transition metal occupying a vertex and providing 2 electrons to cluster bonding (e.g. $CpCoC_2B_{10}H_{12}$, Figure 4.9).[19] Interestingly the carbon atoms do not occupy positions directly opposite one another , the lowest energy structure, but are separated by only one boron atom.

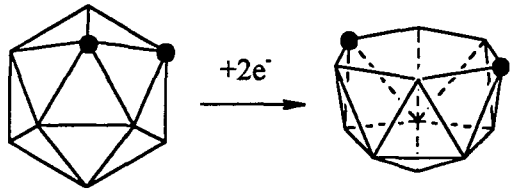

Figure 4.8 Expansion from 12 vertex *closo*-cluster to 13 vertex *nido*-cluster

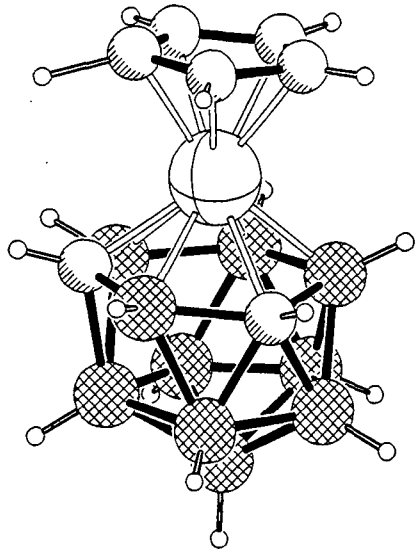

Figure 4.9 Molecular structure of $CpCoC_2B_{10}H_{12}$

The same effect has been noted in a compound with two carborane cages joined by a bond between two of the cage carbon atoms. The reduction of "bis-carborane" (1-1'-bi-*ortho*-carborane $(C_2B_{10}H_{11})_2$) with sodium napthalide gave an anion in which the cages had opened up to give a C-C bond length of 2.41Å and a short C-C bond of 1.38Å between the two carbon atoms indicating multiple bond character (Figure 4.10).[20]

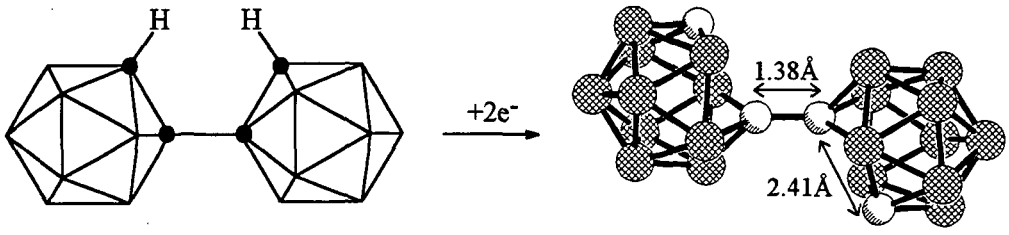

Figure 4.10 Reduction of biscarborane

This can also be rationalised by a consideration of the molecular orbitals. In the anion $PhCbO^-$ the C=O unit can be considered as a ligand to the open face of a $CPhB_{10}H_{10}^-$ *nido* residue. The frontier orbitals for a $CB_{10}H_{11}^-$ fragment have been determined[21] (Figure 4.11), for clarity only the open face of the cluster is shown. Labels for orbitals are derived from those in the $B_{11}H_{11}^{2-}$ fragment in which the $5e_1(x)$ and $5e_1(y)$ are degenerate. The presence of the C atom in this open face lowers the energy of the $5e_1(x)$ in which it is involved due to a higher electronegativity. These orbitals consisting of the tangential p-orbitals are reminiscent of those for the cyclopentadienyl ligand. They are, however, different in that they are non-degenerate and are angled inwards.

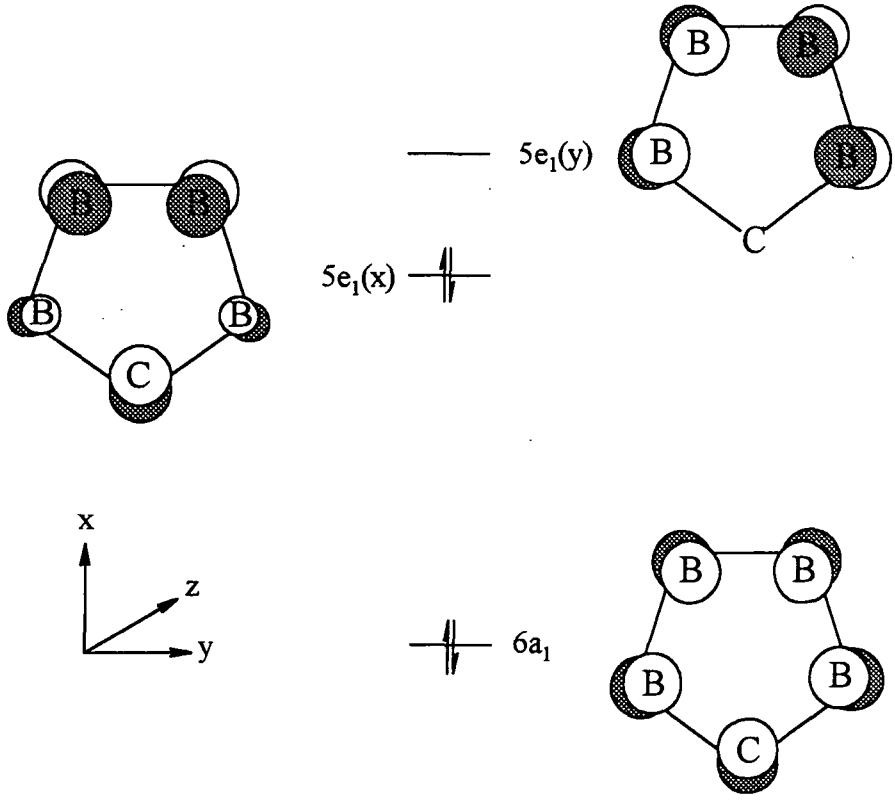

Figure 4.11 Frontier orbitals for $CRB_{10}H_{10}^-$ involved in bonding to the C atom itself involved in *exo* π-bonding

Now consider an sp hybridised C atom capping this open face. The sp hybrid pointing inwards is of correct symmetry for a σ-interaction with the "$6a_1$" cluster orbital. The p_x and p_y orbitals on C are of correct symmetry for a π-interaction with the $5e_1(x)$ and $5e_1(y)$ respectively (Figure 4.12).

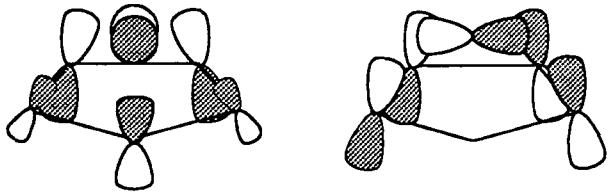

Figure 4.12 Interaction between cage and tangential orbitals

Because the $5e_1(x)$ is lower in energy the greatest interaction will be between the $5e_1(x)$ and p_x and the energy of the resulting $5e_1(x)$-p_x orbital will be lower in energy than the 5e1(y)-p_y orbital (Figure 4.13).

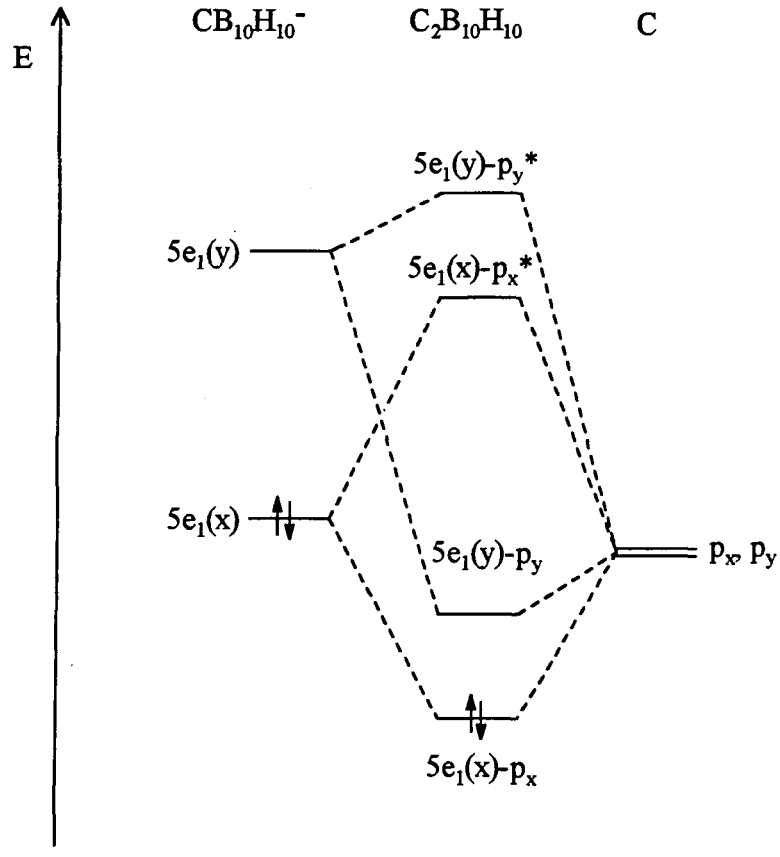

Figure 4.13 Interaction diagram for $RCB_{10}H_{10}^-$ and C (only MO's involved in the formation of the π-bond are shown). Arbitrary vertical scale (energy)

Now consider an oxygen atom bonding to this $RC_2B_{10}H_{10}^-$ fragment, we shall consider this to be sp hybridised although the arguments here remain unchanged if other hybridisation states are considered. The formation of the π-bond between O and C will involve the tangential p-orbitals on O and the $5e_1(x)$-p_x and 5e1(y)-p_y on the cluster. As this O-p_x orbital is closer in energy to the $5e_1(x)$-p_x than the O-p_y is to the 5e1(y)-p_y the major contribution to cluster-O π-bonding involves the p_x orbital on the O substituent (Figure 4.14).

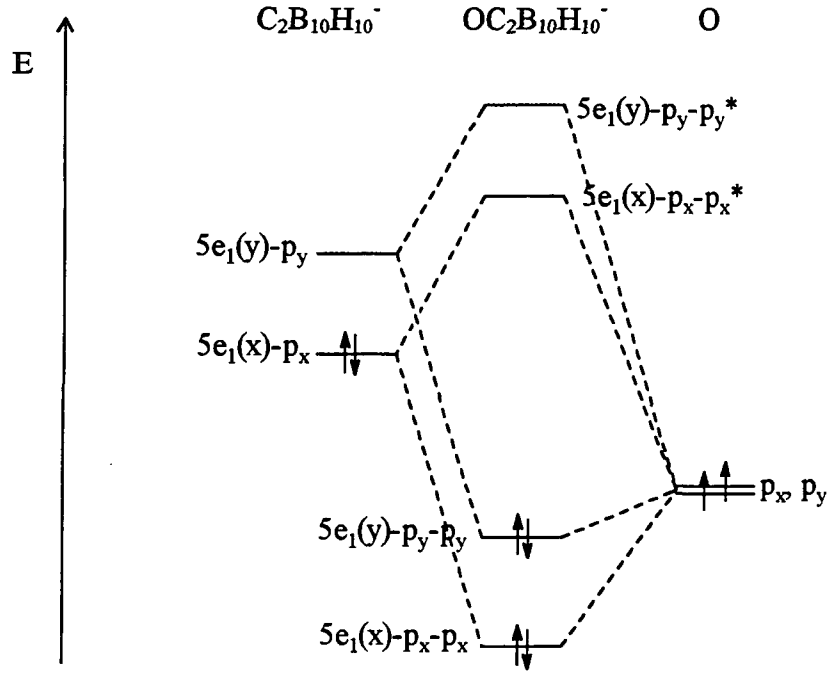

Figure 4.14 Interaction diagram for $RC_2B_{10}H_{10}^-$ and O

Both the $5e_1(x)$ and $5e_1(y)$ become incorporated into the occupied levels. Some of the $5e_1(x)$-p_x combination is incorporated into an unoccupied level. Hence cluster bonding loses some $5e_1(x)$-p_x character, bonding with respect to the two C cluster atoms, and gains some $5e_1(y)$-p_y character, non-bonding with respect to the two C cluster atoms. Bonding between the C cluster atoms is weakened resulting in the lengthening observed in the anion $PhCbO^-$. Clearly the greater the interaction between the lone pair and the cage the greater this effect will be. This can be viewed in an alternative manner. The greater the interaction of the C-p_x in *exo* bonding the less it can contribute to cluster bonding and hence the C-p_y will become increasingly involved, leading to the lengthening of the C-C bond.

Similar observations have been made for compounds bearing sulphur substituents with both the $PhCbS^-$ [22] and CbS_2H^- [23] anions showing shortened C-S distances and lengthened C-C cluster bonds.

Similar exo π-bonding effects have also been reported for metallaboranes substituted at a boron atom. In the cluster 1-Cp-4-(NEt_2)-1-$RhB_{10}H_9$ the N atom bonded to a cluster boron atom shows a planar conformation and short B-N bond (1.43Å) indicative of B-

N π-bonding. NMR studies also show restricted rotation about the B-N bond. A lengthening of the Rh-B bond is also observed.[24]

This chapter investigates these effects further in compounds with π-donor substituents on one of the carbon atoms of an *ortho*-carborane cage.

4.6 Nitrogen Substituted Carboranes

4.6.1 Introduction

This section describes the synthesis and structural characterisation of both novel and previously reported *ortho*-carboranes bearing a nitrogen substituent on one carbon atom (C1) and either a methyl or phenyl group on the other (C2). These compounds reveal similar exo-π-bonding to the previously mentioned anions despite the fact that many are neutral. However, the variety of the substituents (Figure 4.15) gives further information on orientational preferences and other factors which influence this *exo*-π-bonding. Sections 4.6.2 to 4.6.7 detail the synthesis of these compounds while Sections 4.6.8 to 4.6.12 discuss the trends observed in these compounds.

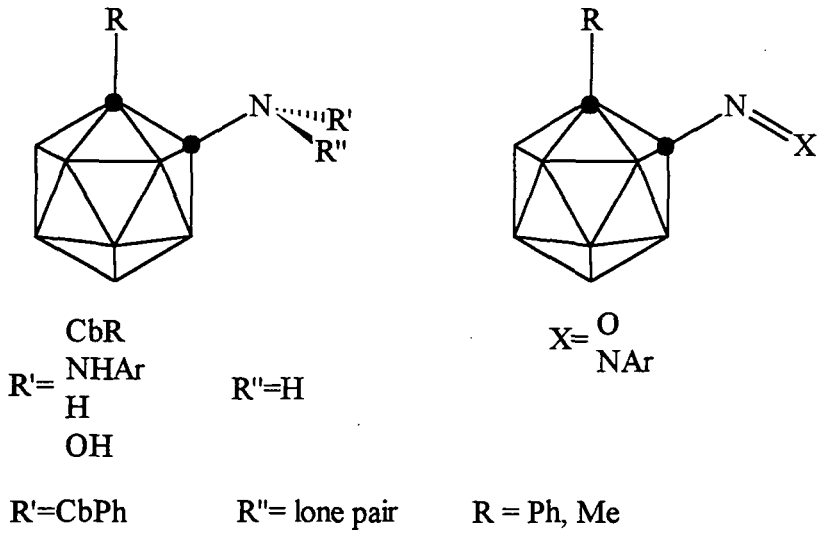

Figure 4.15 Compounds described in this chapter

4.6.2 Reaction of Lithio-Carboranes with Nitrosyl Chloride

There are several reports in the literature regarding the reaction of lithio-carboranes with nitrosyl chloride (NOCl).[25] These reports reveal the formation of either nitroso-carboranes RCbNO or dicarboranyl amines $(RCb)_2NH$ (Scheme 4.2) although no reports mention the isolation of both from a single reaction.

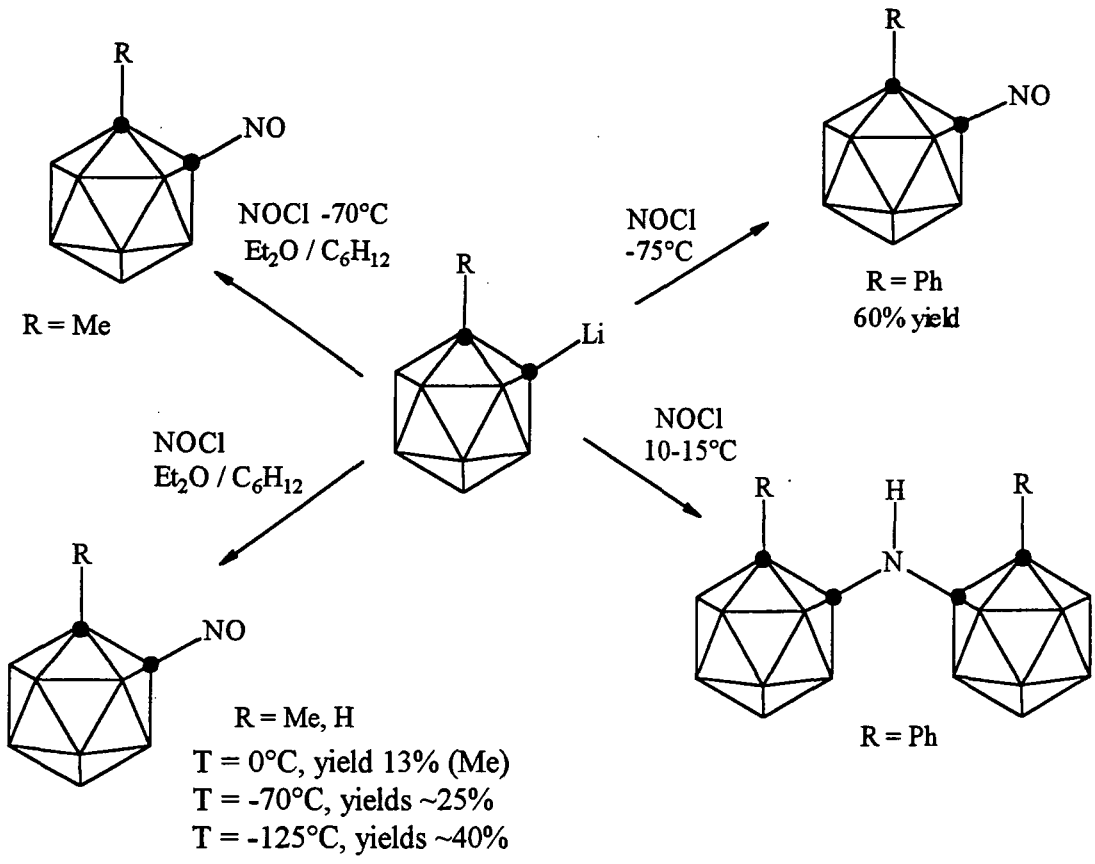

Scheme 4.2 Reaction of lithio-carboranes with NOCl

Recent work[26] has shown that the reaction between PhCbLi and NOCl yields $(PhCb)_2NH$ at -40°C in Et_2O/dme. When the reaction was carried out at -78°C small amounts of PhCbNO were also isolated. The crystal structures of $(PhCb)_2NH$ and the corresponding anion $(PhCb)_2N^-$ have been determined[26] and reveal substantial C-N multiple bonding which is greater in the anion. The orientations found in these compounds confirm previous assumptions about orbital interactions in the anion $PhCbO^-$ and are discussed further in section 4.6.8.

It appears that the yields of the nitroso compounds are greater at lower reaction temperatures, higher temperatures yielding the dicarboranyl amines. The use of dme as a solvent also appears to favour the formation of the dicarboranyl amines. On the basis of these observations a mechanism has been proposed (Scheme 4.3).[26]

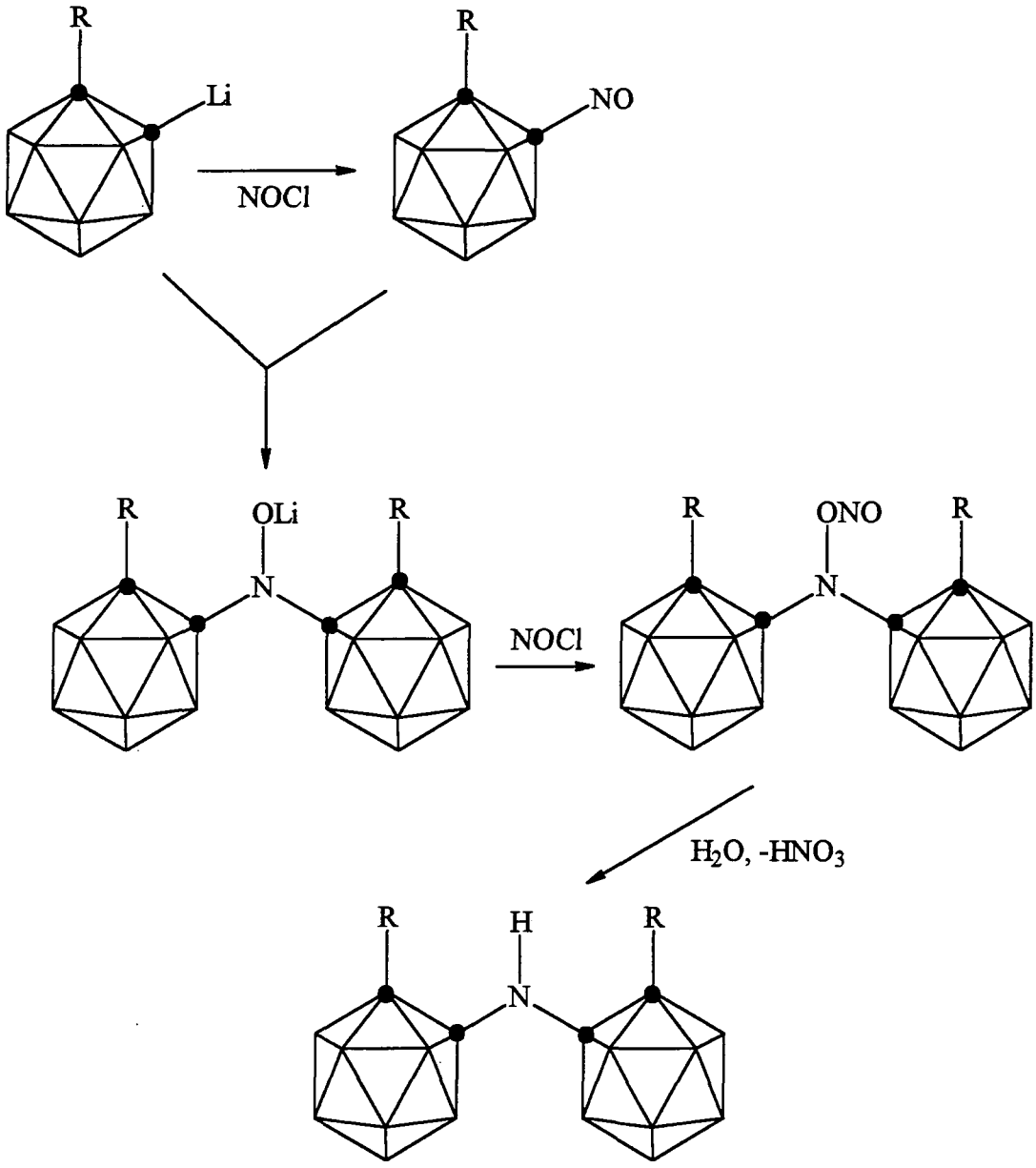

Scheme 4.3 Mechanism for the formation of dicarboranyl amines

4.6.2.1 Synthesis of Dicarboranyl Amines and Nitroso-Carboranes

A series of reactions was undertaken to investigate the reaction of both MeCbLi and PhCbLi with NOCl under a variety of conditions. The general procedure involved the addition of a solution of the appropriate lithio-carborane to an excess of NOCl in solution at the required temperature over a period of 30 mins. In all cases the solution immediately became dark green. After a basic work up the volatile nitroso compounds were easily separated from the involatile amines by sublimation.

The products obtained and corresponding yields are given in Table 4.1. In many cases both the nitroso compound and corresponding amine were isolated from the same reaction. The reactions with no dme present yielded mainly the nitroso carboranes PhCbNO **20** and MeCbNO **21** although in most cases small amounts of the corresponding amine $(PhCb)_2NH$ **22** or $(MeCb)_2NH$ **23** were also isolated. The presence of dme resulted in the formation ultimately of only the amines **22** and **23** although a green colour was observed during the reaction indicating that the nitroso compounds were formed initially. In contrast to previous reports the temperature at which the reaction was carried out appears to have little effect on the products obtained, the main factor being the reaction solvent.

Substituent R		Phenyl		Methyl	
Solvent	Temp. °C	Nitroso **20**	Amine **22**	Nitroso **21**	Amine **23**
dme/Et_2O	-40	0	55	0	65
C_5H_{12}/Et_2O	-40	61	10	69	11
C_5H_{12}/Et_2O	-117	42	0	77	22

Table 4.1 % Yields for reaction of RCbLi with NOCl

The isolation of both the amines and nitroso compounds from one reaction is consistent with the proposed mechanism. The relative yields will be determined by the relative rates of reaction of RCbLi with both NOCl and RCbNO. The reaction involving two molecules of RCbLi to form the amine is favoured by the presence of the bidentate dme which may stabilise dimeric or more highly associated lithium complexes in solution.

*4.6.2.2 Molecular Structure of Bis-(2-methyl)-1-*orthocarboranylamine

Crystals of $(MeCb)_2NH$ **23** were obtained by slowly cooling a solution in hexane from 60°C to room temperature. These proved to be suitable for structural characterisation by X-ray diffraction and the structure was solved by Prof. W. Clegg of Newcastle University. The molecular structure is shown in Figure 4.16 and selected bond lengths and angles in Table 4.2.

The two cages display small differences in bond lengths and angles for equivalent atoms, differences which arise from crystal packing effects. There is a non-

crystallographic two-fold rotation axis through the N-H bond. The conformation adopted in the crystal is equivalent to that found in both $(PhCb)_2NH$ **22** and its anion $(PhCb)_2NK^+$·18-C-6 **24** formed by the deprotonation of **22** with KO^tBu (Figure 4.17). The bonds around the nitrogen atom are found to be coplanar, this plane being perpendicular to that containing the N and C cluster atoms. This implies sp^2 hybridisation of the N atom, the lone pair in a p-orbital being in the plane of the C-C cluster bond and N atom.

Whilst the C-N bond distances in amines **22** and **23** are comparable, the C-C distance in **22** is longer by 0.05Å. This can be attributed to a combination of the greater steric bulk of the phenyl group and to π-donation from the phenyl group to the cage.

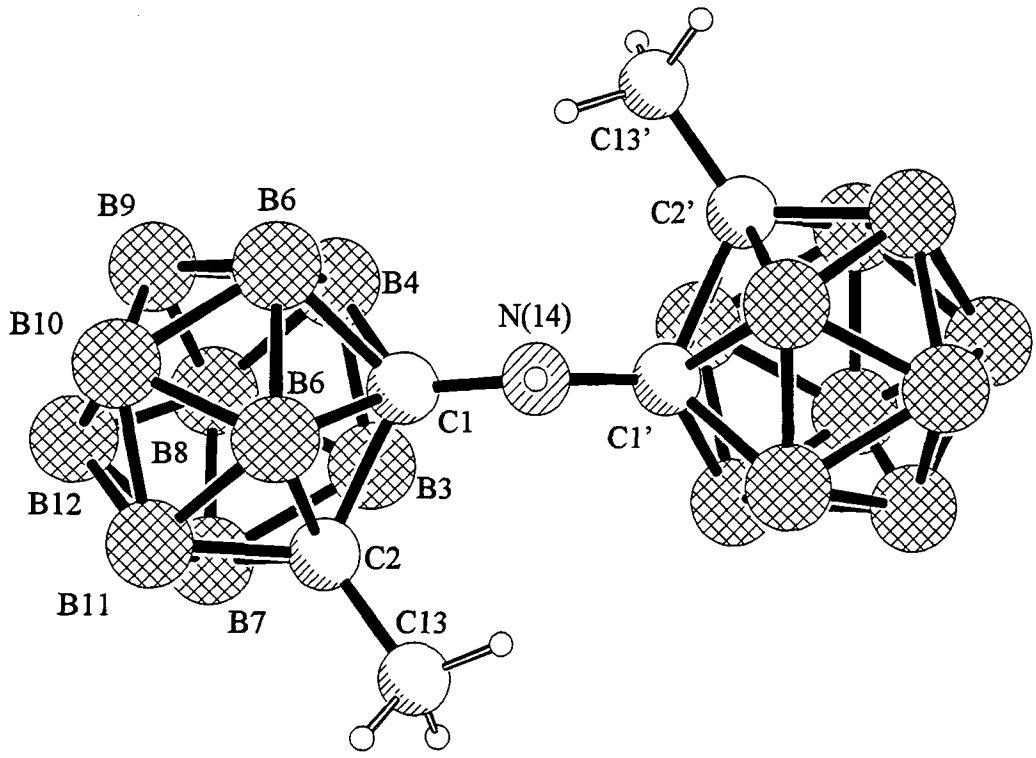

Figure 4.16 **Conformation of $(MeCb)_2NH$ 23 (BH's omitted for clarity, viewed down NH bond)**

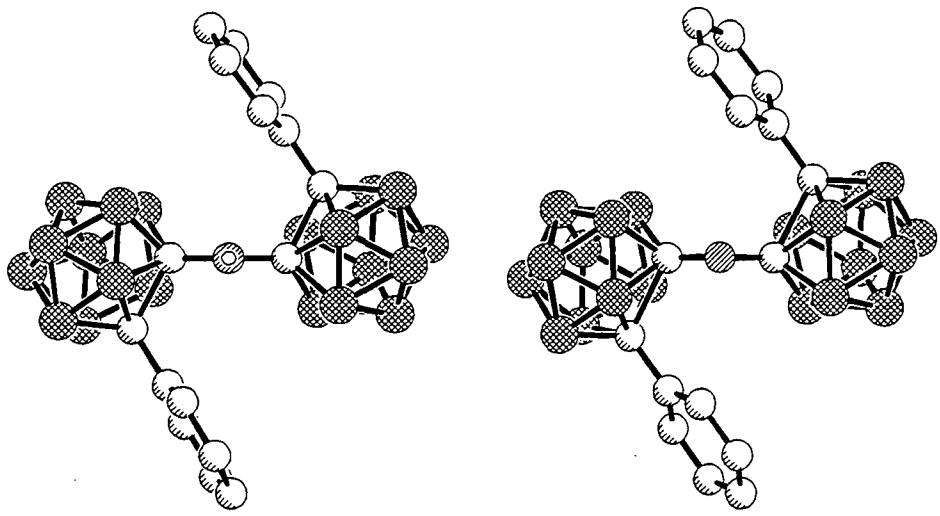

Figure 4.17 **Conformations of $(PhCb)_2NH$ 22 and $[(PhCb)_2N]^-$ 24 (ref. 26. BH's and CH's omitted for clarity, same numbering scheme as 23)**

Atoms	$(MeCb)_2NH$ **23**	$(PhCb)_2NH$ **22**	$(PhCb)_2N^-$ **24**
C1-N14	1.410(4)	1.405(2)	1.350(4)
C1-C2	1.750(4)	1.798(3)	1.987(3)
C2-C13	1.512(4)	1.504(3)	1.491(4)
C1-B3	1.719(4)	1.714(3)	1.786(4)
C1-B4	1.696(2)	1.697(3)	1.685(5)
C1-B5	1.704(3)	1.704(3)	1.677(5)
C1-B6	1.716(2)	1.740(3)	1.788(4)
C2-B3	1.724(4)	1.736(3)	1.736(3)
B3-B4	1.794(5)	1.792(3)	1.792(3)
B4-B5	1.778(5)	1.779(3)	1.779(3)
B5-B6	1.788(5)	1.782(3)	1.782(3)
C2-B6	1.725(4)	1.721(3)	1.721(3)
C1-N14-C1'	131.1(2)	132.0(2)	127.0(2)
N14-C1-C2	117.2(2)	117.09(14)	118.8(2)
N14-C1-B3	123.3(2)	124.15(15)	127.9(3)
N14-C1-B4	127.4(2)	127.8(2)	132.7(2)
N14-C1-B5	119.1(2)	118.5(2)	120.4(2)
N14-C1-B6	111.1(2)	110.85(14)	111.3(2)
C13-C2-C1	117.0(2)	117.94(14)	116.7(2)
C13-C2-B3	117.4(2)	115.99(15)	115.0(3)
C13-C2-B7	122.9(2)	122.3(2)	122.4(2)
C13-C2-B11	122.2(2)	123.9(2)	125.3(2)
C13-C2-B6	116.8(2)	119.6(2)	120.1(3)

Table 4.2 Selected bond lengths and angles for $(MeCb)_2NH$ 23, $(PhCb)_2NH$ 22 and $[(PhCb)_2N]^-$ 24 (averages for equivalent bonds)

*4.6.2.3 Molecular Structure of 1-Nitroso-2-Phenyl-*Orthocarborane

Crystals of PhCbNO **20** were obtained by sublimation (40°C, 0.001 mbar) onto a water cooled probe. These crystals proved suitable for an X-ray diffraction structural study and the structure was solved by Prof. W. Clegg and Dr M.R.J. Elsegood of Newcastle University. The molecular structure is shown in Figure 4.18 and selected bond lengths and angles given in Table 4.3. Although crystals of MeCbNO were obtained in a similar manner they were too soft to be removed from the surface of the probe.

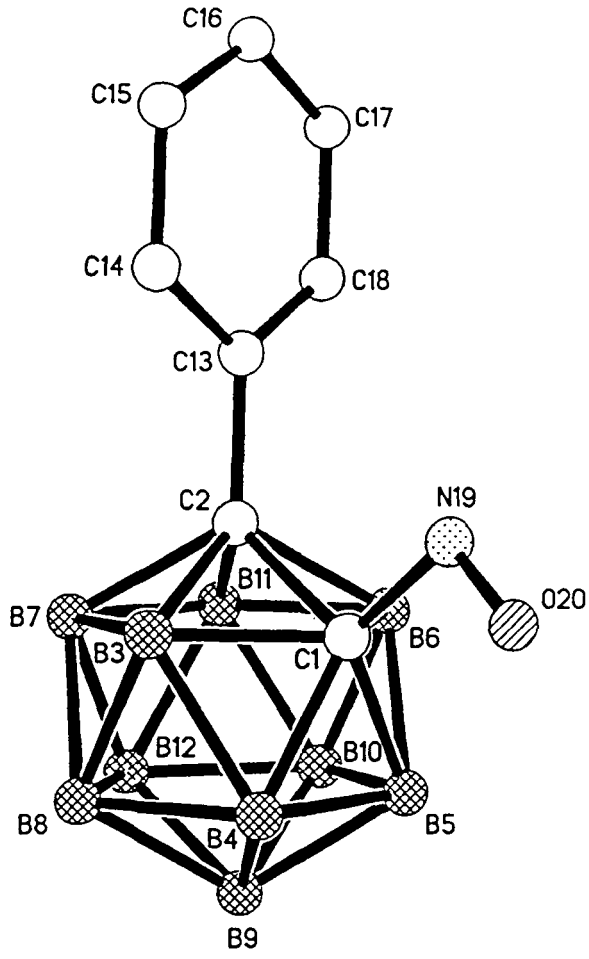

Figure 4.18 Molecular Structure of PhCbNO 20

Atoms	Bond Length / Å	Atoms	Bond Angle / °
C-N	1.490(2)	C1-N-O	113.0(2)
N-O	1.182(2)		
		N-C1-C2	112.14(12)
C1-C2	1.677(2)	N-C1-B3	114.65(13)
C2-C13	1.510(2)	N-C1-B4	123.99(13)
C1-B3	1.704(2)	N-C1-B5	123.49(13)
C1-B4	1.702(2)	N-C1-B6	114.14(13)
C1-B5	1.704(2)		
C1-B6	1.708(2)	C13-C2-C1	120.32(12)
C2-B3	1.743(2)	C13-C2-B3	118.70(13)
B3-B4	1.785(2)	C13-C2-B7	121.66(13)
B4-B5	1.779(3)	C13-C2-B11	121.08(13)
B5-B6	1.787(3)	C13-C2-B6	117.21(12)
C2-B6	1.738(2)		

Table 4.3 Selected bond lengths and angles for PhCbNO 20

The N=O bond lies approximately parallel to the C-C cluster bond and the plane of the phenyl ring lies perpendicular to this. The C-N bond length of 1.490(2) Å long is comparable to that in azoalkanes of 1.493 Å but longer than that in nitrosobenzenes (~1.21 - 1.45Å). The C-C cluster bond at 1.677(2)Å is relatively unperturbed, being only slightly lengthened from that in PhCbH of 1.640(5) and shorter than that in PhCbMe of 1.696(5)Å. The C1-N-O bond angle is comparable to that in aryl nitroso compounds of ~113°. This implies that the NO is acting as a one electron ligand to the cage, and not a three electron ligand as found in many metal complexes.[27]

4.6.3 AZO-CARBORANES

The reaction of lithio-carboranes with PhN_2BF_4 is reported to give azocarboranes RCbN=NPh in good yields.[28] This was carried out with MeCbLi to give MeCbN=NPh **25** in good yield (Equation 4.2) as a yellow crystalline solid.

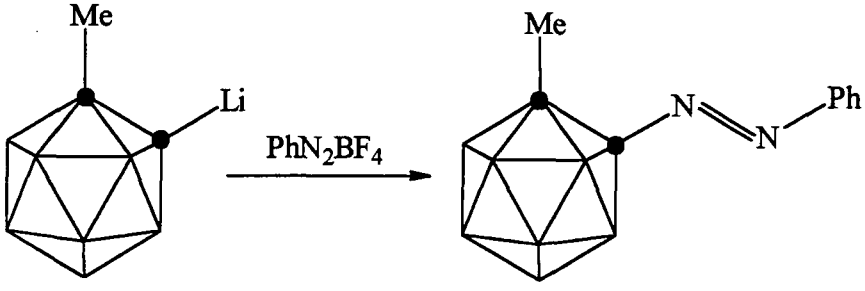

Equation 4.2

The structure of the related compound $PhCbN_2Tol$ **26** (Tol = 4-MeC_6H_4) is known[29] and is shown in Figure 4.19. Selected bond lengths and angles are given in Table 4.4.

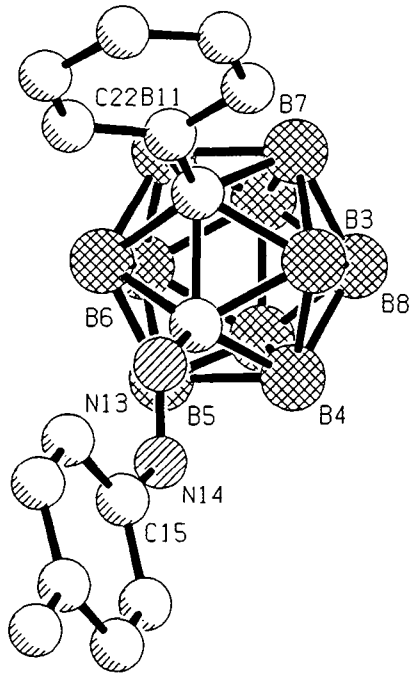

Figure 4.19 Molecular structure of PhCbTol 26

The molecule adopts a trans configuration with the N=N bond lying parallel to the C-C cluster bond. This orientation is equivalent to that found in PhCbNO **20**. Selected bond lengths and angles for **26** and also Fmes-N=N-Ph **1** and azobenzene are given in Table 4.5. There is little difference in C-N bond lengths from the azo-benzenes. Likewise the N=N bond lengths and C-N-N bonds angles are all similar. The cage C-C bond length of 1.690(2)Å is slightly longer than that in PhCbH of 1.640(2)Å.

Atoms	Bond Length / Å	Atoms	Bond Angle / °
C1-C2	1.690(2)	N13-C1-C2	111.3(1)
C1-N13	1.450(2)	N13-C1-B3	116.2(1)
C1-N13	1.450(2)	N13-C1-B4	126.2(1)
C15-N14	1.431(2)	N13-C1-B5	124.0(1)
N13-N14	1.251(2)	N13-C1-B6	112.8(1)
		C22-C2-C1	118.7(1)
		C22-C2-B3	119.0(1)
		C22-C2-B7	123.3(1)
		C22-C2-B11	121.7(1)
		C22-C2-B6	116.3(1)

Table 4.4 Selected bond lengths and angles for PhCbN=NTol 26

Compound	PhCb-N=N-Tol		Fmes-N=N-Ph		$(PhN)_2$
Parameter	PhCb-N	Ph-N	Fmes-N	Ph-N	
C-N	1.450(2)	1.431(2)	1.443(7)	1.453(8)	1.428(2)
N=N	1.251		1.226(6)		1.247(2)
C-N-N	112.9(1)	112.8(1)	112.6(5)	112.7(5)	114.1(1)

Table 4.5 Selected bond lengths and angles for azo compounds

4.6.4 HYDRAZO-CARBORANES

Hydrazocarboranes are reported to be formed by hydrogenation with $Pd/BaSO_4$ or Raney-Ni catalyst or reduction with Sn/HCl. Both PhCbNHNHPh and MeCbNHNHPh are reported.[28]

Reduction of azo-carboranes MeCbN=NPh **25** and PhCbN=NTol **26** gave the corresponding hydrazo-carboranes MeCbNHNHPh **27** and the previously unreported PhCbNHNHTol **28** in good yield (Equation 4.3). These compounds were found to be stable towards oxidation in air and unlike Fmes-NHNHPh and $(PhNH)_2$ showed no tendency to oxidise back to the azo compounds.

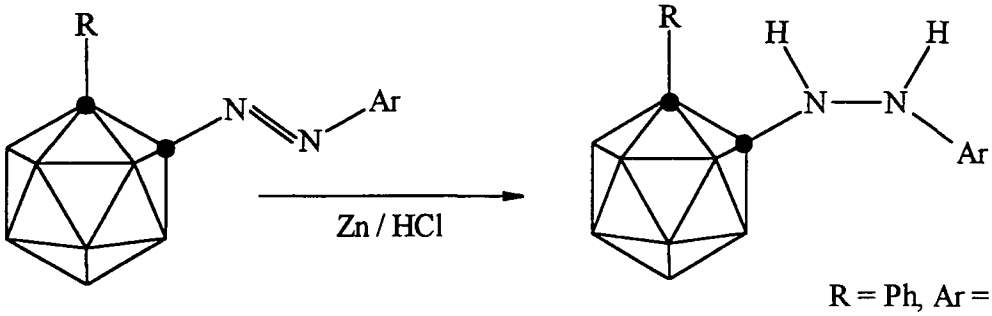

R = Ph, Ar = Tol
R = Me, Ar = Ph

Equation 4.3

4.6.4.1 MOLECULAR STRUCTURE OF 1-(2-METHYL-CARBORANYL)-2-PHENYL-HYDRAZINE

Crystals of MeCbNHNHPh **27** were obtained by cooling a warm solution of **27** in hexane to room temperature. These proved to be suitable for an X-ray structure determination and the structure was solved by Prof. W. Clegg and Dr M.R.J Elsegood

at Newcastle University. The molecular structure is shown in Figure 4.20 and selected bond lengths and angles given in Table 4.6.†

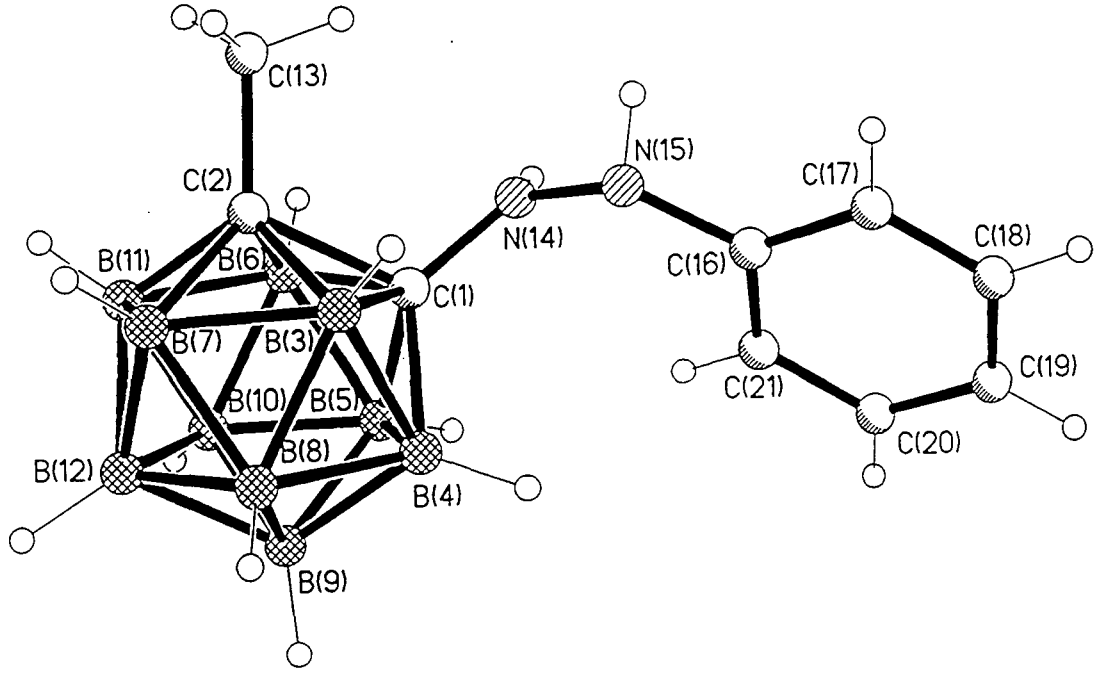

Figure 4.20 Molecular structure of MeCbNHNHPh 27

Atoms	Bond Distance / Å	Atoms	Bond Angle / Å
C1-C2	1.770(2)	N1-C1-C2	115.93(13)
C1-N1	1.387(2)	N1-C1-B3	117.84(14)
C16-N2	1.406(2)	N1-C1-B4	125.52(13)
C1-C13	1.511(2)	N1-C1-B5	123.91(14)
		N1-C1-B6	115.21(13)
		C13-C2-C1	116.22(14)
		C13-C2-B3	116.8(2)
		C13-C2-B7	123.6(2)
		C13-C2-B11	122.9(2)
		C13-C2-B6	116.3(2)

Table 4.6 Selected bond lengths and angles for MeCbNHNHPh 27

† The X-ray structure of PhCbNHNHTol **28** has recently been determined by W. Clegg and M.R.J. Elsegood. Although the results for this compound were obtained too late to be included in this discussion the Cb-N bond length (1.401(2)Å) and the C-C cluster bond length (1.778(3)Å) are similar to those in **27**. The orientation of the N-lone pair with respect to the cage is analogous in both compounds. Hence the discussion in this Chapter of the structures of N-substituted compounds is not altered by this recent result. The X-ray data for **28** are given in Appendix C.

The conformation found in the solid is equivalent to that for the dicarboranyl amines **22** and **23**. Although the N coordination is non-planar there is extensive flattening from a pyramidal geometry. Again the lone pair is in the plane of the C-C cluster bond. The orientation of the phenyl group is analogous to that in both FmesNHNHPh and 1,2-diphenylhydrazine.

Compound	MeCbNHNHPh		FmesNHNHPh		$(PhNH)_2$
	PhCb	Ph	Fmes	Ph	
Parameter					
C-N	1.387(2)	1.406(2)	1.398(4)	1.411(4)	1.386(4)
C-N-H	117(2)	113.6(12)	117(2)	115.5(3)	
C-N-N	118.83(13)	119.18(14)	119.0(3)	119.1(3)	
N-N-H	120(2)	112.5(12)	116(2)	115.5(3)	
$\Sigma\angle N$	356(5)	345.3(26)	352(7)	350(9)	352

Table 4.7 Selected bond lengths and angles for hydrazo compounds

The carboranyl C-N bond is shorter than the phenyl C-N bond by 0.019Å, although comparable to that in hydrazobenzene in which N-C π-bonding has been established, suggesting that there is greater cage-N π-bonding than Ph-N π-bonding. On the basis of coordination number of the carbon atoms it might be expected that the Cb-N bond involving 6-coordinate carbon would be longer than the Ph-N bond involving 3-coordinate carbon.[30] The orientation of the phenyl ring is analogous to that in **3** and hydrazobenzene with the lone pair on nitrogen parallel to the aromatic π-system.

4.6.5 CARBORANYL HYDROXYLAMINES

Hydroxylamines are reportedly formed by the reduction of nitrosocarboranes with tin and conc. HCl in ethanol at 20°C, both MeCbNHOH and HCbNHOH being reported. As nitroso carboranes react readily with ethanol this appears to be a poor choice of solvent. This reaction was carried out in a two phase system with MeCbNO **21**, Sn, conc. HCl and diethyl ether with vigorous stirring. The solution was rapidly decolourised and upon work up a good yield of compound MeCbNHOH **29** was obtained (Equation 4.4).

Catalytic hydrogenation of **21** with 5% Pd on C catalyst was found to give improved yields of **29**. PhCbNHOH **30**, previously unreported, was subsequently synthesised by this method from PhCbNO **20**.

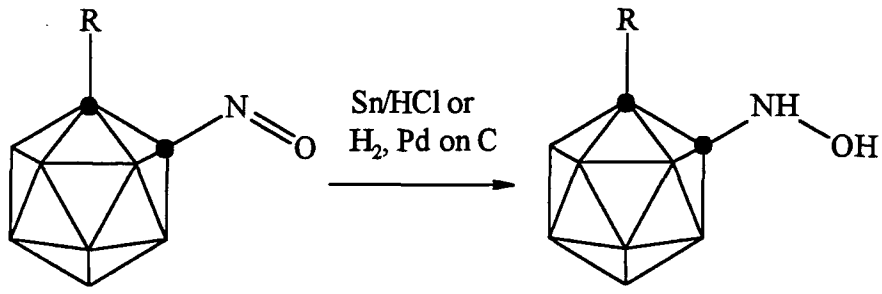

Equation 4.4

The X-ray structure of PhCbNHOH has recently been determined by Prof. W. Clegg and Dr M.R.J. Elsegood at Newcastle University. Although the results for this compound were determined too late to be included in this discussion the Cb-N bond length (1.423(3)Å) and C-C cluster bond length (1.737(3)Å) are as would have been predicted on the basis of the ^{11}B NMR shift of B12 (see pages 127 and 128). The X-ray data are given in Appendix C.

4.6.6 PRIMARY CARBORANYL AMINES

Several methods are reported in the literature for the synthesis of primary carboranyl amines; these are summarised in Scheme 4.4.

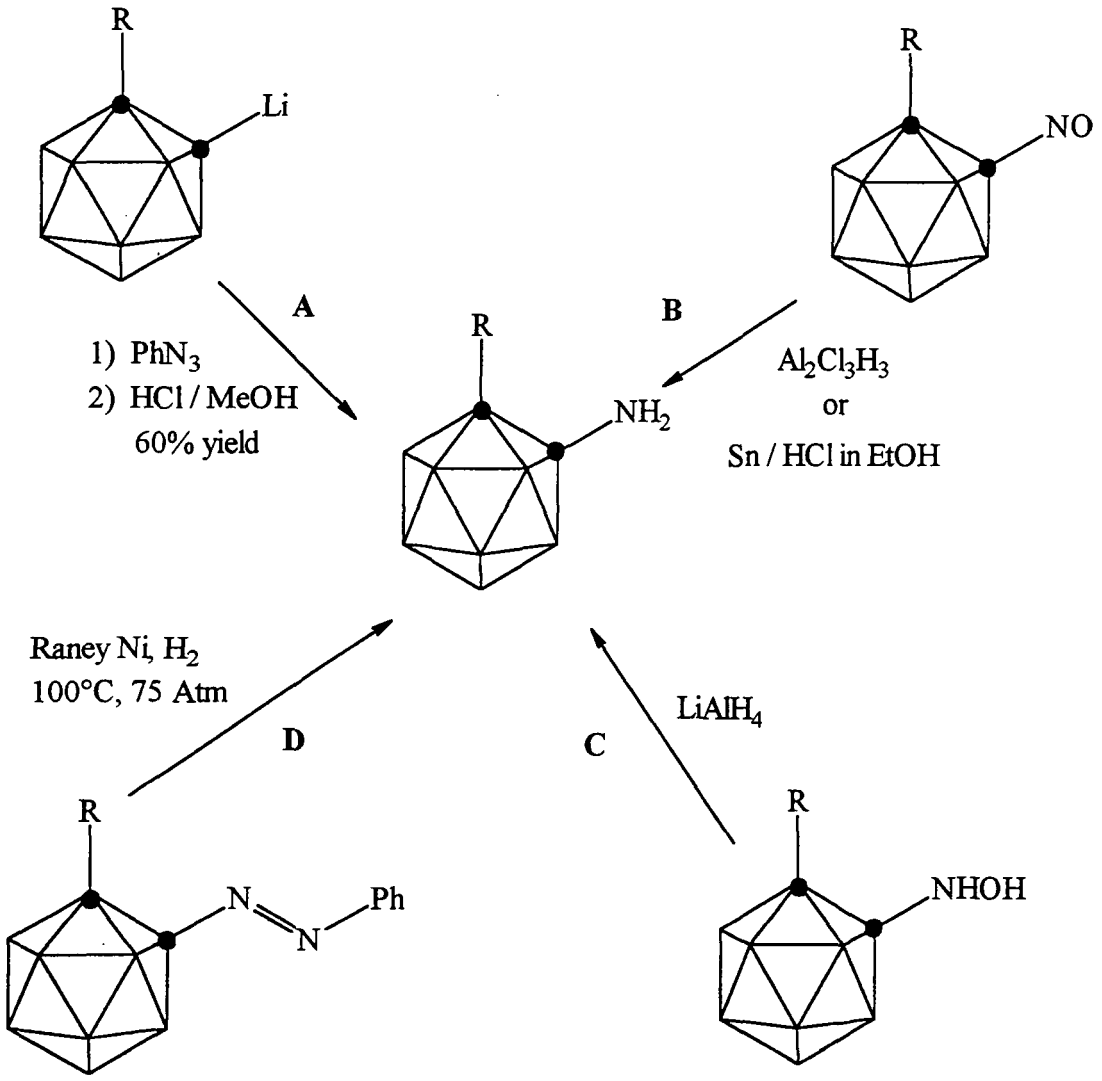

Scheme 4.4 Syntheses of primary carboranyl amines

Previous attempts to synthesise $PhCbNH_2$ by the reduction of PhCbN=NTol with Raney Ni (Route D[31]) resulted in the isolation of an insoluble material with no trace of the amine $PhCbNH_2$.[29] Attempts were made to reduce MeCbN=NPh to the corresponding primary amine by hydrogenation with 5% Pd on C catalyst (1 Atmos H_2) in both dioxane and acidified ethanoic acid. Partial conversion to MeCbNHNHPh was detected but no $MeCbNH_2$ was observed.

Reduction of MeCbNO with $Al_2Cl_3H_3$ (route B[32]) was attempted. The solution was rapidly decolourised but on work up no *closo*-carborane was isolated. The IR spectrum of the product indicated that the cage had degraded to a nido residue but no pure products could be isolated.

Reduction of MeCbNHOH with $LiAlH_4$ (Route C[32]) similarly led to degradation of the cage, although small amounts of $MeCbNH_2$ were isolated. Route A[33] involving the synthesis of a carboranyl triazene (RCbNH-N=NPh) was not attempted.

Due to the reactivity of nitroso carboranes towards ethanol, reduction of RCbNO with Sn/HCl in this solvent was not attempted. Reduction of MeCbNHOH **29** with ethanol, Sn and HCl gave moderate yields of $MeCbNH_2$ **31**. This method was modified by the replacement of the ethanol solvent with dme, thus preventing degradation of the cage by the alcohol and led to the isolation of $MeCbNH_2$ **31** in good yield and $PhCbNH_2$ **32** in moderate yield by the reduction of the corresponding nitroso-carboranes.

*4.6.6.1 Molecular Structure of 1-Amino-2-Phenyl-*ORTHO*carborane*

Crystals of $PhCbNH_2$ were obtained by cooling a solution in hexane to 5°C. The structure of these was determined by X-ray diffraction by Prof. W. Clegg and Dr M.R.J. Elsegood at Newcastle University. The molecular structure is shown in Figure 4.21 and selected bond lengths and angles in Table 4.8.

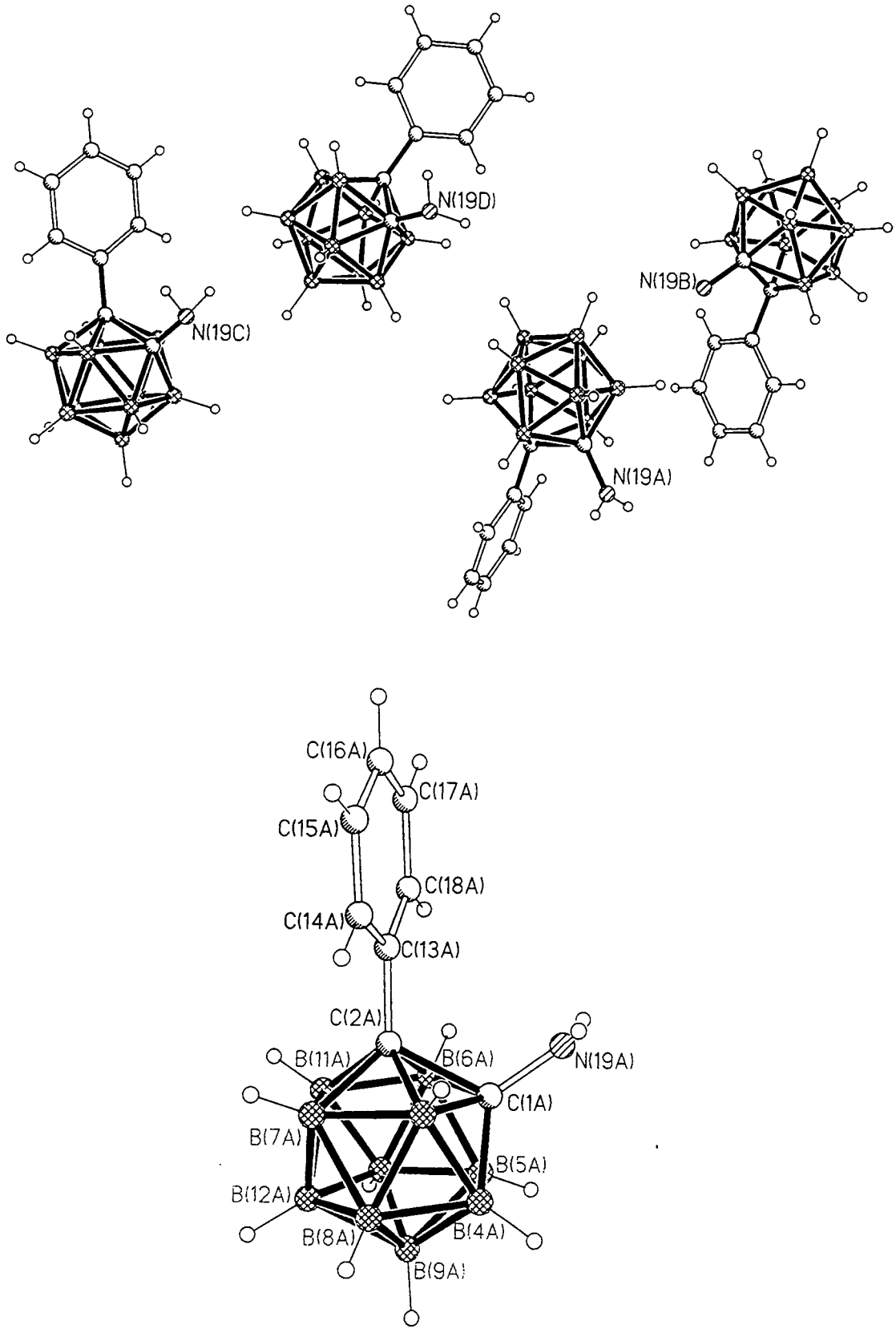

Figure 4.21 Molecular structure of $PhCbNH_2$ 13 showing all four molecules (1) and molecule A with numbering (2)

Molecule:	A	B	C	D	Average
Atoms					
C1-N1	1.392(2)	1.403(3)	1.391(3)	1.404(3)	1.396(3)
C1-C2	1.785(3)	1.765(3)	1.745(3)	1.774(3)	1.767(3)
C2-C13	1.501(3)	1.498(3)	1.506(3)	1.498(3)	1.501(3)
N1-C1-C2	118.49(16)	115.93(17)	119.34(16)	199.75(17)	118.38(17)
N1-C1-B3	118.75(18)	118.0(2)	118.83(17)	119.36(18)	118.7(2)
N1-C1-B4	123.50(18)	124.93(19)	121.53(18)	121.84(18)	123.0(2)
N1-C1-B5	122.11(18)	123.5(2)	120.82(17)	120.71(18)	121.8(2)
N1-C1-B6	116.69(18)	115.9(2)	117.65(17)	117.88(17)	117.03(2)
C13-C2-C1	118.12(15)	118.15(15)	116.7(15)	116.23(15)	117.3(2)
C13-C2-B3	116.08(17)	118.66(17)	114.96(16)	114.64(16)	116.1(2)
C13-C2-B7	121.49(17)	123.44(18)	121.83(16)	122.14(16)	122.2(2)
C13-C2-B11	123.46(17)	122.27(17)	125.15(16)	125.82(17)	124.2(2)
C13-C2-B6	119.19(17)	117.37(17)	119.88(16)	120.06(16)	119.1(2)

Table 4.8 Selected bond lengths and angles in $PhCbNH_2$

Four crystallographically independent molecules (A, B, C and D) were found in the unit cell. The amino hydrogen atoms were located on three of these by applying similarity restraints, those on molecule B were not located due to high thermal motion. All four compounds have similar C-N bond distances, ranging from 1.391(3)Å to 1.404(3)Å. There is slightly more variation in the C-C cluster bond lengths which range from 1.745(3)Å to 1.785(3)Å. This corresponds to a significant lengthening of this bond from that in PhCbH (1.640(5)Å).

Although the errors in the positions of the hydrogen atoms are large the nitrogen coordination appears to be analogous to that in the secondary amines $(MeCb)_2NH$ and $(PhCb)_2NH$ and also MeCbNHNHPh with the lone pair on N in the plane of the C-C cluster bond. To determine the position of the hydrogen atoms with more certainty *ab initio* calculations have been carried out to determine the most likely positions of the hydrogen atoms in the absence of crystal packing and intramolecular interactions.

Coordinates used were those of molecule D from the X-ray study, all atomic positions other than those of the two amine H's were fixed, these hydrogens being fully optimised. A planar N environment was initially assumed, the amino H's lying in the plane defined by the two cluster C atoms and the N. Optimisation at the RHF/STO-

3G level produced a structure with pyramidal N, the lone pair in the plane of the C-C cluster bond and the amine H's leaning away from the phenyl ring (Figure 4.22A). This is different to the crystal structure in that the X-ray structure shows the hydrogens to lean towards the phenyl ring (Figure 4.22 1,2 and 3) although the lone pair is in the plane of the C-C cluster bond. If the calculation is repeated with the H's starting in the positions indicated by the X-ray structure this conformation is retained (Figure 4.22C), the total energy of this structure being only 0.21 $kJmol^{-1}$ higher than that with the amino H's pointing away from the ring. If both of these ab initio geometries are optimised at the higher RHF/3-21G* level the two structures obtained (Figure 4.22B and D) are similar to the respective STO-3G geometries but are virtually identical in energy, the structure equivalent to that found in the solid being lower in energy by only 0.04 $kJmol^{-1}$, virtually negligible. On the basis of these calculations there appears to be little preference for a structure with the H's pointing towards the phenyl or away from it. The important point however is that these calculations confirm that the lone pair is again in the plane of the C-C cluster bond as indicated by the X-ray structures. Table 4.9 summarises geometric parameters for these *ab initio* geometries.

The bond angles around the N atom (~335°) reveal a pyramidal geometry somewhat flattened from that in ammonia (107°) and comparable to that in aniline (344(11)°). As STO-3G geometries tend to underestimate such angles, and 3-21G* to overestimate, it is likely that the actual angle lies between the two.

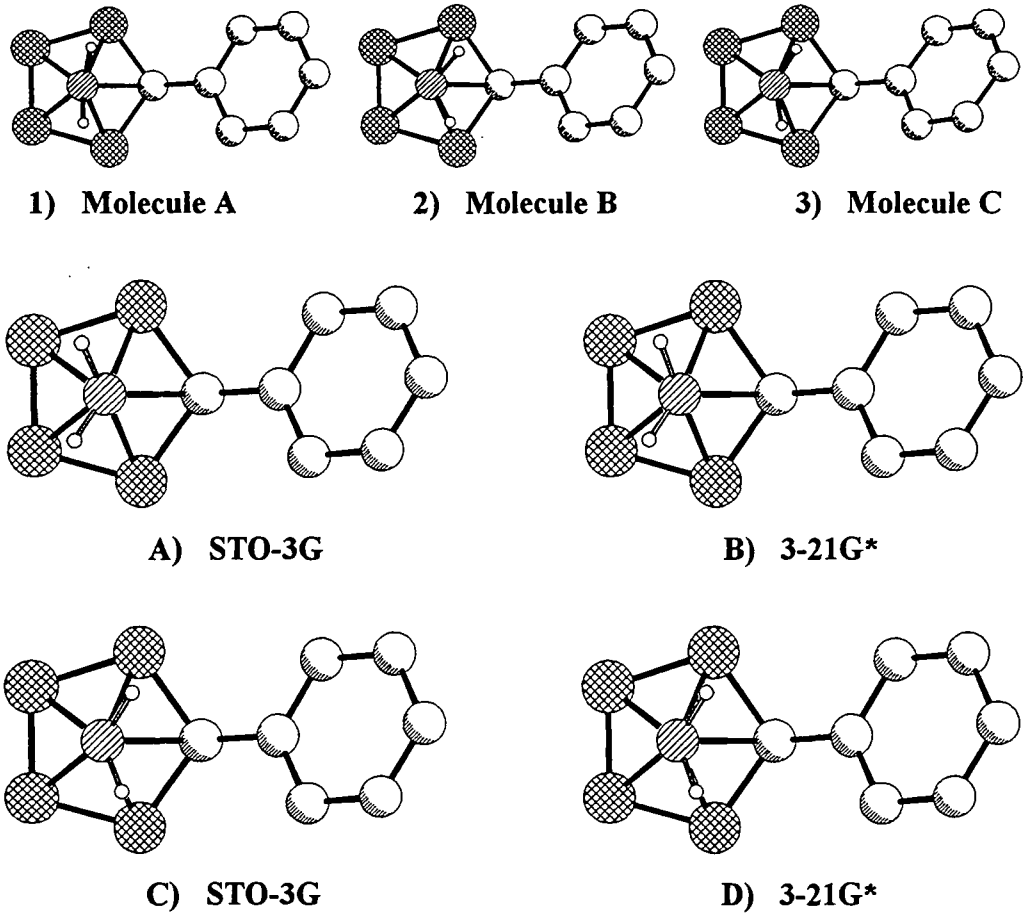

Figure 4.22 NH_2 **orientations in X-ray and calculated structures of** $PhCbNH_2$

	X-ray (Average)	STO-3G (A)	3-21G* (B)	STO-3G (C)	3-21G* (D)
N-H1	1.008(14)	1.025	1.006	1.025	1.006
N-H2	1.005(14)	1.025	1.005	1.025	1.005
C1-N-H1	113.5(11)	111.92	112.78	113.72	113.83
C1-N-H2	115.0(11)	111.64	112.27	113.60	113.80
H1-N-H2	115.8(17)	114.34	110.93	110.64	110.94
$\Sigma\angle N$	344.3(39)	334.20	335.98	337.96	338.57
C2-C1-N-H1	63	114.34	110.42	58.78	58.84
C2-C1-N-H2	-77	122.00	-123.38	-68.96	-69.61
Total Energy	-	-606.5988	-611.1641	-606.5966	-611.1644

Table 4.9 Bond lengths / Å, angles / ° and total energies / eV for X-ray, STO-3G and 3-21G* geometries of NH_2 groups in $PhCbNH_2$

4.6.7 Deprotonation of N-Substituted Carboranes

Deprotonation of $(PhCb)_2NH$ with KO^tBu yields the corresponding anion $(PhCb)_2N^-$ **24** which has several features of interest.[26] Anions of other N substituted carboranes would also be of interest and attempts were made to synthesise such species. Treatment of PhCbNHOH, MeCbNHNHPh and $PhCbNH_2$ with proton sponge did not remove a proton, the parent materials being recovered. This is consistent with previous attempts to deprotonate $(PhCb)_2NH$ using this method.

Treatment of $MeCbNH_2$ with KO^tBu resulted in the isolation of a white solid. ^1H and ^{11}B NMR and IR spectroscopy indicated that this product consisted of a mixture of *nido* species. A pure sample was never obtained and the identity of the product remains a mystery. Attempts to deprotonate $PhCbNH_2$ with both ^nBuLi and the ylide Ph_3PCH_2 gave similar results with a mixture of *nido* species being detected.

The reason for this facile degradation is not obvious. The formation of an anion $[RCbNR']^-$ and delocalisation of the charge onto the cage would be expected to make the cage less susceptible to nucleophilic attack and hence more resistant to degradation to a *nido* species. It may be that the anion formed acts as a nucleophile on another cage, thus leading to a mixture of products.

4.6.8 EXO-π-BONDING BETWEEN N-SUBSTITUENTS AND CARBORANES

The compounds $(MeCb)_2NH$ **23**, $(PhCb)_2NH$ **22**, MeCbNHNHPh **27** and $PhCbNH_2$ **32** are all similar in many respects being of the form RCbNR'R" (R = Me, Ph; R' = H; R" = H, NHPh, CbR). Hence it is not surprising that they have many features in common. The anion $(PhCb)_2N^-$ **24** can also be considered to be analogous to these compounds, the H having been removed without significant changes in the conformation (i.e. R' = CbPh, R" = lone pair).

The N environments are, despite large errors in the positions of the H atoms, clearly less pyramidal than that in ammonia. The C-N bond lengths are shortened from that for a single C-N bond (1.469Å in alkyl amines) being closer to those found in aryl amines ($C\text{-}N(sp^2)H_2$ 1.355Å, $C\text{-}N(sp^3)H_2$ 1.394Å). The C-C cluster bonds are all lengthened from that of 1.63Å in the parent *ortho*-carborane cage[13], ranging from 1.677Å in PhCbNO **20** to 1.987Å in anion **24**. Both C-N and C-C bond lengths and angles indicate significant delocalisation of the lone pair onto the carborane cage in the same manner as the $PhCbO^-$ anion. There is a flattening of the nitrogen environment in the same manner to that observed in aromatic systems (Chapter 2). These geometric parameters are summarised in Table 4.10, also included are data for $PhCbN_2Tol$ and PhCbNO.

Compound	C-N / Å	$\Sigma\angle N°$	C-C / Å
$(PhCb)_2NH$	1.405(2)	360	1.798(3)
$(MeCb)_2NH$	1.410(2)	360	1.798(3)
PhCbNO	1.490(2)	113.0(2)	1.677(2)
$(PhCb)_2N^-$	1.350(4)	127.0(2)	1.987(3)
$PhCbN_2Tol$	1.450(2)	112.9(1)	1.690(2)
MeCbNHNHPh	1.387(2)	356	1.770(2)
$PhCbNH_2$	1396(3)	344	1.767(3)

Table 4.10 Bond lengths and angles for RCbNR'R" compounds

All of these compounds have analogous orientations, the lone pair in the same plane as the p_x orbital (see Figure 4.10) on the cluster carbon atom (Figure 4.23). This confirms the assumption for $PhCbO^-$ that the π-interaction between the cage and *exo*-atom involves primarily the p_x orbitals. The lower energy of the C-p_x orbital allows

strongest π-bonding when the N lone pair is aligned with the C-p_x as opposed to C-p_y and this dictates the orientation of these substituents relative to the cage.

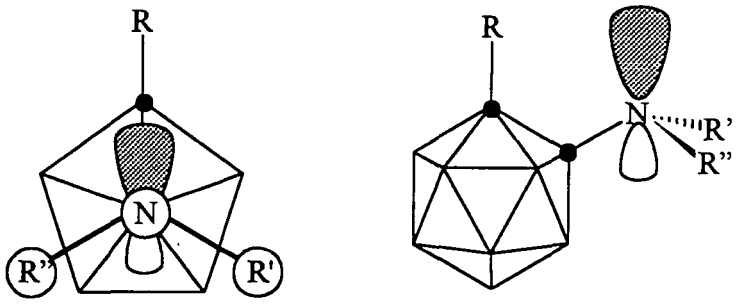

Figure 4.23 Orientation in RCbNR'R"

The compounds PhCbNO and $PhCbN_2Tol$ are also related, being of the form PhCbN=X (X = O, NTol), and adopt analogous conformations with the N=X bond parallel to the C-C cluster bond. The C-N bonds between the cluster and substituent are far longer than those in the RCbNR'R" compounds, being closer to that for a C-N single bond. The cage also shows less distortion, the C-C bond length being closer to that for an unperturbed cage. In both compounds the C1-N-X bond angle is less than the angle of 120° for sp^2 N showing no tendency towards the linear conformation that would have been expected had the NX unit functioned as a 3 electron ligand. This is also observed in azobenzenes and nitrosobenzenes and can be explained in terms of VSEPR, the lone pair having a greater steric effect than the electrons in the bonds to N.

These compounds offer the possibility for an interaction between the cage with both the lone pair on N and the π-system of the N=X bond (Figure 4.24).

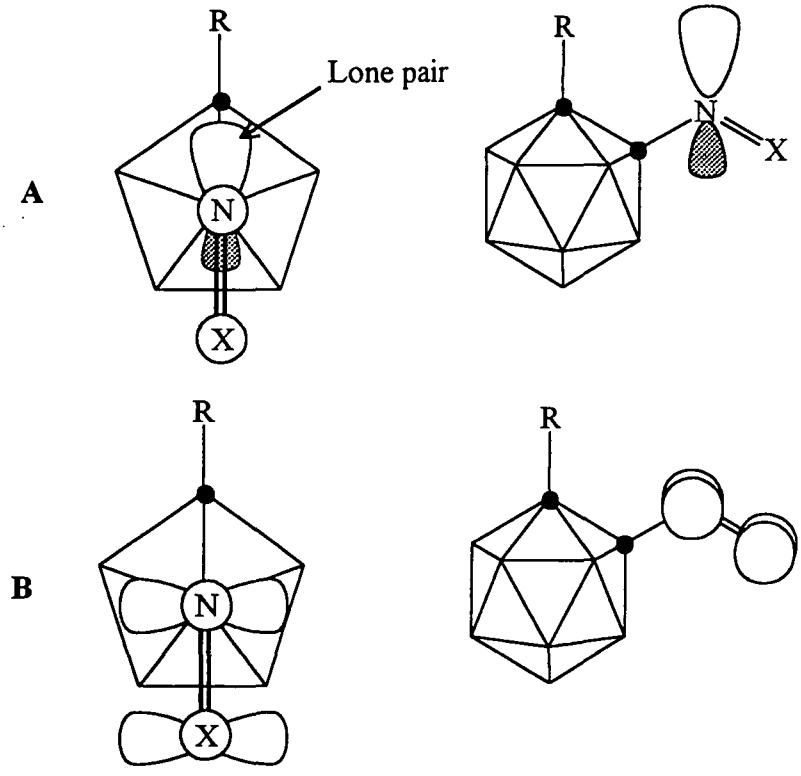

Figure 4.24 Orientation of both N lone pair (A) and N=X π-system (B) in RCbN=X

Bonding in nitrosobenzenes is similar to that in azobenzenes with the preferred orientation in the absence of steric effects being with the NO group lying in the plane of the ring (Figure 4.25A), analogous to the orientation in sterically unhindered azobenzenes.[34] The nitroso group in this orientation is associated with a withdrawal of π-electrons from the aromatic system, viewed as a transfer of electrons from the aromatic π-system to the nitroso π* orbital.[35] Calculations suggest that if the NO group is constrained to lie perpendicular to the ring (Figure 4.25B), electron donation to the ring will occur due to donation of the lone pair onto the ring as observed in azobenzenes. This had been confirmed by ^{13}C NMR of nitrosobenzenes with bulky *ortho*-substituents in which the nitroso group is forced through steric interactions into an orthogonal conformation.[36]

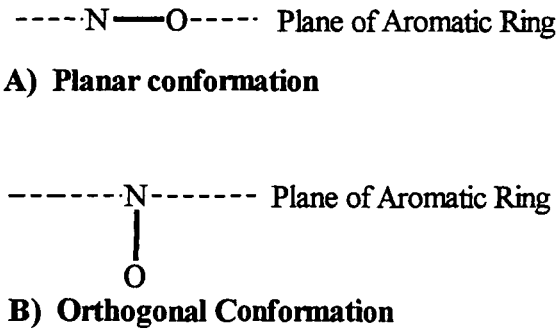

Figure 4.25 Conformations in nitrosobenzenes

Unlike the aromatic system where there is only one p-orbital with which the substituent can interact (i.e. the π-system) and hence which the lone pair and N=X π-system compete for, the carborane system has two orthogonal p-orbitals. The orientation adopted aligns the lone pair with the C-p_x with which the interaction will be strongest due to proximity in energy. The N=X π-system is aligned with the C-p_y on carbon (Figure 4.24B), this interaction being stronger than with the C-px, again due to proximity in energy between N=X π* orbital and the C-p_y.

To aid the comparison of the bonding within this series of calculations AM1 calculations using MOPAC 5.0 have been carried out using the coordinates determined by X-ray diffraction without further optimisation. Selected bond orders with corresponding σ and π contributions are given in Table 4.11.

Compound	C-N Bond				C-C Bond	
	Bond Length / Å	Bond Order	σ-Bond Order	π-Bond Order	Bond Length / Å	Bond Order
$(PhCb)_2NH$ **22**	1.405(2)	1.038	0.914	0.124	1.798(3)	0.453
$(MeCb)_2NH$ **23**	1.410(2)	1.026	0.913	0.113	1.750(4)	0.506
MeCbNHNHPh **27**	1.387(2)	1.057	0.929	0.128	1.770(2)	0.486
MeCbNHNHPh **27**	1.406(2)	1.033	0.917	0.116	-	-
$PhCb_2N$ **24**	1.350(4)	1.295	0.938	0.357	1.987(3)	0.235
$PhCbNH_2$ **32**	1.396(3)	1.088	0.961	0.127	1.767(3)	0.462
PhCbNO **20**	1.490(2)	0.921	0.865	0.056	1.677(2)	0.605
$PhCbN_2Tol$ **26**	1.450(2)	0.998	0.928	0.070	1.690(2)	0.590
$PhCbN_2Tol$ **26**	1.431(1)	1.024	0.924	0.100	-	-

Table 4.11 Calculated bond orders for RCbNR'R" and RCbN=X compounds

It is clear from the calculated π-bond order that all of these compounds show some degree of π-bonding between the substituent and the cage. This is least in PhCbNO and greatest in $PhCb_2N^-$ **24**, this order being consistent with that established by C-N bond lengths.

An increase in π-bonding will cause a reduction in the contribution of the $5e_1(x)$ cluster orbital to cluster bonding and an increasing contribution from the $5e_1(y)$ orbital which will cause a lengthening of the C-C cluster bond. As the C-N π-bond order increases the contribution from the $5e_1(x)$ will decrease and so the C-C bond length should be closely related to the order of the exo-π-bond. This is shown in Figure 4.26 with the C-C bond lengthening as the C-N bond shortens. Steric effects will cause small perturbations in this order. Similar C-N distances in amines **22** and **23** but differing C-C distances can be attributed to a combination of differing steric and electronic effects of the methyl and phenyl substituents on C2.

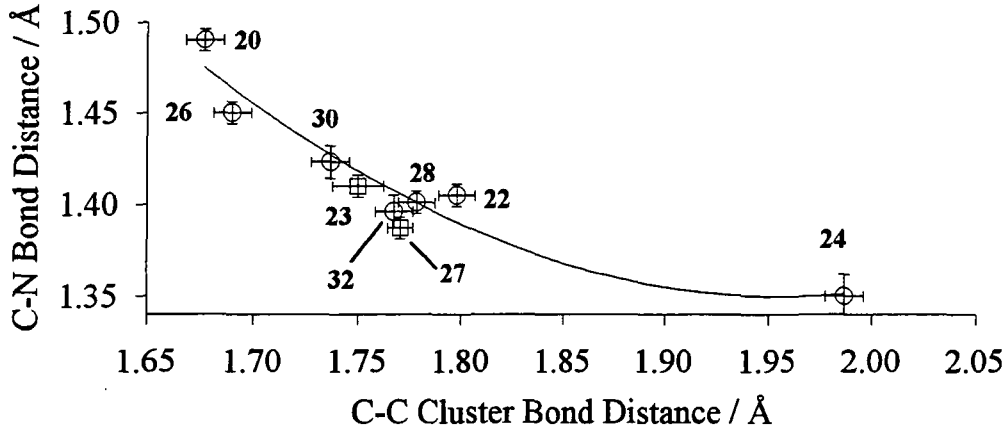

Figure 4.26 C-C bond length vs C-N bond length

Such calculations also reveal the nature of the π-bonding in PhCbNO **20** and $PhCbN_2Tol$ **26**. Most of the π-bonding arises from interaction of the N=X π-system with the cage (71% in **20**, 64% in **26**), the lone pair playing a lesser role. Such π-bonding involving the C-p_y will not affect the C-C bond in the same way as π-bonding involving the C-p_x, but would be expected to lengthen the C-B bonds. These effects, however, are small, no significant difference being seen in C-B bond lengths in this

series of compounds. The involvement of π-bonding involving C-p_y is discussed further in Chapter 5.

This interaction involving the π-system of the N=X bond can be viewed as a withdrawal of electrons from the cluster. Due to the electron deficient nature of the cage such effects should be of lesser magnitude than in electron rich aromatic systems. This is consistent with the smaller C-N π-bond order between the cage and azo linkage than to the aromatic ring in the same compound, the same trend observed in $FmesN_2Ph$ **1**. This also explains the long C-N bond in PhCbNO **20** compared to that in nitrosobenzenes.

4.6.9 ANTIPODAL EFFECTS

It has been shown for other systems that the Antipodal shift - the NMR shift of the boron atom directly opposite the substituted cage C atom - is dependent on the electron donor capacity of the substituent.[14] The degree of π-bonding to the cage will also depend on this π-donor capacity and hence the Antipodal shift should be related to the degree of *exo*-π-bonding and hence to the C-N and C-C bond lengths.

For such a comparison to be made the ^{11}B NMR shift for the Antipodal atom (^{11}B δ-B12) must be reliably assigned. ^{11}B NMR resonances for this series of compounds are displayed in Figure 4.27 for Ph substituted carboranes and Figure 4.28 for Me substituted carboranes. Although the two peaks corresponding to B9 and B12 are readily identified from the peak intensities it is impossible to unambiguously assign each without assumptions being made. It can be seen in Figure 4.27 and Figure 4.28 that one of these peaks appears in approximately the same place in all compounds. This corresponds to B9, antipodal to the Ph or Me group in PhCbH and MeCbH respectively. This peak would be expected to change little in these series of compounds as the substituent on C2, i.e. the Me or Ph group, remains unchanged. Likewise, in comparing two compounds MeCbX and PhCbX it would be expected that B12 opposite X would change little in its NMR shift, B9 opposite the Me or Ph group experiencing the greatest change due to the differing antipodal effect of the Ph or Me group. ^{11}B NMR shifts for B9 and B12 have been assigned on this basis, the peak closest to that of B9 in the parent compound RCbH being assigned to B9, the other peak, similar in frequency between the two compounds PhCbX and MeCbX assigned to B12. ^{11}B NMR shifts for B9 and B12 are summarised in Table 4.12.

Both the nitroso and azo compounds show some degree of increase in shielding despite electron withdrawal onto the N substituent. It may be that the antipodal effect responds only to π-donation to the cage and not π-withdrawal.

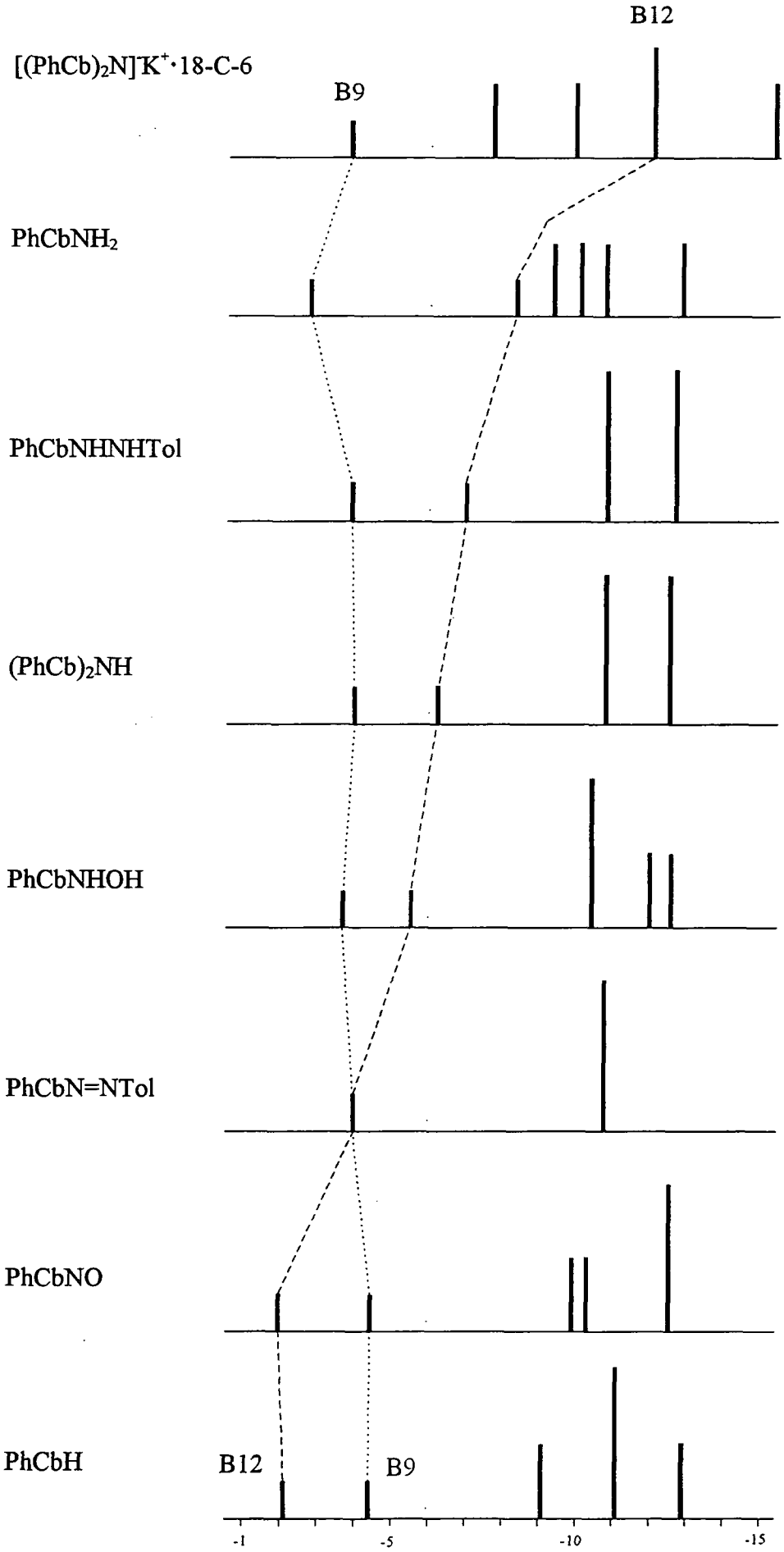

Figure 4.27 NMR shifts for phenyl-*ortho*-carboranes

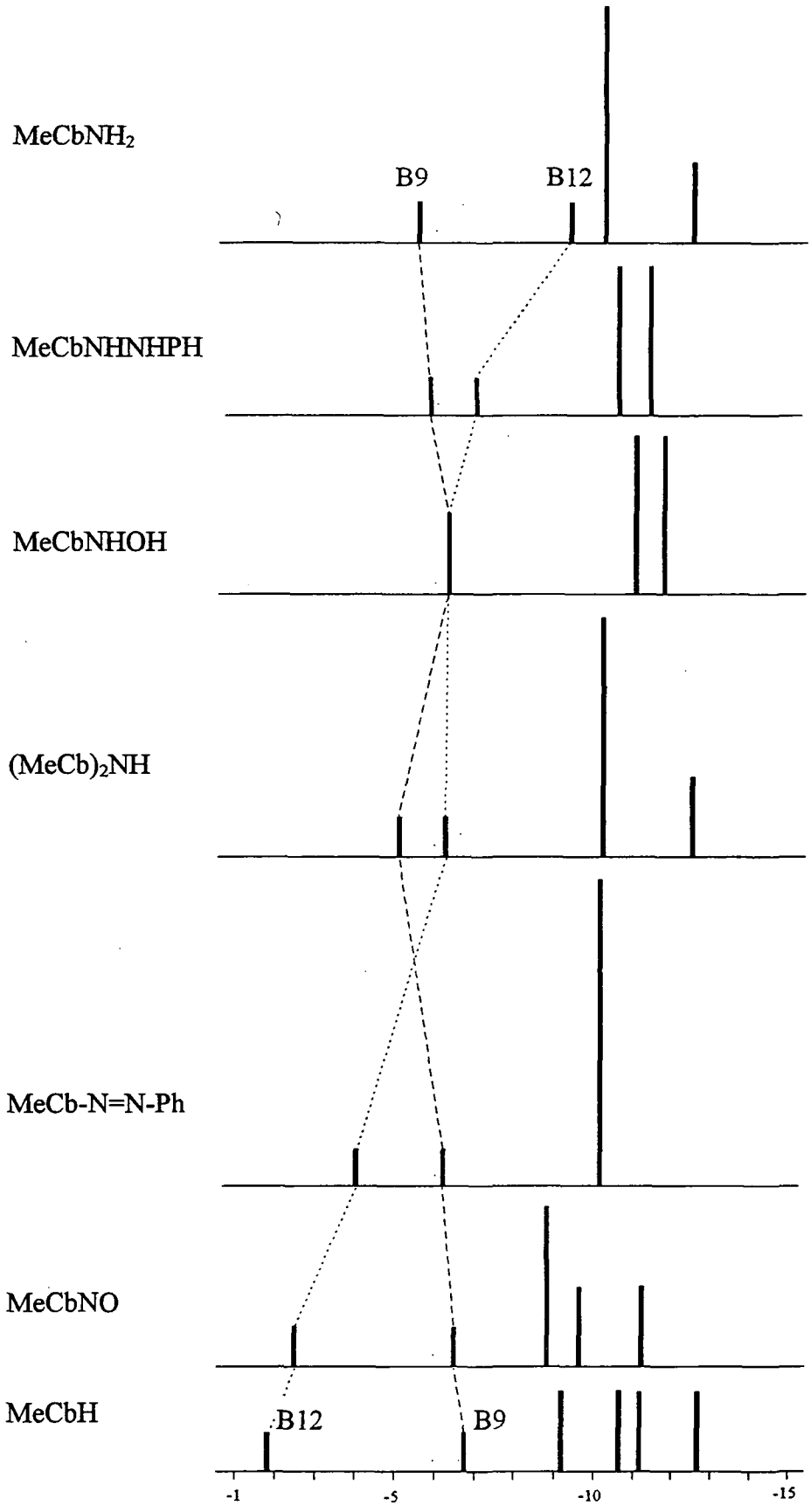

Figure 4.28 NMR shifts for methyl-*ortho*-carboranes

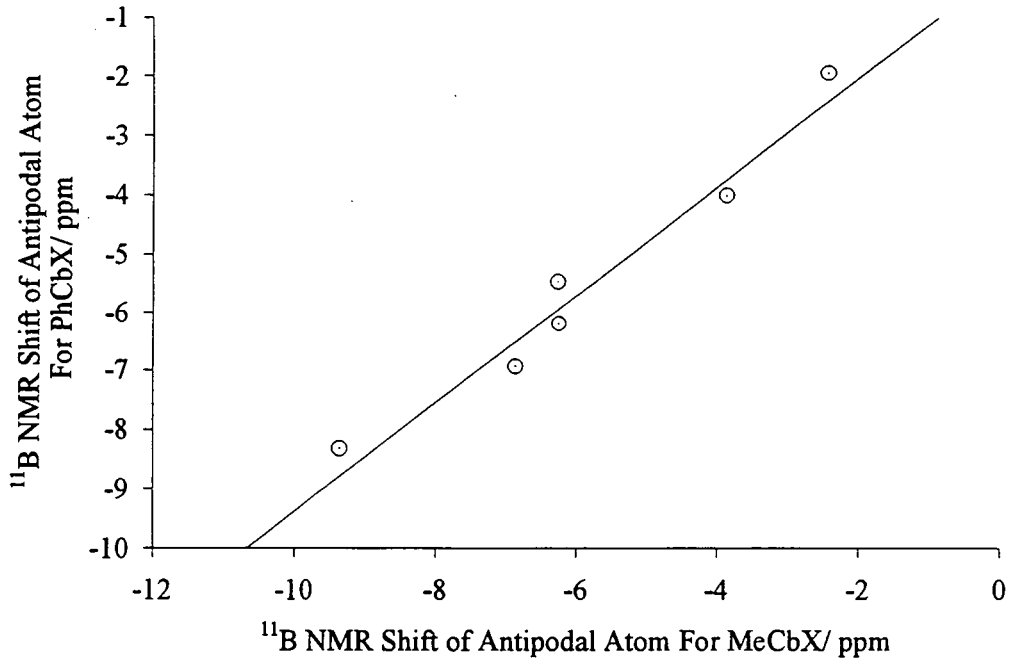

Figure 4.29 Antipodal shifts for Me and Ph substituted carboranes

Compound	δ B9	δ B12	δ B_{ave}	α-B9	α-B12	δ H12
$(MeCb)_2NH$	-5.05	-6.25	-9.57	+4.52	+3.32	+2.12
$(PhCb)_2NH$	-3.95	-6.19	-10.29	+6.34	+4.10	+2.18
$(PhCb)_2N^-$	-3.83	-11.97	-10.62	+6.79	-1.35	+1.72
MeCbNO	-6.64	-2.43	-8.59	+1.95	+6.16	+2.50
PhCbNO	-4.40	-1.95	-9.70	+5.30	+7.75	+2.58
$MeCbN_2Ph$	-6.08	-3.87	-10.00	+3.92	+6.13	+2.42
$PhCbN_2Tol$	-4.01	-4.01	-9.37	+5.36	+5.36	+2.39
MeCbNHNHPh	-5.82	-6.87	-10.13	+4.31	+3.26	+2.07
PhCbNHNHTol	-3.88	-6.94	-10.42	+6.54	+3.48	+2.28
MeCbNHOH	-6.26	-6.26	-10.85	+5.53	+0.78	+1.94
PhCbNHOH	-3.64	-5.47	-9.94	+6.30	+4.47	+2.28
$MeCbNH_2$	-5.48	-9.36	-10.19	+4.71	+0.83	+1.98
$PhCbNH_2$	-2.71	-8.32	-9.61	+6.90	+1.29	+2.18

Table 4.12 ^{11}B and ^{1}H NMR shifts for B12 in RCbX / ppm

The antipodal shift increases as π-bonding increases, displayed by plots of the shift vs C-N bond lengths (Figure 4.30), C-N π-bond orders (Figure 4.31) and C-C bond lengths (Figure 4.32). These graphs show the close relationship between the degree of *exo*-π-bonding and the ^{11}B NMR shift of the antipodal atom. This is in full agreement with previous work showing that such shifts are related to electron donation to the cluster. Hence the ^{11}B NMR gives an accurate indication of degree of exo-π-bonding and this can be used to assess such effects in compounds which have not been structurally characterised.

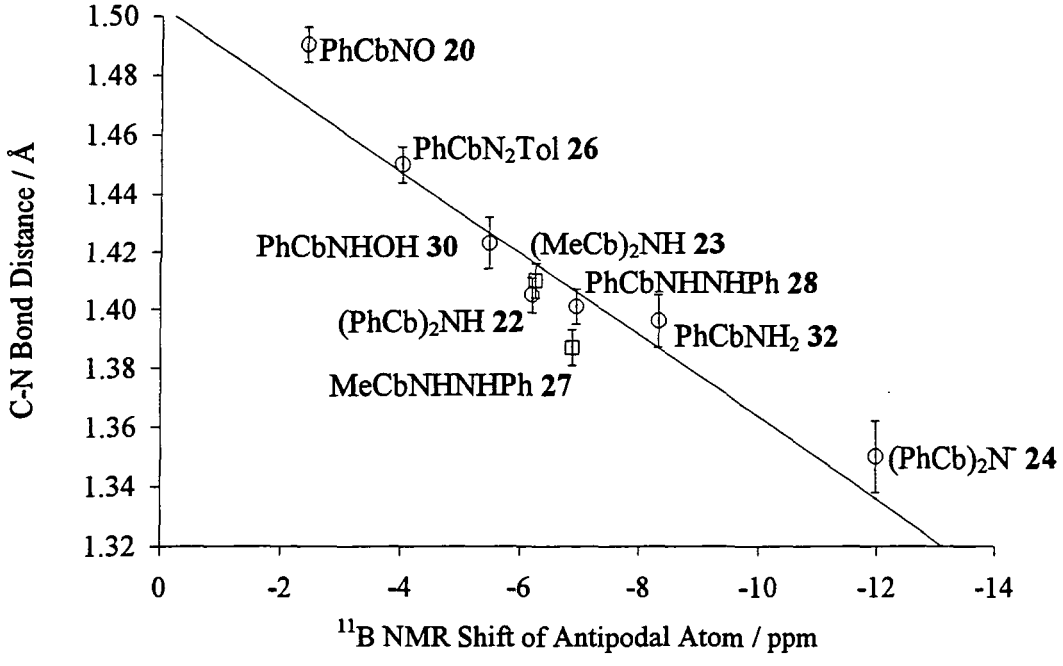

Figure 4.30 ^{11}B shift of B12 (ppm) vs C-N bond length / Å

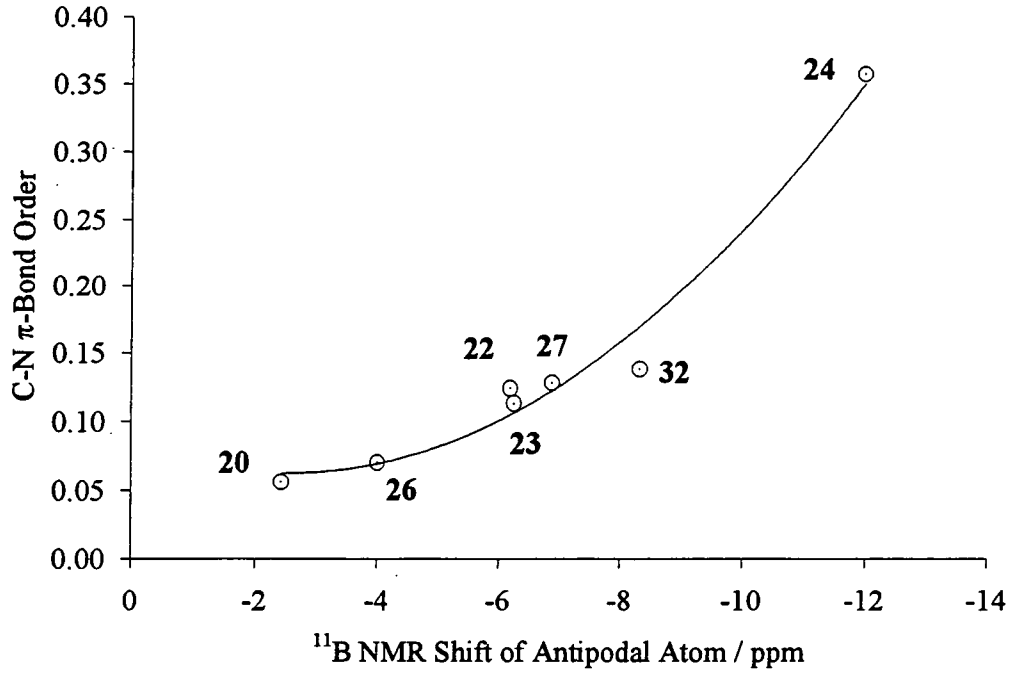

Figure 4.31 **^{11}B shift of B12 (ppm) vs C-N π-bond order**

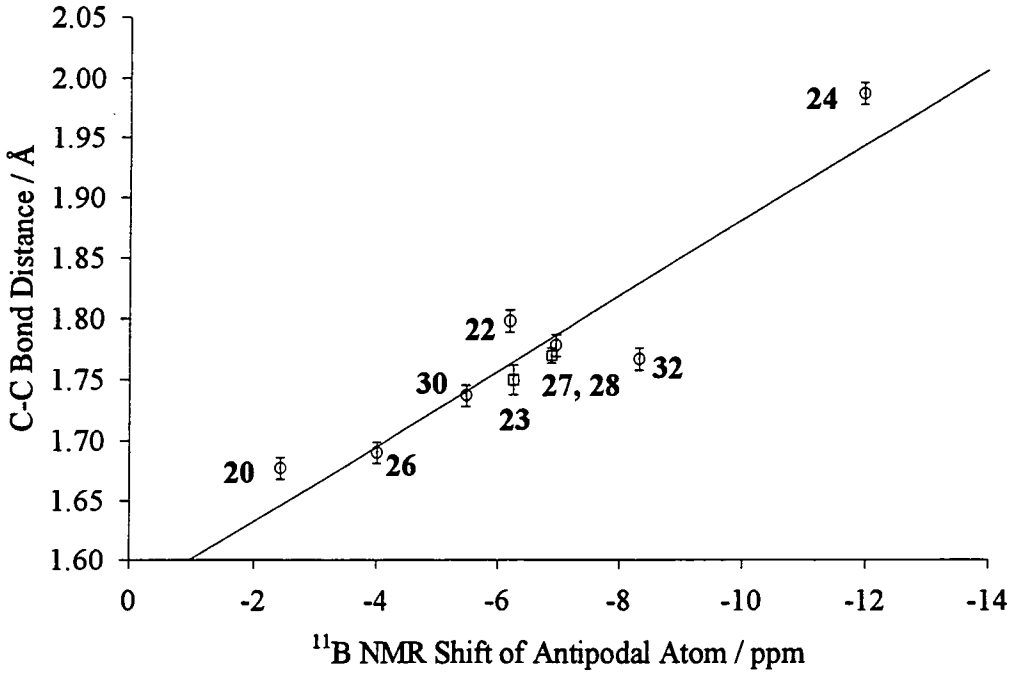

Figure 4.32 **^{11}B shift of B12 (ppm) vs C-C bond length / Å**

Previous work on such systems suggests that the weighted average of the ^{11}B shift (δ-B_{ave}) of all of the cage boron atoms can be related to the π-donating ability of the cage substituents.[37] Figure 4.33 and Figure 4.34 show that for these compounds the correlation with C-N and C-C bond lengths is poor although the general trend is still discernible.

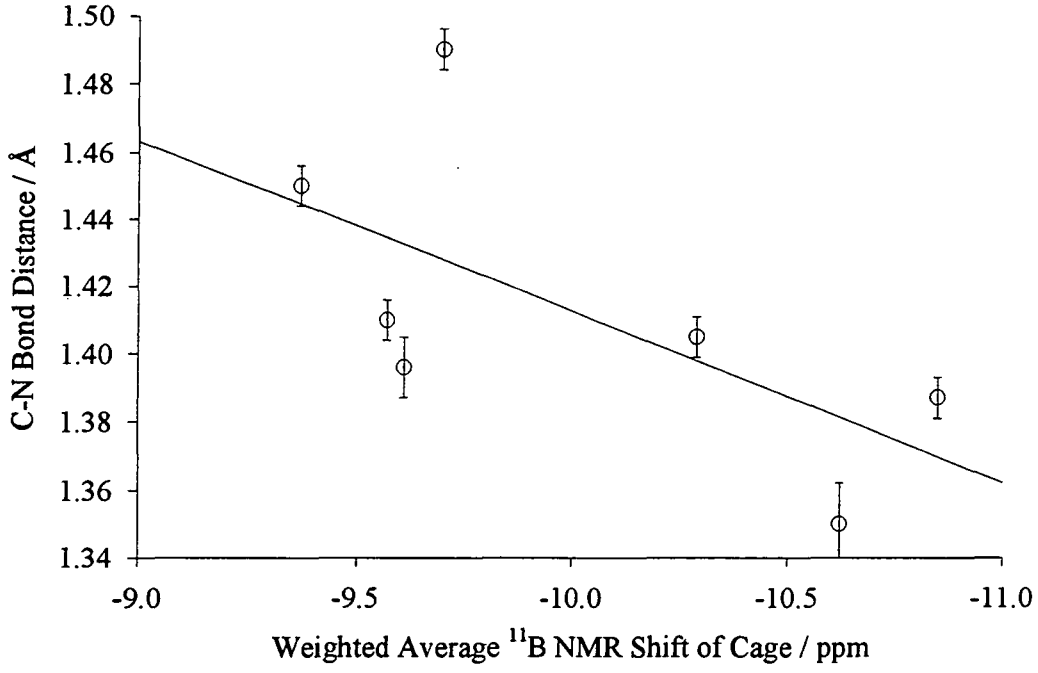

Figure 4.33

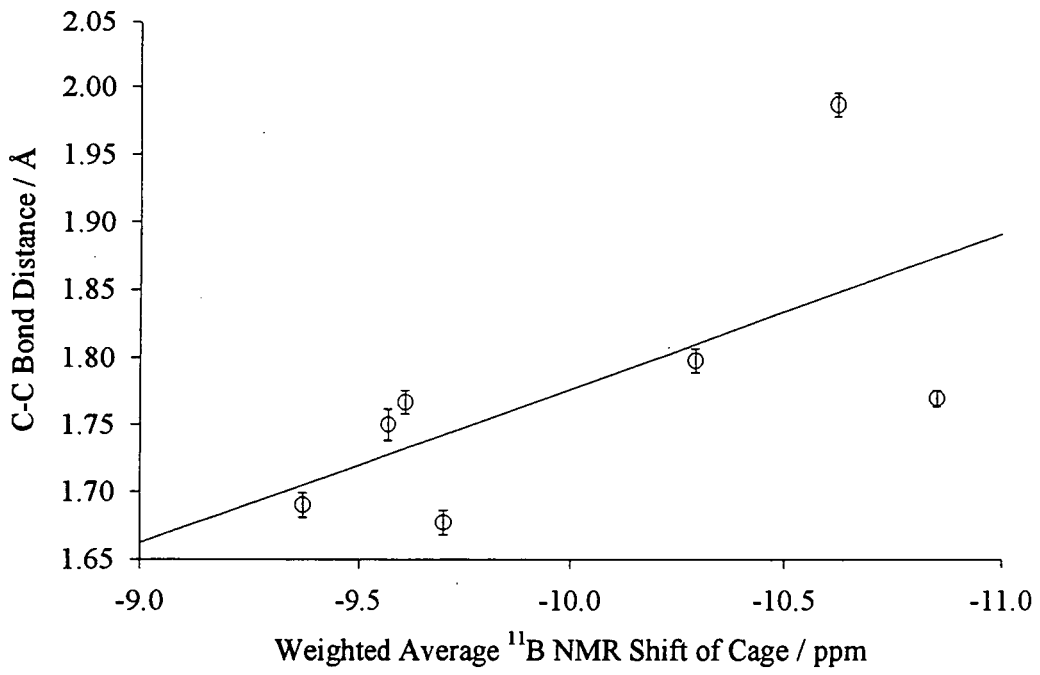

Figure 4.34

The Antipodal shift can be expressed as the difference between δ ^{11}B of B12 and δ $^{11}B_{ave}$ (α-B12), previous studies having found that such corrections aided the comparison of shifts.[37] Figure 4.35 and Figure 4.36 show a correlation between C-N and C-C distances and α-B12 similar to that for δ B12. There is no apparent improvement in considering the α-shift as opposed to the uncorrected ^{11}B shift in this series. Such treatments would have obvious advantages when comparing data from different sources where referencing of spectra was unsure or unreliable as the α-shift is unrelated to the absolute values, depending solely on the separation of peaks.

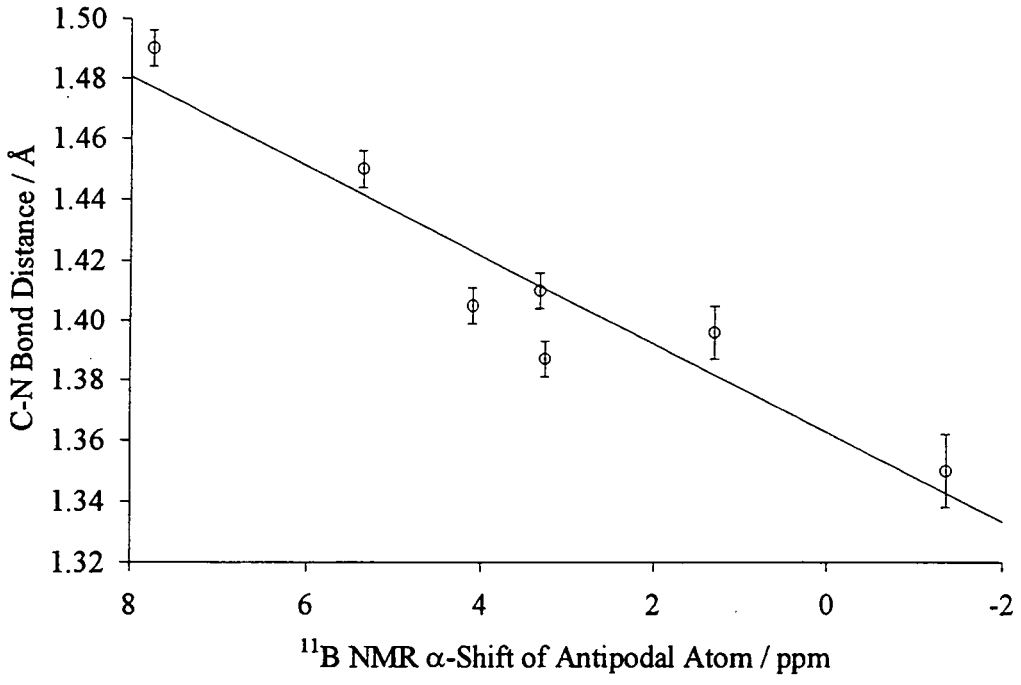

Figure 4.35

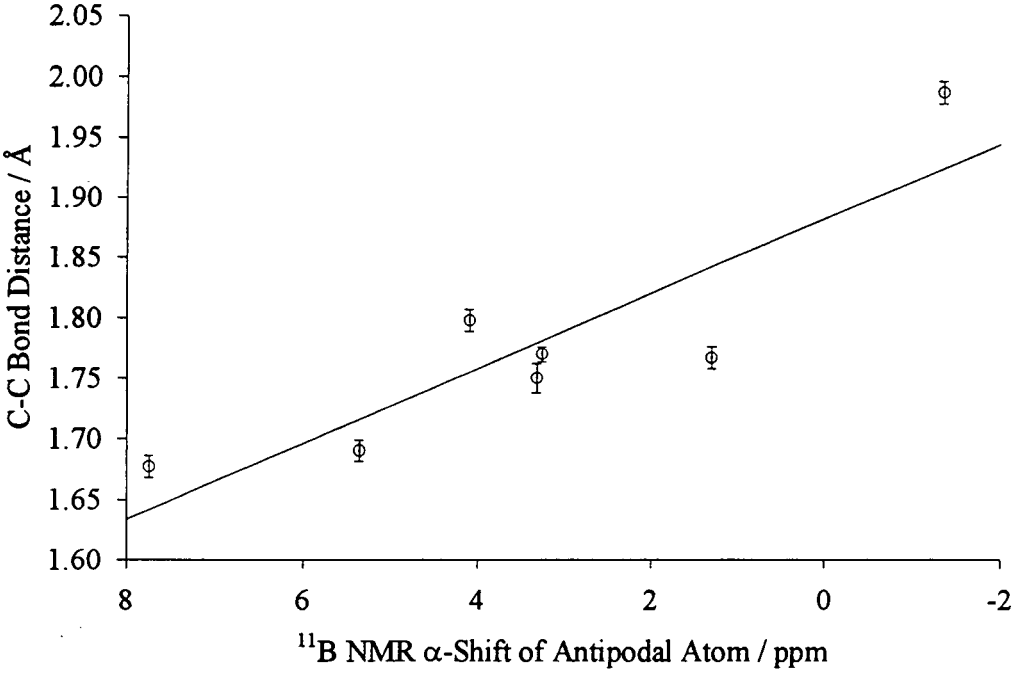

Figure 4.36

The shifts of the BH protons revealed by $^{1}H\{^{11}B\}$ NMR can be assigned using ^{1}H-^{11}B HETCOR experiments. The shifts of the Hs bonded to the antipodal B (^{1}H δ-H12) are seen to show the same relationship with both C-N and C-C distance as δ B12, decreasing frequency of the antipodal H with increased π-bonding to the cage suggesting increased shielding (Figure 4.37 and Figure 4.38). There is a close correlation between ^{11}B δ B12 and ^{1}H δ H12 (Figure 4.39). It appears that charge transfer to the antipodal B atom also affects the shielding of this H atom.

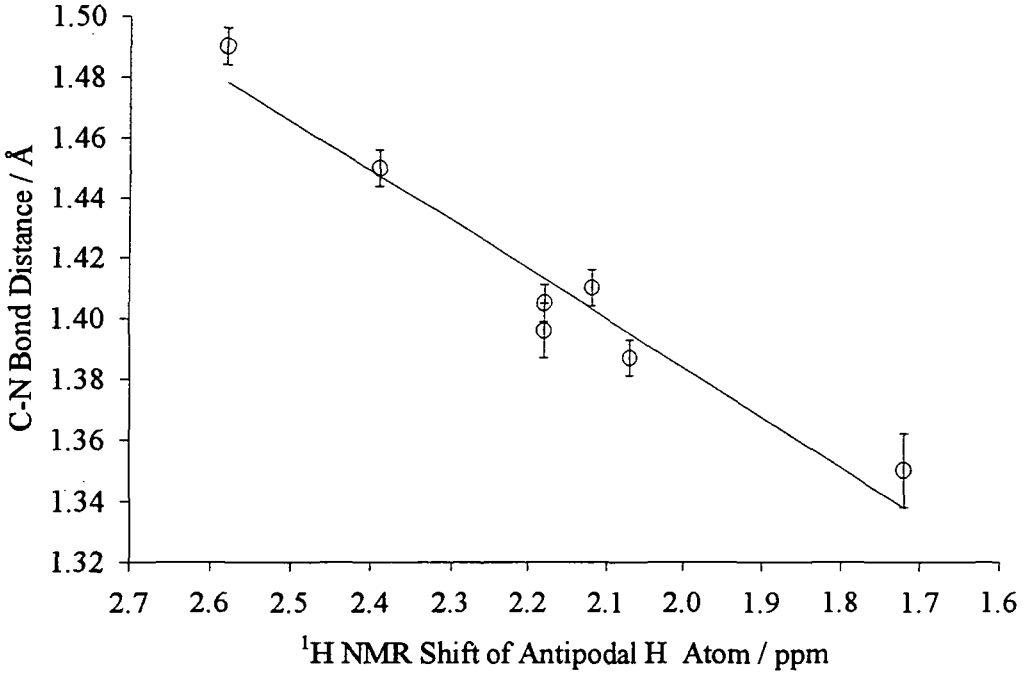

Figure 4.37

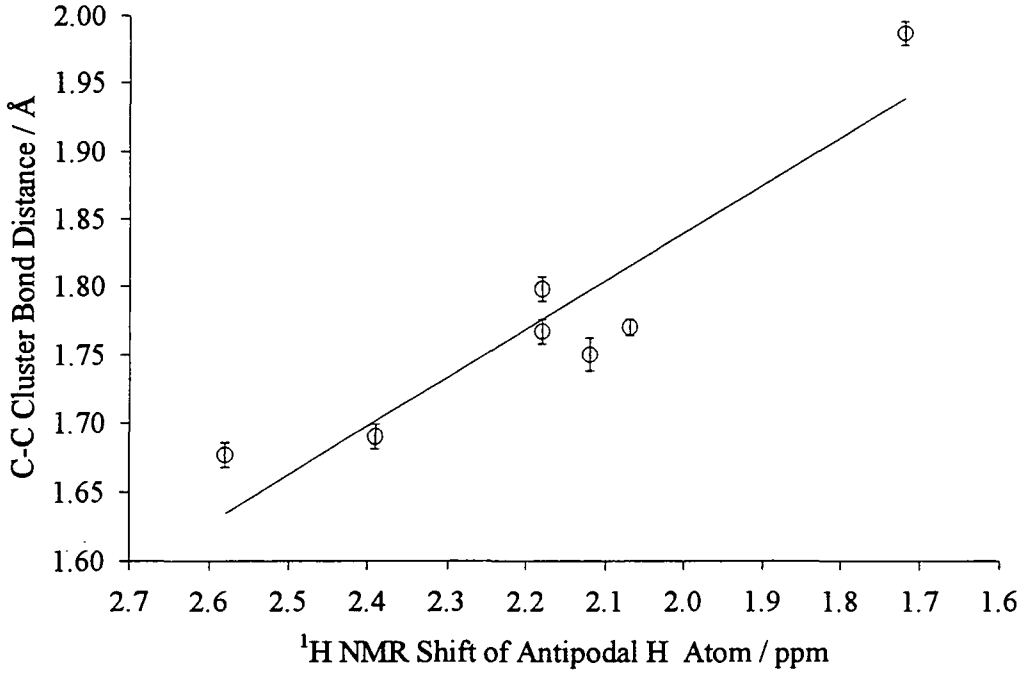

Figure 4.38

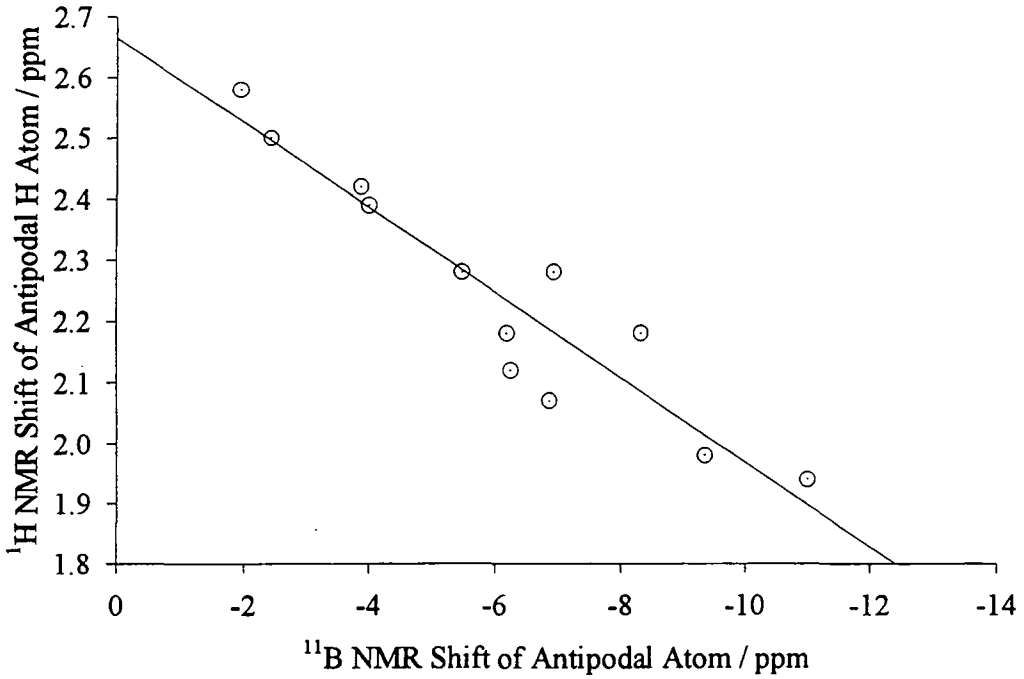

Figure 4.39

4.6.10 CHARGE DENSITIES

Charge densities calculated by Mulliken Population Analyses are somewhat arbitrary and must be treated with caution. They can however be useful in treating a series of similar compounds. Table 4.13 summarises charge densities calculated by the AM1 method for this series of nitrogen substituted carboranes for the carborane cage, the RCb fragment, the NHR' or N=X fragment and the R group. Table 4.14 contains charges on selected atoms.

Compound	N=X / NR'R"	RCb	R	Cb	C-N π-bond
$(MeCb)_2NH$	–0.070	+0.035	+0.122	–0.087	0.113
$(PhCb)_2NH$	–0.055	+0.028	+0.216	–0.188	0.124
$(PhCb)_2N^-$	–0.303	–0.349	+0.027	–0.376	0.357
$PhCbNH_2$	+0.075	-0.075	+0.039	-0.114	0.127
MeCbNHNHPh	–0.004	+0.004	+0.158	–0.162	0.128
PhCbN=NTol	+0.081	–0.081	+0.063	–0.144	0.070
PhCbN=O	+0.097	–0.097	+0.068	–0.165	0.056

Table 4.13 Charge Densities on Selected Groups

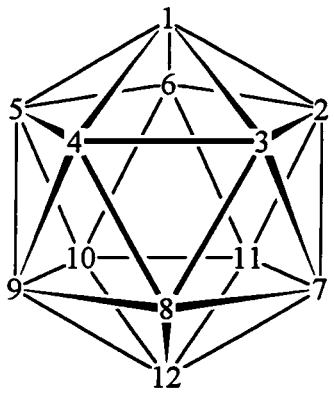

Compound	20	22	23	24	26	27	32
Atom							
C1	–0.355	–0.065	–0.080	+0.006	–0.207	–0.096	–0.108
C2	–0.162	–0.196	–0.248	–0.253	–0.166	–0.301	–0.218
B3	+0.018	–0.011	–0.008	–0.043	+0.014	+0.009	–0.038
B4	–0.028	–0.028	–0.035	–0.042	–0.022	–0.031	–0.010
B5	–0.021	–0.050	–0.056	–0.036	–0.024	–0.044	–0.020
B6	+0.018	–0.044	–0.025	–0.017	–0.000	–0.034	–0.043
B7	–0.025	–0.038	–0.031	–0.041	–0.039	–0.028	–0.031
B8	–0.093	–0.095	–0.087	–0.116	–0.101	–0.080	–0.091
B9	–0.060	–0.057	–0.058	–0.074	–0.063	–0.047	–0.064
B10	–0.091	–0.086	–0.087	–0.117	–0.093	–0.072	–0.091
B11	–0.042	–0.011	–0.027	–0.017	–0.028	–0.019	–0.015
B12	–0.061	–0.061	–0.063	–0.090	–0.061	–0.058	–0.068
H12	+0.069	+0.073	+0.072	+0.042	+0.068	+0.071	+0.069

Table 4.14 Charge densities on cage atoms

There is no obvious trend observed in the charges on the Cb or RCb group other than that the anion $(PhCb)_2N^-$ **24** as expected has the greatest charge. This reflects the fact that both resonance and inductive effects will determine the charge on the cage. The charge on C1 however does follow a clear trend, being most positive in the anion $(PhCb)_2N^-$ **24** and becoming more negative with reducing π-bond to the cage. The opposite trend is observed in the charge on C2, this becoming more negative with increased π-bonding.

As previously observed no trend is observed between ^{11}B δ B12 and the charge on B12. It has been suggested that these shifts can be related to the electron densities in the radial and tangential p-orbitals. If the radial and tangential p-orbitals (p_r and p_t) are considered separately (Table 4.15) it can be seen that the differences in these electron

densities are small, only the anion **24** showing a significant difference. However, a straight line of best fit drawn through these two series of points (Figure 4.40) shows the previously established trend, with p_t increasing and p_r decreasing with increasing shielding, p_t showing the greatest change. The changes in charge densities are too small for any trend to be observed with any reliability. Previous studies have involved a much greater range of chemical shifts giving larger differences in charge densities.

Compound	B-p_r	B-p_t	B-p_x	B-p_y	C-p_x	C-p_y
1	0.7294	1.1573	0.5822	0.5751	0.9495	1.1041
3	0.7255	1.1605	0.5884	0.5721	0.8891	1.0889
4	0.7279	1.1661	0.5911	0.5750	0.9007	1.0946
5	0.7233	1.2103	0.6132	0.5971	0.8258	0.9974
7	0.7278	1.1598	0.5821	0.5777	0.9301	1.0821
8	0.7260	1.1656	0.5919	0.5737	0.8915	1.0956
13	0.7305	1.1587	0.5770	0.5817	0.9246	1.0446

Table 4.15 Electron densities in radial and tangential p-orbitals

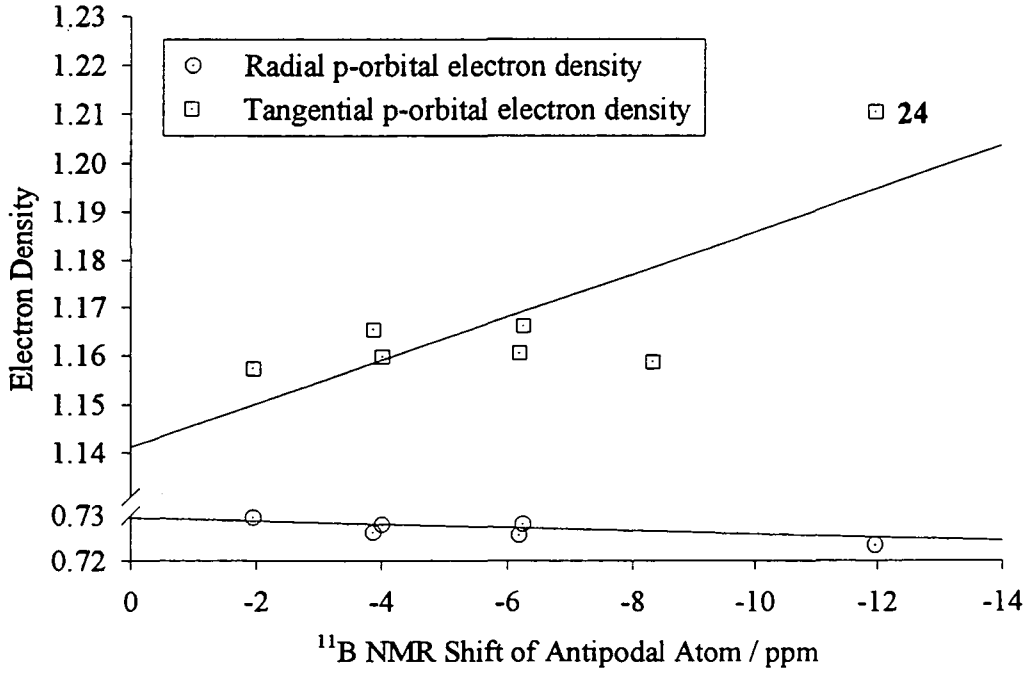

Figure 4.40 Electron density in radial and tangential p-orbitals vs ^{11}B δ-B12

There appears to be no correlation between the charge on the H bonded to B12 and the ^{1}H shift of this atom. Although there are differences in the charges on this H atom they do not explain the ^{1}H NMR shifts in terms of nuclear shielding. As this shift is not related to a change in the charge on the H atom, it may be related to shielding associated with an increase in electron density on the surrounding atoms.

In all cases the substituent R on C2 carries a positive charge indicating electron withdrawal from these substituents. In the compounds $(MeCb)_2NH$ and $(PhCb)_2NH$ the positive charge on the Ph is greater than on the methyl, possibly due to π-bonding to the cage not possible for methyl groups. In all Ph substituted carboranes these calculations give a π-bond order of approximately 0.05 between the phenyl ring and cage. These phenyl rings are orientated so that the aromatic π-system is aligned with the C-p_x on C2. However, this orientation of the ring is not believed to be the lowest energy state in either the solid or gas phase for the parent compound PhCbH.[38] Steric interactions in these compounds will be significant in favouring this orientation in substituted species.[39]

4.6.11 Factors Influencing Exo-π-Bonding

Bond lengths, associated bond orders and ^{11}B NMR shifts of the antipodal atom can be used to assess the degree of *exo*-π-bonding in a series of substituted carboranes. Figure 4.41 shows these compounds in descending order of C-N *exo*-π-bond.

$(PhCb)_2N^-$	Decreasing π-bond order ↓	$MeCbNH_2$
$PhCbNH_2$		MeCbNHNHPh
PhCbNHNHPh		MeCbNHOH
$(PhCb)_2NH$		$(MeCb)_2NH$
PhCbNHOH		$MeCbN_2Ph$
$PhCbN_2Tol$		MeCbNO
PhCbNO		

Figure 4.41

The most π-bonding is displayed by the anion $(PhCb)_2N^-$. This is due to the greater availability of electron charge for delocalisation.

Less π-bonding is seen in the RCbN=X compounds than the RCbNR'R" compounds. This can be attributed to the hybridisation of the lone pair on N, p-p π-

overlap will be more efficient than sp^2-p overlap. In RCbNR'R" species rehybridisation occurs from pyramidal sp^3 N (as in ammonia) towards sp^2 N with the lone pair orbital gaining an increasing amount of p-character. This increases π-overlap between the lone pair and C p_x orbital. This is a similar effect to that observed in anilines, aniline itself have a flattened although still pyramidal N, $FmesNH_2$ **2** being planar.

This rehybridisation is not seen in RCbNX species, the C1-N-X angles showing no signs of increasing to indicate rehybridisation from sp^2 to sp which would increase the p-character of the lone pair and increase π-overlap with the cage. This is due to the greater energy difference between sp and sp^2 than between sp^2 and sp^3. The reduction in energy of the molecule due to the formation of the π-bond is clearly of sufficient magnitude to justify the rehybridisation of the N from sp^3 to sp^2 in RCbNR'R" compounds but not sp^2 to sp in RCbNX compounds. Likewise, the anion $(PhCb)_2N^-$ retains an sp^2 N and shows no tendency to rehybridise to sp to provide two p orbitals for π-bonding.

The electronegativity of the other atoms attached to the N also has an effect on the degree of π-bonding. In the RCbNX compounds the nitroso displays significantly less π-bonding than the azo compounds. This is due to the more electronegative O atom reducing the electron density on the donor N by an inductive electron withdrawal and hence reducing the π-donor capacity of the N atom. This is also observed for RCbNR'R" with RCbNHNHAr displaying less π-bonding than $RCbNH_2$, and RCbNHOH less than RCbNHNHAr. If ^{11}B δ B12 is plotted against the sum of the Pauling electronegativities of the substituents on N this relationship is clear, with two series evident for RCbNX and RCbNR'R" (Figure 4.42). As electronegativity effects are transmitted through bonds it might be expected that doubly bonded substituents might have a greater effect. If this is taken in to account by counting doubly bonded atoms twice all points are seen to fall on the same line (Figure 4.43).

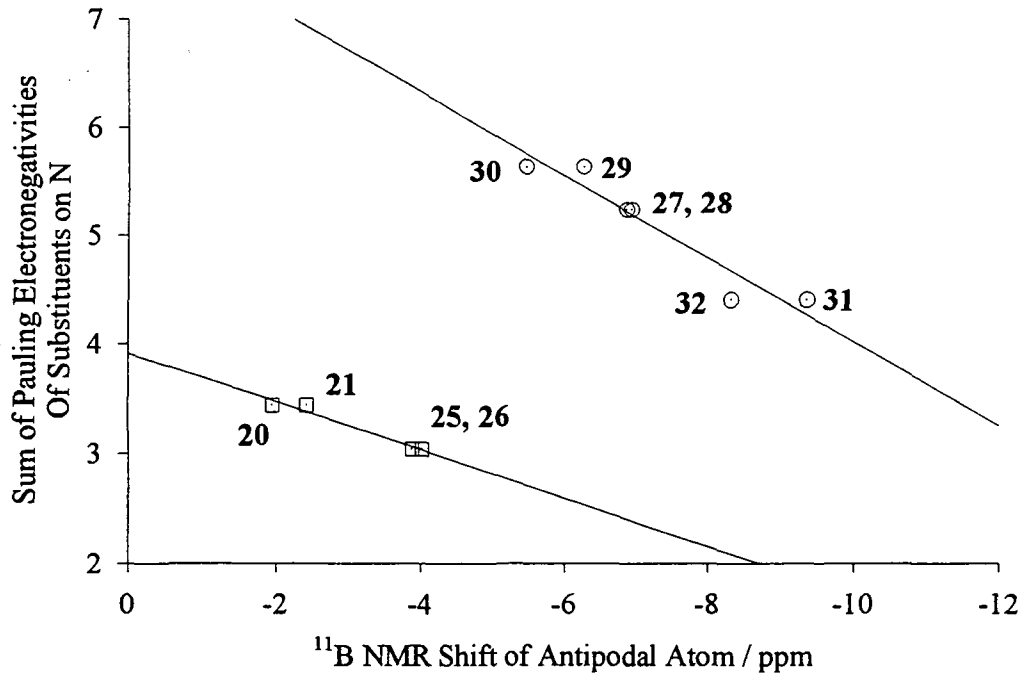

Figure 4.42

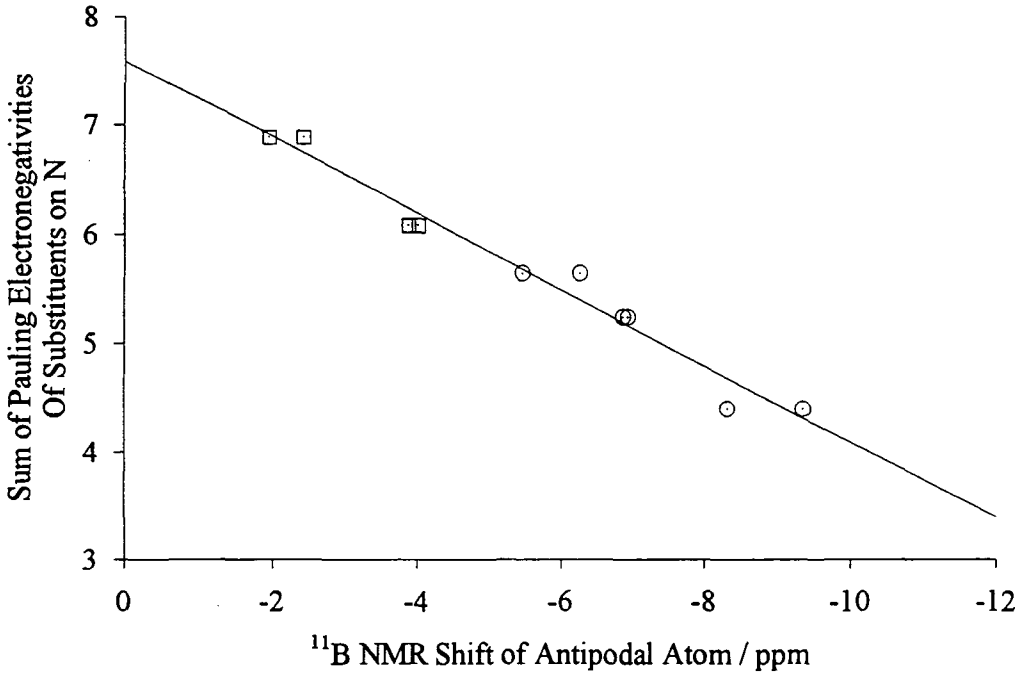

Figure 4.43

4.6.12 Intramolecular Interactions

All compounds characterised by X-ray diffraction have substituents on C2 so that the carbon atoms can be distinguished from the boron atoms. So far it has been assumed that this substituent has no effect on the orientation of the nitrogen substituent. However, it is clearly a possibility that such intramolecular interactions could have an effect. As X-ray structures of compounds unsubstituted at C2 cannot be obtained with a reliable assignment of C2 a series of molecular orbital geometry optimisation calculations have been carried out to assess the effect of intramolecular interactions.

4.6.12.1 Intramolecular Interactions in Primary Amines

AM1 calculations have been carried out on $HCbNH_2$. Energies and π-bond orders were calculated for a variety of orientations of the NH_2 group (defined by the dihedral angle C2-C1-N-H for one of the H atoms). Due to poor treatment of the carborane cage using this method the cage coordinates were not optimised although the coordinates of the subsituents were optimised. The cage coordinates used were those of an ideal icosahedron with all cluster bonds of 1.77Å and all exo bonds to H 1.19Å. Figure 4.44 shows the variation in energy (relative to the minimum) and C-N π-bond order for this compound.

It can be seen that there are two energy minima corresponding to the orientations with the lone pair in the plane of the C-C cluster bond. As expected these energy minima correspond to the maximum π-bonds.

The calculation was repeated with both methyl and phenyl substituents on C2, the positions of these groups being optimised. Although there is some change in the relative energies the overall appearance of the profiles remains unchanged, the energy minima corresponding to the same orientation of the amino substituent (see Appendix A for graphs). Similar calculations repeated for hydroxylamines HCbNHOH, MeCbNHOH and PhCbNHOH gave similar results (Also see Appendix A).

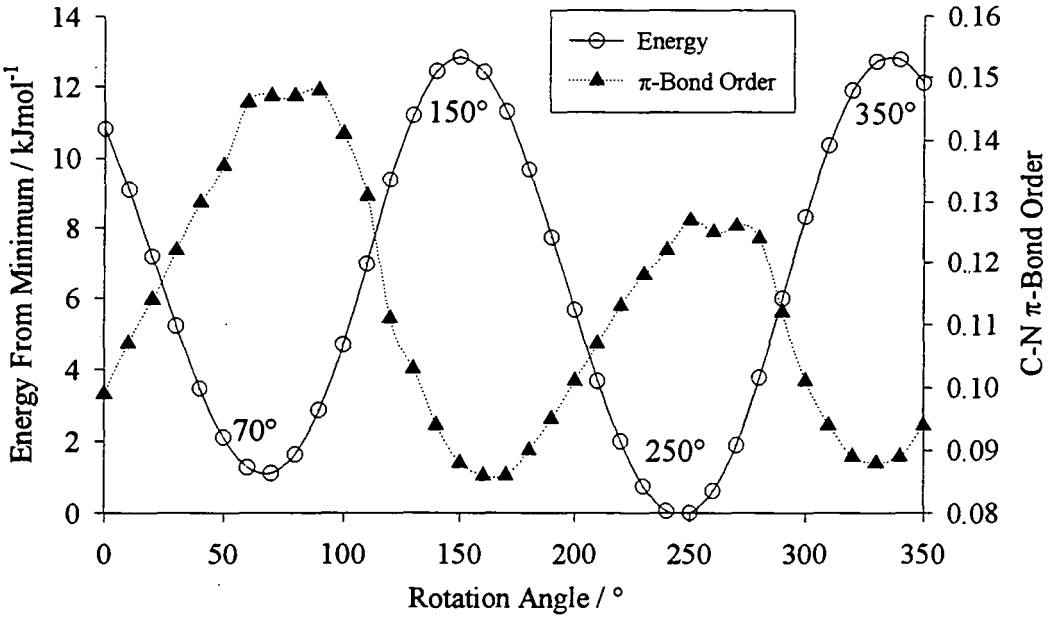

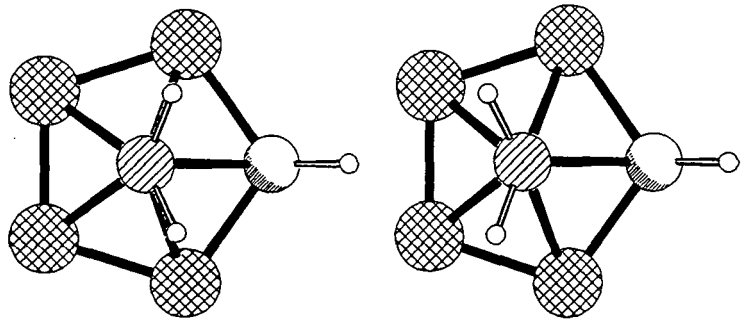

Preferred Orientations

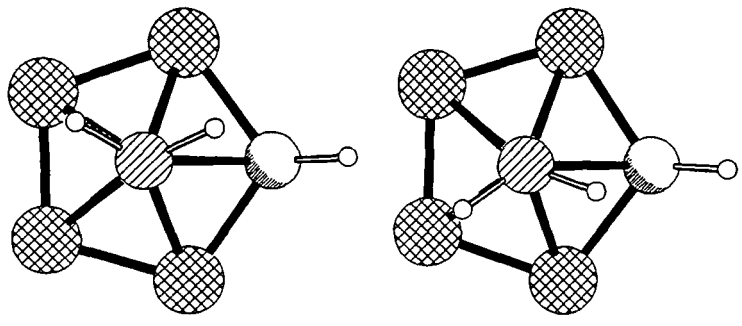

Least Favourable Orientations

Figure 4.44 **Energy and C-N π-bond profiles for rotation of NH_2 group about C-N bond in $HCbNH_2$. Pictures show a view down the N-C bond, the lower half of the molecule and H's on B are omitted.**

While useful, these calculations are at a relatively low level and the use of an ideal cage will clearly affect these results in some manner. *Ab initio* calculations have been carried out on the simpler unsubstituted compound $HCbNH_2$ to gain some idea of the validity of these results.

Calculations were initially carried out at the RHF/STO-3G level. Atomic positions for the cage were taken to be those from molecule D of $PhCbNH_2$ with the phenyl group replaced by a hydrogen. All atomic positions were optimised.

If the NH_2 group is assumed to be planar with this plane parallel to the C-C bond, the conformation opposite to that found in the solid state structure of $PhCbNH_2$, this conformation is retained after optimisation. However, if the plane of the NH_2 group is turned through just 10° optimisation results in a structure with pyramidal nitrogen and the lone pair in the C-N plane, H atoms pointing away from the CH (Figure 4.45A). The energy of this geometry is lower than that in the previous geometry by 1.7 $kJmol^{-1}$. Further optimisation at the higher RHF/3-21G level retains this conformation although the nitrogen environment is more nearly planar (Figure 4.45B). The C-N bond length from the 3-21G geometry is identical within experimental error to that found in the solid state structure of $PhCbNH_2$. The C-C bond is somewhat shorter (0.06Å), this is to be expected in an unsubstituted carborane due to both steric and electronic effects. Selected data for these geometries are given in Table 4.16. For comparison, average values for the solid state structure of $PhCbNH_2$ are also given.

If the H atoms of the amino group are initially placed pointing towards the CH, equivalent to the solid state structure of $PhCbNH_2$, optimisation at the RHF/STO-3G level retains this structure (Figure 4.45C), although the energy of the system is higher than that of the previous STO-3G geometry. Further optimisation at the RHF/3-21G level causes inversion of the N centre resulting in a structure almost identical to the previous 3-21G geometry. These results confirm those of the AM1 calculation, that the equilibrium structure in the gas phase of $HCbNH_2$ has the lone pair in the C-C-N plane and amino Hs pointing away from the CH. The preference for this structure as opposed to that with the amino H's pointing towards the CH may arise from electrostatic interactions between the positively charged H on C2 and the positively

charged amino Hs. The major factor in determining the orientation does appear to be the formation of the π-bond.

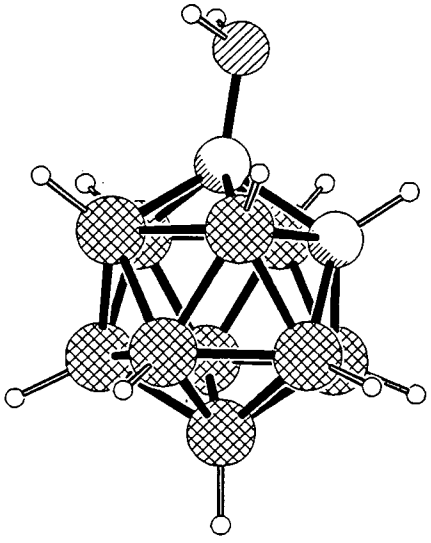

A) STO-3G

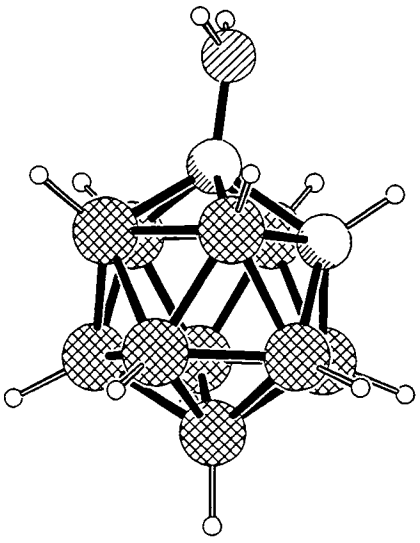

B) 3-21G

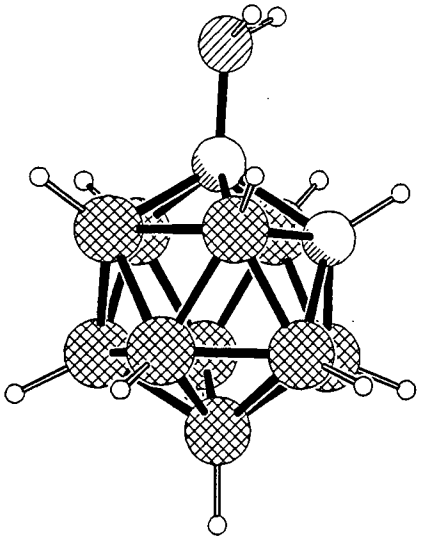

C) STO-3G

Figure 4.45 ***Ab initio*** **geometries of $HCbNH_2$**

	STO-3G (A)	3-21G (B)	STO-3G (C)	$PhCbNH_2$
C-N	1.459	1.399	1.451	1.396(3)
C-C	1.675	1.705	1.688	1.767(3)
$N-H_A$	1.031	0.999	1.029	1.008(14)
$N-H_B$	1.031	0.999	1.029	1.005(14)
$C-N-H_A$	108.70	117.30	110.81	113.5(11)
$C-N-H_B$	108.70	117.30	110.81	115.0(11)
H_A-N-H_B	107.25	116.24	108.74	115.8(17)
$C2-C1-N-H_A$	-121.92	-107.22	60.38	63
$C2-C1-N-H_B$	121.87	107.22	-60.43	-77
N-C1-C2	114.6	116.2	120.3	118.38(17)
N-C1-B3	115.5	115.8	117.8	118.7(2)
N-C1-B4	125.2	124.0	120.9	123.0(2)
N-C1-B5	125.2	124.0	121.0	121.8(2)
N-C1-B6	115.5	115.8	117.8	177.03(2)
$\Sigma\angle N$	324.45	350.84	330.36	344
Total Energy / eV	-379.967	-382.462	-379.962	-

Table 4.16 Selected data of *ab initio* geometries of $HCbNH_2$

4.6.12.2 Intramolecular Interactions in Nitroso-Carboranes

AM1 calculations have been carried out on HCbNO in the same manner as the previous calculations with optimisation of the NO substituent and an ideal cage. The results of these calculations are shown in Figure 4.46. The energy profile again reveals that the most stable conformations are those where π-bonding is maximised and is analogous to that found in the solid state structure of PhCbNO **1**. The calculation was repeated for MeCbNO and PhCbNO giving similar results (see Appendix A).

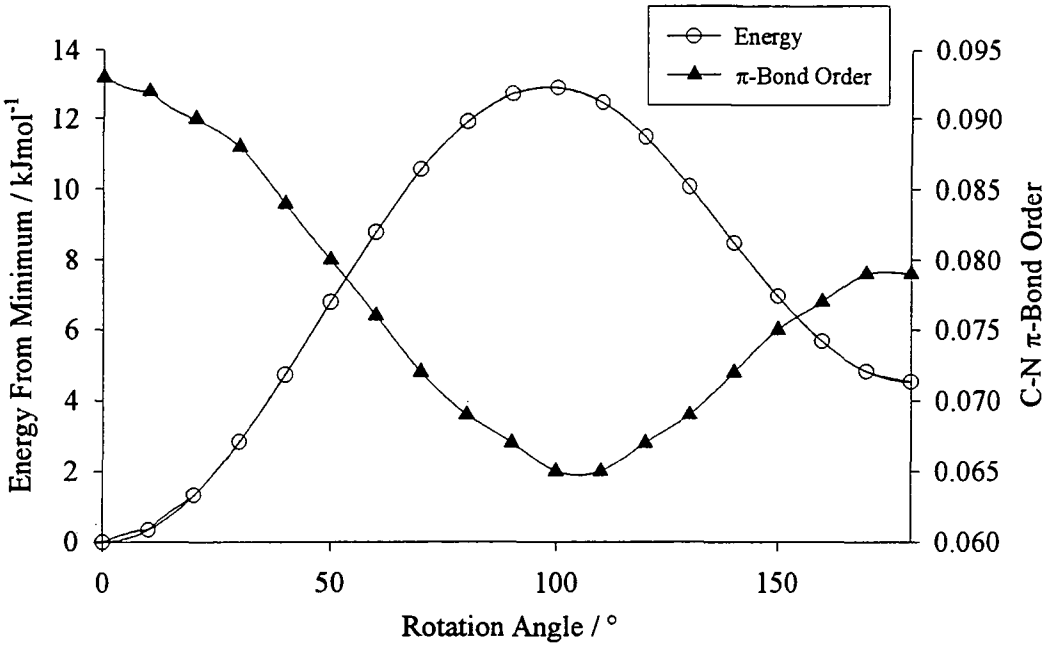

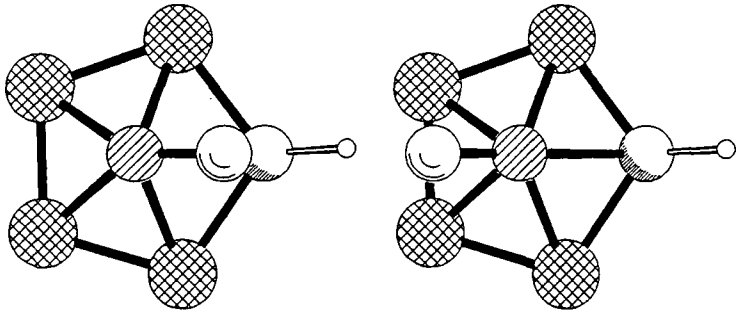

0° 180°

Favoured Orientations

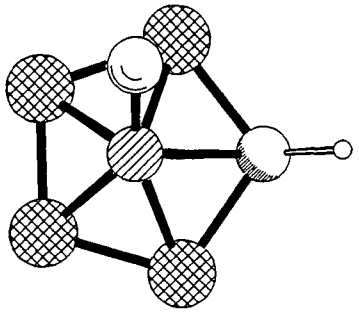

90°

Least Favourable Orientation

Figure 4.46 **Energy and C-N π-bond profiles for rotation of NO group about C-N bond in HCbNO. Pictures show a view down the N-C bond, the lower half of the molecule and H's on B are omitted.**

Ab initio calculations have been performed on the unsubstituted compound HCbNO. The initial cage geometry was taken to be that of PhCbNO from the solid state structure with the phenyl group replaced by a H. The NO group was placed perpendicular to the C-C bond. After optimisation of all atomic positions the equilibrium geometry was found to be analogous to that of PhCbNO in the solid state with the NO group parallel to the C-C bond and pointing away from C2. Further optimisation at the RHF/3-21G level retains this conformation with only minor changes in bond lengths and angles (Figure 4.47). The C-N bond length from the 3-21G geometry is slightly shorter than that in the solid state structure of PhCbNO and the C1-N-O angle somewhat smaller. Selected data for these geometries are given in Table 4.17. Also included are data for the solid state structure of PhCbNO for comparison.

If the initial conformation is taken to be that with the NO group pointing towards the CH this geometry is retained upon optimisation at the RHF/STO-3G level, and when further optimised at the RHF/3-21G level this conformation is retained and found to have an energy very slightly lower than the previous 3-21G geometry.

The AM1 and *ab initio* calculations are in agreement that ideally the NO group will lie in the N-C-C plane. They are in disagreement over the direction of this NO group, the more reliable *ab initio* calculations indicate that it makes little difference in the absence of steric effects whether this group points towards C2 or away. This will be altered if a bulky group is placed on C2.

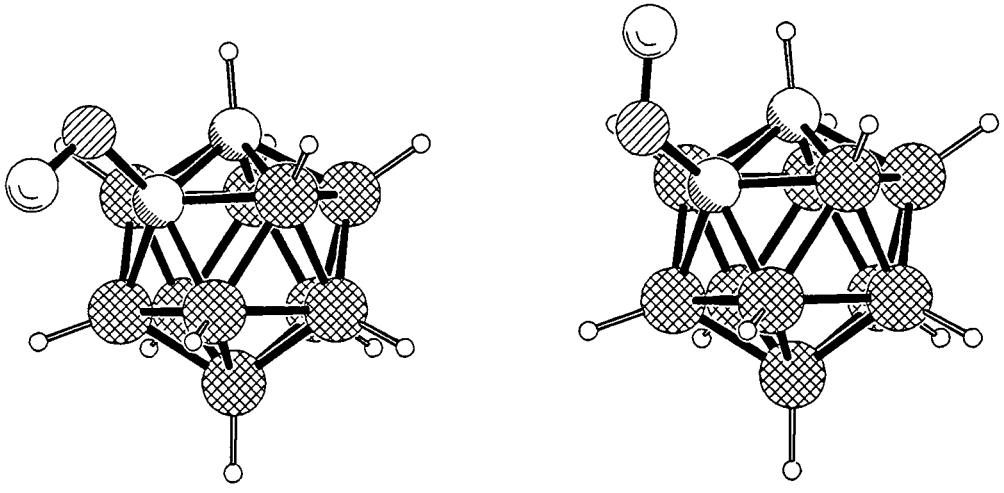

Figure 4.47 3-21G geometries of HCbNO

	STO-3G (A)	3-21G (B)	STO-3G (C)	3-21G (D)	PhCbNO
C-N	1.537	1.463	1.537	1.461	1.490(2)
N-O	1.227	1.212	1.227	1.214	1.182(2)
C1-C2	1.640	1.625	1.647	1.634	1.677(2)
C2-H	1.080	1.070	1.080	1.066	-
C1-N-O	111.25	113.22	111.80	113.87	113.0(2)
N-C1-C2	112.97	112.65	119.85	118.34	112.14(12)
N-C1-B3	114.40	113.40	116.87	115.96	114.65(13)
N-C1-B4	124.70	123.23	119.40	118.87	123.99(13)
N-C1-B5	124.77	123.19	119.44	118.82	123.49(13)
N-C1-B6	114.48	113.35	116.91	115.93	114.14(13)
C2-C1-N-O	180.03	179.94	0.02	0.01	164.67
Total Energy	-452.576	-455.627	-452.574	-455.629	-

Table 4.17 Selected data for *ab initio* geometries of HCbNO

4.6.12.3 Angle of Substituent to Cage

In all of the structures of N-substituted carboranes described in this chapter the two substituents on C1 and C2 can be seen to bend towards each other. This would seem unlikely to be due to single cause as it is observed in both methyl and phenyl substituted cages which are very different in nature. Although this could be attributed to crystal packing effects this seems unlikely as similar observations are made in the *ab initio* geometries calculated for $HCbNH_2$ and HCbNO and can be seen clearly in Figure 4.45. It is possible that intramolecular interactions are responsible for this, possibilities are illustrated in Figure 4.48. These include CH···N hydrogen bonds for species with H or Me on C2 or incipient nucleophilic attack for phenyl substituted species, both of which will be enhanced through the electron withdrawing nature of the cage.

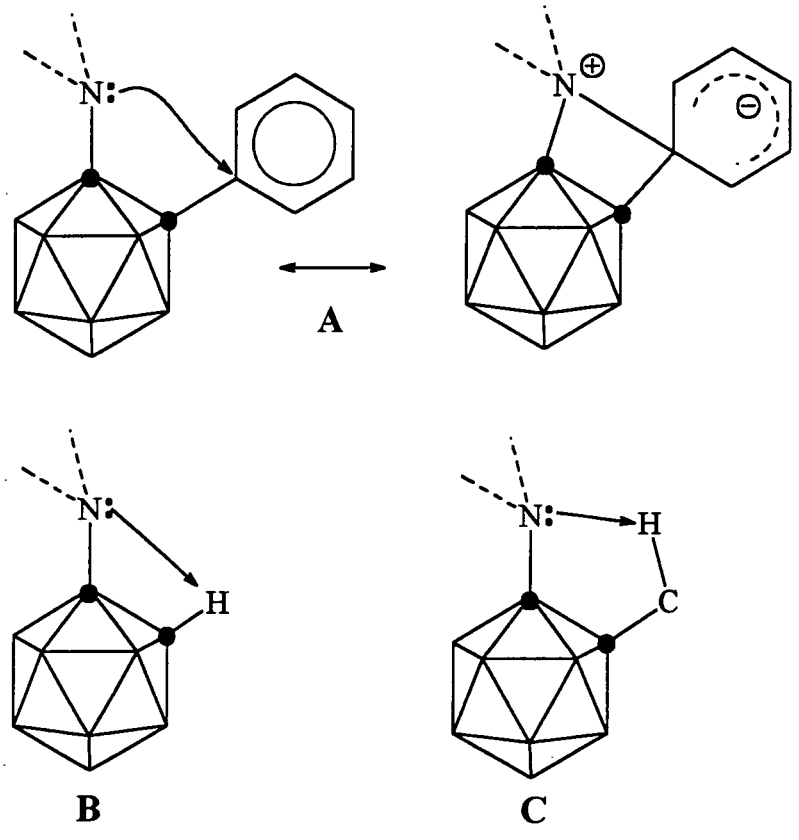

Figure 4.48

4.6.12.4 Conclusions From Molecular Modelling Studies

Comparison between AM1 studies using ideal cages and both X-ray structures and *ab initio* calculations reveals that such calculations can provide valuable information on the orientations of such groups. The AM1 calculations appear adequate for the

location of minima and maxima in energies although the relative energies of these are inaccurate.

Both AM1 and *ab initio* calculations on the carboranes unsubstituted at C2 indicate that the orientations of substituents in the crystal structures are dominated by electronic interactions with the cage and not steric interactions between the N substituent and either Me or Ph substituent which is there to aid crystallographic determination.

4.7 OXYGEN-SUBSTITUTED CARBORANES

Relatively few oxygen substituted carboranes are known being restricted to the C-hydroxy *ortho*[40] and *meta*-carboranes[29] and the anion of PhCbOH[17]. Of these the anion $PhCbO^-PS^+$ has been mentioned previously as displaying considerable π-bonding between the oxygen and carborane cage. Recent work has determined the structure of the parent compound PhCbOH as a hydrate and reveals that this compound also displays considerable exo-π-bonding.[41] The position of the hydrogen is in a plane perpendicular to the C-C cluster bond implying a lone pair in a p-orbital aligned with the C-p_x in a manner analogous to that in the nitrogen systems. The C-O distance in this compound (1.366(2)Å), while longer than in the anion is shorter than a single C-O bond (1.432Å) and comparable to that in phenols (1.362Å). The C-C cluster bond in this compound is lengthened to 1.723(3)Å.

Parameter	PhCbOH	$PhCbO^-$
C-O distance	1.366(2)	1.245(3)
C-C distance	1.723(3)	2.001(3)
C-O π-bond	0.103	0.706
C-C Bond order	0.532	0.174
^{11}B δ B12	-11.40	-21.06
$^{11}B_{ave}$ B12	-11.24	-11.21
^{11}B α-B12	-0.24	-9.85
Electron density in p_r	0.7287	0.7187
Electron density in p_t	1.1170	1.2345

Table 4.18 Selected data for oxygen substituted carboranes

AM1 calculations on these compounds using the atomic coordinates from the X-ray diffraction experiments reveal, as expected, a significant π-bond order between the C and O, far greater in the anion $PhCbO^-$ than the parent alcohol. These calculations confirm the assumption that it is the C-p_x orbital which is involved primarily in exo-π-bonding, 70% of this π-bond being attributed to interaction between the p_x orbitals on both C and O in anion $PhCbO^-$ and 72% in OH.

Figure 4.49 reveals a similar trend to that in the nitrogen system with the C-C bond lengthening as the C-O bond shortens. This is again due to increasing exo-π-bonding involving the C-p_x reducing the contribution of the $5e_1(x)$ orbital to cluster bonding. A similar trend is observed if the degree of exo-π-bonding is considered (Figure 4.50) with the point for PhCbOH falling on the line for the nitrogen system.

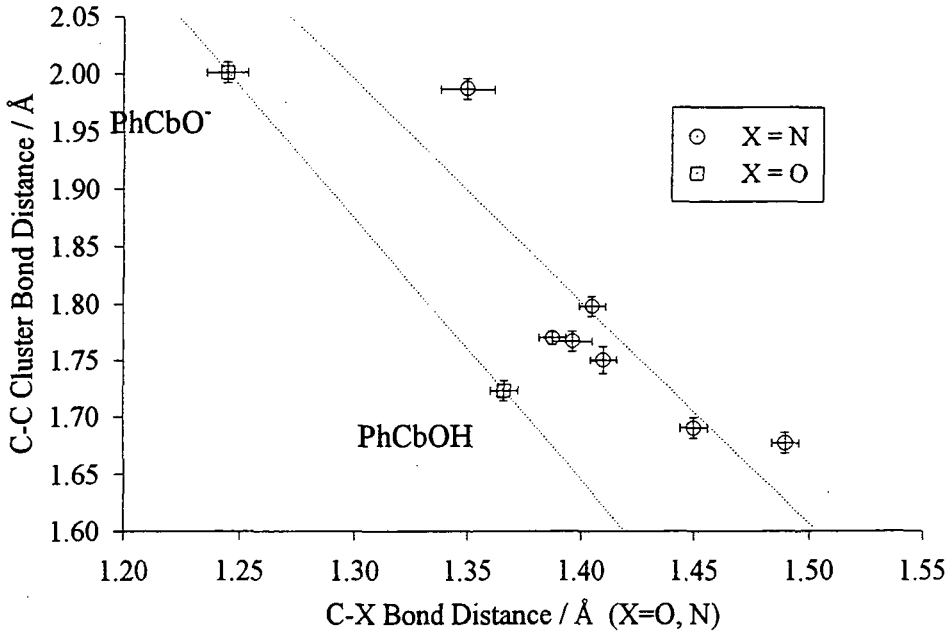

Figure 4.49

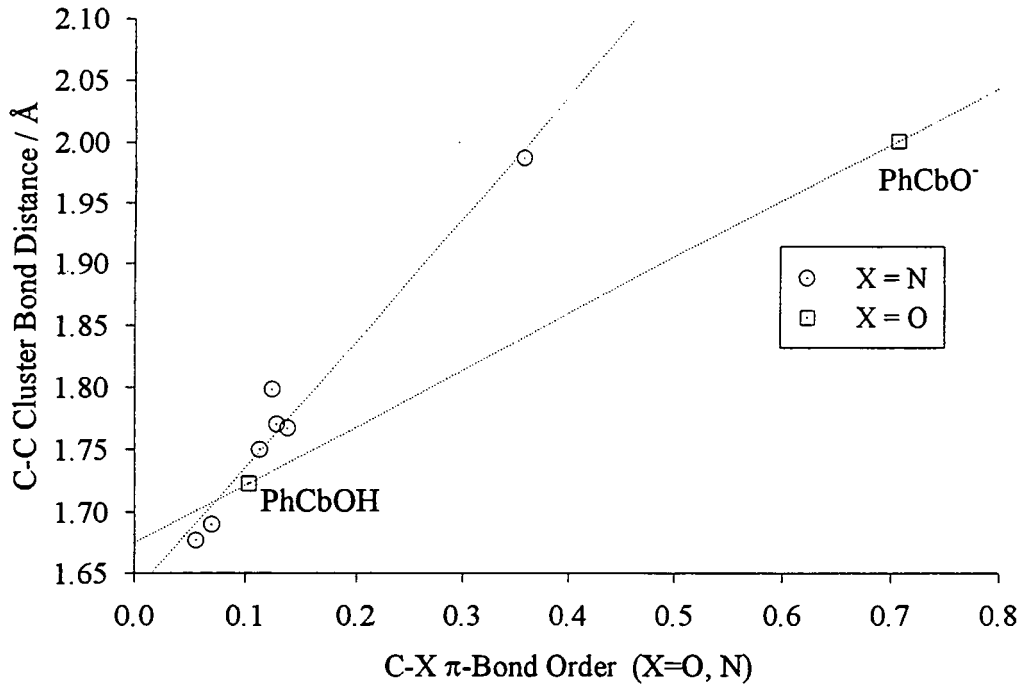

Figure 4.50 C-X π-bond order vs C-C cluster bond distance

Similar trends are also observed in the ^{11}B NMR of the antipodal atom with the anion having a more pronounced antipodal shift than the parent compound. Figure 4.52 shows a plot of ^{11}B δ B12 vs C-X distance (X = O, N). Remarkably these points all appear to fall on one line, although this may arise from coincidence. The points for a plot of ^{11}B δ B12 vs C-C cluster bond distance form two separate lines which appear to have a similar gradient, although the paucity of data for the oxygen system hinders such comparisons. If the antipodal shift is considered to indicate the degree of π-delocalisation onto the cage, it might be expected that these points would fall on the same line with a given lengthening of the C-C distance being caused by a given amount of charge delocalised onto the cage. The fact that this is not seen may be reflective of π-bonding in the O system involving the C-p_y which will result in an antipodal shift in the same manner as the C-p_x but affect the C-C bond differently. This is, however, not supported by a plot of ^{11}B δ B12 vs C-X π-bond order (Figure 4.51). Other factors than the C-X π-bond order are clearly involved in the antipodal shift.

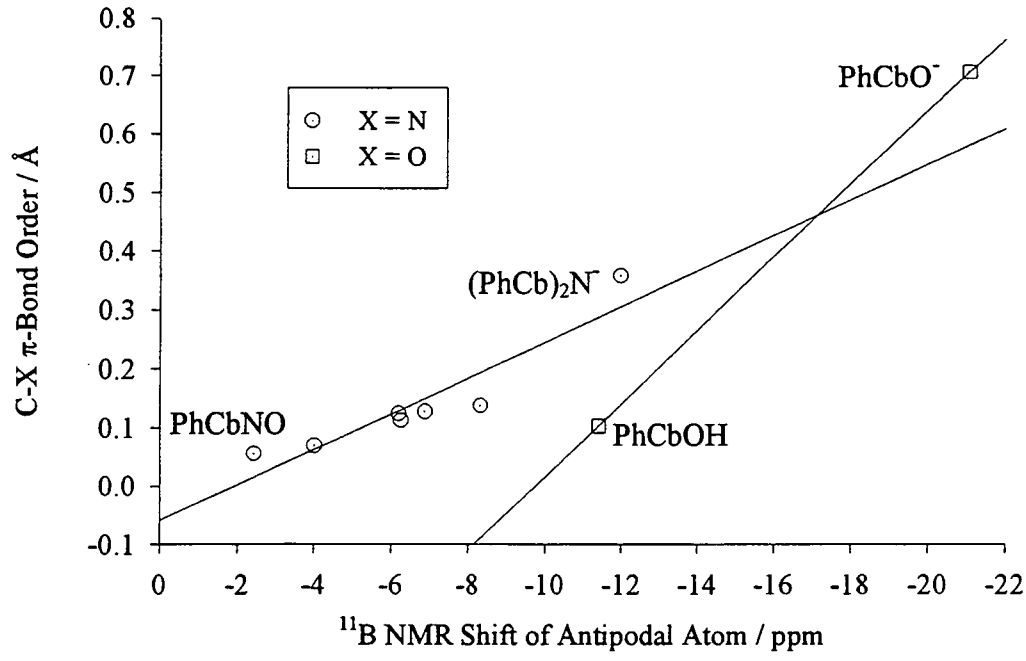

Figure 4.51

Plots of ^{11}B α-shifts of B12 reveal the same trends as ^{11}B δ B12 with no apparent improvement (Figure 4.54 and Figure 4.55).

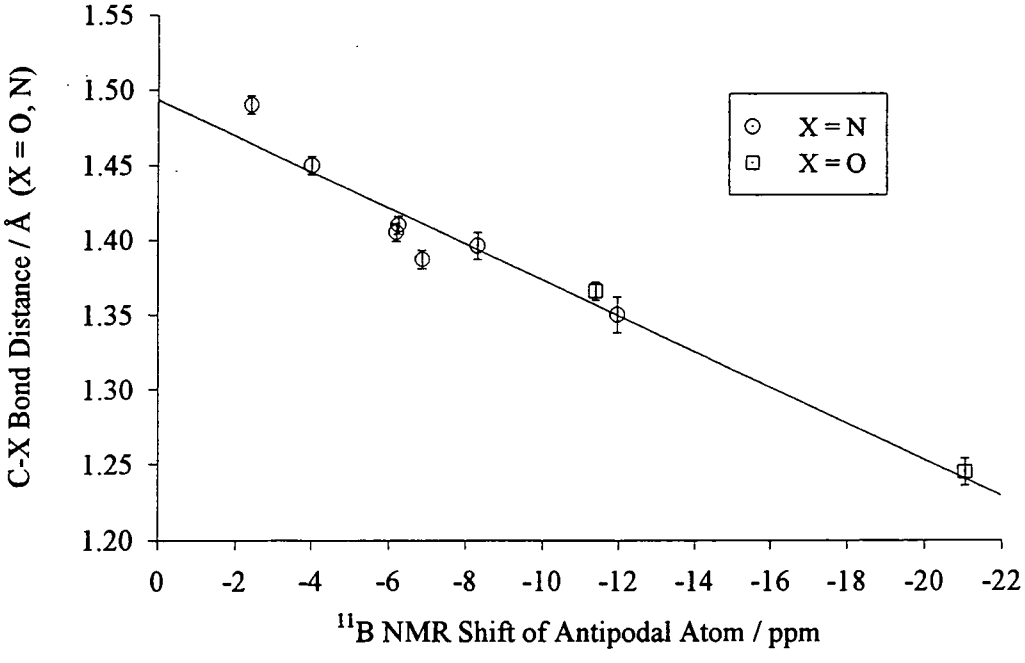

Figure 4.52

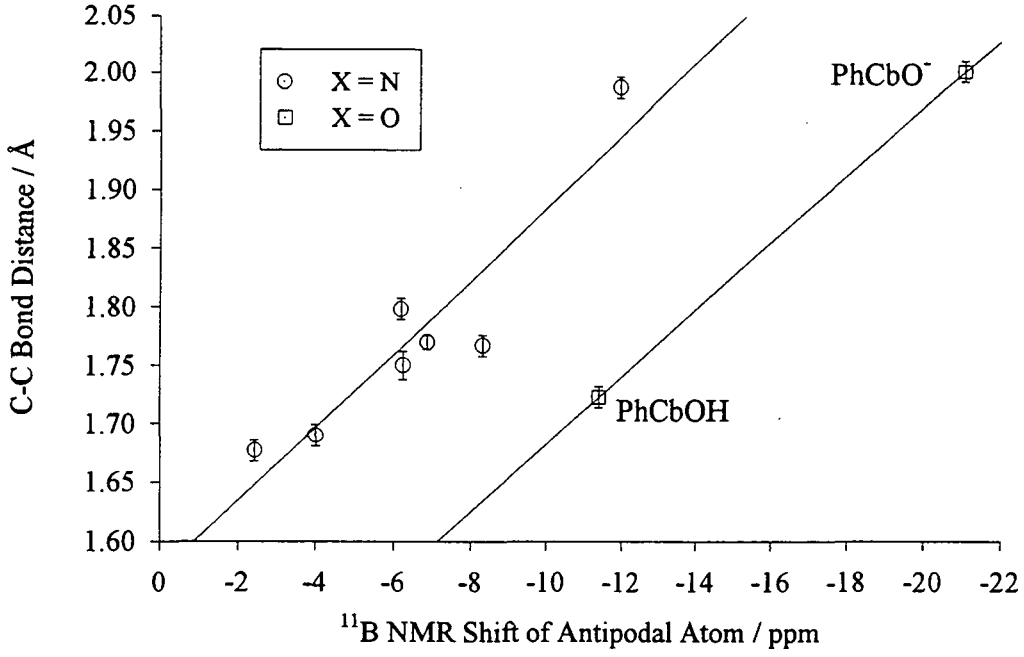

Figure 4.53

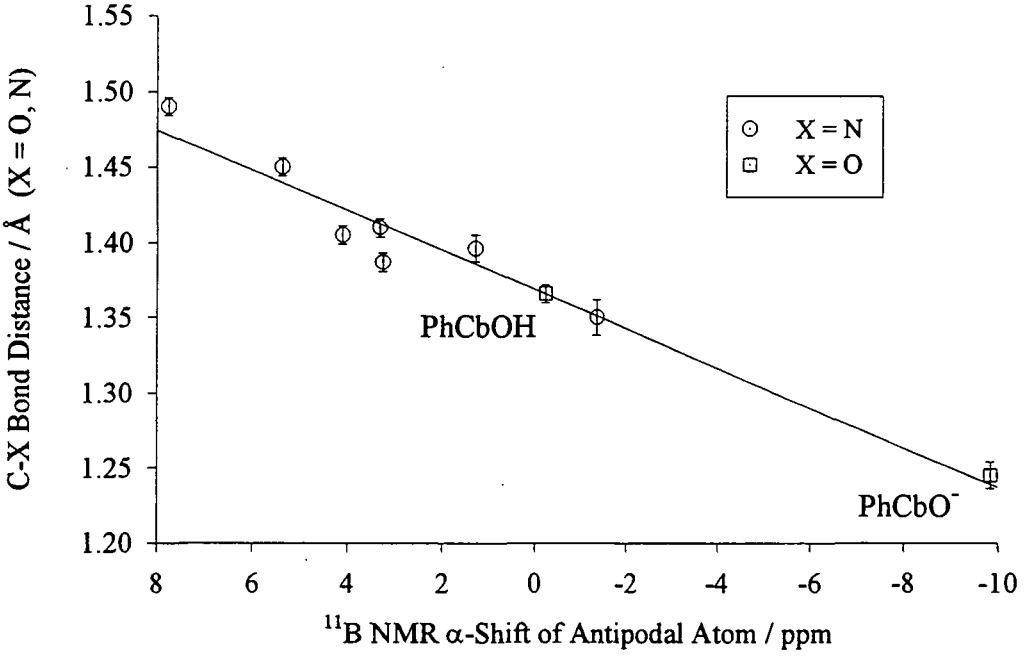

Figure 4.54

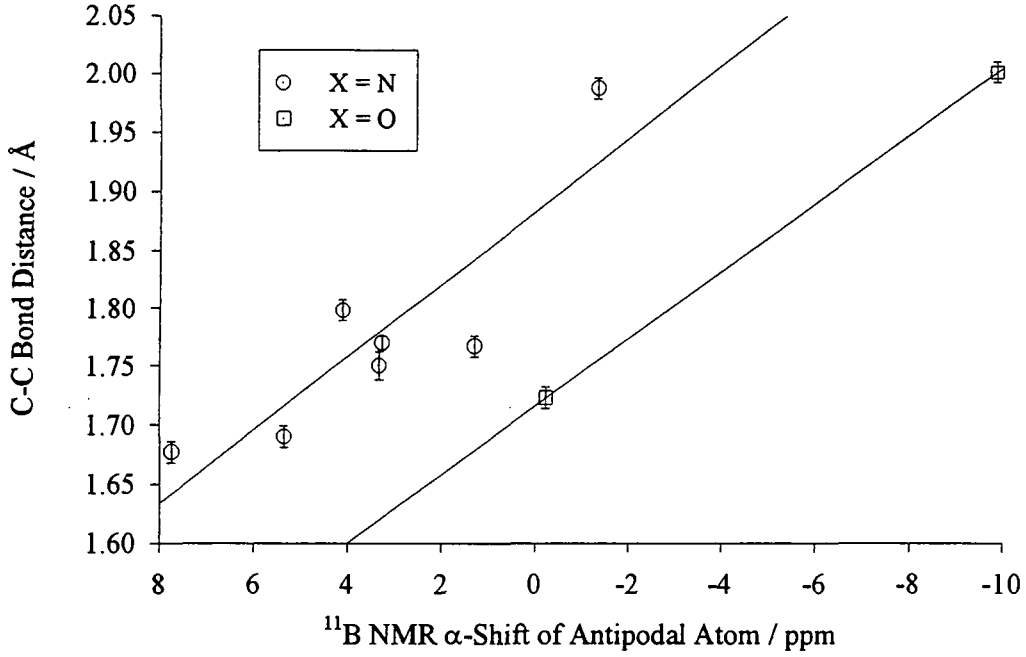
2.05
2.00
1.95
1.90
1.85
1.80
1.75
1.70
1.65
1.60
C-C Bond Distance / Å
X = N
X = O
8
6
4
2
0
-2
-4
-6
-8
-10
11B NMR α-Shift of Antipodal Atom / ppm

Figure 4.55

4.8 SULPHUR-SUBSTITUTED CARBORANES

Much work has been carried out on sulphur substituted carboranes which are easy to synthesise. Of these, the anion $PhCbS^-PS^+$ has already been referred to as displaying substantial *exo*-π-bonding between the S and carborane cage with both shortened C-S and lengthened C-C bonds. Teixidor and co-workers have synthesised a range of sulphur-substituted *ortho*-carboranes which display a lengthening of the C-C cluster bonds which they attribute to a *withdrawal* of electrons from the carborane cage into vacant d-orbitals on S. This is opposite to that used to rationalise the trends observed in the nitrogen and oxygen systems already discussed.

An AM1 calculation on the anion $PhCbS^-PS^+$ using the atomic coordinates from the X-ray structure reveals that, as in $PhCbO^-$, it is the p_x orbitals which are most important in the formation of this exo-π-bond, although the difference is less than for $PhCbO^-$, with the p_x orbitals being responsible for 56% of this π-bond.

Also known is the anion $[S_2HC_2B_{10}H_{10}]^-PSH^+$ (CbS_2H^-) (Figure 4.56), formed by the deprotonation of the dithiol $Cb(SH)_2$. Again, this anion displays exo-π-bonding although the conformation is clearly not determined by this interaction as in the nitrogen system, the H is constrained by S···H···S hydrogen bonding to lie between the two sulphur atoms.

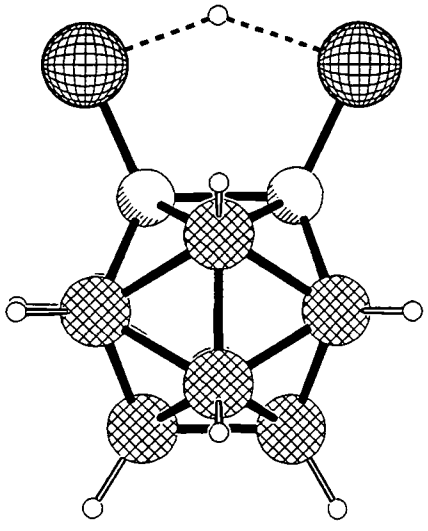

Figure 4.56 Molecular structure of CbS_2^- (cation omitted for clarity)

A number of neutral species have also been structurally characterised, these include the series $Cb(S)_nCb$ (n = 1,[42] 2,[43] 3[44]). The C-S distances in these compounds (~1.79Å) are comparable to those found in aryl thiols (1.768Å). The C-C cluster bonds are somewhat longer than those found in the parent carborane. The conformations in these compounds are found to be analogous to one another (Figure 4.57), the SX bond (X = CbPh, SCbPh, S_2CbPh) being approximately perpendicular to the C-C bond.

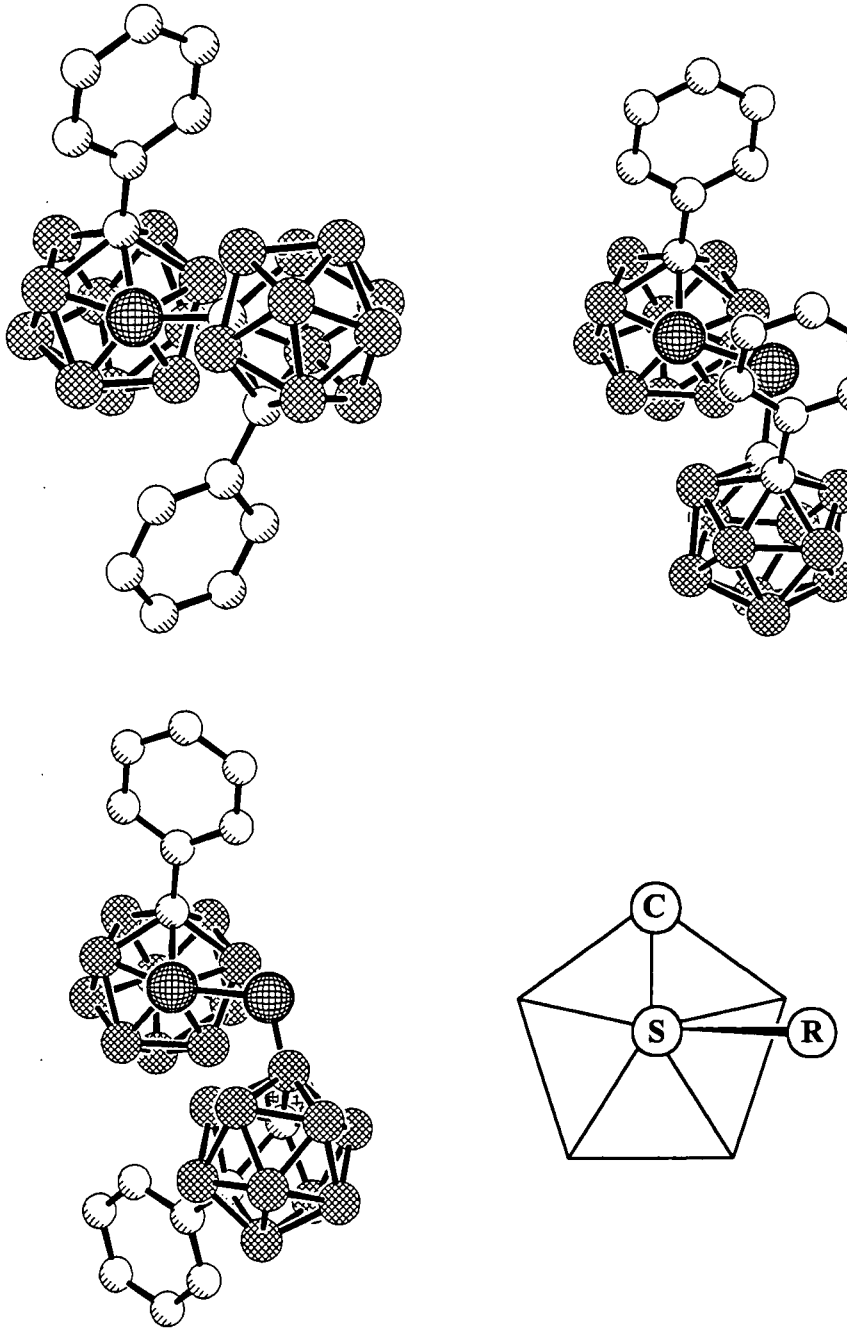

Figure 4.57 Conformations in Cb_2S_n (viewed down S-C bond)

This cannot be rationalised on steric grounds and must arise from an electronic interaction c.f. conformations in the nitrogen system. The bond angles at S are all approximately 105° indicating sp^3 hybridisation. The orientation adopted will maximise π-bonding between the lone pairs on S and the C-p_x.

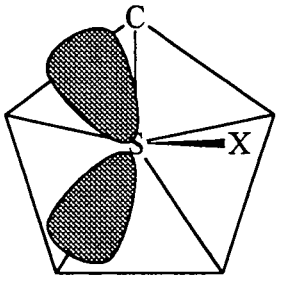

Figure 4.58 Orientation of lone pairs in Cb_2S_n

An AM1 calculation on HCbSH has been performed to confirm this. As with the calculations in Section 4.6.12, the coordinates for the cage were taken to be those of an ideal icosahedron. For each orientation in the calculation the position of the SH substituent was optimised with the exception of the C2-C1-S-H dihedral angle used to define the geometry. The results (Figure 4.59) show that the energy minimum occurs with the SH bond in a plane perpendicular to the S-C-C plane, a conformation analogous to that found in the compounds $PhCb_2S_n$. This conformation coincides with maximum π-bonding.

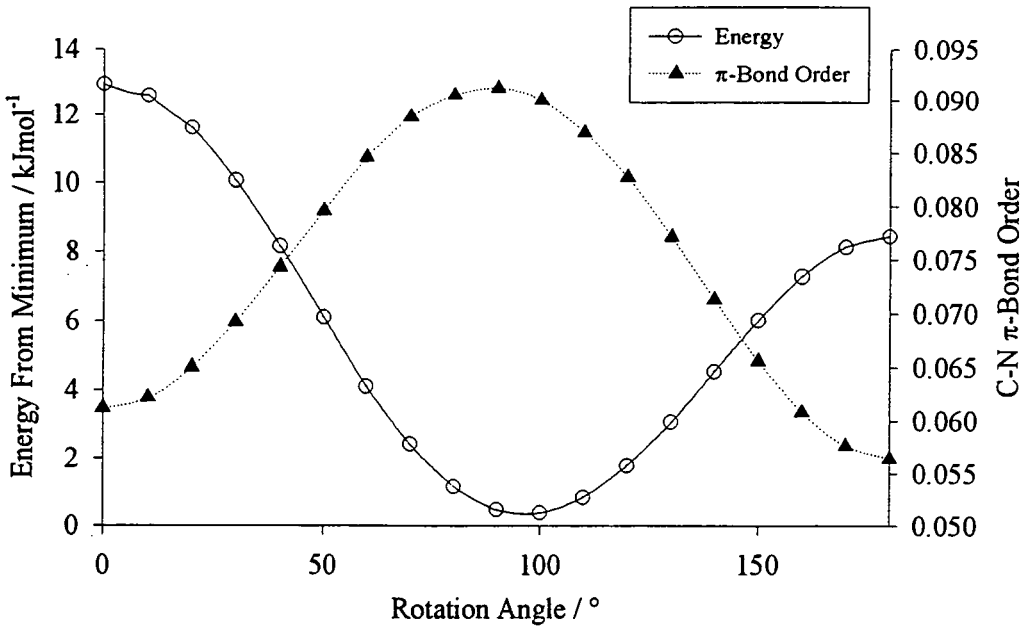

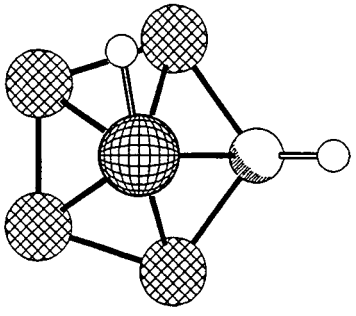

100° **Preferred Orientation**

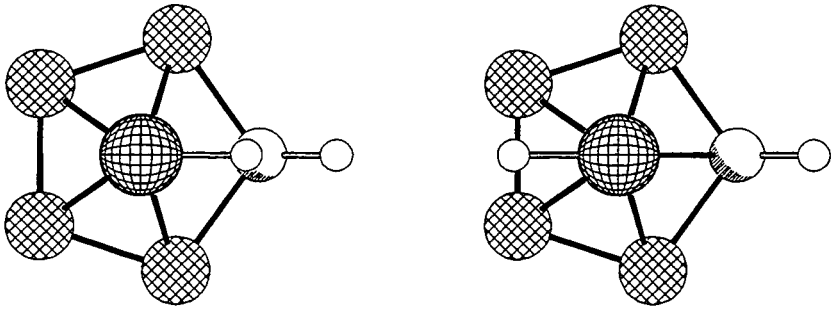

0° 100°

Least Favourable Orientation

Figure 4.59 **Energy and C-S π-bond profile for rotation of SH in HCbSH about the exo C-S bond. Pictures viewed down C-S bond, lower half of cage and H's on B omitted**

The sulphoxide $PhCb_2SO$ is also known and has been structurally characterised.[45] The C-S bond length (1.859(3)Å) is somewhat longer than in the series of sulphides and comparable to aryl systems. Again the orientation of the lone pair suggests alignment of the lone pair with the C-p_x, suggesting the possibility of exo-π-bonding.

AM1 calculations have been carried out on these compounds to investigate further these exo-π-bonding effects. In all compounds there is some degree of π-bonding. The calculations also suggest that there is significant π-bonding involving the C-p_y although that involving the C-p_x is greatest in all cases as indicated by the solid state structures. Results of these calculations are collected in Table 4.19.

	$PhCbS^-$	CbS_2^-	$PhCb_2S$	$PhCb_2S_2$	$PhCb_2S_3$	$PhCb_2SO$
C-S / Å	1.729(4)	1.733(6)	1.788(2)	1.793(4)	1.788(2)	1.859(3)
C-C / Å	1.835(5)	1.771(8)	1.755(3)	1.752(4)	1.735(3)	1.729(3)
C-S π-bond order	0.276	0.132	0.069	0.051	0.051	0.027
C-C bond order	0.391	0.465	0.542	0.519	0.548	0.697
% π-bond to C-p_x	56	71	58	59	55	56
% π-bond to C-p_y	44	29	42	41	45	44
^{11}B δ B12	-11.99	+2.11	+1.32	NA†	NA†	+1.32
^{11}B α-B12	-5.96	+6.08	+8.45	NA†	NA†	+9.37

Table 4.19 Selected data for S substituted carboranes

As with the N system there is a correlation between the C-S distance and the C-C cluster bond distance (Figure 4.60), although this trend is less obvious than in the N system, the relative differences between bond lengths being smaller. Also included are data for two other systems (Figure 4.62). A plot of C-C bond distance against the C-S π-bond order shows a similar trend (Figure 4.61).

† ^{11}B NMR spectra are not available for these compounds due to low solubility

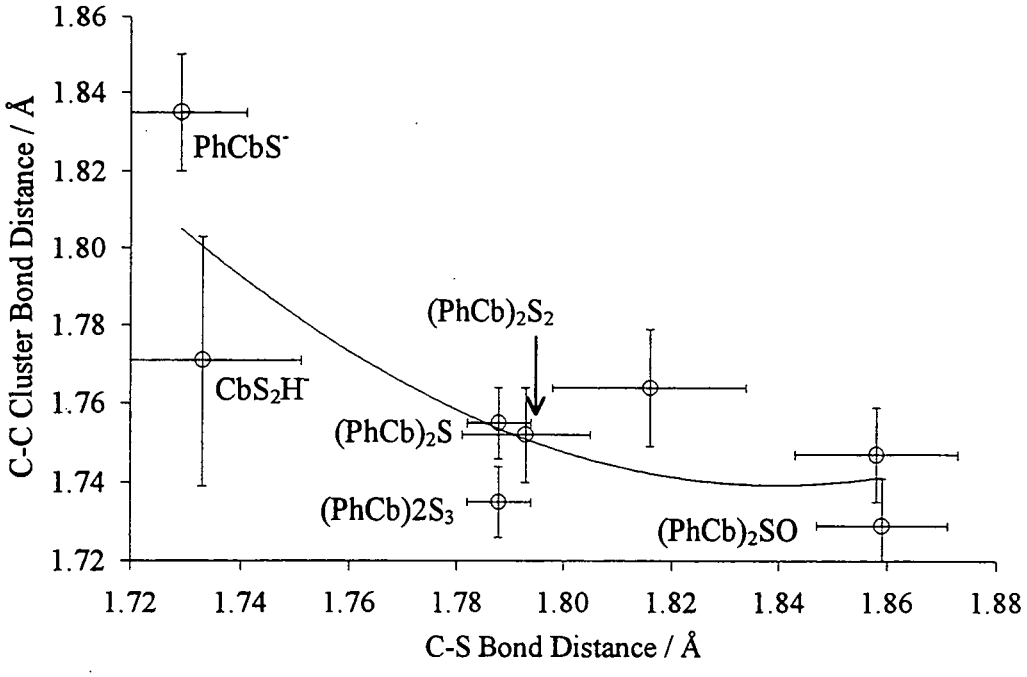

Figure 4.60 C-S bond length vs C-C cluster bond length

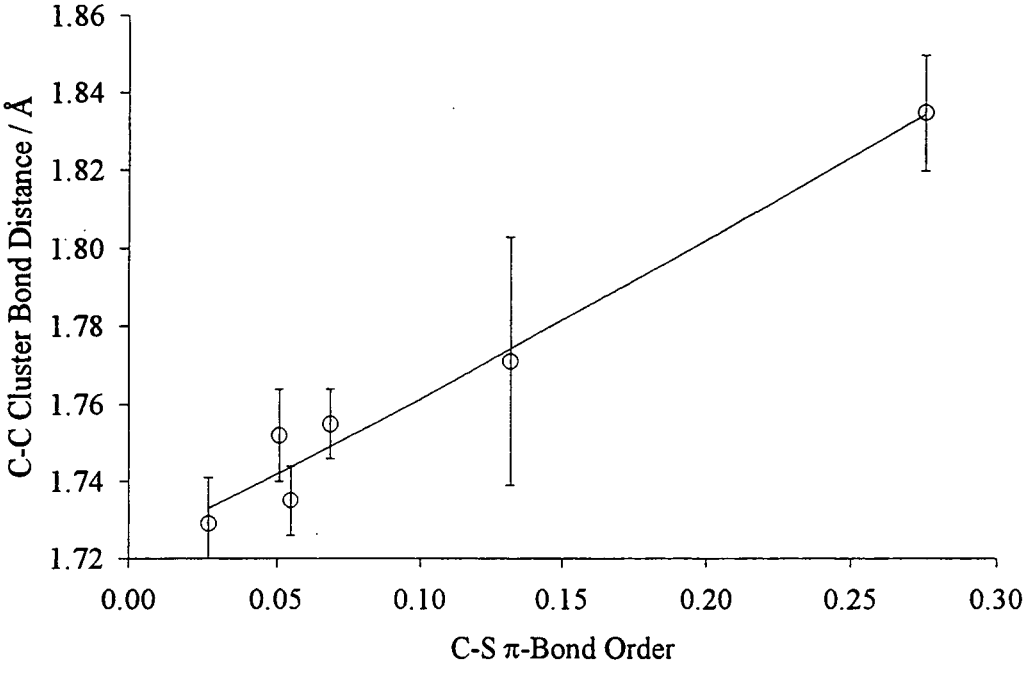

Figure 4.61 C-S π-bond order vs C-C bond length

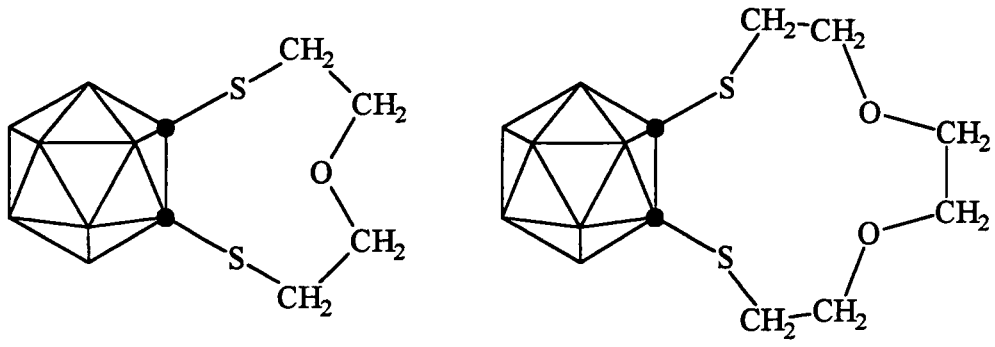

Figure 4.62 Other S substituted carboranes

A plot of the ^{11}B δ B12 vs C-S bond length shows a similar trend to the previous systems, although NMR data on these compounds is limited (Figure 4.63). Points for CbS_2H^- show a consistent deviation from trends in the others points. This reflects the different nature of this compound, others having a phenyl group on C2. The plot of ^{11}B α-B12 vs C-S distance gives points which are considerably closer to a single line (Figure 4.64). A plot of the C-C bond length against ^{11}B δ B12 shows a good correlation in the expected manner.(Figure 4.65)

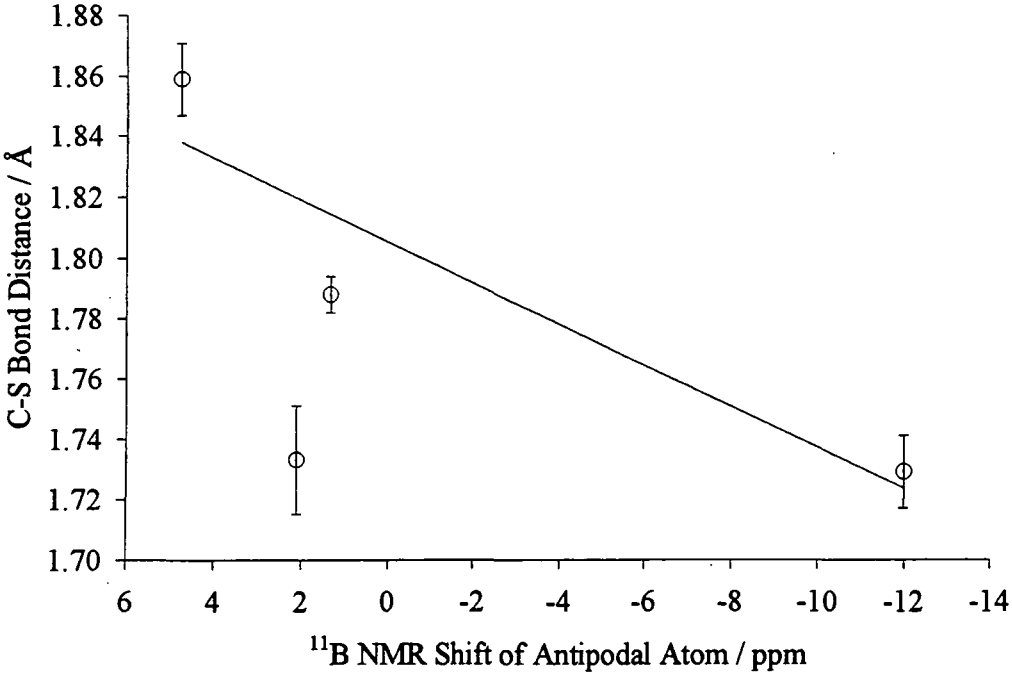

Figure 4.63 ^{11}B δ-B12 vs C-S bond distance

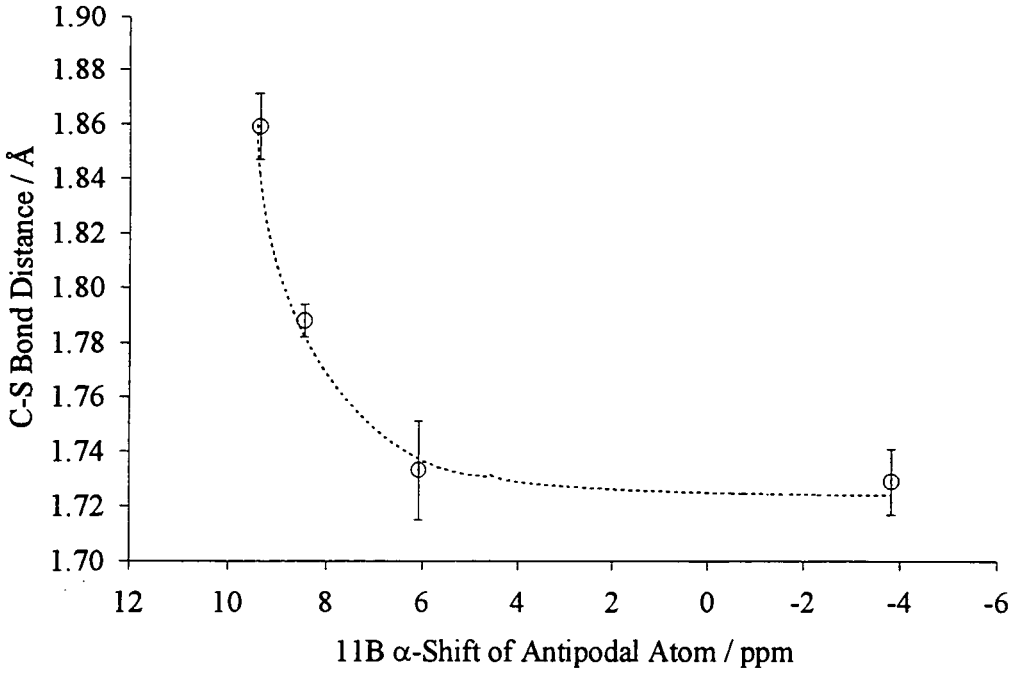

Figure 4.64 **^{11}B δ-B12 vs C-S bond distance**

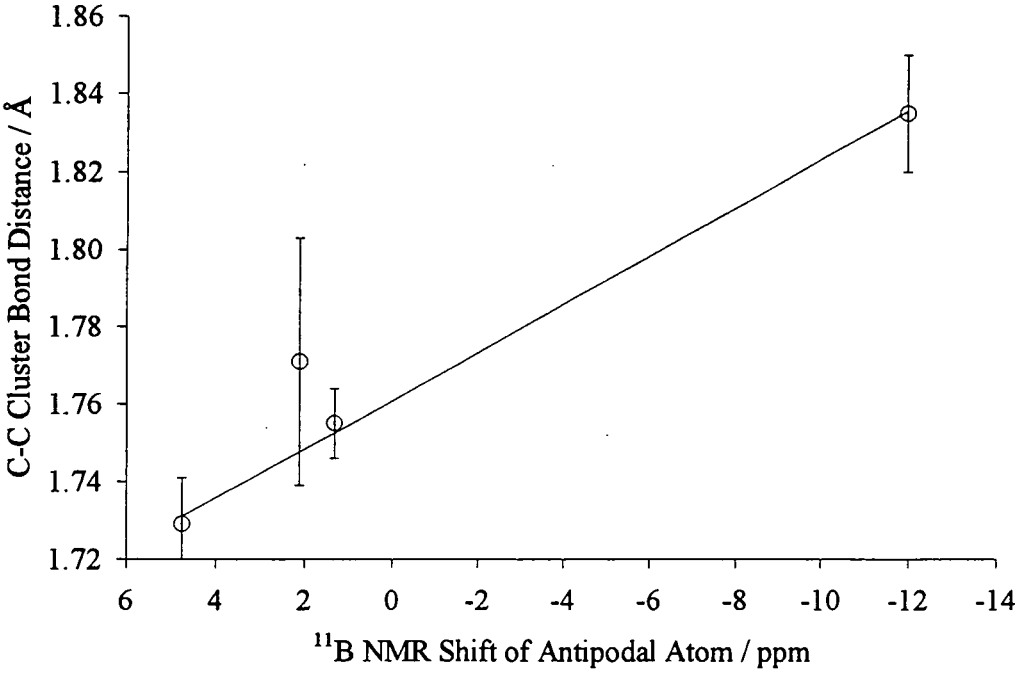

Figure 4.65 **^{11}B δ-B12 vs C-C bond distance**

Comparison of NMR data with both the O and N systems reveals an interesting trend. A plot of ^{11}B δ B12 against the C-C bond distance shows 2 parallel lines for the O and N systems, but a line of different gradient for the S system (Figure 4.66). A plot of ^{11}B δ B12 against the C-S bond distance shows a single line through the N and O systems and a different line of similar gradient for the S system (Figure 4.67). Also included are data for phosphorus-substituted carboranes (see Section 4.9). A plot of ^{11}B δ B12 against the C-X π-bond order gives different gradients for all three lines (Figure 4.68). Clearly the ^{11}B δ B12 values can only be related directly to the degree of π-bonding to the cage (and related parameters such as bond lengths) when considering similar systems. Other factors related to the nature of the substituent also appear to affect the ^{11}B δ B12.

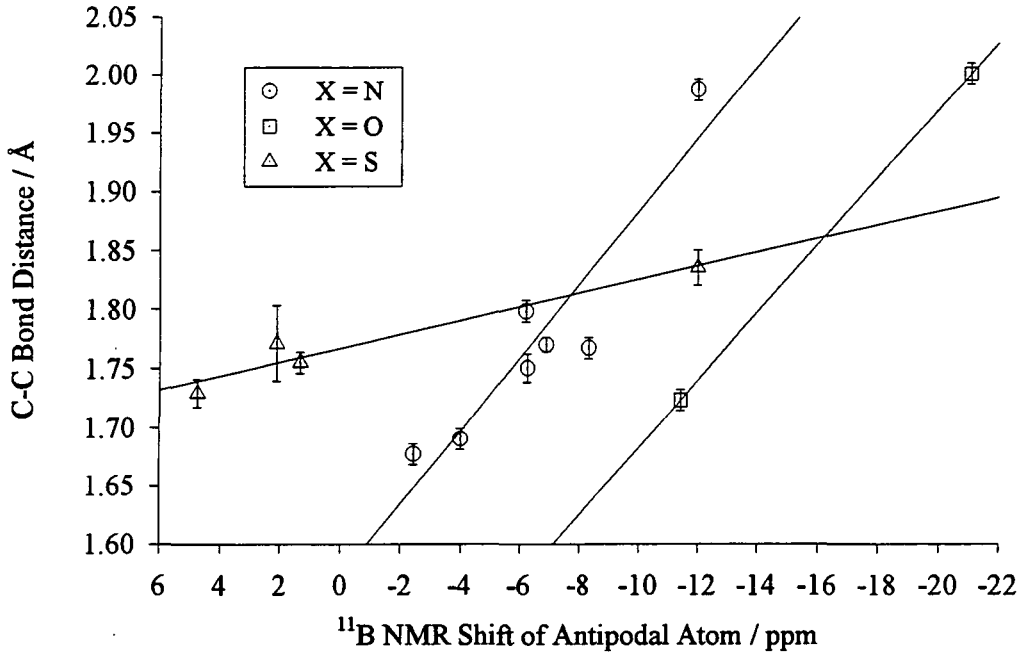

Figure 4.66 ^{11}B δ-B12 vs C-C bond distance

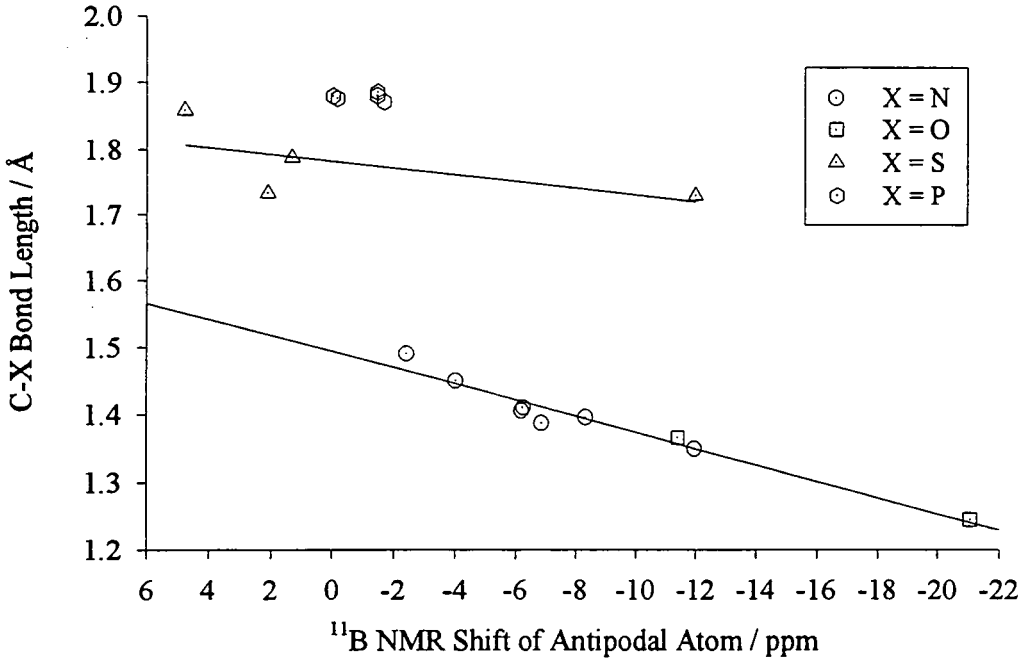

Figure 4.67 ^{11}**B δ-B12 vs C-C bond length**

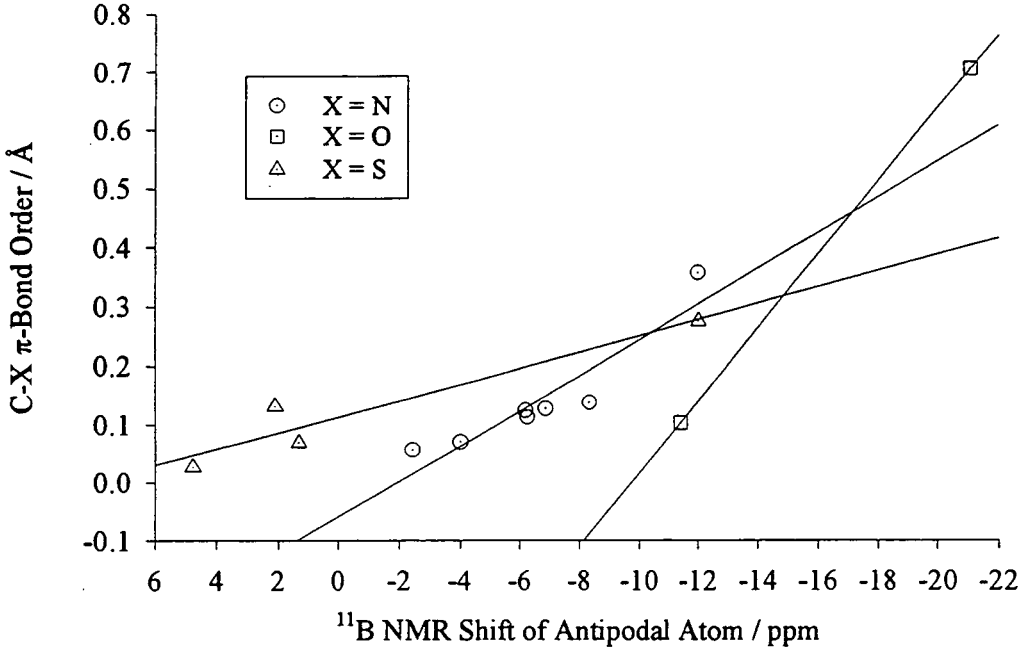

Figure 4.68 ^{11}**B δ-B12 vs C-X π-bond order**

4.8.1.1 D-ORBITAL INVOLVEMENT

It has been suggested that the carborane cage can interact with S substituents either by donation from a lone pair on sulphur onto the cage or in the reverse direction from the cage into an unfilled d-orbital on S (Figure 4.69).

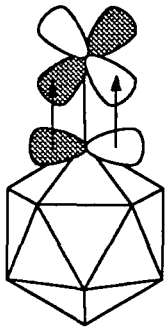

Figure 4.69 Interaction of d-orbital with cage

To determine whether this is significant in the bonding *ab initio* calculations have been carried out at the RHF/3-21G* level. The anion $HCbS^-$ was studied in this manner, coordinates used being those of $PhCbS^-PS^+$ with the phenyl group replaced by H. Also studied was HCbSH with coordinates based on $PhCb_2S$, with one carborane cage and the remaining phenyl group replaced by H. These simplifications reduce the time required for the calculation considerably without affecting the result greatly.

In both cases these calculations show the d-orbitals on sulphur participate very little, these functions containing ~0.04 electrons. There seems to be little involvement of d-orbitals in the bonding *exo* to the cage. This is not surprising as donation of electrons from the electron deficient cage would be expected to be small. It appears that *exo*-π-bonding between sulphur substituents and the carborane cage is essentially of the same nature as that in the nitrogen and oxygen systems.

4.9 PHOSPHORUS SUBSTITUTED CARBORANES

As exo-π-bonding is observed between N, O or S and the carborane cage it would be expected that similar bonding would occur between phosphorus substituents and the cage. However, it has already been noted by Teixidor[46] that phosphorus-substituted carboranes show little lengthening of the C-C cluster bond implying little π-bonding between the cage and substituent. In comparing compounds of the form 1,2-$(SR)_2$-$C_2B_{10}H_{10}$ and 1,2-$(PR_2)_2$-$C_2B_{10}H_{10}$ the sulphur substituted cage will have the greater C-C distance despite the smaller size of the S atom and hence this lengthening cannot be due to steric factors. A study of the solid state structures of such compounds in the literature[47] reveals little variation in C-P distances, this distance being approximately 1.88Å regardless of other groups on P. This is greater than that found in similar aromatic systems (1.836Å) or alkyl systems (1.855Å). These differences reflect the coordination number of the carbon atom to which the phosphorus is attached, higher coordination numbers having greater C-P distances. There is a wider range of C-C cluster bond lengths in these compounds although this can be attributed to steric effects.

^{11}B NMR data, found in the N, O and S systems to give a good indication of the degree *exo*-π-bond, show little variation in ^{11}B δ-B12 in a range of P substituted *ortho*-carboranes despite the variation in substituents on the P. Again this suggests little P-C π-bonding.

Although these data suggest little C-P π-bonding the orientations adopted in the solid state of these compounds correspond to those in which exo-π-bonding will be maximised i.e. the lone pair is aligned with the C-C bond. Although in many compounds this could be attributed to steric effects the compound $HCbPPh_2$, in which C2 has been located, shows the same conformation despite the absence of such steric effects.

An AM1 calculation performed on $MeCbPPh_2$, using coordinates from the crystal structure of this compound reveals a C-P π-bond order of 0.02, far smaller than observed in any of the N, O or S systems investigated in this chapter. While it is possible that this π-bonding interaction is sufficient to affect the conformation in such

compounds the effect appears to be small, too small to have a significant effect on either bond distances or ^{11}B NMR shifts.

4.10 Comparisons Between Carboranyl and Aryl π-Acids

Carboranes are often compared to aromatic systems and it is therefore not surprising that similarities exist in trends observed in interactions *exo* to both phenyl rings and aromatic clusters.

Similar trends are observed in C-N bond lengths and π-bond orders in both the carboranyl system studied in this chapter and the 'fluoromes' system discussed in Chapter 2. In both systems the electronegativity of atoms attached to the nitrogen substituent appear to the most important factor in determining the π-bond order.

The *exo*-π-bond formation has an effect on the bonding in the ring or cluster, the C-C bonds adjacent to the point of substitution are seen to lengthen. Both effects can be described in similar terms, the greater the π-symmetry orbitals on C become involved in exo-π-bonding the less they can be involved in ring / cluster bonding.

Similarities also exist in the NMR frequencies of the atoms directly opposite responding to the formation of the exo-π-bond. Such similarities between mesomeric and antipodal effects have been previously commented on.

In both the ring and cluster systems these π-bonds govern the orientation of the substituent relative to the ring or cage. For amines and amine derivatives the lone pair is found to align with either the C-p_x orbital in the carborane system or the aromatic π-system in the fluoromes compounds. The situation is somewhat different for nitroso or azo compounds in which the interaction can be with either the lone pair or π-system for the aromatic rings, but with both for the carborane system.

4.11 CONCLUSIONS

Substituents on carborane cages bearing lone pairs can interact with the cage via dative π-bonds. These π-bonds will form preferentially with the p_x orbital on the C, i.e. that pointing towards the other cage C atom. This will result in orientational preferences in the structures of such compounds, the substituents will adopt a conformation which maximises these π-bonding interactions. Such interactions with the cage cause changes in cluster bonding and result in a lengthening of the C-C distance. The extent of this lengthening increases with increased interaction with the cage. Such interactions occur to some extent with N, O and S substituents. It is possible that such interactions occur with phosphorus substituents but are much weaker.

This π-electron donation to the cage causes a shift in the ^{11}B NMR of the B atom antipodal to the substituent. This can be attributed to an increase in electron density in the tangential orbitals of this atom. Hence this shift gives a good indication of the degree of exo-π-bonding to the cage and allows the investigation of such bonding in compounds where structural data are not available.

The ^{1}H NMR shift of the H attached to the antipodal B atom also responds in a similar manner to the ^{11}B shift. Calculations reveal that this is not due to an increase in electron density on this atom.

The withdrawal of electrons from the substituent onto the cage will clearly affect the properties of these compounds as ligands. The reduction of electron density on this atom will reduce the electron donating capacity of these ligands. This combined with the bulk of the cage would be expected to produce unusual metal complexes. The next chapter investigates some of these compounds as ligands.

4.12 REFERENCES

1 H.C. Longuet-Higgins, *J. Chem. Phys*, **1949**, *46*, 275.

2 W.N. Lipscomb, *Adv. Inorg. Chem. Radiochem.*, **1950**, *117*, 1.

3 K. Wade, "Electron Deficient Clusters", Nelson, 1971.

4 K. Wade, *Chem. Commun.*, **1971**, *791*; K. Wade, Adv. Inorg. Chem. Radiochem., **1976**, *18*, 1.

5 H.C. Longuet-Higgins and M. de V. Roberts, *Proc. Roy. Soc. London., Ser A*, **1955**, *230*, 110.

6 For a comprehensive review see R.N. Grimes, "Carboranes", *Academic Press, New York*, **1970**, pp54-192.

7 D. Grafstein, J. Dvorak, *Inorg. Chem.*, **1963**, *2*, 1128-1133; S. Papetti, T.L. Heying, *J. Am. Chem. Soc.*, **1964**, *86*, 2295.

8 R.E. Williams in Electron Deficient Boron and Carbon Clusters, G.A. Olah, K. Wade, E.E. Williams, 1991, John Wiley & Sons, Inc.

9 M.M. Fein, D. Grafstein, J.E. Paustian, J. Bobinski, B.M. Lichstein, N. Mayes, N. Schwartz, M.S. Cohen, *Inorg. Chem.*, **1963**, *2*, 1115.

10 T.L. Heying, J.W. Ager Jr, D.J. Mangold, H.L. Goldstein, M. Hillman, R.J. Polak, J.W. Szymanski, *Inorg. Chem.*, **1963**, *2*, 1089; M.F. Hawthorne, T.D. Andrews, P.M. Garrett, F.P. Olsen, M. Reintjes, F.N. Tebbe, L.F. Warren, P.A. Wegner and D.C. Young, *Inorganic Syntheses*, **1967**, 91.

11 T.L. Heying and S. Papetti, *Inorg. Chem.*, **1963**, *2*, 1097.

12 F.A. Gomez, S.E. Johnson, M.F. Hawthorne, *J. Amer. Chem. Soc*, **1991**, *113*, 5915.

13 M.G. Davidson, T.G. Hibbert, J.A.K. Howard and K. Wade, *unpublished results.*

14 S. Hermánek, *Chem. Rev.*, **1992**, *92*, 325-362.

15 S. Hermánek, J. Plešek, V. Gregor, B. Stibr, *J. Chem. Soc., Chem. Commun.*, **1977**, 561.

16 S. Hermánek, D. Hnyk, Z. Havlas, *J. Chem. Soc. Chem. Commun.*, **1989**, 1859.

17 D.A. Brown, W. Clegg, H.M. Colquhuon, J.A. Daniels, I.R. Stephenson and K. Wade, *J. Chem. Soc. Chem. Commun*, **1987**, 889.

18 L.I. Zakharkin, V.N. Kalinin, L.S. Podvisotskaya, *Izvestiya Akademii Nauk. SSSR, Seriya Khimideskaya*, **1967**, *10*, 2310.

19 G.B. Dunks, M.M. McKown and M.F. Hawthorne, *J. Am. Chem. Soc*, **1971**, *93*, 2541; M.R. Churchill and B.G. DeBoer, *J. Chem. Soc. Chem. Commun.*, **1972**, 1326; R. Khattar, C.B. Knobler and M.F. Hawthorne, *J. Am. Chem,. Soc.*, **1990**, 112, 4962; F.Y. Lo, C.E. Strouse, K.P. Callahan, C.B. Knobler,

M.F. Hawthorne; Sihai Li, D.F. Mullica, E.L. Sappenfield, F.G.A. Stone, *J. Organomet. Chem.*, **1994**, *467*, 95.

20 T.D. Getman, C.B. Knobler and M.E. Hawthorne, *J. Amer. Chem. Soc.*, **1990**, *112*, 4592.

21 M. P. Mingos, *J. Chem. Soc. Dalton*, **1977**, 602.

22 R. Coult, M.A. Fox, W.R. Gill, K. Wade and W. Clegg, *Polyhedron*, **1992**, *11*, 2717.

23 R. Copley, R. Coult, M.A. Fox, W.R. Gill, J.A.K. Howard, K. Wade, *unpublished work.*

24 E.J. Ditzel, X.L.R. Fontaine, N.N. Greenwood, J.D. Kennedy and Mark Thornton-Pett, *J. Chem. Soc., Chem. Commun*, **1989**, 1115.

25 L.I. Zakharkin and V.N. Kalinin, *Dokl. Akad. Nauk SSSR*, **1965**, *164*, 577; J.M. Kauffman, J. Green, M.S. Cohen, M.M. Fein and E.L. Cottrill, *J. Amer. Chem. Soc.*, **1964**, *86*, 4210; L.I. Zakharkin and G.G. Zhigareva, *Bull. Acad. Sci. USSR., Div. Chem Sci*, **1989**, 179.

26 W. Clegg, J.A.H MacBride and K.Wade, *unpublished results.*

27 For a discussion of the NO ligand see R.H. Crabtree, "The Organometallic Chemistry of the Transition Metals", John Wiley and Sons, New York, 1988.

28 V.N. Kalinin, G.G. Zhigareva and L.I.Zakharkin, *Synth. Inorg. Metal-Org.* Chem., **1972**, *2*, 105.

29 M.A. Fox, PhD thesis, Durham University, 1991.

30 W. Clegg, R. Coult, M.A. Fox, W.R. Gill, J.A.H. MacBride and K. Wade, *Polyhedron*, **1993**, *12*, 2711.

31 L.I. Zakharkin and G.G. Zhigareva, *Bull. Acad. Sci. USSR., Div. Chem Sci*, **1989**, 179.

32 L.I. Zakharkin and G.G. Zhigareva, *J. Gen. Chem. USSR*, **1975**, 1268.

33 L.A. Polyakova, K.A. Bilevich, V.I. Bregadze and O. Yu. Oklobystin, *Bull. Acad. Sci. USSR, Div. Chem. Sci*, **1972**, 1846.

34 See Chapter 2 for a more detailed discussion of azobenzenes.

35 W.J. Hehre, L. Radom and J.A. Pople, *J. Am. Chem. Soc.*, **1972**, *94*, 1496.

36 B.G. Gowenlock, M. Cameron, A.S.F. Boyd, M. Al-Tahou and P. McKenna, *Can. J. Chem*, **1994**, *72*, 516.

37 I.R. Stephenson, PhD Thesis, 1988, Durham University.

38 P.T. Brain, J. Cowie, D.J. Donohoe, Drahomír Hnyk, D.W.H. Rankin, D. Reed, B.D. Reid, H.E. Robertson, A.J. Welch, M. Hofmann and P.v.R. Schleyer, *Inorg. Chem.*, **1996**, *35*, 1701.

39 T.D. McGrath and A.J. Welch, *Acta Cryst*, **1995**, *C51*, 646; T.D. McGrath and A.J. Welch, *Acta Cryst*, **1995**, *C51*, 649; T.D. McGrath and A.J. Welch, *Acta Cryst*, **1995**, *C51*, 651; T.D. McGrath and A.J. Welch, *Acta Cryst*, **1995**, *C51*, 654.

40 L.I. Zakharkin and G.G. Zhigareva, *J. Gen. Chem. USSR*, **1970**, *40*, 2318; L.I. Zakharkin, G.G. Zhigareva, *J. Gen. Chem. USSR*, **1969**, *39*, 1856; L.I. Zakharkin, G.G. Zhigareva, *Bull. Acad. Sci. USSR., Div. Chem. Sci*, **1970**, 2153; L.I. Zakharkin, G.G. Zhigareva, *J. Gen. Chem. USSR*, **1975**, *45*, 1268.

41 L.A. Boyd, W. Clegg and K.Wade, unpublished work.

42 W. Clegg, R.S. Grimditch, J.A.H. MacBride and K. Wade, *unpublished results.*

43 W. Clegg, W.R. Gill and K. Wade, *unpublished results.*

44 W. Clegg, M.A. Fox and K. Wade, *unpublished results.*

45 A.S. Batsanov, T.G. Hibbert, J.A.K. Howard and K. Wade, *unpublished work*

46 F. Teixidor and C. Viñas, IMEBORON 9, **1996.**

47 Rosario Nùñez Aguilera, Tesis Doctoral, l'Institut de Ciència de Materials de Barcelona; R. Kivekäs, R. Sillanpää, F. Teixidor, C. Viñas, Rosario Nùñez, *Acta Cryst*, **1994**, *C50*, 2027; R. Kivekäs, F. Teixidor, C. Viñas, Rosario Nùñez, *Acta Cryst.* **1995**, *C51*, 1868; R. Kivekäs, R. Sillanpää, F. Teixidor, C. Viñas, Rosario Nùñez, Mar Abad, *Acta Cryst*, **1995**, *C51*, 1864.

Chapter Five

Ligand Systems Containing Icosahedral Carboranes

5.1 INTRODUCTION

There are many examples of metal complexes, both main group and transition metals, containing carboranes. Of these the most numerous are those in which the metal occupies a vertex in a polyhedral cluster (e.g. $CpCoC_2B_{10}H_{10}$, Figure 4.9). The structures of such compounds can be rationalised and predicted in the same way as boranes and carboranes by considering the number of skeletal electrons pairs. The number of electrons provided by the metal for cluster bonding is (v+x-2) for main groups elements and (v+x-12) for transition metals, were v is the number of valence electrons on the metal and x is the number of electrons provided by the ligands to the metal.[1] Much work has been carried out on such clusters and these systems have not been investigated further in this thesis.

Another common class of carborane-containing complex is that in which the carborane is bound to a metal by a direct M-C or M-B σ-bond.[2] These compounds include *ortho*-carboranes bonded to metal atoms through either one carbon atom, both carbon atoms[3] or bridging between two metals.[4,5] Some examples of these are shown in Figure 5.1.[3,4,6]

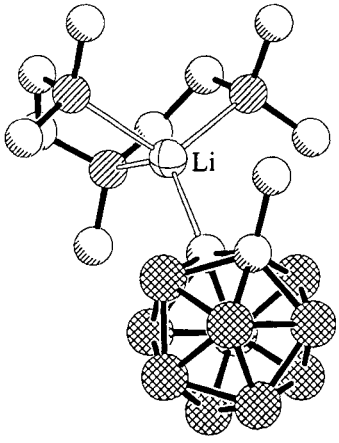

MeCbLi·PMDETA

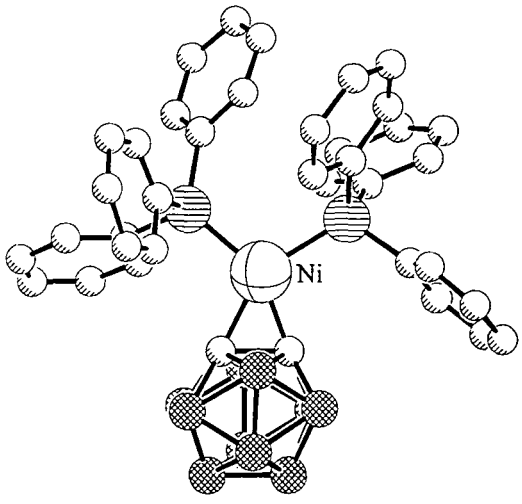

$Ni(1,2\text{-}C_2B_{10}H_{10})(PPh_3)_2$

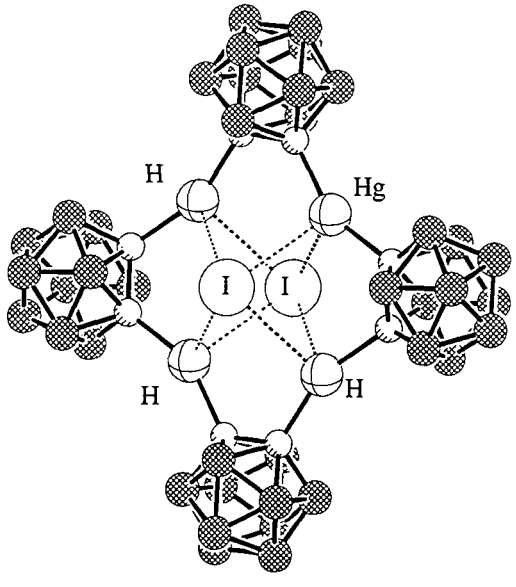

$[(HgC_2B_{10}H_{10})_4I_2][AsPh_4]$ (cation omitted)

Figure 5.1 Examples of M-C σ-bonded carboranes (H's omitted)

Cone angles[7] for such carboranyl ligands have been calculated from the X-ray structure of LiCbMe·PMDETA (Figure 5.1).[6] These values for carborane cages bearing H and Me on the cage C are given in Table 5.1. Also included are values for a phenyl substituted carborane cage, calculated in the same manner to the original values using the molecular structure of PhCbNO **1** as an example of a relatively unperturbed carborane cage. While the unsubstituted carborane is spherical, both methyl and phenyl carboranes are not, having a cone angle at the smallest point equal

to that for the unsubstituted cage, values given in Table 5.1 being values at the widest point.

M-C / Å	1.60	1.95	2.18	2.45
R				
H	154°	140°	132°	120°
Me	169°	158°	149°	138°
Ph	182°	170°	163°	154°

Table 5.1 **Cone angles for carboranyl ligands in M-Cb-R for a variety of M-C distances**

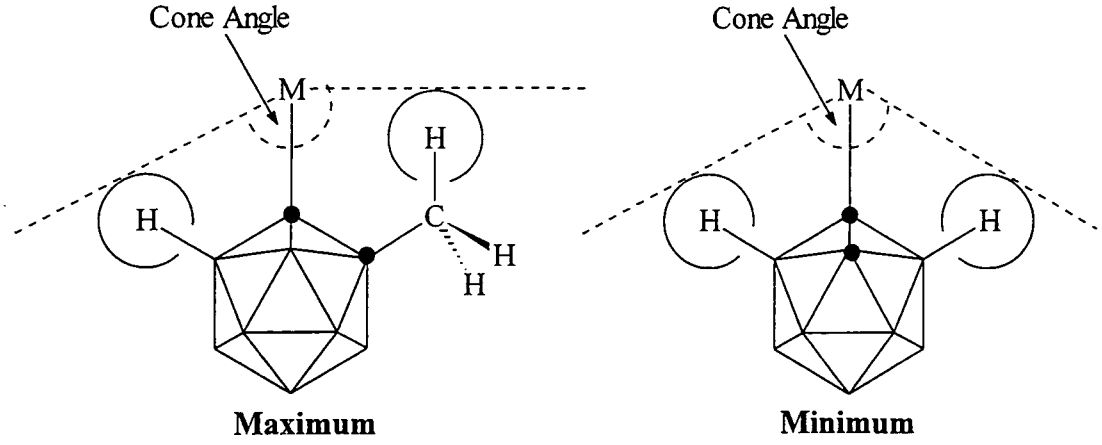

Figure 5.2 **Variation in cone angle for an MeCb ligand**

There are fewer examples of carboranes bound to metals via another atom. For *ortho*-carboranes most examples are S or P substituted carboranes. The example shown in Figure 5.3 has both chelating P and S substituted carboranyl ligands.[8] There are also a number of examples of *nido*-7-CX-8-R-B_9H_{10} species bound to a transition metal via X, where X = SR, PR_2 (Figure 5.4).

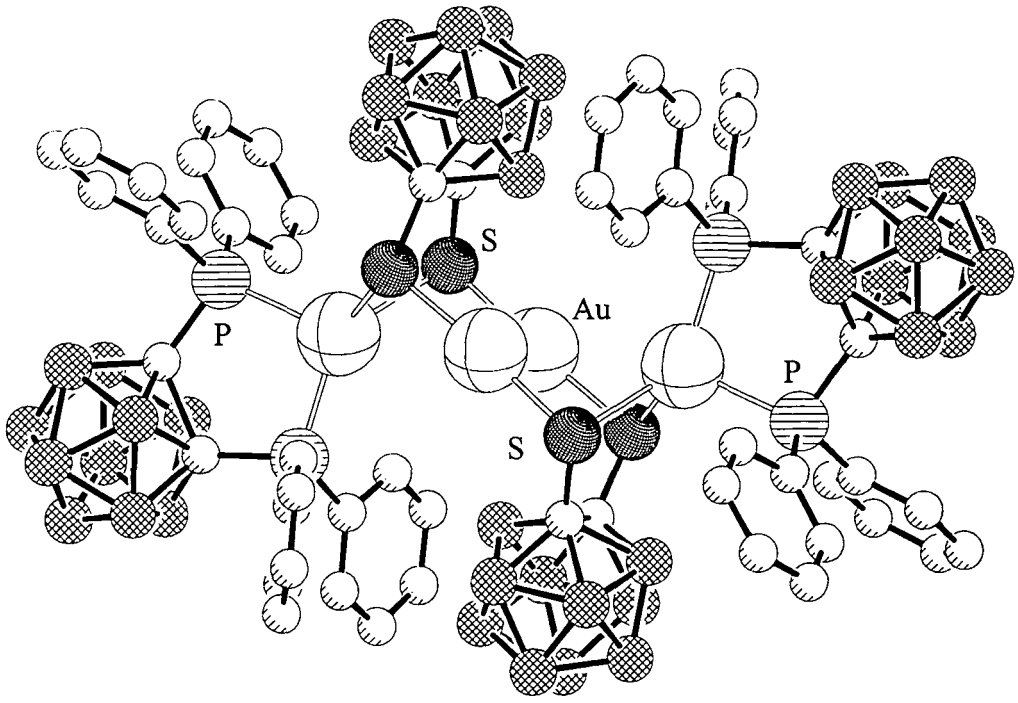

Figure 5.3 $Au_2[Au(1,2\text{-}(PPh_2)_2\text{-}C_2B_{10}H_{10})(1,2\text{-}S_2\text{-}C_2B_{10}H_{10})]_2$

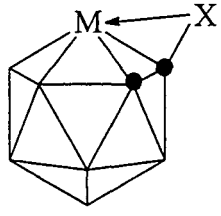

Figure 5.4

There are, however, no examples of *ortho*-carboranes bonded to a metal via an oxygen atom and only a single example coordinated through nitrogen (Figure 5.5), although not the N attached directly to the cage.[9] This chapter describes the synthesis of novel metal complexes containing carboranes. Although problems were encountered due to unexpected degradation of the cage and isolation of mixtures of products two new types of ligand have been synthesised and structurally characterised.

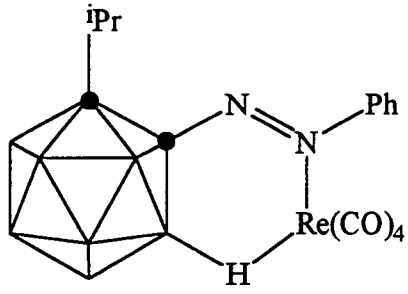

Figure 5.5

5.2 IMIDO LIGANDS CONTAINING CARBORANES

5.2.1 SYNTHESIS OF [Mo(NCbMe)$_2$Cl$_4$][Et$_3$NH]$_2$

Work reviewed in Chapter Four has shown that both the electronic and steric nature of imido ligands can alter the reactivity of a metal complex. Carboranes, being bulky and electron withdrawing, offer potential for a novel type of imido ligand with interesting properties. Of the many methods of synthesising imido complexes, that described in Chapter Three using Na_2MoO_4 and a primary amine is one of the most convenient , the carboranyl amine being accessible.

The reaction of Na_2MoO_4 and $MeCbNH_2$ **31** in the presence of dme, Et_3N and TMSCl gave a yellow solution from which red crystals were obtained. When these crystals were redissolved a yellow solution was again obtained. This was shown by X-ray crystallography to be $[Mo(NCbMe)_2Cl_4]^{2-}[Et_3NH]_2^+$ **33** in the solid state.

$$\begin{aligned} &Na_2MoO_4 + 2MeCbNH_2 \\ &+ 4Et_3N + 11TMSCl \end{aligned} \xrightarrow{70°C,\ 12\ hrs} \begin{aligned} &3TMSCl + 2HNEt_3Cl \\ &+ 4TMS_2O + 2NaCl \\ &+ [Mo(NCbMe)_2Cl_4]^{2-}[Et_3NH]_2^+ \end{aligned}$$

33

Equation 5.1

The carboranyl amine displays a difference in reactivity to that for the majority of amines which form products of the form $Mo(NR)_2Cl_2$·dme. This may be due to the bulk and electron withdrawing nature of the carboranyl group and can be compared to the reactivity of $FmesNH_2$ **1**, also bulky and electron withdrawing, which also reacts differently to most amines, producing $Mo(NFmes)_2(OTMS)_2$ under similar conditions.

The colour change on dissolution may suggest dissociation into $Mo(NCbMe)_2Cl_2$ and Et_3NHCl.

It would appear that this salt is produced by the reaction of $Mo(NCbMe)_2Cl_2$, the formation of which is feasible under these conditions, with Et_3NHCl which is normally produced in such reactions. It seems possible that the electron withdrawing nature of the carborane promotes the addition of Cl^- to the metal centre thus increasing the formal electron count of the metal from 16 to 20 electrons.

5.2.2 Molecular Structure of $[Mo(NCbMe)_2Cl_4][Et_3NH]_2$

The diffusion of Et_2O into a thf solution of **33** gave red crystals which proved to be suitable for an X-ray diffraction study. The structure was solved by Prof. W. Clegg and Dr M.R.J. Elsegood of Newcastle University. The molecular structure is shown in Figure 5.6 and selected bond lengths and angles are collected in Table 5.2. Figure 5.7 shows a stereographic representation of **33**. This may be viewed by focussing on a distant object and then placing the diagram in the line of vision.

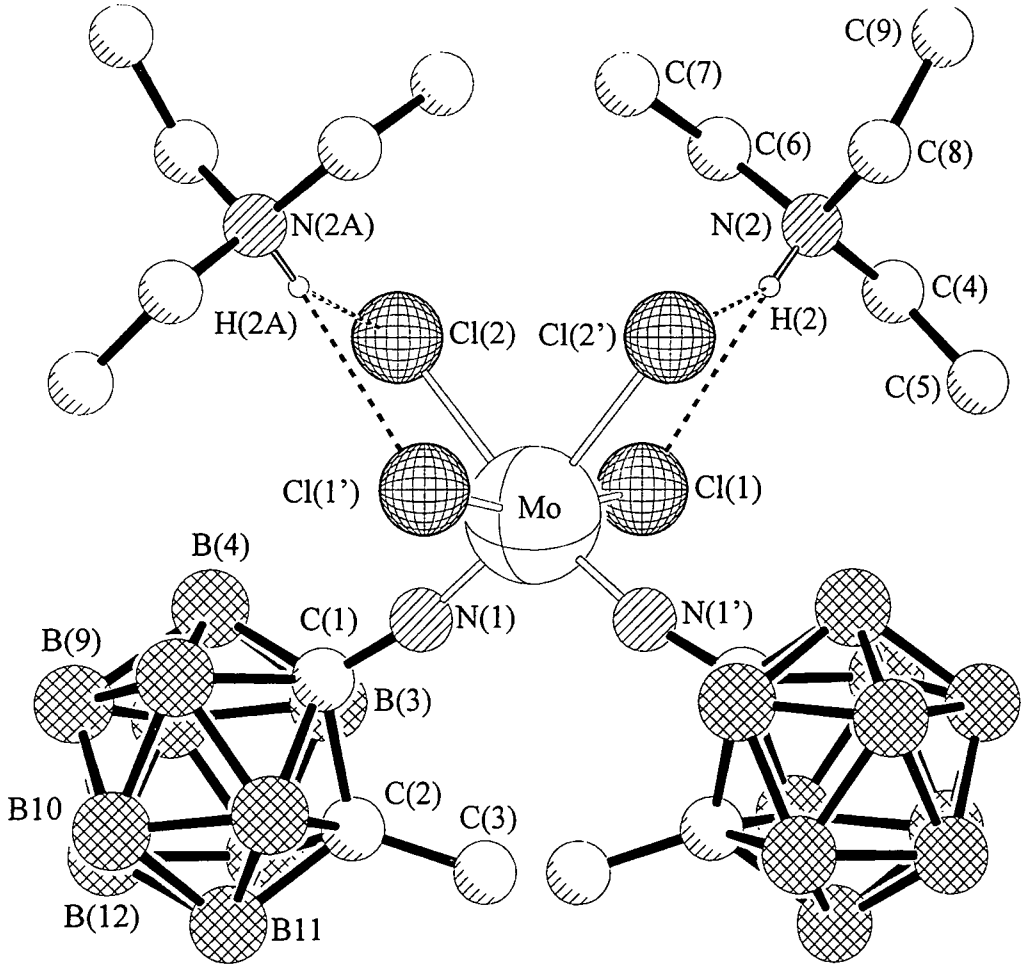

Figure 5.6 Molecular structure of 33

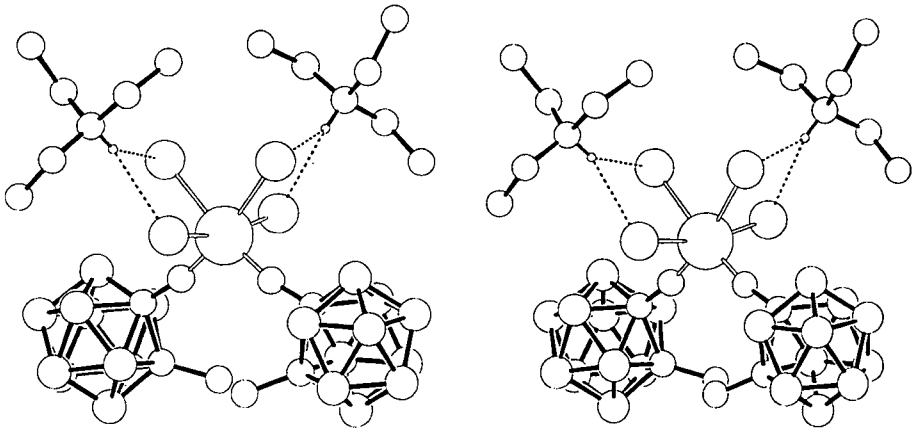

Figure 5.7 Stereographic representation of 33

Atoms	Bond Length / Å	Atoms	Bond Angles / °
C(1)-N(1)	1.364(2)	C(1)-N(1)-Mo	168.87(13)
N(1)-Mo	1.778(2)	N(1)-Mo-N(1')	102.41(10)
Mo-Cl(1)	2.4232(7)	Cl(1)-Mo-Cl(1')	166.87(3)
Mo-Cl(2)	2.5292(5)	Cl(2)-Mo-Cl(2')	82.92(3)
C(1)-C(2)	1.746(2)	Cl(1)-Mo-Cl(2)	85.53(2)

Table 5.2 Selected bond lengths and angles for 33

The structure is octahedral with the N-Mo-N angle distorted from that of an ideal octahedron to 102.41(10)° similar to that in compounds of the form $Mo(NR)_2Cl_2 \cdot dme$. The Mo-Cl bonds opposite the imido ligands are longer than the other Mo-Cl bonds by about 0.1Å. This is attributed to the trans effect of the π-donor imido ligands. The C-N-Mo angle of 168.9° is typical of 'linear' imido groups, bending in such a way as to maximise the distance between the two bulky cages.

There is a bifurcated NH···Cl hydrogen bond between the anion and cation, the H···Cl distances being about 2.5Å (Figure 5.8). This is comparable to normal NH···Cl distances of 2.40Å.[10]

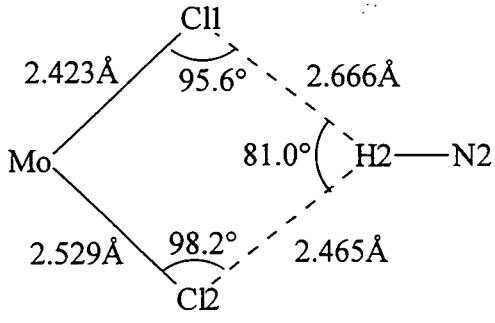

Figure 5.8 Hydrogen bonding in 33

The C1-N1 bond (1.364(2)Å) is shorter than those in all the N compounds discussed in Chapter 4 except in anion $(PhCb)_2N^-$ **24**. Although the solid state structure of the parent compound $MeCbNH_2$ **31** could not be determined it is presumed to be similar to that for $PhCbNH_2$ **32** although the C-C cluster bond would be expected to be somewhat shorter. The C-N distance in **32** is 1.396(3)Å, significantly longer than that in the imido ligand, indicating significantly more C-N π-bonding in **33**. This is

opposite to the aryl systems discussed in Chapter Three in which the C-N bond distance in the imido species is greater than in the corresponding amine. This is because the carborane can interact with two orthogonal lone pairs whereas the aromatic ring can only interact with one. Hence the formation of the imido species in the carborane case provides an extra p-orbital on N with which the cage can interact whereas for the aryl system the lone pair becomes shared with the metal. The C-C cluster bond in **33** does not, however, show the lengthening which would be expected to accompany this exo-π-bonding, although it is lengthened from that in the unperturbed cage. This is shown in Figure 5.9 , the point for **33** falling off the line through the points for the other nitrogen substituted carboranes. This indicates a difference in C-N π-bonding compared to that in the other compounds. This difference arises due to the fact that in all the other compounds there is only one p-orbital available for the formation of the *exo*-π-bond. In the imido ligand there are two such orbitals, and although this interaction is expected to be greatest for that in the plane of the C-C cluster bond it is expected that the other p-orbital will interact to some extent with the p_y on C1 (see Figure 4.10 for the definition of p_x and p_y). This will cause a shortening of the C-N bond but will not lengthen the C-C cluster bond. Hence this C-C bond will be shorter than might be expected on the basis of the C-N bond length.

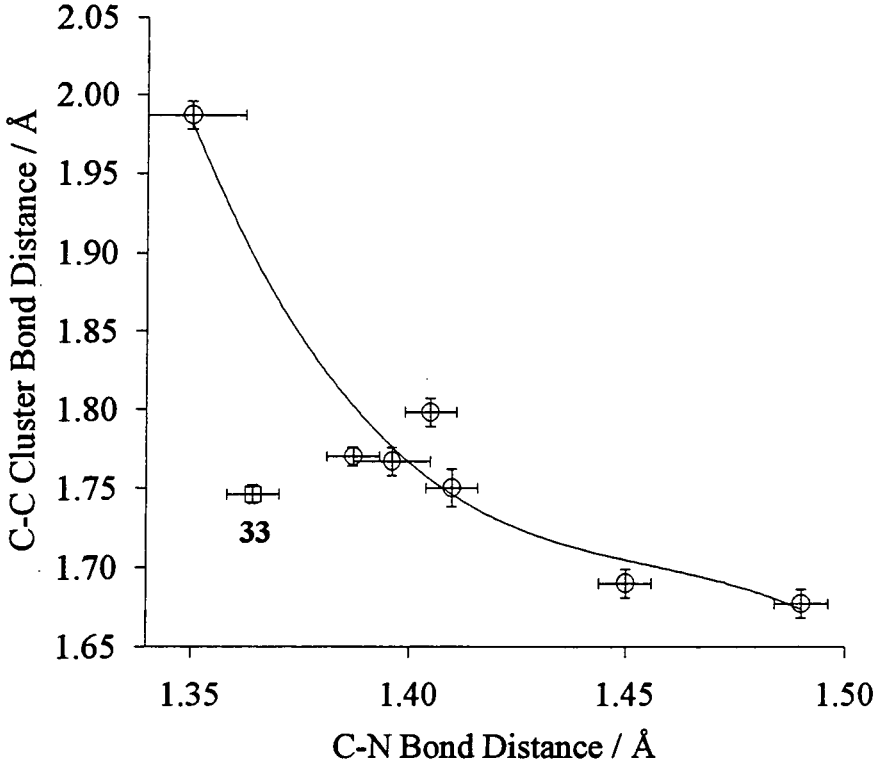

Figure 5.9 C-N vs C-C bond distances

This π-bonding involving the C-p_y cage orbital will affect cage bonding in a different way to that involving the C-p_x. The changes in bond lengths resulting from this can be predicted using similar arguments to those used previously by considering the $5e_1(x)$ and $5e_1(y)$ frontier orbitals. Exo bonding involving C-p_y will reduce the relative contribution of the $5e_1(y)$ orbital to cluster bonding, hence increasing the contribution from $5e_1(x)$. Both are bonding with respect to C1 and B4/B5 (Figure 5.10), hence little change in these bond lengths is expected. $5e_1(x)$ is bonding with respect to C1 and C2 but the $5e_1(y)$ is not, hence the C-C cluster bond should shorten as π-bonding to C-p_y increases. The coefficients on B3/B6 in the $5e_1(x)$ orbital are smaller than in the $5e_1(y)$ and so this bond would be expected to lengthen as the $5e_1(y)$ becomes less significant.

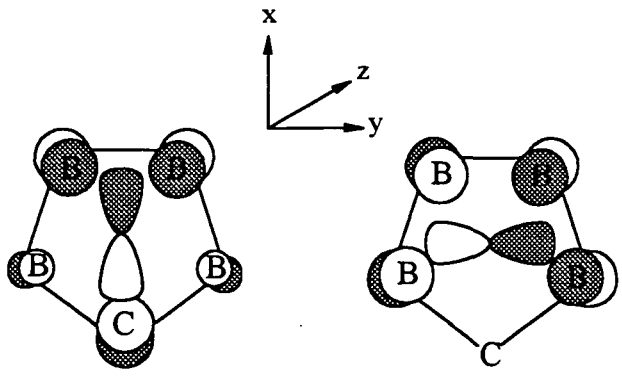

$5e_1(x)$ $5e_1(y)$

Figure 5.10

These changes are reflected in the *ab initio* geometry optimisation calculations carried out in Chapter Four. Table 5.3 compares bond lengths to C1 for STO-3G geometries for HCbH (Figure 5.11A) and $HCbNH_2$ with the N lone pair interacting with the C-p_x (pyramidal N, Figure 5.11B) and with the C-p_y (planar N, Figure 5.11C). As predicted above exo-π-bonding involving C-p_y causes a shortening of C1-C2 and lengthening of C1-B3 and C1-B6 bonds.

Compound	A	B	C
Bond			
C1-C2	1.635	1.675	1.628
C1-B3/6	1.701	1.734	1.771
C1-B4/5	1.701	1.712	1.715
C2-B3/6	1.729	1.716	1.734
B5-B6 / B3-B4	1.782	1.785	1.769
B4-B5	1.787	1.781	1.801

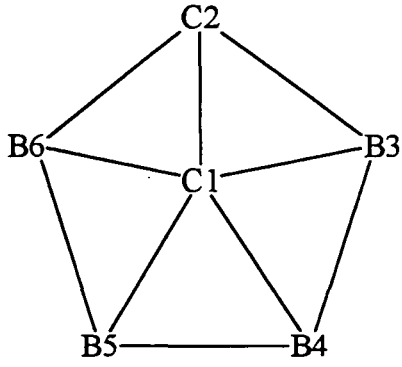

Table 5.3 Bond lengths / Å for STO-3G geometries of HCbH and $HCbNH_2$

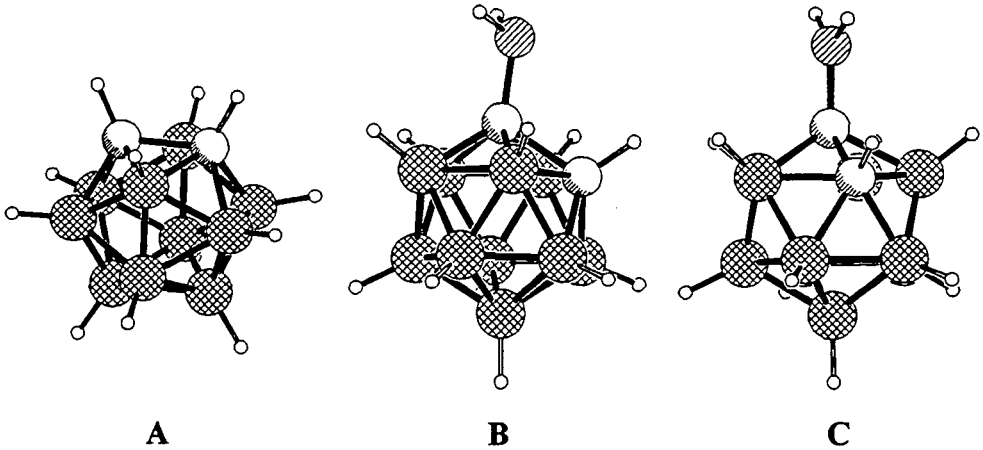

A **B** **C**

Figure 5.11

It would be expected that the bond lengths to C1 in **33** would also show this trend. Table 5.4 gives corresponding bond lengths determined by X-ray diffraction for *ortho*-carborane[11] and **33**. Data for $PhCbNH_2$ **32** are also included as an example of a compound with exo-π-bonding involving solely the C-p_x. The same trend is indeed discernible, **33** having significantly longer C1-B3 and C1-B6 bonds than either **32** or parent *ortho*-carborane.

Compound	HCbH	**33**	**32**
Bond			
C1-C2	1.630(6)	1.746(2)	1.767(3)
C1-B3/6	1.711(7)	1.740(3)	1.715(3)
C1-B4/5	1.693(7)	1.693(3)	1.699(3)
C2-B3/6	1.711(7)	1.728(3)	1.722(3)
B5-B6 / B3-B4	1.772(8)	1.782(3)	1.773(4)
B4-B5	1.777(8)	1.778(3)	1.773(4)

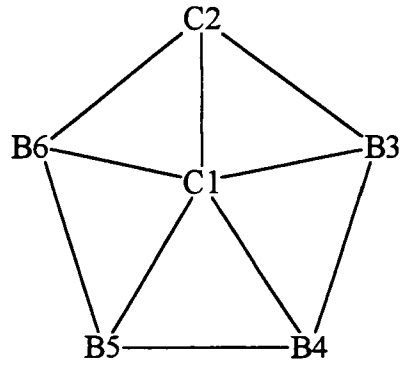

Table 5.4

There is no example of a carborane bearing a strong π-donor in which the lone pair is constrained only to interact with the C-p_y. Such a compound as that shown in Figure 5.12 would be an example of such bonding and should possess lengthened C1-B3/B6 bonds and a shortened C1-C2 bond.

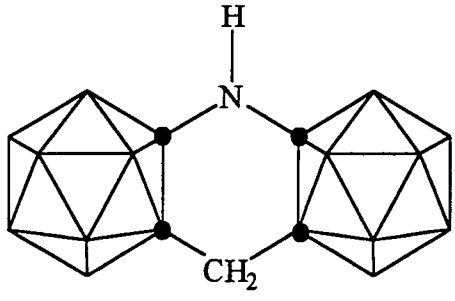

Figure 5.12

In Chapter Four it was shown that there is a close correlation between the C-N *exo* π-bond order and the ^{11}B NMR shift of the antipodal B atom i.e. that directly opposite the N substituent. Figure 5.13 shows that the point for 33 falls on the line for C-C bond lengths vs ^{11}B δ-B12. However, this point does not fall on the line for C-N bond lengths vs ^{11}B δ-B12 (Figure 5.14). The observed chemical shift of -6.75 ppm would correspond to an expected C-N bond length of ~1.40Å. Due to the possibility that the species in solution (on which the NMR measurement is made) is different to that in the solid such comparisons may be invalid. $Mo(NCbMe)_2Cl_2$, the species possibly present in solution should show more N-Mo π-bonding due to a lower electron count on the metal, and hence less N-C π-bonding.

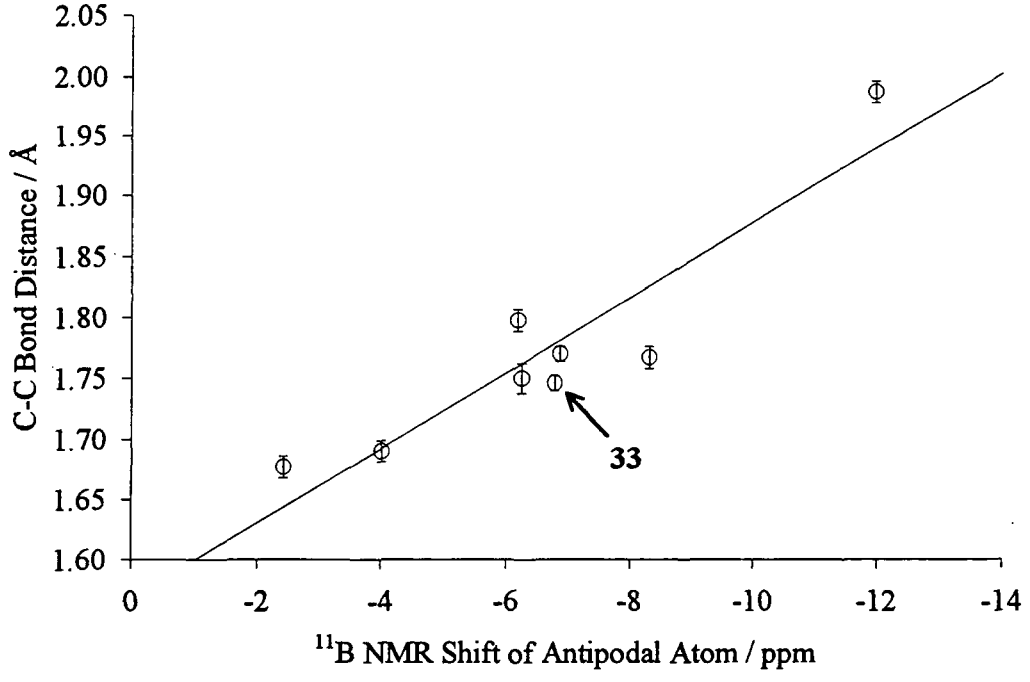

Figure 5.13

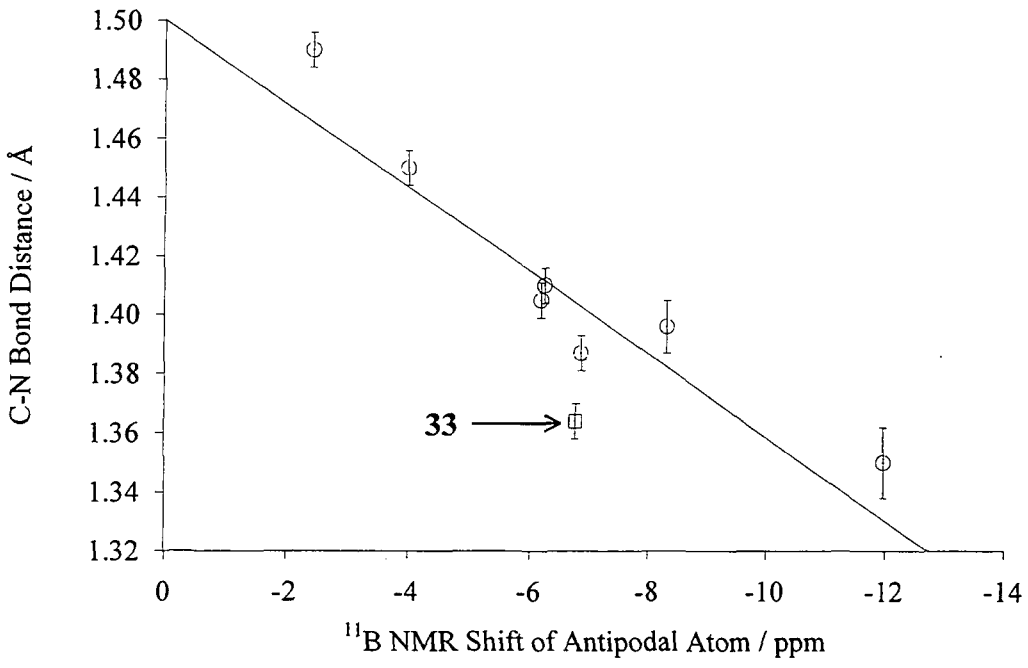

Figure 5.14

Whereas an alkyl imido ligand will provide two degenerate p-orbitals for N-Mo π-bonding this will not be the case for this carboranyl ligand as interactions between the cage and N p-orbitals will remove this degeneracy. The p-orbital which interacts least with the cage will be of higher energy than the other and hence preferable for Mo-N π-bonding, this will be the p-orbital perpendicular to the C-C cluster bond. This should be reflected in the orientation of the cage with respect to the metal centre.

π-Donor ligands can be divided into several classes (see Chapter One). This complex can be described in terms of two Π_2, ligands, i.e. ligands having two non-degenerate π-symmetry orbitals. Although these 'rules' do not explicitly cover this class of compound they can be adapted to include such complexes. Three Cl atoms can be treated as one atom, thus reducing the system to a triad. If one imido ligand is treated as a dominant Π_2 donor the orientation of the other relative to this can be predicted. It is often difficult to predict which π-orbital in a Π_2, ligand will dominate. However, it is likely that the p-orbital on N perpendicular to the C-C cluster bond will dominate being that which interacts least strongly with the cage and therefore most strongly with the metal. This p-orbital would be expected to "underline" the other imido

ligand. Hence the C-C cluster bond of each cage should point towards the other cage. Figure 5.15A shows that this is the case, the cages turning so that the C-C bonds are nearly pointing towards each other, the methyl groups on C2 being as close as steric interactions will allow (Figure 5.15B). An orientation with the methyl groups on the opposite sides of the cage could attain the desired conformation without interference between the methyl groups (Figure 5.16). This conformation is made unfavourable by steric repulsions between the methyl groups and chlorine ligands (Figure 5.17). As with all molecular structures in the solid state the chance exists that crystal packing effects and intermolecular interactions may affect the conformation.

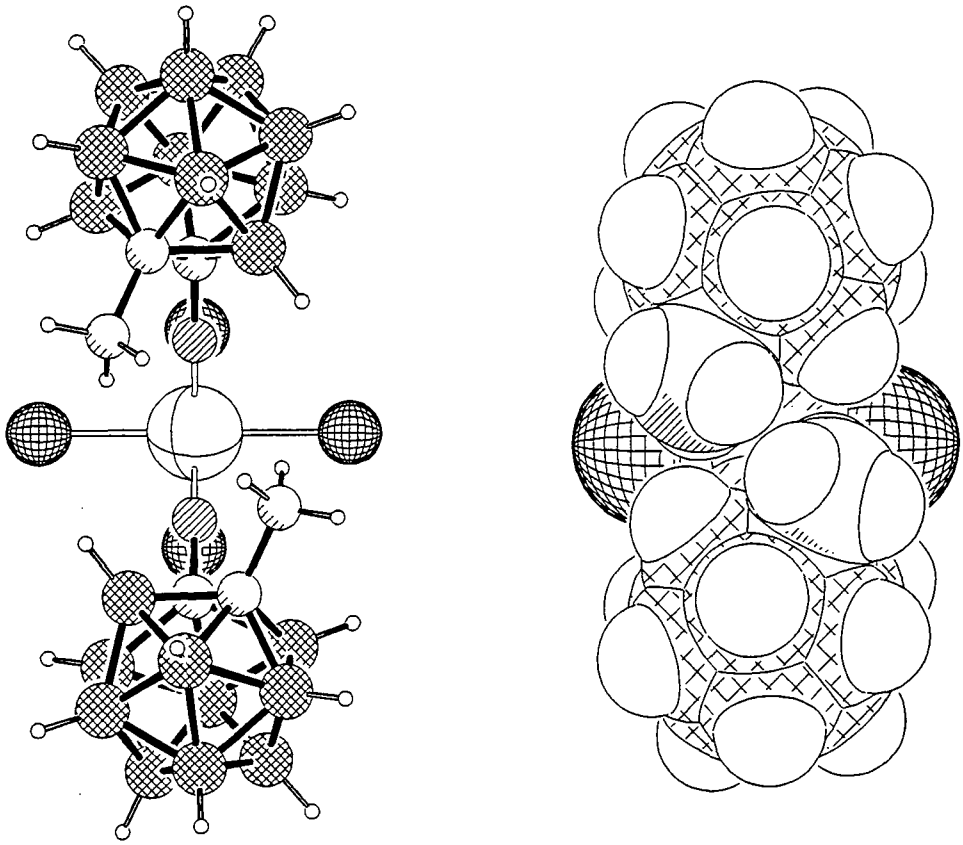

A **B**

Figure 5.15 Molecular structure of 33, cations omitted

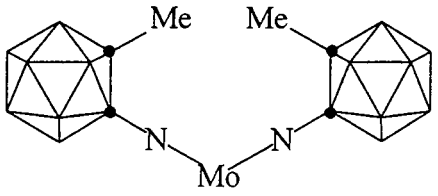

Conformation Found In Crystal

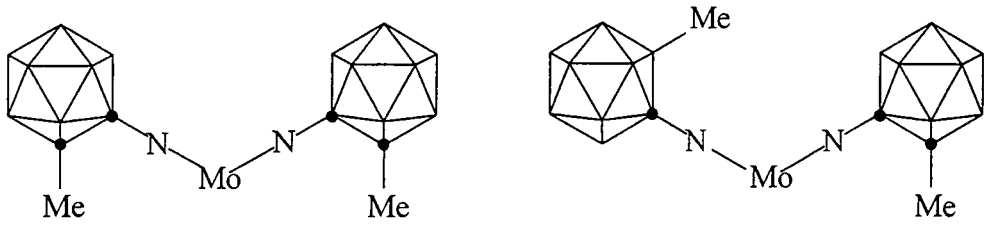

Other possible conformation

Figure 5.16 Conformation of cages in 33

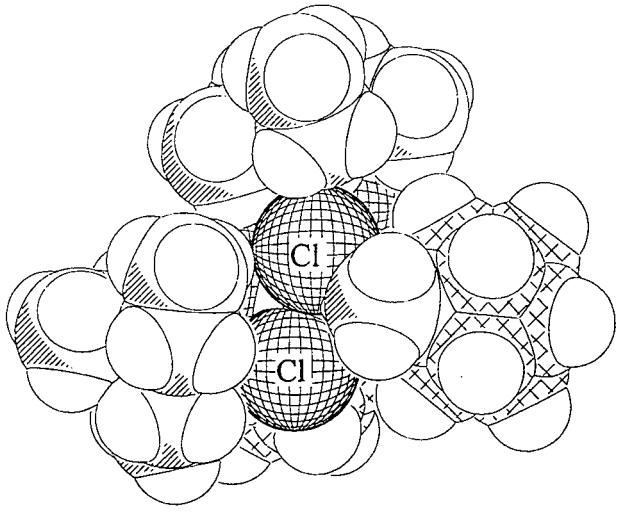

Figure 5.17 Steric interactions between Me and Cl in the opposite orientation to that adopted

Extended Hückel calculations have been carried out to investigate the conformation in this compound further. The coordinates for the crystal structure were taken with the methyl group on C2 replaced by H. Calculations were performed for a variety of orientations varying only in the orientation of the cage relative to the metal centre as defined by the C2-C1-Mo-N1A torsional angle (154° in the solid state structure). The energies obtained by this method (Figure 5.18) for these conformations confirm that the preferred conformation in the absence of steric repulsions associated with the methyl group is that with the C-C axis of the cage pointing towards the other imido

ligand. The Reduced Overlap Populations which give a measure of bond order (Figure 5.19) confirm that this orientation will maximise Mo-N bonding. The maximum in Mo-N bonding corresponds to a minimum in N-C1 bonding reflecting competition for the p-orbitals on N.

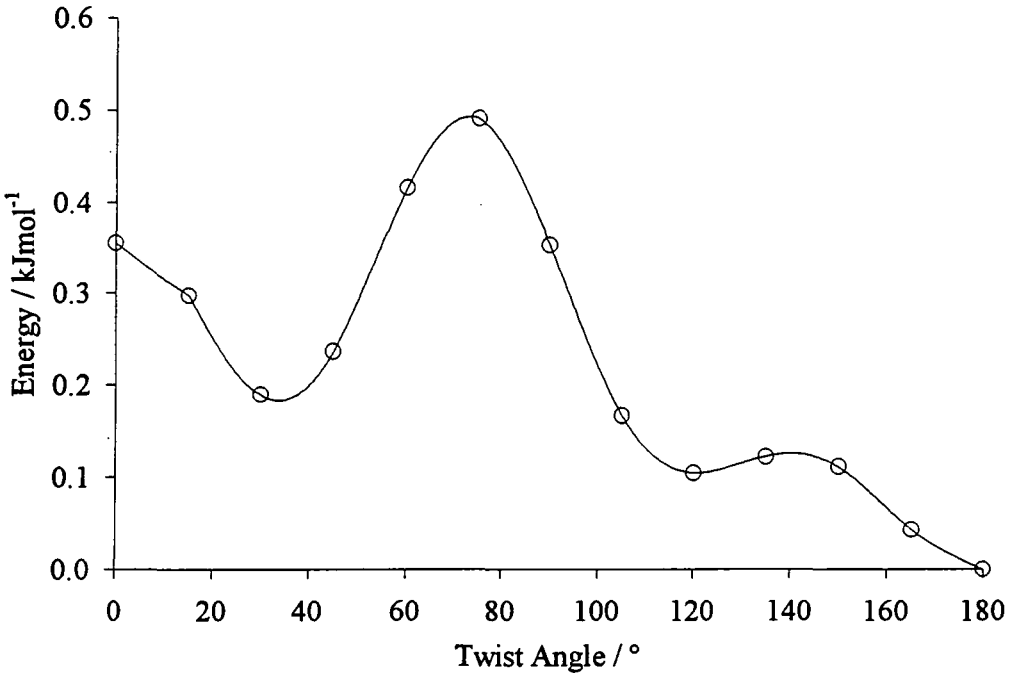

Figure 5.18 Variation in energy with orientation of carborane cage

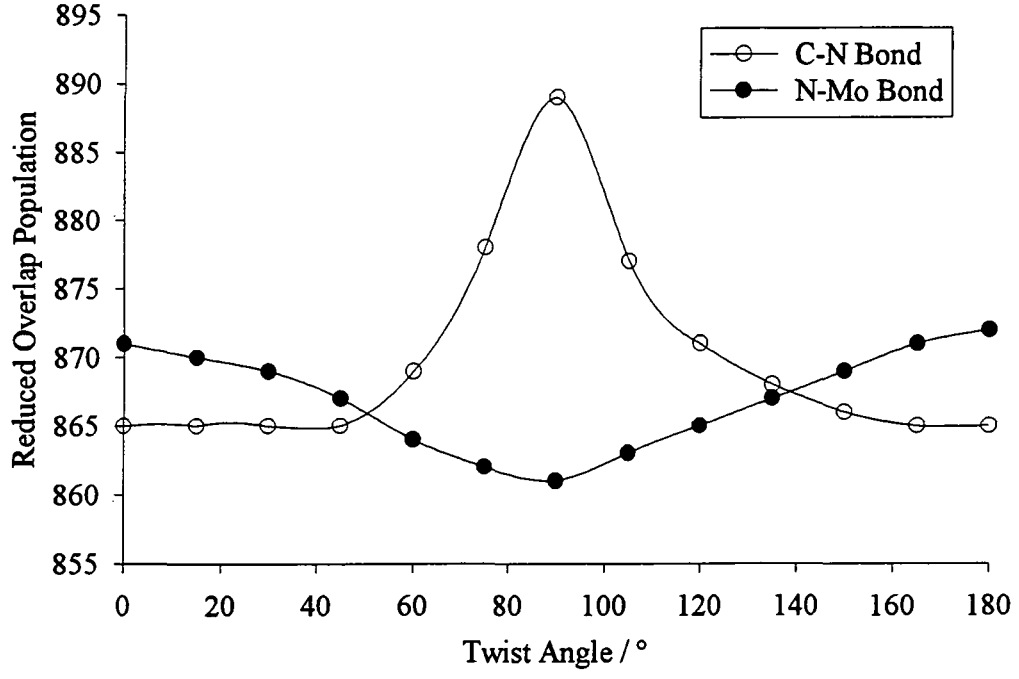

Figure 5.19 Variation in Reduced Overlap Populations with orientation of carborane cage

5.2.3 THE REACTION BETWEEN $Cp_2Zr(NMe_2)_2$ AND $MeCbNH_2$

There is a number of examples of imido ligands in Group 4 metals, both terminal and bridging, although bridging ligands are the most common. Bulky groups tend to stabilise terminal imido ligands for these metals.

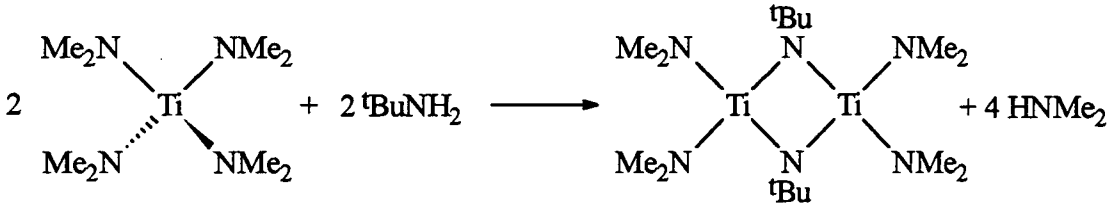

Figure 5.20

One method of synthesising such compounds is by the reaction of dialkylamides with primary amines (Figure 5.20).[12] Such a reaction was carried out between $Cp_2Zr(NMe_2)_2$ and $MeCbNH_2$ and resulted in the formation of an orange solid. This was shown by ^1H NMR to be a mixture of products, the nature of which could not be determined. Me_2NH was apparent in the ^1H NMR, presumably coordinated to the metal centre. No other NH environment was evident in either ^1H NMR or IR spectra indicating that both amine hydrogen atoms had been replaced. The ^{11}B NMR was complex indicating the presence of more than one cage environment, although both this and the IR confirmed that the cage had remained *closo*. Two possible structures are suggested in Figure 5.21 including either terminal or bridging imido groups.

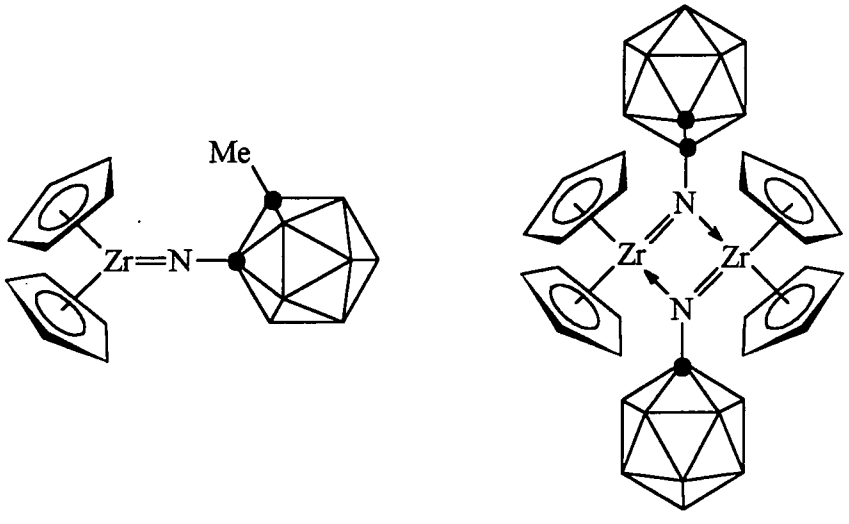

(Such structures including coordinated Me_2NH are also possible)

Figure 5.21

5.3 Attempted Syntheses of Other Carborane-Containing N-Donor Ligands

The synthesis of metal amides by amide exchange has been mentioned previously in Chapter 1. Attempts were made to synthesise a carboranyl amide by this method, reactants being summarised in Equation 5.2. In all cases a mixture of products which could not be separated was obtained. IR and ^{11}B NMR spectra indicated that the carborane cage has degraded to a *nido*-cage. No NH peak was visible in the IR indicating that amide exchange has occurred. The probable reason for the degradation of the cage is nucleophilic attack by the liberated Me_2NH.

$Zr(NMe_2)_4 + (RCb)_2NH \longrightarrow Zr(NMe_2)_3[N(CbR)_2] + Me_2NH$ R = Ph, Me

$Ti(NMe_2)_4 + (PhCb)_2NH \longrightarrow Zr(NMe_2)_3[N(CbR)_2] + Me_2NH$

$Cp_2Zr(NMe_2)_2 + (PhCb)_2NH \longrightarrow Zr(NMe_2)_3[N(CbR)_2] + Me_2NH$

Equation 5.2

A similar reaction was carried out employing $Cp_2Zr(NMe_2)_2$ and MeCbNHNHPh. An orange crystalline material was obtained which was shown by ^1H and ^{13}C NMR to be a mixture of products. Again no NH peaks were evident in the IR implying that proton exchange had occurred to give products similar to that in Figure 5.22. Complexes of this type have previously been formed by the reaction of Cp_2ZrCl_2 with 1,2-dilithio-1,2-diphenylhydrazine, the crystal structure of $Cp_2Zr(N_2Ph_2)(thf)$ having been determined.[13]

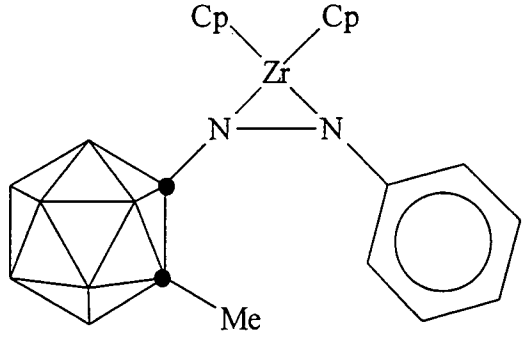

Figure 5.22

5.4 OXYGEN LIGANDS CONTAINING CARBORANES

There are many examples known of alkoxides and aryloxides. Both steric and electronic effects of susbstituent groups are known to influence the structures and reactivity of such complexes. The compounds RCbOH offer the potential for the formation of carboranyl analogues of such systems, the anion $PhCbO^-$ representing the free ligand.

Alkoxide exchange has proved to be an efficient and reliable method for synthesising new alkoxide species (Equation 5.3). Such reactions constitute equilibria and the isolation of a pure product relies on the ability to force the equilibrium over to a single product. This is readily achieved if the alcohol displaced is volatile and can be removed under reduced pressure, whereas the alcohol being substituted onto the metal is involatile. Thus the equilibrium can be forced over to the desired product by the removal of the displaced alcohol.

$$M(OR)_2 + 2R'OH \rightleftharpoons M(OR)(OR') + ROH + R'OH \rightleftharpoons M(OR')_2 + 2ROH$$

Equation 5.3

5.4.1 SYNTHESIS OF $Mo(NAr^i)_2(OCbPh)_2$

The treatment of $Mo(NAr^i)_2(O^tBu)_2$ with two equivalents of PhCbOH in pentane resulted in the formation of an orange precipitate. This proved to be $Mo(NAr^i)_2(OCbPh)_2$ **34**, the insolubility of this compound in pentane allowing its isolation in high yield and purity by displacing the equilibrium towards the product.

$$Mo(NAr^i)_2(O^tBu)_2 + 2PhCbOH \longrightarrow 2^tBuOH +$$

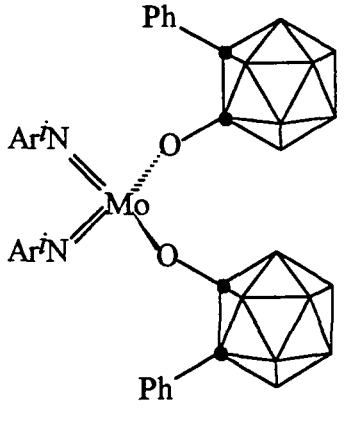

34

Equation 5.4

The similar complex $Mo(NAr^{i})_2(OCbMe)_2$ **35** was synthesised in the same manner from $Mo(NAr^{i})_2(O^{t}Bu)_2$ and MeCbOH.

A similar reaction with $Cp_2Zr(NMe_2)_2$ and two equivalents of PhCbOH gave an off-white solid which appeared from ^{1}H NMR to be the desired product $Cp_2Zr(OCbPh)_2$. Again the antipodal B atom is difficult to locate in the ^{11}B NMR spectrum. The C-O stretch in the IR is in a similar position to that in both PhCbOH and **34** and it seems likely that C-O and C-C bond lengths, and hence C-O π-bond order in this compound would be similar to those in **34**.

5.4.1.1 Molecular Structure of $Mo(NAr^{i})_2(OCbPh)_2$

After 48 hours at room temperature the reaction between $Mo(NAr^{i})_2(O^{t}Bu)_2$ and PhCbOH had appeared to finish. The solution was filtered, and upon standing crystals of **34** formed which proved to be suitable for an X-ray diffraction structure determination. The structure was solved by Prof. W. Clegg and Dr M.R.J. Elsegood of Newcastle University. The molecular structure is shown in Figure 5.23 and selected bond lengths and angles collected in Table 5.5.

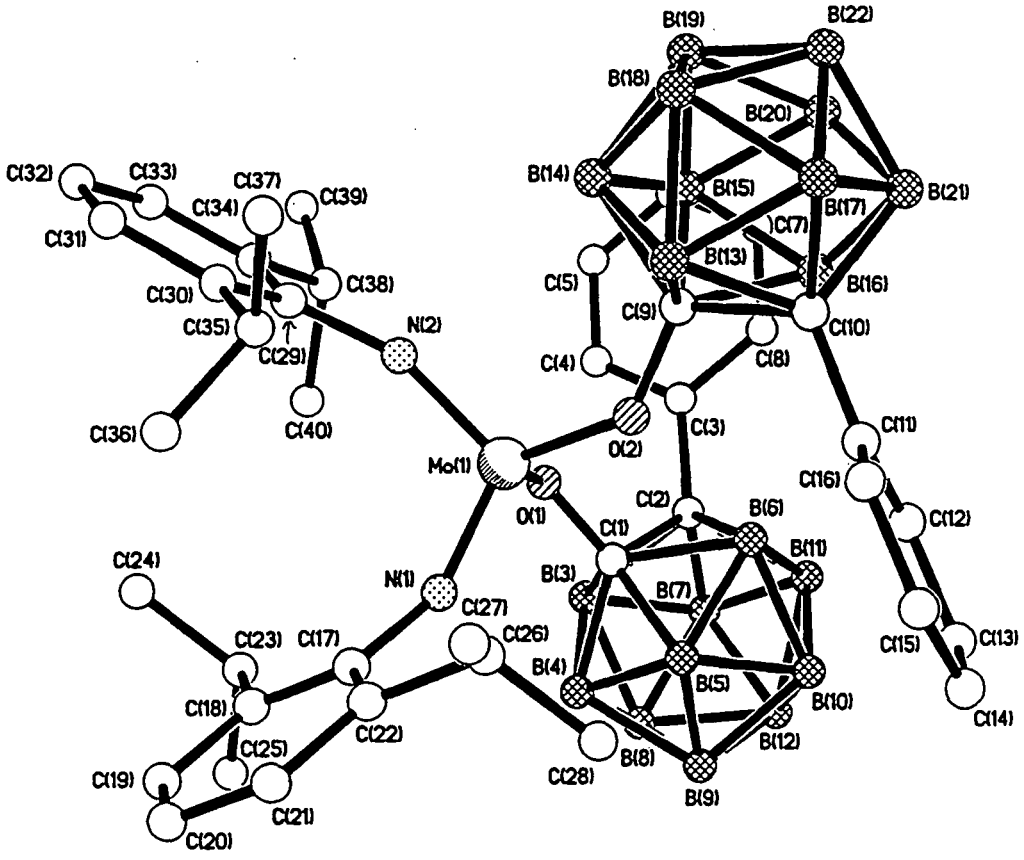

Figure 5.23 Molecular structure of 34

Atoms	Bond Length / Å	Atoms	Bond Angles / °
Mo-O1	1.9517(11)	N2-Mo-N1	108.06(6)
Mo-O2	1.9424(11)	N1-Mo-O2	106.67(6)
Mo-N1	1.7421(13)	N1-Mo-O1	111.61(6)
Mo-N2	1.7369(14)	N2-Mo-O2	110.86(6)
C1-C2	1.708(2)	N2-Mo-O1	102.68(6)
C9-C10	1.710(2)	O2-Mo-O1	116.72(5)
C1-O1	1.3498(19)	C1-O1-Mo	125.53(10)
C9-O2	1.3504(19)	C9-O2-Mo	133.76(10)
C17-N1	1.397(2)	C17-N1-Mo	158.06(12)
C29-N2	1.398(2)	C29-N2-Mo	160.54(12)

Table 5.5 Selected bond lengths and angles in 34

The geometry adopted is distorted tetrahedral, the greatest deviation from an ideal tetrahedron being the O-Mo-O angle of 116.7° reflecting repulsion between the two bulky cages.

The C-O bond to the cage (1.3498(19)Å) and C-C bond within the cage (1.708(2)Å) are surprisingly close to those found in the parent alcohol PhCbOH (1.366(2)Å and 1.723(3)Å respectively), so although there appears to be some degree of *exo*-π-bond formation there is far less than in the anion $PhCbO^-PS^+$, and slightly less than even the parent alcohol. The ^{11}B NMR shift could not be determined for the antipodal atom as most of the peaks form a single very broad peak. The C=O stretching frequencies in the IR are similar (1230 cm^{-1} in PhCbOH and 1225 cm^{-1} in **34**) indicating similar bond strengths.[14]

The Mo-O-C bond angles imply sp^2 hybridisation of the O indicating one 'lone pair' in a p-orbital and another in an sp^2 orbital. The p-orbital will form the strongest π-bonds to either the metal or carborane as p-d π-overlap will be greater than sp^2-d π-overlap. It is the sp^2 lone pair on O that is aligned with the C-p_x of the cage unlike the parent alcohol PhCbOH. This may be the reason for the relatively small C-O π-bond order. It may be that this orientation is adopted due to steric constraints, this conformation placing the phenyl ring as far as possible away from the rest of the molecule.

There are few $Mo(NR)_2(OR')_2$ structures known with which to compare this structure. $Mo(N^tBu)_2(O^tBu)_2$ has been structurally characterised and has Mo-O bond lengths of around 1.87Å, shorter than those in **34**. This is attributed to O-C π-bonding in **34** which will reduce the availability of the p-orbitals on O for π-bonding and hence lengthen the Mo-O bond. Likewise, compounds containing Mo-OC_6F_5 typically have Mo-O distances of 1.90 - 2.10Å and C-O distances of 1.32 - 1.37Å, comparable to those in **34**. This again is due to an interaction between the lone pairs on O and the ring.[15] The Mo-O-C bond angle in **34** (average 129.6°) is smaller than that found in most alkoxides, typically 140°. This is probably caused by repulsion between the phenyl ring on C2 bending away from the rest of the molecule. It has been estimated that a Mo-O single bond should be around 2.00-2.05Å.[16] On this basis it would appear that there is little Mo-O π-bonding in **34**.

This complex can be described in terms of two Π_2 ligands, the imido ligands, and two Π_2, ligands, the carborane ligands. The imido ligands will be the strongest π-donors and hence should determine the orientation of the other ligands. The dominant π-

orbital on O should be the p-orbital and this should point between the imido ligands. This is more or less the conformation found in the solid, shown clearly in Figure 5.24 in which the lone pairs in p-orbitals on O lie horizontally. In such a crowded molecule steric effects will also be important although it is difficult to predict which orientation will minimise steric crowding. There is a slight difference between the orientations of the two cages which is no doubt due to either crystal packing or steric effects. The structure of a related complex with a less bulky substituent on C2 of the carborane, either Me or H, would help to assess the importance of steric factors in determining the adopted conformation. Such compounds may tolerate a greater C-O-Mo angle hence allowing more C-O π-bonding.

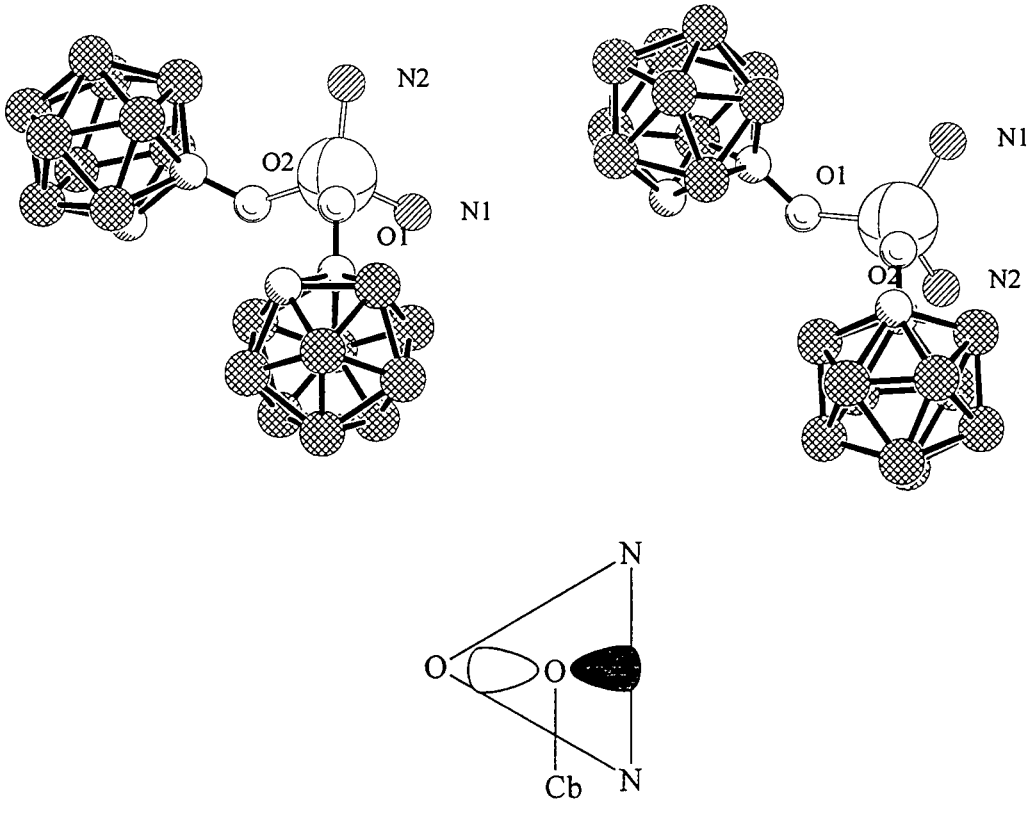

Figure 5.24 Conformation in 34, viewed down O-Mo bond, phenyl and imido groups removed for clarity.

5.5 Synthesis of Compounds Containing Carboranes and Mo-C σ-Bonds

5.5.1 Synthesis of $Mo(NR)_2(CbMe)_2$ Species

The reaction of lithio-carboranes with metal chlorides yields compounds with a carborane cage bound to a metal by a M-C σ-bond. While such compounds are known for many transition metals, none are known for molybdenum.

The reaction of both $Mo(N^tBu)_2Cl_2$·dme and $Mo(NAr^i)_2Cl_2$·dme with two equivalents of LiCbMe gave the corresponding compounds $Mo(N^tBu)_2(CbMe)_2$ **36** and $Mo(NAr^i)_2(CbMe)_2$ **37**.

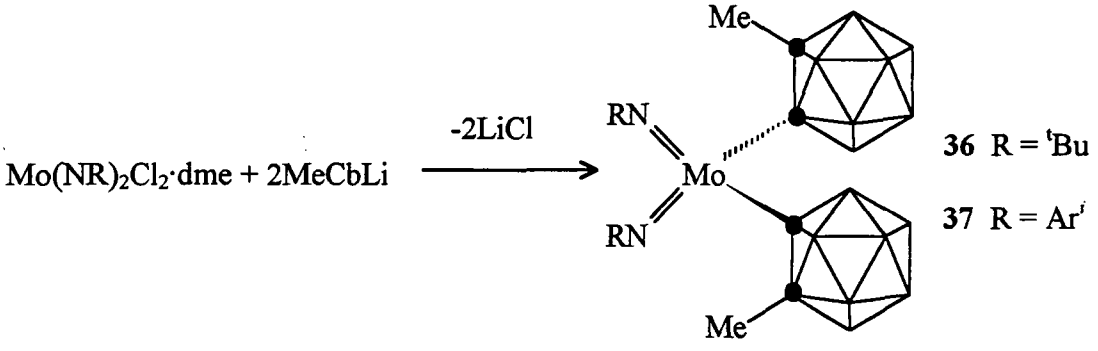

Equation 5.5

5.5.2 Synthesis of Species Containing Chelating Carboranes

These reactions were repeated employing one equivalent of LiCbLi in place of two equivalents of MeCbLi. The reaction with $Mo(N^tBu)_2Cl_2$·dme gave an orange crystalline product (**39**) in low yield. ^1H NMR indicated this to be a mixture of products, three ^{t}Bu environments being evident, two of which are of equal intensity. No carboranyl CH was evident in either ^1H NMR or IR spectra indicating that both C atoms of the cage are bonded to the metal. Mass spectral analysis shows the presence of a species corresponding to the dimer $[Mo(N^tBu)_2(C_2B_{10}H_{10})]_2$ but no sign of the monomer. The products obtained appear to be a mixture of dimeric products, possible structures of which are shown in Figure 5.25. A mixture of two such products would give ^1H NMR signals of the type observed, structure **A** giving rise to one ^{t}Bu signal, structure **B** giving two of equal intensity.

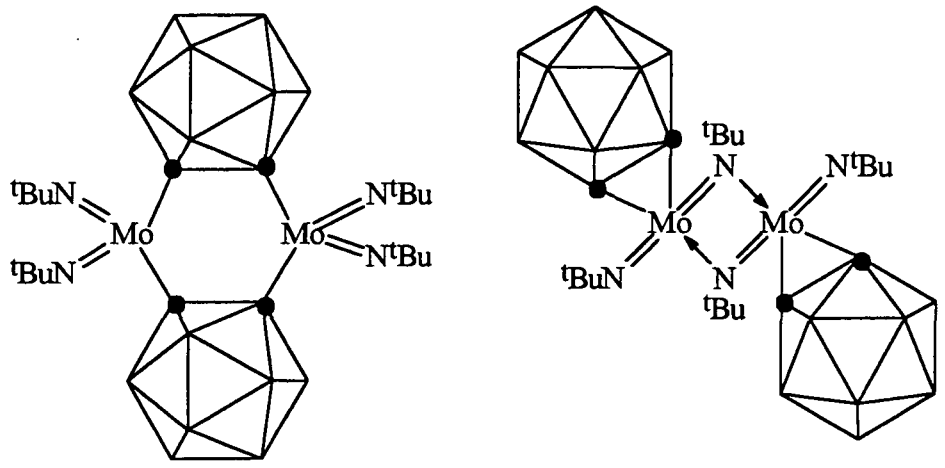

A B

Figure 5.25 Proposed structures for [Mo(NtBu)$_2$Cb]$_2$ - 39A and 39B

The reaction with Mo(NAr^i)$_2$Cl$_2$·dme and LiCbLi gave a red crystalline solid in good yield **38**. The mass spectrum of this product showed only the monomer Mo(NAr^i)$_2$($C_2B_{10}H_{10}$) (Figure 5.26). The monomer is preferred in this case due to the greater steric bulk of the aryl imido ligands.

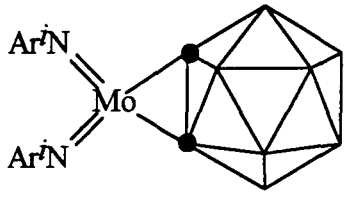

Figure 5.26 Proposed structure for 38

The ^{11}B NMR for **38**, unlike those for **36** and **37**, is very broad, two peaks of relative intensity 2:8 being evident. The reason for this broad appearance is not clear.

5.6 CONCLUSIONS

Two novel types of carboranyl ligand have been synthesised. The carboranyl imido species **33** shows greater C-N π-bonding than the parent amine **31**. The carboranyl oxide **34** however shows slightly less C-O π-bonding than the parent alcohol. The orientations of the cage relative to the metal centre can be rationalised in terms of competition for π-symmetry metal orbitals, although with such bulky ligands steric factors will also be important in determining orientations. The π-interactions between cage and substituent remove the degeneracy of the lone pairs on the donor atom and hence affect the orientation of the cage.

It has been demonstrated that exchange between metal amides and carboranes bearing substituents with acidic hydrogens can generate metal complexes containing carboranes. Although no pure products were obtained there is no reason to believe that further efforts would not result in success. The structures presented in this thesis show that such compounds are likely to show features of considerable interest. Further information on conformations in such compounds may clarify whether electronic or steric effects are responsible for the orientations observed. Other compounds in Chapter Four, for example RCbNO and $RCbN_2Ar$, are also potential ligands which remain to be investigated.

Novel complexes containing carboranes σ-bonded to Mo have also been synthesised including both bridging and chelating ortho-carboranes.

5.7 REFERENCES

1 K.Wade, Adv. Inorg. Chem. Radiochem., 1976, 18, 1; see also M.E. O'Neill and K. Wade, Metal Interactions with Boron Clusters, Ed. R.N. Grimes,1982, Plenum Press, New York.

2 S. Bresadola, Metal Interactions with Boron Clusters, Ed. R.N. Grimes,1982, Plenum Press, New York.

3 A.A. Sayler, H. Beall and J.F. Sieckhaus, *J. Am. Chem. Soc*, **1973**, *95*, 5790.

4 X. Yang, C.B. Knobler, Z. Zheng and M.F. Hawthorne, *J. Am. Chem. Soc*, **1994**, *116*, 7142.

5 X. Yang, Z. Zheng, C.B. Knobler and M.F. Hawthorne, *J. Am. Chem. Soc.*, **1993**, *115*, 193.

6 W. Clegg, D.A. Brown, S.J. Bryan, K. Wade, *Polyhedron*, **1984**, *3*, 307.

7 C.A. Tolman, *J. Am. Chem. Soc.* **1970**, *92*, 2956.

8 Rosario Nùñez, Tesis Doctoral, 1996, L'Institut de Ciència de Materials de Barcelona.

9 A.I. Yanovskii, Yu T. Struchkov, V.N. Kalinin, A.V. Usatov, L.I. Zakharkin, *Koord. Khim.*, **1982**, *8*, 240.

10 W.C. Hamilton, J.C. Ibers, "Hydrogen Bonding in Solids", W.A. Benjamin, New York, 1968.

11 M.G. Davidson, T.G. Hibbert, J.A.K. Howard and K. Wade, unpublished results.

12 D.C. Bradley and E.G. Torrible, *Can. J. Chem.*, **1963**, *41*, 134.

13 P.J. Walsh, F.J. Hollander and R.G. Bergman, *J. Am. Chem. Soc.* **1990**, *112*, 894.

14 W.A. Nugent, J.M. Mayer, "Metal-Ligand Multiple Bonds", John Wiley and Sons, Inc, 1988, New York, pp122.

15 R.G Abbott, F.A. Cotton, L.R. Falvello, *Inorg Chem*, **1990**, *29*, 514.

16 T.W. Coffindaffer, I.P. Rothwell and J.C. Huffman, *Inorg. Chem.*, **1983**, *22*, 2907.

Chapter Six

Experimental Details

6.1 General Experimental Techniques

All manipulations of air or moisture sensitive compounds were performed on a conventional vacuum / nitrogen line using standard Schlenk and cannula techniques or in a nitrogen filled dry box. When required, solvents were dried by prolonged reflux over an appropriate drying agent prior to distillation and deoxygenated by a freeze-thaw process. Drying agents used were sodium metal (toluene, heptane), lithium aluminium hydride (pentane, diethyl ether), potassium metal (1,2-dimethoxyethane), calcium hydride (dichloromethane, acetonitrile) and sodium benzophenone ketyl (tetrahydrofuran). NMR solvents when required dry were vacuum distilled from a suitable drying agent immediately prior to use. These drying agents were di(phosphorus(V)pentoxide) (d_6-benzene, d_8-toluene, d_3-chloroform, d_{12}-cyclohexane, d_2-dichloromethane, d_8-tetrahydrofuran) and calcium hydride (d_3-acetonitrile).

Elemental analyses were performed by the microanalytical services within the university.

Infrared spectra were recorded on Perkin Elmer 1600FT and 577 spectrometers as either KBr discs or Nujol mull (CsI windows). Abbreviations used are s (strong), m (medium), w (weak), br (broad) and sh (shoulder).

Melting points were measured in capillary tubes with an Electrothermal 9200 heating block.

Mass spectra were recorded on a VG 7070E Organic Mass Spectrometer using either electrical ionisation (EI) or chemical ionisation with ammonia (CI). [M] is used to denote the molecular ion.

NMR spectra were recorded on the following machines at frequencies listed unless stated otherwise: Bruker AMX500, 1H (500.14 MHz), ^{11}B (160.46 MHz); Varian VXR400, ^{1}H (399.95 MHz), ^{13}C (100.58 MHz), ^{31}P (161.90 MHz), ^{19}F (376.32 MHz): Bruker AC250, ^{11}B (80.25 MHz). Chemical shifts are quoted as δ in ppm. ^{1}H NMR spectra were referenced to the residual protio impurity in the solvent (C_6D_6, 7.15 ppm; $CDCl_3$, 7.26 ppm; CD_3CN, 2.34 ppm; CD_2Cl_2, 5.25 ppm). ^{13}C NMR spectra were referenced to the solvent resonance (C_6D_6, 128.0 ppm; $CDCl_3$, 77.0 ppm). ^{19}F, ^{31}P and ^{11}B NMR spectra were referenced externally to $CFCl_3$, 85% H_3PO_4 and

$BF_3 \cdot Et_2O$ respectively. Unless stated otherwise all spectra were recorded at ambient temperature. The following abbreviations have been used for multiplicities: s (singlet), d (doublet), t (triplet), q (quartet), sept (septet), br (broad), m (unresolved multiplet).

Unless otherwise stated chemicals used and not described here were purchased commercially (Aldrich).

AM1 Calculations were carried out using MOPAC 5.0[1] (Chapter 2 and Section 4.6.12) or MOPAC 6.0[2] (Sections 4.6.8, 4.7 and 4.8). The keyword PRECISE was used for all geometry optimisation experiments. *Ab initio* calculations were carried out using GAMESS-UK[3]. Extended Hückel calculations were carried out using CACAO.[4]

6.2 EXPERIMENTAL DETAILS TO CHAPTER TWO

6.2.1 SYNTHESIS OF 1,3,5-TRIS(TRIFLUOROMETHYL)BENZENE ('FLUOROMES')

1,3,5-tris(trifluoromethyl)benzene was prepared by a previously published procedure[5] employing trimesic acid ($1,3,5\text{-}(CO_2H)_2C_6H_3$) and SF_4 heated to 150°C for 20hrs in a steel autoclave. Effluent gases were neutralised by passage over 10% NaOH solution. Prior to use it was washed with 10% NaOH solution, dried over $MgSO_4$, distilled using a Vigreux column (1 atoms., 118-120°C) and stored over 4Å molecular sieves.

$^{13}C[^1H]$ NMR ($CDCl_3$, 100 MHz)

δ 133.07 (q, $^2J_{CF}$ 34.3 Hz, $\underline{C}CF_3$), 125.93 (d, $^1J_{CH}$ 165.8 Hz, $\underline{C}H$), 122.68 (q, $^1J_{CF}$ 271.2 Hz)

6.2.2 SYNTHESIS OF 2,4,6-TRIS(TRIFLUOROMETHYL)AZOBENZENE - 1

A solution of $1\text{-Li-}2,4,6(CF_3)_3C_6H_2$ was prepared by the addition of ^{n}BuLi (28.2 ml, 1.6M in hexanes, 45.0 mmol) to a solution of FmesH (12.7g, 45.0 mmol) in Et_2O (100 ml) at -78°C under dry nitrogen. The solution became yellow and was allowed to come to room temperature and stirred for 4 hrs.

The solution was cooled to -78°C and PhN_2BF_4 (10.0g, 52 mmol) added via a solids addition side arm. On allowing the mixture to come to room temperature a dark red solution and pale precipitate formed. The solution was stirred for 14 hrs. The solution was washed with water (3x100ml), dried over $MgSO_4$, and evaporated to leave a red oil. This was crystallised from hexane at -35°C to yield red crystalline **1**. Concentration of the hexane and cooling to -30°C yielded further crops. Total yield was 9.5g (56%).

^1H NMR (400 MHz, $CDCl_3$)

δ 8.23 (s, 2H, Fmes-$\underline{H}$); 7.92-7.95 (rm, 2H, Phenyl-$\underline{H}$); 7.60-7.62 (rm, 3H, Phenyl-$\underline{H}$)

^{19}F NMR (376 MHz, $CDCl_3$)

δ -57.91 (s, 6F, *o*-$C\underline{F}_3$); -62.80 (s, 3F, *p*-$C\underline{F}_3$)

$^{13}C\{^1H\}$ NMR (100 MHz, $CDCl_3$)

δ 122.07 (q $^1J_{CF}$=274.8 Hz, *o*-$\underline{C}F_3$); 122.57 (q, $^1J_{CF}$=272.8 Hz, *p*-CF_3); 123.57 (s, Phenyl *m*-$\underline{C}H$); 124.01 (q, $^2J_{CF}$=33.6 Hz, *p*-$\underline{C}CF_3$); 127.81 (s, Fmes *m*-$\underline{C}H$); 129.43 (s, *o*-$\underline{C}H$); 129.85 (q $^2J_{CF}$=34.7 Hz, *o*-$\underline{C}CF_3$); 133.37 (s, *p*-$\underline{C}H$); 152.50 (s, *i*-$\underline{C}$), 154.96 (s, *i*-$\underline{C}$)

$^{13}C[^1H]$ NMR (100 MHz, $CDCl_3$)

δ 122.07 (q of d, $^1J_{CF}$=274.8 Hz, $^3J_{CH}$=4.9 Hz, *o*-$\underline{C}F_3$); 122.57 (q of t, $^1J_{CF}$=272.8 Hz, *p*-CF_3); 123.57 (d of ps t, $^1J_{CH}$=162.9 Hz, $^3J_{CH}$=6.5 Hz, Phenyl *m*-$\underline{C}H$); 124.01 (q, $^2J_{CF}$=33.6 Hz, *p*-$\underline{C}CF_3$); 127.81 (d, $^1J_{CH}$=170.0 Hz, Fmes *m*-$\underline{C}H$); 129.43 (d of d, $^1J_{CH}$=161.8 Hz, $^3J_{CH}$=6.8 Hz, *o*-$\underline{C}H$); 129.85 (q $^2J_{CF}$=34.7 Hz, *o*-$\underline{C}CF_3$); 133.37 (d of t, $^1J_{CH}$=161.7 Hz, $^3J_{CH}$=7.8 Hz, , *p*-$\underline{C}H$); 152.50 (t, $^3J_{CH}$=7.0 Hz, *i*-$\underline{C}$), 154.96 (t, $^2J_{CH}$=7.6Hz, *i*-$\underline{C}$)

Mass Spectral Data (EI^+, m/z)

$[MH]^+$ 387; $[PhNH_2]^+$ 94

Infra Red Data (KBr)

3070(w), 2961.6(w), 2936(w), 2874(w), CH stretches; 1630.76(m), 1594.85(s), 1500.46(m), 1464.39(s), 1452.2(m), 1384.5(m), 1309.12(m), 1276.79(s); 1213.11(s), 1191.11(s), 1147.1(s, br), CF bands; 1076.6(m), 1019.65(m), 916.55(m), 870.8(w), 839.9(m), 780.7(m), 759.7(m), 685.2(s), 664.7(m), 432.8(w)

Elemental Analysis (Obtained, Theoretical)

N%, 6.90 (7.25); C% 46.92 (46.63), H% 1.92 (1.81)

6.2.3 SYNTHESIS OF 1-AMINO-2,4,6-TRIFLUOROMETHYLBENZENE - 2

A solution of azobenzene **1** (8.40g, 21.8 mmol) in ethanol (10ml) was degassed by a freeze-thaw process and warmed to 70°C under an atmosphere of hydrogen in a water filled hydrogenation apparatus. When equilibrium had been obtained and the volume of hydrogen present was constant a suspension of palladium catalyst (0.5g, 5% Pd on C) in ethanol (3ml) was injected through a rubber septum. When hydrogen uptake ceased the solution was filtered and poured into water (200ml). The sticky yellow precipitate was filtered off, dissolved in the minimum volume of pentane required (~15ml), washed with water and dried over Na_2SO_4. The solution was filtered and the drying agent washed with a small amount of pentane. On cooling the combined pentane fractions to -78°C a yellow crystalline product was formed. This was filtered

off and dried under a flow of nitrogen. It was then sublimed (25°C, 1 atmos, water cooled probe) to yield white crystals of pure **2** (4.48g, 69%).

^{1}H NMR (400 MHz, $CDCl_3$)

δ 5.05 (br, 2H, $N\underline{H}_2$); 7.86 (s, 2H, Fmes-$\underline{H}$)

^{19}F NMR (376 MHz, $CDCl_3$)

δ -62.00 (s, 3F, p-$C\underline{F}_3$); -63.58 (s, 6F, o-$C\underline{F}_3$)

^{13}C{^{1}H} NMR (100 MHz, $CDCl_3$)

δ 115.30 (q, $^{2}J_{CF}$ 31.0 Hz, *o*-$\underline{C}$); 118.60 (q, $^{2}J_{CF}$ 34.5 Hz, *p*-$\underline{C}$); 123.30 (q, $^{1}J_{CF}$ 269.2 Hz, *p*-$\underline{C}F_3$), 123.48 (q, $^{1}J_{CF}$ 271.3 Hz, *o*-$\underline{C}F_3$); 127.95 (s, *m*-$\underline{C}$); 145.06 (s, *i*-$\underline{C}$)

^{13}C[^{1}H] NMR (100 MHz, $CDCl_3$)

δ 115.30 (q of t, $^{2}J_{CF}$ 31.0 Hz, *o*-$\underline{C}$); 118.60 (q, $^{2}J_{CF}$ 34.5 Hz, *p*-$\underline{C}$); 123.30 (q of t, $^{1}J_{CF}$ 269.2 Hz, *p*-$\underline{C}F_3$), 123.48 (q of d, $^{1}J_{CF}$ 271.3 Hz, $^{3}J_{CH}$ 5.6 Hz *o*-$\underline{C}F_3$); 127.95 (d, $^{1}J_{CH}$ 165 Hz, *m*-$\underline{C}$); 145.06 (s, *i*-$\underline{C}$)

Mass Spectral Data (EI^{+}, m/z)

$[M]^{+}$ 297

Infra Red Data (KBr, cm^{-1})

3560.28(w), 3467.05(m), N-H stretches; 2963.02, C-H stretch; 1655.66, NH_2 scissor; 1602.83(w), 1508.9(m), 1342.7(m), 1261.8(s), 1098.9(s,br), 921.1(m), 884.5(m), 802.6(s), 684.96(s), 657.9(s)

Elemental Analysis (Obtained, Theoretical)

N%, 5.00 (4.71); C% 36.36 (36.36), H% 1.19 (1.34)

6.2.4 Synthesis of 2,4,6-Tris(Trifluoromethyl)-1,2-Diphenylhydrazine - 3

Azobenzene **1** (0.90g, 2.33 mmol) in diethyl ether (25 ml) was stirred with conc. HCl (10 ml) and zinc dust (1.0g, 15 mmol) for 15 mins. The red colouration disappeared rapidly. The solution was diluted with diethyl ether (50 ml), washed with water (2x100 ml), dried over Na_2SO_4, evaporated to dryness and recrystallised from hexane to yield white crystals of **2** (yield 0.75g, 83%).

^{1}H NMR (400 MHz, $CDCl_3$)

δ 8.02 (s, 2H, fluoromes C<u>H</u>), 7.27 (t, $^{3}J_{HH}$ 6.8 Hz, 2H, phenyl *m*-C<u>H</u>), 6.95 (t, $^{3}J_{HH}$ 7.4 Hz, 2H, phenyl *p*-C<u>H</u>), 6.81 (d, $^{3}J_{HH}$ 8.0 Hz, 2H, phenyl *o*-C<u>H</u>).

^{19}F NMR (376 MHz, $CDCl_3$)

δ -58.94 (s, 6F, *o*-C<u>F</u>$_3$); -62.20 (s, 3F, *p*-C<u>F</u>$_3$)

^{13}C{^{1}H} NMR (100 MHz, $CDCl_3$)

δ 148.23 (s, *i*-<u>C</u>), 146.94 (s, *i*-<u>C</u>), 129.45 (s, phenyl *o*-<u>C</u>H), 129.14 (s, fluoromes *m*-<u>C</u>H), 123.39 (q, $^{1}J_{CF}$ 271.2 Hz, *o*-<u>C</u>F$_3$), 123.16 (q, $^{1}J_{CF}$ 269.7 Hz, *p*-<u>C</u>F$_3$), 121.44 (s, *p*-<u>C</u>H), 120.63 (q, $^{2}J_{CF}$ 34.5 Hz, *p*-<u>C</u>CF$_3$), 116.66 (q, , $^{2}J_{CF}$ 32.0 Hz, *o*-<u>C</u>CF$_3$), 112.67 (s, phenyl *m*-<u>C</u>H)

^{13}C[^{1}H] NMR (100 MHz, $CDCl_3$)

δ 148.23 (d, $^{2}J_{CH}$ 7.2 Hz, *i*-<u>C</u>), 146.94 (t, $^{2}J_{CH}$ 10.2 Hz, *i*-<u>C</u>), 129.45 (d of d, $^{1}J_{CH}$ 159.3 Hz, $^{2}J_{CH}$ 8.3 Hz phenyl *o*-<u>C</u>H), 129.14 (d, $^{1}J_{CH}$ 164.9 Hz, Fmes *m*-<u>C</u>H), 123.39 (q of d, $^{1}J_{CF}$ 271.2 Hz, $^{3}J_{CH}$ 5.6 Hz *o*-<u>C</u>F$_3$), 123.16 (q of d, $^{1}J_{CF}$ 269.7 Hz, $^{3}J_{CH}$ 5.2 Hz, *p*-<u>C</u>F$_3$), 121.44 (d of t, $^{1}J_{CH}$ 160.5 Hz, $^{2}J_{CH}$ 7.4 Hz, *p*-<u>C</u>H), 120.63 (q, $^{2}J_{CF}$ 34.5 Hz, *p*-<u>C</u>CF$_3$), 116.66 (q of d, $^{2}J_{CF}$ 32.0 Hz, $^{2}J_{CH}$ 3.5 Hz, *o*-<u>C</u>CF$_3$), 112.67 (d, $^{1}J_{CH}$ 157 Hz, phenyl *m*-<u>C</u>H)

Mass Spectral Data (EI^+, m/z)

m/e 388 $[M]^+$; $[M - PhN]^+$ 297; $[M - FmesNH]^+$

Infra Red Data (KBr, cm^{-1})

3376.7(m), 3112(w), 2962.9 (m), 1637.1(m), 1637.8(m), 1528.1(w), 1482.8(m), 1372.9(s), 1305.9(s), 1274.8(s), 1206.1(s), 1169.4(s), 1133.8(s), 1107.4(s), 1024.6(s), 920.5(m), 849.4(w), 801.5(s), 753.2(m), 693.0(m), 658.7(w), 590.0(w)

Elemental Analysis (Obtained, Theoretical)

N% 6.93 (7.22), C% 46.85 (46.39), H% 2.37 (2.32)

6.3 Experimental Details to Chapter Three

6.3.1 Synthesis of $Mo(NFmes)_2(OTMS)_2$ - 8

Et_3N (1.43 ml, 10.3 mmol), TMSCl (3.60 ml, 28.6 mmol) and a solution of amine **2** (1.53 g, 5.15 mmol) were added sequentially to a stirred solution of Na_2MoO_4 (0.530g, 2.57 mmol) in dme (50ml). On warming to ca. 70°C the solution became orange with a copious pale precipitate. The solution was stirred at this temperature for 20 hrs. The solution was then filtered and the precipitate washed with Et_2O (2 x 10ml). The solvent was then removed *in vacuo* to yield a brown oil (2.0g, 90%) which was shown by ^1H NMR to be $Mo(NFmes)_2(OTMS)_2$ with no impurities evident. This oil was distilled (120 °C, 0.01 mbar) to yield a yellow/orange oil (1.2 g, 54%)

^1H NMR Data (200 MHz, $CDCl_3$)

δ 7.65 (s, 4H, Fmes-H); 0.28 (s, 18H, $OSi(CH_3)_3$)

^{19}F NMR Data (376 MHz, $CDCl_3$)

δ -61.24 (s, *o*-CF_3), -62.36(s, *p*-CF_3).

$^{13}C\{^1H\}$ NMR Data (100 MHz, $CDCl_3$)

δ 153.20 (s, *i*-C), 126.93 (s, *m*-CH), 125.62 (q, $^2J_{CF}$ 31.1 Hz, *o*-CCF_3), 125.51 (q, $^2J_{CF}$ 34.3 Hz, *p*-CCF_3), 123.05 (q, $^1J_{CF}$ 272 Hz, *p*-CF_3), 122.75 (q, $^1J_{CF}$ 274 Hz, *o*-CF_3), 1.25 (s, $Si(CH_3)_3$)

$^{13}C[^1H]$ NMR (100 MHz, $CDCl_3$)

δ 153.20 (s, *i*-C), 126.93 (s, *m*-CH), 125.62 (q, $^2J_{CF}$ 31.1 Hz, *o*-CCF_3), 125.51 (q, $^2J_{CF}$ 34.3 Hz, *p*-CCF_3), 123.05 (q of t, $^1J_{CF}$ 272 Hz, *p*-CF_3), 122.75 (q of d, $^1J_{CF}$ 274 Hz, *o*-CF_3), 1.25 (q, $^1J_{CH}$ 118.7 Hz, $Si(CH_3)_3$)

Mass Spectral Data (EI^+, m/z)

$[M]^+$ 864; $[M\text{-}OTMS]^+$ 755; $[M\text{-}OTMS\text{-}Me]^+$ 730; $[M\text{-}NArF\text{-}F]^+$ 590

Isotopes patterns are considtent with those calculated for $Mo(NFmes)_2(OTMS)_2$

Infra Red Data (CsI)

3106(w), Ar C-H stretches; 2961.9(s), 2908(w), TMS C-H stretches, 1653.2(w), 1627.3(m); 1578.7(m); 1464.3(m); 1380.8(m); 1327.0(m); 1305.9(m); 1259.9(s); 1204.4(m); 1132.5(m); 1074.9(s); 1018.65(m); 942.2(m); 916.8(m); 800.64(s, br), Ar skeleton; 700.9(m); 684.7(m); 666.2(m); 515.3(w); 439.9(w)

Elemental Analysis (Obtained, Theoretical)

N%, 2.83 (3.24); C% 32.27 (33.34), H% 2.59 (2.56)

6.3.2 SYNTHESIS OF $Mo(NFtol)_2Cl_2$·dme - 9

Et_3N (27.1 ml, 194.4 mmol), TMSCl (68.0 ml, 534.6 mmol) and $FtolNH_2$ (12.2 ml, 97.2 mmol) were added sequentially to a stirred solution of Na_2MoO_4 (10.0g, 48.6 mmol) in dme (50ml). On warming to ca. 70°C the solution became orange after 10 minutes with a copious pale precipitate becoming deep red after heating for 1 hr. The solution was stirred at this temperature for a further 19 hrs. The solution was then filtered and the precipitate washed with Et_2O (2 x 50ml). The solvent was then removed *in vacuo* to yield a red solid (20.2g, 72%).

^{1}H NMR Data (400 MHz, $CDCl_3$)

3.90 (s, 6H, $OC\underline{H}_3$); 4.02 (s, 4H, $OC\underline{H}_2$); 7.12 (t, $^3J_{HH}$ 7.6 Hz, 2H, *m*-C$\underline{H}$CHCN); 7.38 (t, $^3J_{HH}$ 8.0 Hz, 2H, *p*-C$\underline{H}$); 7.53 (d, $^3J_{HH}$ 8.0Hz, 4H, *o*-C$\underline{H}$ and *m*-C$\underline{H}$-C(CF_3))

^{19}F NMR Data (376 MHz, $CDCl_3$)

60.98 (s, $C\underline{F}_3$)

^{13}C{^{1}H} NMR Data (100 MHz, $CDCl_3$)

63.61 (s, $OC\underline{H}_3$); 71.44 (s, $OC\underline{H}_2$); 119.14 (q, $^2J_{CF}$ 31.3 Hz, *o*-$\underline{C}(CF_3)$); 122.79 (q, $^1J_{CF}$ 271.6 Hz, $\underline{C}F_3$); 125.14 (q, $^3J_{CF}$ 5.1 Hz, m-$\underline{C}$H-C(CF_3)); 126.10 (s, *m*-$\underline{C}$HCHCN); 127.41 (s, *p*-$\underline{C}$H); 132.12 (s, *o*-$\underline{C}$H); 152.35 (s, *i*-$\underline{C}$N)

^{13}C NMR Data, ^{1}H Coupled (100 MHz, $CDCl_3$)

63.61 (q, $^1J_{CH}$ 145.5 Hz, $OC\underline{H}_3$); 71.44 (t, $^1J_{CH}$ 146.4 Hz, $OC\underline{H}_2$); 119.14 (q of t, $^2J_{CF}$ 31.3 Hz, *o*-$\underline{C}(CF_3)$); 122.79 (q of d, $^1J_{CF}$ 271.6 Hz, $^2J_{CH}$ 4.5 Hz, $\underline{C}F_3$); 125.14 (br d, $^1J_{CH}$ 163.1 Hz, *m*-$\underline{C}$H-C(CF_3)); 126.10 (d of d, $^1J_{CH}$ 128.2 Hz, $^2J_{CH}$ 8.0 Hz, *m*-$\underline{C}$HCHCN); 127.41 (d of d, $^1J_{CH}$ 132.4 Hz, $^2J_{CH}$ 7.6 Hz, *p*-$\underline{C}$H); 132.12 (d of d, $^1J_{CH}$ 161.9 Hz, $^2J_{CH}$ 7.9 Hz, *o*-$\underline{C}$H); 152.35 (s, *i*-$\underline{C}$N)

Mass Spectral Data (CI^+, m/z)

$[M]^+$ 575; $[M - DME]^+$ 485; $[M - DME - Cl]^+$ 450

Infra Red Data (CsI, Nujol)

1587.2(m); 1564.6(m); 1321(br, s); 1257.3(s); 1173.1(s); 1103.0(s); 1058.4(s); 1029.2(s, br); 973.2(m); 860.1(m); 772.1(s); 722.75(m); 636.9(m); 593.9(m); 564.3(m); 504.4(m); 476.8(m) 429.2(w)

Elemental Analysis (Obtained, Theoretical)

N%, 4.43 (4.87); C% 37.49 (37.59), H% 3.07 (3.15)

6.3.3 Synthesis Of $Mo(NFxyl)_2Cl_2$·dme - 10

Et_3N (6.1 ml, 43.6 mmol), TMSCl (15.3 ml, 120 mmol) and $FxylNH_2$ (5.0 g, 21.8 mmol) were added sequentially to a stirred solution of Na_2MoO_4 (2.25 g, 10.9 mmol) in dme (100 ml). On warming to ca. 70°C the solution became deep red with a copious pale precipitate. The solution was stirred at this temperature for 20 hrs. The solution was then filtered and the precipitate washed with Et_2O (2 x 50ml). The solvent was then removed *in vacuo* to yield a dark red solid (1.63 g, 21%).

^1H NMR Data (400 MHz, $CDCl_3$)

δ 7.60 (s, 4H, *o*-C<u>H</u>); 7.34 (s, 2H, *p*-C<u>H</u>); 3.32 (s, 6H, OC<u>H</u>$_3$); 3.08 (s, 4H, OC<u>H</u>$_2$)

^{19}F NMR Data (376 MHz, $CDCl_3$)

δ 63.16 (s, C<u>F</u>$_3$)

$^{13}C[^1H]$ NMR (125 MHz, $CDCl_3$)

δ 62.38 (s, O<u>C</u>H$_3$); 70.11 (s, O<u>C</u>H$_2$); 119.06 (s, p-<u>C</u>H); 121.15 (s, o-<u>C</u>H); 121.76 (q, $^1J_{CF}$ 273.3 Hz, <u>C</u>F$_3$); 131.46 (q, $^3J_{CF}$ 33.9 Hz, <u>C</u>-CF$_3$); 155.05 (s, i-<u>C</u>N)

$^{13}C[^1H]$ NMR (125MHz, $CDCl_3$)

δ 62.38 (q, $^1J_{CH}$ 181.9 Hz, O<u>C</u>H$_3$); 70.11 (t, $^1J_{CH}$ 187.0 Hz, O<u>C</u>H$_2$); 119.06 (d, $^1J_{CH}$ 210.0 Hz, *p*-<u>C</u>H); 121.15 (d, $^1J_{CH}$ 205.0 Hz, *o*-<u>C</u>H); 121.76 (q, $^1J_{CF}$ 273.3 Hz, <u>C</u>F$_3$); 131.46 (q, $^3J_{CF}$ 33.9 Hz, <u>C</u>-CF$_3$); 155.05 (s, *i*-<u>C</u>N)

Mass Spectral Data (CI, m/z)

$[M]^+$ 711; $[M - DME]^+$ 622; $[FxylNH_2]^+$ 229

Infra Red Data (Nujol, CsI, cm^{-1})

1594.8(s); 1279.0(s), 1260.6(s); 1163.7(m, br); 1129.0(s, br); 1045.5(s, br); 888.9(m); 861.9(m); 800.0(s, br); 722.9(w); 681.6(m); 557.1(w); 438.1(m)

Elemental Analysis (Obtained, Theoretical)

N%, 3.62 (3.94); C% 33.01 (33.78), H% 2.17 (2.27)

6.3.4 SYNTHESIS OF $Mo(NFmes)_2Cl_2$ - 11

BCl_3 (5.55 ml, 1M in heptane, 5.54 mmol) was added via syringe to a solution of $Mo(NFmes)_2(OTMS)_2$ **8** (1.20g 1.38 mmol) in CH_2Cl_2 (10 ml) at 0°C. The solution instantly turned red and was allowed to come to room temperature with stirring over 2 hrs. The solvent was removed *in vacuo* and the product extracted with heptane at *ca* 70°C leaving a small amount of dark solid. The solvent was removed *in vacuo* to yield $Mo(NFmes)_2Cl_2$ as a red solid (0.85 g, 81%) which was shown by ^1H NMR to contain no protic impurites. Crystals suitable for x-ray diffraction were grown from a pentane solution cooled to -25°C. Subsequent experiments showed that this reaction carried out with crude **8** produced **11** in only slightly reduced yield. This is advantageous in that losses of **8** associated with the problems of distilling a viscous oil are removed, increasing the overall yield of conversion of amine **2** to **11**.

^1H NMR (400 MHz, $CDCl_3$)

δ 8.08 (s, m-C<u>H</u>)

^{19}F NMR (376 MHz, $CDCl_3$)

δ -60.44 (s, 6F, o-C<u>F</u>$_3$); -62.91 (s, 3F, p-C<u>F</u>$_3$)

$^{13}C[^1H]$ NMR (100 MHz, $CDCl_3$)

δ 121.45 (q, $^1J_{CF}$ 273.3 Hz, *o*-<u>C</u>F_3); 122.09 (q, $^1J_{CF}$ 271.6 Hz, *p*-<u>C</u>F_3); 126.55 (q, $^3J_{CF}$ 33.0 Hz, *o*-<u>C</u>(CF_3)); 127.11 (s, m-<u>C</u>H); 129.26 (q, $^3J_{CF}$ 34.0 Hz, *p*-<u>C</u>(CF_3)); 152.46 (s, *i*-<u>C</u>N)

$^{13}C\{^1H\}$ NMR (100 MHz, $CDCl_3$)

δ 121.45 (q, $^1J_{CF}$ 273.3 Hz, *o*-<u>C</u>F_3); 122.09 (q, $^1J_{CF}$ 271.6 Hz, *p*-<u>C</u>F_3); 126.55 (q, $^3J_{CF}$ 33.0 Hz, *o*-<u>C</u>(CF_3)); 127.11 (d, $^1J_{CH}$ 171.5 Hz, *m*-<u>C</u>H); 129.26 (q, $^3J_{CF}$ 34.0 Hz, *p*-<u>C</u>(CF_3)); 152.46 (s, *i*-<u>C</u>N)

Mass Spectral Data (EI^+, m/z)

$[M]^+$ 757; $[M - F]^+$ 738 $[M - Cl]^+$ 722; $[M - Cl-F]^+$ 703; $[M - NAr^F]^+$ 462

Infra Red Data (Nujol, CsI)

1626.5(m); 1582.6(m); 1459.67(s); 1377.4(s); 1340.6(s); 1302.4(s); 1274.7(s); 1209.2(s); 1135.6(s, br); 1077.8(s); 985.5(m); 918.9(m); 855.4(m); 843.2(m); 801.0(m, br), Ar skeleton; 736.3(w); 519.2(w); 380(w, br), M-Cl stretch

Elemental Analysis (Obtained, Theoretical)

N%, 3.35 (3.70); C% 28.46 (28.56), H% 0.49 (0.53)

6.3.5 SYNTHESIS OF $Mo(NFmes)_2Cl_2 \cdot 2py$ - 12

Pyridine (1.0 ml, 1.2 mmol) was added via syringe to a solution of **11** (0.20 g , 0.26 mmol) in pentane (10ml). The solution turned immediately from red to dark purple. On cooling to -25°C a dark purple solid formed (220 g, 92%). Crystals suitable for X-ray diffraction were grown from a solution of pentane at *ca* 40°C cooled slowly to room temperature.

^1H NMR Data (400 MHz, $CDCl_3$)

δ 7.36 (br, 4H, pyridine m-C*H*); 7.86 (br, 2H, pyridine p-C*H*); 7.99 (s, 4H, Ar^FH); 8.902 (br, 4H, pyridine o-C*H*)

^{19}F NMR Data (387 MHz, $CDCl_3$)

δ -58.41 (s, 6F, o-$C\underline{F}_3$); -62.61 (s, 3F, p-$C\underline{F}_3$)

$^{13}C\{^1H\}$ NMR (100 MHz, $CDCl_3$)

δ 121.76 (q, $^1J_{CF}$ 272.7Hz, o-$\underline{C}F_3$); 122.72 (q, $^1J_{CF}$ 270Hz, p-$\underline{C}F_3$); 124.36 (q, $^3J_{CF}$ 32 Hz, o-$\underline{C}CF_3$); 125.10 (q, $^3J_{CF}$ 34 Hz, p-$\underline{C}CF_3$); ca 124 (br, Py p-$\underline{C}H$); 127.30 (s, Ar^F m-$\underline{C}H$); 138 (br, Py m-$\underline{C}H$); 151 (br, Py o-$\underline{C}H$); 152.56 (s, Ar^F i-$\underline{C}$)

$^{13}C[^1H]$ (MHz, $CDCl_3$)

δ 121.76 (q of d, $^1J_{CF}$ 272.7 Hz, $^3J_{CH}$ 5.3 Hz *o*-$\underline{C}F_3$); 122.72 (q of t, $^1J_{CF}$ 270Hz, *p*-$\underline{C}F_3$); 124.36 (q, $^3J_{CF}$ 32 Hz, *o*-$\underline{C}CF_3$); 125.10 (q, $^3J_{CF}$ 34 Hz, *p*-$\underline{C}CF_3$); ca 124 (br, py *p*-$\underline{C}H$); 127.30 (d, $^1J_{CH}$ 169.2 Hz, Fmes *m*-$\underline{C}H$); 138 (br d, $^1J_{CH}$ 168 Hz, Py *m*-$\underline{C}H$); 151 (br d, $^1J_{CH}$ 155Hz, py *o*-$\underline{C}H$); 152.56 (s, Fmes *i*-$\underline{C}$)

Mass Spectral Data (EI, m/z)

$[Mo(NFmes)_2Cl_2]^+$ 757; $[py]^+$ 79

Infra Red Data (Nujol, CsI)

1625.8(s), 1603.8(m); 1569.6(m); 1489.1(w); 1282(s, br); 1224.5(m); 1198.8(s); 1131.6(s, br); 1066.8(s, br); 953.7(m); 912.4(m); 851.7(m); 841.5(m); 800(m, br), Ar skeleton; 773.3(m); 695.1(s); 672.5(m); 629.2(m); 445.8(m)

Elemental Analysis (Obtained, Theoretical)

N%, 6.10 (6.12); C% 36.37 (36.74), H% 1.59 (1.54)

6.3.6 SYNTHESIS OF $Mo(NFmes)_2Cl_2$·dme and $Mo(NFmes)_2Cl_2$.2dme - 13 and 14

Dme (2ml) was added via a syringe to a solution of dichloride **11** (220mg, 0.29 mmol) in pentane (10ml). On standing for 24 hrs a red crystalline solid formed which changed to an orange powder within 48 hrs. The solution was cooled to -25°C to yield both a red crystalline solid and orange powder. Both orange powders were shown to be identical (total yield 150 mg, 55%) and of the form $Mo(NFmes)_2Cl_2$.2dme **14**. The red crystalline solid proved to be $Mo(NFmes)_2Cl_2$·dme **13** (100mg, 41%)

Data for 13

^{1}H NMR Data (400 MHz, $CDCl_3$)

δ 8.04 (s, 4H, Fmes-H), 4.02 (s, 4H, OCH_2), 3.80 (s, 6H, OCH_3)

^{19}F NMR Data (387 MHz, $CDCl_3$)

δ -58.42 (s, 12F, *o*-CF_3), -62.81 (s, 6F, *p*-CF_3)

^{13}C{^{1}H} NMR (100 MHz, $CDCl_3$)

δ 152.15 (s, *i*-C), 127.28 (s, *m*-CH), 126.68 (q, $^2J_{CF}$ 34.5Hz, *p*-CCF_3), 125.52 (q, $^2J_{CF}$ 32.6 Hz, *o*-CCF_3), 122.30 (q, $^1J_{CF}$ 270.8 Hz, *p*-CF_3), 121.52 (q, $^1J_{CF}$ 272.7 Hz, *o*-CF_3), 71.70 (s, OCH_3), 63.71 (s, OCH_2)

^{13}C[^{1}H] NMR (MHz, $CDCl_3$)

δ 152.15 (s, *i*-C), 127.28 (s, *m*-CH), 126.68 (q, $^2J_{CF}$ 34.5Hz, *p*-CCF_3), 125.52 (q, $^2J_{CF}$ 32.6 Hz, *o*-CCF_3), 122.30 (q, $^1J_{CF}$ 270.8 Hz, *p*-CF_3), 121.52 (q, $^1J_{CF}$ 272.7 Hz, *o*-CF_3), 71.70 (t, $^1J_{CH}$ 148.9 Hz, OCH_3), 63.71 (t, $^1J_{CH}$ 148.9 Hz, OCH_2)

Data for 14

^{1}H NMR Data (400 MHz, $CDCl_3$)

δ 8.17 (s, 4H, Fmes-H), 4.03 (s, 8H, OCH_2), 3.95 (s, 12H, OCH_3)

^{19}F NMR Data (387 MHz, $CDCl_3$)

δ -57.92 (s, 12F, *o*-C$\underline{F}_3$), -62.89 (s, 6F, p-C$\underline{F}_3$)

^{13}C{^{1}H} NMR (100 MHz, $CDCl_3$)

δ 152.20 (s, *i*-C), 128.50 (q, $^2J_{CF}$ 34.5 Hz, *p*-$\underline{C}CF_3$), 127.48 (s, *m*-$\underline{C}H$), 127.16 (q, $^2J_{CF}$ 32.6 Hz, *o*-$\underline{C}CF_3$), 122.30 (q, $^1J_{CF}$ 271.2 Hz, *p*-CF_3) 121.73 (q, $^1J_{CF}$ 273.1 Hz, *o*-$\underline{C}F_3$), 71.44 (s, O$\underline{C}H_2$), 64.43 (s, O$\underline{C}H_3$)

^{13}C[^{1}H] NMR (MHz, $CDCl_3$)

δ 152.20 (s, *i*-C), 128.50 (q, $^2J_{CF}$ 34.5 Hz, *p*-$\underline{C}CF_3$), 127.48 (d, $^1J_{CH}$ 166.5 Hz, *m*-$\underline{C}H$), 127.16 (q, $^2J_{CF}$ 32.6 Hz, *o*-$\underline{C}CF_3$), 122.30 (q, $^1J_{CF}$ 271.2 Hz, *p*-CF_3) 121.73 (q, $^1J_{CF}$ 273.1 Hz, *o*-$\underline{C}F_3$), 71.44 (t, $^1J_{CH}$ 147.9 Hz, O$\underline{C}H_2$), 64.43 (q, $^1J_{CH}$ 146.3 Hz, O$\underline{C}H_3$)

6.3.7 SYNTHESIS OF $Mo(NFtol)_2(PMe_3)_3$ - 15

Magnesium turnings (0.5g, 0.02 mol) were activated by drying under vacuum. Dichloride **9** (1.00g, 1.74 mmol) was added and the vessel evacuated and cooled to -196°C. THF (30ml) and PMe_3 (0.6 ml, 0.01 mol) were added by vacuum transfer. The vessel was allowed to warm to room temperature with stirring. On melting of the solvent a red solution formed which turned purple when the vessel reached room temperature. After stirring for one hour the solution became green. The solution was stirred for a further 14hrs.

The solvent was removed *in vacuo* and the product extracted with pentane (3x50ml) to give a green solution. On cooling to -30°C green crystals were formed which turned to an orange powder on drying under nitrogen. Further crops of crystals, some of which were suitable for X-ray diffraction, were obtained by reduction and cooling of the solution. Total yield 650mg (66.3%).

^{1}H NMR (400 MHz, C_6D_6)

δ 1.05 (br s, 27H, P(C$\underline{H}_3$)$_3$); 6.46 (t, $^3J_{HH}$ 7.4 Hz, 2H, *m*-C$\underline{H}$(CHCN)); 6.72 (d, $^3J_{HH}$ 8.0 Hz, 2H, *o*-C$\underline{H}$); 7.07 (t, $^3J_{HH}$ 7.6 Hz, 2H, *p*-C$\underline{H}$); 7.45 (d, $^3J_{HH}$ 8.0 Hz, 2H, *m*-C$\underline{H}$C(CF3))

^{19}F NMR Data (376 MHz, C_6D_6)

δ -61.16 (s, C$\underline{F}_3$)

^{31}P NMR Data (162 MHz, C_6D_6)

δ 31.67 (s, 1P, equatorial $\underline{P}Me_3$); -3.70 (s, 2P, axial $\underline{P}Me_3$)

$^{13}C\{^{1}H\}$ NMR (100 MHz, C_6D_6)

δ 18.14 (br s, *axial* P($\underline{C}H_3$)); 22.99 (br s, *equatorial* P($\underline{C}H_3$)); 115.18 (q, $^{2}J_{CF}$ 27.0 Hz, $\underline{C}(CF_3)$); 115.65 (s, m-CH(CHCN)); 126.29 (q, $^{3}J_{CF}$ 5.3 Hz, m-$\underline{C}H(CCF_3)$); 126.29 (q, $^{1}J_{CF}$ 270.6 Hz, $\underline{C}F_3$); 127.50 (s, o-$\underline{C}H$); 132.02 (s, p-$\underline{C}H$); 156.38 (s, i-$\underline{C}N$). Assigments of some of the Ar C's are cautious guesses.

^{13}C NMR Data, ^{1}H Coupled (100 MHz, C_6D_6)

δ 18.1 (br m, *axial* P($\underline{C}H_3$)); ~23 (br m, *equatorial* P($\underline{C}H_3$)); 115.18 (q of m, $^{2}J_{CF}$ 27.0Hz, $\underline{C}(CF_3)$); 115.65 (d of d, $^{1}J_{CH}$ 163.0 Hz, $^{2}J_{CH}$ 8.5 Hz, *m*-CH(CHCN)); 126.29 (d of m, $^{1}J_{CH}$ 158.3 Hz, *m*-$\underline{C}H(CCF_3)$); 126.29 (q of m, $^{1}J_{CF}$ 270.6 Hz, $\underline{C}F_3$); 127.50 (d of d, $^{1}J_{CH}$ 158.7 Hz, $^{3}J_{CH}$ 7.24 Hz *o*-$\underline{C}H$); 132.02 (d of d, $^{1}J_{CH}$ 156.0 Hz, $^{3}J_{CH}$ 8.8 Hz, *p*-$\underline{C}H$); 156.38 (s, *i*-$\underline{C}N$)

Mass Spectral Data (EI+, m/z)

$[PMe_3]^+$ 76

Infra Red Data (KBr, nujol, cm-1)

1584.9s; 1538.6s, 1335.7s, 1307.4s, 1214.5m, 1102.6s (br), 10233s, 941.3s, 800.6s, 745.2s, 666.47m, 631.1m

Elemental Analysis (Obtained, Theoretical)

N%, 4.31 (4.36); C% 42.59 (42.99), H% 5.30 (5.45)

6.3.8 SYNTHESIS OF $Mo(NFmes)_2(PMe_3)_3$ - 16

Zinc dust (0.05g, 0.76 mmol) was heated under vacuum to form a mirror. Dichloride **11** was added and thf (10ml) and PMe_3 (0.1ml, 1.9 mmol) were condensed onto the mixture. On warming to room temperature a red solution formed, from which after the removal of solvent under vacuum, extraction with pentane (3×20ml), reduction in volume and cooling to -25°C red/green dichroic crystals of **16** were obtained (210 mg, 67%)

^{1}H NMR (400 MHz, C_6D_6)

δ 0.99 (s, 27H, P($C\underline{H}_3$)$_3$), 7.85 (s, 4H, Fmes $\underline{H}$).

^{19}F NMR (376 MHz, C_6D_6)

δ -58.65 (s, 6F, *o*-$C\underline{F}_3$), -60.57 (s, 6F, *o*-$C\underline{F}_3$), -61.39 (s, 6F, *p*-$C\underline{F}_3$).

^{31}P NMR (162 MHz, C_6D_6)

δ 17.60 (s, 1P, *equatorial* P($C\underline{H}_3$)$_3$), -7.17 (s, 2P, *axial* P($C\underline{H}_3$)$_3$).

$^{13}C\{^1H\}$ NMR (100 MHz, C_6D_6)

δ 157.24 (s, *i*-C), 127.99 (s, *m*-CH), 124.70 (q, $^1J_{CF}$ 269 Hz, *p*-CF_3), 116.92 (q, $^2J_{CF}$ 34.2 Hz, *p*-CCF_3), 18.82 (br, *axial* $P(CH_3)_3$), 17.21 (br, *equatorial* $P(CH_3)_3$)

Infra Red Data (KBr, nujol, cm-1)

1622.7(m), 1555.5(w), 1545.3(w), 1456.4(s), 1375.9(s), 1259.15(s), 1171.6(s), 1156.5(s), 1104.6(s), 1058.6(s), 949.4(m), 911.1(m), 837.0(m), 801.4(m), 721.1(m), 684.7(m), 670.1(w), 572.8(w), 477.2(w), 450.6(w).

Elemental Analysis (Obtained, Theoretical)

C% 36.37 (36.74); N% 6.10 (6.12); H% 1.59 (1.54)

6.3.9 Synthesis of $Mo(NFxyl)_2(PMe_3)_2$ - 17

Magnesium turnings (0.3g, 12.4 mmol) were activated by drying under vacuum. Dichloride **10** (1.00g, 1.74 mmol) was added and the vessel evacuated and cooled to -196°C. THF (20ml) and PMe_3 (0.6 ml, 5.0 mmol) were added by vacuum transfer. The vessel was allowed to warm to room temperature with stirring. On melting of the solvent a red solution formed which turned purple when the vessel reached room temperature. After stirring for one hour the solution became orange/brown. The solution was stirred for a further 14hrs.

The solvent was removed *in vacuo* and the product extracted with pentane (3x50ml) and cooled to -30°C to give a small amount of dark orange solid (50mg, 10%)

^1H NMR (400 MHz, C_6D_6)

δ 7.00 (s, 2H, *p*-CH), 6.72 (s, 4H, m-CH), 0.95 (s, 18H, $P(CH_3)_3$)

^{19}F NMR (376 MHz, C_6D_6)

δ -63.07 (s, CF_3)

^{31}P NMR (162 MHz, C_6D_6)

δ -9.13 (s, PMe_3)

$^{13}C\{^1H\}$ NMR (100 MHz, C_6D_6)

161.5 (s, *i*-C), 132.21 (q, $^2J_{CF}$ 31.6 Hz, *m*-CCF_3), 125.02 (q, $^1J_{CF}$ 272.1 Hz, CF_3), 118.72 (s, *o*-CH)

Infra Red Data (KBr, nujol, cm-1)

1732w, 1577s, 1453s, 1418s, 1372s, 1298m, 1270s, 1160s, 1121s, 1079s, 996s, 938s, 861m, 843m, 819m, 745s, 729m, 715m, 696m

Elemental Analysis (Obtained, Theoretical)

C% 37.61 (39.11); N% 3.50 (4.00); H% 3.02 (3.42)

6.3.10 SYNTHESIS OF $Mo(NFmes)_2(PMe_3)_2(C_2H_4)$ - 18

THF (20ml) and PMe_3 (0.2 ml, 1.9 mmol) were condensed onto dichloride **11** (0.48g, 0.63 mmol) in an ampoule at -196°C under vacuum. The temperature was raised to -78°C and dry nitrogen admitted. A purple solution was formed. Et_2Zn (0.64 ml of a 1.0M solution in hexanes, 0.64 mmol) was added via a syringe to the stirred solution. The solution was cautiously warmed to room temprature with regular venting to release any pressure buildup. After stirring for 15 mins the soution turned blue. The solution was stirred for 16hrs. The solution remained blue.

The solvent was removed *in vacuo* and the product extracted with pentane (2x100ml). The solution was reduced and cooled to -25°C. A dark blue crystalline solid formed (270mg, 49%).

^{1}H NMR Data (400 MHz, C_6D_6)

δ 0.91 (t, J 7.6 Hz, 18H, $PC\underline{H}_3$); 1.85 (s, 4H, $C_2\underline{H}_4$); 7.65 (s, 2H, Fmes-$\underline{H}$); 7.78 (s, 2H, Fmes-$\underline{H}$)

^{19}F NMR Data (376 MHz, C_6D_6)

δ -58.25 (s, 3F, *o*-$C\underline{F}_3$); -61.58 (s, 3F, *o*-$C\underline{F}_3$); -63.85 (s, 3F, *p*-$C\underline{F}_3$)

^{31}P NMR Data (162 MHz, C_6D_6)

δ -3.91 (s, $\underline{P}Me_3$)

^{13}C{^{1}H} NMR (100 MHz, C_6D_6)

δ 155.03 (s, *i*-$\underline{C}$), 127.44 (s, *m*-$\underline{C}H$), 124.34 (q, $^1J_{CF}$ 269.3 Hz, *o*-$\underline{C}F_3$), 123.76 (q, $^1J_{CF}$ 271.2 Hz, *p*-$\underline{C}F_3$), 121.42 (q, $^2J_{CF}$ 28.4, *p*-$\underline{C}CF_3$), 118.93 (q, $^2J_{CF}$ 34.1 Hz, *o*-$\underline{C}CF_3$), 42.49 (s, $\underline{C}_2H_4$), 15.80 (t, J 11Hz, $P(\underline{C}H_3)_3$)

Infra Red Data (Nujol, CsI, cm^{-1})

1642.5m, 1554.2m, 1187.9s, 1061.0s, 932.3s, 843.5s, 776.6m, 722,8m, 684.6s

Elemental Analysis (Obtained, Theoretical)

N%, 3.50 (3.23); C% 36.38 (36.05), H% 2.98 (3.02)

6.3.11 PREPARATION OF $Mo(NFtol)_2(PMe_3)_2(C_2H_4)$ - 19

THF (20ml) and PMe_3 (0.3 ml, 2.9 mmol) were condensed onto **9** (0.50g, 0.87 mmol) in an ampoule at -196°C under vacuum. The temperature was raised to -78°C and dry nitrogen admitted. A purple solution was formed. Et_2Zn (0.87ml of a 1.0M solution in hexanes, 0.87 mmol) was added via a syringe to the stirred solution. The solution was cautiously warmed to room temperature with regular venting to release any pressure build up. After stirring for 10 mins the solution turned blue, turning purple after 30 mins. The solution was stirred for 16hrs.

The solvent was removed *in vacuo* and the product extracted with pentane (2x100ml). The solution was reduced and cooled to -25°C. A dark purple crystalline solid formed (235mg, 45%).

^{1}H NMR (400 MHz, C_6D_6)

δ 0.96 (s, 18H, $PC\underline{H}_3$); 1.79 (s, 4H, $C_2\underline{H}_4$); 6.42 (t, $^3J_{HH}$ 7.6 Hz, 2H, Ftol C$\underline{H}$); 6.78 (d, $^3J_{HH}$ 7.2 Hz, 2H, *o*-C$\underline{H}$); 7.07 (t, $^3J_{HH}$ 7.2 Hz, 2H, Ftol C$\underline{H}$); 7.33 (d, $^3J_{HH}$ 8.0 Hz, 2H, *m*-C$\underline{H}$C(CF3))

^{19}F NMR (376 MHz, C_6D_6)

δ -62.91 (s, $C\underline{F}_3$)

^{13}C{^{1}H} NMR (100 MHz, C_6D_6)

δ 14.9 (t, J 10.0 Hz, $PC\underline{H}_3$); 34.0 (s, $C_2\underline{H}_4$); 116.23 (q, $^2J_{CF}$ 27.7 Hz, $\underline{C}CF_3$); 117.35 (s, Ftol $\underline{C}$); 126 (s, Ftol $\underline{C}$); 126.32 (q, $^3J_{CF}$ 5.3 Hz, $\underline{C}HC(CF_3)$); 125.25 (q, $^1J_{CF}$ 270.8 Hz, $\underline{C}F_3$); 132.18 (s, Ftol $\underline{C}$); 154.72 (s, *i*-$\underline{C}$)

^{13}C[^{1}H] NMR (MHz, C_6D_6)

δ 14.9 (q, $^1J_{CH}$ 128.4 Hz, $PC\underline{H}_3$); 34.04 (t, $^1J_{CH}$ 156.5 Hz, $C_2\underline{H}_4$); 116.23 (q of t, $^2J_{CF}$ 27.7 Hz, $^3J_{CH}$ 6.1 Hz $\underline{C}CF_3$); 117.35 (d of d, $^1J_{CH}$ 162.5, $^3J_{CH}$ 8.3 Hz, Ar $\underline{C}$H); 126 (d of d, $^1J_{CH}$ 130.1 Hz, $^3J_{CH}$ 7.6, Ar $\underline{C}$H); 126.32 (d of m, $^1J_{CH}$ 158.5 Hz, $\underline{C}HC(CF_3)$); 125.25 (q of t, $^1J_{CF}$ 270.8 Hz, $^3J_{CH}$ 4.2 Hz, $\underline{C}F_3$); 132.18 (d of d, $^1J_{CH}$ 156.0 Hz, $^3J_{CH}$ 8.7 Hz, Ar $\underline{C}$H); 154.72 (t, $^2J_{CH}$ 7.5 Hz, *i*-$\underline{C}$)

Mass Spectral Data (CI^+, m/z)

$[PMe_3]^+$ 76

Infra Red Data (Nujol, CsI, cm^{-1})

1584.9m, 1543.4m, 1338.8s, 1305.7s, 1275.7s, 1262.3s, 1234.7s, 1158.6s, 1046.6s, 1024.8s, 9433.2s, 800.3s, 752.6m, 723.1m, 668.8w, 632.9w

Elemental Analysis (Obtained, Theoretical)

N%, 5.07 (4.71); C% 44.18 (44.46), H% 4.88 (5.09)

6.4 EXPERIMENTAL DETAILS TO CHAPTER FOUR

$B_{10}H_{12}.2DMS$[6], phenyl-*ortho*carborane[7] and methyl-*ortho*carborane[6] were prepared by literature methods. *Ortho*carborane was obtained commercially (KatChem) and sublimed prior to use. Carboranes give a broad peak in the mass spectrum due to the presence of both ^{10}B and ^{11}B. Such data are expressed as X-Y; Z where X and Y are the limits of the range observed and Z is the m/e ration of the most intense peak. Theoretical isotope patterns are given in brackets.

6.4.1 SYNTHESIS OF SECONDARY CARBORANYL AMINES AND NITROSOCARBORANES

The following describes a typical synthesis of $(MeCb)_2NH$ and MeCbNO. MeCbLi was prepared by the addition of ^{n}BuLi (7.71 ml, 1.6M in hexanes) to a solution of methyl*ortho*caborane (1.95g. 0.0123 mol) in diethyl ether (20ml) at 0°C. The solution was brought to room temperature and stirred for 30 mins. NOCl (5 ml) was condensed under reduced pressure into a calibrated tube and transferred into 20ml of pentane and nitrogen admitted. This NOCl solution was cooled to 40°C and the MeCbLi added over a period of 30 mins maintaining the temperature of the solution at -40°C. The solution was allowed to come to room temperature overnight to give a dark green solution with white precipitate. This was added in portions to a 10% $KHCO_3$ solution (300ml) to give a blue organic layer diluted with diethyl ether (200ml) and washed with water (2 × 100ml). The organic phase was dried ($MgSO_4$) and evaporated at room temperature under reduced pressure (water pump) to give a blue solid. Higher temperatures would result in the evaporation of the volatile nitrosocarboranes. Blue MeCbNO (1.12g, 49%) was sublimed out of this solid residue (40°C, 0.01 mbar) to leave a white solid which was recrystallised from hot hexane to yield $(MeCb)_2NH$ (0.71g, 35%).

A similar procedure was used with variation of solvent and temperature, and with PhCbLi in place of MeCbLi. These conditions and corresponding yields are given in Table 6.1.

Substituent R		Phenyl		Methyl	
Solvent	Temp. °C	Nitroso **20**	Amine **22**	Nitroso **21**	Amine **23**
dme/Et_2O	-40	0	55	0	65
C_5H_{12}/Et_2O	-40	61	10	69	11
C_5H_{12}/Et_2O	-117	42	0	77	22

Table 6.1 Yields of carboranylamines and nitrosocarboranes

6.4.1.1 Characterisation Data for Bis-2-Phenyl-1-orthocarboranyl-amine (PhCb)$_2$NH - 22

These data have been previously measured[8] (except $^1H\{^{11}B\}$ NMR) and are included here for reference purposes.

$^1H[^{11}B]$ NMR Data (400 MHz, $CDCl_3$)

δ 7.36-7.59 (m, 10H, PhCb), 4.46 (s, br, 1H, NH), 0.9-4.1 (m, br, 20H, BH)

$^{13}C\{^1H\}$ NMR Data (100 MHz, $CDCl_3$)

δ 131.3 (*p*-CH Phenyl), 129.6 (*i*-CH Phenyl), 129.9 and 131.7 (o- and m-CH Phenyl), 94.4 (carborane C2), 90.3 (carborane C1)

$^{11}B\{^1H\}$ NMR Data (160 Mhz, $CDCl_3$)

δ -3.95 (s, 1B, B9), -6.19 (s, 1B, B12), -12.51 and -10.69 (d, 8B, B3, 4, 5, 6, 7, 8, 10, 11)

$^1H\{^{11}B\}$ NMR Data (500 MHz, $CDCl_3$) (only BH referred to)

δ 2.65 (s, 2H, H3, 6), 2.22 (s, 2H, H4, 5 or H7, 11 or H8, 10), 2.18 (s, 1H, H12), 2.12 (s, 1H, H9), 1.94 (s, 4H, H4, 5 or H7, 11 or H8, 10)

Infra Red Data (KBr disc, cm^{-1})

3391 (NH), 3062w, 2989w (Ar. CH); 2654, 2633, 2602s, 2584 (BH); 1508 (NH); 1495, 1447 (Ar. skeleton); 1306s (CN); 1069; 1039; 1004; 798; 755, 689 (Phenyl); 729 (carborane skeleton)

Melting Point 205.5-207°C

6.4.1.2 Characterisation of 1-Nitroso-2-Phenyl-orthocarborane - 20

$^1H[^{11}B]$ NMR Data (400 MHz, $CDCl_3$)

δ 7.85 (d, $^3J_{HH}$ 8Hz, 2H, *o*-CH phenyl), 7.50 (t, $^3J_{HH}$ 7.4 Hz, 1H, *p*-CH phenyl), 7.42 (t, $^3J_{HH}$ 7.8 Hz, 2H, *m*-CH phenyl), 1.2-3.8 (m, br, 10H, BH)

$^{13}C\{^{1}H\}$ NMR Data (100 MHz, $CDCl_3$)

δ 131.07 (d of t, $^{1}J_{CH}$ 158.9 Hz, $^{2}J_{CH}$ 6.7 Hz, *m*-C phenyl), 130.09 (d of t, $^{1}J_{CH}$ 161.2 Hz, $^{2}J_{CH}$ 7.4 Hz, *m*-C phenyl), 128.85 (d of d, $^{1}J_{CH}$ 161.5 Hz, $^{2}J_{CH}$ 7.6 Hz, *o*-C phenyl), 114.07 (carborane C1), 81.29 (carborane C2)

$^{11}B\{^{1}H\}$ NMR Data (160 Mhz, $CDCl_3$)

δ -1.95 (s, 1B, B12), -4.40 (s, 1B, B9), -9.82 (s, 2B, B7, 11), -10.36 (s, 2B, B8, 10), -12.56 (s, 2B, B3, 4, 5, 6)

These peaks are assigned on the basis of a ^{11}B COSY experiment.

$^{1}H\{^{11}B\}$ NMR Data (500 MHz, $CDCl_3$) (only BH referred to)

δ 2.90 (s, 2H, H4, 5), 2.58 (s, 3H, H7, 11, 12), 2.26 (s, 3H, H8, 9, 10), 1.99 (s, 2H, H3, 6)

These peaks are assigned on the basis of a ^{1}H-^{11}B HETCOR experiment.

Infra Red Data (KBr disc, cm^{-1})

3098, 3072 (Ar CH); 2577br (BH); 1560s (NO), 1493m, 1446m; 1340w; 1270w, 1059s; 897; 867m; 753s; 724w (carborane skeleton), 688.8s

Mass Spectral Data (EI^{+}, m/z)

$[M]^{+}$ 245-253; 249 (245-252; 249)

Elemental Analysis (Observed (Theoretical))

C% 38.87 (38.53), H% 6.03 (6.07), N% 5.22 (5.62)

Melting Point 43-44°C (lit.[9] 54-55°C)

6.4.1.3 Characterisation Data for Bis-2-Methyl-1-orthocarboranyl-amime $(MeCb)_2NH$ - 23

$^{1}H[^{11}B]$ NMR Data (400 MHz, $CDCl_3$)

δ 4.84 (s, br, 1H, N<u>H</u>), 2.10 (s, 6H, C<u>H</u>$_3$), 1.0-3.9 (m, br, 20H, B<u>H</u>)

$^{13}C\{^{1}H\}$ NMR Data (100 MHz, $CDCl_3$)

δ 90.86 (carborane C1), 81.81 (carborane C2), 22.11 (<u>C</u>H_3)

$^{11}B\{^{1}H\}$ NMR Data (160 Mhz, $CDCl_3$)

δ -6.25 (s, 1B, B12), -5.05 (s, 1B, B9), -10.20 (s, 6B, B3, 4, 5, 6, 7, 11), -11.62 (s, 2B, B8, 10)

$^{1}H\{^{11}B\}$ NMR Data (500 MHz, $CDCl_3$) (only BH referred to)

δ 2.41 (s, 2H, H4, 5 or H7, 11), 2.31 (s, 2H, B3, 6), 2.20 (s, 2H, H4, 5 or H7, 11), 2.18 (s, 1H, H12), 2.12 (s, 1H, H9), 2.00 (s, 2H, H8, 10)

These peaks are assigned on the basis of a ^{1}H-^{11}B HETCOR experiment. The peak at δ 2.31 does not appear coupled to any B atom. This is commonly observed for B/H3, 6 and has hence been assigned to these atoms. The cross peak between ^{1}H δ 2.00 and ^{11}B δ -11.62 appears far stronger than any other; this is observed for B/H8, 10 and has hence been assigned to these atoms. Although the ^{11}B NMR peaks for B9 and B12 are close, the peak at 6.25 ppm is assigned to B12 as it is closest to the corresponding peak in $(PhCb)_2NH$.

Infra Red Data (KBr disc, cm^{-1})

3389 (NH); 2963, 2943 (methyl CH), 2680w, 2670w, 2606, 2573, 2541 (BH); 1496, 1383 (methyl CH), 1297 (CN); 1261; 1084; 1029; 800; 727 (carborane skeleton); 475; 416

Mass Spectral Data (EI^+, m/z)

$[M]^+$ 333-313; 329; (324-333; 329)

Elemental Analysis (Observed (Theoretical))

C% 21.35 (21.88), H% 8.32 (8.20), N% 3.98 (4.25)

Melting Point 205.5-207°C

6.4.1.4 Characterisation of 1-Nitroso-2-Methyl-orthocarborane - 21

$^{1}H[^{11}B]$ NMR Data (400 MHz, $CDCl_3$)

δ 2.70 (s, 3H, $C\underline{H}_3$), 1.1-3.2 (m, br, 10H, $B\underline{H}$)

$^{13}C\{^{1}H\}$ NMR Data (100 MHz, $CDCl_3$)

δ 111.64 (s, carborane C1), 73.26 (s, carborane C2), 22.97 (s, $\underline{C}H_3$)

$^{11}B\{^{1}H\}$ NMR Data (160 Mhz, $CDCl_3$)

δ -2.43 (s, 1B, B12), -6.64 (s, 1B, B9), -8.81 (s, 4B, B7, 8, 10, 11), -9.58 (s, 2B, B3, 6), -11.19 (s, 2B, 4,5)

$^{1}H\{^{11}B\}$ NMR Data (500 MHz, $CDCl_3$) (only BH referred to)

δ 2.53 (s, 2H. H7, 11), 2.50 (s, 1H, H12), 2.41 (s, 2H, H3, 6), 2.19 (s, 2H, H8, 10), 2.08 (s, 1H, H9), 1.88 (s, 2H, H4, 5)

Infra Red Data (KBr disc, cm^{-1})

δ 3105.8w, 3062.6w, 2948w (methyl CH); 2599s, br (BH); 1567s (NO); 1445; 1389; 1111.4; 1046.4; 1022; 948; 921; 892; 721.4m (carborane skeleton); 697w, 640w, 540w

Mass Spectral Data (EI^+, m/z)

$[M]^+$ 186-190; 188, (183-190; 188)

Elemental Analysis (Observed (Theoretical))

C% 38.87 (38.53), H% 6.03 (6.07), N% 5.22 (5.62)

Melting Point

Attempts to measure the melting point of this compound resulted in evaporation of the nitroso compound to leave a colourless residue which melted at 208-210°C, the temperature reported in the literature as the melting point of MeCbNO. A DSC scan showed a broad exotherm at 230°C and the residue was shown by IR to consist of boric acid and *closo*-carborane products.

6.4.1.5 Characterisation Data for Potassium-18-crown-6 salt of bis-2-phenyl-1-orthocarboranyl amide - 24

These data have been previously measured (except $^1H\{^{11}B\}$ NMR) and are included here for reference purposes. A sample of $(PhCb)_2N^-$ for the measurement of the $^1H\{^{11}B\}$ and ^1H-^{11}B spectra was kindly provided by Dr J.A.H. MacBride.

$^1H[^{11}B]$ NMR Data (400 MHz, CD_3CN)

δ 7.15-7.37 (m, 10H, phenyl), 3.47 (s, 24H, 18-C-6), 0.9-3.3 (m, br, 20H, BH)

$^{13}C\{^1H\}$ NMR Data (100 MHz, CD_3CN)

δ 137.7 (s, *i*-C phenyl), 129.3 (*p*-C phenyl), 128.8 and 131.1 (*o*-C and *m*-C phenyl), 89.9 (carborane C2), 70.9 (18-C-6)

$^{11}B\{^1H\}$ NMR Data (160 Mhz, CD_3CN)

δ -3.83 (br, 1B, B9), -7.65 (br, 2B, B7, 11), -9.89 (br, 2B, B3, 6), -11.97 (br, 3B, B4, 5, 12), -15.70 (br, 2B, B8, 10)

$^1H\{^{11}B\}$ NMR Data (500 MHz, CD_3CN) (only BH referred to)

δ 2.68 (s, 2H, H3, 6), 2.13 (s, 5H, H4, 5, 7, 11, 9), 1.72 (s, 1H, H12), 1.58 (s, 2H, H8, 10)

These peaks are assigned on the basis of a ^1H-^{11}B HETCOR experiment.

Infra Red Data (KBr disc, cm^{-1})

3062w (Ar. CH), 2899, 1472, 1351, 1108, 966, 838 (18-crown-6); 2575s, 2555s (BH), 1495 (Ar. skeleton); 1395s, br (CN), 1284; 1248; 1072; 1039; 1004w; 775, 883w, 806w, 775w; 745, 691 (phenyl o.o.p); 732 (carborane skeleton); 643w; 570w

Melting Point 254-257°C

6.4.2 SYNTHESIS OF MeCbN$_2$Ph - 25

A solution of MeCbLi was prepared by the addition of ^{n}BuLi (5.05 ml, 2.52M in hexanes) to a solution of MeCbH (2.00g, 0.0127 mol) in diethyl ether (100ml) at 0°C. The solution was allowing to come to room temperature and stirred for 30 mins. PhN_2BF_4 was added as a solid over a period of 30 mins and stirred overnight to give a red cloudy solution. Water (100ml) was added and the organic layer separated and washed with water (100ml). The organic layer was dried ($MgSO_4$) and evaporated to leave a brown resisdue which was recrystallised from hexane to give orange crystals of $MeCbN_2Ph$ (1.78g, 50%)

^{1}H[^{11}B] NMR Data (400 MHz, $CDCl_3$)

δ 7.82-7.80 (m, 2H, phenyl), 7.61-7.51, 2.30 (s, 3H, C<u>H</u>$_3$), 1.5-3.2 (m, br, 10H, B<u>H</u>)

^{13}C[^{1}H] NMR Data (100 MHz, $CDCl_3$)

δ 151.12 (s, *i*-C phenyl), 133.52 (d of t, $^1J_{CH}$ 161.2 Hz, $^2J_{CH}$ 7.8 Hz, *p*-C phenyl), 129.40 (d of d, $^1J_{CH}$ 161.2 Hz, $^2J_{CH}$ 7.6 Hz, *o*-C phenyl), 123.57 (d of t, $^1J_{CH}$ 161.2 Hz, $^2J_{CH}$ 6.1 Hz, *m*-C phenyl), 95.72 (s, carborane C1), 73.86 (s, carborane C2), 22.46 (q, $^1J_{CH}$ 131.8 Hz, C<u>H</u>$_3$)

^{11}B{^{1}H} NMR Data (160 Mhz, $CDCl_3$)

δ -3.87 (s, 1B, B12), -6.08 (s, 1B, B9), -10.13 (s, 10B, B3, 4, 5, 6, 7, 8, 10, 11)

^{1}H{^{11}B} NMR Data (500 MHz, $CDCl_3$) (only BH referred to)

δ 2.50 (s, 2H, H8, 10), 2.40 (s, 3H, B12 and H3,6 or H4, 5 or H7, 11), 2.20 (s, 5H, H12 and H3,6 or H4, 5 or H7, 11)

Mass Spectral Data (EI^+, m/z)

[M]+ 259-266; 263 (258-265; 262)

Elemental Analysis (Observed (Theoretical))

C% 41.07 (41.22), H% 7.04 (6.87), N% 10.57 (10.69)

Melting Point 122.5-123.5°C (Lit. 121-122°C)[10]

6.4.3 DATA FOR PhCbN$_2$Tol - 26

These data (other than ^{1}H{^{11}B}) have been reported elsewhere[11] and are included for reference purposes. A sample of $PhCbN_2Ph$ was kindly provided by Dr M.A. Fox for measurement of the ^{1}H{^{11}B} NMR spectra.

$^{1}H[^{11}B]$ NMR Data (400 MHz, $CDCl_3$)

δ 7.16-7.72 (d of d, 4H, tolyl), 7.32-7.51 (m, 5H, phenyl), 2.37 (s, 3H, C$\underline{H}_3$), 1.0-4.0 (m, br, 10H, B$\underline{H}$)

$^{13}C[^{1}H]$ NMR Data (100 MHz, $CDCl_3$)

δ 149.11, 144.40, 131.09, 130.44, 130.18, 129.82, 128.22, 123.45 (aromatic C's); 98.83 (carborane C1), 81.80 (carborane C2); 21.56 (s, $\underline{C}H_3$)

$^{11}B\{^{1}H\}$ NMR Data (160 Mhz, $CDCl_3$)

δ -4.01 (s, 2B, B9, 12), -10.71 (s, 8B, B3, 4, 5, 6, 7, 8, 10, 11)

$^{1}H\{^{11}B\}$ NMR Data (500 MHz, $CDCl_3$) (only BH referred to)

δ 2.95, 2.57, 2.53 (s, 8H, H3, 4, 5, 6, 7, 8, 10, 11), 2.39 (s, 2H, H9, 12)

6.4.4 Synthesis of MeCbNHNHPh - 27

$LiAlH_4$ (0.3g, 8.0 mmol) was added to a solution of $MeCbN_2Ph$ (0.50g, 1.91 mmol) in diethyl ether (20 ml) and stirred for 20hr. Wet diethyl ether was added followed by water (10ml) and dilute HCl until all lithium salts had dissolved. The organic layer was washed with water (2 × 50ml), dried ($MgSO_4$) and evaporated to leave a pale yellow solid. This was recrystallised from hot hexane to yield colourless crystals of MeCbNHNHPh (0.41g, 82%).

$^{1}H[^{11}B]$ NMR Data (400 MHz, $CDCl_3$)

δ 7.164 (t, $^{3}J_{CH}$ 7.0 Hz, 2H, *m*-C$\underline{H}$ phenyl), 6.82 (t, $^{3}J_{CH}$ 7.2 Hz, 1H, *p*-C$\underline{H}$ phenyl), 6.77 (d, $^{3}J_{CH}$ 8.4 Hz, 2H, *o*-C$\underline{H}$ phenyl), 5.58 (s, br, 1H, N$\underline{H}$), 4.77 (s, br, 1H, N$\underline{H}$), 2.00 (s, 3H, CH_3), 1.4-3.0 (m, br, 10H, B$\underline{H}$)

$^{13}C[^{1}H]$ NMR Data (100 MHz, $CDCl_3$)

δ 147.30 (s, *i*-C Phenyl), 129.32 (d, $^{1}J_{CH}$ 157.8 Hz, phenyl C), 121.03 (d, $^{1}J_{CH}$ 160.0 Hz, phenyl C), 112.99 (d, $^{1}J_{CH}$ 156.3 Hz, phenyl C), 96.65 (s, carborane C1), 80.93 (s, carborane C2), 22.12 (q, $^{1}J_{CH}$ 130.4Hz, CH_3)

$^{11}B\{^{1}H\}$ NMR Data (160 Mhz, $CDCl_3$)

δ -5.82 (s, 1B, B9), -6.87 (s, 1B, B12), -10.66 (s, 4B, B3, 6 or B4, 5 or B7, 11 or B8, 10), -11.49 (s, 4B, B3, 6 or B4, 5 or B7, 11 or B8, 10)

$^{1}H\{^{11}B\}$ NMR Data (500 MHz, $CDCl_3$) (only BH referred to)

δ 2.43 (s, 2H, H3,6 or H4, 5 or H7, 11 or H8, 10), 2.15 (s, 2H, H3,6 or H4, 5 or H7, 11 or H8, 10), 2.12 (s, 3H, B9 and H3,6 or H4, 5 or H7, 11 or H8, 10), 2.07 (s, 1H, H12), 1.96 (s, 2H, H3,6 or H4, 5 or H7, 11 or H8, 10)

Infra Red Data (KBr disc, cm^{-1})

3360, 3322 (NH stretches); 3125 (phenyl CH); 2933 (methyl CH); 2615, 2580, 2559 (BH); 1601; 1497; 1454m; 1380w; 1287w; 1251m; 1156w; 1019m,br; 886w; 754s; 725w (carborane skeleton); 696m; 584w

Mass Spectral Data (EI^+, m/z)

$[M]^+$ 260-267; 264, (260-267; 264)

Elemental Analysis (Observed (Theoretical))

C% 40.69 (40.91), H% 7.82 (7.58), N% 10.28 (10.61)

Melting Point 142-144°C (Lit. 143-144°C)[10]

6.4.5 SYNTHESIS OF PhCbNHNHTol - 28

$PhCbN_2Tol$ (0.73g) was dissolved in ethanol (20ml). Zinc dust (3.5g) was added and 20ml conc HCl added dropwise. The solution was stirred overnight becoming colourless. This was poured into water (200ml) forming a white precipitate which was extracted with diethyl ether (3 × 50ml). The organic layer was washed with water, dried (Na_2SO_4) and evaporated. The residue was recrystallised form hexane to give pale yellow crystals of $PhCbN_2H_2Tol$ (0.65g, 89%) which proved suitable for an X-ray diffraction experiment.

$^1H[^{11}B]$ NMR Data (400 MHz, $CDCl_3$)

δ 7.69 (d, $^3J_{HH}$ 8.0 Hz, 2H, *o*-C<u>H</u> phenyl), 7.53 (t, $^3J_{HH}$ 7.8 Hz, 1H, *p*-C<u>H</u> phenyl), 7.40 (t, $^3J_{HH}$ 8.0 Hz, 2H, *m*-C<u>H</u> phenyl), 6.82 (d, $^3J_{HH}$ 8.4 Hz, 2H, C<u>H</u> tolyl), 6.17 (d, $^3J_{HH}$ 8.4 Hz, 2H, C<u>H</u> tolyl), 5.32 (s, br, 1H, N<u>H</u>), 4.81 (s, br, 1H, N<u>H</u>), 2.21 (s, 3H, CH_3), 1.5-3.5 (m, br, 10H, B<u>H</u>)

$^{13}C[^1H]$ NMR Data (100 MHz, $CDCl_3$)

δ 144.71 (t, $^2J_{CH}$ 7.6 Hz, *i*-C), 131.68 (t, $^1J_{CH}$ 158.9 Hz, o-C or m-C phenyl), 131.02 (d, $^3J_{CH}$ 10.0Hz, i-C), 130.54 (t, $^1J_{CH}$ 161.2 Hz, o-C or m-C phenyl), 129.91 (d, $^3J_{CH}$ 6.5 Hz), 128.63 (d of d, $^1J_{CH}$ 160.9 Hz, $^2J_{CH}$ 7.6 Hz, tolyl <u>C</u>H), 129.35 (m, *p*-C phenyl), 112.52 (d, $^1J_{CH}$ 156.2 Hz, tolyl <u>C</u>H), 102.18 (s, carborane C1), 89.86 (carborane C2), 20.34 (t, $^1J_{CH}$ 125.4 Hz, <u>C</u>H_3)

$^{11}B\{^1H\}$ NMR Data (160 Mhz, $CDCl_3$)

δ -3.88 (s, 1B, B9), -6.94 (s, 1B, B12), -10.74 (s, 2B, B3, 6 or B4, 5 or B7, 11), -12.60 (s, 4B, B8,10 and B4,5 or B7, 11)

$^1H\{^{11}B\}$ NMR Data (500 MHz, $CDCl_3$) (only BH referred to)

δ 2.78 (s, 2H, H3, 6), 2.54 (s, 2H, H4,5 or H7, 11), 2.38 (s, 1H, H9), 2.28 (s, 1H, H12), 2.10 (s, 2H, H8, 10)

Infra Red Data (KBr disc, cm^{-1})

3312s (NH), 3120, 3105 (CH phenyl/ tolyl); 2950 (CH, methyl); 2663, 2628, 2592, 2584, 2571, 2550 (BH), 1610w, 1514s; 1262m; 1239m, br; 1106br; 1028br; 1002w; 814s, br; 754w; 724w (carborane skeleton); 689s; 661m; 636w; 558w; 507m

Mass Spectral Data (EI^+, m/z)

$[M]^+$ 336-343; 340 (336-343; 340)

Elemental Analysis (Observed (Theoretical))

C% 53.00 (52.78), H% 7.02 (7.04), N% 8.08 (8.21)

Melting Point 148-149.5°C

6.4.6 SYNTHESIS OF MeCbNHOH - 29

MeCbNO (0.22g) was dissolved in p-dioxane (10 ml), 5% Pd / C (40 mg) added, and the solution degassed by a freeze-thaw process. Hydrogen was admitted and the uptake of hydrogen measured using a standard water filled hydrogentation apparatus. 25 ml of hydrogen were used over a period of 6 hrs after which time hydrogen uptake ceased. The solution was filtered and evaporated to leave a white solid which proved to be pure MeCbNHOH (210 mg, 95%).

$^1H[^{11}B]$ NMR Data (400 MHz, $CDCl_3$)

δ 5.94 (s, br, 1H, N<u>H</u>OH), 5.70 (d, $^3J_{HH}$ 3 Hz, NHO<u>H</u>), 2.01 (s, 3H, C<u>H</u>$_3$), 0.5-4.0 (m, br, 10H, B<u>H</u>)

$^{13}C[^1H]$ NMR Data (100 MHz, $CDCl_3$)

δ 94.52 (s, carborane C1), 78.57 (s, carborane C2), 21.64 (s, <u>C</u>H_3)

$^{11}B\{^1H\}$ NMR Data (160 Mhz, $CDCl_3$)

δ -6.26 (s, 2B, B9, 12), -11.01 (s, 5B, B3, 6 or B4, 5), -11.79 (s, 4B, B8, 10 and B4, 5 or B7, 11)

$^1H\{^{11}B\}$ NMR Data (500 MHz, $CDCl_3$) (only BH referred to)

δ 2.36 (s, 2H, B3, 6), 2.08 (s, 2H, B4, 5), 2.00 (s, 4H, B9, B12 and B7, 11 or B4, 5), 1.94 (s, 2H, B8, 10)

Infra Red Data (KBr disc, cm^{-1})

3240s, 3290sh (NH and OH); 2966, 2914, 2857 (CH methyl); 2579 (BH); 1453w; 1254s, 1116s; 1080m; 1045w; 870s, 724w (carborane skeleton), 612w

Mass Spectral Data (EI^+, m/z)

$[M]^+$ 185-192; 189 (185-192; 189)

Elemental Analysis (Observed (Theoretical))

C% 19.41 (19.05), H% 8.12 (7.94), N% 6.17 (7.41)

Melting Point °C

6.4.7 SYNTHESIS OF PhCbNHOH - 30

The procedure used was identical to that above for MeCbNHOH using PhCbNO (3.86g) and 5% Pd / C (0.40g) giving a yield of 3.37g of PhCbNHOH (87%)

$^1H[^{11}B]$ NMR Data (400 MHz, $CDCl_3$)

δ 7.21-7.62 (m, 5H, phenyl), 5.58 (s, 1H, NHOH), 5.07 (s, 1H, NHOH), 1.1-3.6 (m, br, 10H, BH)

$^{13}C[^1H]$ NMR Data (100 MHz, $CDCl_3$)

δ 131.30 (d of t, $^1J_{CH}$ 159.0 Hz, $^2J_{CH}$ 6.1 Hz, *m*-CH phenyl), 130.82 (d of t, $^1J_{CH}$ 161.2 Hz, $^2J_{CH}$ 7.3 Hz, *p*-CH phenyl), 131.30 (d of d, $^1J_{CH}$ 161.1 Hz, $^2J_{CH}$ 7.5 Hz, *o*-CH phenyl), 96.25 (s, carborane C1), 86.46 (s, carborane C2)

$^{11}B\{^1H\}$ NMR Data (160 Mhz, $CDCl_3$)

δ -3.64 (s, 1B, B9), -5.47 (s, 1B, B12), -10.38 (s, 4B, B4, 5 and B7, 11), -11.90 (s, 2B, B8, 10); -12.47 (s, 2B, B3, 6)

$^1H\{^{11}B\}$ NMR Data (500 MHz, $CDCl_3$) (only BH referred to)

δ 2.73 (s, 2H, B3, 6), 2.42 (s, 2H, B4, 5 or B7, 11), 2.32 (s, 3H, B9 and B4, 5 or B7, 11), 2.28 (s, 1H, H12), 2.07 (s, 2H, H8, 10)

Infra Red Data (KBr disc, cm^{-1})

3532, 3463, 3280 (NH and OH), 3061 (CH phenyl), 2574br (BH); 1493m; 1446s; 1382br; 1337w, br; 1259w; 1193w; 1160w; 1071s; 1003s; 841w; 792m; 756m; 724m; 689s; 667w; 571w; 485w

Mass Spectral Data (EI^+, m/z)

$[M]^+$ 247-255; 251 (247-254; 251)

Elemental Analysis (Observed (Theoretical))

C% 38.25 (38.19), H% 6.77 (7.19), N% 5.58 (5.41)

Melting Point 95-96°C

6.4.8 SYNTHESIS OF MeCbNH$_2$ - 31

MeCbNO (1.50g) was dissolved in dme (25 ml) and tin powder (1.50g) added. Conc. HCl (25 ml) was added dropwise and the solution stirred for 15 mins after which time the blue colour had disappeared. The solution was heated to 95°C for 3 hrs, cooled to room temperature and diluted with diethyl ether (100ml). The solution was washed with water (3 × 50 ml), dried (Na_2SO_4) and evaporated. The white residue was sublimed to yield MeCbNH$_2$ (1.10g, 79%).

^{1}H[^{11}B] NMR Data (400 MHz, $CDCl_3$)

δ 2.99 (s, br, 2H, N$\underline{H}_2$), 2.04 (s, 3H, C$\underline{H}_3$)

^{13}C[^{1}H] NMR Data (100 MHz, $CDCl_3$)

δ 91.05 (s, carborane C2), 78.92 (s, carborane C1), 21.08 (s, $\underline{C}H_3$)

^{11}B{^{1}H} NMR Data (160 Mhz, $CDCl_3$)

δ -5.48 (s, 1B, B9), -9.36 (s, 1B, B12), -9.76 (s, 2B, B4, 5), -10.64 (s, 4B, B3, 6 and B7, 11), -12.50 (s, 2B, B8, 10)

^{1}H{^{11}B} NMR Data (500 MHz, $CDCl_3$) (only BH referred to)

δ 3.00 (s, 2H, H4, 5), 2.41 (s, 2H, H7, 11), 2.20 (s, 1H, H9), 2.02 (s, 2H, H3, 6), 1.98 (s, 1H, H12), 1.95 (s, 2H, H8, 10)

Infra Red Data (KBr disc, cm^{-1})

3306w, 3219br (NH); 2939w (CH methyl); 2671, 2634, 2602, 2580 (BH); 1596w; 1491; 1451; 1221br; 1079; 1026; 1002; 864; 809; 764; 729w; 714w; 700; 652w

Mass Spectral Data (EI$^+$, m/z)

[M]$^+$ 169-176; 173 (169-176; 173)

Elemental Analysis (Observed (Theoretical))

C% 20.89 (20.81), H% 8.98 (8.67), N% 7.07 (8.09)

Melting Point 301-302°C (lit. 302-303°C)[12]

6.4.9 SYNTHESIS OF PhCbNH$_2$ - 32

The method used was the same as that for MeCbNH$_2$ employing PhCbNO (0.50g, 2.0 mmol) and tin (0.50g, 4.0 mmol) yielding 0.27g PhCbNH$_2$, 57%.

$^{1}H[^{11}B]$ NMR Data (400 MHz, $CDCl_3$)

δ 7.35-7.70 (m, 5H, phenyl), 2.89 (s, br, 2H, NH_2) 1.1-3.5 (m, br, 10H, BH)

$^{13}C[^{1}H]$ NMR Data (100 MHz, $CDCl_3$)

δ 131.51 (s, *m*-C phenyl), 130.54 (s, *p*-C phenyl), 128.70 (s, *o*-C phenyl), 129.86 (s, i-C phenyl)

$^{11}B\{^{1}H\}$ NMR Data (160 Mhz, $CDCl_3$)

δ -12.70 (s, 2B, B8, 10), -10.62 (s, 2B, B3, 6),-9.99 (s, 2B, B7, 11), -9.23 (s, 2B, B3, 6), -8.32 (s, 1B, B12), -2.71 (s, 1B, B9)

$^{1}H\{^{11}B\}$ NMR Data (500 MHz, $CDCl_3$) (only BH referred to)

δ 2.71 (s, 3H, H9 and H3, 6), 2.52 (s, 2H, H4, 5), 2.44 (s, 2H, H7, 11), 2.18 (s, 1H, H12), 2.07 (s, 2H, H8, 10)

Infra Red Data (KBr disc, cm^{-1})

3461d, 3370d (NH); 3060w (CH phenyl); 2594br, 2564br (BH); 1956w; 1605s, 1579w; 1492; 1445; 1389w; 1337w; 1289br; 1249br; 1191m; 1159; 1070s; 1033; 1002; 940; 882; 841; 801; 755s; 726s; 690s; 649w; 597w; 571m; 509w; 484m

Mass Spectral Data (EI^+, m/z)

$[M]^+$ 231-237; 235 (231-238; 235)

Elemental Analysis (Observed (Theoretical))

C% 40.09 (40.85), H% 7.38 (7.23), N% 5.41 (5.96)

Melting Point 93.5-94.5°C (Lit. 97-98°C)[13]

6.5 EXPERIMENTAL DETAILS TO CHAPTER FIVE

6.5.1 SYNTHESIS OF [Mo(NCbMe)$_2$Cl$_4$][Et$_3$NH]$_2$ - 33

Et_3N (0.81ml, 5.81 mmol) and TMSCl (2.03ml, 15.98 mmol) were added sequentially to a suspension of Na_2MoO_4 (0.30g, 1.45 mmol) in dme (20ml). A solution of $MeCbNH_2$ (0.50g, 2.89 mmol) in dme 10 ml was added and the solution warmed to 70°C. After 30 mins the solution became yellow and cloudy. Heating was continued for 12 hrs. The solution was filtered and solvent removed *in vacuo* to yield a brown solid. This was dissolved in thf and red crystals obtained by the slow diffusion of Et_2O into the thf solution. Yield (0.59g, 22%)

^{1}H[^{11}B] NMR Data (400 MHz, CD_2Cl_2)

δ ~10 (br s, 2H, N<u>H</u>), 3.15 (q, $^3J_{HH}$ 6.8 Hz, 12H, C<u>H</u>$_2$CH$_3$), 2.16 (s, 6H, carborane-C<u>H</u>$_3$), 1.40 (t, $^3J_{HH}$ 7.0 Hz, 18H, CH$_2$C<u>H</u>$_3$), 1.5-3.0 (br s, B<u>H</u>)

^{13}C[^{1}H] NMR Data (100 MHz, CD_2Cl_2)

δ 100.40 (carborane C1), 79.63 (carborane C2), 47.09 (<u>C</u>H$_2$CH$_3$), 22.94 (carborane <u>C</u>H$_3$), 9.24 (CH$_2$<u>C</u>H$_3$)

^{11}B{^{1}H} NMR Data (160 Mhz, CD_2Cl_2)

δ -5.42 (s, 1B, B9), -6.78 (s, 1B, B12), -11.01 (s, 8B, B3, 4, 5, 6, 7, 8, 10, 11)

Infra Red Data (Nujol, cm^{-1})

3488w (NH); 2611, 2588 (BH strectches); 1607w, 1260s; 1154m; 1030s; 950m, 856s; 803s; 723s, 616w; 560w; 528w

Elemental Analysis (Observed (Theoretical))

C% 29.75 (27.98), H% 7.99 (7.68), N% 7.71 (7.64)

6.5.2 SYNTHESIS OF Mo(NAr^i)$_2$(OCbPh)$_2$ - 34

Pentane was condensed onto a mixture of PhCbOH (0.34g, 1.69 mmol) and Mo(NAr^i)$_2$(O^{t}Bu)$_2$ (0.43, 0.85 mmol) under vacuum. The vessel was allowed to come to room temperature and nitrogen admitted. The red solution formed soon became cloudy with the formation of an orange precipitate and was stirred overnight. The solvent was removed *in vacuo* to remove ^{t}BuOH and fresh pentane condensed onto the solid. The solution was stirred for a further 20 hours. The solution was filtered and

the solid dried to give $Mo(NAr^i)_2(OCbPh)_2$. On standing several large red crystals of $Mo(NAr^i)_2(OCbPh)_2$ formed. Total yield (1.32g, 85%)

$^1H[^{11}B]$ NMR Data (400 MHz, C_6D_6)

δ 7.69 (d, $^3J_{HH}$ 7.2 Hz, 2H, carborane Ph), 7.56 (t, $^3J_{HH}$ 7.4 Hz, 1H, carborane Ph), 7.48 (t, $^3J_{HH}$ 7.6 Hz, 2H, carborane Ph), 7.0-7.1 (m, 3H, Ar^i C<u>H</u>'s), 2.99 (sept, $^3J_{HH}$ 6.8 Hz, 2H, C<u>H</u>$(CH_3)_2$), 0.94 (d $^3J_{HH}$, 12H, $CH_2(C\underline{H}_3)_2$), 3.0-1.4 (br m, 10H, B<u>H</u>)

$^{13}C\{^1H\}$ NMR Data (100 MHz, $CDCl_3$)

δ 153.56 (s, aryl *i*-<u>C</u>), 143.95 (s, aryl *o*-<u>C</u>), 131.12 (d, $^1J_{CH}$ 159.7, phenyl <u>C</u>H), 130.69 (d, $^1J_{CH}$ 153.6, phenyl <u>C</u>H), 130.34 (s, Phenyl *i*-C), 128.91 (d, $^1J_{CH}$ 160.1 phenyl <u>C</u>H), 123.4 (d, $^1J_{CH}$ 157Hz, phenyl <u>C</u>H), 111.42 (s, carborane C1), 84.85 (s, carborane C2), 28.61 (d, $^1J_{CH}$ 124 Hz, <u>C</u>H$(CH_3)_2$), 23.48 (q, $^1J_{CH}$ 94 Hz, CH$(\underline{C}H_3)_2$)

$^{11}B\{^1H\}$ NMR Data (160 MHz, $CDCl_3$)

-2.38 (1B, B9), -7.89 and -10.44 (9B, B3, 4, 5, 6, 7, 8, 10, 11, 12)

Infra Red Data (KBr disc, cm^{-1})

3020, 2961, 2924 (CH stretches); 2570br (BH); 1457m; 1225s (C-O); 1100w; 1070w; 1032m, 946w; 778w; 750m; 688m; 661w; 613w

Elemental Analysis (Observed (Theoretical))

C% 52.12 (52.39), H% 7.05 (7.03), N% 2.92 (3.05)

6.5.3 SYNTHESIS OF $Mo(NAr^i)_2(OCbMe)_2$ - 35

MeCbOH (0.18g, 1.0 mmol) and $Mo(NAr^i)_2(O^tBu)_2$ (0.30, 0.50 mmol) were mixed and diethyl ether (20ml) added to give a red solution. This was stirred for 10 hrs, the solvent removed in vacuo and replaced by an equal quantity of the same solvent. This was repeated three times. The solvent was removed and the red solid formed dissolved in pentane. On cooling to -25°C a red solid formed (0.19g, 48%).

$^1H[^{11}B]$ NMR Data (400 MHz, $CDCl_3$)

δ 6.83 (s, 3H, aryl C<u>H</u>), 3.33 (sept $^3J_{HH}$ 6.8 Hz, 2H, C<u>H</u>$(CH_3)_2$), 1.78 (s, 3H, carborane C<u>H</u>$_3$), 1.01 (d, $^3J_{HH}$ 6.8 Hz, 12H, CH$(C\underline{H}_3)_2$)

$^{13}C[^1H]$ NMR Data (100 MHz, $CDCl_3$)

δ 154.14 (s, aryl *i*-<u>C</u>), 143.96 (s, aryl o-<u>C</u>), 129.37 (d, $^1J_{CH}$ 160.0 Hz, aryl <u>C</u>H), 123.38 (d, $^1J_{CH}$ 158.1 Hz, aryl <u>C</u>H), 108.16 (s, carborane C1), 77.42 (s, carborane C2), 29.23 (d, $^1J_{CH}$ 127Hz, <u>C</u>H$(CH_3)_2$), 23.42 (q, $^1J_{CH}$ 117Hz, CH$(\underline{C}H_3)_2$), 21.12 (q, $^1J_{CH}$ 133Hz, carborane CH_3)

Infra Red Data (Nujol, cm^{-1})

2586 (BH stretches); 1457m, 1388w; 1362w; 1237br (C-O stretch); 1170s; 1086; 1016; 981s; 941s; 853s; 793s; 750w; 655s

Mass Spectral Data (EI^+, m/z)

$[M\text{-}OCbMe]^+$ 612-624; 620 (612-626; 620)

$[M\text{-}2NAr^i]^+$ 445-426; 441 (450-434; 443)

Elemental Analysis (Observed (Theoretical))

C% 45.34 (45.44), H% 7.69 (7.63), N% 3.15 (3.53)

6.5.4 SYNTHESIS OF $Mo(N^tBu)_2(CbMe)_2$ - 36

A solution of LiCbMe was prepared by the addition of ^{n}BuLi (3.1ml 1.6M in hexanes, 5.0 mmol) to MeCbH (0.79g, 5.0 mmol) in Et_2O (20ml) at 0°C. The solution was allowed to come to room tempearature and stirred for 30 mins, then added dropwise to a solution of $Mo((N^tBu)_2Cl_2\cdot dme$ (1.0g, 2.51 mmol) in Et_2O (20ml) at -78°C over half an hour. The solution was allowed to come to room temperature slowly, a white prepciptate being seen to form at -45°C. The solution was stirred for 14 hrs and was then filtered, reduced to approximately half volume and cooled to -25°C to give a green solid (0.51, 37%).

$^1H[^{11}B]$ NMR Data (400 MHz, C_6D_6)

δ 2.23 (s, 6H, carborane $\underline{C}H_3$), 1.52 (s, 18H, ^{t}Bu), 4.0-1.5 (br m, 20H, B$\underline{H}$)

$^{13}C\{^1H\}$ NMR Data (100 MHz, $CDCl_3$)

δ 97.2 (carborane $\underline{C}$-Mo), 75.1 (carborane $\underline{C}$-Me), 59.6 ($\underline{C}Me_3$), 30.9 ($C\underline{C}H_3$), 28.9 (carborane CH_3)

Infra Red Data (Nujol, cm^{-1})

2572s (BH), 1261m; 1225.9m; 1189.2s; 1094.5s; 1037.3m; 1018.2s; 921.9w; 802m; 743m; 725s

$^{11}B\{^1H\}$ NMR Data (160 MHz, $CDCl_3$)

δ -4.57 (s, 1B, B12), -9.87 (s, 1B, B9), -11.29 (s, 2B), -12.74 (s, 6B)

Mass Spectral Data (EI^+, m/z)

$[M]^+$ 560-544; 553 (560-544; 553)

Elemental Analysis (Observed (Theoretical))

C% 29.61 (30.43), H% 7.86 (8.02), N% 5.07 (4.51)

6.5.5 SYNTHESIS OF $Mo(NAr^{i})_2(CbMe)_2$ - 37

A solution of LiCbMe was prepared by the addition of ^{n}BuLi (2.84 ml 1.6M in hexanes, 4.6 mmol) to MeCbH (0.72g, 4.6 mmol) in Et_2O (20ml) at 0°C. The solution was allowed to come to room temperature and stirred for 30 mins, then added dropwise to a solution of $Mo((NAr^{i})_2Cl_2$·dme (1.13g, 2.29 mmol) in Et_2O (20ml) at -78°C over half an hour. The solution was allowed to come to room temperature slowly, a white prepiciptate being seen to form at -45°C. The solution was stirred for 14 hrs and was then filtered, reduced to approximately half volume and cooled to -25°C to give a red solid (0.76, 43%).

$^{1}H[^{11}B]$ NMR Data (400 MHz, C_6D_6)

δ 7.1-7.3 (m, 6H, aryl C<u>H</u>), 3.48 (sept, $^{3}J_{HH}$ 6.9Hz, C<u>H</u>Me$_2$), 2.36 (s, 6H, carborane C<u>H</u>$_3$), 1.06 (d, $^{3}J_{HH}$ 6.9 Hz, CH(C<u>H</u>$_3$)$_2$)

$^{13}C\{^{1}H\}$ NMR Data (100 MHz, $CDCl_3$)

153.05, 146.22, 130.30, 124.25 (aryl C), 99.06 (carborane <u>C</u>-Mo), 78.79 (carborane <u>C</u>-CH$_3$), 28.77 (<u>C</u>HMe$_2$), 27.72 (CH(<u>C</u>H$_3$)$_2$), 24.52 (<u>C</u>H$_3$)

Infra Red Data (Nujol, cm^{-1})

2724w; 2573s (BH); 1585w, 1261s, 1219w; 1091s; 1019s; 976w; 930w; 799s; 753m; 726s

$^{11}B\{^{1}H\}$ NMR Data (160 MHz, $CDCl_3$)

δ 0.38 (s, 1B, B12), -4.91 (s, 1B, B9), -6.65 (s, 2B), -8.55 (s, 6B)

Mass Spectral Data (EI^{+}, m/z)

$[M]^{+}$ 758-766; 762 (752-768; 761)

Elemental Analysis (Observed (Theoretical))

C% 46.73 (47.36), H% 8.00 (7.95), N% 3.45 (3.68)

6.5.6 SYNTHESIS OF $Mo(NAr^{i})_2(Cb)$ - 38

A solution of LiCbLi was prepared by the addition of ^{n}BuLi (2.00 ml 1.6M in hexanes, 4.6 mmol) to *ortho*-carborane (0.234g, 1.62 mmol) in Et_2O (20ml) at 0°C. The solution was allowed to come to room temperature and stirred for 30 mins, then added dropwise to a solution of $Mo((NAr^{i})_2Cl_2$·dme (0.98g, 1.62 mmol) in Et_2O (20ml) at -78°C over half an hour. The solution was stirred for 14 hrs and was then

filtered, reduced to approximately half volume and cooled to -25°C to give a red solid (0.2g, 21%).

$^{1}H[^{11}B]$ NMR Data (200 MHz, C_6D_6)

δ 6.85 (m, 6H, aryl C<u>H</u>), 3.63 (sept $^{3}J_{HH}$ 6.7 Hz, 4H, C<u>H</u>$(CH_3)_2$), 1.09 (d, $^{3}J_{HH}$, 6.7 Hz, CH$(C\underline{H}_3)_2$)

Infra Red Data (Nujol, cm^{-1})

2560br (BH), 1583m; 1260s; 1157w; 1098m; 1066s; 1016s; 979m; 932m; 861w; 797s; 757s; 748s; 722s; 625w; 530w

$^{11}B\{^{1}H\}$ NMR Data (160 MHz, $CDCl_3$)

δ -1.96 (2B, B9 and B12), -10.54 (8B)

Mass Spectral Data (EI^+, m/z)

$[M]^+$ 584-593; 588 (581-595; 589)

Elemental Analysis (Observed (Theoretical))

C% 52.47 (52.97), H% 7.32 (7.47), N% 4.60 (4.75)

6.5.7 SYNTHESIS OF $Mo(N^tBu)_2(Cb)$ - 39

A solution of LiCbLi was prepared by the addition of ^{n}BuLi (9.46 ml 1.6M in hexanes, 15 mmol) to *ortho*-carborane (1.09g, 7.57 mmol) in Et_2O (20ml) at 0°C. The solution was allowed to come to room tempearature and stirred for 30 mins, then added dropwise to a solution of $Mo((N^tBu)_2Cl_2 \cdot dme$ (3.02g, 7.57 mmol) in Et_2O (20ml) at -78°C over half an hour. The solution became dark orange / brown was stirred for 14 hrs and was then filtered and the solvent removed *in vacuo* to give a brown oil. This was washed with 10 ml Et_2O to give an orange solid which was recrystallised from hot toluene to give an orange microcrystalline solid (0.20g, 3.5%).

$^{1}H[^{11}B]$ NMR Data (400 MHz, $CDCl_3$)

δ 1.57 (s, 1H, C$(C\underline{H}_3)_3$), 1.52 (s, 1H, C$(C\underline{H}_3)_3$), 1.49 (s, 7H, C$(C\underline{H}_3)_3$), 1.1-3.2 (br m, 5H, B<u>H</u>)

Infra Red Data (Nujol, cm^{-1})

2560br (BH), 1583m; 1260s; 1157w; 1098m; 1066s; 1016s; 979m; 932m; 861w; 797s; 757s; 748s; 722s; 625w; 530w

Mass Spectral Data (EI^+, m/z)

$[M]^+$ 750-771; 762 (747-767; 761)

Elemental Analysis (Observed (Theoretical))

C% 32.19 (31.58), H% 7.45 (7.37), N% 7.20 (7.37)

6.6 REFERENCES

1 J.J.P. Stewart, QCPE 455, Mopac 5.0, Frank Seiler Research Lab., USAF Academy, Colorado.

2 J.J.P. Stewart, QCPE 455, Mopac 6.0, Frank Seiler Research Lab., USAF Academy, Colorado.

3 GAMESS-UK is a package of ab initio programs written by M.F. Guest, J.H. van Lenthe, J. Kendrick, K. Schöffel, P. Sherwood and R.J. Harrison with contributions from R.D. Amos, R.J. Buenker, M. Dupuis, N.C. Handy, I.H. Hillier, P.J. Knowles, V. Bonaeie-Koutecky, W. von Niessen, V.R. Saunders and A. Stone. The package is derived from the original GAMESS code due to M. Dupuis, D. Spangler and J. Wendoloski, NRCC Software Catalog. Vol 1, Program No. QG01 (GAMESS), 1980.

4 C. Mealli and D.M. Proserpio, *J. Chem. Edu.*, **1990**, *67*, 399. Revisions by K. Linn, A. Sironi and J.A. Lopez.

5 G.E. Carr, R.D. Chambers, T.F. Holmes and D.G. Parker, *J. Organomet. Chem.*, **1987**, *325*, 13.

6 T.L. Heying, J.W. Ager Jr, D.J. Mangold, H.L. Goldstein, M. Hillman, R.J. Polak, J.W. Szymanski, *Inorg. Chem.*, **1963**, *2*, 1089; M.F. Hawthorne, T.D. Andrews, P.M. Garrett, F.P. Olsen, M. Reintjes, F.N. Tebbe, L.F. Warren, P.A. Wegner and D.C. Young, *Inorganic Syntheses*, **1967**, 91.

7 M.M. Fein, D. Grafstein, J.E. Paustian, J. Bobinski, B.M. Lichstein, N. Mayes, N.N. Schwartz, M.S. Cohen, *Inorg. Chem.*, **1963**, *2*, 1115.

8 J.A.H. MacBride and K. Wade, unpublished results.

9 L.I. Zakharkin and V.N. Kalinin, *Dokl. Acad. Nauk. SSSR*, **1965**, *164*, 577; C.A. 63: 18134f.

10 V.N. Kalinin, G.G. Zhigareva, L.I. Zakharkin, *Syn. Inorg. Metal-Org. Chem.*, **1972**, *2*, 105.

11 M.A. Fox, PhD Thesis, University of Durham, 1991.

12 L.I. Zakharkin and G.G. Zhigareva, *J. Gen. Chem. USSR*, **1975**, 1268.

13 L.I. Zakharkin and V.N. Kalinin, *Dokl. Akad. Nauk. SSSR*, **1965**, *164*, 577.

Appendix A

Additional Data From Chapter Two

A.1 AM1 CALCULATIONS ON 2,4,6-TRIS(TRIFLUOROMETHYL)AZOBENZENE

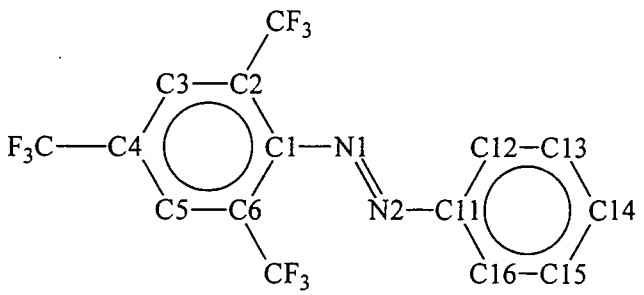

Atoms	X-ray Structure	Calculated Geometry	Atoms	X-ray Structure	Calculated Geometry
N1-N2	1.228(6)	1.226	C1-N1-N2	112.6(5)	120.3
C1-N1	1.443(7)	1.434	C1-N2-N1	112.7(5)	120.5
C11-N2	1.453(8)	1.434			
			C6-C1-C2	118.8(5)	118.5
C1-C2	1.401(7)	1.414	C1-C2-C3	120.7(5)	120.6
C2-C3	1.384(8)	1.394	C2-C3-C4	120.1(5)	119.9
C3-C4	1.380(7)	1.394	C3-C4-C5	120.0(5)	120.5
C4-C5	1.384(7)	1.394	C4-C5-C6	120.8(5)	120.0
C5-C6	1.391(8)	1.394	C5-C6-C1	119.5(5)	120.5
C6-C1	1.406(7)	1.413			
			C16-C11-C12	121.0(6)	119.3
C11-C12	1.388(9)	1.410	C11-C12-C13	119.3(7)	120.0
C12-C13	1.385(9)	1.392	C12-C13-C14	119.8(8)	120.5
C13-C14	1.379(12)	1.394	C13-C14-C15	120.9(7)	119.9
C14-C15	1.371(11)	1.395	C14-C15-C16	120.0(7)	120.5
C15-C16	1.394(10)	1.392	C15-C16-C11	118.9(8)	119.8
C16-C11	1.381(9)	1.413			
			C6-C1-N1-N2	52.5	81.9
			C12-C11-N2-N1	6.5	4.4

Table A.1 Selected Bond lengths (Å) Angles (°) and Torsional Angles (°) for both the X-ray and calculated structure of 1

Bond	X-ray Structure			Calculated Structure		
	Bond Order	π-Bond Order	σ-Bond Order	Bond Order	π-Bond Order	σ-Bond Order
N1-N2	1.890	0.917	0.973	1.877	0.916	0.961
		Fluoromes Group				
C1-N1	1.003	0.081	0.922	1.013	0.097	0.916
C1-C2	1.358	0.418	0.940	1.339	0.406	0.933
C1-C6	1.353	0.418	0.935	1.342	0.411	0.931
Average	1.356	0.418	0.938	1.341	0.409	0.932
C2-C3	1.412	0.457	0.955	1.412	0.461	0.951
C5-C6	1.409	0.454	0.955	1.406	0.455	0.951
Average	1.411	0.456	0.955	1.409	0.458	0.951
C3-C4	1.400	0.442	0.960	1.389	0.437	0.952
C5-C6	1.402	0.446	0.956	1.395	0.443	0.952
Average	1.401	0.444	0.958	1.392	0.440	0.952
		Phenyl Group				
C11-N2	1.004	0.089	0.915	1.017	0.107	0.910
C11-C12	1.356	0.407	0.949	1.353	0.413	0.940
C11-C16	1.388	0.435	0.953	1.549	0.407	1.142
Average	1.372	0.421	0.951	1.451	0.410	1.041
C12-C13	1.445	0.481	0.964	1.430	0.472	0.958
C15-C16	1.410	0.448	0.962	1.435	0.478	0.957
Average	1.428	0.465	0.963	1.433	0.475	0.958
C13-C14	1.403	0.437	0.966	1.410	0.452	0.958
C14-C15	1.437	0.470	0.967	1.405	0.447	0.958
Average	1.420	0.454	0.967	1.408	0.450	0.958

Table A.2 Selected Calculated Bond Orders for 1

Atom	X-ray Structure	Calculated Structure	Atom	X-ray Structure	Calculated Structure
N1	–0.062	–0.088	N2	–0.002	+0.004
	Fluoromes			*Phenyl*	
C1	+0.078	+0.119	C11	–0.086	–0.074
C2	–0.186	–0.175	C12	–0.068	–0.086
C3	+0.019	–0.001	C13	–0.121	–0.142
C4	–0.229	–0.187	C14	–0.088	–0.092
C5	+0.017	–0.001	C15	–0.127	–0.146
C6	–0.192	–0.181	C16	–0.053	–0.060
C7	+0.512	+0.475	N=N	-0.063	-0.084
C8	+0.561	+0.473	Ph	+0.105	0.135
C9	+0.510	+0.473	Fmes	-0.042	-0.051
C7*F*	–0.155	–0.156			
C8*F*	–0.167	–0.158			
C9*F*	–0.154	–0.155			

Table A.3 Atomic charges for both X-ray and calculated structures 1

A.2 AM1 CALCULATIONS ON 2,4,6-TRIS(TRIFLUOROMETHYL)ANILINE

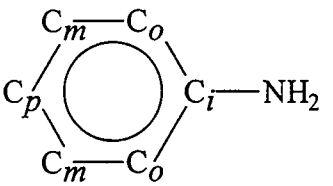

Parameter	X-ray Structure	Calculated Structure	Parameter	X-ray Structure	Calculated Structure
N-C_i	1.358(7)	1.360	N-C_i-C_o	121.6(4)	121.5
C_i-C_o	1.413(7)	1.430	C_o-C_i-C_o	116.8(4)	117.1
C_o-C_m	1.378(7)	1.389	C_i-C_o-C_m	121.4(4)	121.0
C_m-C_p	1.387(7)	1.396	C_o-C_m-C_p	120.8(4)	120.4
			C_m-C_p-C_m	119.1(4)	120.0
			H-N-H	123(4)	118.7
			H-N-C_i	119(5)	120.6
			$\sum\angle N$	360.0	358.0

Table A.4 Comparison of geometries for both X-ray and calculated structures of 2

Atoms	Bond Order	π-Bond Order	σ-Bond Order	Atoms	Bond Order	π-Bond Order	σ-Bond Order
	Molecule 1				*Molecule 2*		
N1-C6	1.244	0.300	0.944	N11-C11	1.243	0.303	0.940
C1-C6	1.253	0.314	0.939	C11-C12	1.245	0.305	0.940
C5-C6	1.248	0.309	0.939	C16-C11	1.260	0.320	0.940
C1-C2	1.436	0.479	0.957	C12-C13	1.446	0.489	0.957
C4-C5	1.441	0.483	0.958	C15-C16	1.416	0.459	0.957
C2-C3	1.376	0.419	0.957	C13-C14	1.363	0.406	0.957
C3-C4	1.377	0.419	0.958	C14-C15	1.396	0.438	0.958
	Averages for Calculated Geometry				*Averages for Both Molecules*		
N-C_i	1.247	0.310	0.937	N-C_i	1.244	0.302	0.942
C_i-C_o	1.242	0.308	0.934	C_i-C_o	1.252	0.312	0.940
C_o-C_m	1.429	0.477	0.952	C_o-C_m	1.435	0.478	0.957
C_m-C_p	1.396	0.421	0.975	C_m-C_p	1.378	0.421	0.958

Table A.5 Selected Bond Orders for X-ray and Calculated Structures of 2

	Atomic Charge	
Atom	X-ray Structure	Calculated Structure
N	–0.356	–0.351
H	+0.251	+0.252
NH_2	+0.146	+0.147
Ipso	+0.239	+0.242
Ortho	–0.306	–0.275
Meta	+0.074	+0.047
Para	–0.287	–0.248
Ortho-CF_3	+0.514	+0.482
Ortho-CF_3	–0.164	–0.163
Para-CF_3	+0.517	0.474
Para-CF_3	–0.164	–0.163

Table A.6 Selected atomic charges for both X-ray and calculated structure of 2 (values are averages for equivalent positions)

A.3 AM1 CALCULATIONS ON 2,4,6-TRIS(TRIFLUOROMETHYL)HYDRAZOBENZENE

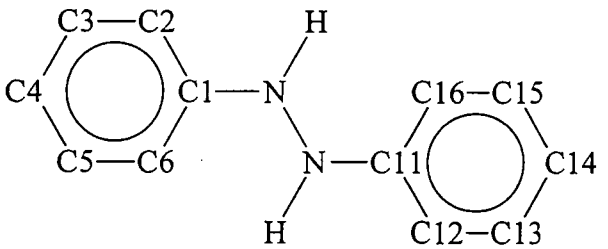

Parameter	X-ray Structure	Calculated Structure	Parameter	X-ray Structure	Calculated Structure
N1-N2	1.398(4)	1.379			
	Fluoromes Group			Phenyl group	
C1-N1	1.388(4)	1.417	C11-N2	1.411(4)	1.436
C1-C2	1.425(4)	1.422	C11-C12	1.398(4)	1.410
C2-C3	1.394(4)	1.395	C12-C13	1.388(4)	1.393
C3-C4	1.385(4)	1.391	C13-C14	1.387(4)	1.393
C4-C5	1.388(4)	1.393	C14-C15	1.380(4)	1.396
C5-C6	1.389(4)	1.394	C15-C16	1.392(4)	1.392
C6-C1	1.417(4)	1.427	C16-C11	1.391(4)	1.409

Table A.7 Comparison between bond lengths / Å in the X-ray structure of 3 (average) and the calculated structure

Parameter	X-ray Structure	Calculated Structure	Parameter	X-ray Structure	Calculated Structure
	Fluoromes Group		C1-N1-N2	119.0(3)	118.2
			C11-N2-N1	119.1(3)	117.9
C2-C1-C6	117.3(3)	117.1	C1-N1-H1	117(2)	111.6
C1-C2-C3	119.5(3)	120.2	C11-N2-H2	115.5(3)	109.9
C2-C3-C4	116.8(3)	121.6	N1-N2-H2	115.5(3)	106.7
C3-C4-C5	119.6(3)	119.4	N2-N1-H1	116(2)	112.2
C4-C5-C6	119.9(3)	120.1			
C5-C6-C1	121.7(3)	121.5	N1-C1-C2	123.2(3)	123.1
			N1-C1-C6	119.5(3)	119.4
	Phenyl group				
			N2-C11-C12	117.6(3)	119.4
C12-C11-C16	119.7(3)	118.8	N2-C11-C16	122.7(3)	121.5
C11-C12-C13	119.9(4)	120.6			
C12-C13-C14	120.5(4)	120.7	$\sum\angle$N1	352(7)	342.0
C13-C14-C15	119.4(3)	119.5	$\sum\angle$N2	350(9)	334.5
C14-C15-C16	120.9(4)	120.6			
C15-C16-C11	119.6(3)	120.3			

Table A.8 Comparison between angles / ° in the X-ray structure of 3 (average) and the calculated structure

Atom	Charge (X-ray Structure)	Charge (Calculated Structure)	Atom	Charge (X-ray Structure)	Charge (Calculated Structure)
	Fluoromes Group		N1	–0.197	–0.208
			N2	–0.209	–0.195
C1	+0.226	+0.225			
C2	–0.232	–0.233		*Phenyl*	
C3	+0.038	+0.038			
C4	–0.261	–0.264	C11	+0.030	+0.030
C5	+0.066	+0.069	C12	–0.152	–0.149
C6	–0.285	–0.286	C13	–0.079	–0.080
			C14	–0.144	–0.143
C7	+0.515	+0.515	C15	–0.411	–0.076
C8	+0.571	+0.573	C16	–0.163	–0.160
C9	+0.499	+0.498			
C7F	–0.159	–0.159	NHNH	+0.035	+0.047
C8F	–0.181	–0.181	Ph	+0.030	+0.037
C9F	–0.160	–0.160	Fmes	-0.056	-0.085

Table A.9 Calculated atomic charges for both X-ray and calculated structures of 3

Atoms	X-ray Structure			Calculated Structure		
	Bond Order	π-Bond Order	σ-Bond Order	Bond Order	π-Bond Order	σ-Bond Order
N1-N2	0.961	0.034	0.927	0.962	0.036	0.926
	Fluoromes Group			Fluoromes Group		
C1-N1	1.128	0.203	0.925	1.097	0.170	0.927
C1-C2	1.294	0.355	0.939	1.311	0.374	0.937
C1-C6	1.286	0.352	0.934	1.291	0.360	0.931
C2-C3	1.428	0.473	0.955	1.415	0.464	0.951
C5-C6	1.417	0.463	0.955	1.417	0.465	0.952
C3-C4	1.384	0.427	0.958	1.385	0.432	0.953
C4-C5	1.389	0.433	0.956	1.386	0.433	0.953
	Phenyl Group			Phenyl Group		
C11-N2	1.019	0.108	0.964	1.012	0.087	0.925
C11-C12	1.350	0.403	0.947	1.365	0.423	0.942
C11-C16	1.379	0.428	0.951	1.365	0.421	0.944
C12-C13	1.442	0.479	0.963	1.424	0.467	0.957
C15-C16	1.413	0.449	0.964	1.427	0.469	0.958
C13-C14	1.405	0.439	0.966	1.414	0.455	0.959
C14-C15	1.435	0.469	0.967	1.409	0.451	0.958

Table A.10 Selected bond orders for both X-ray and calculated structures of 3

Although there are small differences in calculated bond orders between the two crystallographically distinct molecules these differences arise from perturbations in the molecules attributed to crystal packing effects as the two are clearly chemically equivalent. Data presented are averages for the two molecules.

A.4 AM1 Calculations on Other Anilines with Trifluoromethyl Substituents

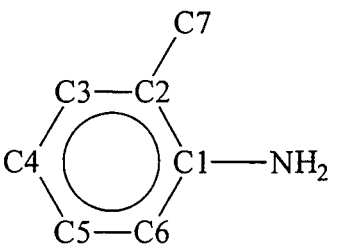

4

Atoms	Bond Angle / °	Atoms	Bond Angle / °
H1-N1-C1	118.2	N1-C1-C2	121.9
H2-N2-C1	118.8	N1-C1-C6	120.4
H1-N1-H2	117.5		
$\Sigma\angle$N	354.5	C2-C1-C6	117.7
		C1-C2-C3	120.5
C7-C2-C1	120.1	C1-C6-C5	120.7
C7-C2-C3	119.4	C2-C3-C4	120.8
		C6-C5-C4	120.9
		C3-C4-C5	119.3

Table A.11 Selected bond angles for calculated structure of 4

Bond	Bond Length / Å	Bond Order	π-Bond Order	σ-Bond Order
N1-C1	1.377	1.150	0.209	0.941
N1-H1	0.990	0.915	-	
N1-H2	0.991	0.909	-	
C1-C2	1.420	1.307	0.371	0.936
C1-C6	1.423	1.290	0.350	0.940
C2-C3	1.396	1.368	0.418	0.950
C5-C6	1.384	1.472	0.512	0.960
C3-C4	1.389	1.452	0.493	0.959
C4-C5	1.398	1.364	0.406	0.958
C2-C7	1.519	1.519	0.029	1.490
C7-F1	1.373	0.957	0.090	0.867
C7-F2	1.376	0.947	0.088	0.859
C7-F3	1.378	0.938	0.084	0.854
H2-F2	2.371	0.001	-	0.001
H2-F3	2.371	0.002	-	0.002

Table A.12 Selected bond lengths and bond orders for calculated structure of 4

Atom	Atomic Charge	Atom	Atomic Charge
N1	–0.370	C1	+0.157
H1	+0.220	C2	–0.252
H2	+0.227	C3	–0.037
		C4	–0.194
C7	+0.472	C5	–0.053
F1	–0.164	C6	–0.218
F2	–0.170		
F3	–0.180	NH_2	+0.078

Table A.13 Atomic charges for calculated structure of 4

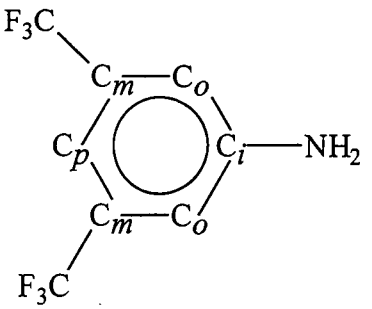

5

Bond	Bond Length / Å	Bond Order	π-Bond Order	σ-Bond Order
N-H	0.994	0.925	-	0.925
N-C_i	1.393	1.107	0.156	0.951
C_i-C_o	1.416	1.334	0.390	0.944
C_o-C_m	1.391	1.414	0.461	0.953
C_m-C_p	1.395	1.395	0.443	0.952
C_m-CF_3	1.526	0.905	0.024	0.881
C-F	1.373	0.954	0.090	0.864

Table A.14 Selected bond lengths and bond orders for calculated structure of 5 (averages for equivalent bonds)

Atoms	Bond Angle / °	Atoms	Bond Angle / °
H-N-H	114.3	N-C_i-C_o	120.7
H-N-C_i	115.4	C_o-C_i-C_o	118.4
$\sum\angle$N	345.2	C_i-C_o-C_m	120.2
		C_o-C_m-C_p	121.3
C_o-C_m-CF_3	119.4	C_m-C_p-C_m	118.8
C_p-C_m-CF_3	119.5		

Table A.15 Selected bond angles for calculated structure of 5 (averages for equivalent bonds)

Atom	Atomic Charge	Atom	Atomic Charge
N	–0.332	C_i	+0.070
H	+0.201	C_o	–0.129
		C_m	–0.121
CF_3	+0.467	C_p	–0.088
CF_3	–0.162		
		NH_2	+0.070

Table A.16 Selected atomic charges for calculated structure of 5 (averages for equivalent atoms)

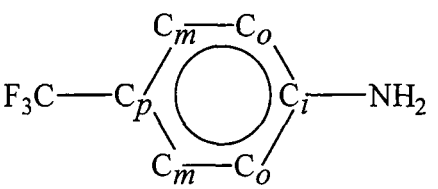

6

Bond	Bond Length / Å	Bond Order	π-Bond Order	σ-Bond Order
N-H	0.993	0.923	-	0.923
$N-C_i$	1.387	1.387	0.174	1.213
C_i-C_o	1.418	1.317	0.374	0.943
C_o-C_m	1.387	1.455	0.496	0.959
C_m-C_p	1.397	1.374	0.422	0.952
C_p-CF_3	1.518	0.914	0.028	0.886
C-F	1.375	0.949	0.088	0.861

Table A.17 Selected bond lengths and bond orders for the calculated structure of 6

Atoms	Bond Angle / °	Atoms	Bond Angle / °
H-N-H	115.2	$N-C_i-C_o$	120.7
$H-N-C_i$	116.3	$C_o-C_i-C_o$	118.4
$\sum\angle N$	347.7	$C_i-C_o-C_m$	120.4
		$C_o-C_m-C_p$	120.4
$C_m-C_p-CF_3$	120.0	$C_m-C_p-C_m$	120.0

Table A.18 Selected bond angles for the calculated structure of 6

Atom	Atomic Charge	Atom	Atomic Charge
N	–0.345	C_i	+0.108
H	+0.203	C_o	–0.209
		C_m	–0.037
$\boldsymbol{C}F_3$	+0.473	C_p	-0.219
$C\boldsymbol{F}_3$	–0.170		
		NH_2	+0.061

Table A.19 Selected atomic charges for 6

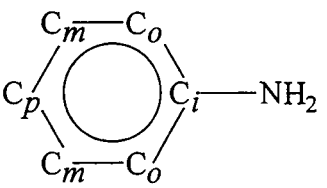

Aniline

Atoms	Bond Length		Atoms	Bonds Angle	
	X-ray Structure	*Calculated Structure*		*X-ray Structure*	*Calculated Structure*
H-N	0.94(5)	0.996	H-N-H	112(5)	113.2
N-C_i	1.392(6)	1.399	H-N-C_i	115(3)	114.3
C_i-C_o	1.396(6)	1.415	$\sum\angle$N	342(11)	341.8
C_o-C_m	1.379(7)	1.390			
C_m-C_p	1.381(7)	1.394	N-C_i-C_o	121.0(4)	120.7
			C_o-C_i-C_o	117.9(4)	118.5
			C_i-C_o-C_p	120.7(4)	120.3
			C_o-C_m-C_p	121.2(5)	120.7
			C_m-C_p-C_m	118.4(5)	119.5

Table A.20 Comparison between bond lengths and angles of X-ray and calculated structures of aniline

X-ray Structure				Calculated Structure			
Atoms	Bond Order	π-Bond Order	σ-Bond Order	Atoms	Bond Order	π-Bond Order	σ-Bond Order
N-H	0.935	-	0.935	N-H	0.933	-	0.933
N-C_i	1.090	0.138	0.952	N-C_i	1.085	0.135	0.950
C_i-C_o	1.347	0.397	0.950	C_i-C_o	1.342	0.399	0.943
C_o-C_m	1.436	0.472	0.964	C_o-C_m	1.432	0.474	0.958
C_m-C_p	1.414	0.450	0.964	C_m-C_p	1.408	0.450	0.958

Table A.21 Calculated bond orders for calculated structure of aniline

Atom	Atomic Charge	
	X-ray Structure	*Calculated Structure*
N	–0.323	–0.329
H	+0.181	+0.183
C_i	+0.053	+0.056
C_o	–0.179	–0.191
C_m	–0.081	–0.093
C_p	–0.172	–0.173
ΣNH_2	+0.039	+0.037

Table A.22 Atomic charges for calculated structure of aniline

A.5 AM1 CALCULATIONS ON OTHER FLUOROMES COMPOUNDS

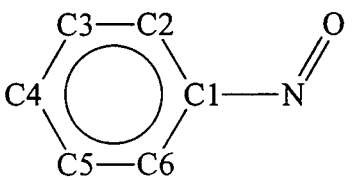

FmesNO

Atoms	Bond Angle / °
C2-C1-C6	118.5
C1-C2-C3	120.9
C1-C6-C5	120.5
C2-C3-C4	119.6
C6-C5-C4	119.9
C3-C4-C5	120.5
C1-N-O	119.7

Table A.23 Selected bond angles for calculated structure of FmesNO

Bond	Bond Length / Å	Bond Order	π-Bond Order	σ-Bond Order
N-C1	1.477	0.910	0.068	0.842
N-O	1.150	2.014	1.013	1.001
C1-C2	1.408	1.368	0.426	0.942
C1-C6	1.410	1.360	0.426	0.934
C2-C3	1.396	1.406	0.456	0.950
C5-C6	1.396	1.406	0.454	0.952
C3-C4	1.394	1.396	0.444	0.952
C4-C5	1.395	1.397	0.446	0.951

Table A.24 Selected bond lengths and bond orders for calculated structure of FmesNO

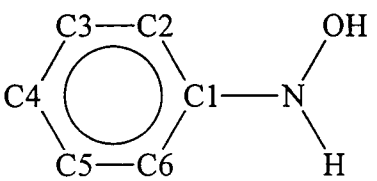

FmesNHOH

Atoms	Bond Angle / °
C2-C1-C6	117.4
C1-C2-C3	120.9
C1-C6-C5	121.1
C2-C3-C4	120.5
C6-C5-C4	120.2
C3-C4-C5	119.9
C1-N-O	115.6

Table A.25 Selected bond angles for calculated structure of FmesNHOH

Bond	Bond Length / Å	Bond Order	π-Bond Order	σ-Bond Order
N-C1	1.421	1.081	0.151	0.930
N-O	1.332	1.006	0.008	0.998
C1-C2	1.418	1.322	0.384	0.938
C1-C6	1.423	1.303	0.368	0.935
C2-C3	1.394	1.409	0.457	0.952
C5-C6	1.391	1.420	0.469	0.951
C3-C4	1.394	1.391	0.439	0.952
C4-C5	1.394	1.382	0.430	0.952

Table A.26 Selected bond lengths and bond orders for calculated structure of FmesNHOH

Appendix B

Additional Data From Chapter Four

B.1 Intramolecular Interactions in Primary Carboranyl Amines

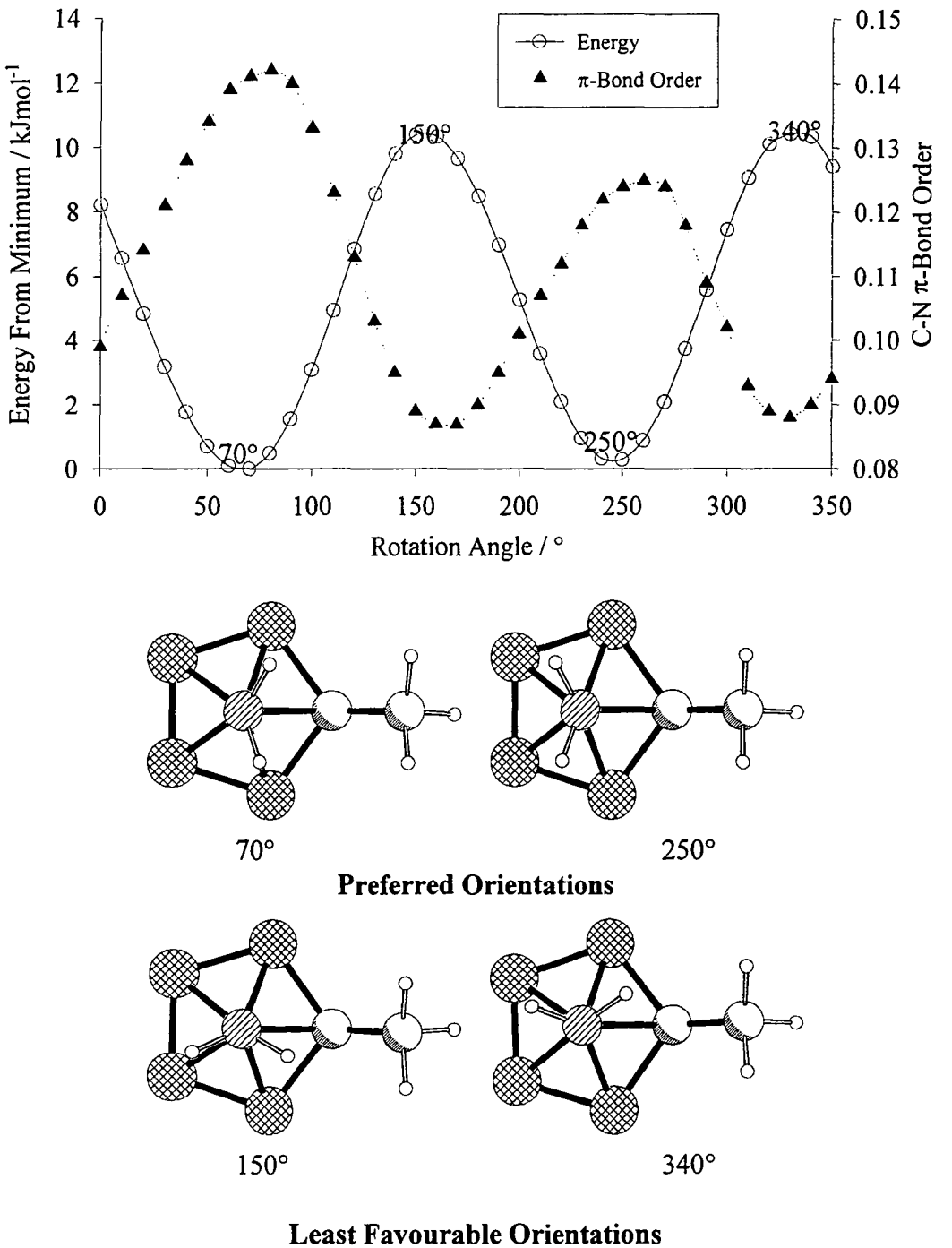

Figure B.1 **Energy and π-bond profiles for roation of the NH_2 group in $MeCbNH_2$ about the C-N axis**

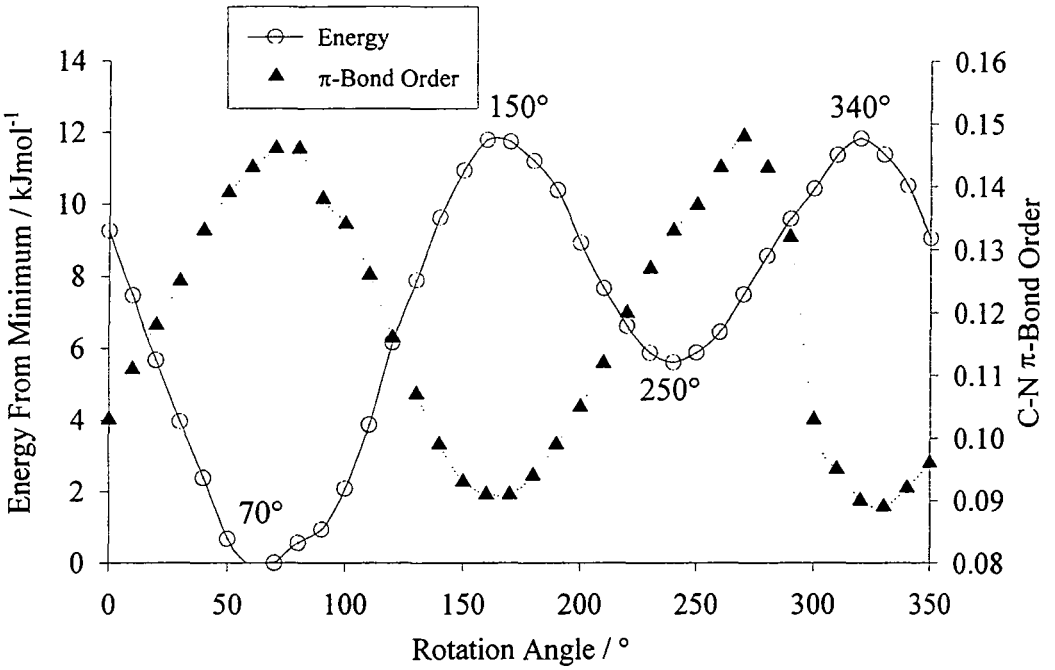

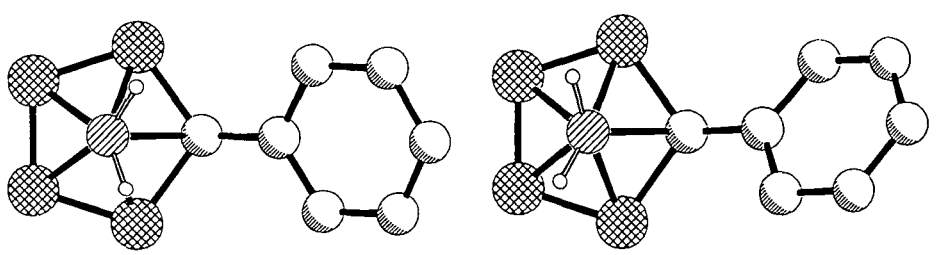

70° 250°

Preferred Orientations

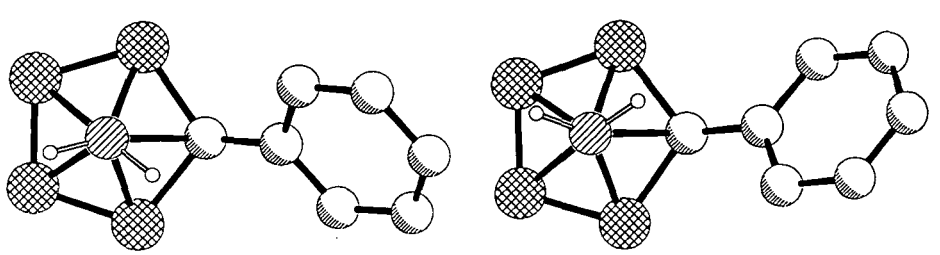

150° 340°

Least Favourable Orientations

Figure B.2 Energy and π-bond profiles for roation of the NH_2 group in $PhCbNH_2$ about the C-N axis

B.2 Intramolecular Interactions in Nitroso Carboranes

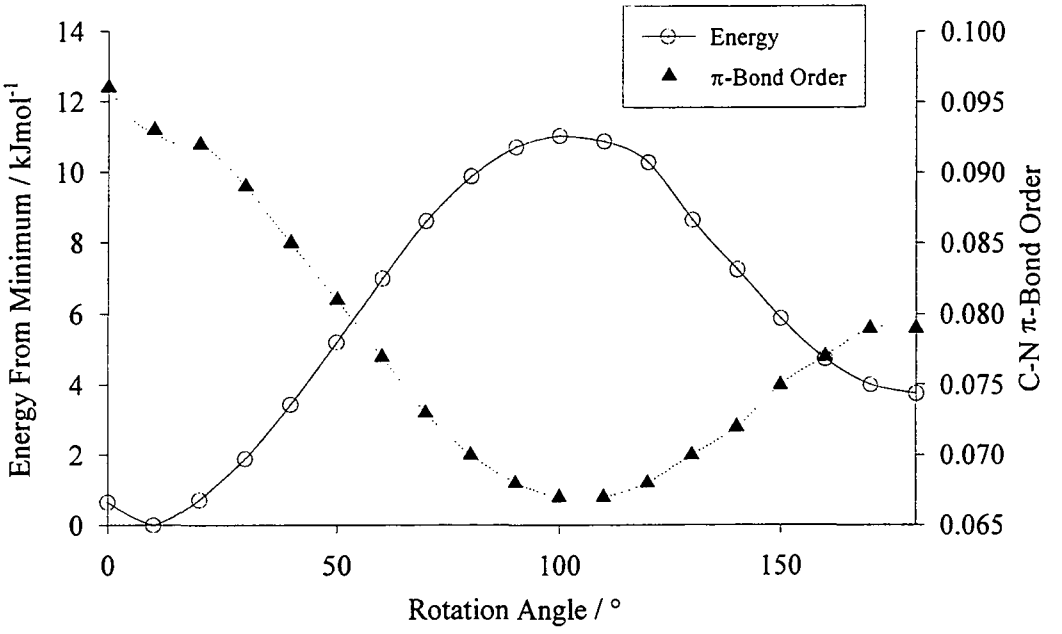

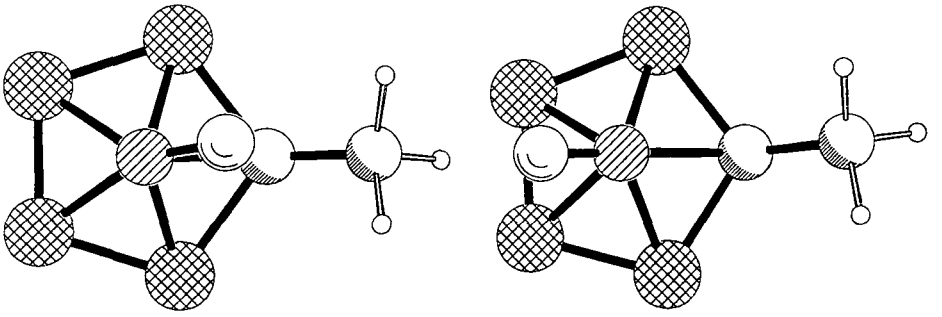

10° 180°

Preferred Orientations

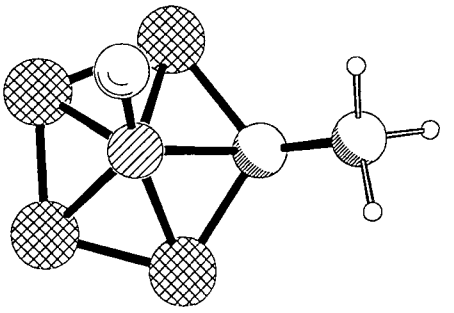

100°

Least Favoured Orientations

Figure B.3 **Energy and π-bond profiles for the rotation of the NO group in MeCbNO about the C-N axis**

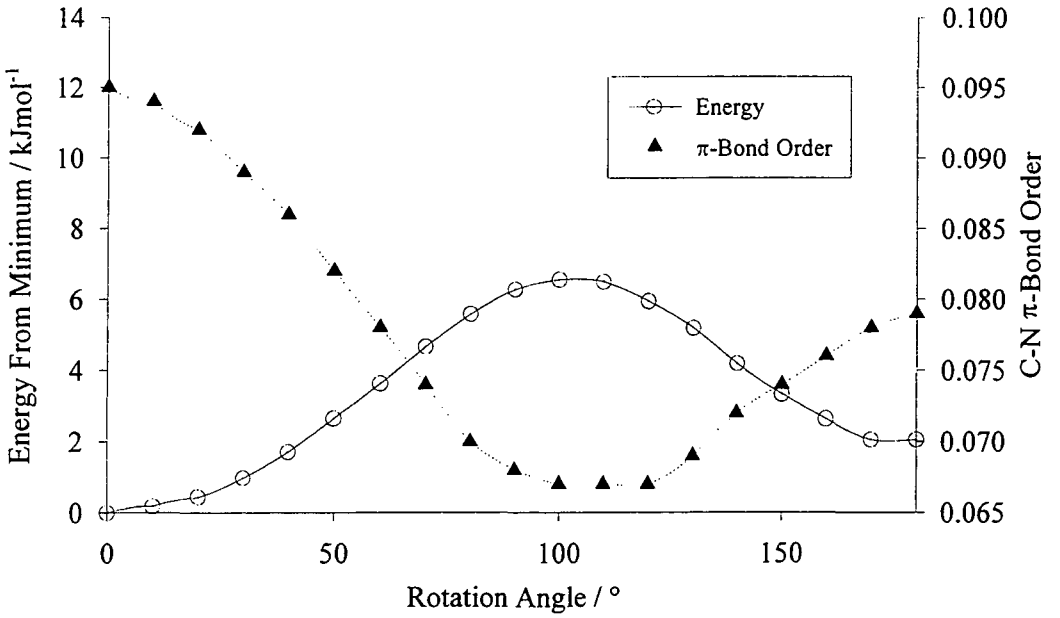

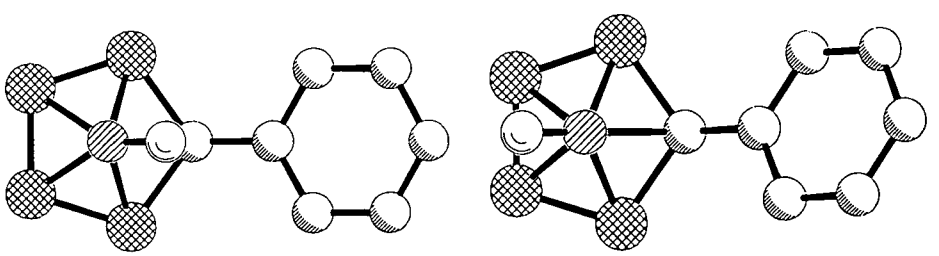

0° 180°

Preferred Orientations

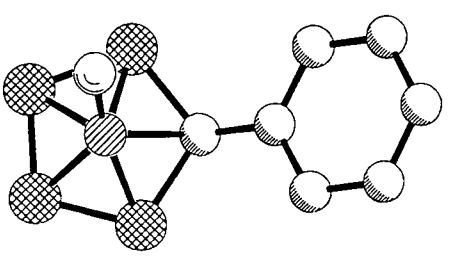

100°

Least Favourable Orientations

Figure B.4 **Energy and π-bond profiles for the rotation of the NO group in MeCbNO about the C-N axis**

B.3 INTRAMOLECULAR INTERACTIONS IN HYDROXYLAMINES

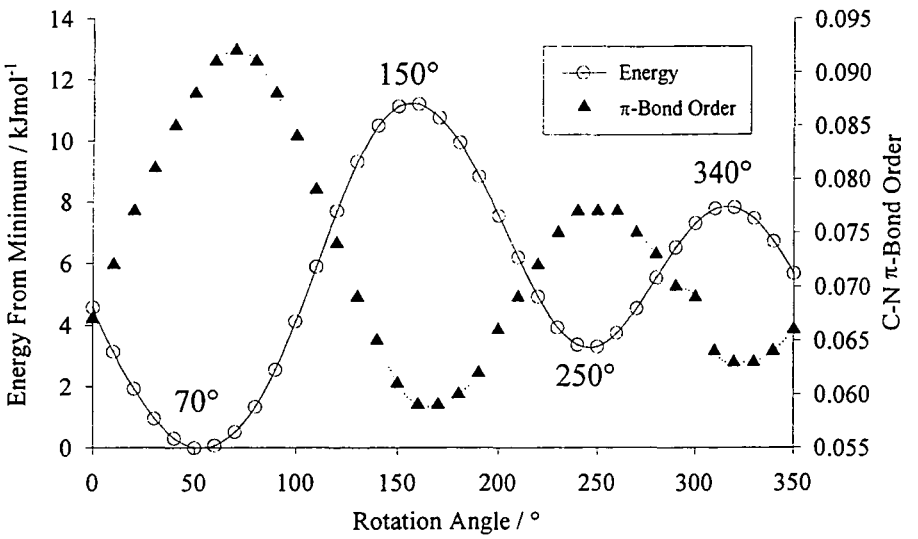

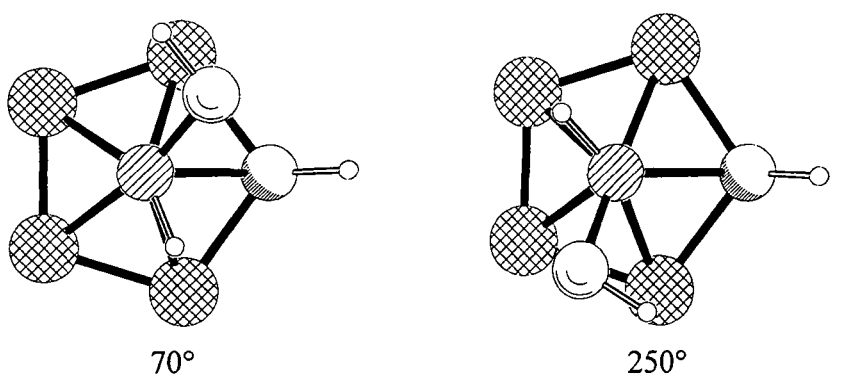

Preferred Orientations

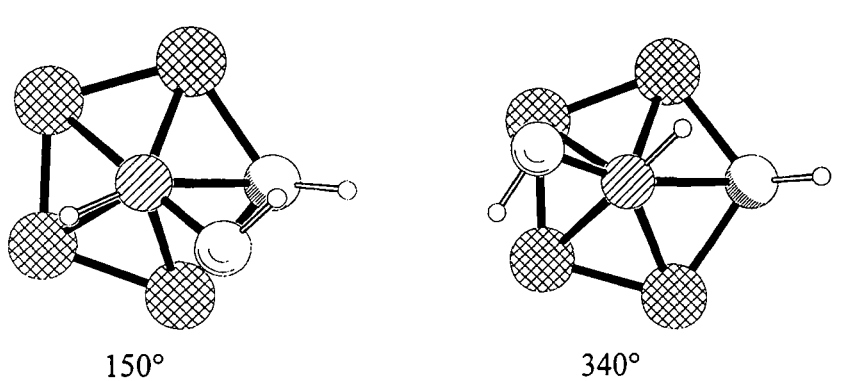

Least Favourable Orientations

Figure B.5 **Energy and π-bond profiles for the rotation of the NO group in HCbNHOH about the C-N axis**

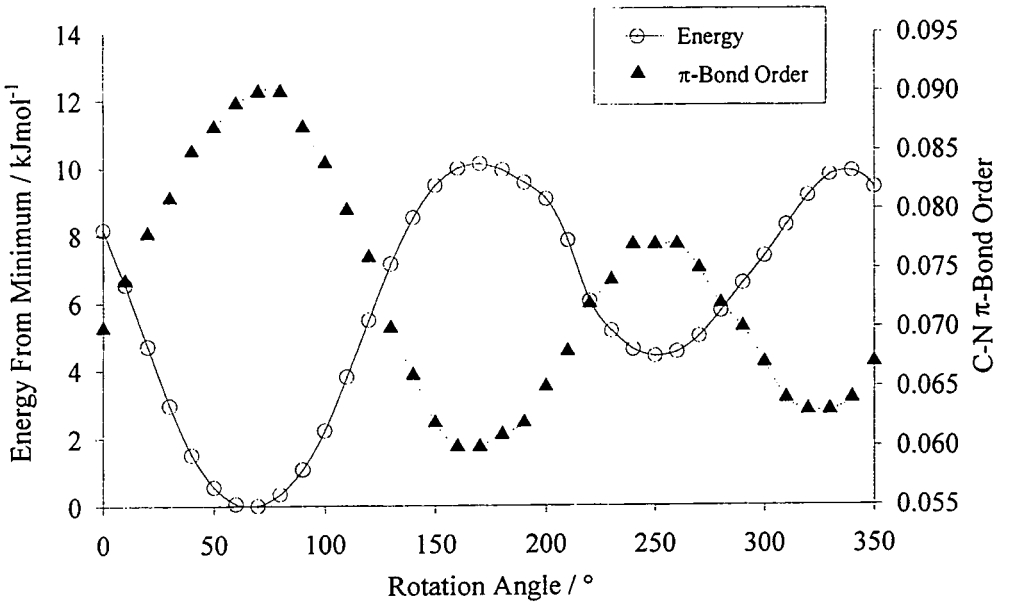

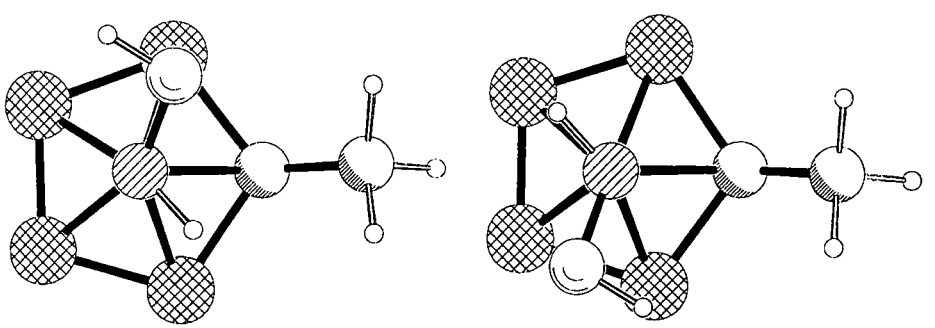

70° 250°

Preferred Orientations

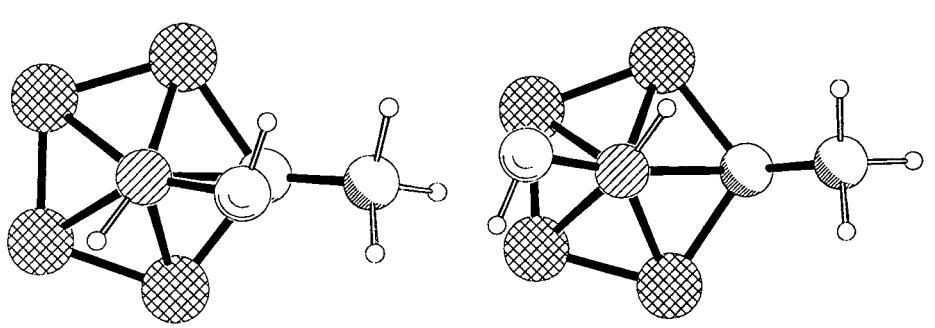

170° 350°

Least Favourable orientations

Figure B.6 **Energy and π-bond profiles for the rotation of the NO group in MeCbNHOH about the C-N axis**

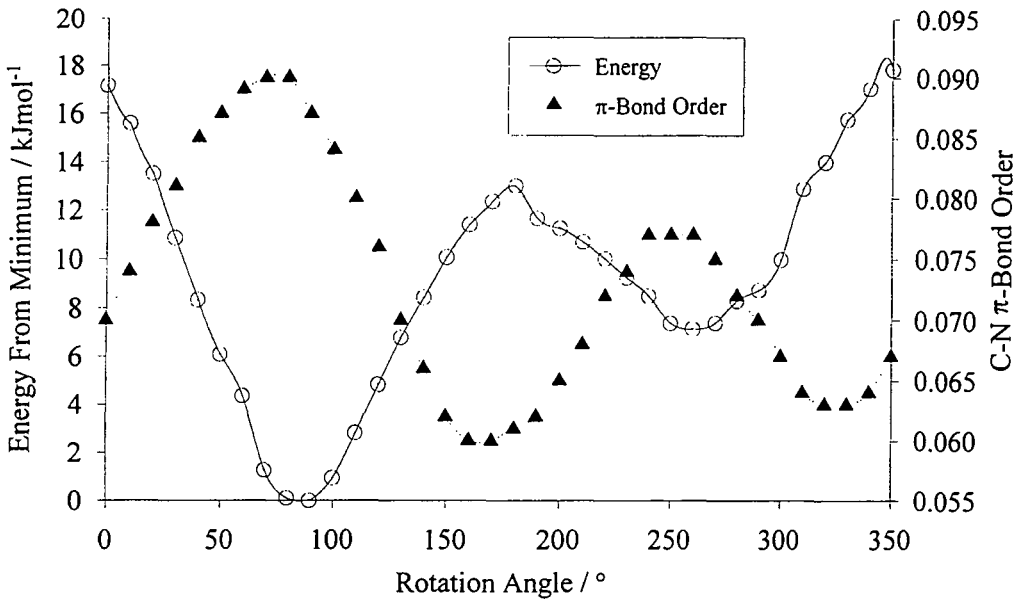

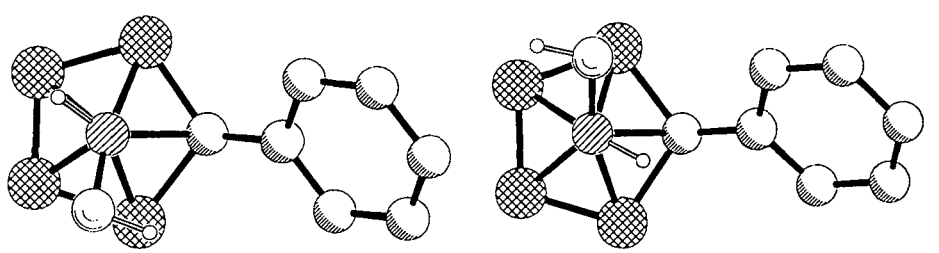

90° 260°

Preferred Orientations

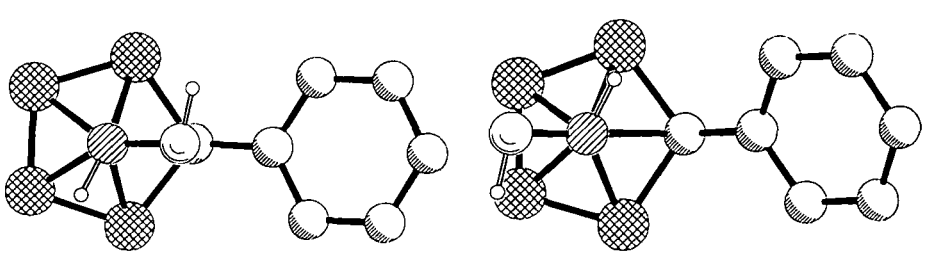

0° 180°

Least Favourable Orientations

Figure B.7 Energy and π-bond profiles for the rotation of the NO group in PhCbNHOH about the C-N axis

Appendix C

Crystal Data

C1 CRYSTAL DATA FOR FmesN$_2$Ph - 1

Empirical Formula	$C_{15}H_7F_9N_2$	
Temperature	190(2)K	
Wavelength	0.71073Å	
Crystal System	Monoclinic	
Space Group	P2(1)/C	
Unit Cell Dimensions	a = 16.842(2)Å	alpha = 90°
	b = 6.3996(6)Å	beta = 113.949(3)°
	c = 15.887(2)Å	gamma = 90°
Crystal Size	0.35 × 0.25 × 0.18 mm	
Final R indices [I>2σ(I)]	R1 = 0.0580	wR2 = 0.1363
R indices (all data)	R1 = 0.0905	wR2 = 0.2000

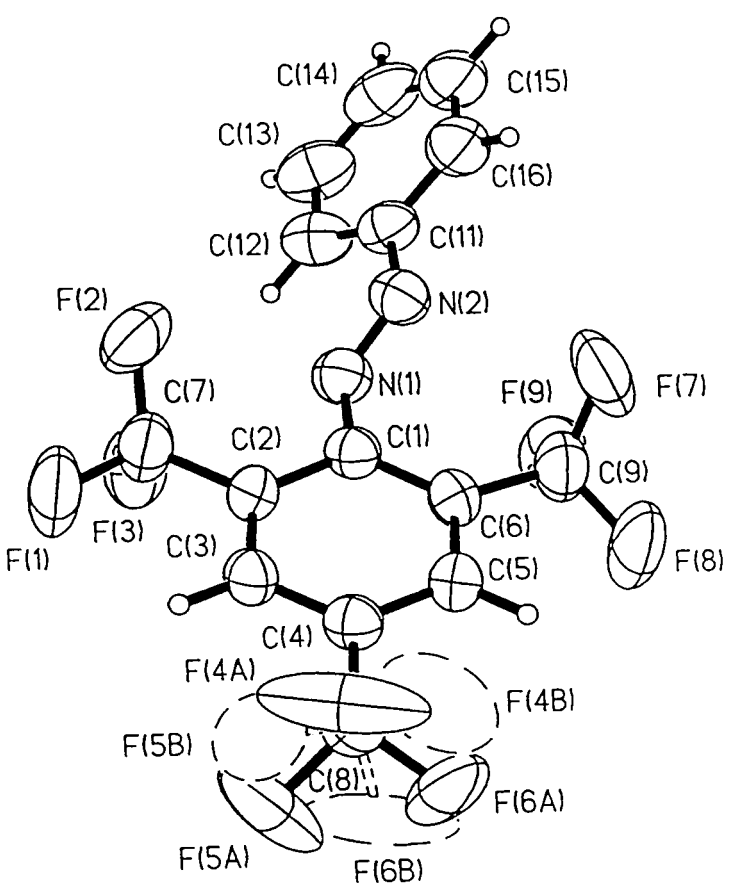

N(1)-N(2)	1.228(6)	N(1)-C(1)	1.443(7)
N(2)-C(11)	1.453(8)	C(1)-C(2)	1.401(7)
C(1)-C(6)	1.406(7)	C(2)-C(3)	1.384(8)
C(2)-C(7)	1.510(8)	C(3)-C(4)	1.380(7)
C(4)-C(5)	1.384(7)	C(4)-C(8)	1.498(8)
C(5)-C(6)	1.391(8)	C(6)-C(9)	1.510(8)
C(7)-F(3)	1.329(8)	C(7)-F(2)	1.334(7)
C(7)-F(1)	1.345(7)	C(8)-F(4A)	1.210(12)
C(8)-F(6B)	1.221(11)	C(8)-F(6A)	1.292(12)
C(8)-F(5B)	1.291(11)	C(8)-F(4B)	1.323(12)
C(8)-F(5A)	1.367(11)	C(9)-F(9)	1.328(9)
C(9)-F(7)	1.332(8)	C(9)-F(8)	1.348(8)
C(11)-C(16)	1.381(9)	C(11)-C(12)	1.388(9)
C(12)-C(13)	1.385(9)	C(13)-C(14)	1.379(12)
C(14)-C(15)	1.371(11)	C(15)-C(16)	1.394(10)
N(2)-N(1)-C(1)	112.6(5)	N(1)-N(2)-C(11)	112.7(5)
C(2)-C(1)-C(6)	118.8(5)	C(2)-C(1)-N(1)	115.9(5)
C(6)-C(1)-N(1)	125.1(5)	C(3)-C(2)-C(1)	120.7(5)
C(3)-C(2)-C(7)	119.5(5)	C(1)-C(2)-C(7)	119.8(5)
C(4)-C(3)-C(2)	120.1(5)	C(3)-C(4)-C(5)	120.0(5)
C(3)-C(4)-C(8)	120.3(5)	C(5)-C(4)-C(8)	119.7(5)
C(4)-C(5)-C(6)	120.8(5)	C(5)-C(6)-C(1)	119.5(5)
C(5)-C(6)-C(9)	117.9(5)	C(1)-C(6)-C(9)	122.5(5)
F(3)-C(7)-F(2)	107.2(5)	F(3)-C(7)-F(1)	105.9(6)
F(2)-C(7)-F(1)	106.2(5)	F(3)-C(7)-C(2)	113.1(5)
F(2)-C(7)-C(2)	112.7(5)	F(1)-C(7)-C(2)	111.3(5)
F(4A)-C(8)-F(6A)	111.0(14)	F(6B)-C(8)-F(5B)	109.2(10)
F(6B)-C(8)-F(4B)	106.7(12)	F(5B)-C(8)-F(4B)	98.9(11)
F(4A)-C(8)-F(5A)	105.5(11)	F(6A)-C(8)-F(5A)	97.3(11)
F(4A)-C(8)-C(4)	117.4(7)	F(6B)-C(8)-C(4)	116.1(7)
F(6A)-C(8)-C(4)	109.7(8)	F(5B)-C(8)-C(4)	116.3(7)
F(4B)-C(8)-C(4)	107.9(6)	F(5A)-C(8)-C(4)	114.0(7)
F(9)-C(9)-F(7)	106.8(6)	F(9)-C(9)-F(8)	106.2(6)
F(7)-C(9)-F(8)	106.2(6)	F(9)-C(9)-C(6)	114.3(6)
F(7)-C(9)-C(6)	112.4(6)	F(8)-C(9)-C(6)	110.5(5)
C(16)-C(11)-C(12)	121.0(6)	C(16)-C(11)-N(2)	113.9(6)
C(12)-C(11)-N(2)	125.0(5)	C(13)-C(12)-C(11)	119.3(7)
C(14)-C(13)-C(12)	119.8(8)	C(15)-C(14)-C(13)	120.9(7)
C(14)-C(15)-C(16)	120.0(7)	C(11)-C(16)-C(15)	118.9(8)

Table Atomic coordinates (x 10^4) and equivalent isotropic displacement parameters (A^2 x 10^3) for 1. U(eq) is defined as one third of the trace of the orthogonalized Uij tensor.

	x	y	z	U(eq)
N(1)	2336(3)	6984(8)	4753(3)	56(1)
N(2)	1562(3)	6868(8)	4602(3)	57(1)
C(1)	2813(3)	5129(8)	5188(3)	45(1)
C(2)	3370(3)	4323(9)	4811(3)	47(1)
C(3)	3896(3)	2621(9)	5208(4)	49(1)
C(4)	3885(3)	1714(8)	5992(4)	46(1)
C(5)	3348(3)	2506(9)	6381(4)	50(1)
C(6)	2813(3)	4211(9)	5992(4)	49(1)
C(7)	3394(4)	5310(11)	3958(4)	65(2)
C(8)	4474(4)	-86(10)	6440(4)	58(2)
C(9)	2293(5)	5088(13)	6493(5)	73(2)
C(11)	1079(4)	8735(10)	4165(4)	57(2)
C(12)	1413(4)	10404(10)	3853(4)	70(2)
C(13)	881(6)	12089(12)	3442(5)	84(2)
C(14)	30(6)	12091(14)	3348(5)	90(3)
C(15)	-298(5)	10445(15)	3658(5)	87(2)
C(16)	226(4)	8729(13)	4066(5)	74(2)
F(1)	3937(3)	4277(8)	3676(3)	99(2)
F(2)	2620(3)	5301(7)	3247(2)	88(1)
F(3)	3670(3)	7277(7)	4088(3)	87(1)
F(4A)	4237(11)	-1810(20)	6124(16)	154(12)
F(5A)	5295(8)	128(28)	6478(18)	126(7)
F(6A)	4680(13)	-58(33)	7317(8)	117(8)
F(4B)	4011(8)	-1523(18)	6637(15)	128(6)
F(5B)	4728(14)	-1191(30)	5915(9)	139(7)
F(6B)	5098(10)	303(20)	7157(13)	149(9)
F(7)	1468(3)	4456(8)	6127(3)	106(2)
F(8)	2624(3)	4437(9)	7376(3)	112(2)
F(9)	2280(3)	7160(7)	6522(3)	87(1)

Table Hydrogen coordinates (x 10^4) and isotropic displacement parameters (A^2 x 10^3)

	x	y	z	U(eq)
H(3)	4266(3)	2078(9)	4941(4)	63(17)
H(5)	3348(3)	1884(9)	6925(4)	53(15)
H(12)	2002(4)	10393(10)	3923(4)	92(24)
H(13)	1102(6)	13241(12)	3224(5)	127(34)
H(14)	-333(6)	13251(14)	3064(5)	105(26)
H(15)	-885(5)	10471(15)	3594(5)	105(27)
H(16)	0(4)	7574(13)	4276(5)	83(24)

C2 CRYSTAL DATA FOR FmesNH$_2$ - 2

Empirical Formula	$C_9H_4F_9N$	
Temperature	150(2)K	
Wavelength	0.71073Å	
Crystal System	Orthorhombic	
Space Group	Pnma	
Unit Cell Dimensions	a = 16.713Å	alpha = 90°
	b = 7.7406Å	beta = 90°
	c = 16.147Å	gamma = 90°
Final R indices [I>2σ(I)]	R1 = 0.0574	wR2 = 0.1905
R indices (all data)	R1 = 0.0620	wR2 = 0.1982

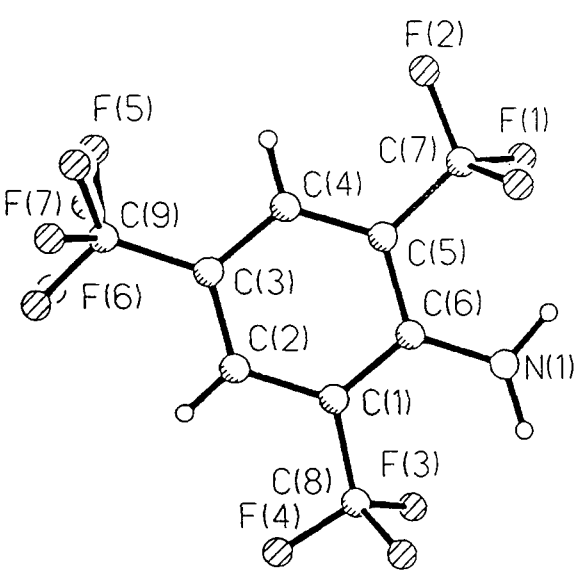

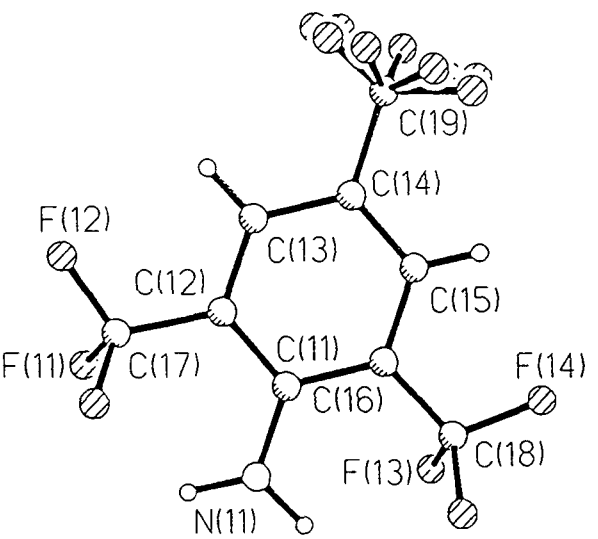

F(1)-C(7)	1.340(4)
F(2)-C(7)	1.325(6)
F(3)-C(8)	1.331(4)
F(4)-C(8)	1.317(7)
F(5)-F(7)	1.094(10)
F(5)-F(5)#1	1.26(2)
F(5)-C(9)	1.298(7)
F(6)-F(6)#1	1.01(2)
F(6)-C(9)	1.295(7)
F(6)-F(7)	1.343(13)
F(7)-C(9)	1.318(7)
N(1)-C(6)	1.358(6)
N(1)-H(1B)	0.98(4)
N(1)-H(1A)	0.96(4)
C(1)-C(2)	1.381(7)
C(1)-C(6)	1.417(7)
C(1)-C(8)	1.504(7)
C(2)-C(3)	1.394(7)
C(2)-H(2)	0.95
C(3)-C(4)	1.386(7)
C(3)-C(9)	1.476(7)
C(4)-C(5)	1.368(7)
C(4)-H(4)	0.95
C(5)-C(6)	1.415(7)
C(5)-C(7)	1.503(7)
C(7)-F(1)#1	1.339(4)
C(8)-F(3)#1	1.331(4)
C(9)-F(5)#1	1.298(7)
C(9)-F(6)#1	1.295(7)
C(9)-F(7)#1	1.318(7)
F(11)-C(17)	1.330(4)
F(12)-C(17)	1.331(7)
F(13)-C(18)	1.324(4)
F(14)-C(18)	1.344(6)
F(15)-F(17)	0.85(3)
F(15)-F(17)#1	0.85(3)
F(15)-C(19)	1.31(2)
F(15)-F(17A)#1	1.40(3)
F(15)-F(17A)	1.40(3)
F(16)-F(18)#1	0.63(4)
F(16)-F(17A)	0.96(3)
F(16)-C(19)	1.342(13)
F(16)-F(17)	1.64(3)
F(16)-F(18)	1.69(3)
F(17)-F(17A)	0.73(3)
F(17)-C(19)	1.33(2)
F(17)-F(17)#1	1.62(5)
F(17A)-C(19)	1.27(2)
F(17A)-F(18)#1	1.49(4)
F(18)-F(16)#1	0.63(4)
F(18)-F(18)#1	1.17(7)
F(18)-C(19)	1.32(2)
F(18)-F(17A)#1	1.49(4)
N(11)-C(11)	1.357(7)
N(11)-H(11B)	1.00(4)
N(11)-H(11A)	0.99(4)
C(11)-C(16)	1.409(6)
C(11)-C(12)	1.409(7)
C(12)-C(13)	1.379(7)
C(12)-C(17)	1.497(7)
C(13)-C(14)	1.391(7)
C(13)-H(13)	0.95
C(14)-C(15)	1.377(7)
C(14)-C(19)	1.492(7)

C(15)-C(14)-C(19)	121.4(4)
C(13)-C(14)-C(19)	119.2(4)
C(14)-C(15)-C(16)	120.8(4)
C(14)-C(15)-H(15)	119.6(3)
C(16)-C(15)-H(15)	119.6(3)
C(15)-C(16)-C(11)	120.8(4)
C(15)-C(16)-C(18)	119.1(4)
C(11)-C(16)-C(18)	120.1(4)
F(12)-C(17)-F(11)#1	106.2(3)
F(12)-C(17)-F(11)	106.2(3)
F(11)#1-C(17)-F(11)	105.2(4)
F(12)-C(17)-C(12)	113.0(5)
F(11)#1-C(17)-C(12)	112.8(3)
F(11)-C(17)-C(12)	112.8(3)
F(13)#1-C(18)-F(13)	105.9(4)
F(13)#1-C(18)-F(14)	105.7(3)
F(13)-C(18)-F(14)	105.7(3)
F(13)#1-C(18)-C(16)	113.2(3)
F(13)-C(18)-C(16)	113.2(3)
F(14)-C(18)-C(16)	112.5(4)
F(17A)#1-C(19)-F(17A)	119(3)
F(17A)#1-C(19)-F(15)	65.7(13)
F(17A)-C(19)-F(15)	65.7(13)
F(17A)#1-C(19)-F(18)#1	115(2)
F(17A)-C(19)-F(18)#1	70(2)
F(15)-C(19)-F(18)#1	126(2)
F(17A)#1-C(19)-F(18)	70(2)
F(17A)-C(19)-F(18)	115(2)
F(15)-C(19)-F(18)	126(2)
F(18)#1-C(19)-F(18)	53(3)
F(17A)#1-C(19)-F(17)#1	32.4(13)
F(17A)-C(19)-F(17)#1	102(2)
F(15)-C(19)-F(17)#1	37.4(12)
F(18)#1-C(19)-F(17)#1	139(2)
F(18)-C(19)-F(17)#1	102(2)
F(17A)#1-C(19)-F(17)	102(2)
F(17A)-C(19)-F(17)	32.4(13)
F(15)-C(19)-F(17)	37.4(12)
F(18)#1-C(19)-F(17)	102(2)
F(18)-C(19)-F(17)	139(2)
F(17)#1-C(19)-F(17)	75(2)
F(17A)#1-C(19)-F(16)	128(2)
F(17A)-C(19)-F(16)	43.1(11)
F(15)-C(19)-F(16)	105.4(8)
F(18)#1-C(19)-F(16)	28(2)
F(18)-C(19)-F(16)	79(2)
F(17)#1-C(19)-F(16)	133.9(13)
F(17)-C(19)-F(16)	75.5(12)
F(17A)#1-C(19)-F(16)#1	43.1(11)
F(17A)-C(19)-F(16)#1	128(2)
F(15)-C(19)-F(16)#1	105.4(8)
F(18)#1-C(19)-F(16)#1	79(2)
F(18)-C(19)-F(16)#1	28(2)
F(17)#1-C(19)-F(16)#1	75.5(11)
F(17)-C(19)-F(16)#1	133.9(13)
F(16)-C(19)-F(16)#1	102(2)
F(17A)#1-C(19)-C(14)	115.9(12)
F(17A)-C(19)-C(14)	115.9(12)
F(15)-C(19)-C(14)	113.8(9)
F(18)#1-C(19)-C(14)	112(2)
F(18)-C(19)-C(14)	112(2)
F(17)#1-C(19)-C(14)	107.6(10)
F(17)-C(19)-C(14)	107.6(10)
F(16)-C(19)-C(14)	114.5(8)
F(16)#1-C(19)-C(14)	114.5(8)

C(15)-C(16)	1.384(7)
C(15)-H(15)	0.95
C(16)-C(18)	1.482(7)
C(17)-F(11)#1	1.330(4)
C(18)-F(13)#1	1.324(4)
C(19)-F(17A)#1	1.27(2)
C(19)-F(18)#1	1.32(2)
C(19)-F(17)#1	1.33(2)
C(19)-F(16)#1	1.342(13)

F(7)-F(5)-F(5)#1	122.3(8)
F(7)-F(5)-C(9)	66.2(5)
F(5)#1-F(5)-C(9)	61.0(4)
F(6)#1-F(6)-C(9)	67.1(4)
F(6)#1-F(6)-F(7)	121.9(5)
C(9)-F(6)-F(7)	59.9(4)
F(5)-F(7)-C(9)	64.3(6)
F(5)-F(7)-F(6)	115.6(8)
C(9)-F(7)-F(6)	58.2(5)
C(6)-N(1)-H(1B)	124(4)
C(6)-N(1)-H(1A)	113(4)
H(1B)-N(1)-H(1A)	124(6)
C(2)-C(1)-C(6)	121.8(4)
C(2)-C(1)-C(8)	118.1(4)
C(6)-C(1)-C(8)	120.2(4)
C(1)-C(2)-C(3)	120.4(4)
C(1)-C(2)-H(2)	119.8(3)
C(3)-C(2)-H(2)	119.8(3)
C(4)-C(3)-C(2)	118.7(4)
C(4)-C(3)-C(9)	120.7(4)
C(2)-C(3)-C(9)	120.7(4)
C(5)-C(4)-C(3)	121.4(4)
C(5)-C(4)-H(4)	119.3(3)
C(3)-C(4)-H(4)	119.3(3)
C(4)-C(5)-C(6)	121.7(4)
C(4)-C(5)-C(7)	119.2(4)
C(6)-C(5)-C(7)	119.1(4)
N(1)-C(6)-C(1)	121.7(4)
N(1)-C(6)-C(5)	122.2(5)
C(1)-C(6)-C(5)	116.1(4)
F(2)-C(7)-F(1)#1	107.1(3)
F(2)-C(7)-F(1)	107.1(3)
F(1)#1-C(7)-F(1)	106.0(4)
F(2)-C(7)-C(5)	112.3(4)
F(1)#1-C(7)-C(5)	112.0(3)
F(1)-C(7)-C(5)	112.0(3)
F(4)-C(8)-F(3)#1	106.9(3)
F(4)-C(8)-F(3)	106.9(3)
F(3)#1-C(8)-F(3)	104.3(4)
F(4)-C(8)-C(1)	112.9(4)
F(3)#1-C(8)-C(1)	112.6(3)
F(3)-C(8)-C(1)	112.6(3)
F(5)#1-C(9)-F(5)	58.1(9)
F(5)#1-C(9)-F(6)#1	105.7(5)
F(5)-C(9)-F(6)#1	130.5(5)
F(5)#1-C(9)-F(6)	130.5(5)
F(5)-C(9)-F(6)	105.7(5)
F(6)#1-C(9)-F(6)	45.8(8)
F(5)#1-C(9)-F(7)	104.2(9)
F(5)-C(9)-F(7)	49.4(5)
F(6)#1-C(9)-F(7)	104.3(8)
F(6)-C(9)-F(7)	61.9(6)
F(5)#1-C(9)-F(7)#1	49.4(5)
F(5)-C(9)-F(7)#1	104.2(9)
F(6)#1-C(9)-F(7)#1	61.9(6)
F(6)-C(9)-F(7)#1	104.3(8)
F(7)-C(9)-F(7)#1	134.5(7)
F(5)#1-C(9)-C(3)	114.5(4)

F(5)-C(9)-C(3)	114.5(4)
F(6)#1-C(9)-C(3)	114.6(4)
F(6)-C(9)-C(3)	114.6(4)
F(7)-C(9)-C(3)	112.5(3)
F(7)#1-C(9)-C(3)	112.5(3)
F(17)-F(15)-F(17)#1	146(3)
F(17)-F(15)-C(19)	73(2)
F(17)#1-F(15)-C(19)	73(2)
F(17)-F(15)-F(17A)#1	126(2)
F(17)#1-F(15)-F(17A)#1	25(2)
C(19)-F(15)-F(17A)#1	55.8(14)
F(17)-F(15)-F(17A)	25(2)
F(17)#1-F(15)-F(17A)	126(2)
C(19)-F(15)-F(17A)	55.8(14)
F(17A)#1-F(15)-F(17A)	103(3)
F(18)#1-F(16)-F(17A)	136(4)
F(18)#1-F(16)-C(19)	74(3)
F(17A)-F(16)-C(19)	64.3(14)
F(18)#1-F(16)-F(17)	124(3)
F(17A)-F(16)-F(17)	12(2)
C(19)-F(16)-F(17)	52.0(8)
F(18)#1-F(16)-F(18)	29(3)
F(17A)-F(16)-F(18)	108(2)
C(19)-F(16)-F(18)	50.0(10)
F(17)-F(16)-F(18)	96.5(14)
F(17A)-F(17)-F(15)	125(5)
F(17A)-F(17)-C(19)	69(3)
F(15)-F(17)-C(19)	70(2)
F(17A)-F(17)-F(17)#1	113(3)
F(15)-F(17)-F(17)#1	17(2)
C(19)-F(17)-F(17)#1	52.6(12)
F(17A)-F(17)-F(16)	16(3)
F(15)-F(17)-F(16)	112(3)
C(19)-F(17)-F(16)	52.5(9)
F(17)#1-F(17)-F(16)	98.2(11)
F(17)-F(17A)-F(16)	151(4)
F(17)-F(17A)-C(19)	79(2)
F(16)-F(17A)-C(19)	73(2)
F(17)-F(17A)-F(15)	30(3)
F(16)-F(17A)-F(15)	126(2)
C(19)-F(17A)-F(15)	58.5(10)
F(17)-F(17A)-F(18)#1	135(4)
F(16)-F(17A)-F(18)#1	17(2)
C(19)-F(17A)-F(18)#1	57(2)
F(15)-F(17A)-F(18)#1	109(2)
F(16)#1-F(18)-F(18)#1	136(4)
F(16)#1-F(18)-C(19)	78(3)
F(18)#1-F(18)-C(19)	64(2)
F(16)#1-F(18)-F(17A)#1	27(2)
F(18)#1-F(18)-F(17A)#1	110(2)
C(19)-F(18)-F(17A)#1	53.4(12)
F(16)#1-F(18)-F(16)	121(4)
F(18)#1-F(18)-F(16)	15.1(12)
C(19)-F(18)-F(16)	51.3(11)
F(17A)#1-F(18)-F(16)	95(2)
C(11)-N(11)-H(11B)	118(4)
C(11)-N(11)-H(11A)	120(5)
H(11B)-N(11)-H(11A)	122(6)
N(11)-C(11)-C(16)	121.4(4)
N(11)-C(11)-C(12)	121.2(4)
C(16)-C(11)-C(12)	117.4(4)
C(13)-C(12)-C(11)	121.1(4)
C(13)-C(12)-C(17)	119.1(4)
C(11)-C(12)-C(17)	119.9(4)
C(14)-C(13)-C(12)	120.5(4)
C(14)-C(13)-H(13)	119.7(3)
C(12)-C(13)-H(13)	119.8(3)
C(15)-C(14)-C(13)	119.4(4)

Table Atomic coordinates (x 10^4) and equivalent isotropic displacement parameters (A^2 x 10^3) for 1. U(eq) is defined as one third of the trace of the orthogonalized Uij tensor.

	x	y	z	U(eq)
F(1)	918(2)	1118(3)	5543(1)	64(1)
F(2)	-137(2)	2500	5906(2)	71(1)
F(3)	3260(1)	1143(3)	7790(2)	72(1)
F(4)	2978(2)	2500	8898(2)	106(2)
F(5)	-640(4)	1686(12)	8782(4)	92(3)
F(6)	262(3)	1848(10)	9656(3)	98(4)
F(7)	-222(7)	930(9)	9158(7)	112(3)
N(1)	2325(3)	2500	6391(3)	51(1)
C(1)	1997(3)	2500	7853(3)	36(1)
C(2)	1435(3)	2500	8480(3)	39(1)
C(3)	620(3)	2500	8294(3)	34(1)
C(4)	388(3)	2500	7471(3)	37(1)
C(5)	939(3)	2500	6845(3)	36(1)
C(6)	1771(3)	2500	7007(3)	37(1)
C(7)	655(3)	2500	5961(3)	50(1)
C(8)	2867(3)	2500	8091(3)	47(1)
C(9)	17(3)	2500	8962(3)	46(1)
F(11)	3304(2)	1135(3)	4502(1)	79(1)
F(12)	2226(2)	2500	4247(2)	99(2)
F(13)	5423(1)	1134(3)	2026(2)	73(1)
F(14)	5048(2)	2500	951(2)	88(1)
F(15)	2319(11)	2500	407(9)	117(16)
F(16)	1590(9)	1153(23)	1254(9)	81(7)
F(17)	2290(13)	1456(33)	559(12)	71(10)
F(17A)	1967(13)	1088(31)	805(19)	86(13)
F(18)	1447(19)	3255(43)	1482(22)	87(22)
N(11)	4622(3)	2500	3509(3)	60(1)
C(11)	4018(3)	2500	2948(3)	35(1)
C(12)	3212(3)	2500	3201(3)	35(1)
C(13)	2599(3)	2500	2629(3)	37(1)
C(14)	2766(3)	2500	1785(3)	34(1)
C(15)	3551(3)	2500	1523(3)	35(1)
C(16)	4172(3)	2500	2090(3)	34(1)
C(17)	3010(3)	2500	4104(3)	53(1)
C(18)	5008(3)	2500	1782(3)	45(1)
C(19)	2090(3)	2500	1181(3)	49(1)

Table Hydrogen coordinates (x 10^4) and isotropic displacement parameters (A^2 x 10^3)

	x	y	z	U(eq)
H(2)	1604(3)	2500	9042(3)	33(12)
H(4)	-166(3)	2500	7338(3)	54(15)
H(13)	2059(3)	2500	2812(3)	50(15)
H(15)	3666(3)	2500	947(3)	12(9)
H(1B)	2901(27)	2500	6486(45)	91(24)
H(1A)	2087(35)	2500	5849(29)	61(18)
H(11B)	5185(29)	2500	3301(43)	85(22)
H(11A)	4500(46)	2500	4111(28)	87(23)

C3 CRYSTAL DATA FOR FmesNHNHPh - 3

Empirical Formula	$C_{15}H_9F_9N_2$	
Temperature	150(2)K	
Wavelength	0.71073Å	
Crystal System	Monoclinic	
Space Group	P2/n (No.13)	
Unit Cell Dimensions	a = 16.5777(10)Å	alpha = 90°
	b = 8.5862(5)Å	beta = 90.263(4)°
	c = 21.3089(10)Å	gamma = 90°
Final R indices [I>2σ(I)]	R1 = 0.0614	wR2 = 0.1404
R indices (all data)	R1 = 0.0867	wR2 = 0.1821

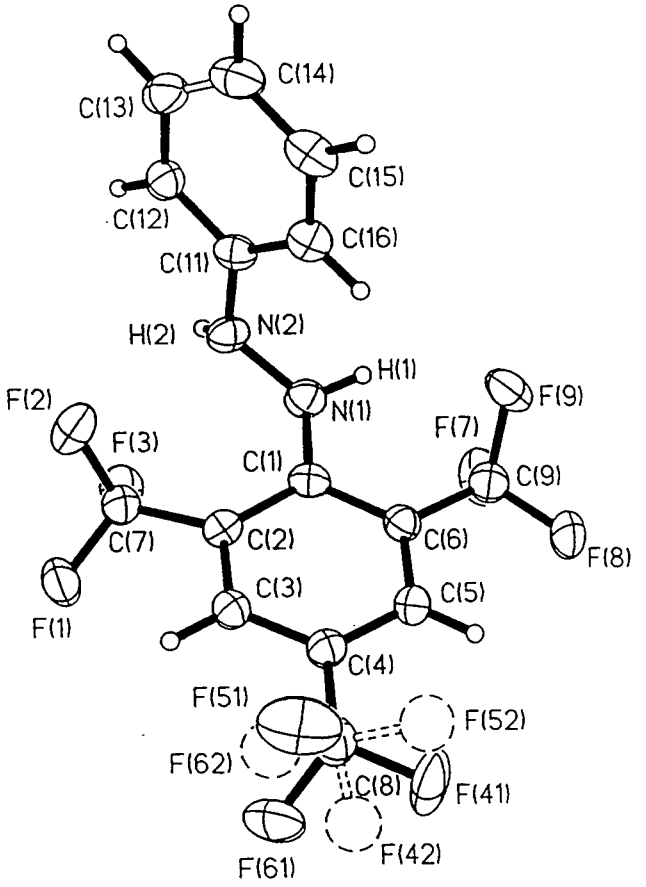

Table Bond lengths [A] and angles [deg]

N(1A)-H(1A)	0.90(4)	N(1A)-C(1A)	1.389(4)
N(1A)-N(2A)	1.395(4)	N(2A)-H(2A)	0.86(4)
N(2A)-C(11A)	1.411(4)	C(1A)-C(6A)	1.413(5)
C(1A)-C(2A)	1.427(4)	C(2A)-C(3A)	1.391(5)
C(2A)-C(7A)	1.503(5)	C(3A)-C(4A)	1.386(5)
C(4A)-C(5A)	1.393(5)	C(4A)-C(8A)	1.482(5)
C(5A)-C(6A)	1.390(5)	C(6A)-C(9A)	1.499(5)
C(7A)-F(2A)	1.340(4)	C(7A)-F(3A)	1.348(4)
C(7A)-F(1A)	1.352(4)	C(8A)-F(42A)	1.15(2)
C(8A)-F(62A)	1.29(2)	C(8A)-F(41A)	1.321(5)
C(8A)-F(51A)	1.332(5)	C(8A)-F(52A)	1.45(2)
C(8A)-F(61A)	1.369(5)	C(9A)-F(7A)	1.339(4)
C(9A)-F(8A)	1.342(4)	C(9A)-F(9A)	1.350(4)
C(11A)-C(16A)	1.394(5)	C(11A)-C(12A)	1.400(5)
C(12A)-C(13A)	1.387(5)	C(13A)-C(14A)	1.383(6)
C(14A)-C(15A)	1.383(6)	C(15A)-C(16A)	1.391(5)
N(1B)-H(1B)	0.92(4)	N(1B)-C(1B)	1.386(4)
N(1B)-N(2B)	1.401(4)	N(2B)-H(2B)	0.86(4)
N(2B)-C(11B)	1.411(4)	C(1B)-C(6B)	1.421(5)
C(1B)-C(2B)	1.423(4)	C(2B)-C(3B)	1.397(5)
C(2B)-C(7B)	1.507(5)	C(3B)-C(4B)	1.384(5)
C(4B)-C(5B)	1.383(5)	C(4B)-C(8B)	1.490(5)
C(5B)-C(6B)	1.389(5)	C(6B)-C(9B)	1.505(5)
C(7B)-F(1B)	1.343(4)	C(7B)-F(2B)	1.344(4)
C(7B)-F(3B)	1.350(4)	C(9B)-F(8B)	1.328(4)
C(9B)-F(9B)	1.346(4)	C(9B)-F(7B)	1.354(4)
C(11B)-C(16B)	1.388(5)	C(11B)-C(12B)	1.395(5)
C(12B)-C(13B)	1.388(5)	C(13B)-C(14B)	1.390(6)
C(14B)-C(15B)	1.377(6)	C(15B)-C(16B)	1.392(5)

H(1A)-N(1A)-C(1A)	116(3)	H(1A)-N(1A)-N(2A)	117(2)
C(1A)-N(1A)-N(2A)	119.4(3)	H(2A)-N(2A)-N(1A)	111(3)
H(2A)-N(2A)-C(11A)	119(3)	N(1A)-N(2A)-C(11A)	118.9(3)
N(1A)-C(1A)-C(6A)	119.5(3)	N(1A)-C(1A)-C(2A)	123.1(3)
C(6A)-C(1A)-C(2A)	117.4(3)	C(3A)-C(2A)-C(1A)	119.3(3)
C(3A)-C(2A)-C(7A)	116.1(3)	C(1A)-C(2A)-C(7A)	124.4(3)
C(4A)-C(3A)-C(2A)	122.1(3)	C(3A)-C(4A)-C(5A)	119.2(3)
C(3A)-C(4A)-C(8A)	120.1(3)	C(5A)-C(4A)-C(8A)	120.6(3)
C(6A)-C(5A)-C(4A)	119.8(3)	C(5A)-C(6A)-C(1A)	121.8(3)
C(5A)-C(6A)-C(9A)	117.5(3)	C(1A)-C(6A)-C(9A)	120.8(3)
F(2A)-C(7A)-F(3A)	107.1(3)	F(2A)-C(7A)-F(1A)	105.6(3)
F(3A)-C(7A)-F(1A)	105.0(3)	F(2A)-C(7A)-C(2A)	115.3(3)
F(3A)-C(7A)-C(2A)	112.9(3)	F(1A)-C(7A)-C(2A)	110.1(3)
F(42A)-C(8A)-F(62A)	108(2)	F(41A)-C(8A)-F(51A)	109.7(4)
F(42A)-C(8A)-F(52A)	101(2)	F(62A)-C(8A)-F(52A)	92(2)
F(41A)-C(8A)-F(61A)	103.5(3)	F(51A)-C(8A)-F(61A)	104.1(3)
F(42A)-C(8A)-C(4A)	124.9(13)	F(62A)-C(8A)-C(4A)	119(2)
F(41A)-C(8A)-C(4A)	113.3(3)	F(51A)-C(8A)-C(4A)	113.3(3)
F(52A)-C(8A)-C(4A)	105.2(10)	F(61A)-C(8A)-C(4A)	112.1(3)
F(7A)-C(9A)-F(8A)	106.5(3)	F(7A)-C(9A)-F(9A)	105.5(3)
F(8A)-C(9A)-F(9A)	105.3(3)	F(7A)-C(9A)-C(6A)	113.0(3)
F(8A)-C(9A)-C(6A)	113.0(3)	F(9A)-C(9A)-C(6A)	112.9(3)
C(16A)-C(11A)-C(12A)	119.7(3)	C(16A)-C(11A)-N(2A)	122.9(3)
C(12A)-C(11A)-N(2A)	117.3(3)	C(13A)-C(12A)-C(11A)	119.6(3)
C(14A)-C(13A)-C(12A)	120.7(4)	C(15A)-C(14A)-C(13A)	119.5(3)
C(14A)-C(15A)-C(16A)	120.8(4)	C(15A)-C(16A)-C(11A)	119.5(3)
H(1B)-N(1B)-C(1B)	118(2)	H(1B)-N(1B)-N(2B)	115(2)
C(1B)-N(1B)-N(2B)	118.6(3)	H(2B)-N(2B)-N(1B)	120(3)
H(2B)-N(2B)-C(11B)	112(3)	N(1B)-N(2B)-C(11B)	119.3(3
N(1B)-C(1B)-C(6B)	119.4(3)	N(1B)-C(1B)-C(2B)	123.3(3

C(6B)-C(1B)-C(2B)	117.3(3)	C(3B)-C(2B)-C(1B)	119.6(3)
C(3B)-C(2B)-C(7B)	115.6(3)	C(1B)-C(2B)-C(7B)	124.7(3)
C(4B)-C(3B)-C(2B)	121.4(3)	C(5B)-C(4B)-C(3B)	120.0(3)
C(5B)-C(4B)-C(8B)	119.5(4)	C(3B)-C(4B)-C(8B)	120.5(3)
C(4B)-C(5B)-C(6B)	119.9(3)	C(5B)-C(6B)-C(1B)	121.6(3)
C(5B)-C(6B)-C(9B)	117.1(3)	C(1B)-C(6B)-C(9B)	121.3(3)
F(1B)-C(7B)-F(2B)	105.8(3)	F(1B)-C(7B)-F(3B)	105.4(3)
F(2B)-C(7B)-F(3B)	106.7(3)	F(1B)-C(7B)-C(2B)	110.1(3)
F(2B)-C(7B)-C(2B)	114.9(3)	F(3B)-C(7B)-C(2B)	113.2(3)
F(8B)-C(9B)-F(9B)	106.5(3)	F(8B)-C(9B)-F(7B)	106.4(3)
F(9B)-C(9B)-F(7B)	105.9(3)	F(8B)-C(9B)-C(6B)	113.0(3)
F(9B)-C(9B)-C(6B)	112.7(3)	F(7B)-C(9B)-C(6B)	111.9(3)
C(16B)-C(11B)-C(12B)	119.6(3)	C(16B)-C(11B)-N(2B)	122.5(3)
C(12B)-C(11B)-N(2B)	117.9(3)	C(13B)-C(12B)-C(11B)	120.1(4)
C(12B)-C(13B)-C(14B)	120.3(4)	C(15B)-C(14B)-C(13B)	119.3(3)
C(14B)-C(15B)-C(16B)	121.0(4)	C(11B)-C(16B)-C(15B)	119.7(3)

Table Atomic coordinates (x 10^4) and equivalent isotropic displacement parameters (A^2 x 10^3) U(eq) is defined as one third of the trace of the orthogonalized Uij tensor.

	x	y	z	U(eq)
N(1A)	8534(2)	4033(4)	1638(1)	32(1)
N(2A)	8126(2)	5454(3)	1623(1)	32(1)
C(1A)	8647(2)	3214(4)	1083(1)	26(1)
C(2A)	8721(2)	3953(4)	486(2)	28(1)
C(3A)	8772(2)	3040(4)	-51(2)	31(1)
C(4A)	8793(2)	1427(4)	-24(2)	31(1)
C(5A)	8796(2)	693(4)	559(2)	30(1)
C(6A)	8727(2)	1576(4)	1103(1)	28(1)
C(7A)	8813(2)	5679(4)	393(2)	35(1)
F(1A)	9168(2)	5971(3)	-165(1)	52(1)
F(2A)	8124(1)	6493(2)	387(1)	45(1)
F(3A)	9301(1)	6346(2)	824(1)	40(1)
C(8A)	8829(3)	502(4)	-611(2)	43(1)
F(41A)	8984(3)	-988(3)	-513(1)	90(1)
F(51A)	8171(2)	644(5)	-967(2)	67(1)
F(61A)	9444(2)	970(4)	-993(1)	57(1)
F(42A)	9400(12)	-97(31)	-801(11)	52(4)
F(52A)	8316(14)	-836(26)	-501(11)	52(4)
F(62A)	8394(15)	934(43)	-1083(14)	52(4)
C(9A)	8729(2)	722(4)	1716(2)	35(1)
F(7A)	9290(1)	1251(3)	2118(1)	50(1)
F(8A)	8863(2)	-811(3)	1652(1)	49(1)
F(9A)	8022(1)	836(3)	2024(1)	48(1)
C(11A)	7286(2)	5468(4)	1726(1)	29(1)
C(12A)	6924(2)	6915(4)	1836(2)	34(1)
C(13A)	6096(2)	7002(5)	1918(2)	41(1)
C(14A)	5622(2)	5677(5)	1886(2)	43(1)
C(15A)	5981(2)	4250(5)	1775(2)	39(1)
C(16A)	6812(2)	4130(4)	1700(2)	33(1)
N(1B)	3634(2)	3185(4)	1643(1)	33(1)
N(2B)	3198(2)	4582(4)	1632(1)	32(1)
C(1B)	3692(2)	2329(4)	1093(1)	29(1)
C(2B)	3701(2)	3018(4)	486(2)	32(1)
C(3B)	3718(2)	2065(4)	-45(2)	37(1)
C(4B)	3760(2)	460(5)	5(2)	38(1)
C(5B)	3809(2)	-230(4)	590(2)	35(1)
C(6B)	3774(2)	684(4)	1128(1)	30(1)
C(7B)	3743(2)	4744(5)	361(2)	38(1)
F(1B)	4018(2)	5006(3)	-221(1)	55(1)
F(2B)	3033(1)	5496(3)	397(1)	48(1)
F(3B)	4259(1)	5498(3)	747(1)	45(1)
C(8B)	3762(3)	-534(5)	-568(2)	54(1)
F(01B)	4304(3)	160(6)	-1027(2)	42(1)
F(02B)	4344(3)	-1711(6)	-521(2)	48(1)
F(03B)	3135(3)	-83(8)	-985(2)	48(1)
F(04B)	3222(4)	-1817(7)	-489(3)	71(2)
F(05B)	3704(13)	72(18)	-1092(6)	86(4)
F(06B)	4350(7)	-709(21)	-871(7)	65(3)
F(07B)	3127(6)	-851(16)	-796(6)	41(3)
F(08B)	3915(9)	-1936(13)	-499(5)	52(3)
C(9B)	3830(2)	-144(5)	1749(2)	38(1)
F(7B)	4442(1)	415(3)	2108(1)	52(1)
F(8B)	3958(2)	-1663(3)	1690(1)	53(1)
F(9B)	3158(1)	15(3)	2095(1)	52(1)

C(11B)	2356(2)	4548(4)	1723(1)	29(1)
C(12B)	1960(2)	5963(4)	1814(2)	36(1)
C(13B)	1128(2)	5997(5)	1880(2)	40(1)
C(14B)	682(2)	4629(5)	1845(2)	44(1)
C(15B)	1076(2)	3237(5)	1750(2)	41(1)
C(16B)	1912(2)	3180(4)	1695(2)	34(1)

Table Hydrogen coordinates (x 10^4) and isotropic displacement parameters (A^2 x 10^3)

	x	y	z	U(eq)
H(1A)	8483(22)	3458(46)	1987(18)	40(11)
H(2A)	8414(25)	6174(52)	1791(19)	51(13)
H(3A)	8790(2)	3537(4)	-449(2)	28(9)
H(5A)	8851(2)	-406(4)	584(2)	19(8)
H(12A)	7243(2)	7832(4)	1860(2)	60(13)
H(13A)	5849(2)	7983(5)	1994(2)	47(11)
H(14A)	5055(2)	5745(5)	1941(2)	51(11)
H(15A)	5657(2)	3339(5)	1753(2)	48(11)
H(16A)	7051(2)	3142(4)	1627(2)	47(11)
H(1B)	3618(20)	2646(42)	2017(17)	32(9)
H(2B)	3411(24)	5426(50)	1780(18)	44(12)
H(3B)	3699(2)	2528(4)	-450(2)	35(9)
H(5B)	3872(2)	-1326(4)	627(2)	54(12)
H(12B)	2260(2)	6905(4)	1832(2)	41(11)
H(13B)	862(2)	6961(5)	1951(2)	49(12)
H(14B)	111(2)	4655(5)	1883(2)	59(13)
H(15B)	774(2)	2298(5)	1725(2)	43(11)
H(16B)	2177(2)	2210(4)	1636(2)	43(11)

C4 CRYSTAL DATA FOR Mo(NFtol)$_2$Cl$_2$·dme - 9

Empirical Formula	$C_{18}H_{18}F_6MoN_2O_2Cl_2$	
Temperature	150(2)K	
Wavelength	0.71073Å	
Crystal System	Monoclinic	
Space Group	P2(1)/c	
Unit Cell Dimensions	a = 7.9613(7)Å	alpha = 90°
	b = 16.750(2)Å	beta = 90.519(4)°
	c = 16.428(2)Å	gamma = 90°
Crystal Size	0.32 × 0.18 × 0.10 mm	
Final R indices [I>2σ(I)]	R1 = 0.0371	wR2 = 0.1040
R indices (all data)	R1 = 0.0412	wR2 = 0.1086

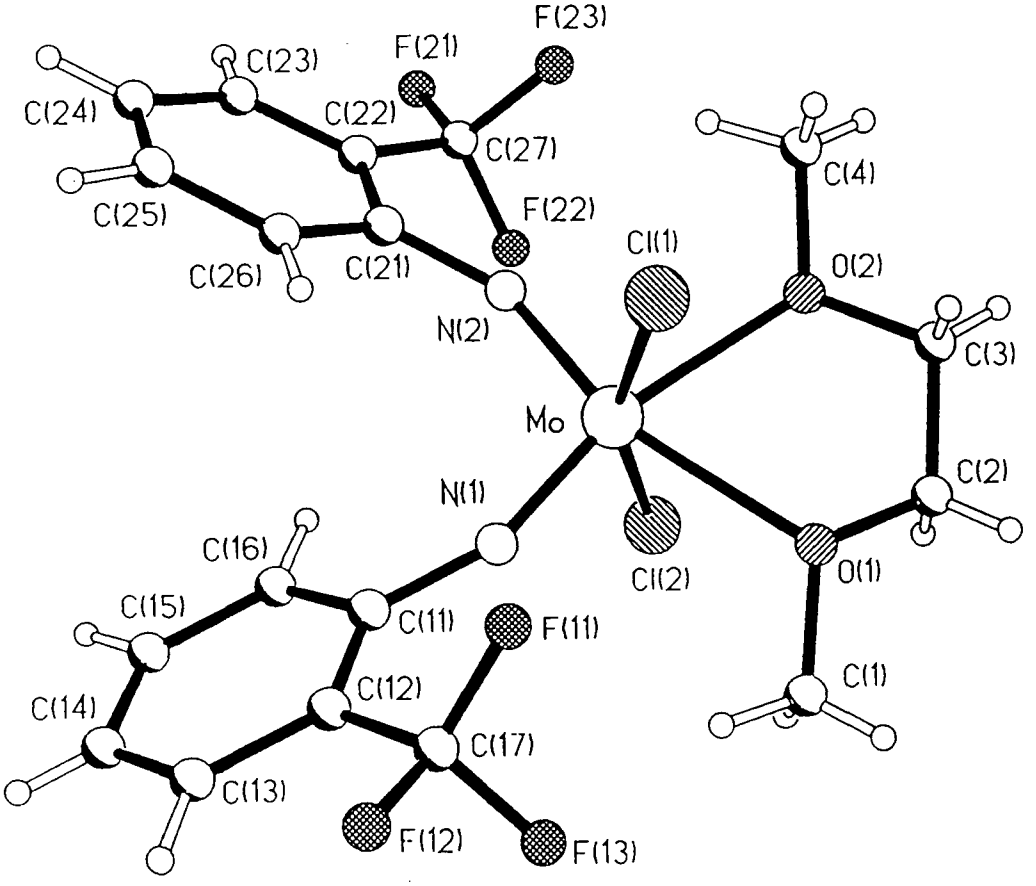

Table Bond lengths [A] and angles [deg]

Mo-N(1)	1.747(3)	Mo-N(2)	1.745(3)
Mo-O(2)	2.345(2)	Mo-O(1)	2.352(2)
Mo-Cl(2)	2.387(1)	Mo-Cl(1)	2.393(1)
O(1)-C(2)	1.439(5)	O(1)-C(1)	1.446(5)
O(2)-C(4)	1.438(5)	O(2)-C(3)	1.450(5)
N(1)-C(11)	1.383(4)	N(2)-C(21)	1.393(4)
C(2)-C(3)	1.479(6)	C(11)-C(16)	1.401(5)
C(11)-C(12)	1.413(5)	C(12)-C(13)	1.389(5)
C(12)-C(17)	1.505(5)	C(13)-C(14)	1.382(6
C(14)-C(15)	1.383(6)	C(15)-C(16)	1.385(5
C(17)-F(12)	1.335(4)	C(17)-F(11)	1.334(4)
C(17)-F(13)	1.344(4)	C(21)-C(26)	1.398(5)
C(21)-C(22)	1.416(5)	C(22)-C(23)	1.392(5
C(22)-C(27)	1.495(5)	C(23)-C(24)	1.390(5)
C(24)-C(25)	1.384(5)	C(25)-C(26)	1.382(5)
C(27)-F(21)	1.334(5)	C(27)-F(22)	1.334(5)
C(27)-F(23)	1.343(5)		

N(1)-Mo-N(2)	102.7(1)	N(1)-Mo-O(2)	164.9(1)
N(2)-Mo-O(2)	92.4(1)	N(1)-Mo-O(1)	95.2(1)
N(2)-Mo-O(1)	162.1(1)	O(2)-Mo-O(1)	69.75(9)
N(1)-Mo-Cl(2)	95.11(9)	N(2)-Mo-Cl(2)	98.46(9)
O(2)-Mo-Cl(2)	83.38(7)	O(1)-Mo-Cl(2)	80.19(6)
N(1)-Mo-Cl(1)	96.35(9)	N(2)-Mo-Cl(1)	94.82(9)
O(2)-Mo-Cl(1)	81.33(7)	O(1)-Mo-Cl(1)	82.62(7)
Cl(2)-Mo-Cl(1)	160.11(4)	C(2)-O(1)-C(1)	111.0(3)
C(2)-O(1)-Mo	114.3(2)	C(1)-O(1)-Mo	117.4(2)
C(4)-O(2)-C(3)	111.3(3)	C(4)-O(2)-Mo	120.0(3)
C(3)-O(2)-Mo	115.3(2)	C(11)-N(1)-Mo	157.0(3)
C(21)-N(2)-Mo	153.6(2)	O(1)-C(2)-C(3)	107.7(4)
O(2)-C(3)-C(2)	108.3(3)	N(1)-C(11)-C(16)	118.9(3)
N(1)-C(11)-C(12)	122.4(3)	C(16)-C(11)-C(12)	118.7(3)
C(13)-C(12)-C(11)	119.7(3)	C(13)-C(12)-C(17)	119.2(3)
C(11)-C(12)-C(17)	121.0(3)	C(14)-C(13)-C(12)	120.4(3)
C(15)-C(14)-C(13)	120.7(4)	C(14)-C(15)-C(16)	119.7(4)
C(15)-C(16)-C(11)	120.9(3)	F(12)-C(17)-F(11)	106.8(3)
F(12)-C(17)-F(13)	105.9(3)	F(11)-C(17)-F(13)	106.6(3)
F(12)-C(17)-C(12)	112.1(3)	F(11)-C(17)-C(12)	113.1(3)
F(13)-C(17)-C(12)	111.9(3)	N(2)-C(21)-C(26)	118.6(3)
N(2)-C(21)-C(22)	122.4(3)	C(26)-C(21)-C(22)	119.0(3)
C(23)-C(22)-C(21)	120.1(3)	C(23)-C(22)-C(27)	119.7(3)
C(21)-C(22)-C(27)	120.2(3)	C(22)-C(23)-C(24)	119.7(3)
C(25)-C(24)-C(23)	120.4(3)	C(26)-C(25)-C(24)	120.5(3)
C(25)-C(26)-C(21)	120.3(3)	F(21)-C(27)-F(22)	106.6(3)
F(21)-C(27)-F(23)	106.3(3)	F(22)-C(27)-F(23)	105.5(3)
F(21)-C(27)-C(22)	112.5(3)	F(22)-C(27)-C(22)	113.6(3)
F(23)-C(27)-C(22)	111.8(3)		

Table Atomic coordinates (x 10^4) and equivalent isotropic displacement parameters (A^2 x 10^3) for 1. U(eq) is defined as one third of the trace of the orthogonalized Uij tensor.

	x	y	z	U(eq)
Mo	870.0(4)	5030.6(2)	2829.7(2)	27.7(1)
Cl(1)	2460(1)	4203.6(5)	3840.4(5)	37.4(2)
Cl(2)	-1453(1)	5754.9(5)	2115.7(5)	38.2(2)
O(1)	-586(3)	5368(2)	3938(2)	36(1)
O(2)	-1219(3)	4074(2)	2981(2)	39(1)
N(1)	2243(3)	5849(2)	2947(2)	30(1)
N(2)	1518(4)	4529(2)	1993(2)	32(1)
C(1)	-708(6)	6206(3)	4134(3)	45(1)
C(2)	-2199(6)	4978(3)	3929(3)	47(1)
C(3)	-1964(6)	4125(3)	3739(3)	46(1)
C(4)	-974(7)	3258(3)	2753(3)	52(1)
C(11)	3419(4)	6390(2)	2731(2)	30(1)
C(12)	4495(4)	6830(2)	3321(2)	32(1)
C(13)	5618(5)	7382(2)	3065(2)	37(1)
C(14)	5679(5)	7507(2)	2238(3)	40(1)
C(15)	4640(5)	7081(2)	1652(2)	38(1)
C(16)	3520(5)	6525(2)	1897(2)	34(1)
C(17)	4411(5)	6727(2)	4225(2)	37(1)
C(21)	2651(4)	4362(2)	1437(2)	27(1)
C(22)	2122(4)	4042(2)	648(2)	30(1)
C(23)	3304(5)	3900(2)	111(2)	34(1)
C(24)	5010(5)	4051(2)	363(2)	37(1)
C(25)	5538(5)	4343(2)	1142(2)	37(1)
C(26)	4373(5)	4513(2)	1671(2)	35(1)
C(27)	305(5)	3825(3)	400(2)	40(1)
F(11)	4303(3)	5964(1)	4447(1)	50(1)
F(12)	5767(3)	7032(1)	4684(1)	45(1)
F(13)	3063(3)	7102(2)	4462(1)	51(1)
F(21)	-13(3)	3613(2)	-388(2)	63(1)
F(22)	-773(3)	4413(2)	512(2)	55(1)
F(23)	-167(3)	3205(2)	835(2)	59(1)

Table Hydrogen coordinates (x 10^4) and isotropic displacement parameters (A^2 x 10^3)

	x	y	z	U(eq)
H(1A)	-1415(59)	6454(23)	3683(30)	52(13)
H(1B)	468(66)	6428(31)	4169(30)	66(15)
H(1C)	-1148(59)	6277(28)	4583(31)	54(13)
H(2A)	-3049(61)	5274(28)	3538(30)	53(12)
H(2B)	-2603(71)	5019(26)	4391(34)	58(16)
H(3A)	-1138(51)	3878(23)	4171(26)	36(10)
H(3B)	-2975(66)	3850(30)	3668(31)	67(15)
H(4A)	-276(68)	3263(30)	2306(33)	74(16)
H(4B)	-2009(67)	3015(31)	2650(32)	68(15)
H(4C)	-240(59)	3000(28)	3157(30)	54(13)
H(13)	6340(54)	7703(25)	3480(26)	46(11)
H(14)	6399(53)	7860(26)	2093(26)	44(12)
H(15)	4717(53)	7171(26)	1051(29)	52(12)
H(16)	2736(52)	6182(25)	1497(26)	44(11)
H(23)	2904(50)	3711(24)	-452(26)	42(11)
H(24)	5820(54)	3939(24)	-2(26)	41(11)
H(25)	6708(56)	4500(25)	1294(26)	48(12)
H(26)	4678(61)	4735(29)	2210(30)	52(12)

C5 CRYSTAL DATA FOR Mo(NFmes)$_2$Cl$_2$ - 11

Empirical Formula	$C_{18}H_4F_{18}MoN_2Cl_2$	
Temperature	150(2)K	
Wavelength	0.71073Å	
Crystal System	Triclinic	
Space Group	P(-1)	
Unit Cell Dimensions	a = 8.917(2)Å	alpha = 96.78(3)°
	b = 9.078(2)Å	beta = 104.08(3)°
	c = 16.050(3)Å	gamma = 103.63(3)°
Crystal Size	0.44 × 0.32 × 0.24 mm	
Final R indices [I>2σ(I)]	R1 = 0.0371	wR2 = 0.0955
R indices (all data)	R1 = 0.0378	wR2 = 0.0962

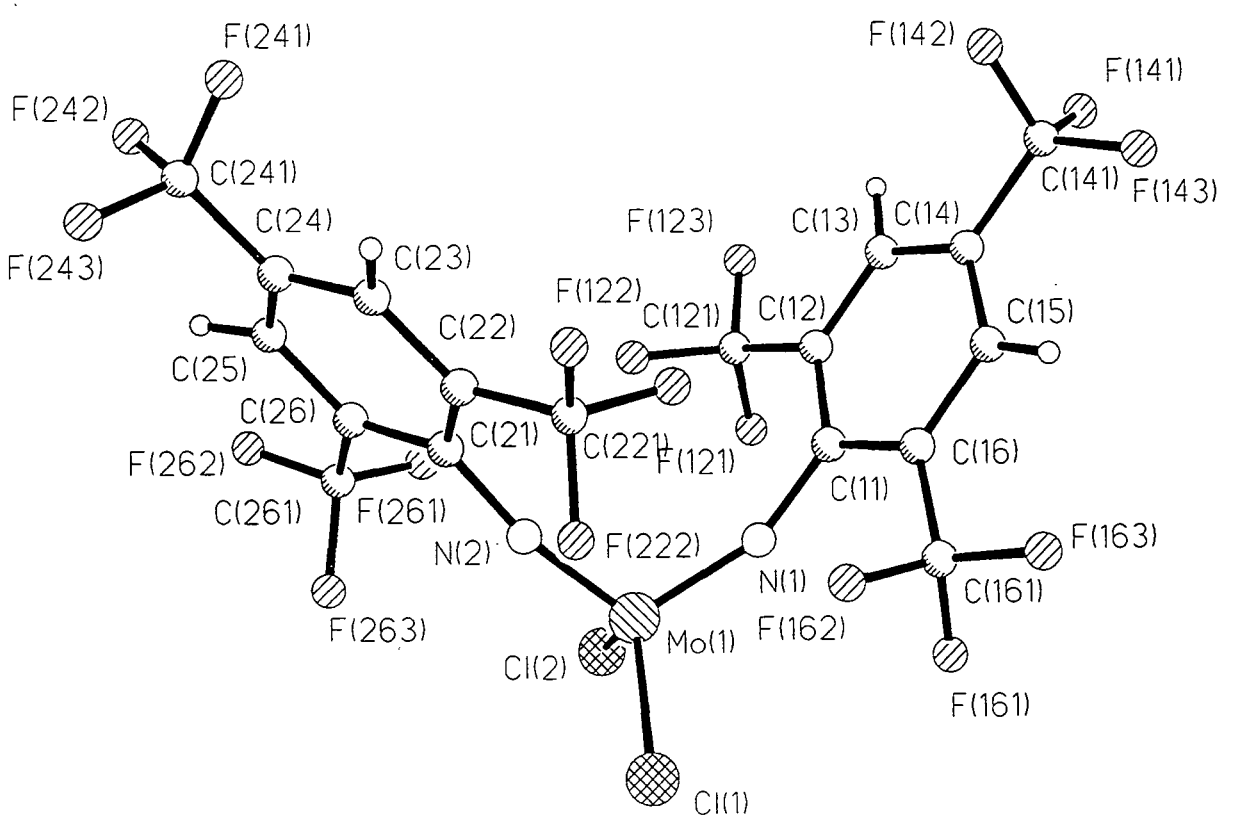

Mo(1)-N(2)	1.736(3)
Mo(1)-N(1)	1.745(3)
Mo(1)-Cl(1)	2.2524(12)
Mo(1)-Cl(2)	2.2588(13)
N(1)-C(11)	1.387(5)
N(2)-C(21)	1.396(5)
C(11)-C(12)	1.405(6)
C(11)-C(16)	1.407(6)
C(12)-C(13)	1.386(6)
C(12)-C(121)	1.506(6)
C(13)-C(14)	1.391(6)
C(14)-C(15)	1.379(6)
C(14)-C(141)	1.498(6)
C(15)-C(16)	1.388(6)
C(16)-C(161)	1.502(6)
C(121)-F(123)	1.323(5)
C(121)-F(121)	1.334(5)
C(121)-F(122)	1.343(5)
C(141)-F(142)	1.300(6)
C(141)-F(141)	1.305(6)
C(141)-F(143)	1.336(6)
C(161)-F(161)	1.333(5)
C(161)-F(163)	1.335(5)
C(161)-F(162)	1.337(5)
C(21)-C(22)	1.401(6)
C(21)-C(26)	1.408(6)
C(22)-C(23)	1.388(6)
C(22)-C(221)	1.507(6)
C(23)-C(24)	1.385(6)
C(24)-C(25)	1.377(6)
C(24)-C(241)	1.497(6)
C(25)-C(26)	1.390(6)
C(26)-C(261)	1.500(6)
C(221)-F(223)	1.336(5)
C(221)-F(221)	1.337(5)
C(221)-F(222)	1.338(5)
C(261)-F(261)	1.337(5)
C(261)-F(263)	1.337(5)
C(261)-F(262)	1.342(5)
C(241)-F(243)	1.313(6)
C(241)-F(241)	1.314(6)
C(241)-F(242)	1.330(6)

N(2)-Mo(1)-N(1)	109.3(2)
N(2)-Mo(1)-Cl(1)	107.32(11)
N(1)-Mo(1)-Cl(1)	107.62(12)
N(2)-Mo(1)-Cl(2)	107.98(11)
N(1)-Mo(1)-Cl(2)	108.94(11)
Cl(1)-Mo(1)-Cl(2)	115.53(6)
C(11)-N(1)-Mo(1)	156.9(3)
C(21)-N(2)-Mo(1)	167.8(3)
N(1)-C(11)-C(12)	120.7(4)
N(1)-C(11)-C(16)	120.5(3)
C(12)-C(11)-C(16)	118.8(4)
C(13)-C(12)-C(11)	120.4(4)
C(13)-C(12)-C(121)	119.2(4)
C(11)-C(12)-C(121)	120.4(4)
C(12)-C(13)-C(14)	120.1(4)
C(15)-C(14)-C(13)	120.1(4)
C(15)-C(14)-C(141)	121.1(4)
C(13)-C(14)-C(141)	118.8(4)
C(14)-C(15)-C(16)	120.7(4)
C(15)-C(16)-C(11)	119.9(4)
C(15)-C(16)-C(161)	119.4(4)

C(11)-C(16)-C(161)	120.6(4)
F(123)-C(121)-F(121)	107.4(4)
F(123)-C(121)-F(122)	106.9(4)
F(121)-C(121)-F(122)	106.6(4)
F(123)-C(121)-C(12)	111.6(4)
F(121)-C(121)-C(12)	111.6(4)
F(122)-C(121)-C(12)	112.3(3)
F(142)-C(141)-F(141)	109.7(5)
F(142)-C(141)-F(143)	104.2(4)
F(141)-C(141)-F(143)	104.4(4)
F(142)-C(141)-C(14)	112.5(4)
F(141)-C(141)-C(14)	112.8(4)
F(143)-C(141)-C(14)	112.5(4)
F(161)-C(161)-F(163)	107.0(3)
F(161)-C(161)-F(162)	106.6(3)
F(163)-C(161)-F(162)	106.5(3)
F(161)-C(161)-C(16)	112.3(3)
F(163)-C(161)-C(16)	112.0(3)
F(162)-C(161)-C(16)	112.0(3)
N(2)-C(21)-C(22)	121.5(4)
N(2)-C(21)-C(26)	119.4(3)
C(22)-C(21)-C(26)	119.0(4)
C(23)-C(22)-C(21)	120.3(4)
C(23)-C(22)-C(221)	119.4(4)
C(21)-C(22)-C(221)	120.4(4)
C(24)-C(23)-C(22)	119.9(4)
C(25)-C(24)-C(23)	120.7(4)
C(25)-C(24)-C(241)	120.2(4)
C(23)-C(24)-C(241)	119.1(4)
C(24)-C(25)-C(26)	120.2(4)
C(25)-C(26)-C(21)	119.9(4)
C(25)-C(26)-C(261)	119.9(4)
C(21)-C(26)-C(261)	120.2(4)
F(223)-C(221)-F(221)	106.9(3)
F(223)-C(221)-F(222)	106.6(3)
F(221)-C(221)-F(222)	107.1(3)
F(223)-C(221)-C(22)	111.9(3)
F(221)-C(221)-C(22)	111.8(3)
F(222)-C(221)-C(22)	112.1(3)
F(261)-C(261)-F(263)	107.1(3)
F(261)-C(261)-F(262)	106.4(3)
F(263)-C(261)-F(262)	106.6(3)
F(261)-C(261)-C(26)	112.3(3)
F(263)-C(261)-C(26)	111.9(3)
F(262)-C(261)-C(26)	112.1(3)
F(243)-C(241)-F(241)	106.8(4)
F(243)-C(241)-F(242)	106.1(5)
F(241)-C(241)-F(242)	105.7(4)
F(243)-C(241)-C(24)	112.4(4)
F(241)-C(241)-C(24)	112.9(4)
F(242)-C(241)-C(24)	112.4(4)

Table Hydrogen coordinates (x 10^4) and isotropic displacement parameters (A^2 x 10^3)

	x	y	z	U(eq)
H(13)	7602(61)	6175(53)	3933(30)	31
H(15)	4103(56)	7823(57)	4446(31)	31
H(23)	2317(56)	4928(59)	-299(31)	32
H(25)	3404(55)	1040(55)	-900(32)	31

Table Atomic coordinates (x 10^4) and equivalent isotropic displacement parameters (A^2 x 10^3) U(eq) is defined as one third of the trace of the orthogonalized Uij tensor.

	x	y	z	U(eq)
Mo(1)	1508(1)	1313(1)	2479(1)	21(1)
Cl(1)	-1063(1)	1184(1)	2439(1)	37(1)
Cl(2)	2302(2)	-807(1)	2763(1)	42(1)
N(1)	2734(4)	2895(4)	3278(2)	22(1)
N(2)	1737(4)	1618(4)	1464(2)	20(1)
C(11)	3837(5)	4329(5)	3612(2)	21(1)
C(12)	5457(5)	4550(5)	3628(2)	23(1)
C(13)	6540(5)	5999(5)	3934(3)	26(1)
C(14)	6033(5)	7239(5)	4243(2)	24(1)
C(15)	4453(5)	7029(5)	4249(3)	26(1)
C(16)	3350(5)	5589(5)	3943(2)	23(1)
C(121)	6044(5)	3213(5)	3325(3)	31(1)
C(141)	7227(6)	8796(5)	4554(3)	36(1)
C(161)	1635(5)	5400(5)	3950(3)	27(1)
F(121)	5735(4)	2072(3)	3764(2)	45(1)
F(122)	5343(3)	2606(3)	2474(2)	38(1)
F(123)	7614(3)	3630(4)	3432(2)	54(1)
F(141)	8527(4)	8778(4)	5137(3)	86(1)
F(142)	7611(6)	9407(4)	3916(2)	94(2)
F(143)	6653(4)	9825(4)	4951(3)	75(1)
F(161)	1107(3)	4246(3)	4341(2)	39(1)
F(162)	637(3)	5099(3)	3142(2)	38(1)
F(163)	1435(3)	6671(3)	4366(2)	49(1)
C(21)	2175(4)	2142(4)	751(2)	20(1)
C(22)	2051(5)	3580(5)	556(3)	23(1)
C(23)	2432(5)	4044(5)	-179(3)	27(1)
C(24)	2934(5)	3083(5)	-722(3)	28(1)
C(25)	3083(5)	1673(5)	-535(3)	26(1)
C(26)	2698(4)	1184(4)	194(3)	21(1)
C(221)	1516(5)	4642(5)	1144(3)	28(1)
C(261)	2800(5)	-380(5)	373(3)	27(1)
C(241)	3282(6)	3581(6)	-1528(3)	39(1)
F(221)	2547(3)	5087(3)	1944(2)	34(1)
F(222)	74(3)	3976(3)	1237(2)	35(1)
F(223)	1396(4)	5925(3)	833(2)	41(1)
F(241)	3940(5)	5073(4)	-1415(2)	76(1)
F(242)	4300(5)	2911(6)	-1795(3)	90(1)
F(243)	1983(4)	3241(5)	-2191(2)	76(1)
F(261)	3874(3)	-300(3)	1133(2)	34(1)
F(262)	3240(3)	-1162(3)	-247(2)	40(1)
F(263)	1387(3)	-1257(3)	403(2)	36(1)

C6 Crystal Data for Mo(NFmes)$_2$Cl$_2$·2py - 12

Empirical Formula	$C_{28}H_{14}F_{18}MoN_4Cl_2$	
Temperature	150(2)K	
Wavelength	0.71073Å	
Crystal System	Monoclinic	
Space Group	P2(1)/n	
Unit Cell Dimensions	a = 8.841(1)Å	alpha = 90°
	b = 17.120(2)Å	beta = 96.77(1)°
	c = 21.634(2)Å	gamma = 90°
Crystal Size	0.36 × 0.30 × 0.20 mm	
Final R indices [I>2σ(I)]	R1 = 0.0434	wR2 = 0.0976
R indices (all data)	R1 = 0.0477	wR2 = 0.1001

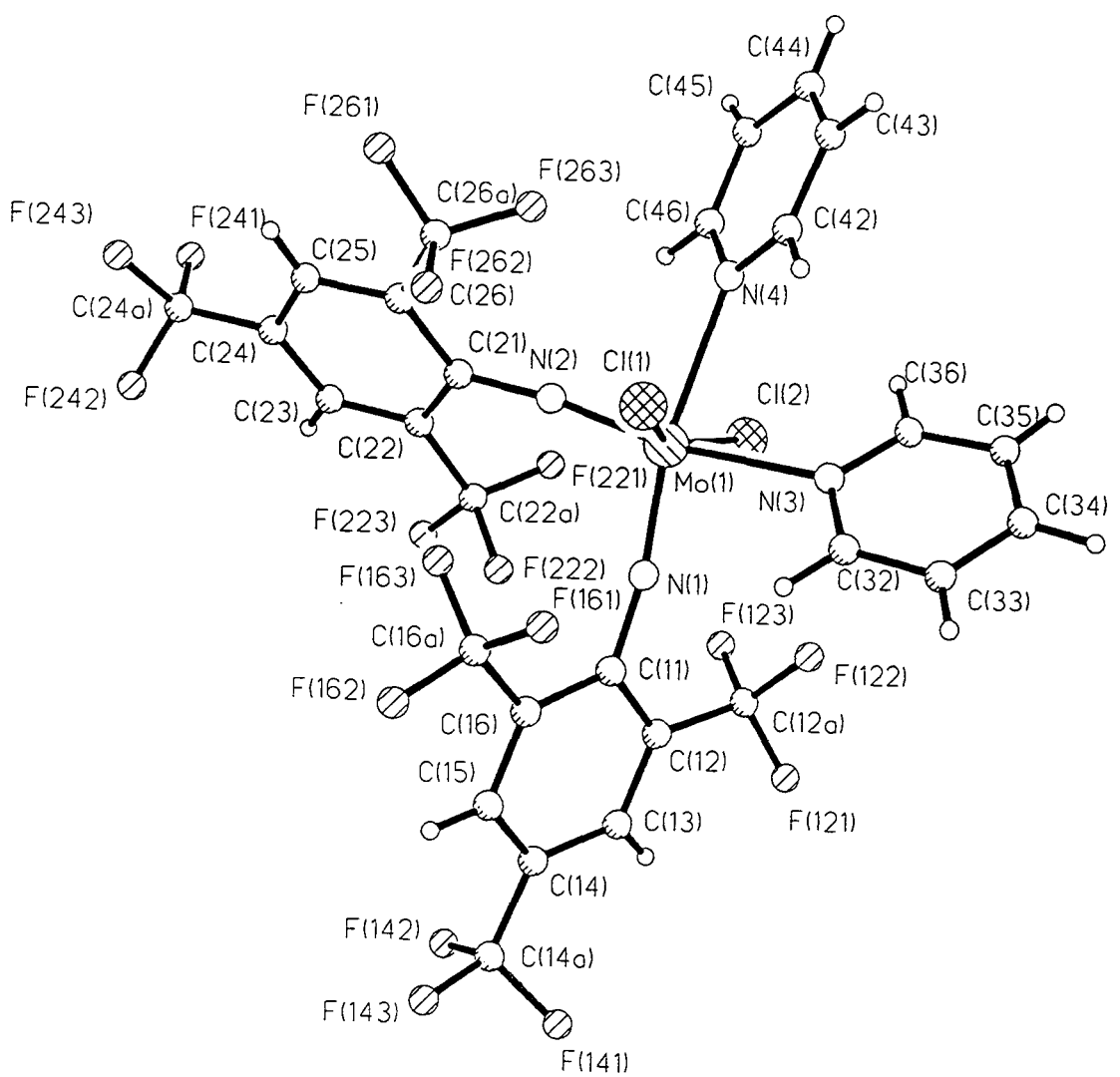

Mo(1)-N(1)	1.774(4)
Mo(1)-N(2)	1.775(4)
Mo(1)-N(3)	2.354(4)
Mo(1)-N(4)	2.385(4)
Mo(1)-Cl(1)	2.3738(13)
Mo(1)-Cl(2)	2.3776(14)
N(1)-C(11)	1.372(6)
N(2)-C(21)	1.379(6)
N(3)-C(32)	1.332(7)
N(3)-C(36)	1.342(6)
C(11)-C(12)	1.415(7)
C(11)-C(16)	1.430(7)
C(12)-C(13)	1.381(7)
C(12)-C(12A)	1.505(7)
C(13)-C(14)	1.393(7)
C(14)-C(15)	1.375(7)
C(14)-C(14A)	1.491(7)
C(15)-C(16)	1.376(7)
C(16)-C(16A)	1.493(7)
C(12A)-F(122)	1.325(6)
C(12A)-F(123)	1.342(6)
C(12A)-F(121)	1.348(6)
C(14A)-F(142)	1.331(6)
C(14A)-F(143)	1.331(6)
C(14A)-F(141)	1.342(6)
C(16A)-F(162)	1.342(6)
C(16A)-F(163)	1.345(6)
C(16A)-F(161)	1.350(6)
C(21)-C(22)	1.414(6)
C(21)-C(26)	1.417(6)
C(22)-C(23)	1.388(7)
C(22)-C(22A)	1.502(7)
C(23)-C(24)	1.385(7)
C(24)-C(25)	1.380(7)
C(24)-C(24A)	1.500(7)
C(25)-C(26)	1.395(7)
C(26)-C(26A)	1.493(6)
C(22A)-F(222)	1.329(6)
C(22A)-F(221)	1.342(6)
C(22A)-F(223)	1.346(5)
C(24A)-F(242)	1.335(6)
C(24A)-F(243)	1.337(6)
C(24A)-F(241)	1.343(6)
C(26A)-F(263)	1.318(6)
C(26A)-F(261)	1.342(6)
C(26A)-F(262)	1.350(6)
C(32)-C(33)	1.383(8)
C(33)-C(34)	1.372(9)
C(34)-C(35)	1.364(9)
C(35)-C(36)	1.380(7)
N(4)-C(42)	1.345(6)
N(4)-C(46)	1.354(6)
C(42)-C(43)	1.373(7)
C(43)-C(44)	1.370(8)
C(44)-C(45)	1.390(8)
C(45)-C(46)	1.371(7)

N(1)-Mo(1)-N(2)	102.4(2)
N(1)-Mo(1)-N(3)	87.6(2)
N(2)-Mo(1)-N(3)	169.9(2)
N(1)-Mo(1)-Cl(1)	98.65(13)
N(2)-Mo(1)-Cl(1)	96.77(12)
N(3)-Mo(1)-Cl(1)	80.09(10)
N(1)-Mo(1)-Cl(2)	98.03(13)

N(2)-Mo(1)-Cl(2)	98.03(12)
N(3)-Mo(1)-Cl(2)	81.80(10)
Cl(1)-Mo(1)-Cl(2)	154.74(5)
N(1)-Mo(1)-N(4)	168.9(2)
N(2)-Mo(1)-N(4)	88.6(2)
N(3)-Mo(1)-N(4)	81.47(13)
Cl(1)-Mo(1)-N(4)	81.48(10)
Cl(2)-Mo(1)-N(4)	78.54(10)
C(11)-N(1)-Mo(1)	168.7(3)
C(21)-N(2)-Mo(1)	172.9(3)
C(32)-N(3)-C(36)	116.9(4)
C(32)-N(3)-Mo(1)	118.0(3)
C(36)-N(3)-Mo(1)	125.1(3)
N(1)-C(11)-C(12)	121.9(4)
N(1)-C(11)-C(16)	121.2(4)
C(12)-C(11)-C(16)	116.9(4)
C(13)-C(12)-C(11)	120.5(4)
C(13)-C(12)-C(12A)	117.9(4)
C(11)-C(12)-C(12A)	121.6(4)
C(12)-C(13)-C(14)	121.4(5)
C(15)-C(14)-C(13)	118.8(5)
C(15)-C(14)-C(14A)	121.4(5)
C(13)-C(14)-C(14A)	119.8(5)
C(14)-C(15)-C(16)	121.5(5)
C(15)-C(16)-C(11)	120.7(5)
C(15)-C(16)-C(16A)	119.5(4)
C(11)-C(16)-C(16A)	119.8(4)
F(122)-C(12A)-F(123)	107.6(4)
F(122)-C(12A)-F(121)	106.7(4)
F(123)-C(12A)-F(121)	105.3(4)
F(122)-C(12A)-C(12)	113.6(4)
F(123)-C(12A)-C(12)	111.6(4)
F(121)-C(12A)-C(12)	111.6(4)
F(142)-C(14A)-F(143)	105.7(5)
F(142)-C(14A)-F(141)	105.3(5)
F(143)-C(14A)-F(141)	107.2(5)
F(142)-C(14A)-C(14)	112.2(5)
F(143)-C(14A)-C(14)	113.4(5)
F(141)-C(14A)-C(14)	112.4(4)
F(162)-C(16A)-F(163)	106.8(4)
F(162)-C(16A)-F(161)	106.2(4)
F(163)-C(16A)-F(161)	106.9(4)
F(162)-C(16A)-C(16)	112.3(4)
F(163)-C(16A)-C(16)	113.2(4)
F(161)-C(16A)-C(16)	111.1(4)
N(2)-C(21)-C(22)	120.7(4)
N(2)-C(21)-C(26)	122.4(4)
C(22)-C(21)-C(26)	116.9(4)
C(23)-C(22)-C(21)	121.1(4)
C(23)-C(22)-C(22A)	118.3(4)
C(21)-C(22)-C(22A)	120.6(4)
C(24)-C(23)-C(22)	120.8(4)
C(25)-C(24)-C(23)	119.5(4)
C(25)-C(24)-C(24A)	121.0(4)
C(23)-C(24)-C(24A)	119.5(4)
C(24)-C(25)-C(26)	120.7(5)
C(25)-C(26)-C(21)	120.9(4)
C(25)-C(26)-C(26A)	117.4(4)
C(21)-C(26)-C(26A)	121.6(4)
F(222)-C(22A)-F(221)	107.3(4)
F(222)-C(22A)-F(223)	106.0(4)
F(221)-C(22A)-F(223)	106.3(4)
F(222)-C(22A)-C(22)	112.7(4)
F(221)-C(22A)-C(22)	112.7(4)
F(223)-C(22A)-C(22)	111.4(4)
F(242)-C(24A)-F(243)	107.1(4)
F(242)-C(24A)-F(241)	106.4(4)
F(243)-C(24A)-F(241)	106.1(4)

Table Atomic coordinates (x 10^4) and equivalent isotropic displacement parameters (A^2 x 10^3) for 1. U(eq) is defined as one third of the trace of the orthogonalized Uij tensor.

	x	y	z	U(eq)
Mo(1)	9600(1)	8507(1)	8696(1)	25(1)
Cl(1)	8574(1)	9241(1)	9479(1)	34(1)
Cl(2)	11475(1)	8183(1)	8036(1)	33(1)
N(1)	9303(4)	7556(2)	8984(2)	27(1)
N(2)	8030(4)	8620(2)	8112(2)	24(1)
N(3)	11764(4)	8591(2)	9440(2)	30(1)
N(4)	10464(4)	9770(2)	8431(2)	29(1)
C(11)	8886(5)	6803(3)	9099(2)	27(1)
C(12)	9847(5)	6160(3)	9015(2)	29(1)
C(13)	9341(6)	5405(3)	9083(2)	36(1)
C(14)	7899(6)	5252(3)	9252(2)	33(1)
C(15)	6987(6)	5871(3)	9373(2)	34(1)
C(16)	7450(5)	6632(3)	9311(2)	29(1)
C(12A)	11421(6)	6271(3)	8830(3)	39(1)
F(121)	12277(3)	5623(2)	8937(2)	62(1)
F(122)	12186(3)	6851(2)	9128(2)	45(1)
F(123)	11381(4)	6409(2)	8217(2)	50(1)
C(14A)	7358(6)	4430(3)	9281(3)	43(1)
F(141)	8451(4)	3945(2)	9535(2)	72(1)
F(142)	6913(4)	4139(2)	8718(2)	62(1)
F(143)	6172(4)	4349(2)	9602(2)	70(1)
C(16A)	6442(5)	7284(3)	9470(2)	36(1)
F(161)	7151(3)	7738(2)	9925(1)	41(1)
F(162)	5167(3)	7023(2)	9683(2)	48(1)
F(163)	6001(3)	7754(2)	8984(1)	43(1)
C(21)	6728(5)	8632(3)	7693(2)	26(1)
C(22)	6378(5)	8004(3)	7276(2)	27(1)
C(23)	5067(5)	8010(3)	6854(2)	29(1)
C(24)	4034(5)	8619(3)	6847(2)	28(1)
C(25)	4343(6)	9241(3)	7248(2)	30(1)
C(26)	5675(5)	9259(3)	7662(2)	24(1)
C(22A)	7424(6)	7313(3)	7277(2)	34(1)
F(221)	8793(3)	7500(2)	7110(2)	50(1)
F(222)	7663(4)	6966(2)	7830(1)	51(1)
F(223)	6843(3)	6760(2)	6874(1)	41(1)
C(24A)	2621(6)	8606(3)	6388(2)	37(1)
F(241)	2931(4)	8791(2)	5813(1)	54(1)
F(242)	1961(4)	7904(2)	6345(2)	53(1)
F(243)	1569(3)	9117(2)	6528(1)	49(1)
C(26A)	5933(5)	9956(3)	8076(2)	34(1)
F(261)	5044(4)	10560(2)	7874(2)	59(1)
F(262)	5584(4)	9801(2)	8654(2)	59(1)
F(263)	7348(3)	10213(2)	8144(2)	48(1)
C(32)	11652(6)	8323(4)	10011(2)	48(2)
C(33)	12841(8)	8353(5)	10487(3)	63(2)
C(34)	14185(7)	8700(4)	10378(3)	54(2)
C(35)	14323(6)	8975(3)	9796(3)	41(1)
C(36)	13103(6)	8905(3)	9339(3)	34(1)
C(42)	10990(5)	10322(3)	8844(2)	31(1)
C(43)	11610(5)	11013(3)	8672(3)	37(1)
C(44)	11682(6)	11165(3)	8055(3)	39(1)
C(45)	11075(6)	10619(3)	7618(3)	36(1)
C(46)	10483(6)	9938(3)	7821(2)	33(1)

Table Hydrogen coordinates (x 10^4) and isotropic displacement parameters (A^2 x 10^3)

	x	y	z	U(eq)
H(13)	9952(61)	5028(33)	9015(24)	43
H(15)	6035(60)	5787(31)	9509(23)	41
H(23)	4874(55)	7609(30)	6569(23)	35
H(25)	3722(57)	9632(31)	7235(23)	36
H(32)	10699(68)	8081(34)	10093(26)	57
H(33)	12739(76)	8136(41)	10851(32)	76
H(34)	15026(71)	8721(35)	10746(28)	65
H(35)	15197(66)	9216(33)	9687(25)	50
H(36)	13173(57)	9092(30)	8929(25)	41
H(42)	10960(56)	10191(30)	9242(24)	37
H(43)	11974(59)	11385(32)	8981(24)	44
H(44)	12078(61)	11623(33)	7919(25)	47
H(45)	11043(58)	10701(32)	7196(25)	44
H(46)	10049(56)	9535(31)	7523(23)	39

Hydrogen atoms are located by difference Fourier maps.

C7 CRYSTAL DATA FOR $Mo(NFtol)_2(PMe_3)_3$ - 15

Empirical Formula	$C_{23}H_{35}F_6MoN_2P_3$	
Temperature	150(2)K	
Wavelength	0.71073Å	
Crystal System	Monoclinic	
Space Group	P2(1)/n	
Unit Cell Dimensions	a = 15.141(1)Å	alpha = 90°
	b = 9.298(1)Å	beta = 100.34(1)°
	c = 21.447(2)Å	gamma = 90°
Crystal Size	0.34 × 0.22 × 0.17 mm	
Final R indices [I>2σ(I)]	R1 = 0.0443	wR2 = 0.1059
R indices (all data)	R1 = 0.0505	wR2 = 0.1103

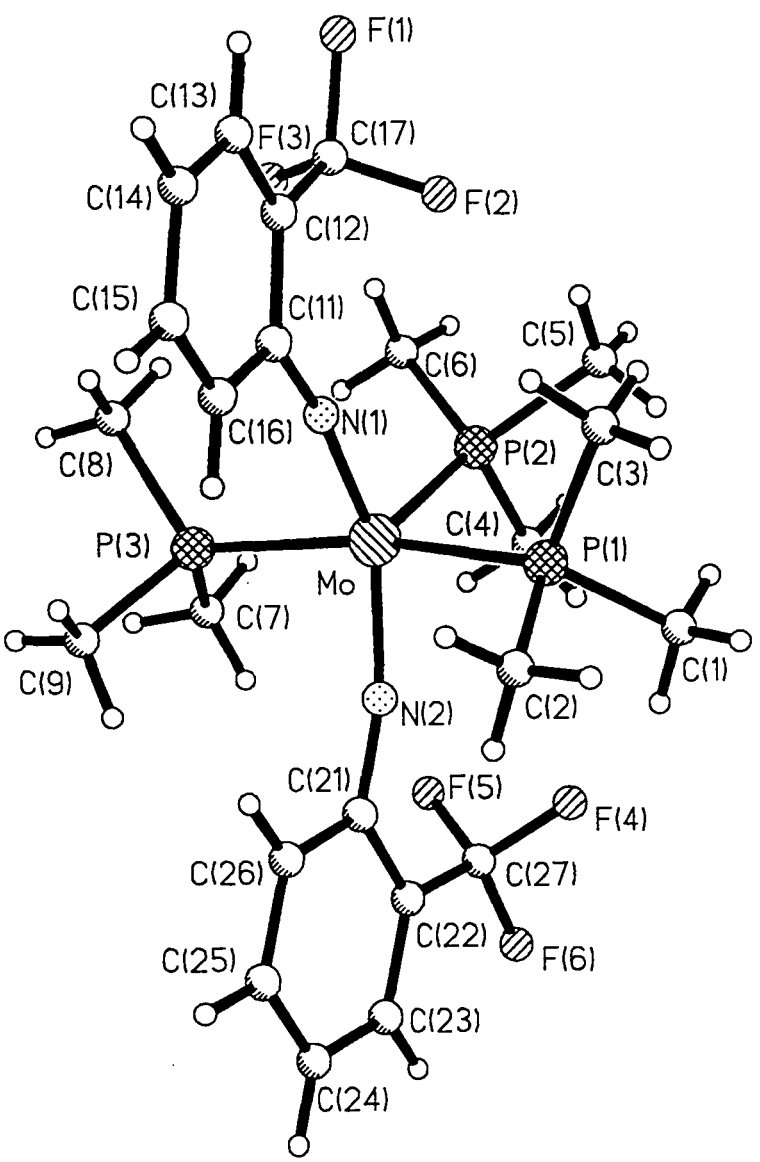

Mo-N(1)	1.826(3)	Mo-N(2)	1.848(3)
Mo-P(2)	2.419(1)	Mo-P(3)	2.481(1)
Mo-P(1)	2.495(1)	P(1)-C(3)	1.813(4)
P(1)-C(2)	1.818(5)	P(1)-C(1)	1.820(5)
P(2)-C(4)	1.814(5)	P(2)-C(6)	1.826(5)
P(2)-C(5)	1.829(5)	P(3)-C(7)	1.818(5)
P(3)-C(9)	1.818(5)	P(3)-C(8)	1.819(4)
N(1)-C(11)	1.376(5)	N(1)-C(11A)	1.42(3)
N(2)-C(21)	1.360(5)	C(11)-C(12)	1.417(6)
C(11)-C(16)	1.424(10)	C(12)-C(13)	1.396(7)
C(12)-C(17)	1.486(8)	C(13)-C(14)	1.378(9)
C(14)-C(15)	1.387(9)	C(15)-C(16)	1.383(8)
C(17)-F(3)	1.335(7)	C(17)-F(2)	1.344(7)
C(17)-F(1)	1.351(8)	C(21)-C(26)	1.416(5)
C(21)-C(22)	1.426(5)	C(22)-C(23)	1.394(6)
C(22)-C(27)	1.477(6)	C(23)-C(24)	1.378(6)
C(24)-C(25)	1.384(6)	C(25)-C(26)	1.384(6)
C(27)-F(6)	1.345(5)	C(27)-F(5)	1.348(5)
C(27)-F(4)	1.360(5)		

N(1)-Mo-N(2)	146.5(2)	N(1)-Mo-P(2)	103.2(1)
N(2)-Mo-P(2)	110.4(1)	N(1)-Mo-P(3)	90.3(1)
N(2)-Mo-P(3)	86.0(1)	P(2)-Mo-P(3)	96.38(4)
N(1)-Mo-P(1)	89.2(1)	N(2)-Mo-P(1)	87.1(1)
P(2)-Mo-P(1)	96.69(4)	P(3)-Mo-P(1)	166.70(4)
C(3)-P(1)-C(2)	101.6(2)	C(3)-P(1)-C(1)	103.1(2)
C(2)-P(1)-C(1)	100.7(3)	C(3)-P(1)-Mo	117.1(2)
C(2)-P(1)-Mo	111.8(2)	C(1)-P(1)-Mo	119.8(2)
C(4)-P(2)-C(6)	101.8(3)	C(4)-P(2)-C(5)	102.0(3)
C(6)-P(2)-C(5)	100.0(3)	C(4)-P(2)-Mo	113.1(2)
C(6)-P(2)-Mo	118.1(2)	C(5)-P(2)-Mo	119.1(2)
C(7)-P(3)-C(9)	101.6(2)	C(7)-P(3)-C(8)	104.5(3)
C(9)-P(3)-C(8)	101.6(2)	C(7)-P(3)-Mo	114.3(2)
C(9)-P(3)-Mo	113.1(2)	C(8)-P(3)-Mo	119.5(2)
C(11)-N(1)-Mo	162.7(3)	C(11A)-N(1)-Mo	156.0(8)
C(21)-N(2)-Mo	160.3(3)	N(1)-C(11)-C(12)	122.4(4)
N(1)-C(11)-C(16)	121.2(4)	C(12)-C(11)-C(16)	116.3(4)
C(13)-C(12)-C(11)	121.5(5)	C(13)-C(12)-C(17)	119.2(6)
C(11)-C(12)-C(17)	119.3(5)	C(14)-C(13)-C(12)	119.9(6)
C(13)-C(14)-C(15)	120.5(5)	C(16)-C(15)-C(14)	120.1(6)
C(15)-C(16)-C(11)	121.6(6)	F(3)-C(17)-F(2)	105.1(5)
F(3)-C(17)-F(1)	105.9(6)	F(2)-C(17)-F(1)	104.9(4)
F(3)-C(17)-C(12)	113.7(4)	F(2)-C(17)-C(12)	113.9(6)
F(1)-C(17)-C(12)	112.5(5)	N(2)-C(21)-C(26)	120.5(3)
N(2)-C(21)-C(22)	123.9(4)	C(26)-C(21)-C(22)	115.6(3)
C(23)-C(22)-C(21)	121.3(4)	C(23)-C(22)-C(27)	119.1(4)
C(21)-C(22)-C(27)	119.6(4)	C(24)-C(23)-C(22)	120.9(4)
C(23)-C(24)-C(25)	119.5(4)	C(26)-C(25)-C(24)	120.4(4)
C(25)-C(26)-C(21)	122.3(4)	F(6)-C(27)-F(5)	105.4(4)
F(6)-C(27)-F(4)	105.1(4)	F(5)-C(27)-F(4)	104.8(4)
F(6)-C(27)-C(22)	113.5(4)	F(5)-C(27)-C(22)	114.1(4)
F(4)-C(27)-C(22)	113.0(4)		

Table Atomic coordinates (x 10^4) and equivalent isotropic displacement parameters (A^2 x 10^3) U(eq) is defined as one third of the trace of the orthogonalized Uij tensor.

	x	y	z	U(eq)
Mo	2430.5(2)	5696.8(4)	3977.4(1)	33.1(1)
P(1)	2831.5(7)	3747(1)	4777.6(5)	38.5(3)
P(2)	853.7(7)	5105(1)	3691.1(6)	47.8(3)
P(3)	2385.1(8)	7844(1)	3285.4(5)	44.0(3)
N(1)	2943(2)	4649(4)	3416(2)	41(1)
N(2)	2614(2)	6978(3)	4647(1)	36(1)
C(1)	2171(4)	3504(6)	5400(2)	68(2)
C(2)	3944(3)	4007(6)	5248(3)	67(2)
C(3)	2917(4)	1938(5)	4479(2)	56(1)
C(4)	157(3)	6063(6)	4158(3)	72(2)
C(5)	497(3)	3243(6)	3765(3)	63(1)
C(6)	286(3)	5494(7)	2884(2)	71(2)
C(7)	1546(4)	9171(5)	3397(2)	60(1)
C(8)	2236(4)	7610(6)	2431(2)	66(1)
C(9)	3411(3)	8902(5)	3445(2)	53(1)
C(11)	3558(3)	3950(5)	3124(2)	40(1)
C(12)	3299(4)	2980(5)	2614(2)	47(1)
C(13)	3934(5)	2208(7)	2352(3)	56(2)
C(14)	4836(5)	2400(6)	2582(3)	64(2)
C(15)	5121(4)	3357(7)	3073(3)	61(2)
C(16)	4498(6)	4120(5)	3339(3)	49(4)
C(17)	2330(4)	2762(6)	2359(4)	54(2)
F(1)	2184(3)	1717(4)	1915(2)	86(1)
F(2)	1846(2)	2366(3)	2798(1)	63(1)
F(3)	1918(2)	3933(4)	2087(1)	68(1)
C(11A)	2989(12)	3550(31)	2964(12)	41(12)
C(12A)	3909(13)	3355(20)	2917(8)	58(16)
C(13A)	4157(18)	2508(26)	2439(10)	14(13)
C(14A)	3518(23)	1832(33)	1999(12)	53(15)
C(15A)	2619(21)	1991(38)	2031(14)	67(23)
C(16A)	2362(15)	2824(40)	2503(15)	46(32)
C(17A)	4615(12)	4087(19)	3370(8)	45(49)
F(1A)	5450(12)	3802(30)	3277(12)	72(15)
F(2A)	4547(17)	5534(19)	3362(11)	57(9)
F(3A)	4609(16)	3711(25)	3983(8)	49(8)
C(21)	3042(3)	7884(4)	5101(2)	36(1)
C(22)	2609(3)	8607(4)	5549(2)	38(1)
C(23)	3084(3)	9520(4)	6006(2)	46(1)
C(24)	3990(3)	9751(5)	6038(2)	49(1)
C(25)	4433(3)	9066(4)	5610(2)	45(1)
C(26)	3973(3)	8151(4)	5156(2)	39(1)
C(27)	1635(3)	8414(5)	5524(2)	53(1)
F(4)	1400(2)	7021(3)	5596(1)	68(1)
F(5)	1126(2)	8832(3)	4972(1)	65(1)
F(6)	1314(2)	9142(3)	5977(1)	69(1)

Table Hydrogen coordinates (x 10^4) and isotropic displacement parameters (A^2 x 10^3)

	x	y	z	U(eq)
H(1A)	1562(8)	3197(39)	5213(3)	101(12)
H(1B)	2143(21)	4419(12)	5623(12)	101(12)
H(1C)	2452(14)	2772(30)	5701(10)	101(12)
H(2A)	3963(8)	4927(19)	5474(13)	87(11)
H(2B)	4392(4)	4014(37)	4970(3)	87(11)
H(2C)	4078(10)	3222(21)	5556(11)	87(11)
H(3A)	3280(17)	1951(7)	4144(10)	75(9)
H(3B)	2317(4)	1565(13)	4307(13)	75(9)
H(3C)	3204(19)	1317(9)	4827(4)	75(9)
H(4A)	363(15)	5865(30)	4610(3)	92(11)
H(4B)	-468(5)	5750(28)	4035(12)	92(11)
H(4C)	198(18)	7098(7)	4081(12)	92(11)
H(5A)	669(20)	2927(13)	4206(4)	89(11)
H(5B)	791(18)	2629(8)	3491(12)	89(11)
H(5C)	-156(4)	3170(9)	3635(15)	89(11)
H(6A)	569(14)	4943(27)	2583(3)	77(10)
H(6B)	331(19)	6524(9)	2798(6)	77(10)
H(6C)	-348(6)	5221(33)	2837(5)	77(10)
H(7A)	1597(13)	9379(23)	3850(3)	67(9)
H(7B)	946(4)	8787(13)	3233(13)	67(9)
H(7C)	1639(12)	10057(12)	3171(11)	67(9)
H(8A)	1659(10)	7139(32)	2278(3)	80(10)
H(8B)	2723(12)	7013(29)	2328(2)	80(10)
H(8C)	2245(22)	8552(6)	2227(2)	80(10)
H(9A)	3917(4)	8317(11)	3363(13)	64(8)
H(9B)	3521(11)	9209(26)	3889(4)	64(8)
H(9C)	3349(8)	9751(17)	3169(10)	64(8)
H(13)	3745(5)	1559(7)	2012(3)	67
H(14)	5262(5)	1872(6)	2398(3)	77
H(15)	5743(4)	3495(7)	3230(3)	73
H(16)	4693(6)	4771(5)	3678(3)	58
H(23)	2779(3)	9993(4)	6298(2)	55
H(24)	4307(3)	10376(5)	6350(2)	59
H(25)	5089(31)	9228(9)	5631(2)	54
H(26)	4291(3)	7688(4)	4869(2)	47

C8 CRYSTAL DATA FOR PhCbNO - 20

Empirical Formula	$C_8H_{15}B_{10}NO$	
Temperature	160(2)K	
Wavelength	0.71073Å	
Crystal System	Monoclinic	
Space Group	P2(1)/n	
Unit Cell Dimensions	a = 10.942(2)Å	alpha = 90°
	b = 8.4999(12)Å	beta = 102.986(4)°
	c = 15.068(2)Å	gamma = 90°
Crystal Size	0.52 × 0.50 × 0.50 mm	
Final R indices [I>2σ(I)]	R1 = 0.0490	wR2 = 0.1327
R indices (all data)	R1 = 0.0578	wR2 = 0.1432

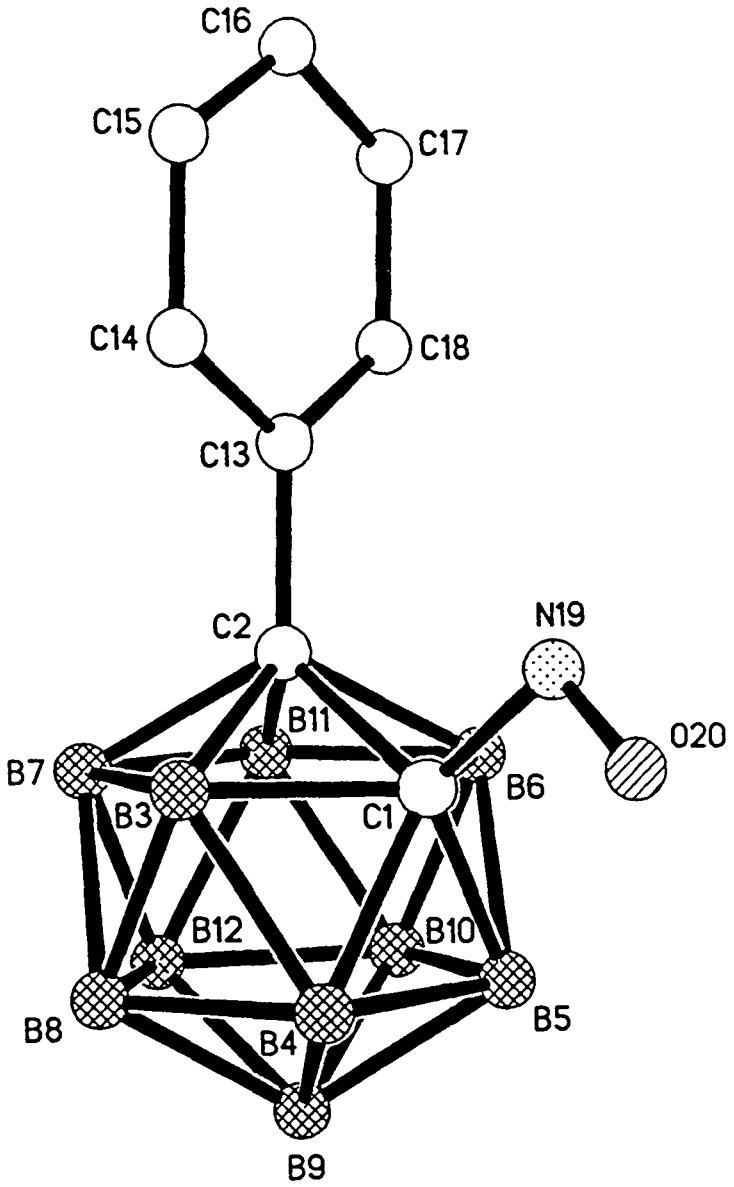

Table Bond lengths (Å) and angles (°)

C(1)-N(19)	1.490(2)	C(1)-C(2)	1.677(2)
C(1)-B(4)	1.702(2)	C(1)-B(3)	1.704(2)
C(1)-B(5)	1.704(2)	C(1)-B(6)	1.708(2)
C(2)-C(13)	1.510(2)	C(2)-B(11)	1.705(2)
C(2)-B(7)	1.710(2)	C(2)-B(6)	1.738(2)
C(2)-B(3)	1.743(2)	B(3)-B(8)	1.767(3)
B(3)-B(7)	1.777(3)	B(3)-B(4)	1.785(2)
B(4)-B(8)	1.773(3)	B(4)-B(9)	1.775(3)
B(4)-B(5)	1.779(3)	B(5)-B(9)	1.775(3)
B(5)-B(10)	1.777(3)	B(5)-B(6)	1.787(3)
B(6)-B(10)	1.765(2)	B(6)-B(11)	1.778(3)
B(7)-B(12)	1.783(3)	B(7)-B(11)	1.783(3)
B(7)-B(8)	1.788(3)	B(8)-B(12)	1.785(3)
B(8)-B(9)	1.789(3)	B(9)-B(12)	1.782(3)
B(9)-B(10)	1.785(3)	B(10)-B(11)	1.782(2)
B(10)-B(12)	1.792(3)	B(11)-B(12)	1.775(2)
C(13)-C(14)	1.381(2)	C(13)-C(18)	1.392(2)
C(14)-C(15)	1.382(2)	C(15)-C(16)	1.379(3)
C(16)-C(17)	1.377(3)	C(17)-C(18)	1.386(2)
N(19)-O(20)	1.182(2)		

N(19)-C(1)-C(2)	112.14(12)	N(19)-C(1)-B(4)	123.99(13)
C(2)-C(1)-B(4)	112.99(12)	N(19)-C(1)-B(3)	114.65(13)
C(2)-C(1)-B(3)	62.05(9)	B(4)-C(1)-B(3)	63.24(10)
N(19)-C(1)-B(5)	123.49(13)	C(2)-C(1)-B(5)	112.92(12)
B(4)-C(1)-B(5)	62.97(10)	B(3)-C(1)-B(5)	115.68(13)
N(19)-C(1)-B(6)	114.14(13)	C(2)-C(1)-B(6)	61.80(9)
B(4)-C(1)-B(6)	115.50(12)	B(3)-C(1)-B(6)	115.32(13)
B(5)-C(1)-B(6)	63.20(10)	C(13)-C(2)-C(1)	120.32(12)
C(13)-C(2)-B(11)	121.08(13)	C(1)-C(2)-B(11)	108.69(12)
C(13)-C(2)-B(7)	121.66(13)	C(1)-C(2)-B(7)	108.68(11)
B(11)-C(2)-B(7)	62.94(10)	C(13)-C(2)-B(6)	117.21(12)
C(1)-C(2)-B(6)	59.97(9)	B(11)-C(2)-B(6)	62.18(10)
B(7)-C(2)-B(6)	113.59(12)	C(13)-C(2)-B(3)	118.70(13)
C(1)-C(2)-B(3)	59.73(9)	B(11)-C(2)-B(3)	113.09(12)
B(7)-C(2)-B(3)	61.96(10)	B(6)-C(2)-B(3)	111.79(12)
C(1)-B(3)-C(2)	58.22(9)	C(1)-B(3)-B(8)	104.15(12)
C(2)-B(3)-B(8)	105.33(13)	C(1)-B(3)-B(7)	104.44(12)
C(2)-B(3)-B(7)	58.12(9)	B(8)-B(3)-B(7)	60.57(10)
C(1)-B(3)-B(4)	58.34(10)	C(2)-B(3)-B(4)	105.99(12)
B(8)-B(3)-B(4)	59.89(10)	B(7)-B(3)-B(4)	108.41(13)
C(1)-B(4)-B(8)	103.95(12)	C(1)-B(4)-B(9)	104.02(12)
B(8)-B(4)-B(9)	60.53(11)	C(1)-B(4)-B(5)	58.56(10)
B(8)-B(4)-B(5)	108.44(14)	B(9)-B(4)-B(5)	59.93(11)
C(1)-B(4)-B(3)	58.43(9)	B(8)-B(4)-B(3)	59.54(10)
B(9)-B(4)-B(3)	107.90(13)	B(5)-B(4)-B(3)	108.05(12)
C(1)-B(5)-B(9)	103.96(13)	C(1)-B(5)-B(10)	103.79(12)
B(9)-B(5)-B(10)	60.33(11)	C(1)-B(5)-B(4)	58.47(10)
B(9)-B(5)-B(4)	59.94(11)	B(10)-B(5)-B(4)	108.15(13)
C(1)-B(5)-B(6)	58.51(9)	B(9)-B(5)-B(6)	107.64(13)
B(10)-B(5)-B(6)	59.35(10)	B(4)-B(5)-B(6)	107.93(12)
C(1)-B(6)-C(2)	58.23(9)	C(1)-B(6)-B(10)	104.15(12)
C(2)-B(6)-B(10)	105.41(12)	C(1)-B(6)-B(11)	104.03(12)
C(2)-B(6)-B(11)	57.98(9)	B(10)-B(6)-B(11)	60.38(10)
C(1)-B(6)-B(5)	58.29(10)	C(2)-B(6)-B(5)	106.09(12)
B(10)-B(6)-B(5)	60.04(10)	B(11)-B(6)-B(5)	108.15(13)
C(2)-B(7)-B(3)	59.92(9)	C(2)-B(7)-B(12)	105.10(12)
B(3)-B(7)-B(12)	107.42(13)	C(2)-B(7)-B(11)	58.38(9)

B(3)-B(7)-B(11)	107.77(12)	B(12)-B(7)-B(11)	59.71(10)
C(2)-B(7)-B(8)	105.84(12)	B(3)-B(7)-B(8)	59.43(10)
B(12)-B(7)-B(8)	59.99(11)	B(11)-B(7)-B(8)	107.64(13)
B(3)-B(8)-B(4)	60.57(10)	B(3)-B(8)-B(12)	107.77(13)
B(4)-B(8)-B(12)	107.79(14)	B(3)-B(8)-B(7)	60.00(10)
B(4)-B(8)-B(7)	108.49(13)	B(12)-B(8)-B(7)	59.87(10)
B(3)-B(8)-B(9)	108.12(13)	B(4)-B(8)-B(9)	59.79(11)
B(12)-B(8)-B(9)	59.84(11)	B(7)-B(8)-B(9)	107.96(13)
B(5)-B(9)-B(4)	60.13(10)	B(5)-B(9)-B(12)	108.18(13)
B(4)-B(9)-B(12)	107.82(13)	B(5)-B(9)-B(10)	59.89(11)
B(4)-B(9)-B(10)	107.95(13)	B(12)-B(9)-B(10)	60.32(11)
B(5)-B(9)-B(8)	107.92(13)	B(4)-B(9)-B(8)	59.68(11)
B(12)-B(9)-B(8)	59.97(11)	B(10)-B(9)-B(8)	108.11(13)
B(6)-B(10)-B(5)	60.61(10)	B(6)-B(10)-B(11)	60.18(10)
B(5)-B(10)-B(11)	108.45(12)	B(6)-B(10)-B(9)	108.21(13)
B(5)-B(10)-B(9)	59.78(10)	B(11)-B(10)-B(9)	107.66(13)
B(6)-B(10)-B(12)	107.74(12)	B(5)-B(10)-B(12)	107.65(13)
B(11)-B(10)-B(12)	59.55(10)	B(9)-B(10)-B(12)	59.76(11)
C(2)-B(11)-B(12)	105.67(12)	C(2)-B(11)-B(6)	59.84(10)
B(12)-B(11)-B(6)	107.94(13)	C(2)-B(11)-B(10)	106.12(12)
B(12)-B(11)-B(10)	60.53(10)	B(6)-B(11)-B(10)	59.44(10)
C(2)-B(11)-B(7)	58.67(10)	B(12)-B(11)-B(7)	60.14(10)
B(6)-B(11)-B(7)	108.25(13)	B(10)-B(11)-B(7)	108.62(12)
B(11)-B(12)-B(9)	108.09(13)	B(11)-B(12)-B(7)	60.15(10)
B(9)-B(12)-B(7)	108.45(13)	B(11)-B(12)-B(8)	108.12(13)
B(9)-B(12)-B(8)	60.18(11)	B(7)-B(12)-B(8)	60.14(10)
B(11)-B(12)-B(10)	59.93(10)	B(9)-B(12)-B(10)	59.92(11)
B(7)-B(12)-B(10)	108.14(12)	B(8)-B(12)-B(10)	107.96(14)
C(14)-C(13)-C(18)	118.9(2)	C(14)-C(13)-C(2)	121.76(14)
C(18)-C(13)-C(2)	119.24(14)	C(13)-C(14)-C(15)	120.4(2)
C(16)-C(15)-C(14)	120.6(2)	C(17)-C(16)-C(15)	119.6(2)
C(16)-C(17)-C(18)	120.1(2)	C(17)-C(18)-C(13)	120.4(2)
O(20)-N(19)-C(1)	113.0(2)		

Table Atomic coordinates (x 10^4) and equivalent isotropic displacement parameters ($Å^2$ x 10^3) for kw51sm. U(eq) is defined as one third of the trace of the orthogonalized U_{ij} tensor.

	x	y	z	U(eq)
C(1)	7605(2)	9183(2)	900.9(11)	24.1(4)
C(2)	7007.5(14)	7599(2)	1314.7(10)	20.5(4)
B(3)	8321(2)	8546(2)	1962.4(12)	25.2(4)
B(4)	9201(2)	9221(2)	1172.4(13)	27.1(4)
B(5)	8351(2)	8731(2)	56.1(12)	27.1(4)
B(6)	6946(2)	7743(2)	154.8(12)	24.3(4)
B(7)	8218(2)	6461(2)	1889.8(13)	25.6(4)
B(8)	9621(2)	7452(2)	1789.5(14)	29.7(5)
B(9)	9639(2)	7552(2)	606.7(14)	28.2(4)
B(10)	8239(2)	6648(2)	-24.9(13)	28.0(4)
B(11)	7374(2)	5967(2)	769.5(12)	24.8(4)
B(12)	9035(2)	5849(2)	1050.7(14)	29.8(4)
C(13)	5781.0(14)	7714(2)	1611.8(11)	23.0(4)
C(14)	5722(2)	8277(2)	2460.9(12)	35.2(4)
C(15)	4590(2)	8329(3)	2721.9(14)	43.4(5)
C(16)	3505(2)	7810(2)	2141.7(14)	37.3(5)
C(17)	3556(2)	7213(2)	1301.4(14)	36.0(4)
C(18)	4688(2)	7165(2)	1033.7(12)	30.9(4)
N(19)	6800(2)	10601(2)	885.9(11)	37.7(4)
O(20)	7321(2)	11784(2)	786.8(11)	54.8(4)

Table Hydrogen atom coordinates (x 10^4) and isotropic displacement parameters ($Å^2$ x 10^3)

	x	y	z	U
H(3)	8323(2)	9196(2)	2609.3(12)	30
H(4)	9793(2)	10308(2)	1303.5(13)	32
H(5)	8387(2)	9498(2)	-542.2(12)	33
H(6)	6052(2)	7869(2)	-375.1(12)	29
H(7)	8167(2)	5721(2)	2495.5(13)	31
H(8)	10507(2)	7358(2)	2330.5(14)	36
H(9)	10535(2)	7516(2)	366.0(14)	34
H(10)	8208(2)	6022(2)	-683.5(13)	34
H(11)	6767(2)	4894(2)	636.8(12)	30
H(12)	9536(2)	4692(2)	1103.3(14)	36
H(14)	6465(2)	8631(2)	2867.9(12)	42
H(15)	4559(2)	8726(3)	3305.8(14)	52
H(16)	2727(2)	7863(2)	2320.9(14)	45
H(17)	2814(2)	6833(2)	904.3(14)	43
H(18)	4718(2)	6756(2)	452.3(12)	37

C9 CRYSTAL DATA FOR (MeCb)$_2$NH - 23

Empirical Formula	$C_6H_{27}B_{20}N$	
Temperature	160(2)K	
Wavelength	0.71073Å	
Crystal System	Monoclinic	
Space Group	P2(1)/n	
Unit Cell Dimensions	a = 11.302(6)Å	alpha = 90°
	b = 12.705(7)Å	beta = 107.03(2)°
	c = 14.167(7)Å	gamma = 90°
Crystal Size	0.52 × 0.48 × 0.16 mm	
Final R indices [I>2σ(I)]	R1 = 0.0757	wR2 = 0.1619
R indices (all data)	R1 = 0.0890	wR2 = 0.1676

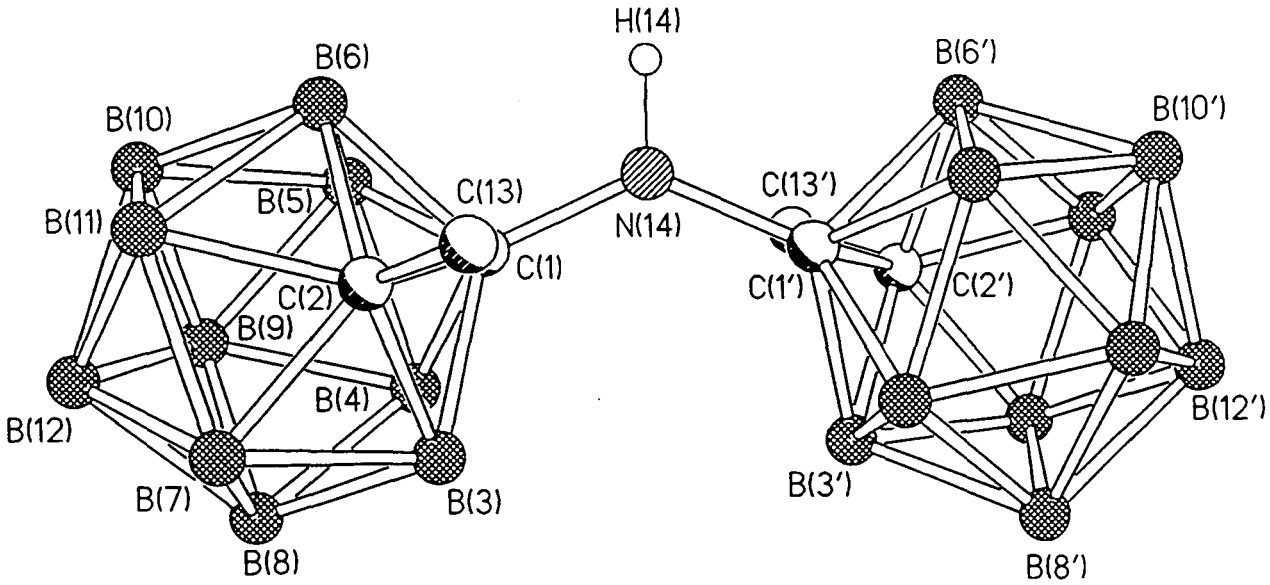

Table Bond lengths (Å) and angles (°)

C(1)-N(14)	1.410(4)	C(1)-B(5)	1.712(4)
C(1)-B(4)	1.713(4)	C(1)-B(3)	1.717(4)
C(1)-B(6)	1.740(4)	C(1)-C(2)	1.752(4)
C(2)-C(13)	1.512(4)	C(2)-B(7)	1.685(4)
C(2)-B(11)	1.696(4)	C(2)-B(6)	1.722(4)
C(2)-B(3)	1.723(4)	B(3)-B(8)	1.774(5)
B(3)-B(7)	1.783(5)	B(3)-B(4)	1.800(4)
B(4)-B(8)	1.773(5)	B(4)-B(9)	1.779(5)
B(4)-B(5)	1.780(5)	B(5)-B(10)	1.777(5)
B(5)-B(9)	1.780(5)	B(5)-B(6)	1.789(4)
B(6)-B(10)	1.770(5)	B(6)-B(11)	1.778(5)
B(7)-B(12)	1.772(5)	B(7)-B(11)	1.777(5)
B(7)-B(8)	1.789(5)	B(8)-B(9)	1.791(5)
B(8)-B(12)	1.794(5)	B(9)-B(12)	1.775(5)
B(9)-B(10)	1.789(5)	B(10)-B(11)	1.781(5)
B(10)-B(12)	1.800(5)	B(11)-B(12)	1.781(5)
C(1')-N(14)	1.409(4)	C(1')-B(4')	1.714(4)
C(1')-B(5')	1.715(4)	C(1')-B(3')	1.721(4)
C(1')-B(6')	1.738(4)	C(1')-C(2')	1.748(4)
C(2')-C(13')	1.515(4)	C(2')-B(7')	1.686(4)
C(2')-B(11')	1.703(4)	C(2')-B(3')	1.724(4)
C(2')-B(6')	1.727(4)	B(3')-B(8')	1.771(5)
B(3')-B(7')	1.784(4)	B(3')-B(4')	1.789(5)
B(4')-B(8')	1.767(5)	B(4')-B(5')	1.775(5)
B(4')-B(9')	1.778(5)	B(5')-B(9')	1.770(5)
B(5')-B(10')	1.773(5)	B(5')-B(6')	1.786(5)
B(6')-B(10')	1.765(5)	B(6')-B(11')	1.775(5)
B(7')-B(11')	1.776(5)	B(7')-B(12')	1.785(5)
B(7')-B(8')	1.786(5)	B(8')-B(9')	1.796(5)
B(8')-B(12')	1.802(5)	B(9')-B(12')	1.776(5)
B(9')-B(10')	1.781(5)	B(10')-B(11')	1.779(5)
B(10')-B(12')	1.793(5)	B(11')-B(12')	1.783(5)

N(14)-C(1)-B(5)	118.8(2)	N(14)-C(1)-B(4)	127.5(2)
B(5)-C(1)-B(4)	62.6(2)	N(14)-C(1)-B(3)	123.4(2)
B(5)-C(1)-B(3)	113.8(2)	B(4)-C(1)-B(3)	63.3(2)
N(14)-C(1)-B(6)	110.7(2)	B(5)-C(1)-B(6)	62.4(2)
B(4)-C(1)-B(6)	113.3(2)	B(3)-C(1)-B(6)	110.8(2)
N(14)-C(1)-C(2)	117.0(2)	B(5)-C(1)-C(2)	108.9(2)
B(4)-C(1)-C(2)	109.6(2)	B(3)-C(1)-C(2)	59.6(2)
B(6)-C(1)-C(2)	59.1(2)	C(13)-C(2)-B(7)	122.7(2)
C(13)-C(2)-B(11)	122.0(2)	B(7)-C(2)-B(11)	63.4(2)
C(13)-C(2)-B(6)	116.7(2)	B(7)-C(2)-B(6)	114.1(2)
B(11)-C(2)-B(6)	62.7(2)	C(13)-C(2)-B(3)	117.3(2)
B(7)-C(2)-B(3)	63.1(2)	B(11)-C(2)-B(3)	114.5(2)
B(6)-C(2)-B(3)	111.4(2)	C(13)-C(2)-C(1)	117.3(2)
B(7)-C(2)-C(1)	109.8(2)	B(11)-C(2)-C(1)	110.2(2)
B(6)-C(2)-C(1)	60.1(2)	B(3)-C(2)-C(1)	59.2(2)
C(1)-B(3)-C(2)	61.2(2)	C(1)-B(3)-B(8)	105.3(2)
C(2)-B(3)-B(8)	105.1(2)	C(1)-B(3)-B(7)	106.9(2)
C(2)-B(3)-B(7)	57.4(2)	B(8)-B(3)-B(7)	60.4(2)
C(1)-B(3)-B(4)	58.3(2)	C(2)-B(3)-B(4)	107.0(2)
B(8)-B(3)-B(4)	59.5(2)	B(7)-B(3)-B(4)	108.0(2)
C(1)-B(4)-B(8)	105.5(2)	C(1)-B(4)-B(9)	105.4(2)
B(8)-B(4)-B(9)	60.6(2)	C(1)-B(4)-B(5)	58.6(2)
B(8)-B(4)-B(5)	108.3(2)	B(9)-B(4)-B(5)	60.0(2)
C(1)-B(4)-B(3)	58.5(2)	B(8)-B(4)-B(3)	59.5(2)
B(9)-B(4)-B(3)	107.2(2)	B(5)-B(4)-B(3)	106.7(2)

C(1)-B(5)-B(10)	106.2(2)	C(1)-B(5)-B(9)	105.4(2)
B(10)-B(5)-B(9)	60.4(2)	C(1)-B(5)-B(4)	58.7(2)
B(10)-B(5)-B(4)	108.6(2)	B(9)-B(5)-B(4)	59.9(2)
C(1)-B(5)-B(6)	59.6(2)	B(10)-B(5)-B(6)	59.5(2)
B(9)-B(5)-B(6)	107.4(2)	B(4)-B(5)-B(6)	107.8(2)
C(2)-B(6)-C(1)	60.8(2)	C(2)-B(6)-B(10)	105.3(2)
C(1)-B(6)-B(10)	105.4(2)	C(2)-B(6)-B(11)	58.0(2)
C(1)-B(6)-B(11)	107.0(2)	B(10)-B(6)-B(11)	60.3(2)
C(2)-B(6)-B(5)	106.7(2)	C(1)-B(6)-B(5)	58.0(2)
B(10)-B(6)-B(5)	59.9(2)	B(11)-B(6)-B(5)	108.4(2)
C(2)-B(7)-B(12)	105.7(2)	C(2)-B(7)-B(11)	58.6(2)
B(12)-B(7)-B(11)	60.2(2)	C(2)-B(7)-B(3)	59.5(2)
B(12)-B(7)-B(3)	107.8(2)	B(11)-B(7)-B(3)	107.8(2)
C(2)-B(7)-B(8)	106.1(2)	B(12)-B(7)-B(8)	60.5(2)
B(11)-B(7)-B(8)	108.6(2)	B(3)-B(7)-B(8)	59.5(2)
B(4)-B(8)-B(3)	61.0(2)	B(4)-B(8)-B(7)	108.9(2)
B(3)-B(8)-B(7)	60.0(2)	B(4)-B(8)-B(9)	59.9(2)
B(3)-B(8)-B(9)	107.9(2)	B(7)-B(8)-B(9)	107.0(2)
B(4)-B(8)-B(12)	107.8(2)	B(3)-B(8)-B(12)	107.3(2)
B(7)-B(8)-B(12)	59.3(2)	B(9)-B(8)-B(12)	59.4(2)
B(12)-B(9)-B(4)	108.4(2)	B(12)-B(9)-B(5)	108.3(2)
B(4)-B(9)-B(5)	60.1(2)	B(12)-B(9)-B(10)	60.7(2)
B(4)-B(9)-B(10)	108.2(2)	B(5)-B(9)-B(10)	59.7(2)
B(12)-B(9)-B(8)	60.4(2)	B(4)-B(9)-B(8)	59.6(2)
B(5)-B(9)-B(8)	107.6(2)	B(10)-B(9)-B(8)	108.5(2)
B(6)-B(10)-B(5)	60.6(2)	B(6)-B(10)-B(11)	60.1(2)
B(5)-B(10)-B(11)	108.7(2)	B(6)-B(10)-B(9)	107.8(2)
B(5)-B(10)-B(9)	59.9(2)	B(11)-B(10)-B(9)	107.6(2)
B(6)-B(10)-B(12)	107.2(2)	B(5)-B(10)-B(12)	107.3(2)
B(11)-B(10)-B(12)	59.7(2)	B(9)-B(10)-B(12)	59.3(2)
C(2)-B(11)-B(7)	58.0(2)	C(2)-B(11)-B(6)	59.4(2)
B(7)-B(11)-B(6)	107.1(2)	C(2)-B(11)-B(10)	105.9(2)
B(7)-B(11)-B(10)	108.3(2)	B(6)-B(11)-B(10)	59.7(2)
C(2)-B(11)-B(12)	104.8(2)	B(7)-B(11)-B(12)	59.7(2)
B(6)-B(11)-B(12)	107.7(2)	B(10)-B(11)-B(12)	60.7(2)
B(7)-B(12)-B(9)	108.5(2)	B(7)-B(12)-B(11)	60.0(2)
B(9)-B(12)-B(11)	108.2(2)	B(7)-B(12)-B(8)	60.2(2)
B(9)-B(12)-B(8)	60.2(2)	B(11)-B(12)-B(8)	108.2(2)
B(7)-B(12)-B(10)	107.6(2)	B(9)-B(12)-B(10)	60.1(2)
B(11)-B(12)-B(10)	59.6(2)	B(8)-B(12)-B(10)	107.9(2)
N(14)-C(1')-B(4')	127.2(2)	N(14)-C(1')-B(5')	119.3(2)
B(4')-C(1')-B(5')	62.3(2)	N(14)-C(1')-B(3')	123.1(2)
B(4')-C(1')-B(3')	62.8(2)	B(5')-C(1')-B(3')	113.3(2)
N(14)-C(1')-B(6')	111.5(2)	B(4')-C(1')-B(6')	112.8(2)
B(5')-C(1')-B(6')	62.3(2)	B(3')-C(1')-B(6')	110.9(2)
N(14)-C(1')-C(2')	117.3(2)	B(4')-C(1')-C(2')	109.2(2)
B(5')-C(1')-C(2')	109.0(2)	B(3')-C(1')-C(2')	59.6(2)
B(6')-C(1')-C(2')	59.4(2)	C(13')-C(2')-B(7')	123.1(2)
C(13')-C(2')-B(11')	122.4(2)	B(7')-C(2')-B(11')	63.2(2)
C(13')-C(2')-B(3')	117.4(2)	B(7')-C(2')-B(3')	63.1(2)
B(11')-C(2')-B(3')	114.3(2)	C(13')-C(2')-B(6')	116.8(2)
B(7')-C(2')-B(6')	113.6(2)	B(11')-C(2')-B(6')	62.3(2)
B(3')-C(2')-B(6')	111.2(2)	C(13')-C(2')-C(1')	117.0(2)
B(7')-C(2')-C(1')	109.9(2)	B(11')-C(2')-C(1')	110.0(2)
B(3')-C(2')-C(1')	59.4(2)	B(6')-C(2')-C(1')	60.0(2)
C(1')-B(3')-C(2')	61.0(2)	C(1')-B(3')-B(8')	105.5(2)
C(2')-B(3')-B(8')	105.2(2)	C(1')-B(3')-B(7')	106.7(2)
C(2')-B(3')-B(7')	57.4(2)	B(8')-B(3')-B(7')	60.3(2)
C(1')-B(3')-B(4')	58.4(2)	C(2')-B(3')-B(4')	106.9(2)
B(8')-B(3')-B(4')	59.5(2)	B(7')-B(3')-B(4')	107.8(2)
C(1')-B(4')-B(8')	106.0(2)	C(1')-B(4')-B(5')	58.9(2)
B(8')-B(4')-B(5')	108.5(2)	C(1')-B(4')-B(9')	105.6(2)

B(8')-B(4')-B(9')	60.9(2)	B(5')-B(4')-B(9')	59.8(2)
C(1')-B(4')-B(3')	58.8(2)	B(8')-B(4')-B(3')	59.7(2)
B(5')-B(4')-B(3')	107.2(2)	B(9')-B(4')-B(3')	107.8(2)
C(1')-B(5')-B(9')	105.9(2)	C(1')-B(5')-B(10')	106.3(2)
B(9')-B(5')-B(10')	60.4(2)	C(1')-B(5')-B(4')	58.8(2)
B(9')-B(5')-B(4')	60.2(2)	B(10')-B(5')-B(4')	108.6(2)
C(1')-B(5')-B(6')	59.5(2)	B(9')-B(5')-B(6')	107.5(2)
B(10')-B(5')-B(6')	59.5(2)	B(4')-B(5')-B(6')	107.7(2)
C(2')-B(6')-C(1')	60.6(2)	C(2')-B(6')-B(10')	105.5(2)
C(1')-B(6')-B(10')	105.6(2)	C(2')-B(6')-B(11')	58.2(2)
C(1')-B(6')-B(11')	107.2(2)	B(10')-B(6')-B(11')	60.3(2)
C(2')-B(6')-B(5')	106.7(2)	C(1')-B(6')-B(5')	58.2(2)
B(10')-B(6')-B(5')	59.9(2)	B(11')-B(6')-B(5')	108.4(2)
C(2')-B(7')-B(11')	58.9(2)	C(2')-B(7')-B(3')	59.5(2)
B(11')-B(7')-B(3')	107.9(2)	C(2')-B(7')-B(12')	106.0(2)
B(11')-B(7')-B(12')	60.1(2)	B(3')-B(7')-B(12')	107.9(2)
C(2')-B(7')-B(8')	106.1(2)	B(11')-B(7')-B(8')	108.6(2)
B(3')-B(7')-B(8')	59.5(2)	B(12')-B(7')-B(8')	60.6(2)
B(4')-B(8')-B(3')	60.7(2)	B(4')-B(8')-B(7')	108.7(2)
B(3')-B(8')-B(7')	60.2(2)	B(4')-B(8')-B(9')	59.9(2)
B(3')-B(8')-B(9')	107.8(2)	B(7')-B(8')-B(9')	107.0(2)
B(4')-B(8')-B(12')	107.7(2)	B(3')-B(8')-B(12')	107.8(2)
B(7')-B(8')-B(12')	59.6(2)	B(9')-B(8')-B(12')	59.1(2)
B(5')-B(9')-B(12')	108.6(2)	B(5')-B(9')-B(4')	60.0(2)
B(12')-B(9')-B(4')	108.4(2)	B(5')-B(9')-B(10')	59.9(2)
B(12')-B(9')-B(10')	60.5(2)	B(4')-B(9')-B(10')	108.0(2)
B(5')-B(9')-B(8')	107.4(2)	B(12')-B(9')-B(8')	60.6(2)
B(4')-B(9')-B(8')	59.3(2)	B(10')-B(9')-B(8')	108.3(2)
B(6')-B(10')-B(5')	60.6(2)	B(6')-B(10')-B(11')	60.1(2)
B(5')-B(10')-B(11')	108.8(2)	B(6')-B(10')-B(9')	107.9(2)
B(5')-B(10')-B(9')	59.7(2)	B(11')-B(10')-B(9')	107.9(2)
B(6')-B(10')-B(12')	107.7(2)	B(5')-B(10')-B(12')	107.7(2)
B(11')-B(10')-B(12')	59.9(2)	B(9')-B(10')-B(12')	59.6(2)
C(2')-B(11')-B(6')	59.5(2)	C(2')-B(11')-B(7')	57.9(2)
B(6')-B(11')-B(7')	107.1(2)	C(2')-B(11')-B(10')	106.0(2)
B(6')-B(11')-B(10')	59.6(2)	B(7')-B(11')-B(10')	108.2(2)
C(2')-B(11')-B(12')	105.3(2)	B(6')-B(11')-B(12')	107.6(2)
B(7')-B(11')-B(12')	60.2(2)	B(10')-B(11')-B(12')	60.4(2)
B(9')-B(12')-B(11')	107.9(2)	B(9')-B(12')-B(7')	108.0(2)
B(11')-B(12')-B(7')	59.7(2)	B(9')-B(12')-B(10')	59.9(2)
B(11')-B(12')-B(10')	59.7(2)	B(7')-B(12')-B(10')	107.2(2)
B(9')-B(12')-B(8')	60.3(2)	B(11')-B(12')-B(8')	107.5(2)
B(7')-B(12')-B(8')	59.7(2)	B(10')-B(12')-B(8')	107.5(2)
C(1')-N(14)-C(1)	131.1(2)		

Table Atomic coordinates (x 10^4) and equivalent isotropic displacement parameters ($Å^2$ x 10^3) for kw48. U(eq) is defined as one third of the trace of the orthogonalized U_{ij} tensor.

	x	y	z	U(eq)
C(1)	916(2)	2578(2)	1676(2)	20.7(7)
C(2)	1155(3)	2255(2)	544(2)	23.4(7)
B(3)	344(3)	1423(2)	1088(2)	23.5(8)
B(4)	1085(3)	1475(3)	2399(2)	25.8(8)
B(5)	2282(3)	2433(3)	2593(2)	24.3(8)
B(6)	2270(3)	2944(3)	1414(2)	23.0(7)
B(7)	1449(3)	958(3)	510(3)	29.8(8)
B(8)	1422(3)	440(3)	1678(3)	29.8(8)
B(9)	2646(3)	1070(3)	2603(3)	29.2(8)
B(10)	3386(3)	1995(3)	2009(2)	26.6(8)
B(11)	2653(3)	1907(3)	714(2)	28.1(8)
B(12)	2862(3)	743(3)	1446(3)	31.3(8)
C(13)	423(3)	2863(2)	-356(2)	28.6(7)
C(1')	-1099(2)	3555(2)	1589(2)	20.8(7)
C(2')	-1540(3)	3595(2)	2673(2)	23.3(7)
B(3')	-1961(3)	2550(3)	1868(2)	24.2(8)
B(4')	-2303(3)	3078(3)	647(2)	25.1(8)
B(5')	-1972(3)	4445(3)	764(2)	26.2(8)
B(6')	-1444(3)	4746(3)	2051(2)	24.2(8)
B(7')	-2997(3)	3138(3)	2453(3)	26.9(8)
B(8')	-3510(3)	2809(3)	1172(2)	28.0(8)
B(9')	-3521(3)	4007(3)	495(3)	29.3(8)
B(10')	-2978(3)	5045(3)	1358(2)	27.8(8)
B(11')	-2675(3)	4509(3)	2566(3)	29.5(8)
B(12')	-3962(3)	4038(3)	1600(3)	29.2(8)
C(13')	-536(3)	3405(2)	3634(2)	28.1(7)
N(14)	174(2)	3466(2)	1691(2)	21.2(6)

Table Hydrogen atom coordinates (x 10^4) and isotropic displacement parameters ($Å^2$ x 10^3)

	x	y	z	U
H(3)	-671(3)	1269(2)	772(2)	28
H(4)	572(3)	1332(3)	2954(2)	31
H(5)	2555(3)	2929(3)	3277(2)	29
H(6)	2509(3)	3784(3)	1312(2)	28
H(7)	1169(3)	472(3)	-179(3)	36
H(8)	1124(3)	-387(3)	1760(3)	36
H(9)	3172(3)	653(3)	3295(3)	35
H(10)	4390(3)	2198(3)	2312(2)	32
H(11)	3173(3)	2053(3)	165(2)	34
H(12)	3522(3)	110(3)	1380(3)	38
H(13A)	-25(14)	3437(10)	-150(2)	43
H(13B)	-169(13)	2391(4)	-803(7)	43
H(13C)	988(3)	3155(13)	-697(8)	43
H(3')	-1586(3)	1735(3)	2052(2)	29
H(4')	-2182(3)	2606(3)	14(2)	30
H(5')	-1624(3)	4878(3)	210(2)	31
H(6')	-729(3)	5366(3)	2356(2)	29
H(7')	-3333(3)	2703(3)	3012(3)	32
H(8')	-4184(3)	2155(3)	885(2)	34
H(9')	-4215(3)	4152(3)	-239(3)	35
H(10')	-3299(3)	5877(3)	1193(2)	33
H(11')	-2794(3)	4984(3)	3198(3)	35
H(12')	-4940(3)	4198(3)	1589(3)	35
H(13D)	274(3)	3402(15)	3511(3)	42
H(13E)	-674(10)	2724(7)	3909(7)	42
H(13F)	-557(12)	3965(8)	4104(5)	42
H(14)	591(27)	4062(26)	1830(21)	25(8)

C10 CRYSTAL DATA FOR MeCbNHNHPh - 27

Empirical Formula	$C_9H_{20}B_{10}N_2$	
Temperature	160(2)K	
Wavelength	0.71073Å	
Crystal System	Monoclinic	
Space Group	P2(1)/n	
Unit Cell Dimensions	a = 8.6912(11)Å	alpha = 90°
	b = 15.568(2)Å	beta = 96.576(1)°
	c = 11.568(2)Å	gamma = 90°
Crystal Size	0.70 × 0.22 × 0.10 mm	
Final R indices [I>2σ(I)]	R1 = 0.0493	wR2 = 0.1144
R indices (all data)	R1 = 0.0699	wR2 = 0.1360

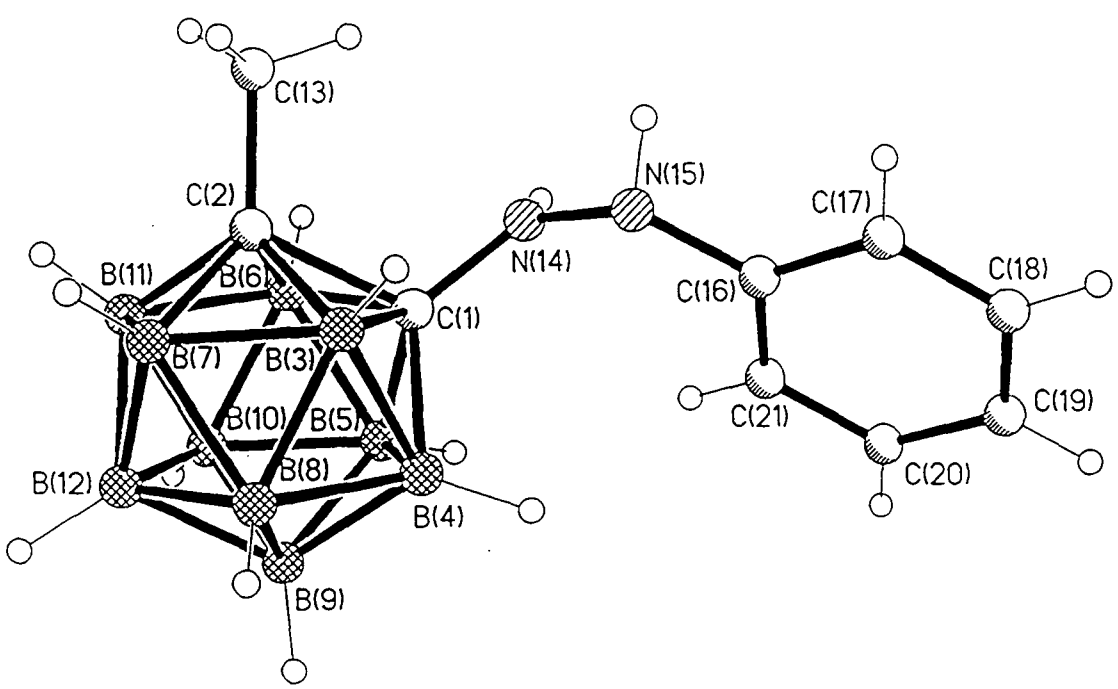

Table Bond lengths (Å) and angles (°)

C(1)-N(14)	1.387(2)	C(1)-B(4)	1.696(2)
C(1)-B(5)	1.704(3)	C(1)-B(6)	1.716(2)
C(1)-B(3)	1.725(2)	C(1)-C(2)	1.770(2)
C(2)-C(13)	1.511(2)	C(2)-B(7)	1.682(2)
C(2)-B(11)	1.686(2)	C(2)-B(6)	1.713(3)
C(2)-B(3)	1.714(2)	B(3)-B(8)	1.770(3)
B(3)-B(7)	1.786(3)	B(3)-B(4)	1.786(3)
B(3)-H(3)	1.07(2)	B(4)-B(8)	1.774(3)
B(4)-B(9)	1.776(3)	B(4)-B(5)	1.779(3)
B(4)-H(4)	1.12(2)	B(5)-B(10)	1.765(3)
B(5)-B(9)	1.772(3)	B(5)-B(6)	1.784(3)
B(5)-H(5)	1.10(2)	B(6)-B(10)	1.768(3)
B(6)-B(11)	1.780(3)	B(6)-H(6)	1.09(2)
B(7)-B(12)	1.763(3)	B(7)-B(11)	1.772(3)
B(7)-B(8)	1.776(3)	B(7)-H(7)	1.11(2)
B(8)-B(9)	1.776(3)	B(8)-B(12)	1.790(3)
B(8)-H(8)	1.11(2)	B(9)-B(12)	1.772(3)
B(9)-B(10)	1.787(3)	B(9)-H(9)	1.11(2)
B(10)-B(11)	1.774(3)	B(10)-B(12)	1.786(3)
B(10)-H(10)	1.05(2)	B(11)-B(12)	1.768(3)
B(11)-H(11)	1.07(2)	B(12)-H(12)	1.12(2)
C(13)-H(13A)	0.99(2)	C(13)-H(13B)	0.91(3)
C(13)-H(13C)	1.00(3)	N(14)-N(15)	1.395(2)
N(14)-H(14)	0.88(2)	N(15)-C(16)	1.406(2)
N(15)-H(15)	0.92(2)	C(16)-C(21)	1.390(2)
C(16)-C(17)	1.399(2)	C(17)-C(18)	1.382(2)
C(17)-H(17)	0.97(2)	C(18)-C(19)	1.385(3)
C(18)-H(18)	0.95(2)	C(19)-C(20)	1.382(3)
C(19)-H(19)	0.98(2)	C(20)-C(21)	1.386(2)
C(20)-H(20)	0.95(2)	C(21)-H(21)	0.93(2)

N(14)-C(1)-B(4)	125.52(13)	N(14)-C(1)-B(5)	123.91(14)
B(4)-C(1)-B(5)	63.09(11)	N(14)-C(1)-B(6)	115.21(13)
B(4)-C(1)-B(6)	113.80(13)	B(5)-C(1)-B(6)	62.88(11)
N(14)-C(1)-B(3)	117.84(14)	B(4)-C(1)-B(3)	62.95(11)
B(5)-C(1)-B(3)	113.62(13)	B(6)-C(1)-B(3)	110.05(12)
N(14)-C(1)-C(2)	115.93(13)	B(4)-C(1)-C(2)	108.78(12)
B(5)-C(1)-C(2)	108.66(12)	B(6)-C(1)-C(2)	58.82(10)
B(3)-C(1)-C(2)	58.72(10)	C(13)-C(2)-B(7)	123.6(2)
C(13)-C(2)-B(11)	122.9(2)	B(7)-C(2)-B(11)	63.48(11)
C(13)-C(2)-B(6)	116.3(2)	B(7)-C(2)-B(6)	114.40(13)
B(11)-C(2)-B(6)	63.17(11)	C(13)-C(2)-B(3)	116.8(2)
B(7)-C(2)-B(3)	63.43(11)	B(11)-C(2)-B(3)	114.82(13)
B(6)-C(2)-B(3)	110.74(13)	C(13)-C(2)-C(1)	116.22(14)
B(7)-C(2)-C(1)	110.01(12)	B(11)-C(2)-C(1)	109.86(12)
B(6)-C(2)-C(1)	59.03(9)	B(3)-C(2)-C(1)	59.31(9)
C(2)-B(3)-C(1)	61.97(10)	C(2)-B(3)-B(8)	104.78(13)
C(1)-B(3)-B(8)	105.10(14)	C(2)-B(3)-B(7)	57.42(10)
C(1)-B(3)-B(7)	107.38(13)	B(8)-B(3)-B(7)	59.92(11)
C(2)-B(3)-B(4)	107.23(13)	C(1)-B(3)-B(4)	57.73(10)
B(8)-B(3)-B(4)	59.83(11)	B(7)-B(3)-B(4)	108.13(14)
C(2)-B(3)-H(3)	116.5(10)	C(1)-B(3)-H(3)	116.8(10)
B(8)-B(3)-H(3)	131.0(10)	B(7)-B(3)-H(3)	123.4(10)
B(4)-B(3)-H(3)	124.5(10)	C(1)-B(4)-B(8)	106.20(13)
C(1)-B(4)-B(9)	105.51(13)	B(8)-B(4)-B(9)	60.03(12)
C(1)-B(4)-B(5)	58.69(10)	B(8)-B(4)-B(5)	107.91(14)
B(9)-B(4)-B(5)	59.80(12)	C(1)-B(4)-B(3)	59.32(10)
B(8)-B(4)-B(3)	59.65(11)	B(9)-B(4)-B(3)	107.14(13)

B(5)-B(4)-B(3)	107.21(13)	C(1)-B(4)-H(4)	116.0(10)
B(8)-B(4)-H(4)	125.5(10)	B(9)-B(4)-H(4)	130.8(10)
B(5)-B(4)-H(4)	122.7(10)	B(3)-B(4)-H(4)	116.0(10)
C(1)-B(5)-B(10)	106.16(13)	C(1)-B(5)-B(9)	105.31(14)
B(10)-B(5)-B(9)	60.70(12)	C(1)-B(5)-B(4)	58.22(10)
B(10)-B(5)-B(4)	108.57(14)	B(9)-B(5)-B(4)	60.03(12)
C(1)-B(5)-B(6)	58.90(10)	B(10)-B(5)-B(6)	59.75(11)
B(9)-B(5)-B(6)	107.42(13)	B(4)-B(5)-B(6)	106.69(13)
C(1)-B(5)-H(5)	114.6(10)	B(10)-B(5)-H(5)	126.9(10)
B(9)-B(5)-H(5)	131.3(10)	B(4)-B(5)-H(5)	121.2(10)
B(6)-B(5)-H(5)	116.4(10)	C(2)-B(6)-C(1)	62.15(10)
C(2)-B(6)-B(10)	105.00(13)	C(1)-B(6)-B(10)	105.50(13)
C(2)-B(6)-B(11)	57.69(10)	C(1)-B(6)-B(11)	108.00(13)
B(10)-B(6)-B(11)	59.99(11)	C(2)-B(6)-B(5)	107.62(13)
C(1)-B(6)-B(5)	58.22(10)	B(10)-B(6)-B(5)	59.59(11)
B(11)-B(6)-B(5)	108.25(13)	C(2)-B(6)-H(6)	116.1(10)
C(1)-B(6)-H(6)	117.3(10)	B(10)-B(6)-H(6)	130.4(10)
B(11)-B(6)-H(6)	122.1(10)	B(5)-B(6)-H(6)	125.3(10)
C(2)-B(7)-B(12)	105.39(13)	C(2)-B(7)-B(11)	58.37(10)
B(12)-B(7)-B(11)	60.00(11)	C(2)-B(7)-B(8)	105.89(13)
B(12)-B(7)-B(8)	60.75(11)	B(11)-B(7)-B(8)	108.47(14)
C(2)-B(7)-B(3)	59.15(10)	B(12)-B(7)-B(3)	107.82(14)
B(11)-B(7)-B(3)	107.26(13)	B(8)-B(7)-B(3)	59.62(11)
C(2)-B(7)-H(7)	118.1(10)	B(12)-B(7)-H(7)	127.7(10)
B(11)-B(7)-H(7)	121.1(10)	B(8)-B(7)-H(7)	125.5(10)
B(3)-B(7)-H(7)	118.6(10)	B(3)-B(8)-B(4)	60.52(11)
B(3)-B(8)-B(7)	60.46(11)	B(4)-B(8)-B(7)	109.11(13)
B(3)-B(8)-B(9)	107.84(13)	B(4)-B(8)-B(9)	60.05(12)
B(7)-B(8)-B(9)	107.56(14)	B(3)-B(8)-B(12)	107.33(13)
B(4)-B(8)-B(12)	107.92(14)	B(7)-B(8)-B(12)	59.28(11)
B(9)-B(8)-B(12)	59.61(11)	B(3)-B(8)-H(8)	121.0(11)
B(4)-B(8)-H(8)	119.7(11)	B(7)-B(8)-H(8)	122.5(11)
B(9)-B(8)-H(8)	121.8(11)	B(12)-B(8)-H(8)	123.7(11)
B(5)-B(9)-B(12)	108.23(13)	B(5)-B(9)-B(8)	108.12(14)
B(12)-B(9)-B(8)	60.59(11)	B(5)-B(9)-B(4)	60.17(11)
B(12)-B(9)-B(4)	108.61(14)	B(8)-B(9)-B(4)	59.92(12)
B(5)-B(9)-B(10)	59.46(11)	B(12)-B(9)-B(10)	60.23(11)
B(8)-B(9)-B(10)	108.22(14)	B(4)-B(9)-B(10)	107.70(13)
B(5)-B(9)-H(9)	120.2(11)	B(12)-B(9)-H(9)	123.3(11)
B(8)-B(9)-H(9)	121.9(11)	B(4)-B(9)-H(9)	119.8(11)
B(10)-B(9)-H(9)	122.8(11)	B(5)-B(10)-B(6)	60.66(11)
B(5)-B(10)-B(11)	109.41(14)	B(6)-B(10)-B(11)	60.35(11)
B(5)-B(10)-B(12)	107.93(14)	B(6)-B(10)-B(12)	107.24(13)
B(11)-B(10)-B(12)	59.55(11)	B(5)-B(10)-B(9)	59.85(11)
B(6)-B(10)-B(9)	107.47(13)	B(11)-B(10)-B(9)	107.59(14)
B(12)-B(10)-B(9)	59.47(11)	B(5)-B(10)-H(10)	120.2(11)
B(6)-B(10)-H(10)	120.6(11)	B(11)-B(10)-H(10)	121.2(10)
B(12)-B(10)-H(10)	123.6(11)	B(9)-B(10)-H(10)	123.2(10)
C(2)-B(11)-B(12)	105.03(13)	C(2)-B(11)-B(7)	58.15(10)
B(12)-B(11)-B(7)	59.75(11)	C(2)-B(11)-B(10)	105.89(12)
B(12)-B(11)-B(10)	60.57(11)	B(7)-B(11)-B(10)	108.12(13)
C(2)-B(11)-B(6)	59.15(10)	B(12)-B(11)-B(6)	107.50(13)
B(7)-B(11)-B(6)	106.90(13)	B(10)-B(11)-B(6)	59.66(11)
C(2)-B(11)-H(11)	117.4(10)	B(12)-B(11)-H(11)	128.7(10)
B(7)-B(11)-H(11)	121.5(10)	B(10)-B(11)-H(11)	125.9(10)
B(6)-B(11)-H(11)	118.1(10)	B(7)-B(12)-B(11)	60.25(11)
B(7)-B(12)-B(9)	108.28(14)	B(11)-B(12)-B(9)	108.53(14)
B(7)-B(12)-B(10)	107.97(13)	B(11)-B(12)-B(10)	59.89(11)
B(9)-B(12)-B(10)	60.30(12)	B(7)-B(12)-B(8)	59.97(12)
B(11)-B(12)-B(8)	108.05(13)	B(9)-B(12)-B(8)	59.80(12)
B(10)-B(12)-B(8)	107.65(13)	B(7)-B(12)-H(12)	122.5(10)
B(11)-B(12)-H(12)	121.5(9)	B(9)-B(12)-H(12)	120.8(9)

B(10)-B(12)-H(12)	120.9(10)	B(8)-B(12)-H(12)	122.6(9)
C(2)-C(13)-H(13A)	108.5(13)	C(2)-C(13)-H(13B)	110(2)
H(13A)-C(13)-H(13B)	115(2)	C(2)-C(13)-H(13C)	109(2)
H(13A)-C(13)-H(13C)	106(2)	H(13B)-C(13)-H(13C)	109(2)
C(1)-N(14)-N(15)	118.83(13)	C(1)-N(14)-H(14)	117(2)
N(15)-N(14)-H(14)	120(2)	N(14)-N(15)-C(16)	119.18(14)
N(14)-N(15)-H(15)	112.5(12)	C(16)-N(15)-H(15)	113.6(12)
C(21)-C(16)-C(17)	119.3(2)	C(21)-C(16)-N(15)	122.87(14)
C(17)-C(16)-N(15)	117.76(14)	C(18)-C(17)-C(16)	120.0(2)
C(18)-C(17)-H(17)	119.3(11)	C(16)-C(17)-H(17)	120.6(11)
C(17)-C(18)-C(19)	120.8(2)	C(17)-C(18)-H(18)	118.4(13)
C(19)-C(18)-H(18)	120.8(12)	C(20)-C(19)-C(18)	119.0(2)
C(20)-C(19)-H(19)	120.9(12)	C(18)-C(19)-H(19)	120.1(12)
C(19)-C(20)-C(21)	121.2(2)	C(19)-C(20)-H(20)	121.6(11)
C(21)-C(20)-H(20)	117.2(11)	C(20)-C(21)-C(16)	119.7(2)
C(20)-C(21)-H(21)	120.8(11)	C(16)-C(21)-H(21)	119.4(11)

Table Atomic coordinates (x 10^4) and equivalent isotropic displacement parameters ($Å^2$ x 10^3) for kw49. U(eq) is defined as one third of the trace of the orthogonalized U_{ij} tensor.

	x	y	z	U(eq)
C(1)	6106(2)	2862.8(10)	4015.3(13)	23.9(3)
C(2)	5071(2)	1890.1(10)	3749.3(14)	27.6(4)
B(3)	6537(2)	1967.4(12)	4869(2)	29.6(4)
B(4)	8006(2)	2630.9(12)	4376(2)	30.8(4)
B(5)	7299(2)	2998.1(13)	2959(2)	31.4(4)
B(6)	5404(2)	2558.6(12)	2628(2)	29.5(4)
B(7)	6291(2)	1049.9(12)	3940(2)	31.1(4)
B(8)	8161(2)	1495.9(13)	4323(2)	34.4(5)
B(9)	8617(2)	2126.7(13)	3129(2)	34.9(5)
B(10)	6996(2)	2099.9(13)	2029(2)	32.9(5)
B(11)	5574(2)	1421.9(12)	2533(2)	28.2(4)
B(12)	7556(2)	1161.3(13)	2861(2)	31.0(4)
C(13)	3437(2)	1877(2)	4076(2)	47.3(6)
N(14)	5305(2)	3526.9(9)	4478.2(13)	31.7(4)
N(15)	5641(2)	3723.0(9)	5656.3(12)	27.9(3)
C(16)	6534(2)	4454.9(9)	5982.9(14)	23.6(3)
C(17)	6532(2)	4757.4(10)	7121.6(14)	26.2(4)
C(18)	7494(2)	5427.8(11)	7517(2)	32.3(4)
C(19)	8447(2)	5818.1(11)	6792(2)	35.8(4)
C(20)	8417(2)	5531.2(11)	5659(2)	34.2(4)
C(21)	7467(2)	4856.5(10)	5247(2)	27.9(4)

Table Hydrogen atom coordinates (x 10^4) and isotropic displacement parameters ($Å^2$ x 10^3)

	x	y	z	U
H(3)	6200(21)	1982(11)	5731(17)	37(5)
H(4)	8645(22)	3055(12)	5045(17)	42(5)
H(5)	7453(21)	3668(12)	2699(16)	39(5)
H(6)	4403(22)	2904(12)	2211(17)	40(5)
H(7)	5856(21)	448(12)	4291(17)	42(5)
H(8)	9073(24)	1162(13)	4913(18)	54(6)
H(9)	9830(26)	2210(14)	2927(19)	60(6)
H(10)	7101(22)	2161(12)	1138(17)	43(5)
H(11)	4691(22)	1079(12)	1997(17)	40(5)
H(12)	8079(20)	595(12)	2451(16)	38(5)
H(13A)	3172(25)	2459(16)	4324(20)	60(7)
H(13B)	3345(32)	1455(18)	4614(25)	83(9)
H(13C)	2705(31)	1753(17)	3363(24)	81(8)
H(14)	4910(26)	3925(15)	3986(20)	59(7)
H(15)	4797(24)	3657(12)	6061(18)	43(5)
H(17)	5887(21)	4489(11)	7647(16)	33(5)
H(18)	7483(23)	5615(13)	8294(19)	47(6)
H(19)	9116(22)	6297(13)	7079(17)	42(5)
H(20)	9026(21)	5793(12)	5127(17)	35(5)
H(21)	7442(20)	4669(11)	4479(17)	32(5)

C11 CRYSTAL DATA FOR PhCbNHNHTol - 28

Crystals of **28** were grown by cooling a warm hexane solution to room temperature. The structure was solved by Prof. W. Clegg and Dr. M.R.J. Elsegood at Newcastle University. The molecular structure is shown below, bond lengths, angles and atomic coordinates are shown on the following pages. The molecules pack in well separated stacks with no unusually short intermolecular contacts (see Figure on next page).

The C-N distance to the carborane cage (1.401(2)Å) and the C-C cluster bond (1.778(3)Å) are similar to those in MeCbNHNHPh **27** (1.387(2)Å and 1.770(2)Å respectively). They are also close to the bond lengths (C-N 1.41Å and C-C 1.77Å) which can be predicted using the ^{11}B NMR shift of the antipodal atom and the relationships illustrated in Figures 4.30 and 4.32 (see pages 127 and 128). The conformations are similar in that the lone pair on the nitrogen attached to the cage lies in the N-C1-C2 plane.

The major difference between **27** and **28** lies in the position of the phenyl or tolyl group bonded to the other nitrogen atom. In **27** the phenyl groups points away from the methyl group on C2. In **28**, however, the tolyl group points towards the phenyl on C2. This may be due to crystal packing effects or CH···π bonding between the ortho-CH or the tolyl group and the π-system of the phenyl group.

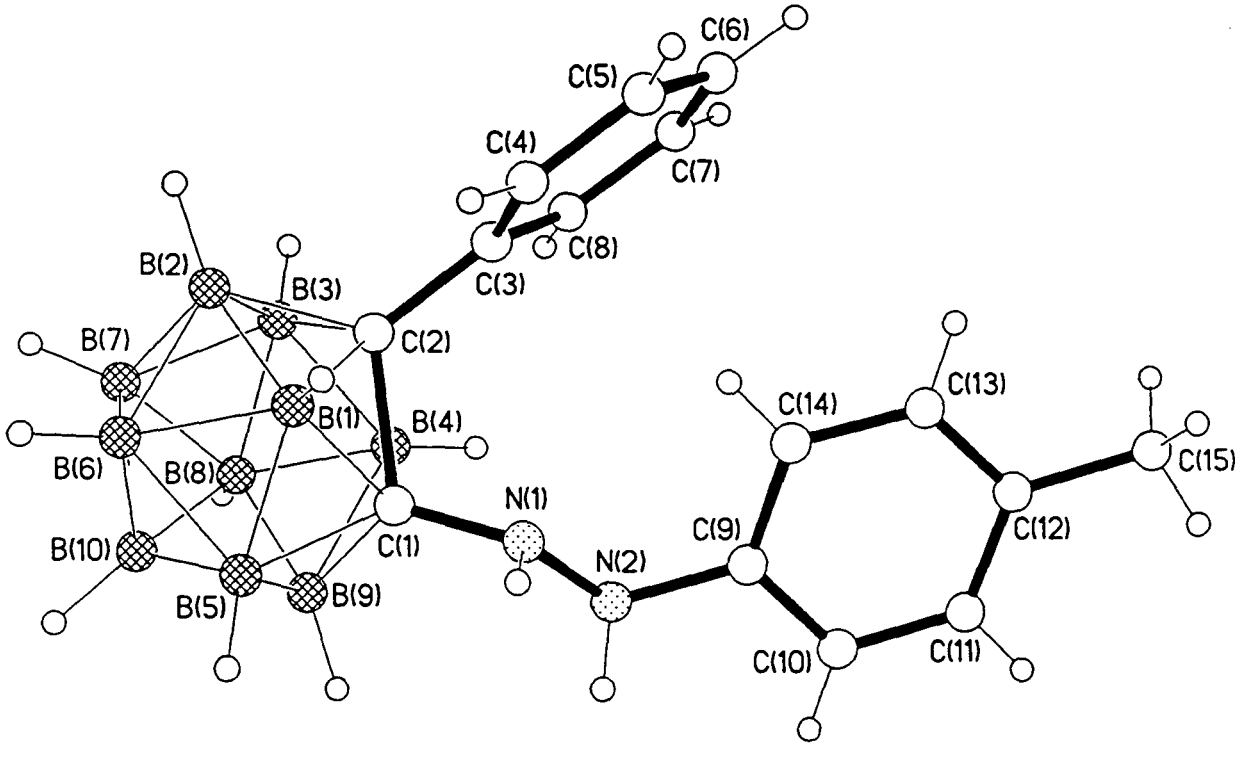

Empirical Formula	$C_{15}H_{24}B_{10}N_2$	
Temperature	160(2)K	
Wavelength	0.71073Å	
Crystal System	Monoclinic	
Space Group	$P2_1/c$	
Unit Cell Dimensions	a = 11.753(6)Å	alpha = 90°
	b = 7.617(4)Å	beta = 104.74(6)°
	c = 21.899(13)Å	gamma = 90°
Crystal Size	0.52 × 0.42 × 0.27 mm	
Final R indices [I>2σ(I)]	R1 = 0.0489	wR2 = 0.1239
R indices (all data)	R1 = 0.0632	wR2 = 0.1369

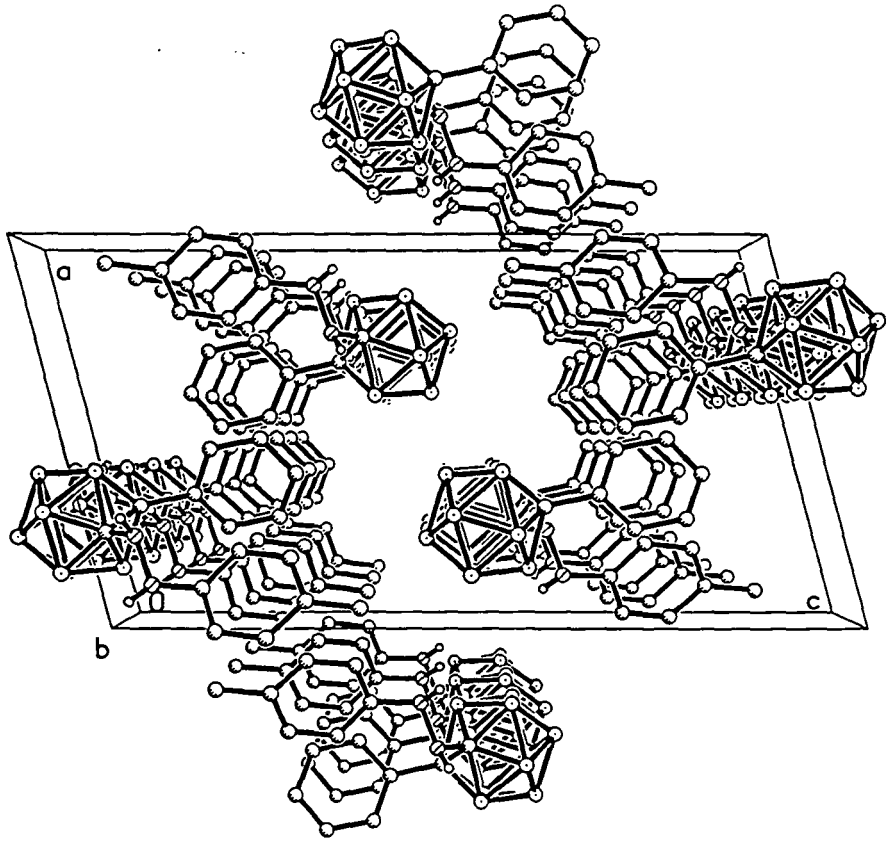

Table 3. Bond lengths (Å) and angles (°) for kw57.

C(1)-N(1)	1.401(2)	C(1)-B(9)	1.705(3)
C(1)-B(5)	1.711(3)	C(1)-B(4)	1.714(3)
C(1)-B(1)	1.724(3)	C(1)-C(2)	1.778(3)
C(2)-C(3)	1.497(3)	C(2)-B(3)	1.684(3)
C(2)-B(2)	1.706(3)	C(2)-B(1)	1.734(3)
C(2)-B(4)	1.739(3)	C(3)-C(4)	1.394(3)
C(3)-C(8)	1.398(3)	C(4)-C(5)	1.390(3)
C(5)-C(6)	1.385(3)	C(6)-C(7)	1.385(3)
C(7)-C(8)	1.383(3)	N(1)-N(2)	1.409(2)
N(2)-C(9)	1.421(3)	C(9)-C(14)	1.390(3)
C(9)-C(10)	1.392(3)	C(10)-C(11)	1.390(3)
C(11)-C(12)	1.390(3)	C(12)-C(13)	1.390(3)
C(12)-C(15)	1.508(3)	C(13)-C(14)	1.389(3)
B(1)-B(6)	1.773(3)	B(1)-B(2)	1.785(3)
B(1)-B(5)	1.786(3)	B(2)-B(6)	1.780(3)
B(2)-B(3)	1.786(3)	B(2)-B(7)	1.788(3)
B(3)-B(8)	1.780(3)	B(3)-B(7)	1.782(3)
B(3)-B(4)	1.784(3)	B(4)-B(8)	1.775(3)
B(4)-B(9)	1.786(3)	B(5)-B(6)	1.773(3)
B(5)-B(10)	1.778(3)	B(5)-B(9)	1.784(3)
B(6)-B(10)	1.784(3)	B(6)-B(7)	1.791(3)
B(7)-B(10)	1.774(3)	B(7)-B(8)	1.797(3)
B(8)-B(9)	1.774(3)	B(8)-B(10)	1.785(3)
B(9)-B(10)	1.789(3)		

N(1)-C(1)-B(9)	126.25(15)	N(1)-C(1)-B(5)	122.62(15)
B(9)-C(1)-B(5)	62.96(12)	N(1)-C(1)-B(4)	119.08(15)
B(9)-C(1)-B(4)	62.98(12)	B(5)-C(1)-B(4)	113.82(14)
N(1)-C(1)-B(1)	113.62(15)	B(9)-C(1)-B(1)	113.78(14)
B(5)-C(1)-B(1)	62.62(12)	B(4)-C(1)-B(1)	110.98(14)
N(1)-C(1)-C(2)	115.17(14)	B(9)-C(1)-C(2)	109.90(14)
B(5)-C(1)-C(2)	109.37(13)	B(4)-C(1)-C(2)	59.69(11)
B(1)-C(1)-C(2)	59.31(11)	C(3)-C(2)-B(3)	122.29(15)
C(3)-C(2)-B(2)	123.51(15)	B(3)-C(2)-B(2)	63.59(12)
C(3)-C(2)-B(1)	119.10(15)	B(3)-C(2)-B(1)	113.24(14)
B(2)-C(2)-B(1)	62.52(12)	C(3)-C(2)-B(4)	116.45(15)
B(3)-C(2)-B(4)	62.78(12)	B(2)-C(2)-B(4)	113.97(14)
B(1)-C(2)-B(4)	109.37(14)	C(3)-C(2)-C(1)	118.16(14)
B(3)-C(2)-C(1)	108.41(14)	B(2)-C(2)-C(1)	108.90(13)
B(1)-C(2)-C(1)	58.80(10)	B(4)-C(2)-C(1)	58.32(11)
C(4)-C(3)-C(8)	119.04(17)	C(4)-C(3)-C(2)	120.98(17)
C(8)-C(3)-C(2)	119.96(17)	C(5)-C(4)-C(3)	119.98(18)
C(6)-C(5)-C(4)	120.5(2)	C(5)-C(6)-C(7)	119.66(18)
C(8)-C(7)-C(6)	120.27(19)	C(7)-C(8)-C(3)	120.45(19)
C(1)-N(1)-N(2)	116.43(15)	N(1)-N(2)-C(9)	115.73(16)
C(14)-C(9)-C(10)	119.13(17)	C(14)-C(9)-N(2)	122.13(17)
C(10)-C(9)-N(2)	118.64(17)	C(11)-C(10)-C(9)	120.28(19)
C(10)-C(11)-C(12)	121.37(18)	C(11)-C(12)-C(13)	117.49(18)
C(11)-C(12)-C(15)	121.53(18)	C(13)-C(12)-C(15)	120.98(19)
C(14)-C(13)-C(12)	122.04(19)	C(13)-C(14)-C(9)	119.67(17)
C(1)-B(1)-C(2)	61.89(11)	C(1)-B(1)-B(6)	105.47(15)
C(2)-B(1)-B(6)	105.47(15)	C(1)-B(1)-B(2)	107.74(14)
C(2)-B(1)-B(2)	57.96(11)	B(6)-B(1)-B(2)	60.04(12)
C(1)-B(1)-B(5)	58.33(11)	C(2)-B(1)-B(5)	108.02(14)
B(6)-B(1)-B(5)	59.77(12)	B(2)-B(1)-B(5)	108.53(15)
C(2)-B(2)-B(6)	106.37(15)	C(2)-B(2)-B(1)	59.51(11)
B(6)-B(2)-B(1)	59.64(12)	C(2)-B(2)-B(3)	57.63(11)
B(6)-B(2)-B(3)	107.51(15)	B(1)-B(2)-B(3)	106.13(14)

C(2)-B(2)-B(7)	105.31(14)	B(6)-B(2)-B(7)	60.28(12)
B(1)-B(2)-B(7)	107.24(15)	B(3)-B(2)-B(7)	59.82(12)
C(2)-B(3)-B(8)	107.21(16)	C(2)-B(3)-B(7)	106.48(14)
B(8)-B(3)-B(7)	60.62(12)	C(2)-B(3)-B(4)	60.10(12)
B(8)-B(3)-B(4)	59.75(12)	B(7)-B(3)-B(4)	108.13(15)
C(2)-B(3)-B(2)	58.78(11)	B(8)-B(3)-B(2)	108.68(15)
B(7)-B(3)-B(2)	60.14(12)	B(4)-B(3)-B(2)	108.01(15)
C(1)-B(4)-C(2)	61.99(11)	C(1)-B(4)-B(8)	105.23(14)
C(2)-B(4)-B(8)	105.06(15)	C(1)-B(4)-B(3)	106.84(14)
C(2)-B(4)-B(3)	57.11(11)	B(8)-B(4)-B(3)	60.01(12)
C(1)-B(4)-B(9)	58.27(12)	C(2)-B(4)-B(9)	108.01(14)
B(8)-B(4)-B(9)	59.77(12)	B(3)-B(4)-B(9)	108.13(15)
C(1)-B(5)-B(6)	106.02(15)	C(1)-B(5)-B(10)	105.39(14)
B(6)-B(5)-B(10)	60.34(13)	C(1)-B(5)-B(9)	58.35(12)
B(6)-B(5)-B(9)	108.60(16)	B(10)-B(5)-B(9)	60.30(12)
C(1)-B(5)-B(1)	59.05(11)	B(6)-B(5)-B(1)	59.76(12)
B(10)-B(5)-B(1)	107.43(16)	B(9)-B(5)-B(1)	107.17(15)
B(1)-B(6)-B(5)	60.48(12)	B(1)-B(6)-B(2)	60.32(12)
B(5)-B(6)-B(2)	109.32(14)	B(1)-B(6)-B(10)	107.70(15)
B(5)-B(6)-B(10)	59.96(12)	B(2)-B(6)-B(10)	108.13(15)
B(1)-B(6)-B(7)	107.61(14)	B(5)-B(6)-B(7)	107.95(15)
B(2)-B(6)-B(7)	60.08(12)	B(10)-B(6)-B(7)	59.48(12)
B(10)-B(7)-B(3)	107.78(15)	B(10)-B(7)-B(2)	108.23(16)
B(3)-B(7)-B(2)	60.04(12)	B(10)-B(7)-B(6)	60.06(13)
B(3)-B(7)-B(6)	107.18(15)	B(2)-B(7)-B(6)	59.64(12)
B(10)-B(7)-B(8)	59.97(12)	B(3)-B(7)-B(8)	59.62(12)
B(2)-B(7)-B(8)	107.81(15)	B(6)-B(7)-B(8)	107.37(16)
B(9)-B(8)-B(4)	60.43(12)	B(9)-B(8)-B(3)	108.84(15)
B(4)-B(8)-B(3)	60.24(12)	B(9)-B(8)-B(10)	60.35(12)
B(4)-B(8)-B(10)	107.95(15)	B(3)-B(8)-B(10)	107.41(15)
B(9)-B(8)-B(7)	108.26(15)	B(4)-B(8)-B(7)	107.84(15)
B(3)-B(8)-B(7)	59.76(12)	B(10)-B(8)-B(7)	59.36(12)
C(1)-B(9)-B(8)	105.63(15)	C(1)-B(9)-B(5)	58.69(12)
B(8)-B(9)-B(5)	107.80(15)	C(1)-B(9)-B(4)	58.75(12)
B(8)-B(9)-B(4)	59.80(12)	B(5)-B(9)-B(4)	107.00(15)
C(1)-B(9)-B(10)	105.16(14)	B(8)-B(9)-B(10)	60.12(12)
B(5)-B(9)-B(10)	59.67(12)	B(4)-B(9)-B(10)	107.28(15)
B(7)-B(10)-B(5)	108.52(16)	B(7)-B(10)-B(6)	60.46(12)
B(5)-B(10)-B(6)	59.70(12)	B(7)-B(10)-B(8)	60.67(12)
B(5)-B(10)-B(8)	107.60(15)	B(6)-B(10)-B(8)	108.22(15)
B(7)-B(10)-B(9)	108.65(15)	B(5)-B(10)-B(9)	60.02(12)
B(6)-B(10)-B(9)	107.87(15)	B(8)-B(10)-B(9)	59.53(12)

Table 2. Atomic coordinates (x 10^4) and equivalent isotropic displacement parameters ($Å^2$ x 10^3) for kw57. U(eq) is defined as one third of the trace of the orthogonalized U_{ij} tensor.

	x	y	z	U(eq)
C(1)	2687.0(15)	-886(2)	659.3(8)	22.5(4)
C(2)	3268.6(15)	-2833(2)	1069.4(8)	22.1(4)
C(3)	3553.8(16)	-2818(2)	1775.8(8)	23.7(4)
C(4)	4622.0(16)	-2154(2)	2132.7(9)	26.5(4)
C(5)	4854.3(18)	-2109(3)	2787.3(9)	31.3(5)
C(6)	4040.4(19)	-2749(3)	3090.7(9)	33.1(5)
C(7)	2996.3(19)	-3469(3)	2738.9(9)	34.2(5)
C(8)	2753.7(17)	-3512(3)	2087.1(9)	29.8(4)
N(1)	2635.2(13)	568(2)	1043.7(7)	26.8(4)
N(2)	1511.2(13)	1037(2)	1107.7(8)	27.3(4)
C(9)	1464.0(15)	1619(2)	1717.4(9)	25.0(4)
C(10)	517.5(16)	2653(3)	1771.3(9)	30.2(4)
C(11)	391.1(17)	3130(3)	2363.0(10)	32.0(5)
C(12)	1203.1(16)	2610(2)	2912.7(9)	28.7(4)
C(13)	2153.8(16)	1605(3)	2848.8(9)	29.6(4)
C(14)	2294.0(16)	1109(2)	2261.8(9)	27.4(4)
C(15)	1065(2)	3115(3)	3555.9(10)	42.7(6)
B(1)	4101.2(17)	-1559(3)	689.5(9)	22.7(4)
B(2)	4097.1(18)	-3899(3)	649.7(10)	24.9(5)
B(3)	2636.7(18)	-4572(3)	639.7(10)	25.9(5)
B(4)	1789.6(17)	-2649(3)	675.0(10)	24.4(5)
B(5)	3146.1(17)	-729(3)	-20.3(9)	25.4(5)
B(6)	4012.8(18)	-2623(3)	-41.1(10)	25.8(5)
B(7)	3088.6(18)	-4510(3)	-77.5(10)	27.7(5)
B(8)	1653.9(18)	-3738(3)	-56.6(10)	27.0(5)
B(9)	1689.7(18)	-1411(3)	-29.2(10)	25.9(5)
B(10)	2513.0(18)	-2564(3)	-485.8(10)	27.5(5)

Table 5. Hydrogen atom coordinates (x 10^4) and isotropic displacement parameters ($Å^2$ x 10^3) for kw57.

	x	y	z	U
H(4)	5191	-1732	1928	32
H(5)	5577	-1636	3028	38
H(6)	4197	-2694	3538	40
H(7)	2445	-3935	2946	41
H(8)	2038	-4016	1849	36
H(1)	3049(18)	1465(30)	962(10)	32
H(2)	1150(19)	1737(30)	818(10)	33
H(10)	-44	3034	1402	36
H(11)	-264	3825	2392	38
H(13)	2725	1247	3218	36
H(14)	2954	425	2233	33
H(15A)	391	3908	3508	64
H(15B)	1780	3708	3794	64
H(15C)	933	2057	3783	64
H(1A)	4893	-808	954	27
H(2A)	4892	-4705	871	30
H(3A)	2459	-5840	857	31
H(4A)	1074	-2619	929	29
H(5A)	3321	543	-236	30
H(6A)	4759	-2592	-273	31
H(7A)	3214	-5734	-336	33
H(8A)	831	-4457	-298	32
H(9A)	900	-594	-251	31
H(10A)	2265	-2517	-1014	33

C12 CRYSTAL DATA FOR PhCbNH$_2$ - 32

Empirical Formula	$C_9H_{20}B_{10}N_2$	
Temperature	160(2)K	
Wavelength	0.71073Å	
Crystal System	Monoclinic	
Space Group	P2(1)/n	
Unit Cell Dimensions	a = 10.6738(7)Å	alpha = 90°
	b = 22.3100(16)Å	beta = 102.677(2)°
	c = 23.3165(16)Å	gamma = 90°
Crystal Size	0.70 × 0.50 × 0.25 mm	
Final R indices [I>2σ(I)]	R1 = 0.0691	wR2 = 0.1952
R indices (all data)	R1 = 0.1071	wR2 = 0.2193

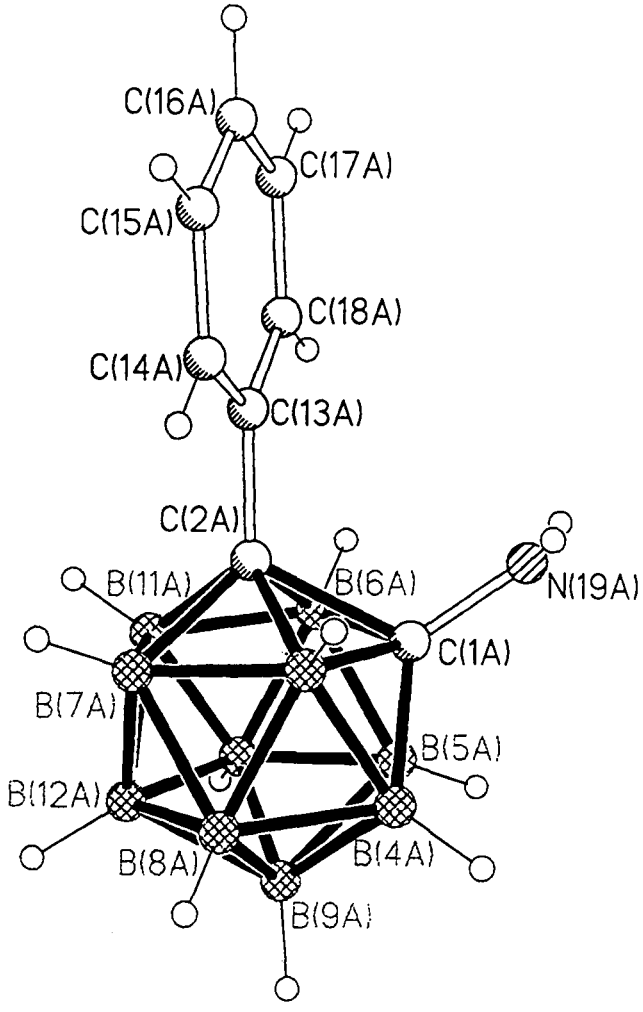

Table 3. Bond lengths (Å) and angles (°) for kw54.

C(1A)-N(19A)	1.392(3)	C(1A)-B(5A)	1.694(3)
C(1A)-B(4A)	1.696(3)	C(1A)-B(3A)	1.719(3)
C(1A)-B(6A)	1.720(3)	C(1A)-C(2A)	1.785(3)
C(2A)-C(13A)	1.501(3)	C(2A)-B(11A)	1.696(3)
C(2A)-B(7A)	1.697(3)	C(2A)-B(6A)	1.717(3)
C(2A)-B(3A)	1.729(3)	B(3A)-B(4A)	1.770(3)
B(3A)-B(8A)	1.778(3)	B(3A)-B(7A)	1.799(3)
B(4A)-B(9A)	1.768(3)	B(4A)-B(8A)	1.773(4)
B(4A)-B(5A)	1.784(4)	B(5A)-B(10A)	1.757(4)
B(5A)-B(6A)	1.768(4)	B(5A)-B(9A)	1.775(3)
B(6A)-B(10A)	1.763(3)	B(6A)-B(11A)	1.782(4)
B(7A)-B(12A)	1.770(3)	B(7A)-B(11A)	1.778(3)
B(7A)-B(8A)	1.779(3)	B(8A)-B(9A)	1.777(4)
B(8A)-B(12A)	1.788(3)	B(9A)-B(12A)	1.763(3)
B(9A)-B(10A)	1.786(4)	B(10A)-B(11A)	1.767(3)
B(10A)-B(12A)	1.790(4)	B(11A)-B(12A)	1.780(3)
C(13A)-C(18A)	1.388(3)	C(13A)-C(14A)	1.395(3)
C(14A)-C(15A)	1.384(3)	C(15A)-C(16A)	1.390(4)
C(16A)-C(17A)	1.372(4)	C(17A)-C(18A)	1.395(3)
N(19A)-H(2A)	0.964(14)	N(19A)-H(1A)	0.973(14)
C(1B)-N(19B)	1.403(3)	C(1B)-B(4B)	1.687(3)
C(1B)-B(5B)	1.695(4)	C(1B)-B(6B)	1.698(3)
C(1B)-B(3B)	1.700(4)	C(1B)-C(2B)	1.765(3)
C(2B)-C(13B)	1.498(3)	C(2B)-B(7B)	1.682(3)
C(2B)-B(11B)	1.686(3)	C(2B)-B(3B)	1.710(3)
C(2B)-B(6B)	1.717(3)	B(3B)-B(8B)	1.763(4)
B(3B)-B(4B)	1.774(4)	B(3B)-B(7B)	1.788(4)
B(4B)-B(5B)	1.755(4)	B(4B)-B(8B)	1.764(4)
B(4B)-B(9B)	1.764(3)	B(5B)-B(10B)	1.737(4)
B(5B)-B(6B)	1.761(3)	B(5B)-B(9B)	1.763(4)
B(6B)-B(10B)	1.747(4)	B(6B)-B(11B)	1.755(4)
B(7B)-B(11B)	1.763(4)	B(7B)-B(12B)	1.779(4)
B(7B)-B(8B)	1.779(4)	B(8B)-B(9B)	1.771(4)
B(8B)-B(12B)	1.801(4)	B(9B)-B(12B)	1.759(4)
B(9B)-B(10B)	1.773(4)	B(10B)-B(12B)	1.771(4)
B(10B)-B(11B)	1.775(4)	B(11B)-B(12B)	1.767(4)
C(13B)-C(14B)	1.389(3)	C(13B)-C(18B)	1.395(3)
C(14B)-C(15B)	1.391(3)	C(15B)-C(16B)	1.376(3)
C(16B)-C(17B)	1.380(3)	C(17B)-C(18B)	1.392(3)
C(1C)-N(19C)	1.391(3)	C(1C)-B(5C)	1.696(3)
C(1C)-B(4C)	1.708(3)	C(1C)-B(3C)	1.712(3)
C(1C)-B(6C)	1.731(3)	C(1C)-C(2C)	1.745(3)
C(2C)-C(13C)	1.506(3)	C(2C)-B(11C)	1.700(3)
C(2C)-B(7C)	1.703(3)	C(2C)-B(6C)	1.707(3)
C(2C)-B(3C)	1.748(3)	B(3C)-B(8C)	1.768(3)
B(3C)-B(4C)	1.771(3)	B(3C)-B(7C)	1.786(3)
B(4C)-B(5C)	1.773(4)	B(4C)-B(8C)	1.777(3)
B(4C)-B(9C)	1.778(3)	B(5C)-B(10C)	1.776(4)
B(5C)-B(6C)	1.776(3)	B(5C)-B(9C)	1.780(4)
B(6C)-B(10C)	1.766(3)	B(6C)-B(11C)	1.774(3)
B(7C)-B(11C)	1.769(3)	B(7C)-B(12C)	1.773(4)
B(7C)-B(8C)	1.784(3)	B(8C)-B(12C)	1.785(4)
B(8C)-B(9C)	1.786(4)	B(9C)-B(12C)	1.778(4)
B(9C)-B(10C)	1.789(4)	B(10C)-B(11C)	1.781(4)
B(10C)-B(12C)	1.789(4)	B(11C)-B(12C)	1.778(3)
C(13C)-C(18C)	1.391(3)	C(13C)-C(14C)	1.393(3)
C(14C)-C(15C)	1.387(3)	C(15C)-C(16C)	1.371(3)
C(16C)-C(17C)	1.370(3)	C(17C)-C(18C)	1.390(3)

N(19C)-H(2C)	1.027(14)	N(19C)-H(1C)	1.038(14)
C(1D)-N(19D)	1.404(3)	C(1D)-B(5D)	1.701(3)
C(1D)-B(4D)	1.712(3)	C(1D)-B(3D)	1.712(3)
C(1D)-B(6D)	1.729(3)	C(1D)-C(2D)	1.774(3)
C(2D)-C(13D)	1.498(3)	C(2D)-B(7D)	1.695(3)
C(2D)-B(11D)	1.696(3)	C(2D)-B(6D)	1.716(3)
C(2D)-B(3D)	1.732(3)	B(3D)-B(8D)	1.766(3)
B(3D)-B(4D)	1.775(3)	B(3D)-B(7D)	1.781(4)
B(4D)-B(8D)	1.763(4)	B(4D)-B(9D)	1.770(4)
B(4D)-B(5D)	1.778(3)	B(5D)-B(9D)	1.772(4)
B(5D)-B(10D)	1.777(4)	B(5D)-B(6D)	1.789(3)
B(6D)-B(10D)	1.765(3)	B(6D)-B(11D)	1.768(3)
B(7D)-B(12D)	1.766(3)	B(7D)-B(11D)	1.777(3)
B(7D)-B(8D)	1.787(4)	B(8D)-B(9D)	1.775(4)
B(8D)-B(12D)	1.783(4)	B(9D)-B(10D)	1.776(4)
B(9D)-B(12D)	1.779(4)	B(10D)-B(11D)	1.779(3)
B(10D)-B(12D)	1.789(3)	B(11D)-B(12D)	1.778(4)
C(13D)-C(18D)	1.383(3)	C(13D)-C(14D)	1.389(3)
C(14D)-C(15D)	1.383(3)	C(15D)-C(16D)	1.373(4)
C(16D)-C(17D)	1.376(3)	C(17D)-C(18D)	1.383(3)
N(19D)-H(2D)	1.015(14)	N(19D)-H(1D)	1.021(14)

N(19A)-C(1A)-B(5A)	122.11(18)	N(19A)-C(1A)-B(4A)	123.50(18)
B(5A)-C(1A)-B(4A)	63.52(14)	N(19A)-C(1A)-B(3A)	118.75(18)
B(5A)-C(1A)-B(3A)	113.55(16)	B(4A)-C(1A)-B(3A)	62.46(14)
N(19A)-C(1A)-B(6A)	116.69(18)	B(5A)-C(1A)-B(6A)	62.39(14)
B(4A)-C(1A)-B(6A)	113.52(16)	B(3A)-C(1A)-B(6A)	109.97(16)
N(19A)-C(1A)-C(2A)	118.49(16)	B(5A)-C(1A)-C(2A)	108.34(15)
B(4A)-C(1A)-C(2A)	108.65(15)	B(3A)-C(1A)-C(2A)	59.08(12)
B(6A)-C(1A)-C(2A)	58.62(12)	C(13A)-C(2A)-B(11A)	123.46(17)
C(13A)-C(2A)-B(7A)	121.49(17)	B(11A)-C(2A)-B(7A)	63.20(13)
C(13A)-C(2A)-B(6A)	119.19(17)	B(11A)-C(2A)-B(6A)	62.97(14)
B(7A)-C(2A)-B(6A)	113.74(16)	C(13A)-C(2A)-B(3A)	116.08(17)
B(11A)-C(2A)-B(3A)	114.06(16)	B(7A)-C(2A)-B(3A)	63.37(13)
B(6A)-C(2A)-B(3A)	109.63(16)	C(13A)-C(2A)-C(1A)	118.12(15)
B(11A)-C(2A)-C(1A)	109.25(15)	B(7A)-C(2A)-C(1A)	109.27(14)
B(6A)-C(2A)-C(1A)	58.78(13)	B(3A)-C(2A)-C(1A)	58.53(12)
C(1A)-B(3A)-C(2A)	62.39(13)	C(1A)-B(3A)-B(4A)	58.13(13)
C(2A)-B(3A)-B(4A)	107.86(17)	C(1A)-B(3A)-B(8A)	105.72(16)
C(2A)-B(3A)-B(8A)	105.07(16)	B(4A)-B(3A)-B(8A)	59.95(13)
C(1A)-B(3A)-B(7A)	107.65(16)	C(2A)-B(3A)-B(7A)	57.46(12)
B(4A)-B(3A)-B(7A)	107.98(16)	B(8A)-B(3A)-B(7A)	59.65(13)
C(1A)-B(4A)-B(9A)	105.66(17)	C(1A)-B(4A)-B(3A)	59.41(13)
B(9A)-B(4A)-B(3A)	107.63(17)	C(1A)-B(4A)-B(8A)	106.95(16)
B(9A)-B(4A)-B(8A)	60.26(14)	B(3A)-B(4A)-B(8A)	60.23(13)
C(1A)-B(4A)-B(5A)	58.20(13)	B(9A)-B(4A)-B(5A)	59.95(14)
B(3A)-B(4A)-B(5A)	106.87(17)	B(8A)-B(4A)-B(5A)	108.21(17)
C(1A)-B(5A)-B(10A)	106.91(17)	C(1A)-B(5A)-B(6A)	59.53(13)
B(10A)-B(5A)-B(6A)	60.01(14)	C(1A)-B(5A)-B(9A)	105.41(17)
B(10A)-B(5A)-B(9A)	60.74(14)	B(6A)-B(5A)-B(9A)	107.73(17)
C(1A)-B(5A)-B(4A)	58.28(13)	B(10A)-B(5A)-B(4A)	108.37(18)
B(6A)-B(5A)-B(4A)	107.05(17)	B(9A)-B(5A)-B(4A)	59.56(14)
C(2A)-B(6A)-C(1A)	62.59(13)	C(2A)-B(6A)-B(10A)	105.31(17)
C(1A)-B(6A)-B(10A)	105.50(17)	C(2A)-B(6A)-B(5A)	108.09(17)
C(1A)-B(6A)-B(5A)	58.09(13)	B(10A)-B(6A)-B(5A)	59.67(14)
C(2A)-B(6A)-B(11A)	57.93(13)	C(1A)-B(6A)-B(11A)	108.29(17)
B(10A)-B(6A)-B(11A)	59.80(14)	B(5A)-B(6A)-B(11A)	108.26(17)
C(2A)-B(7A)-B(12A)	105.73(16)	C(2A)-B(7A)-B(11A)	58.37(12)
B(12A)-B(7A)-B(11A)	60.24(13)	C(2A)-B(7A)-B(8A)	106.36(16)
B(12A)-B(7A)-B(8A)	60.49(13)	B(11A)-B(7A)-B(8A)	108.54(17)
C(2A)-B(7A)-B(3A)	59.17(12)	B(12A)-B(7A)-B(3A)	107.29(16)
B(11A)-B(7A)-B(3A)	106.86(16)	B(8A)-B(7A)-B(3A)	59.57(13)

B(4A)-B(8A)-B(9A)	59.73(14)	B(4A)-B(8A)-B(3A)	59.81(13)
B(9A)-B(8A)-B(3A)	106.88(17)	B(4A)-B(8A)-B(7A)	108.78(16)
B(9A)-B(8A)-B(7A)	107.15(17)	B(3A)-B(8A)-B(7A)	60.79(13)
B(4A)-B(8A)-B(12A)	107.55(18)	B(9A)-B(8A)-B(12A)	59.27(14)
B(3A)-B(8A)-B(12A)	107.46(16)	B(7A)-B(8A)-B(12A)	59.50(13)
B(12A)-B(9A)-B(4A)	108.89(17)	B(12A)-B(9A)-B(5A)	108.42(17)
B(4A)-B(9A)-B(5A)	60.48(14)	B(12A)-B(9A)-B(8A)	60.66(14)
B(4A)-B(9A)-B(8A)	60.01(14)	B(5A)-B(9A)-B(8A)	108.43(16)
B(12A)-B(9A)-B(10A)	60.60(14)	B(4A)-B(9A)-B(10A)	107.82(17)
B(5A)-B(9A)-B(10A)	59.13(14)	B(8A)-B(9A)-B(10A)	108.52(17)
B(5A)-B(10A)-B(6A)	60.32(14)	B(5A)-B(10A)-B(11A)	109.46(17)
B(6A)-B(10A)-B(11A)	60.65(14)	B(5A)-B(10A)-B(9A)	60.13(14)
B(6A)-B(10A)-B(9A)	107.49(17)	B(11A)-B(10A)-B(9A)	107.68(17)
B(5A)-B(10A)-B(12A)	108.00(18)	B(6A)-B(10A)-B(12A)	107.80(17)
B(11A)-B(10A)-B(12A)	60.04(13)	B(9A)-B(10A)-B(12A)	59.07(14)
C(2A)-B(11A)-B(10A)	106.03(17)	C(2A)-B(11A)-B(7A)	58.44(12)
B(10A)-B(11A)-B(7A)	108.08(17)	C(2A)-B(11A)-B(12A)	105.33(17)
B(10A)-B(11A)-B(12A)	60.62(14)	B(7A)-B(11A)-B(12A)	59.67(13)
C(2A)-B(11A)-B(6A)	59.10(13)	B(10A)-B(11A)-B(6A)	59.55(13)
B(7A)-B(11A)-B(6A)	106.85(17)	B(12A)-B(11A)-B(6A)	107.39(17)
B(9A)-B(12A)-B(7A)	108.19(16)	B(9A)-B(12A)-B(11A)	108.12(17)
B(7A)-B(12A)-B(11A)	60.10(13)	B(9A)-B(12A)-B(8A)	60.06(14)
B(7A)-B(12A)-B(8A)	60.01(13)	B(11A)-B(12A)-B(8A)	108.04(16)
B(9A)-B(12A)-B(10A)	60.33(14)	B(7A)-B(12A)-B(10A)	107.41(16)
B(11A)-B(12A)-B(10A)	59.34(13)	B(8A)-B(12A)-B(10A)	107.84(17)
C(18A)-C(13A)-C(14A)	119.4(2)	C(18A)-C(13A)-C(2A)	121.6(2)
C(14A)-C(13A)-C(2A)	118.9(2)	C(15A)-C(14A)-C(13A)	120.5(2)
C(14A)-C(15A)-C(16A)	119.9(2)	C(17A)-C(16A)-C(15A)	119.7(2)
C(16A)-C(17A)-C(18A)	121.0(3)	C(13A)-C(18A)-C(17A)	119.5(2)
H(2A)-N(19A)-H(1A)	127.1(17)	H(2A)-N(19A)-C(1A)	118.5(12)
H(1A)-N(19A)-C(1A)	112.9(11)	N(19B)-C(1B)-B(4B)	124.93(19)
N(19B)-C(1B)-B(5B)	123.5(2)	B(4B)-C(1B)-B(5B)	62.54(15)
N(19B)-C(1B)-B(6B)	115.9(2)	B(4B)-C(1B)-B(6B)	113.14(17)
B(5B)-C(1B)-B(6B)	62.52(14)	N(19B)-C(1B)-B(3B)	118.0(2)
B(4B)-C(1B)-B(3B)	63.16(16)	B(5B)-C(1B)-B(3B)	113.47(18)
B(6B)-C(1B)-B(3B)	110.35(18)	N(19B)-C(1B)-C(2B)	115.93(17)
B(4B)-C(1B)-C(2B)	109.57(17)	B(5B)-C(1B)-C(2B)	109.36(16)
B(6B)-C(1B)-C(2B)	59.43(12)	B(3B)-C(1B)-C(2B)	59.12(13)
C(13B)-C(2B)-B(7B)	123.44(18)	C(13B)-C(2B)-B(11B)	122.27(17)
B(7B)-C(2B)-B(11B)	63.14(16)	C(13B)-C(2B)-B(3B)	118.66(17)
B(7B)-C(2B)-B(3B)	63.60(16)	B(11B)-C(2B)-B(3B)	113.83(17)
C(13B)-C(2B)-B(6B)	117.37(17)	B(7B)-C(2B)-B(6B)	112.79(17)
B(11B)-C(2B)-B(6B)	62.07(14)	B(3B)-C(2B)-B(6B)	108.96(17)
C(13B)-C(2B)-C(1B)	118.15(15)	B(7B)-C(2B)-C(1B)	109.27(16)
B(11B)-C(2B)-C(1B)	108.41(15)	B(3B)-C(2B)-C(1B)	58.56(14)
B(6B)-C(2B)-C(1B)	58.36(13)	C(1B)-B(3B)-C(2B)	62.32(13)
C(1B)-B(3B)-B(8B)	105.56(18)	C(2B)-B(3B)-B(8B)	105.59(19)
C(1B)-B(3B)-B(4B)	58.06(15)	C(2B)-B(3B)-B(4B)	108.09(18)
B(8B)-B(3B)-B(4B)	59.85(15)	C(1B)-B(3B)-B(7B)	107.38(18)
C(2B)-B(3B)-B(7B)	57.44(14)	B(8B)-B(3B)-B(7B)	60.13(16)
B(4B)-B(3B)-B(7B)	108.19(19)	C(1B)-B(4B)-B(5B)	58.95(15)
C(1B)-B(4B)-B(8B)	106.06(18)	B(5B)-B(4B)-B(8B)	108.22(19)
C(1B)-B(4B)-B(9B)	106.02(18)	B(5B)-B(4B)-B(9B)	60.13(15)
B(8B)-B(4B)-B(9B)	60.26(16)	C(1B)-B(4B)-B(3B)	58.78(14)
B(5B)-B(4B)-B(3B)	107.09(17)	B(8B)-B(4B)-B(3B)	59.77(16)
B(9B)-B(4B)-B(3B)	107.50(19)	C(1B)-B(5B)-B(10B)	106.57(17)
C(1B)-B(5B)-B(4B)	58.51(14)	B(10B)-B(5B)-B(4B)	109.07(19)
C(1B)-B(5B)-B(6B)	58.83(14)	B(10B)-B(5B)-B(6B)	59.95(15)
B(4B)-B(5B)-B(6B)	106.93(18)	C(1B)-B(5B)-B(9B)	105.73(19)
B(10B)-B(5B)-B(9B)	60.87(15)	B(4B)-B(5B)-B(9B)	60.19(14)
B(6B)-B(5B)-B(9B)	107.65(18)	C(1B)-B(6B)-C(2B)	62.21(14)
C(1B)-B(6B)-B(10B)	105.94(17)	C(2B)-B(6B)-B(10B)	106.45(18)

C(1B)-B(6B)-B(11B)	108.30(18)	C(2B)-B(6B)-B(11B)	58.08(13)
B(10B)-B(6B)-B(11B)	60.89(15)	C(1B)-B(6B)-B(5B)	58.65(14)
C(2B)-B(6B)-B(5B)	108.52(18)	B(10B)-B(6B)-B(5B)	59.34(14)
B(11B)-B(6B)-B(5B)	108.84(18)	C(2B)-B(7B)-B(11B)	58.53(14)
C(2B)-B(7B)-B(12B)	105.78(19)	B(11B)-B(7B)-B(12B)	59.86(16)
C(2B)-B(7B)-B(8B)	106.09(19)	B(11B)-B(7B)-B(8B)	108.22(19)
B(12B)-B(7B)-B(8B)	60.83(16)	C(2B)-B(7B)-B(3B)	58.96(14)
B(11B)-B(7B)-B(3B)	106.50(18)	B(12B)-B(7B)-B(3B)	107.23(19)
B(8B)-B(7B)-B(3B)	59.24(16)	B(3B)-B(8B)-B(4B)	60.39(16)
B(3B)-B(8B)-B(9B)	107.68(19)	B(4B)-B(8B)-B(9B)	59.87(15)
B(3B)-B(8B)-B(7B)	60.63(15)	B(4B)-B(8B)-B(7B)	109.02(18)
B(9B)-B(8B)-B(7B)	107.5(2)	B(3B)-B(8B)-B(12B)	107.34(19)
B(4B)-B(8B)-B(12B)	107.1(2)	B(9B)-B(8B)-B(12B)	58.99(15)
B(7B)-B(8B)-B(12B)	59.58(16)	B(12B)-B(9B)-B(5B)	107.74(18)
B(12B)-B(9B)-B(4B)	109.02(18)	B(5B)-B(9B)-B(4B)	59.69(15)
B(12B)-B(9B)-B(8B)	61.35(17)	B(5B)-B(9B)-B(8B)	107.56(18)
B(4B)-B(9B)-B(8B)	59.86(16)	B(12B)-B(9B)-B(10B)	60.20(16)
B(5B)-B(9B)-B(10B)	58.82(15)	B(4B)-B(9B)-B(10B)	107.03(17)
B(8B)-B(9B)-B(10B)	108.40(18)	B(5B)-B(10B)-B(6B)	60.71(15)
B(5B)-B(10B)-B(12B)	108.38(19)	B(6B)-B(10B)-B(12B)	107.29(18)
B(5B)-B(10B)-B(9B)	60.31(14)	B(6B)-B(10B)-B(9B)	107.80(18)
B(12B)-B(10B)-B(9B)	59.50(15)	B(5B)-B(10B)-B(11B)	109.02(18)
B(6B)-B(10B)-B(11B)	59.76(14)	B(12B)-B(10B)-B(11B)	59.78(15)
B(9B)-B(10B)-B(11B)	107.60(19)	C(2B)-B(11B)-B(6B)	59.84(13)
C(2B)-B(11B)-B(7B)	58.33(14)	B(6B)-B(11B)-B(7B)	107.18(18)
C(2B)-B(11B)-B(12B)	106.14(18)	B(6B)-B(11B)-B(12B)	107.15(17)
B(7B)-B(11B)-B(12B)	60.51(16)	C(2B)-B(11B)-B(10B)	106.61(17)
B(6B)-B(11B)-B(10B)	59.35(15)	B(7B)-B(11B)-B(10B)	108.23(18)
B(12B)-B(11B)-B(10B)	60.02(15)	B(9B)-B(12B)-B(11B)	108.56(19)
B(9B)-B(12B)-B(10B)	60.30(15)	B(11B)-B(12B)-B(10B)	60.20(15)
B(9B)-B(12B)-B(7B)	108.03(19)	B(11B)-B(12B)-B(7B)	59.64(15)
B(10B)-B(12B)-B(7B)	107.69(18)	B(9B)-B(12B)-B(8B)	59.66(15)
B(11B)-B(12B)-B(8B)	107.07(18)	B(10B)-B(12B)-B(8B)	107.16(19)
B(7B)-B(12B)-B(8B)	59.59(16)	C(14B)-C(13B)-C(18B)	118.57(19)
C(14B)-C(13B)-C(2B)	121.09(19)	C(18B)-C(13B)-C(2B)	120.30(18)
C(13B)-C(14B)-C(15B)	120.6(2)	C(16B)-C(15B)-C(14B)	120.4(2)
C(15B)-C(16B)-C(17B)	119.6(2)	C(16B)-C(17B)-C(18B)	120.4(2)
C(17B)-C(18B)-C(13B)	120.4(2)	N(19C)-C(1C)-B(5C)	120.82(17)
N(19C)-C(1C)-B(4C)	121.53(18)	B(5C)-C(1C)-B(4C)	62.79(14)
N(19C)-C(1C)-B(3C)	118.83(17)	B(5C)-C(1C)-B(3C)	113.25(16)
B(4C)-C(1C)-B(3C)	62.38(13)	N(19C)-C(1C)-B(6C)	117.65(17)
B(5C)-C(1C)-B(6C)	62.45(13)	B(4C)-C(1C)-B(6C)	113.35(16)
B(3C)-C(1C)-B(6C)	111.01(15)	N(19C)-C(1C)-C(2C)	119.34(16)
B(5C)-C(1C)-C(2C)	109.19(15)	B(4C)-C(1C)-C(2C)	110.28(15)
B(3C)-C(1C)-C(2C)	60.73(11)	B(6C)-C(1C)-C(2C)	58.84(12)
C(13C)-C(2C)-B(11C)	125.15(16)	C(13C)-C(2C)-B(7C)	121.83(16)
B(11C)-C(2C)-B(7C)	62.64(13)	C(13C)-C(2C)-B(6C)	119.88(16)
B(11C)-C(2C)-B(6C)	62.74(13)	B(7C)-C(2C)-B(6C)	113.20(16)
C(13C)-C(2C)-C(1C)	116.74(15)	B(11C)-C(2C)-C(1C)	109.97(15)
B(7C)-C(2C)-C(1C)	108.86(14)	B(6C)-C(2C)-C(1C)	60.15(12)
C(13C)-C(2C)-B(3C)	114.96(16)	B(11C)-C(2C)-B(3C)	112.99(15)
B(7C)-C(2C)-B(3C)	62.31(12)	B(6C)-C(2C)-B(3C)	110.38(15)
C(1C)-C(2C)-B(3C)	58.68(11)	C(1C)-B(3C)-C(2C)	60.59(11)
C(1C)-B(3C)-B(8C)	106.02(16)	C(2C)-B(3C)-B(8C)	105.43(16)
C(1C)-B(3C)-B(4C)	58.71(12)	C(2C)-B(3C)-B(4C)	107.29(16)
B(8C)-B(3C)-B(4C)	60.28(13)	C(1C)-B(3C)-B(7C)	106.63(16)
C(2C)-B(3C)-B(7C)	57.61(12)	B(8C)-B(3C)-B(7C)	60.27(13)
B(4C)-B(3C)-B(7C)	108.59(17)	C(1C)-B(4C)-B(3C)	58.91(12)
C(1C)-B(4C)-B(5C)	58.27(13)	B(3C)-B(4C)-B(5C)	106.82(16)
C(1C)-B(4C)-B(8C)	105.78(16)	B(3C)-B(4C)-B(8C)	59.78(13)
B(5C)-B(4C)-B(8C)	108.03(17)	C(1C)-B(4C)-B(9C)	105.51(17)
B(3C)-B(4C)-B(9C)	107.63(17)	B(5C)-B(4C)-B(9C)	60.15(14)

B(8C)-B(4C)-B(9C)	60.32(14)	C(1C)-B(5C)-B(4C)	58.94(13)
C(1C)-B(5C)-B(10C)	106.61(16)	B(4C)-B(5C)-B(10C)	108.66(17)
C(1C)-B(5C)-B(6C)	59.74(12)	B(4C)-B(5C)-B(6C)	108.08(16)
B(10C)-B(5C)-B(6C)	59.64(13)	C(1C)-B(5C)-B(9C)	105.96(17)
B(4C)-B(5C)-B(9C)	60.07(14)	B(10C)-B(5C)-B(9C)	60.42(14)
B(6C)-B(5C)-B(9C)	107.74(17)	C(2C)-B(6C)-C(1C)	61.00(12)
C(2C)-B(6C)-B(10C)	106.18(16)	C(1C)-B(6C)-B(10C)	105.51(16)
C(2C)-B(6C)-B(11C)	58.42(12)	C(1C)-B(6C)-B(11C)	107.24(16)
B(10C)-B(6C)-B(11C)	60.40(14)	C(2C)-B(6C)-B(5C)	107.22(16)
C(1C)-B(6C)-B(5C)	57.81(12)	B(10C)-B(6C)-B(5C)	60.17(13)
B(11C)-B(6C)-B(5C)	108.62(17)	C(2C)-B(7C)-B(11C)	58.60(12)
C(2C)-B(7C)-B(12C)	105.84(17)	B(11C)-B(7C)-B(12C)	60.25(14)
C(2C)-B(7C)-B(8C)	106.65(16)	B(11C)-B(7C)-B(8C)	108.60(18)
B(12C)-B(7C)-B(8C)	60.23(14)	C(2C)-B(7C)-B(3C)	60.08(12)
B(11C)-B(7C)-B(3C)	107.95(16)	B(12C)-B(7C)-B(3C)	107.35(17)
B(8C)-B(7C)-B(3C)	59.36(13)	B(3C)-B(8C)-B(4C)	59.95(13)
B(3C)-B(8C)-B(7C)	60.36(13)	B(4C)-B(8C)-B(7C)	108.40(16)
B(3C)-B(8C)-B(12C)	107.63(16)	B(4C)-B(8C)-B(12C)	107.89(18)
B(7C)-B(8C)-B(12C)	59.58(14)	B(3C)-B(8C)-B(9C)	107.43(17)
B(4C)-B(8C)-B(9C)	59.89(14)	B(7C)-B(8C)-B(9C)	107.49(17)
B(12C)-B(8C)-B(9C)	59.74(14)	B(4C)-B(9C)-B(12C)	108.10(18)
B(4C)-B(9C)-B(5C)	59.79(13)	B(12C)-B(9C)-B(5C)	107.74(17)
B(4C)-B(9C)-B(8C)	59.80(14)	B(12C)-B(9C)-B(8C)	60.10(14)
B(5C)-B(9C)-B(8C)	107.33(17)	B(4C)-B(9C)-B(10C)	107.85(17)
B(12C)-B(9C)-B(10C)	60.21(14)	B(5C)-B(9C)-B(10C)	59.69(14)
B(8C)-B(9C)-B(10C)	107.95(17)	B(6C)-B(10C)-B(5C)	60.20(13)
B(6C)-B(10C)-B(11C)	60.00(13)	B(5C)-B(10C)-B(11C)	108.33(16)
B(6C)-B(10C)-B(9C)	107.76(17)	B(5C)-B(10C)-B(9C)	59.89(14)
B(11C)-B(10C)-B(9C)	107.84(18)	B(6C)-B(10C)-B(12C)	107.23(17)
B(5C)-B(10C)-B(12C)	107.42(17)	B(11C)-B(10C)-B(12C)	59.72(14)
B(9C)-B(10C)-B(12C)	59.60(14)	C(2C)-B(11C)-B(7C)	58.76(12)
C(2C)-B(11C)-B(6C)	58.84(12)	B(7C)-B(11C)-B(6C)	106.97(16)
C(2C)-B(11C)-B(12C)	105.76(16)	B(7C)-B(11C)-B(12C)	59.99(14)
B(6C)-B(11C)-B(12C)	107.43(17)	C(2C)-B(11C)-B(10C)	105.88(16)
B(7C)-B(11C)-B(10C)	108.11(17)	B(6C)-B(11C)-B(10C)	59.60(13)
B(12C)-B(11C)-B(10C)	60.38(14)	B(7C)-B(12C)-B(11C)	59.76(13)
B(7C)-B(12C)-B(9C)	108.32(17)	B(11C)-B(12C)-B(9C)	108.46(17)
B(7C)-B(12C)-B(8C)	60.19(14)	B(11C)-B(12C)-B(8C)	108.18(17)
B(9C)-B(12C)-B(8C)	60.16(14)	B(7C)-B(12C)-B(10C)	107.54(16)
B(11C)-B(12C)-B(10C)	59.90(14)	B(9C)-B(12C)-B(10C)	60.20(14)
B(8C)-B(12C)-B(10C)	108.00(17)	C(18C)-C(13C)-C(14C)	117.78(19)
C(18C)-C(13C)-C(2C)	121.90(18)	C(14C)-C(13C)-C(2C)	120.31(18)
C(15C)-C(14C)-C(13C)	120.6(2)	C(16C)-C(15C)-C(14C)	120.8(2)
C(17C)-C(16C)-C(15C)	119.5(2)	C(16C)-C(17C)-C(18C)	120.3(2)
C(17C)-C(18C)-C(13C)	121.0(2)	H(2C)-N(19C)-H(1C)	102.8(16)
H(2C)-N(19C)-C(1C)	113.5(11)	H(1C)-N(19C)-C(1C)	111.7(11)
N(19D)-C(1D)-B(5D)	120.71(18)	N(19D)-C(1D)-B(4D)	121.84(18)
B(5D)-C(1D)-B(4D)	62.81(13)	N(19D)-C(1D)-B(3D)	119.36(18)
B(5D)-C(1D)-B(3D)	113.13(16)	B(4D)-C(1D)-B(3D)	62.44(14)
N(19D)-C(1D)-B(6D)	117.88(17)	B(5D)-C(1D)-B(6D)	62.85(13)
B(4D)-C(1D)-B(6D)	113.17(16)	B(3D)-C(1D)-B(6D)	109.80(15)
N(19D)-C(1D)-C(2D)	119.75(17)	B(5D)-C(1D)-C(2D)	109.21(15)
B(4D)-C(1D)-C(2D)	109.38(15)	B(3D)-C(1D)-C(2D)	59.53(12)
B(6D)-C(1D)-C(2D)	58.63(11)	C(13D)-C(2D)-B(7D)	122.14(16)
C(13D)-C(2D)-B(11D)	125.82(17)	B(7D)-C(2D)-B(11D)	63.22(13)
C(13D)-C(2D)-B(6D)	120.06(16)	B(7D)-C(2D)-B(6D)	113.21(16)
B(11D)-C(2D)-B(6D)	62.44(13)	C(13D)-C(2D)-B(3D)	114.64(16)
B(7D)-C(2D)-B(3D)	62.62(14)	B(11D)-C(2D)-B(3D)	113.33(16)
B(6D)-C(2D)-B(3D)	109.55(15)	C(13D)-C(2D)-C(1D)	116.23(15)
B(7D)-C(2D)-C(1D)	108.93(15)	B(11D)-C(2D)-C(1D)	109.37(15)
B(6D)-C(2D)-C(1D)	59.39(11)	B(3D)-C(2D)-C(1D)	58.47(12)
C(1D)-B(3D)-C(2D)	62.00(12)	C(1D)-B(3D)-B(8D)	105.93(16)

C(2D)-B(3D)-B(8D)	105.80(16)	C(1D)-B(3D)-B(4D)	58.75(13)
C(2D)-B(3D)-B(4D)	108.43(16)	B(8D)-B(3D)-B(4D)	59.71(14)
C(1D)-B(3D)-B(7D)	107.82(16)	C(2D)-B(3D)-B(7D)	57.69(12)
B(8D)-B(3D)-B(7D)	60.50(14)	B(4D)-B(3D)-B(7D)	108.83(17)
C(1D)-B(4D)-B(8D)	106.12(17)	C(1D)-B(4D)-B(9D)	105.22(17)
B(8D)-B(4D)-B(9D)	60.32(14)	C(1D)-B(4D)-B(3D)	58.81(13)
B(8D)-B(4D)-B(3D)	59.89(14)	B(9D)-B(4D)-B(3D)	107.19(18)
C(1D)-B(4D)-B(5D)	58.31(13)	B(8D)-B(4D)-B(5D)	108.21(18)
B(9D)-B(4D)-B(5D)	59.91(14)	B(3D)-B(4D)-B(5D)	106.59(16)
C(1D)-B(5D)-B(9D)	105.60(17)	C(1D)-B(5D)-B(10D)	106.14(17)
B(9D)-B(5D)-B(10D)	60.05(15)	C(1D)-B(5D)-B(4D)	58.89(13)
B(9D)-B(5D)-B(4D)	59.82(14)	B(10D)-B(5D)-B(4D)	108.00(18)
C(1D)-B(5D)-B(6D)	59.35(12)	B(9D)-B(5D)-B(6D)	106.84(18)
B(10D)-B(5D)-B(6D)	59.32(13)	B(4D)-B(5D)-B(6D)	107.27(16)
C(2D)-B(6D)-C(1D)	61.98(12)	C(2D)-B(6D)-B(10D)	105.96(16)
C(1D)-B(6D)-B(10D)	105.46(16)	C(2D)-B(6D)-B(11D)	58.24(12)
C(1D)-B(6D)-B(11D)	108.11(16)	B(10D)-B(6D)-B(11D)	60.46(14)
C(2D)-B(6D)-B(5D)	107.86(16)	C(1D)-B(6D)-B(5D)	57.80(12)
B(10D)-B(6D)-B(5D)	60.00(14)	B(11D)-B(6D)-B(5D)	109.00(17)
C(2D)-B(7D)-B(12D)	105.94(16)	C(2D)-B(7D)-B(11D)	58.41(12)
B(12D)-B(7D)-B(11D)	60.23(14)	C(2D)-B(7D)-B(3D)	59.69(12)
B(12D)-B(7D)-B(3D)	107.25(17)	B(11D)-B(7D)-B(3D)	107.17(16)
C(2D)-B(7D)-B(8D)	106.44(17)	B(12D)-B(7D)-B(8D)	60.26(14)
B(11D)-B(7D)-B(8D)	108.22(17)	B(3D)-B(7D)-B(8D)	59.33(14)
B(4D)-B(8D)-B(3D)	60.40(14)	B(4D)-B(8D)-B(9D)	60.06(14)
B(3D)-B(8D)-B(9D)	107.38(17)	B(4D)-B(8D)-B(12D)	108.50(17)
B(3D)-B(8D)-B(12D)	107.15(17)	B(9D)-B(8D)-B(12D)	59.99(15)
B(4D)-B(8D)-B(7D)	109.12(17)	B(3D)-B(8D)-B(7D)	60.17(13)
B(9D)-B(8D)-B(7D)	107.57(18)	B(12D)-B(8D)-B(7D)	59.29(14)
B(4D)-B(9D)-B(5D)	60.27(14)	B(4D)-B(9D)-B(8D)	59.63(14)
B(5D)-B(9D)-B(8D)	107.94(17)	B(4D)-B(9D)-B(10D)	108.40(17)
B(5D)-B(9D)-B(10D)	60.11(14)	B(8D)-B(9D)-B(10D)	108.30(18)
B(4D)-B(9D)-B(12D)	108.36(17)	B(5D)-B(9D)-B(12D)	108.64(18)
B(8D)-B(9D)-B(12D)	60.25(15)	B(10D)-B(9D)-B(12D)	60.44(14)
B(6D)-B(10D)-B(9D)	107.73(17)	B(6D)-B(10D)-B(5D)	60.67(13)
B(9D)-B(10D)-B(5D)	59.83(14)	B(6D)-B(10D)-B(11D)	59.88(13)
B(9D)-B(10D)-B(11D)	108.15(17)	B(5D)-B(10D)-B(11D)	109.08(17)
B(6D)-B(10D)-B(12D)	107.11(16)	B(9D)-B(10D)-B(12D)	59.87(15)
B(5D)-B(10D)-B(12D)	107.96(17)	B(11D)-B(10D)-B(12D)	59.77(14)
C(2D)-B(11D)-B(6D)	59.32(12)	C(2D)-B(11D)-B(7D)	58.37(12)
B(6D)-B(11D)-B(7D)	106.86(16)	C(2D)-B(11D)-B(12D)	105.38(17)
B(6D)-B(11D)-B(12D)	107.44(17)	B(7D)-B(11D)-B(12D)	59.56(14)
C(2D)-B(11D)-B(10D)	106.19(16)	B(6D)-B(11D)-B(10D)	59.67(13)
B(7D)-B(11D)-B(10D)	107.74(18)	B(12D)-B(11D)-B(10D)	60.41(14)
B(7D)-B(12D)-B(11D)	60.21(13)	B(7D)-B(12D)-B(9D)	108.31(18)
B(11D)-B(12D)-B(9D)	108.04(18)	B(7D)-B(12D)-B(8D)	60.45(14)
B(11D)-B(12D)-B(8D)	108.34(17)	B(9D)-B(12D)-B(8D)	59.77(15)
B(7D)-B(12D)-B(10D)	107.78(17)	B(11D)-B(12D)-B(10D)	59.82(14)
B(9D)-B(12D)-B(10D)	59.69(14)	B(8D)-B(12D)-B(10D)	107.33(18)
C(18D)-C(13D)-C(14D)	118.2(2)	C(18D)-C(13D)-C(2D)	122.32(19)
C(14D)-C(13D)-C(2D)	119.46(18)	C(15D)-C(14D)-C(13D)	121.0(2)
C(16D)-C(15D)-C(14D)	120.2(2)	C(15D)-C(16D)-C(17D)	119.4(2)
C(16D)-C(17D)-C(18D)	120.6(2)	C(13D)-C(18D)-C(17D)	120.6(2)
H(2D)-N(19D)-H(1D)	117.5(16)	H(2D)-N(19D)-C(1D)	114.9(11)
H(1D)-N(19D)-C(1D)	114.0(11)		

Table Atomic coordinates (x 10^4) and equivalent isotropic displacement parameters ($Å^2$ x 10^3) for kw54. U(eq) is defined as one third of the trace of the orthogonalized U_{ij} tensor.

	x	y	z	U(eq)
C(1A)	9516.7(19)	6633.5(10)	2444.0(9)	27.9(5)
C(2A)	9739.6(18)	6167.3(9)	1851.9(9)	23.4(4)
B(3A)	8848(2)	6819.8(10)	1726.9(11)	27.5(5)
B(4A)	7984(2)	6890.2(11)	2290.6(11)	31.1(6)
B(5A)	8480(2)	6286.4(12)	2790.7(11)	32.1(6)
B(6A)	9628(2)	5867.0(11)	2516.8(11)	29.8(5)
B(7A)	8349(2)	6135.6(11)	1334.3(10)	26.1(5)
B(8A)	7220(2)	6583.3(11)	1601.3(11)	29.1(5)
B(9A)	7004(2)	6247.7(12)	2264.0(11)	30.5(5)
B(10A)	8033(2)	5609.6(12)	2416.7(11)	32.1(6)
B(11A)	8844(2)	5537.1(11)	1836.2(11)	28.9(5)
B(12A)	7220(2)	5786.1(11)	1679.8(11)	28.0(5)
C(13A)	11021.0(19)	6180.3(9)	1686.4(9)	28.1(5)
C(14A)	11136(2)	6482.7(10)	1176.8(10)	34.8(5)
C(15A)	12296(2)	6491.8(12)	1003.7(12)	45.1(7)
C(16A)	13360(2)	6204.8(13)	1342.7(13)	50.1(7)
C(17A)	13247(2)	5904.6(12)	1842.3(13)	47.7(7)
C(18A)	12081(2)	5886.5(10)	2019.0(11)	36.4(5)
N(19A)	10556.6(18)	6965.7(9)	2747.9(9)	38.9(5)
C(1B)	4212(2)	7978.5(10)	2261.3(10)	34.5(5)
C(2B)	4564.7(18)	8583.3(9)	1835.2(8)	23.2(4)
B(3B)	4519(3)	8673.2(14)	2558.7(11)	40.6(7)
B(4B)	3264(2)	8218.1(13)	2706.3(12)	37.3(6)
B(5B)	2624(3)	7816.8(12)	2060.9(12)	36.1(6)
B(6B)	3500(2)	8030.6(12)	1536.4(12)	32.8(6)
B(7B)	3832(3)	9205.1(12)	2005.2(14)	41.4(7)
B(8B)	3004(3)	8988.8(13)	2556.6(14)	44.8(7)
B(9B)	1820(2)	8458.0(12)	2238.4(11)	30.9(5)
B(10B)	1965(2)	8318.4(14)	1507.0(12)	38.6(6)
B(11B)	3200(2)	8790.0(12)	1363.4(11)	33.3(6)
B(12B)	2157(3)	9053.3(13)	1800.9(14)	42.6(7)
C(13B)	5842.1(18)	8589.2(9)	1668.5(9)	25.2(4)
C(14B)	6897(2)	8869.4(10)	2021.2(10)	31.7(5)
C(15B)	8065(2)	8894.8(11)	1849.6(11)	39.3(6)
C(16B)	8195(2)	8637.4(11)	1329.7(11)	40.0(6)
C(17B)	7156(2)	8355.6(11)	975.1(11)	40.5(6)
C(18B)	5982(2)	8329.5(10)	1141.9(10)	33.0(5)
N(19B)	5171(2)	7540.5(11)	2409.9(11)	64.1(8)
C(1C)	9454.7(18)	1645.7(9)	1120.0(9)	24.5(4)
C(2C)	8909.1(18)	1045.2(8)	652.0(8)	21.9(4)
B(3C)	10004(2)	938.9(10)	1320.9(10)	23.4(5)
B(4C)	11051(2)	1564.1(11)	1428.5(11)	28.1(5)
B(5C)	10499(2)	2059.8(11)	832.1(11)	29.2(5)
B(6C)	9134(2)	1730.4(10)	364.0(10)	24.9(5)
B(7C)	10152(2)	563.7(11)	662.5(10)	27.3(5)
B(8C)	11524(2)	884.0(12)	1140.6(11)	29.6(5)
B(9C)	11840(2)	1585.6(12)	831.5(11)	32.7(6)
B(10C)	10644(2)	1698.1(12)	171.1(11)	31.6(6)
B(11C)	9618(2)	1059.2(11)	66.8(10)	27.1(5)
B(12C)	11289(2)	966.8(12)	363.0(11)	31.8(6)
C(13C)	7568.8(18)	824.8(9)	637.1(8)	23.0(4)

C(14C)	7376(2)	273.5(10)	884.2(11)	36.6(5)
C(15C)	6145(2)	75.8(11)	886.7(11)	43.5(6)
C(16C)	5094(2)	418.7(11)	648.2(10)	37.7(6)
C(17C)	5263(2)	960.8(11)	399.4(11)	39.1(6)
C(18C)	6490(2)	1162.4(10)	389.0(10)	32.8(5)
N(19C)	8621.1(19)	1918.0(9)	1423.0(9)	37.8(5)
C(1D)	5156(2)	3939.9(9)	1284.2(9)	26.2(4)
C(2D)	3981.0(18)	3824.8(8)	626.5(8)	22.1(4)
B(3D)	4461(2)	3250.5(10)	1125.9(11)	27.0(5)
B(4D)	6133(2)	3324.4(11)	1421.4(12)	31.3(6)
B(5D)	6629(2)	3993.3(11)	1120.3(11)	29.7(5)
B(6D)	5243(2)	4304.7(10)	639.6(10)	24.8(5)
B(7D)	4207(2)	3139.1(10)	352.6(11)	28.2(5)
B(8D)	5571(2)	2820.2(11)	839.8(12)	34.1(6)
B(9D)	6911(2)	3286.9(12)	825.1(12)	34.8(6)
B(10D)	6376(2)	3898.7(11)	346.8(11)	30.6(5)
B(11D)	4706(2)	3804.8(11)	48.2(10)	27.9(5)
B(12D)	5725(3)	3165.9(11)	169.0(12)	34.5(6)
C(13D)	2669.3(19)	4068.9(9)	616.7(9)	25.0(4)
C(14D)	1646(2)	3675.9(11)	581.4(12)	41.0(6)
C(15D)	430(2)	3885.0(12)	589.4(13)	48.2(7)
C(16D)	221(2)	4487.7(12)	642.5(11)	43.9(6)
C(17D)	1224(2)	4882.1(11)	672.3(12)	46.1(6)
C(18D)	2438(2)	4675.8(10)	654.4(11)	38.4(6)
N(19D)	4852(2)	4282.1(10)	1740.3(9)	41.9(5)

Table Hydrogen atom coordinates (x 10^4) and isotropic displacement parameters ($Å^2$ x 10^3)

	x	y	z	U
H(3A)	9172	7221	1510	33
H(4A)	7697	7338	2438	37
H(5A)	8524	6329	3273	39
H(6A)	10464	5646	2816	36
H(7A)	8305	6087	852	31
H(8A)	6433	6829	1294	35
H(9A)	6057	6267	2396	37
H(10A)	7782	5206	2654	39
H(11A)	9130	5089	1690	35
H(12A)	6420	5502	1428	34
H(14A)	10413	6684	947	42
H(15A)	12364	6694	653	54
H(16A)	14161	6216	1229	60
H(17A)	13974	5706	2072	57
H(18A)	12013	5675	2364	44
H(1A)	10718(19)	7324(8)	2537(9)	47
H(2A)	11125(17)	6784(9)	3081(8)	47
H(3B)	5401	8774	2905	49
H(4B)	3289	8026	3152	45
H(5B)	2219	7355	2074	43
H(6B)	3716	7706	1205	39
H(7B)	4226	9668	1989	50
H(8B)	2862	9310	2906	54
H(9B)	877	8432	2373	37
H(10B)	1121	8188	1152	46
H(11B)	3177	8973	914	40
H(12B)	1435	9415	1644	51
H(14B)	6821	9045	2383	38
H(15B)	8777	9091	2093	47
H(16B)	8996	8654	1215	48
H(17B)	7243	8178	615	49
H(18B)	5273	8134	896	40
H(3C)	9759	694	1701	28
H(4C)	11522	1730	1878	34
H(5C)	10600	2557	887	35
H(6C)	8318	2007	116	30
H(7C)	10027	67	610	33
H(8C)	12310	598	1401	35
H(9C)	12838	1765	884	39
H(10C)	10848	1956	-210	38
H(11C)	9147	893	-382	33
H(12C)	11930	739	109	38
H(14C)	8094	31	1052	44
H(15C)	6029	-302	1056	52
H(16C)	4255	281	655	45
H(17C)	4537	1200	233	47
H(18C)	6593	1536	210	39
H(1C)	8187(18)	1606(9)	1647(9)	45
H(2C)	7851(16)	2123(9)	1153(8)	45
H(3D)	3804	3052	1390	32
H(4D)	6598	3163	1873	38
H(5D)	7423	4280	1373	36

H(6D)	5105	4801	583	30
H(7D)	3404	2855	104	34
H(8D)	5670	2324	910	41
H(9D)	7905	3101	879	42
H(10D)	7017	4122	90	37
H(11D)	4243	3966	-403	34
H(12D)	5934	2899	-206	41
H(14D)	1783	3257	551	49
H(15D)	-263	3611	558	58
H(16D)	-609	4631	658	53
H(17D)	1083	5300	706	55
H(18D)	3118	4954	668	46
H(1D)	4106(19)	4115(9)	1900(9)	50
H(2D)	4887(21)	4732(6)	1685(10)	50

C13 Crystal Data for [Mo(NCbMe)$_2$Cl$_4$][Et$_3$NH]$_2$ - 33

Empirical Formula	$C_{18}H_{58}B_{20}Cl_4MoN_4$	
Temperature	160(2)K	
Wavelength	0.71073Å	
Crystal System	Monoclinic	
Space Group	C2/c	
Unit Cell Dimensions	a = 24.054(4)Å	alpha = 90°
	b = 11.771(2)Å	beta = 101.71(2)°
	c = 14.137(3)Å	gamma = 90°
Crystal Size	0.35 × 0.33 × 0.15 mm	
Final R indices [I>2σ(I)]	R1 = 0.0235	wR2 = 0.0582
R indices (all data)	R1 = 0.0280	wR2 = 0.0613

The numbering scheme used here is non-standard and different to that used in Chapter Five for this compound.

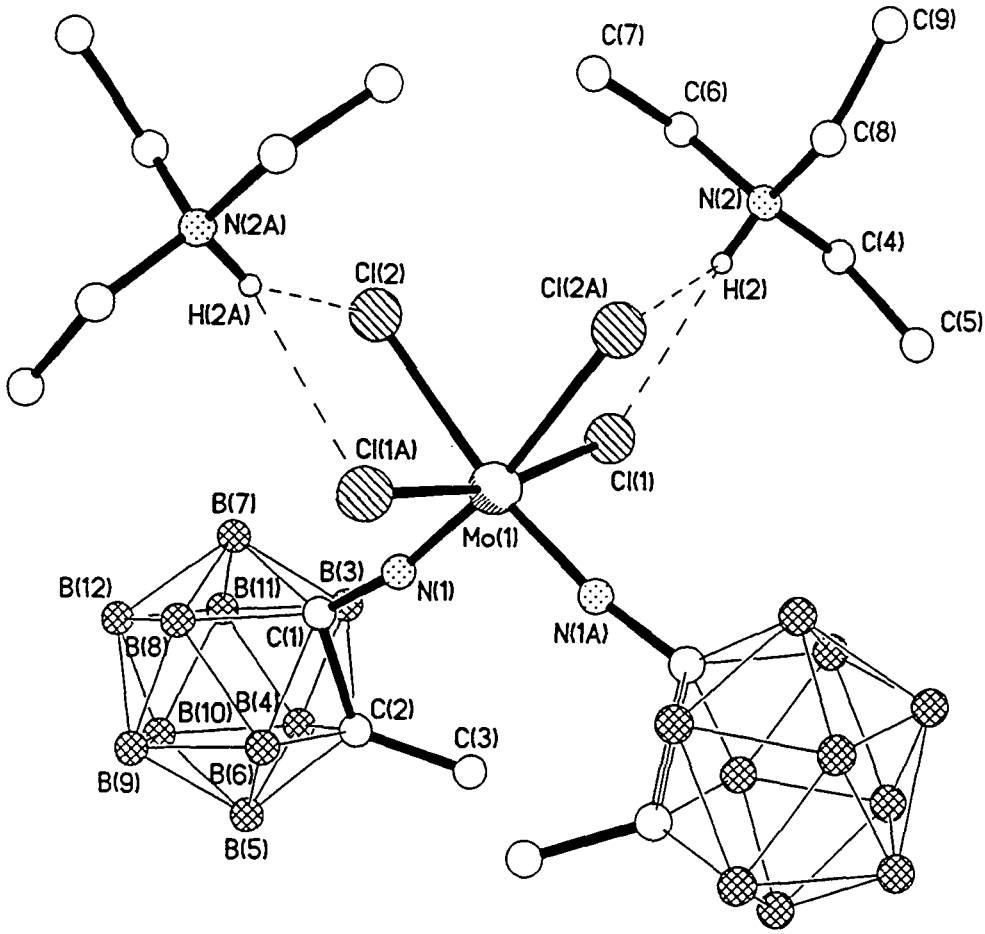

Table Bond lengths (Å) and angles (°)

Mo(1)-N(1)	1.778(2)	Mo(1)-N(1')	1.778(2)
Mo(1)-Cl(1)	2.4232(7)	Mo(1)-Cl(1')	2.4232(7)
Mo(1)-Cl(2')	2.5292(5)	Mo(1)-Cl(2)	2.5292(5)
N(1)-C(1)	1.364(2)	C(1)-B(8)	1.704(3)
C(1)-B(7)	1.724(3)	C(1)-B(3)	1.730(3)
C(1)-C(2)	1.746(2)	C(1)-B(6)	1.751(3)
C(2)-C(3)	1.510(3)	C(2)-B(4)	1.693(3)
C(2)-B(5)	1.693(3)	C(2)-B(6)	1.720(3)
C(2)-B(3)	1.735(3)	B(3)-B(11)	1.775(3)
B(3)-B(7)	1.786(3)	B(3)-B(4)	1.788(3)
B(4)-B(5)	1.778(3)	B(4)-B(10)	1.780(3)
B(4)-B(11)	1.780(3)	B(5)-B(6)	1.775(3)
B(5)-B(10)	1.776(3)	B(5)-B(9)	1.777(3)
B(6)-B(9)	1.761(3)	B(6)-B(8)	1.795(3)
B(7)-B(12)	1.775(3)	B(7)-B(11)	1.777(3)
B(7)-B(8)	1.795(3)	B(8)-B(12)	1.782(3)
B(8)-B(9)	1.783(3)	B(9)-B(10)	1.790(3)
B(9)-B(12)	1.792(3)	B(10)-B(12)	1.786(3)
B(10)-B(11)	1.789(3)	B(11)-B(12)	1.783(3)
N(2)-C(8)	1.505(2)	N(2)-C(4)	1.506(2)
N(2)-C(6)	1.509(2)	C(4)-C(5)	1.512(3)
C(6)-C(7)	1.507(3)	C(8)-C(9)	1.514(3)

N(1)-Mo(1)-N(1')	102.41(10)	N(1)-Mo(1)-Cl(1)	93.99(5)
N(1')-Mo(1)-Cl(1)	94.22(5)	N(1)-Mo(1)-Cl(1')	94.22(5)
N(1')-Mo(1)-Cl(1')	93.99(5)	Cl(1)-Mo(1)-Cl(1')	166.87(3)
N(1)-Mo(1)-Cl(2')	170.24(5)	N(1')-Mo(1)-Cl(2')	87.34(5)
Cl(1)-Mo(1)-Cl(2')	84.64(2)	Cl(1')-Mo(1)-Cl(2')	85.53(2)
N(1)-Mo(1)-Cl(2)	87.34(5)	N(1')-Mo(1)-Cl(2)	170.24(5)
Cl(1)-Mo(1)-Cl(2)	85.53(2)	Cl(1')-Mo(1)-Cl(2)	84.64(2)
Cl(2')-Mo(1)-Cl(2)	82.92(3)	C(1)-N(1)-Mo(1)	168.87(13)
N(1)-C(1)-B(8)	123.6(2)	N(1)-C(1)-B(7)	125.3(2)
B(8)-C(1)-B(7)	63.13(12)	N(1)-C(1)-B(3)	117.7(2)
B(8)-C(1)-B(3)	113.54(15)	B(7)-C(1)-B(3)	62.28(12)
N(1)-C(1)-C(2)	115.85(14)	B(8)-C(1)-C(2)	108.88(14)
B(7)-C(1)-C(2)	109.15(14)	B(3)-C(1)-C(2)	59.89(11)
N(1)-C(1)-B(6)	115.51(15)	B(8)-C(1)-B(6)	62.58(12)
B(7)-C(1)-B(6)	113.51(14)	B(3)-C(1)-B(6)	110.84(14)
C(2)-C(1)-B(6)	58.92(11)	C(3)-C(2)-B(4)	122.2(2)
C(3)-C(2)-B(5)	123.9(2)	B(4)-C(2)-B(5)	63.33(13)
C(3)-C(2)-B(6)	117.6(2)	B(4)-C(2)-B(6)	114.39(15)
B(5)-C(2)-B(6)	62.67(13)	C(3)-C(2)-B(3)	115.2(2)
B(4)-C(2)-B(3)	62.84(13)	B(5)-C(2)-B(3)	114.44(15)
B(6)-C(2)-B(3)	112.12(14)	C(3)-C(2)-C(1)	115.88(15)
B(4)-C(2)-C(1)	110.23(14)	B(5)-C(2)-C(1)	110.73(14)
B(6)-C(2)-C(1)	60.69(11)	B(3)-C(2)-C(1)	59.61(11)
C(1)-B(3)-C(2)	60.49(11)	C(1)-B(3)-B(11)	105.39(15)
C(2)-B(3)-B(11)	104.40(15)	C(1)-B(3)-B(7)	58.69(11)
C(2)-B(3)-B(7)	106.81(15)	B(11)-B(3)-B(7)	59.89(12)
C(1)-B(3)-B(4)	106.6(2)	C(2)-B(3)-B(4)	57.42(12)
B(11)-B(3)-B(4)	59.95(12)	B(7)-B(3)-B(4)	108.3(2)
C(2)-B(4)-B(5)	58.34(12)	C(2)-B(4)-B(10)	105.1(2)
B(5)-B(4)-B(10)	59.90(13)	C(2)-B(4)-B(11)	106.0(2)
B(5)-B(4)-B(11)	108.3(2)	B(10)-B(4)-B(11)	60.36(13)
C(2)-B(4)-B(3)	59.74(12)	B(5)-B(4)-B(3)	107.9(2)
B(10)-B(4)-B(3)	107.8(2)	B(11)-B(4)-B(3)	59.66(12)
C(2)-B(5)-B(6)	59.39(12)	C(2)-B(5)-B(10)	105.3(2)
B(6)-B(5)-B(10)	108.0(2)	C(2)-B(5)-B(9)	105.4(2)

B(6)-B(5)-B(9)	59.46(13)	B(10)-B(5)-B(9)	60.50(13)
C(2)-B(5)-B(4)	58.32(12)	B(6)-B(5)-B(4)	107.7(2)
B(10)-B(5)-B(4)	60.10(13)	B(9)-B(5)-B(4)	108.2(2)
C(2)-B(6)-C(1)	60.39(11)	C(2)-B(6)-B(9)	105.0(2)
C(1)-B(6)-B(9)	104.94(15)	C(2)-B(6)-B(5)	57.93(12)
C(1)-B(6)-B(5)	106.7(2)	B(9)-B(6)-B(5)	60.31(13)
C(2)-B(6)-B(8)	105.96(15)	C(1)-B(6)-B(8)	57.42(11)
B(9)-B(6)-B(8)	60.18(12)	B(5)-B(6)-B(8)	108.5(2)
C(1)-B(7)-B(12)	104.82(15)	C(1)-B(7)-B(11)	105.54(15)
B(12)-B(7)-B(11)	60.25(13)	C(1)-B(7)-B(3)	59.04(11)
B(12)-B(7)-B(3)	107.4(2)	B(11)-B(7)-B(3)	59.73(12)
C(1)-B(7)-B(8)	57.88(11)	B(12)-B(7)-B(8)	59.88(12)
B(11)-B(7)-B(8)	107.8(2)	B(3)-B(7)-B(8)	106.69(15)
C(1)-B(8)-B(12)	105.4(2)	C(1)-B(8)-B(9)	106.0(2)
B(12)-B(8)-B(9)	60.35(13)	C(1)-B(8)-B(7)	58.98(12)
B(12)-B(8)-B(7)	59.52(12)	B(9)-B(8)-B(7)	108.1(2)
C(1)-B(8)-B(6)	60.00(11)	B(12)-B(8)-B(6)	107.2(2)
B(9)-B(8)-B(6)	58.98(12)	B(7)-B(8)-B(6)	108.1(2)
B(6)-B(9)-B(5)	60.23(13)	B(6)-B(9)-B(8)	60.84(12)
B(5)-B(9)-B(8)	108.9(2)	B(6)-B(9)-B(10)	108.0(2)
B(5)-B(9)-B(10)	59.73(13)	B(8)-B(9)-B(10)	108.0(2)
B(6)-B(9)-B(12)	108.2(2)	B(5)-B(9)-B(12)	107.8(2)
B(8)-B(9)-B(12)	59.79(13)	B(10)-B(9)-B(12)	59.82(13)
B(5)-B(10)-B(4)	60.00(13)	B(5)-B(10)-B(12)	108.1(2)
B(4)-B(10)-B(12)	107.8(2)	B(5)-B(10)-B(11)	107.9(2)
B(4)-B(10)-B(11)	59.83(13)	B(12)-B(10)-B(11)	59.83(13)
B(5)-B(10)-B(9)	59.77(13)	B(4)-B(10)-B(9)	107.5(2)
B(12)-B(10)-B(9)	60.16(13)	B(11)-B(10)-B(9)	107.7(2)
B(3)-B(11)-B(7)	60.38(12)	B(3)-B(11)-B(4)	60.39(12)
B(7)-B(11)-B(4)	109.1(2)	B(3)-B(11)-B(12)	107.6(2)
B(7)-B(11)-B(12)	59.82(12)	B(4)-B(11)-B(12)	107.9(2)
B(3)-B(11)-B(10)	108.0(2)	B(7)-B(11)-B(10)	108.4(2)
B(4)-B(11)-B(10)	59.82(13)	B(12)-B(11)-B(10)	59.99(13)
B(7)-B(12)-B(8)	60.59(12)	B(7)-B(12)-B(11)	59.94(12)
B(8)-B(12)-B(11)	108.08(15)	B(7)-B(12)-B(10)	108.7(2)
B(8)-B(12)-B(10)	108.3(2)	B(11)-B(12)-B(10)	60.18(13)
B(7)-B(12)-B(9)	108.51(15)	B(8)-B(12)-B(9)	59.86(13)
B(11)-B(12)-B(9)	107.9(2)	B(10)-B(12)-B(9)	60.02(13)
C(8)-N(2)-C(4)	113.98(14)	C(8)-N(2)-C(6)	113.24(15)
C(4)-N(2)-C(6)	109.77(15)	N(2)-C(4)-C(5)	113.0(2)
C(7)-C(6)-N(2)	113.2(2)	N(2)-C(8)-C(9)	113.6(2)

Symmetry transformations used to generate equivalent atoms:

': -x,y,-z+1/2

Table 2. Atomic coordinates (x 10^4) and equivalent isotropic displacement parameters ($Å^2$ x 10^3) for kw55. U(eq) is defined as one third of the trace of the orthogonalized U_{ij} tensor.

	x	y	z	U(eq)
Mo(1)	0	2544.3(2)	2500	14.94(8)
Cl(1)	-365.9(2)	2309.0(4)	783.7(3)	23.59(12)
Cl(2)	666.8(2)	934.1(4)	2319.2(3)	21.92(12)
N(1)	548.8(6)	3490.8(13)	2336.2(11)	18.0(3)
C(1)	1028.6(7)	4029.0(15)	2199.3(13)	17.6(4)
C(2)	930.5(8)	5379(2)	1681.1(14)	20.4(4)
C(3)	323.0(8)	5777(2)	1393(2)	30.2(5)
B(3)	1108.8(9)	4239(2)	1023(2)	22.2(5)
B(4)	1413.8(10)	5619(2)	984(2)	24.9(5)
B(5)	1481.3(10)	6242(2)	2148(2)	26.3(5)
B(6)	1215.5(9)	5253(2)	2895(2)	21.4(5)
B(7)	1596.0(9)	3382(2)	1845(2)	21.4(5)
B(8)	1655.0(9)	4008(2)	3018(2)	22.2(5)
B(9)	1953.7(9)	5391(2)	2988(2)	24.9(5)
B(10)	2082.9(9)	5624(2)	1800(2)	24.6(5)
B(11)	1850.5(9)	4386(2)	1095(2)	23.3(5)
B(12)	2190.0(9)	4245(2)	2334(2)	23.4(5)
N(2)	-1155.3(6)	-92.3(13)	531.5(11)	19.7(3)
C(4)	-1473.6(8)	514(2)	-352.2(14)	25.7(4)
C(5)	-1910.7(9)	1342(2)	-131(2)	33.8(5)
C(6)	-680.9(8)	-788(2)	272.7(15)	26.5(4)
C(7)	-318.6(9)	-1369(2)	1131(2)	31.8(5)
C(8)	-1529.5(8)	-762(2)	1061.3(14)	22.5(4)
C(9)	-1786.8(9)	-1810(2)	522(2)	29.7(5)

Table Hydrogen atom coordinates (x 10^4) and isotropic displacement parameters ($Å^2$ x 10^3)

	x	y	z	U
H(3A)	257(2)	6395(9)	1822(7)	45
H(3B)	66.6(8)	5144(4)	1446(10)	45
H(3C)	251(2)	6051(12)	725(4)	45
H(3)	813.5(9)	3862(2)	385(2)	27
H(4)	1328.6(10)	6145(2)	310(2)	30
H(5)	1442.9(10)	7181(2)	2245(2)	32
H(6)	991.3(9)	5537(2)	3475(2)	26
H(7)	1633.9(9)	2444(2)	1740(2)	26
H(8)	1729.5(9)	3479(2)	3690(2)	27
H(9)	2230.9(9)	5769(2)	3645(2)	30
H(10)	2446.8(9)	6154(2)	1670(2)	30
H(11)	2058.2(9)	4105(2)	494(2)	28
H(12)	2625.3(9)	3872(2)	2556(2)	28
H(2)	-983.7(6)	468.3(13)	955.7(11)	24
H(4A)	-1665.9(8)	-55(2)	-822.1(14)	31
H(4B)	-1198.9(8)	931(2)	-657.9(14)	31
H(5A)	-2234(3)	920(2)	16(11)	51
H(5B)	-2040(5)	1833(9)	-691(4)	51
H(5C)	-1741(2)	1808(9)	428(7)	51
H(6A)	-845.9(8)	-1370(2)	-208.3(15)	32
H(6B)	-437.4(8)	-285(2)	-31.7(15)	32
H(7A)	12(4)	-1715(11)	938(3)	48
H(7B)	-542(2)	-1959(9)	1371(7)	48
H(7C)	-190(5)	-809(3)	1642(4)	48
H(8A)	-1839.6(8)	-264(2)	1181.6(14)	27
H(8B)	-1303.2(8)	-997(2)	1696.4(14)	27
H(9A)	-2042(5)	-2180(7)	887(6)	44
H(9B)	-1483.6(10)	-2338(6)	447(10)	44
H(9C)	-2002(5)	-1589(2)	-117(4)	44

C14 Crystal Data for $Mo(NAr^{i})_2(OCbPh)_2$ - 34

Empirical Formula	$C_{40}H_{64}B_{20}MoN_2O_2$	
Temperature	160(2)K	
Wavelength	0.71073Å	
Crystal System	Triclinic	
Space Group	$P\bar{1}$	
Unit Cell Dimensions	a = 13.1462(11)Å	alpha = 76.930(2)°
	b = 13.6145(12)Å	beta = 67.555(2)°
	c = 16.9491(15)Å	gamma = 61.590(2)°
Crystal Size	0.66 × 0.51 × 0.46 mm	
Final R indices [I>2σ(I)]	R1 = 0.0273	wR2 = 0.0675
R indices (all data)	R1 = 0.0328	wR2 = 0.0715

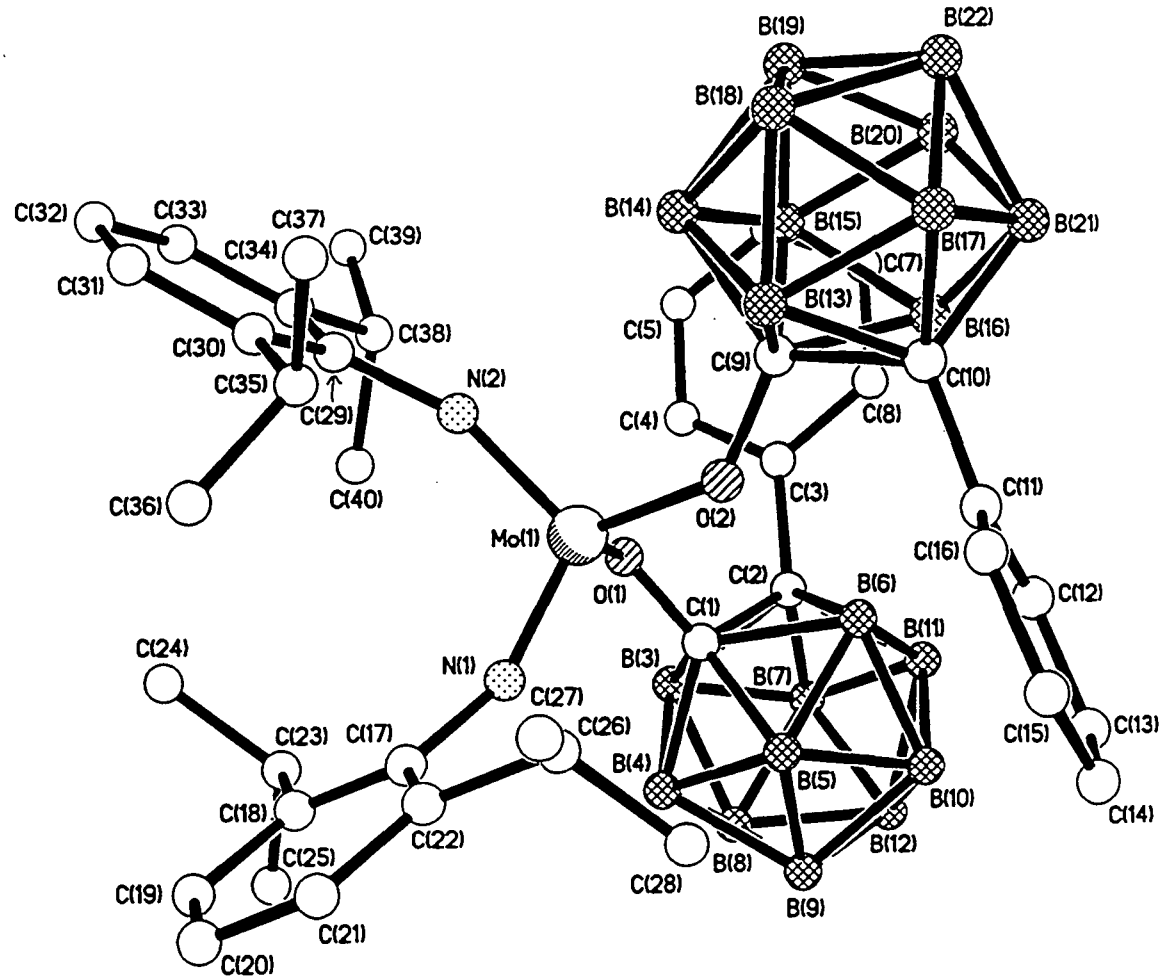

Table Bond lengths (Å) and angles (°)

Mo(1)-N(2)	1.7369(14)	Mo(1)-N(1)	1.7421(13)
Mo(1)-O(2)	1.9424(11)	Mo(1)-O(1)	1.9517(11)
O(1)-C(1)	1.3498(19)	C(1)-B(4)	1.698(3)
C(1)-B(5)	1.705(2)	C(1)-C(2)	1.708(2)
C(1)-B(3)	1.722(2)	C(1)-B(6)	1.737(2)
C(2)-C(3)	1.511(2)	C(2)-B(11)	1.714(3)
C(2)-B(7)	1.715(3)	C(2)-B(6)	1.728(2)
C(2)-B(3)	1.734(3)	C(3)-C(4)	1.386(3)
C(3)-C(8)	1.391(3)	C(4)-C(5)	1.393(3)
C(5)-C(6)	1.371(3)	C(6)-C(7)	1.378(3)
C(7)-C(8)	1.389(3)	B(3)-B(8)	1.769(3)
B(3)-B(7)	1.773(3)	B(3)-B(4)	1.781(3)
B(4)-B(8)	1.774(3)	B(4)-B(9)	1.777(3)
B(4)-B(5)	1.786(3)	B(5)-B(6)	1.770(3)
B(5)-B(9)	1.774(3)	B(5)-B(10)	1.779(3)
B(6)-B(10)	1.762(3)	B(6)-B(11)	1.774(3)
B(7)-B(8)	1.780(3)	B(7)-B(11)	1.781(3)
B(7)-B(12)	1.785(3)	B(8)-B(12)	1.781(3)
B(8)-B(9)	1.782(3)	B(9)-B(12)	1.778(3)
B(9)-B(10)	1.791(3)	B(10)-B(11)	1.782(3)
B(10)-B(12)	1.783(3)	B(11)-B(12)	1.779(3)
O(2)-C(9)	1.3504(19)	C(9)-B(14)	1.701(2)
C(9)-B(15)	1.706(2)	C(9)-C(10)	1.710(2)
C(9)-B(13)	1.729(2)	C(9)-B(16)	1.734(2)
C(10)-C(11)	1.508(2)	C(10)-B(21)	1.708(3)
C(10)-B(17)	1.712(2)	C(10)-B(16)	1.732(2)
C(10)-B(13)	1.734(2)	C(11)-C(12)	1.391(2)
C(11)-C(16)	1.394(2)	C(12)-C(13)	1.389(3)
C(13)-C(14)	1.378(3)	C(14)-C(15)	1.380(3)
C(15)-C(16)	1.391(3)	B(13)-B(18)	1.767(3)
B(13)-B(17)	1.775(3)	B(13)-B(14)	1.783(3)
B(14)-B(19)	1.770(3)	B(14)-B(18)	1.775(3)
B(14)-B(15)	1.778(3)	B(15)-B(16)	1.771(3)
B(15)-B(20)	1.776(3)	B(15)-B(19)	1.779(3)
B(16)-B(21)	1.764(3)	B(16)-B(20)	1.768(3)
B(17)-B(21)	1.773(3)	B(17)-B(18)	1.777(3)
B(17)-B(22)	1.778(3)	B(18)-B(19)	1.785(3)
B(18)-B(22)	1.789(3)	B(19)-B(20)	1.781(3)
B(19)-B(22)	1.783(3)	B(20)-B(21)	1.775(3)
B(20)-B(22)	1.781(3)	B(21)-B(22)	1.780(3)
N(1)-C(17)	1.397(2)	C(17)-C(18)	1.406(2)
C(17)-C(22)	1.413(2)	C(18)-C(19)	1.396(3)
C(18)-C(23)	1.513(3)	C(19)-C(20)	1.377(3)
C(20)-C(21)	1.382(3)	C(21)-C(22)	1.391(2)
C(22)-C(26)	1.514(2)	C(23)-C(25)	1.533(3)
C(23)-C(24)	1.534(3)	C(26)-C(27)	1.525(2)
C(26)-C(28)	1.529(3)	N(2)-C(29)	1.398(2)
C(29)-C(30)	1.409(2)	C(29)-C(34)	1.417(2)
C(30)-C(31)	1.399(2)	C(30)-C(35)	1.515(2)
C(31)-C(32)	1.378(3)	C(32)-C(33)	1.387(3)
C(33)-C(34)	1.394(2)	C(34)-C(38)	1.515(2)
C(35)-C(36)	1.533(3)	C(35)-C(37)	1.535(3)
C(38)-C(39)	1.531(2)	C(38)-C(40)	1.536(3)

N(2)-Mo(1)-N(1)	108.06(6)	N(2)-Mo(1)-O(2)	110.86(6)
N(1)-Mo(1)-O(2)	106.67(6)	N(2)-Mo(1)-O(1)	102.68(6)
N(1)-Mo(1)-O(1)	111.61(6)	O(2)-Mo(1)-O(1)	116.72(5)
C(1)-O(1)-Mo(1)	125.53(10)	O(1)-C(1)-B(4)	124.07(14)

O(1)-C(1)-B(5)	124.22(13)	B(4)-C(1)-B(5)	63.33(11)
O(1)-C(1)-C(2)	114.30(13)	B(4)-C(1)-C(2)	111.02(12)
B(5)-C(1)-C(2)	110.22(12)	O(1)-C(1)-B(3)	115.96(13)
B(4)-C(1)-B(3)	62.76(11)	B(5)-C(1)-B(3)	114.29(13)
C(2)-C(1)-B(3)	60.75(10)	O(1)-C(1)-B(6)	116.34(13)
B(4)-C(1)-B(6)	113.75(13)	B(5)-C(1)-B(6)	61.89(11)
C(2)-C(1)-B(6)	60.21(10)	B(3)-C(1)-B(6)	112.21(13)
C(3)-C(2)-C(1)	117.96(13)	C(3)-C(2)-B(11)	120.86(14)
C(1)-C(2)-B(11)	109.91(12)	C(3)-C(2)-B(7)	124.07(13)
C(1)-C(2)-B(7)	109.26(13)	B(11)-C(2)-B(7)	62.57(11)
C(3)-C(2)-B(6)	115.21(13)	C(1)-C(2)-B(6)	60.75(10)
B(11)-C(2)-B(6)	62.06(11)	B(7)-C(2)-B(6)	113.00(13)
C(3)-C(2)-B(3)	119.84(14)	C(1)-C(2)-B(3)	60.03(10)
B(11)-C(2)-B(3)	113.06(13)	B(7)-C(2)-B(3)	61.85(11)
B(6)-C(2)-B(3)	112.06(13)	C(4)-C(3)-C(8)	118.35(17)
C(4)-C(3)-C(2)	122.01(16)	C(8)-C(3)-C(2)	119.63(16)
C(3)-C(4)-C(5)	120.3(2)	C(6)-C(5)-C(4)	120.9(2)
C(5)-C(6)-C(7)	119.49(19)	C(6)-C(7)-C(8)	120.1(2)
C(7)-C(8)-C(3)	120.91(19)	C(1)-B(3)-C(2)	59.23(10)
C(1)-B(3)-B(8)	104.72(13)	C(2)-B(3)-B(8)	105.44(14)
C(1)-B(3)-B(7)	106.01(13)	C(2)-B(3)-B(7)	58.55(10)
B(8)-B(3)-B(7)	60.32(12)	C(1)-B(3)-B(4)	57.98(10)
C(2)-B(3)-B(4)	106.00(13)	B(8)-B(3)-B(4)	59.97(11)
B(7)-B(3)-B(4)	108.42(14)	C(1)-B(4)-B(8)	105.49(14)
C(1)-B(4)-B(9)	105.11(13)	B(8)-B(4)-B(9)	60.25(12)
C(1)-B(4)-B(3)	59.26(10)	B(8)-B(4)-B(3)	59.68(11)
B(9)-B(4)-B(3)	107.78(14)	C(1)-B(4)-B(5)	58.52(10)
B(8)-B(4)-B(5)	107.79(14)	B(9)-B(4)-B(5)	59.72(11)
B(3)-B(4)-B(5)	107.58(13)	C(1)-B(5)-B(6)	59.96(10)
C(1)-B(5)-B(9)	104.94(13)	B(6)-B(5)-B(9)	107.83(13)
C(1)-B(5)-B(10)	106.01(13)	B(6)-B(5)-B(10)	59.53(11)
B(9)-B(5)-B(10)	60.53(11)	C(1)-B(5)-B(4)	58.15(10)
B(6)-B(5)-B(4)	107.99(13)	B(9)-B(5)-B(4)	59.87(11)
B(10)-B(5)-B(4)	108.40(14)	C(2)-B(6)-C(1)	59.04(9)
C(2)-B(6)-B(10)	106.05(13)	C(1)-B(6)-B(10)	105.34(13)
C(2)-B(6)-B(5)	106.28(13)	C(1)-B(6)-B(5)	58.15(10)
B(10)-B(6)-B(5)	60.47(11)	C(2)-B(6)-B(11)	58.56(10)
C(1)-B(6)-B(11)	105.79(13)	B(10)-B(6)-B(11)	60.50(11)
B(5)-B(6)-B(11)	108.72(14)	C(2)-B(7)-B(3)	59.59(10)
C(2)-B(7)-B(8)	105.78(13)	B(3)-B(7)-B(8)	59.74(11)
C(2)-B(7)-B(11)	58.67(10)	B(3)-B(7)-B(11)	108.06(13)
B(8)-B(7)-B(11)	107.96(14)	C(2)-B(7)-B(12)	105.20(13)
B(3)-B(7)-B(12)	107.67(14)	B(8)-B(7)-B(12)	59.97(12)
B(11)-B(7)-B(12)	59.87(11)	B(3)-B(8)-B(4)	60.34(11)
B(3)-B(8)-B(7)	59.94(11)	B(4)-B(8)-B(7)	108.41(14)
B(3)-B(8)-B(12)	107.98(14)	B(4)-B(8)-B(12)	108.03(14)
B(7)-B(8)-B(12)	60.16(12)	B(3)-B(8)-B(9)	108.05(14)
B(4)-B(8)-B(9)	59.94(11)	B(7)-B(8)-B(9)	108.11(14)
B(12)-B(8)-B(9)	59.87(12)	B(5)-B(9)-B(4)	60.41(11)
B(5)-B(9)-B(12)	107.87(14)	B(4)-B(9)-B(12)	108.06(14)
B(5)-B(9)-B(8)	107.98(14)	B(4)-B(9)-B(8)	59.81(12)
B(12)-B(9)-B(8)	60.03(12)	B(5)-B(9)-B(10)	59.87(11)
B(4)-B(9)-B(10)	108.30(14)	B(12)-B(9)-B(10)	59.96(11)
B(8)-B(9)-B(10)	107.96(14)	B(6)-B(10)-B(5)	59.99(11)
B(6)-B(10)-B(11)	60.08(11)	B(5)-B(10)-B(11)	108.01(13)
B(6)-B(10)-B(12)	107.65(13)	B(5)-B(10)-B(12)	107.44(14)
B(11)-B(10)-B(12)	59.87(11)	B(6)-B(10)-B(9)	107.46(13)
B(5)-B(10)-B(9)	59.61(11)	B(11)-B(10)-B(9)	107.62(14)
B(12)-B(10)-B(9)	59.68(12)	C(2)-B(11)-B(6)	59.37(10)
C(2)-B(11)-B(12)	105.52(14)	B(6)-B(11)-B(12)	107.30(14)
C(2)-B(11)-B(7)	58.77(10)	B(6)-B(11)-B(7)	107.76(13)
B(12)-B(11)-B(7)	60.18(11)	C(2)-B(11)-B(10)	105.82(13)

B(6)-B(11)-B(10)	59.41(11)	B(12)-B(11)-B(10)	60.11(11)
B(7)-B(11)-B(10)	108.34(14)	B(9)-B(12)-B(11)	108.27(14)
B(9)-B(12)-B(8)	60.10(12)	B(11)-B(12)-B(8)	107.96(14)
B(9)-B(12)-B(10)	60.36(11)	B(11)-B(12)-B(10)	60.02(11)
B(8)-B(12)-B(10)	108.34(14)	B(9)-B(12)-B(7)	108.07(14)
B(11)-B(12)-B(7)	59.95(11)	B(8)-B(12)-B(7)	59.88(12)
B(10)-B(12)-B(7)	108.08(14)	C(9)-O(2)-Mo(1)	133.76(10)
O(2)-C(9)-B(14)	124.37(13)	O(2)-C(9)-B(15)	124.04(14)
B(14)-C(9)-B(15)	62.92(11)	O(2)-C(9)-C(10)	114.61(12)
B(14)-C(9)-C(10)	110.59(12)	B(15)-C(9)-C(10)	110.27(12)
O(2)-C(9)-B(13)	116.33(13)	B(14)-C(9)-B(13)	62.63(11)
B(15)-C(9)-B(13)	113.98(13)	C(10)-C(9)-B(13)	60.56(10)
O(2)-C(9)-B(16)	116.33(13)	B(14)-C(9)-B(16)	113.32(13)
B(15)-C(9)-B(16)	61.96(11)	C(10)-C(9)-B(16)	60.38(10)
B(13)-C(9)-B(16)	112.13(12)	C(11)-C(10)-B(21)	122.71(13)
C(11)-C(10)-C(9)	119.02(12)	B(21)-C(10)-C(9)	109.43(12)
C(11)-C(10)-B(17)	120.96(13)	B(21)-C(10)-B(17)	62.47(11)
C(9)-C(10)-B(17)	109.40(12)	C(11)-C(10)-B(16)	119.39(13)
B(21)-C(10)-B(16)	61.69(11)	C(9)-C(10)-B(16)	60.49(10)
B(17)-C(10)-B(16)	112.68(13)	C(11)-C(10)-B(13)	116.52(13)
B(21)-C(10)-B(13)	112.97(13)	C(9)-C(10)-B(13)	60.26(10)
B(17)-C(10)-B(13)	62.00(11)	B(16)-C(10)-B(13)	111.98(12)
C(12)-C(11)-C(16)	118.63(16)	C(12)-C(11)-C(10)	121.84(15)
C(16)-C(11)-C(10)	119.49(15)	C(13)-C(12)-C(11)	120.35(18)
C(14)-C(13)-C(12)	120.61(19)	C(13)-C(14)-C(15)	119.66(18)
C(14)-C(15)-C(16)	120.10(18)	C(15)-C(16)-C(11)	120.63(17)
C(9)-B(13)-C(10)	59.18(9)	C(9)-B(13)-B(18)	104.96(13)
C(10)-B(13)-B(18)	105.54(13)	C(9)-B(13)-B(17)	105.68(13)
C(10)-B(13)-B(17)	58.37(10)	B(18)-B(13)-B(17)	60.24(11)
C(9)-B(13)-B(14)	57.90(10)	C(10)-B(13)-B(14)	105.73(13)
B(18)-B(13)-B(14)	60.03(11)	B(17)-B(13)-B(14)	107.92(14)
C(9)-B(14)-B(19)	105.66(13)	C(9)-B(14)-B(18)	105.80(13)
B(19)-B(14)-B(18)	60.47(11)	C(9)-B(14)-B(15)	58.70(10)
B(19)-B(14)-B(15)	60.17(11)	B(18)-B(14)-B(15)	108.43(14)
C(9)-B(14)-B(13)	59.47(10)	B(19)-B(14)-B(13)	107.99(13)
B(18)-B(14)-B(13)	59.54(11)	B(15)-B(14)-B(13)	108.01(13)
C(9)-B(15)-B(16)	59.78(10)	C(9)-B(15)-B(20)	105.97(13)
B(16)-B(15)-B(20)	59.77(11)	C(9)-B(15)-B(14)	58.38(10)
B(16)-B(15)-B(14)	107.89(13)	B(20)-B(15)-B(14)	107.90(14)
C(9)-B(15)-B(19)	105.04(13)	B(16)-B(15)-B(19)	107.77(14)
B(20)-B(15)-B(19)	60.15(11)	B(14)-B(15)-B(19)	59.70(11)
C(10)-B(16)-C(9)	59.13(9)	C(10)-B(16)-B(21)	58.48(10)
C(9)-B(16)-B(21)	105.81(13)	C(10)-B(16)-B(20)	105.74(13)
C(9)-B(16)-B(20)	105.17(13)	B(21)-B(16)-B(20)	60.34(11)
C(10)-B(16)-B(15)	106.30(13)	C(9)-B(16)-B(15)	58.25(10)
B(21)-B(16)-B(15)	108.53(14)	B(20)-B(16)-B(15)	60.26(11)
C(10)-B(17)-B(21)	58.66(10)	C(10)-B(17)-B(13)	59.63(10)
B(21)-B(17)-B(13)	107.97(13)	C(10)-B(17)-B(18)	106.06(13)
B(21)-B(17)-B(18)	108.27(14)	B(13)-B(17)-B(18)	59.65(11)
C(10)-B(17)-B(22)	105.90(14)	B(21)-B(17)-B(22)	60.15(11)
B(13)-B(17)-B(22)	108.16(14)	B(18)-B(17)-B(22)	60.43(11)
B(13)-B(18)-B(14)	60.44(11)	B(13)-B(18)-B(17)	60.11(11)
B(14)-B(18)-B(17)	108.14(13)	B(13)-B(18)-B(19)	108.04(13)
B(14)-B(18)-B(19)	59.62(11)	B(17)-B(18)-B(19)	107.65(14)
B(13)-B(18)-B(22)	108.04(14)	B(14)-B(18)-B(22)	107.66(14)
B(17)-B(18)-B(22)	59.82(11)	B(19)-B(18)-B(22)	59.82(11)
B(14)-B(19)-B(15)	60.14(11)	B(14)-B(19)-B(20)	108.02(13)
B(15)-B(19)-B(20)	59.87(11)	B(14)-B(19)-B(22)	108.20(14)
B(15)-B(19)-B(22)	107.98(14)	B(20)-B(19)-B(22)	59.95(11)
B(14)-B(19)-B(18)	59.91(11)	B(15)-B(19)-B(18)	107.97(13)
B(20)-B(19)-B(18)	107.99(14)	B(22)-B(19)-B(18)	60.20(12)
B(16)-B(20)-B(21)	59.73(11)	B(16)-B(20)-B(15)	59.97(11)

B(21)-B(20)-B(15)	107.81(13)	B(16)-B(20)-B(22)	107.92(14)
B(21)-B(20)-B(22)	60.08(11)	B(15)-B(20)-B(22)	108.16(14)
B(16)-B(20)-B(19)	107.79(13)	B(21)-B(20)-B(19)	107.86(14)
B(15)-B(20)-B(19)	59.99(11)	B(22)-B(20)-B(19)	60.05(11)
C(10)-B(21)-B(16)	59.83(10)	C(10)-B(21)-B(17)	58.86(10)
B(16)-B(21)-B(17)	108.25(13)	C(10)-B(21)-B(20)	106.47(13)
B(16)-B(21)-B(20)	59.93(11)	B(17)-B(21)-B(20)	108.22(14)
C(10)-B(21)-B(22)	105.99(13)	B(16)-B(21)-B(22)	108.12(14)
B(17)-B(21)-B(22)	60.07(11)	B(20)-B(21)-B(22)	60.12(12)
B(17)-B(22)-B(21)	59.78(11)	B(17)-B(22)-B(20)	107.73(13)
B(21)-B(22)-B(20)	59.80(11)	B(17)-B(22)-B(19)	107.72(14)
B(21)-B(22)-B(19)	107.60(14)	B(20)-B(22)-B(19)	59.99(11)
B(17)-B(22)-B(18)	59.75(11)	B(21)-B(22)-B(18)	107.44(14)
B(20)-B(22)-B(18)	107.84(14)	B(19)-B(22)-B(18)	59.98(11)
C(17)-N(1)-Mo(1)	158.06(12)	N(1)-C(17)-C(18)	120.65(15)
N(1)-C(17)-C(22)	117.17(14)	C(18)-C(17)-C(22)	122.18(15)
C(19)-C(18)-C(17)	117.45(17)	C(19)-C(18)-C(23)	120.23(16)
C(17)-C(18)-C(23)	122.30(15)	C(20)-C(19)-C(18)	121.18(18)
C(19)-C(20)-C(21)	120.58(17)	C(20)-C(21)-C(22)	121.14(17)
C(21)-C(22)-C(17)	117.46(16)	C(21)-C(22)-C(26)	122.54(16)
C(17)-C(22)-C(26)	119.99(14)	C(18)-C(23)-C(25)	111.48(18)
C(18)-C(23)-C(24)	110.86(18)	C(25)-C(23)-C(24)	110.57(18)
C(22)-C(26)-C(27)	113.73(15)	C(22)-C(26)-C(28)	110.19(14)
C(27)-C(26)-C(28)	111.01(15)	C(29)-N(2)-Mo(1)	160.54(12)
N(2)-C(29)-C(30)	120.78(14)	N(2)-C(29)-C(34)	116.70(15)
C(30)-C(29)-C(34)	122.48(15)	C(31)-C(30)-C(29)	116.98(16)
C(31)-C(30)-C(35)	119.47(16)	C(29)-C(30)-C(35)	123.55(15)
C(32)-C(31)-C(30)	121.58(17)	C(31)-C(32)-C(33)	120.57(16)
C(32)-C(33)-C(34)	120.98(17)	C(33)-C(34)-C(29)	117.41(16)
C(33)-C(34)-C(38)	122.25(16)	C(29)-C(34)-C(38)	120.31(15)
C(30)-C(35)-C(36)	111.03(15)	C(30)-C(35)-C(37)	112.00(15)
C(36)-C(35)-C(37)	109.77(16)	C(34)-C(38)-C(39)	113.02(15)
C(34)-C(38)-C(40)	110.57(15)	C(39)-C(38)-C(40)	109.62(15)

Table Atomic coordinates (x 10^4) and equivalent isotropic displacement parameters ($Å^2$ x 10^3) for kw53. U(eq) is defined as one third of the trace of the orthogonalized U_{ij} tensor.

	x	y	z	U(eq)
Mo(1)	2145.13(12)	2699.27(11)	7409.78(8)	16.56(5)
O(1)	778.1(10)	3063.1(10)	7023.3(7)	23.5(2)
C(1)	-409.6(14)	3679.5(14)	7441.6(10)	20.5(3)
C(2)	-1378.6(14)	3205.3(13)	7400.1(10)	20.6(3)
C(3)	-829.2(15)	2142.1(14)	6950.0(11)	23.5(3)
C(4)	-342(2)	2109.5(17)	6067.3(13)	37.5(4)
C(5)	139(2)	1117(2)	5675.7(15)	47.1(5)
C(6)	144.9(18)	156.4(17)	6152.6(15)	39.9(5)
C(7)	-329(2)	174.8(17)	7030.7(15)	43.3(5)
C(8)	-814.8(19)	1161.7(16)	7427.6(13)	36.3(4)
B(3)	-1334.0(18)	4413.4(16)	6812.6(13)	24.7(4)
B(4)	-1079.1(19)	5096.6(16)	7449.9(13)	26.3(4)
B(5)	-927.9(18)	4234.0(17)	8402.7(12)	23.8(4)
B(6)	-1092.7(17)	3036.5(16)	8347.9(12)	22.6(4)
B(7)	-2735.7(18)	4323.1(17)	7377.9(13)	26.9(4)
B(8)	-2575.0(19)	5530.0(17)	7432.5(14)	29.4(4)
B(9)	-2325.8(19)	5421.6(17)	8417.6(13)	27.2(4)
B(10)	-2330.5(18)	4137.9(17)	8975.1(12)	25.7(4)
B(11)	-2587.2(18)	3467.0(17)	8329.2(13)	25.8(4)
B(12)	-3351.7(18)	4948.2(17)	8374.9(14)	28.9(4)
O(2)	2210.4(11)	1772.1(9)	8461.2(7)	23.3(2)
C(9)	2716.4(14)	657.0(13)	8639.2(10)	19.5(3)
C(10)	2426.9(14)	268.0(13)	9705.5(10)	19.4(3)
C(11)	1688.8(15)	1163.3(13)	10346.4(10)	22.2(3)
C(12)	449.6(16)	1834.8(16)	10483.0(12)	31.7(4)
C(13)	-210.6(18)	2628.9(17)	11096.1(14)	39.7(5)
C(14)	349.0(19)	2759.7(17)	11580.8(13)	37.2(4)
C(15)	1576.9(19)	2094.2(17)	11455.7(12)	35.2(4)
C(16)	2247.4(17)	1302.9(15)	10838.2(11)	28.4(4)
B(13)	3873.9(17)	146.4(16)	9081.7(12)	23.1(4)
B(14)	4126.4(17)	-247.2(16)	8065.0(12)	23.3(4)
B(15)	2785.0(18)	-301.4(17)	8099.6(12)	25.1(4)
B(16)	1713.0(17)	49.5(16)	9133.5(12)	22.7(4)
B(17)	3656.5(18)	-918.0(16)	9855.3(13)	25.6(4)
B(18)	4743.5(18)	-1269.7(16)	8821.5(13)	26.5(4)
B(19)	4073.0(18)	-1553.3(16)	8213.1(13)	25.6(4)
B(20)	2573.7(19)	-1368.4(17)	8874.7(13)	27.5(4)
B(21)	2320.0(18)	-970.7(16)	9885.4(13)	25.5(4)
B(22)	3783.3(19)	-1975.0(16)	9321.4(13)	28.5(4)
N(1)	2202.4(12)	3900.2(11)	7546.7(8)	19.7(3)
C(17)	2705.7(14)	4634.5(13)	7464.4(10)	20.4(3)
C(18)	2770.2(17)	5390.6(15)	6749.5(11)	27.2(4)
C(19)	3303(2)	6085.9(17)	6704.0(13)	36.9(4)
C(20)	3733(2)	6042.0(17)	7341.7(14)	39.2(5)
C(21)	3649.1(17)	5302.3(16)	8045.0(13)	31.8(4)
C(22)	3141.3(14)	4577.6(14)	8125.0(11)	22.4(3)
C(23)	2318(2)	5444.0(17)	6035.7(12)	35.4(4)
C(24)	3385(2)	5038(2)	5207.7(14)	49.4(6)
C(25)	1373(3)	6626(2)	5886.9(17)	56.0(6)
C(26)	3025.2(16)	3763.9(15)	8890.0(11)	25.4(3)
C(27)	3987.7(18)	3398.7(19)	9321.0(13)	37.9(5)

C(28)	1738.5(17)	4250.2(18)	9531.5(12)	35.1(4)
N(2)	3403.9(12)	2026.3(11)	6551.3(8)	20.7(3)
C(29)	4458.1(14)	1816.3(13)	5842.0(10)	20.6(3)
C(30)	5541.2(15)	1693.0(14)	5922.9(11)	23.9(3)
C(31)	6566.0(16)	1441.2(15)	5187.4(12)	30.4(4)
C(32)	6520.0(17)	1318.1(16)	4418.5(12)	35.0(4)
C(33)	5444.1(18)	1445.8(16)	4351.3(11)	31.5(4)
C(34)	4386.7(16)	1698.3(14)	5057.6(10)	24.0(3)
C(35)	5644.5(16)	1806.9(16)	6754.7(11)	28.2(4)
C(36)	5912.7(19)	2807.0(18)	6690.1(14)	38.8(5)
C(37)	6626.3(19)	739.6(18)	7025.9(14)	39.9(5)
C(38)	3186.1(16)	1884.1(14)	4997.9(11)	26.0(3)
C(39)	3348(2)	1316.8(17)	4246.6(12)	35.0(4)
C(40)	2353.9(18)	3139.7(16)	4933.7(12)	33.4(4)

Table Hydrogen atom coordinates (x 10^4) and isotropic displacement parameters ($Å^2$ x 10^3)

	x	y	z	U
H(4)	-337	2767	5728	45
H(5)	467	1105	5070	56
H(6)	473	-516	5880	48
H(7)	-323	-489	7365	52
H(8)	-1142	1167	8033	44
H(3)	-988	4479	6097	30
H(4A)	-574	5628	7155	32
H(5A)	-320	4194	8737	29
H(6A)	-584	2201	8636	27
H(7A)	-3326	4345	7036	32
H(8A)	-3069	6359	7129	35
H(9)	-2654	6178	8766	33
H(10)	-2659	4043	9690	31
H(11)	-3081	2925	8613	31
H(12)	-4360	5394	8696	35
H(12A)	53	1750	10155	38
H(13)	-1056	3086	11182	48
H(14)	-108	3305	11999	45
H(15)	1965	2177	11792	42
H(16)	3094	853	10751	34
H(13A)	4283	665	9155	28
H(14A)	4718	2	7461	28
H(15A)	2486	-86	7522	30
H(16A)	707	506	9241	27
H(17)	3937	-1116	10440	31
H(18)	5749	-1705	8719	32
H(19)	4637	-2179	7707	31
H(20)	2144	-1871	8807	33
H(21)	1714	-1201	10491	31
H(22)	4154	-2877	9548	34
H(19A)	3370	6598	6225	44
H(20A)	4090	6524	7298	47
H(21A)	3943	5289	8481	38
H(23)	1912	4931	6209	43
H(24A)	3072	5081	4755	74
H(24B)	3949	4262	5303	74
H(24C)	3817	5512	5036	74
H(25A)	1033	6615	5467	84
H(25B)	1765	7134	5672	84
H(25C)	715	6884	6427	84
H(26)	3139	3078	8679	30
H(27A)	3913	2818	9771	57
H(27B)	3866	4043	9573	57
H(27C)	4803	3101	8896	57
H(28A)	1650	3689	9996	53
H(28B)	1138	4460	9243	53
H(28C)	1603	4913	9766	53
H(31)	7311	1353	5219	37
H(32)	7231	1144	3930	42
H(33)	5427	1360	3816	38
H(35)	4842	1944	7210	34
H(36A)	5927	2890	7245	58

H(36B)	5275	3489	6527	58
H(36C)	6707	2682	6257	58
H(37A)	6609	819	7592	60
H(37B)	7431	619	6610	60
H(37C)	6465	99	7049	60
H(38)	2768	1557	5537	31
H(39A)	2559	1370	4288	52
H(39B)	3930	528	4263	52
H(39C)	3657	1690	3708	52
H(40A)	1580	3244	4901	50
H(40B)	2755	3486	4419	50
H(40C)	2196	3490	5440	50

C15 CRYSTAL DATA FOR PhCbNHOH·dioxane - 30

Empirical Formula	$C_{10}H_{21}B_{10}NO_2$	
Temperature	160(2)K	
Wavelength	0.71073Å	
Crystal System	Monoclinic	
Space Group	$P2_1/c$	
Unit Cell Dimensions	a = 12.3940(10)Å	alpha = 90°
	b = 6.7140(10)Å	beta = 94.30(2)°
	c = 19.498(2)Å	gamma = 90°
Crystal Size	0.46 × 0.34 × 0.19 mm	
Final R indices [I>2σ(I)]	R1 = 0.0480	wR2 = 0.1126
R indices (all data)	R1 = 0.0698	wR2 = 0.1339

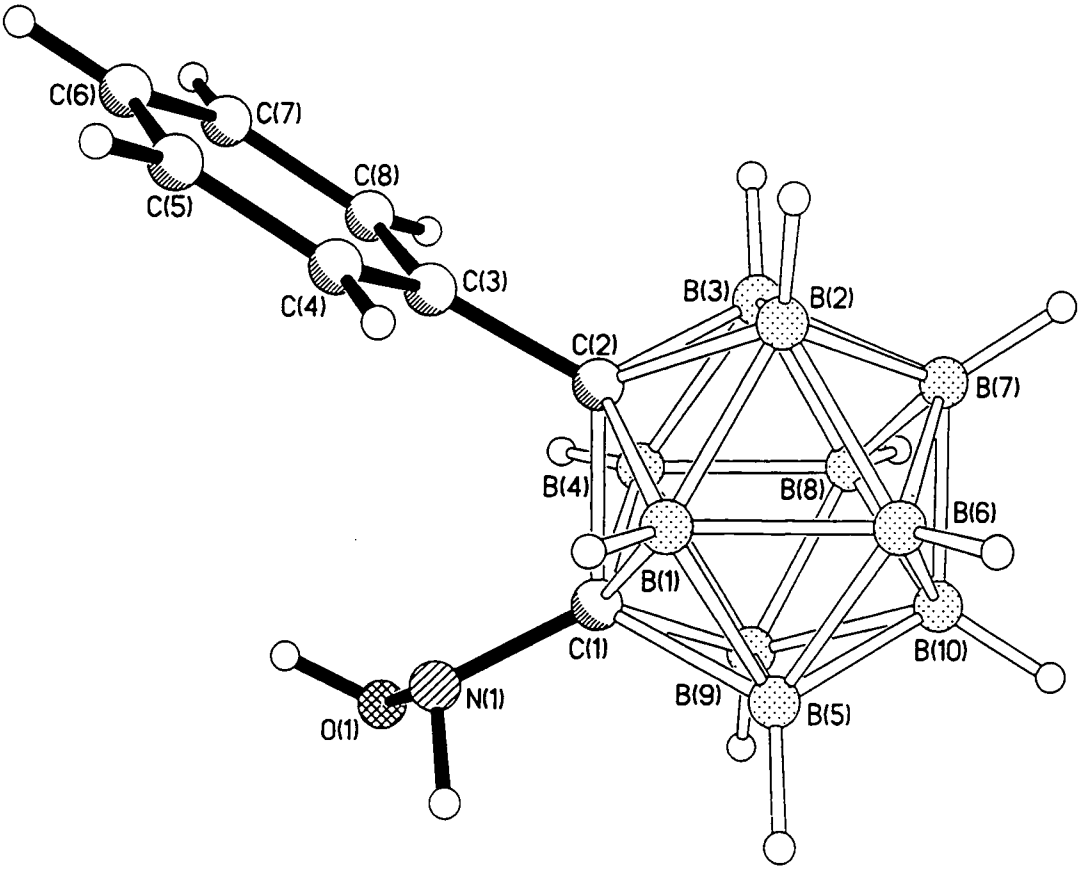

Table Hydrogen atom coordinates (x 10^4) and isotropic displacement parameters ($Å^2$ x 10^3) for kw58.

	x	y	z	U
H(1A)	9721(22)	-99(42)	3389(16)	54(8)
H(1B)	9341(21)	2735(42)	2632(13)	49(8)
H(4)	6322(2)	2604(4)	3373.0(11)	37
H(5)	5951(2)	2119(4)	4515.1(11)	42
H(6)	6185(2)	-987(4)	5022.6(11)	41
H(7)	6820(2)	-3630(4)	4398.1(11)	43
H(8)	7216(2)	-3173(3)	3256.2(11)	36
H(1)	6952(2)	3764(4)	2430.5(12)	28
H(2)	5138(2)	1052(4)	1987.8(12)	29
H(3)	6034(2)	-3029(4)	1982.8(11)	29
H(4A)	8376(2)	-2752(4)	2423.4(12)	27
H(5A)	8536(2)	3629(4)	1368.5(11)	28
H(6A)	6201(2)	3451(4)	957.9(12)	30
H(7A)	5638(2)	-796(4)	675.4(12)	31
H(8A)	7643(2)	-3204(4)	939.4(12)	30
H(9)	9427(2)	-462(4)	1358.2(11)	28
H(10)	7723(2)	780(4)	290.3(12)	30
H(9A)	8610(2)	1071(4)	4915.3(12)	46
H(9B)	9117(2)	2455(4)	4351.6(12)	46
H(10A)	10820(2)	2318(4)	4968.4(11)	42
H(10B)	9939(2)	3160(4)	5455.4(11)	42

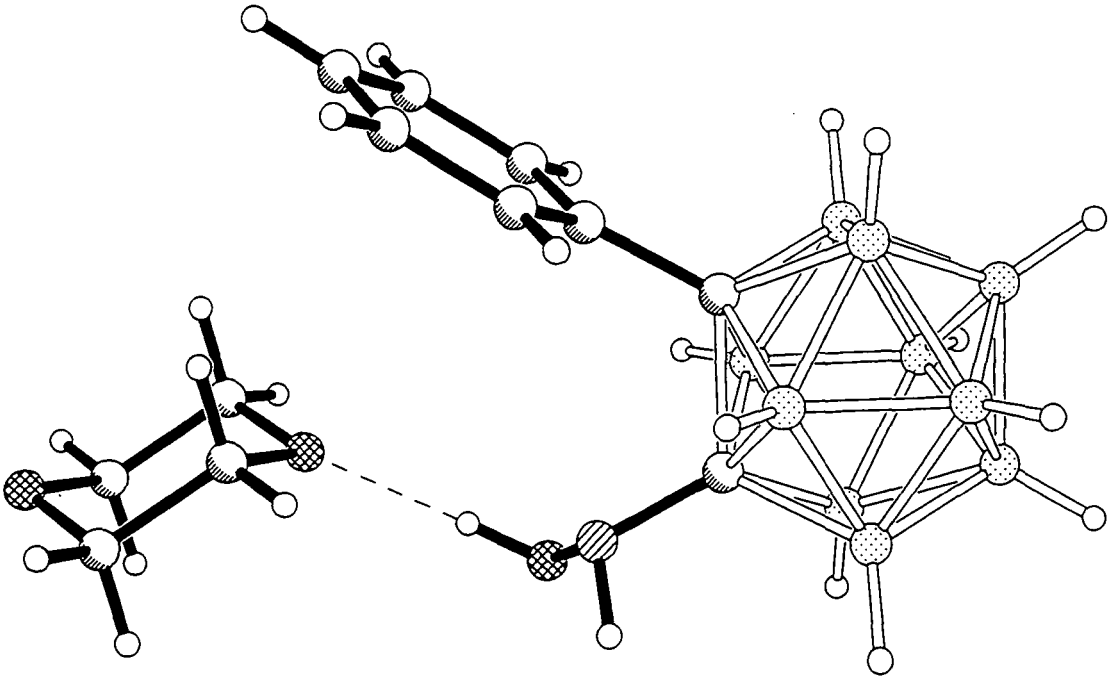

O(1)-N(1)	1.435(2)	N(1)-C(1)	1.423(3)
C(1)-B(9)	1.701(3)	C(1)-B(5)	1.701(3)
C(1)-B(4)	1.715(3)	C(1)-B(1)	1.729(3)
C(1)-C(2)	1.737(3)	C(2)-C(3)	1.506(3)
C(2)-B(3)	1.700(3)	C(2)-B(2)	1.705(3)
C(2)-B(1)	1.728(3)	C(2)-B(4)	1.735(3)
C(3)-C(4)	1.388(3)	C(3)-C(8)	1.389(3)
C(4)-C(5)	1.385(3)	C(5)-C(6)	1.371(3)
C(6)-C(7)	1.374(3)	C(7)-C(8)	1.388(3)
B(1)-B(6)	1.764(3)	B(1)-B(5)	1.778(3)
B(1)-B(2)	1.781(3)	B(2)-B(7)	1.771(3)
B(2)-B(3)	1.777(3)	B(2)-B(6)	1.781(3)
B(3)-B(7)	1.778(3)	B(3)-B(8)	1.779(3)
B(3)-B(4)	1.786(3)	B(4)-B(8)	1.777(3)
B(4)-B(9)	1.781(3)	B(5)-B(6)	1.773(3)
B(5)-B(10)	1.774(3)	B(5)-B(9)	1.781(3)
B(6)-B(10)	1.788(3)	B(6)-B(7)	1.788(3)
B(7)-B(10)	1.774(3)	B(7)-B(8)	1.790(3)
B(8)-B(9)	1.771(3)	B(8)-B(10)	1.781(3)
B(9)-B(10)	1.783(3)	O(2)-C(10#1)	1.429(3)
O(2)-C(9)	1.432(3)	C(9)-C(10)	1.502(3)
C(10)-O(2#1)	1.429(3)		

C(1)-N(1)-O(1)	110.7(2)	N(1)-C(1)-B(9)	126.0(2)
N(1)-C(1)-B(5)	120.8(2)	B(9)-C(1)-B(5)	63.14(13)
N(1)-C(1)-B(4)	120.2(2)	B(9)-C(1)-B(4)	62.83(13)
B(5)-C(1)-B(4)	114.2(2)	N(1)-C(1)-B(1)	112.6(2)
B(9)-C(1)-B(1)	113.9(2)	B(5)-C(1)-B(1)	62.42(13)
B(4)-C(1)-B(1)	112.0(2)	N(1)-C(1)-C(2)	115.7(2)
B(9)-C(1)-C(2)	110.36(15)	B(5)-C(1)-C(2)	109.82(15)
B(4)-C(1)-C(2)	60.35(12)	B(1)-C(1)-C(2)	59.79(12)
C(3)-C(2)-B(3)	121.0(2)	C(3)-C(2)-B(2)	121.9(2)
B(3)-C(2)-B(2)	62.91(13)	C(3)-C(2)-B(1)	118.9(2)
B(3)-C(2)-B(1)	113.4(2)	B(2)-C(2)-B(1)	62.51(13)
C(3)-C(2)-B(4)	117.0(2)	B(3)-C(2)-B(4)	62.64(13)
B(2)-C(2)-B(4)	113.7(2)	B(1)-C(2)-B(4)	111.07(15)
C(3)-C(2)-C(1)	119.4(2)	B(3)-C(2)-C(1)	109.06(14)
B(2)-C(2)-C(1)	109.56(15)	B(1)-C(2)-C(1)	59.88(12)
B(4)-C(2)-C(1)	59.21(12)	C(4)-C(3)-C(8)	119.0(2)
C(4)-C(3)-C(2)	121.0(2)	C(8)-C(3)-C(2)	119.8(2)
C(5)-C(4)-C(3)	120.1(2)	C(6)-C(5)-C(4)	120.5(2)
C(5)-C(6)-C(7)	119.9(2)	C(6)-C(7)-C(8)	120.3(2)
C(7)-C(8)-C(3)	120.1(2)	C(2)-B(1)-C(1)	60.32(12)
C(2)-B(1)-B(6)	105.7(2)	C(1)-B(1)-B(6)	105.3(2)
C(2)-B(1)-B(5)	106.7(2)	C(1)-B(1)-B(5)	58.01(12)
B(6)-B(1)-B(5)	60.09(13)	C(2)-B(1)-B(2)	58.12(13)
C(1)-B(1)-B(2)	106.4(2)	B(6)-B(1)-B(2)	60.30(13)
B(5)-B(1)-B(2)	108.3(2)	C(2)-B(2)-B(7)	105.6(2)
C(2)-B(2)-B(3)	58.42(12)	B(7)-B(2)-B(3)	60.15(13)
C(2)-B(2)-B(6)	106.0(2)	B(7)-B(2)-B(6)	60.46(13)
B(3)-B(2)-B(6)	108.3(2)	C(2)-B(2)-B(1)	59.37(12)
B(7)-B(2)-B(1)	107.5(2)	B(3)-B(2)-B(1)	107.3(2)
B(6)-B(2)-B(1)	59.36(13)	C(2)-B(3)-B(2)	58.68(13)
C(2)-B(3)-B(7)	105.5(2)	B(2)-B(3)-B(7)	59.75(13)
C(2)-B(3)-B(8)	106.2(2)	B(2)-B(3)-B(8)	108.2(2)
B(7)-B(3)-B(8)	60.43(13)	C(2)-B(3)-B(4)	59.64(12)
B(2)-B(3)-B(4)	107.9(2)	B(7)-B(3)-B(4)	107.9(2)
B(8)-B(3)-B(4)	59.80(13)	C(1)-B(4)-C(2)	60.44(12)

C(1)-B(4)-B(8)	104.7(2)	C(2)-B(4)-B(8)	104.8(2)
C(1)-B(4)-B(9)	58.18(12)	C(2)-B(4)-B(9)	106.8(2)
B(8)-B(4)-B(9)	59.70(13)	C(1)-B(4)-B(3)	106.1(2)
C(2)-B(4)-B(3)	57.72(12)	B(8)-B(4)-B(3)	59.91(13)
B(9)-B(4)-B(3)	107.9(2)	C(1)-B(5)-B(6)	106.1(2)
C(1)-B(5)-B(10)	105.4(2)	B(6)-B(5)-B(10)	60.54(14)
C(1)-B(5)-B(1)	59.58(12)	B(6)-B(5)-B(1)	59.57(13)
B(10)-B(5)-B(1)	107.7(2)	C(1)-B(5)-B(9)	58.42(12)
B(6)-B(5)-B(9)	108.8(2)	B(10)-B(5)-B(9)	60.19(14)
B(1)-B(5)-B(9)	107.8(2)	B(1)-B(6)-B(5)	60.34(13)
B(1)-B(6)-B(2)	60.33(13)	B(5)-B(6)-B(2)	108.5(2)
B(1)-B(6)-B(10)	107.7(2)	B(5)-B(6)-B(10)	59.75(13)
B(2)-B(6)-B(10)	107.4(2)	B(1)-B(6)-B(7)	107.5(2)
B(5)-B(6)-B(7)	107.4(2)	B(2)-B(6)-B(7)	59.50(13)
B(10)-B(6)-B(7)	59.47(13)	B(2)-B(7)-B(10)	108.5(2)
B(2)-B(7)-B(3)	60.09(13)	B(10)-B(7)-B(3)	108.1(2)
B(2)-B(7)-B(6)	60.04(13)	B(10)-B(7)-B(6)	60.26(14)
B(3)-B(7)-B(6)	107.9(2)	B(2)-B(7)-B(8)	108.0(2)
B(10)-B(7)-B(8)	59.97(13)	B(3)-B(7)-B(8)	59.82(13)
B(6)-B(7)-B(8)	107.9(2)	B(9)-B(8)-B(4)	60.24(13)
B(9)-B(8)-B(3)	108.7(2)	B(4)-B(8)-B(3)	60.29(13)
B(9)-B(8)-B(10)	60.24(14)	B(4)-B(8)-B(10)	108.0(2)
B(3)-B(8)-B(10)	107.7(2)	B(9)-B(8)-B(7)	108.1(2)
B(4)-B(8)-B(7)	107.8(2)	B(3)-B(8)-B(7)	59.75(13)
B(10)-B(8)-B(7)	59.56(13)	C(1)-B(9)-B(8)	105.6(2)
C(1)-B(9)-B(4)	58.99(12)	B(8)-B(9)-B(4)	60.06(13)
C(1)-B(9)-B(5)	58.43(12)	B(8)-B(9)-B(5)	107.8(2)
B(4)-B(9)-B(5)	107.3(2)	C(1)-B(9)-B(10)	105.0(2)
B(8)-B(9)-B(10)	60.18(14)	B(4)-B(9)-B(10)	107.8(2)
B(5)-B(9)-B(10)	59.71(13)	B(5)-B(10)-B(7)	108.0(2)
B(5)-B(10)-B(8)	107.7(2)	B(7)-B(10)-B(8)	60.47(14)
B(5)-B(10)-B(9)	60.11(13)	B(7)-B(10)-B(9)	108.3(2)
B(8)-B(10)-B(9)	59.59(13)	B(5)-B(10)-B(6)	59.71(13)
B(7)-B(10)-B(6)	60.27(13)	B(8)-B(10)-B(6)	108.3(2)
B(9)-B(10)-B(6)	108.0(2)	C(10#1)-O(2)-C(9)	109.8(2)
O(2)-C(9)-C(10)	110.2(2)	O(2#1)-C(10)-C(9)	110.2(2)

Symmetry transformations used to generate equivalent atoms:

#1: -x+2,-y,-z+1

Table Atomic coordinates (x 10^4) and equivalent isotropic displacement parameters ($Å^2$ x 10^3) for kw58. U(eq) is defined as one third of the trace of the orthogonalized U_{ij} tensor.

	x	y	z	U(eq)
O(1)	9777.9(11)	114(2)	2933.0(8)	28.7(4)
N(1)	8956.3(13)	1585(3)	2773.8(8)	23.8(4)
C(1)	8227(2)	935(3)	2220.4(10)	20.6(4)
C(2)	6995(2)	13(3)	2450.3(10)	21.3(5)
C(3)	6809(2)	-236(3)	3199.9(10)	22.8(5)
C(4)	6429(2)	1330(4)	3578.9(11)	31.2(5)
C(5)	6205(2)	1038(4)	4256.9(11)	34.8(6)
C(6)	6346(2)	-796(4)	4558.5(11)	34.5(6)
C(7)	6721(2)	-2359(4)	4188.5(11)	35.9(6)
C(8)	6955(2)	-2089(3)	3509.5(11)	30.0(5)
B(1)	7075(2)	2392(4)	2119.2(12)	22.9(5)
B(2)	5989(2)	754(4)	1860.9(12)	24.4(5)
B(3)	6528(2)	-1699(4)	1857.7(11)	24.0(5)
B(4)	7939(2)	-1551(4)	2115.8(12)	22.9(5)
B(5)	8036(2)	2302(4)	1486.9(11)	23.6(5)
B(6)	6630(2)	2195(4)	1241.2(12)	25.3(5)
B(7)	6293(2)	-357(4)	1074.3(12)	25.7(5)
B(8)	7499(2)	-1804(4)	1231.3(12)	25.3(5)
B(9)	8574(2)	-157(4)	1481.2(11)	23.4(5)
B(10)	7550(2)	592(4)	842.3(12)	25.3(5)
O(2)	9588.3(13)	-383(3)	4320.0(7)	36.7(4)
C(9)	9275(2)	1354(4)	4681.8(12)	38.7(6)
C(10)	10166(2)	1968(4)	5204.3(11)	35.3(6)

Appendix D

Courses, Lectures, Colloquia and Conferences Attended

D1 First Year Induction Courses: October 1993

The course consists of one hour lectures on the services available in the department.

1. Department Safety
2. Safety Matters
3. Electrical Appliances and Infrared Spectroscopy
4. Chromatography and Microanalysis
5. Atomic Absorption and Inorganic Analysis
6. Library Facilities
7. Mass Spectroscopy
8. Nuclear Magnetic Resonance
9. Glass Blowing Techniques
10. Introduction to Computing Facilities

D2 Examined Lecture Courses: October 1993 to April 1994

Three courses were attended consisting of 6 one hour lectures followed by a written examination in each.

1. "Diffraction and Scattering Methods", Prof. J.A.K. Howard (6 hours)
2. "Organometallic Chemistry", Prof. V.C. Gibson (3 hours) and Prof. D. Parker (3 hours)
3. "NMR Techniques", Dr. A. Kenwright (6 hours)

D3 RESEARCH COLLOQUIA, SEMINARS AND LECTURES ORGANISED BY THE DEPARTMENT OF CHEMISTRY

Only lectures attended by the author are shown.

During the period 1993 - 1994 (August 1 - July 31)

October 4 Prof. F.J. Feher, University of California, Irvine, USA
Bridging the Gap between Surfaces and Solution with Sessilquioxanes

October 20 Dr. P. Quayle, University of Manchester
Aspects of Aqueous ROMP Chemistry

October 21 Prof. R. Adams, University of South Carolina, USA
Chemistry of Metal Carbonyl Cluster Complexes : Development of Cluster Based Alkyne Hydrogenation Catalysts

October 27 Dr. R.A.L. Jones, Cavendish Laboratory, Cambridge
Perambulating Polymers

January 26 Prof. J. Evans, University of Southampton
Shining Light on Catalysts

February 16 Prof. K.H. Theopold, University of Delaware, USA
Paramagnetic Chromium Alkyls : Synthesis and Reactivity

February 23 Prof. P.M. Maitlis, University of Sheffield
Across the Border : From Homogeneous to Heterogeneous Catalysis

1994 - 1995 (August 1 - July 31)

October 5 Prof. N. L. Owen, Brigham Young University, Utah, USA
Determining Molecular Structure - the INADEQUATE NMR way

October 19 Prof. N. Bartlett, University of California

Some Aspects of Ag(II) and Ag(III) Chemistry

November 3 Prof. B. F. G. Johnson, Edinburgh University
Arene-metal Clusters

November 9 Dr G. Hogarth, University College, London
New Vistas in Metal-imido Chemistry

February 1 Dr T. Cosgrove, Bristol University
Polymers do it at Interfaces

February 8 Dr D. O'Hare, Oxford University
Synthesis and Solid-state Properties of Poly-, Oligo- and Multidecker Metallocenes

March 1 Dr M. Rosseinsky, Oxford University
Fullerene Intercalation Chemistry

March 22 Dr M. Taylor, University of Auckland, New Zealand
Structural Methods in Main-group Chemistry

1995 - 1996 (August 1 - July 31)

October 13 Prof. R. Schmutzler, Univ Braunschweig, FRG.
Calixarene-Phosphorus Chemistry: A New Dimension in Phosphorus Chemistry

November 15 Dr Andrea Sella, UCL, London
Chemistry of Lanthanides with Polypyrazoylborate Ligands

November 17 Prof. David Bergbreiter, Texas A&M, USA
Design of Smart Catalysts, Substrates and Surfaces from Simple Polymers

November 22 Prof. I Soutar, Lancaster University

A Water of Glass? Luminescence Studies of Water-Soluble Polymers.

November 29 Prof. Dennis Tuck, University of Windsor, Ontario, Canada
New Indium Coordination Chemistry

December 8 Professor M.T. Reetz, Max Planck Institut, Mulheim
Perkin Regional Meeting

January 31 Dr J. Penfold, Rutherford Appleton Laboratory,
Soft Soap and Surfaces

February 21 Dr C R Pulham , Univ. Edinburgh
Heavy Metal Hydrides - an exploration of the chemistry of stannanes and plumbanes

February 28 Prof. E. W. Randall, Queen Mary & Westfield College
New Perspectives in NMR Imaging

March 7 Dr D.S. Wright, University of Cambridge
Synthetic Applications of Me_2N-p-Block Metal Reagents

D4 CONFERENCES AND SYMPOSIA ATTENDED

Posters† and papers‡ presented.

†"*The Royal Scoiety of Chemistry, Annual Chemical Congress*", Heriot-watt University, Edinburgh, 10-13 April 1995

"*ISOM 11*", University of Durham, Durham, 10-14 July, 1995

‡"*Intraboron 15*", University of Leeds, Leeds, 11-13 September 1995

†"*ICI Poster Competition*", University of Durham, Durham, December 1995

‡"*North East Graduate Symposium*", Swallow Hotel, Seaburn, April 1996

†"*IMEBORON 9*", Ruprecht-Karls-Univerisität, Heidelberg, Germany, 14-18 July, 1996

"And as that is really the end of the story, and I am very tired after that last sentence, I think I shall stop there."

A.A. Milne in "Winnie-the-Pooh"